IDENTIFICATION OF BIOACTIVE SECONDARY METABOLITES FROM MANGROVE PLANT *AVICENNIA LANATA* AND ITS ENDOPHYTIC FUNGI BY USING METABOLOMICS

A THESIS PRESENTED FOR THE DEGREE OF DOCTOR OF
PHILOSOPHY IN
THE FACULTY OF SCIENCE
THE UNIVERSITY OF STRATHCLYDE

NOOR WINI BINTI MAZLAN
B.Sc., M.Sc.

Strathclyde Institute of Pharmacy and Biomedical Sciences
University of Strathclyde

November 2015

This thesis is the result of the author's original research. It has been composed by the author and has not been previously submitted for examination which has led to the award of a degree.

The copyright of this thesis belongs to the author under the terms of the United Kingdom Copyright Acts as qualified by University of Strathclyde Regulation 3.50. Due acknowledgement must always be made of the use of any material contained in, or derived from, this thesis.

Signed:

Date:

ACKNOWLEDMENT

<div align="center">**Table of Contents**</div>

LIST OF FIGURES

LIST OF TABLES

LIST OF ABBREVIATION AND SYMBOLS

$[\alpha]_D^{20}$	optical rotation at 20°C
μg	micro gram
μM	micro molar
δ_C	carbon chemical shift in ppm
δ_H	proton chemical shift in ppm
^{13}C NMR	carbon-13 nuclear magnetic resonance
^{1}H NMR	proton nuclear magnetic resonance
A-549	adenocarcinomic human alveolar basal epithelial cells
Acetone-d_6	deuterated acetone
ACN	acetonitrile
ADC	antibody-drug conjugates
B16 10F7	mouse melanoma cell line
BEL-7402	human liver cancer cell
BLAST	basic local alignment search tool
CCRF-CEM	human leukaemia cell
CD	circular dichroism
CDCl$_3$	deuterated chloroform
CHCl$_3$	chloroform
cm	centimetre
CMAC	continuous manufacturing and crystallisation
CNS	central nervous system
COSY	correlation spectroscopy
COX-2	cyclooxygenase-2
Da	Dalton
DCM	dichloromethane
DEPT	distortionless enhancement by polarization transfer
DMSO-d_6	deuterated dimethyl sulfoxide
DNA	deoxyribonucleic acid
DNP	Dictionary of Natural Products
DMEM	Dulbecco's modified Eagle's medium
EA	ethyl acetate
ECACC	European Collection of Cell Cultures
EC$_{50}$	half maximal effective concentration
EMA	European Medicines Agency
ESI	electrospray ionization
EU	European Union
FDA	Food and Drugs Administration
FDPM	Forestry Department Peninsular Malaysia
FT-IR	Fourier transformed infrared spectroscopy
g	gram
gGAPDH	enzyme glycosomal glyceraldehyde 3-phosphate
g/mol	mass in grams/molecular weight
GC	gas chromatography
GC-MS	gas chromatography-mass spectrometry
GPS	Global Positioning System
H	hexane

HAT	human African trypanosomiasis
HeLa	human cervical cancer cell line
HepG-2	human hepatoma cell line
HIV-1	human immunodeficiency virus related to viruses found in chimpanzees and gorillas living in western Africa
HL-60	human leukaemia cell
HMBC	heteronuclear multiple bond coherence
HMQC	heteronuclear multiple quantum coherence
HPLC	high performance liquid chromatography
HSQC	heteronuclear single quantum correlation
HRFT-LCMS	high resolution fourier transform liquid chromatography-mass spectrometry
HMI-9	human serum medium for trypanosome
H4IIE-C3	rat hepatoma cells
H37Ra	*Mycobacterium tuberculosis* cell
IC_{50}	half minimal (50%) inhibitory concentration (IC) of a substance
IC_{k50}	drug concentration needed to lower the growth constant (kc) by 50%.
$IR\nu_{max}$ (KBr)	Infrared, maximum wavelength measured in potassium bromide
ITS1	forward primer
ITS4	reverse primer
J	coupling constant in Hertz (Hz)
KB	human epidermoid carcinoma of the nasopharynx cell culture
KI	*Plasmodium falciparum* cell
kg	kilogram
km	kilometer
KOH	potassium hydroxide
K-562	human chronic myeloid leukaemia
L	liter
L-929	mouse fibroblast cell lines
m	meter
m/z	mass-to-charge ratio
MCPBA	*meta*-chloroperbenzoic acid
MCF-7	estrogen receptor-positive human breast cell cancer
MDA-MB-435	estrogen receptor-negative human breast cell cancer
MEOH	methanol
MHz	megahertz
MIC	minimum inhibition concentration
mL	milliliter
MOLT-4	human acute lymphoblastic leukaemia cell
MPLC	medium pressure liquid chromatography
mRNA	messenger ribonucleic acid
MS/MS	mass spectrometry/mass spectrometry
MVDA	multivariate data analysis
NADH	nicotinamide adenine dinucleotide (reduced form)
NaOH	sodium hydroxide

HCl	hydrochloric acid
n-BuOH	normal butanol
NCBI	National Centre for Biotechnology Information
NECT	nifurtimox/eflornithine
NF-κ B	nuclear factor kappa-light-chain-enhancer of activated B cells
NMR	nuclear magnetic resonance
NOESY	nuclear overhausser enhancement spectroscopy
NRK-49F	normal rat kidney fibroblast
OPLS-DA	orthogonal partial least square-discriminant analysis
P-388	murine leukaemia cell
PC-3	human prostatic cancer cell line
PCA	principal component analysis
PCR	polymerase chain reaction
PNT-2A	human normal prostatic epithelial cell line
ppm	parts per million
RAW 264.7	macrophage-like, Abelson leukaemia virus transformed cell line derived from mice
ROS	reactive oxygen species
Rt	retention time
SIMCA	soft independent modelling of class analogy
TBE/EDTA	tri-borate/ethylenediaminetetraacetic acid
SW626	ovarian adenocarcinoma cell lines
TGF-β1	transforming growth factor beta 1
TLC	thin layer chromatography
TNF-α	tumour necrosis factor alpha
UV	ultraviolet
U-937	monocytic lymphoma cells
WHO	World Health Organization
WiDr	colic adenocarcinoma cell

ABSTRACT

The discovery of new secondary metabolites from plants and endophytes has become more challenging in natural products chemistry. Different approaches have been applied in order to increase the production of bioactive metabolites from microbial sources. Bacteria and fungi interact within the host plant and stimulate competition for nutrients and spaces which is regarded as a major ecological factor that induces production of bioactive secondary metabolites.

Prior to this study, metabolomics has been applied to identify and preliminarily screen the production of bioactive secondary metabolites from three strains: *A. aculeatus*, *L. theobromae*, and *Fusarium* sp. inoculated in both solid rice and liquid culture media at different growth stages 7, 15 and 30 days. High resolution mass spectrometry and NMR spectroscopy were used as metabolomics profiling tools. The spectral data was processed by utilizing the quantitative expression analysis software Xcalibur, Mzmine 2.10, *in house* MS-Excel macro coupled with Antimarin (Antibase and Marinlit) and Dictionary of Natural Products databases for dereplication studies. SIMCA P+ 13.0 was used to prove that the optimized models were statistically sound.

In this study, isolation and fractionation of bioactive natural products was done on the crude organic extract of the mangrove plant *Avicennia lanata* by using several high-throughput chromatographic techniques which yielded three new derivatives of naphthofuranquinone along with three known congeners, triterpenes and sterol compounds. Meanwhile, four pure endophytic fungal strains were also isolated from the root, stem, stem barks and leaf parts of *A. lanata.* The fungi were identified by DNA extraction, PCR amplification and sequencing by using polymerase chain reaction (PCR) and the universal ITS primers. The voucher specimens of all strains were deposited in Natural Product Metabolomics Laboratory (SIPBS, University of Strathclyde). The isolated endophytic fungi from the mangrove plant *A. lanata* were identified as *Aspergillus aculeatus* obtained from the leaf part; *Lasiodiplodia*

theobromae from the stem; *Aspergillus flavipes* from the stem bark and *Fusarium* sp. from the root part.

Metabolomic profiling of *Fusarium* sp. extract from the 15-days solid culture (FRC15) yielded four 1,4-naphthoquinone with naphthazarin structures and ergosterol peroxide. Meanwhile, isolation work of bioactive metabolites on the crude extract of a 30 day solid rice culture of *A. aculeatus* afforded two new metabolites, aspergillusenone and 2-(3,4-dihydroxyphenyl)-*N*,*N*-dimethylacetamide, along with four known simple phenolics, secalonic acid A and ergosterol peroxide. The investigation for other potential bioactive compounds was carried out on the endophytic fungus *L. theobromae* grown on the 15-day solid rice culture (LTRC15) which produced mellein along with its three derivatives and two other phenolic compounds. Structure elucidation of the isolated secondary metabolites was established using 1D and 2D-NMR and HRESI-MS.

Except for taraxerone, taraxerol, stigmasterol and β-sitosterol, all isolated compounds from the mangrove plant *A. lanata* and its fungal endophyte showed significant anti-trypanosomal activity to *T. b. brucei*. In this study, it proved that metabolomics approach is an essential tool to identify biomarkers from mangrove plant and its endophytic fungi to target the isolation of potential anti-trypanosomal effective drugs.

CHAPTER 1

1.   Introduction

1.1   Marine natural products

Most of the natural product-derived remedies originate from the terrestrial environment. Nevertheless, in relation to chemical structures novelty marine sources are remarkable compared with terrestrial natural products (Kong *et al.*, 2010). The oceans possess more than 70% of the earth's surface representing 34 of the 36 phyla of marine plants and animals (Pomponi, 1999, Jimeno, 2002, Kijjoa and Sawangwong, 2004). The diversity in marine species is noticeably valuable, particularly in the way they adapt to extreme conditions including high salinity, low oxygen, nutrient limitation, and high temperatures which led them to evolve the ability to synthesise unique functional metabolites to protect them not only from environmental stress but also from predators, infection and competition for space (Pomponi, 1999). Marine biodiversity has been shown to be the reservoir of numerous chemical and structural features with potential biological activities primarily from sponges, cnidarians, tunicates (ascidians), bryozoans, molluscs, red, green and brown algae, marine bacteria and cyanobacteria, mangroves and mangrove-derived endophytic fungi (Blunt *et al.*, 2015). In recent years, many unique and important marine-derived secondary metabolites with diverse bioactivities have been isolated, some of which are being tested in last phases of pre-clinical studies and clinical trials in the development of new pharmaceutical drugs (Donia and Hamann, 2003, Rawat *et al.*, 2006, Haefner, 2003, Yonghong, 2012).

1.2   Latest commercial marine drugs in the market

To date, eight marine-derived drugs have been approved and registered by the Food and Drugs Administration (FDA) and European Medicines Agency (EMA). The first FDA-approved marine-derived drug was cephalosporin C, a class of bactericidal antibiotics that include the β-lactam ring structurally related to (D-4-amino-4-carboxy-n-butyl)penicillin which was isolated from the *Acremonium* fungi

and was first structurally characterized in 1961 (Abraham and Newton, 1961). It was marketed in 1964 as cefolatin, the first-generation cephalosporin antibiotic (Hameed and Robinson, 2002). Later in 1969, cytarabine (Ara-C) under the trade name Cytosar®, was introduced as an anti-cancer drug and eight years later vidarabine, Ara-A under the trade name Vira-A® was approved as an anti-viral agent. Ara-C and Ara-A are synthetic pyrimidine and purine nucleosides, respectively, which are derivatives of naturally occurring nucleosides isolated from the Caribbean sponge *Tethya crypta* (Mayer *et al.*, 2010). Ziconotide (SNX-111) was first introduced in America in 2004 under the trade name Prialt® (produced by Elan Pharmaceuticals) to treat severe and chronic pain for patients who need intrathecal analgesia, and two months later the drug was also approved by the European Commission. Ziconotide (ω-conotoxin) is naturally occurring peptide isolated from the venom of cone snail *Conus magus* which was initially investigated in the late 1960s by Baldomero Olivera. The fifth drug was trabectedin (ecteinascidin-743/ET-743) that is marketed under the trade name Yondelis® (produced by PharmaMar/Johnson & Johnson/OrthoBiotech), which is awaiting FDA approval but had gained approval in the EU in 2007. Currently in 2015 the drug is used in Japan as an anti-cancer drug to treat soft tissue sarcoma and relapsed ovarian cancer. The initial screening tests were carried out by the National Cancer Institute on the extracts of the Caribbean tunicate *Ecteinascidia turbinate*, which possessed anti-tumour activity (Lichter *et al.*, 1972). Later, the pure molecule was isolated and characterised for the first time by Wright *et al.*, 1990, Rinehart *et al.*, 1990. Omega-3-acid ethyl ester is naturally occurring in fish and was approved by the FDA in 2004 (developed by Reliant Pharmaceuticals) and marketed under the trade name Lovaza® (produced by Glaxo-SmithKline) in 2007. It was originally called Omacor, and contains a highly purified and concentrated omega-3 polyunsaturated fatty acid preparation to lower very high triglyceride levels (Breivik *et al.*, 1997). Another drug in the market is eribulin mesylate (E7389) for metastatic breast cancer (Huyck *et al.*, 2011, Shetty and Gupta, 2014) which was approved by the FDA in 2010 under the trade name Halaven™ (produced by Eisai Co., Ltd.). The naturally occurring lead compound was a macro-cyclic ketone analogue of halichondrin B which was first isolated from the Japanese marine sponge *Halichondria okadai* Kadota (Uemura *et al.*, 1985, Hirata and

Uemura, 1986). Other halichondrin analogues have also been found in other sponge genera like *Axinella*, *Phakellia* and *Lissodendoryx* (Swami *et al.*, 2012). Eribulin has been approved in 40 countries (Shetty and Gupta, 2014).

1.3   Mangrove family

The term "mangroves" refer to an assemblage of tropical trees and shrubs that grows in the intertidal zone (Khoon, 1987). Mangroves are described as woody plants that grow at the interface between land and sea in tropical and sub-tropical latitudes (Kathiresan and Bingham, 2001). These plants and their associated microbes, fungi, plants and animals constitute the mangrove forest community or '*mangal*'. Duke defined a mangrove as a tree, shrub, palm or ground fern, generally exceeding one half meter in height and which normally grows above mean sea level in the intertidal zone of marine coastal environments or estuarine margins (Duke and Pinzon, 1992). The word mangrove came from the Portuguese word "*mangue*" and the English word "*grove.*" The corresponding French words are "*manglier*" and "*paletuvier*" while the Spanish term is "*manglar*" (Macnae, 1968). Dutch use "*vloedbosschen*" for the mangrove community and "*mangrove*" for the individual trees. The word "*mangro*" is a common name for *Rhizophora* in Surinam (Chapman, 1976). It is believed that all these words originated from the Malaysian word, "*manggi-manggi*" meaning "above the soil." Somehow, this word is no longer used in Malaysia but is used in Eastern Indonesia referring to *Avicennia* species.

1.3.1   Distribution of mangroves

In 2010, Southeast Asia contributed 33% to the world's total mangrove area, in which the largest mangrove forest was located in Indonesia and Malaysia as amongst the top twelve countries with the largest extents of mangroves in the world (Spalding, 2010) (Figure 1.1). The Malaysian mangrove forest is a unique ecosystem (Figure 1.2), the second largest after peat swamp forest located at the bottom elevation which is equivalent to the sea level (Hamdan, 2012). The mangrove forest is generally found along sheltered coasts where it grows abundantly in saline soil and
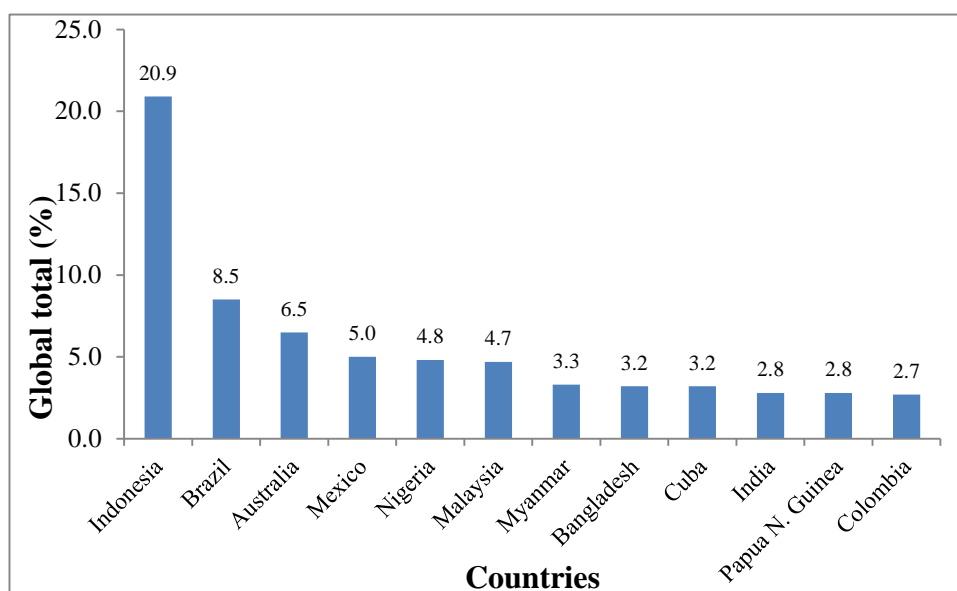
Figure 1.1: The top 12 countries with the largest mangrove area in the world (Spalding, 2010).

briny water dominated mostly by Rhizophoraceae family trees. Next is the peat swamp forest which was formed as sediment and organic substances deposited by rivers are trapped behind the mangroves over hundreds of years, gradually building up a layer of waterlogged, acidic, anaerobic conditions and peat soil. The lowland dipterocarp forest is 300 m above sea level, followed by the hill dipterocarp forest (300 m to 1200 m above sea level). These two types of forest are rich in biological diversity and form the most abundance forest types in Malaysia. Next is the montane forest located at the highest latitude which is greater than 1200 m above sea level. Mangrove plants are categorized into two groups: true mangrove and semi-mangrove plants (Jun Wu *et al.*, 2008). The true mangrove plants are restricted to the typical intertidal mangrove habitats whereas semi-mangrove plants grow on the landward fringe mangrove habitat or in terrestrial marginal zones subjected to irregular high tides. Worldwide, there are 84 mangrove plant species in which 70 species are true mangroves and 14 species are semi-mangroves.

In Peninsular Malaysia, mangroves occur mostly in sheltered areas along the west coast in the states of Perlis, Pulau Pinang, Kedah, Perak, Selangor, Negeri Sembilan, Melaka and Johor which have been recorded by Global Positioning System (GPS) (Hamdan, 2012). The abundance of the mangrove forest on the west coast is due
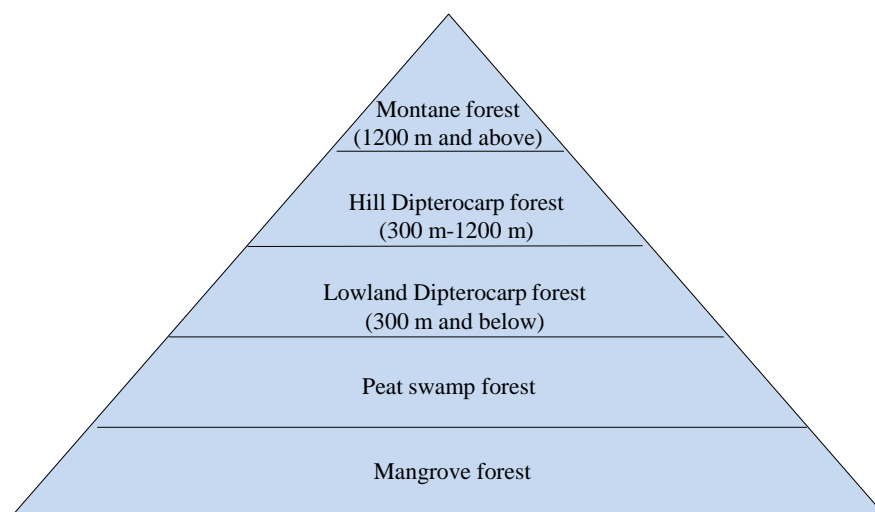
Figure 1.2: Tropical rainforests in Malaysia based on altitudinal height (Hamdan, 2012).

to the sheltering effect from the Island of Sumatra which provides relatively calm seas in the Straits of Melaka. The fine silt and clay discharged from rivers leads to the deposition of mud along the coast, and forms higher substrate for the mangroves to grow. In contrast, the mangrove distribution is less on the east coast (Terengganu, Pahang, Johor and Kelantan) facing the South China Sea (Figure 1.3), which typically extend 0.5−1 km inland (Ibrahim *et al.*, 2000). Perak possesses the greatest abundance of mangrove forest with 37.6%, followed by Johor (20.6%) and Selangor (19.6%).

1.3.2   Functions and value of mangroves

The mangrove forest is an important habitat for aquatic and terrestrial micro and macro organisms. It is an important breeding ground for many tropical commercial fish species, crabs, prawns and other marine animals particularly in terms of providing food and shelter. Mangroves provide habitat for marine species - fishes, molluscs, crustaceans and other vertebrates which contribute to the commercial fishing industry among local people and even to the national economy. In world usages, the mangroves have been explored mostly in economic sector for construction of dwellings, furniture, rafts, boats, fences, fishing gear, paddles as well as production of tannins for dying and leather production (Bandaranayake, 1998).

Figure 1.3: Distribution of mangrove areas in Peninsular Malaysia

The abundance of mangrove forest was recorded using Global Positioning System (GPS) equipment. The mangrove locations on the west coast are found in Perlis, Pulau Pinang, Kedah, Perak, Selangor, Negeri Sembilan, Melaka and Johor facing the Strait of Melaka. Meanwhile on the east coast, mangrove are sheltered in Terengganu, Pahang, Mersing, Johor and small areas in Kelantan in which these locations are facing the South China Sea (Hamdan, 2012).

Mangrove wood with its high content of tannin in is used as timber for its durability for example; *Avicennia marina, Bruguiera cylindrica, B. parviflora, Xylocarpus granatum* and *Sonneratia apetala* stems are used for construction of houses. Meanwhile, mangrove twigs also are used for making charcoal and firewood due to high calorific value and they burn producing high heat without generating smoke.

Some of the mangrove plant parts are used for food purposes; for example, fruits of *Bruguiera gymnorhiza, Phoenix paludosa, Sonneratia alba, S. caseolaris* and *Terminalia catappa* are used as vegetables (Bandaranayake, 1998, Pattanaik *et al.*, 2008). The mangroves are also used for natural functions such as the control of coastal erosion, protection of coastal land and stabilization of sediments. Apart from the above uses, mangrove plants are known to possess medicinal value and have been used traditionally to treat ailments of various diseases by local people. The coastal communities fully or partially depend upon mangrove plants for curing numerous diseases. Extracts of *Ipomoea pescaprae* are used to treat headache and various types of inflammation including jelly fish sting dermatitis. They make cigarettes which are prepared from the chopped stem bark of *I. pescaprae* and were smoked to relieve pain in sinusitis. In Indo-China, the leaves and young shoots are crushed, mixed with alcohol and applied on the back in cases of lumbago, and are used to relieve rheumatic pains and are incorporated in baths to treat scabies (Bandaranayake, 1998). In East Africa, the young bitter-tasting fruit of *Xylocarpus molluscensis* is used in folk medicine as an aphrodisiac (Bandaranayake, 2002).

1.4 Bioactive secondary metabolites isolated from mangrove *Avicennia* sp.

Mangrove plants as well as their endophytic fungi exhibit unique chemical diversity from various classes of compounds with promising biological activities (Blunt *et al.*, 2015, Jing Xu, 2015, Newman and Cragg, 2012, Newman and Cragg, 2004). *Avicennia* is the only mangrove genus belonging to the Avicenniaceae family which is the most abundant in mangrove ecosystems and widely distributed on the tropical and subtropical coastlines. About eight to ten species have been recorded worldwide

(Duke *et al.*, 1998) and Table 1.2 shows the global distribution of the genus *Avicennia*.

Table 1.1: *Avicennia* species and its global distribution
(Duke *et al.*, 1998)

Avicennia sp.	Southeast USA	Central/South America	Africa	South Asia	Malay Archipelago	East Asia	Australia	Southwest Pacific
A. alba				✓	✓	✓		
A. balanophora							✓	
A. bicolor		✓						
A. eucalyptifolia							✓	
A. germinans	✓	✓						
A. lanata					✓			
A. marina			✓	✓	✓	✓	✓	✓
A. officinalis					✓	✓	✓	
A. schaueriana		✓						
A. africana			✓					

The first phytochemical study on *Avicennia* sp. revealed lapachol (**1.1**) which has been isolated from Indian and West African *A. tomentosa* (Bournot, 1913). Various classes of chemical components have been isolated from this genus including naphthoquinones, iridoid glucosides, sterols, flavones, diterpenes and triterpenes from the leaves, roots, twigs and stem bark.

1.4.1   Naphthoquinones

Avicennia alba collected in Singapore yielded avicequinones A-C (**1.2**-**1.4**) and avicenols A-C (**1.5**-**1.7**) which were isolated from the stem barks (Ito *et al.*, 2000). Han and his colleagues identified twelve naphthoquinones namely avicennone A–G (**1.8**–**1.14**), avicequinone A (**1.2**), C (**1.4**), stenocarpoquinone B (**1.15**), and avicenol A (**1.5**) and C (**1.7**) from twigs of *A. marina* collected from the coast of Xiamen, China (Han *et al.*, 2007). A study on lapachol (**1.1**) isolated from dried twigs of *A. lanata* (synonym *A. rumphiana*) collected in Singapore revealed that this compound is able to hinder the development of hypertrophic scars (Matsui *et al.*, 2011). All the naphthoquinone types of compounds are listed in Figure 1.4.
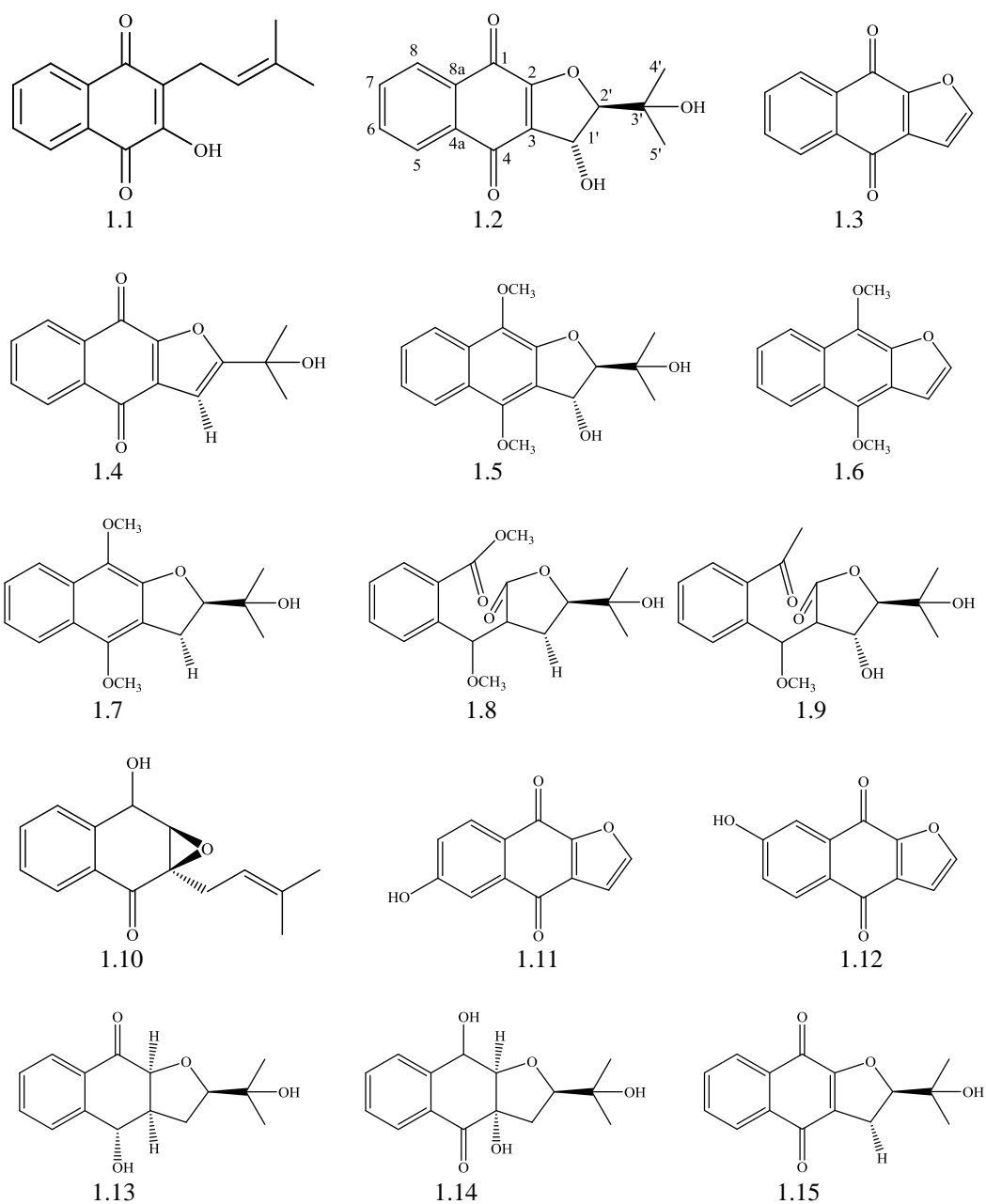
Figure 1.4: Naphthoquinone derived compounds isolated from *Avicennia* sp.

1.4.2 Iridoid glucosides

The occurrence of iridoid glucosides in some *Avicennia* species was reported from *A. marina, A. officinalis* and *A. germinans*. The iridoid glucosides which have been isolated from *Avicennia* species are shown in Figure 1.5. In 1985, König and her co-workers isolated 2'-cinnamoylmussaenoside (**1.16**), l0-*O*-(5-Phenyl-2,4-pentadienoyl) geniposide (**1.17**), 7-*0*-(5-phenyl-2,4-pentadienoyl)-8-epiloganin (**1.18**), geniposide (**1.19**), and mussaenoside (**1.20**) from a methylated leaf extract of

A. marina collected from Ceylon (König and Rimpler, 1985). Later, they identified more iridoid glucosoides: avicennioside (**1.21**), 7-*O*-cinnamoyl-8-epiloganic acid sodium salt (**1.23**), geniposidic acid (**1.24**), and 2'-cinnamoylmussaenosidic acid (**1.25**) from the air-dried leaves of *A. officinalis* collected from Sri Lanka (König *et al.*, 1987). Later, the structure of avicennioside (**1.21**) was revised to linarioside (**1.22**) (Demuth *et al.*, 1989, Nass and Rimpler, 1996). Fauvel and his colleagues described two iridoid glucosides from the leaves of *A. germinans* collected from Cayenne, Guyana (Fauvel *et al.*, 1995) namely; 2'-caffeoylmussaenosidic acid (**1.26**) and 2'-cinnamoylmussaenosidic acid (**1.25**) which earlier had been isolated from the leaves of *A. officinalis* (König *et al.*, 1987). These compounds (**1.25** and **1.26**) were reported again from the leaves of *A. germinans* collected from Libreville, Gabon (Fauvel *et al.*, 1997). Fauvel also reported 2'-coumaroylmussaenosidic acid (**1.27a** and **1.27b**) from the leaves of *A. germinans* collected from Libreville; its two isomeric forms differing from each other on the geometry of the double bond of the 2'-coumaroyl group were analysed and confirmed by their NMR spectra and molecular models (Fauvel *et al.*, 1999). Aerial parts of *A. marina* from Hainan island (Feng *et al.*, 2006) yielded three iridoid glucosides, namely, 2'-*O*-[(2*E*,4*E*)-5-phenylpenta-2,4-dienoyl]mussaenosidic acid (**1.28**), 2'-O-(4-methoxycinnamoyl)mussaenosidic acid (**1.29**), and 2'-*O*-coumaroylmussaenosidic acid (**1.30**). A chemical investigation on the fruits of *A. marina* gave three phenylethyl glycosides: marinoids J–L (**1.31–1.33**), and marinoid M, a cinnamoyl glycoside (**1.34**) (Gao *et al.*, 2014).

1.16 R$_1$ = CH$_3$ R$_2$ = H   R$_3$ = H
1.25 R$_1$ = H   R$_2$ = H   R$_3$ = H
1.26 R$_1$ = H   R$_2$ = OH   R$_3$ = OH

1.17 R = CH$_3$
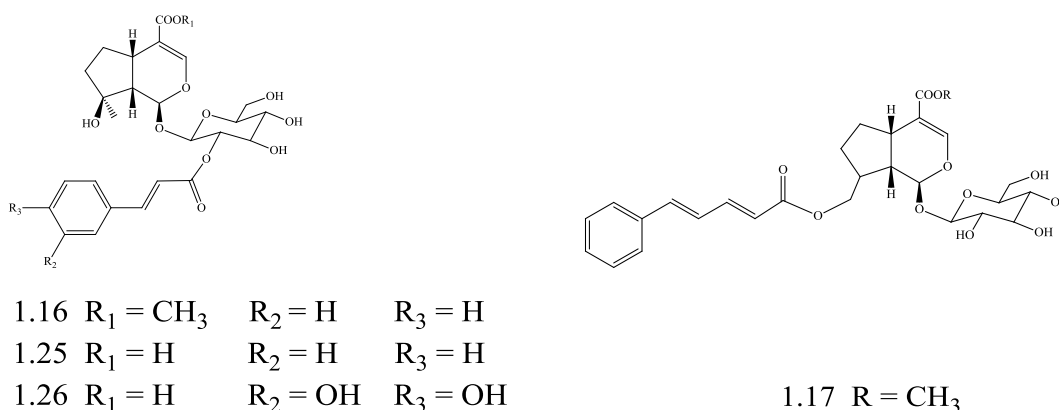
Figure 1.5: Iridoid glucosides isolated from *Avicennia* sp.

1.19 R = CH$_3$
1.24 R = H

1.18
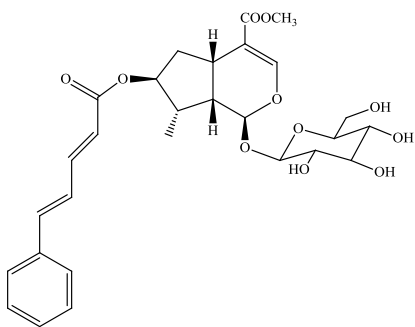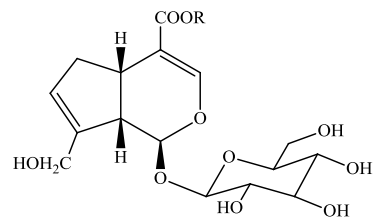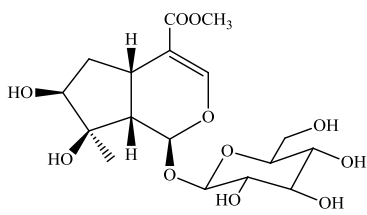
1.20
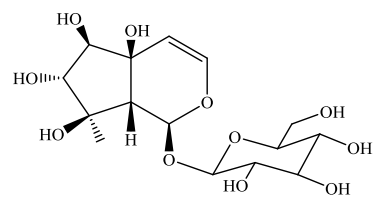
1.21
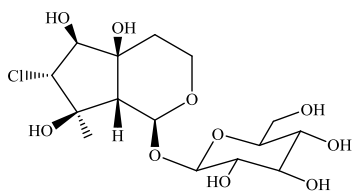
1.22
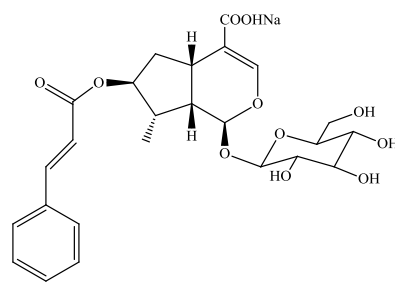
1.23
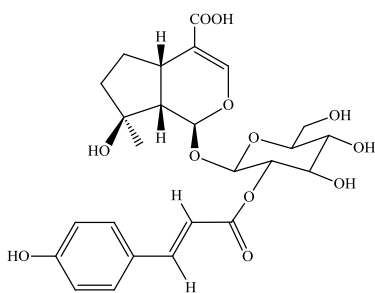
1.27a
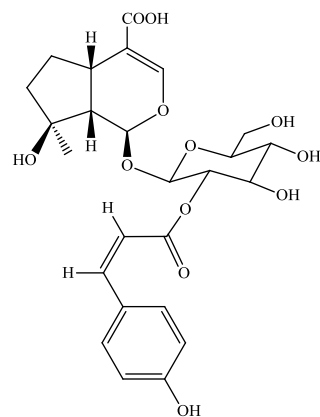
1.27b

Figure 1.5: Cont'd. Iridoid glucosides isolated from *Avicennia* sp.

11

1.28

1.29

1.30

1.31 R$_1$ = OH   R$_2$ = OH   R$_3$ = H
1.32 R$_1$ = H   R$_2$ = H   R$_3$ = OH

1.33

1.34
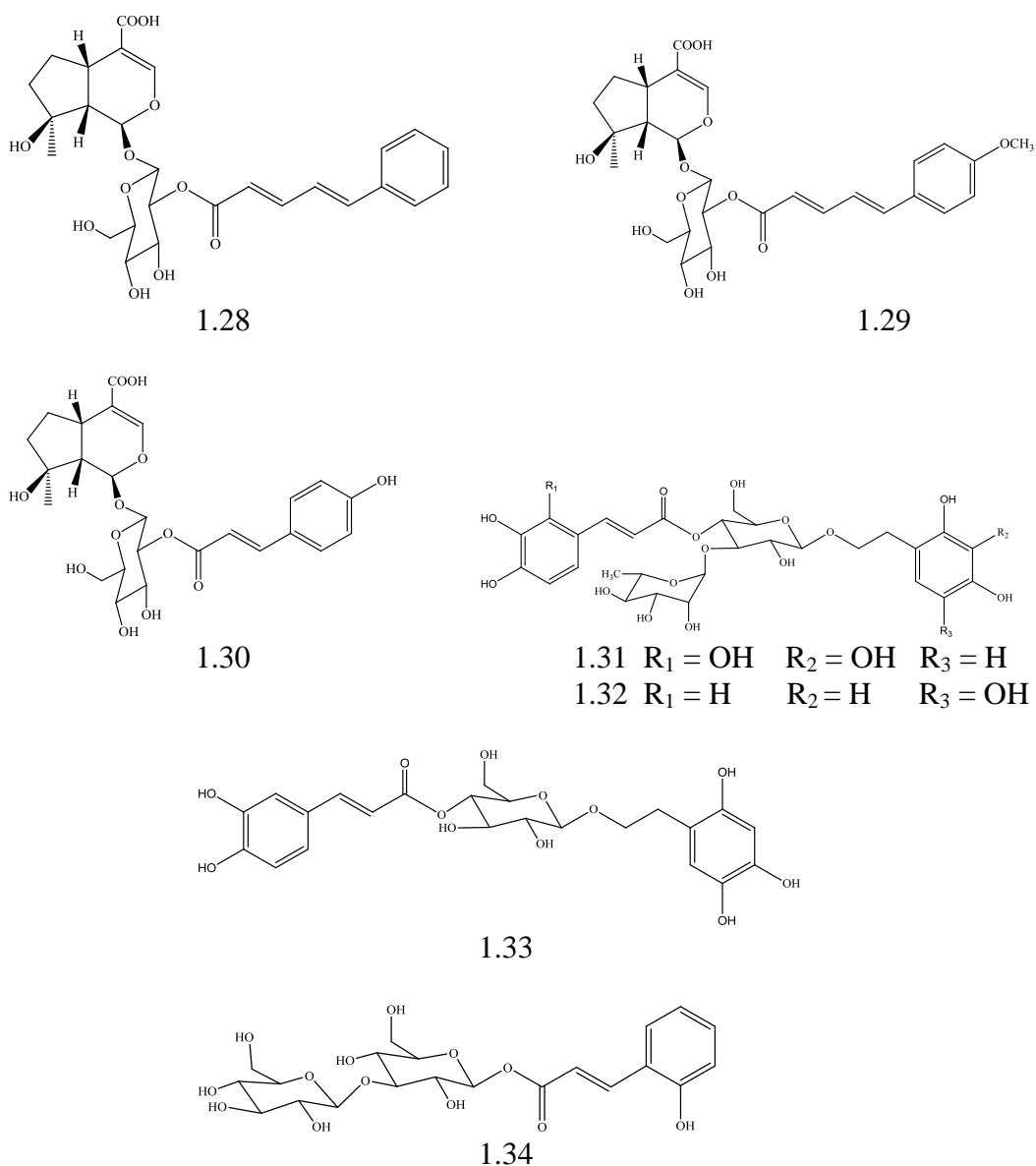
Figure 1.5: Cont'd. Iridoid glucosides isolated from *Avicennia* sp.

1.4.3   Diterpenoids

A study by Subrahmanyam and his co-workers successfully identified seven labdanes *viz.* rhizophorin-A (**1.35**), *ent*-(13*S*)-2,3-seco-14-labden-2,8-olide-3-oic acid (**1.36**), ribenone (**1.37**), ent-16-hydroxy-3-oxo-13-epi-manoyl oxide (**1.38**), *ent*-15-hydroxy-labda-8(17),13*E*-dien-3-one (**1.39**), *ent*-3α,15-dihydroxylabda-8(17),13*E*-diene (**1.40**), excoecarin A (**1.41**), and rhizophorin-B (**1.42**) from the roots of *Avicennia officinalis* Linn from India (Subrahmanyam *et al.*, 2006). The compounds are shown in Figure 1.6.
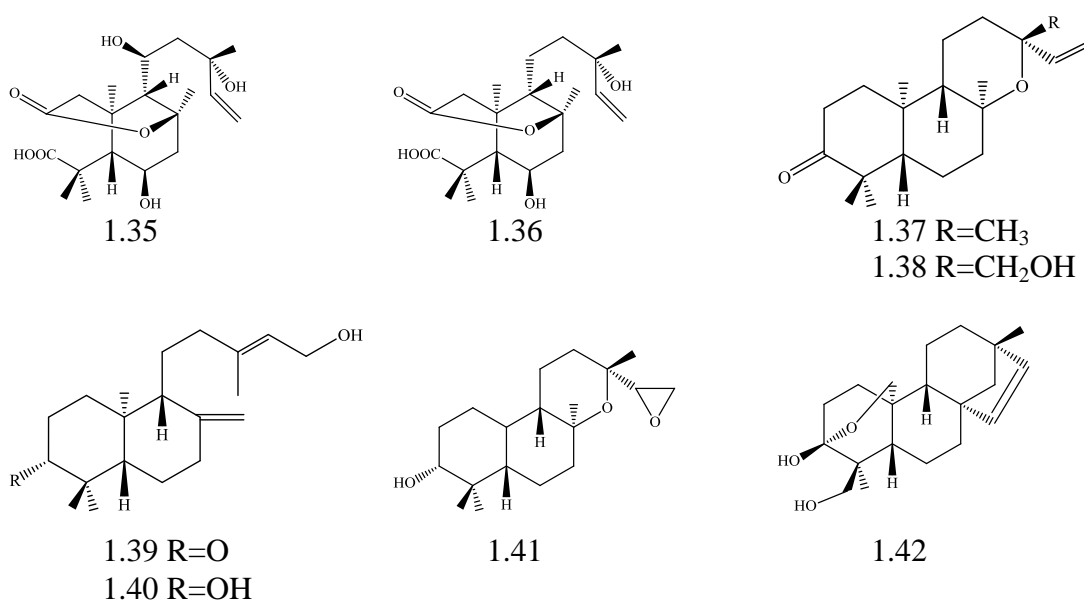
Figure 1.6: Selected diterpenoids group isolated from *Avicennia* sp.

1.4.4 Triterpenoids and sterols

Various types of triterpenoids and sterols also have been isolated and characterised from *Avicennia* species as listed in Figure 1.7. A phyto-chemical investigation of the dried bark of *A. marina* collected from Newcastle, New South Wales yielded betulinic acid (**1.43**), taraxerol (**1.44**) and taraxerone (**1.45**) (Bell and Duewell, 1961). Isolation work on pneumatophores (aerial roots) of the grey mangrove *A. marina* collected from Karachi Harbour, Pakistan gave two sterols, stigmasterol-3-*O*-β-ᴅ-galactopyranoside (**1.46**) which possessed anti-glycation activity and stigmasterol (**1.47**) as well as three triterpenoids, lupeol (**1.48**) and betulinic acid (**1.43**), taraxerol (**1.44**) (Mahera *et al.*, 2011). Majumdar and his colleagues also isolated betulinic acid (**1.43**), taraxerol (**1.44**), taraxerone (**1.45**), β-amyrin (**1.49**) and betulin (**1.50**) from the stem bark and leaves of *A. officinalis* and *A. tomentosa* collected in India (Majumdar and Ghosh, 1979). Meanwhile, Ghosh and his co-workers identified six triterpenes, β-amyrin (**1.49**), betulin (**1.50**), α-amyrin (**1.51**), lupeol (**1.48**), oleanolic acid (**1.52**), ursolic acid (**1.53**) and five sterols, cholesterol (**1.54**), campesterol (**1.55**), stigmasterol (**1.47**), β-sitosterol (**1.56**), 24-ethyl-cholest-5α-7-en-3-β-ol (**1.57**) from the leaves of *A. officinalis* collected in India (Ghosh *et al.*, 1985).

13
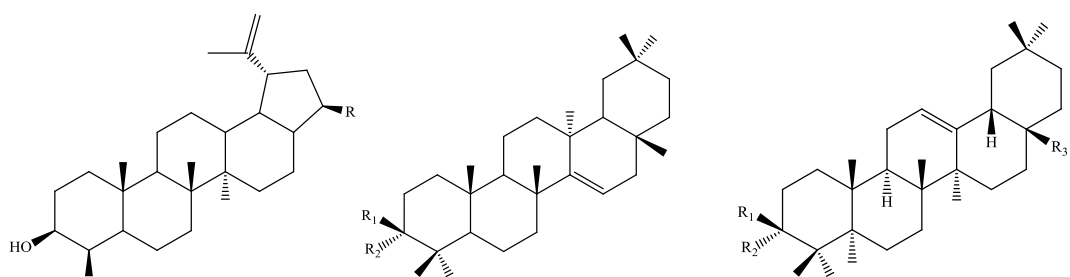
1.43 R = COOH

1.48 R = CH$_3$ 1.44 R$_1$ = OH   R$_2$ = H 1.49 R$_1$ = OH   R$_2$ = H   R$_3$ = CH$_3$

1.50 R = CH$_2$OH   1.45 R$_1$ + R$_2$ = O   1.52 R$_1$ = OH   R$_2$ = H   R$_3$ = COOH
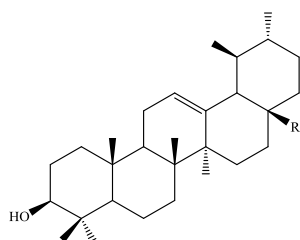
1.51 R = CH$_3$
1.53 R = COOH
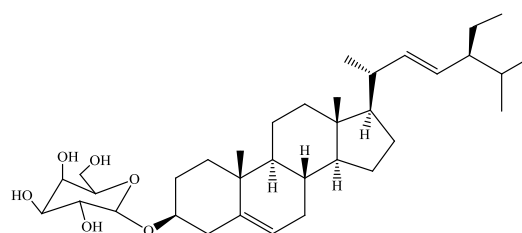
1.46
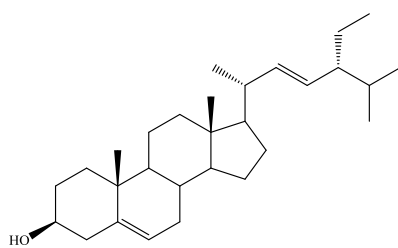
1.47
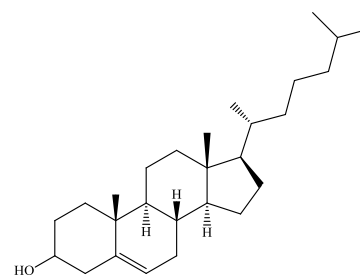
1.54
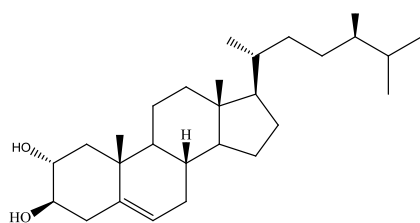
1.55
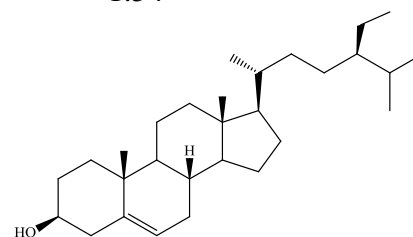
1.56
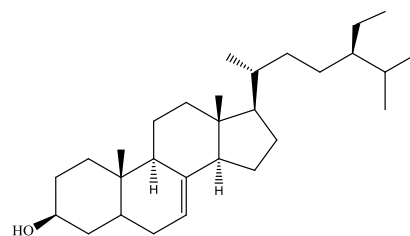
1.57

Figure 1.7: Triterpenoids and sterols isolated from *Avicennia* sp.

14

1.4.5 Flavones

Investigation on aerial parts of *A. marina* (Feng *et al.*, 2006) collected from China resulted in the isolation of four flavones: 2-phenyl-4*H*-1-benzopyran-4-one)4',5-dihydroxy-3',7-dimethoxyflavone (**1.58**), 4',5-dihydroxy-3',5',7-trimethoxy-flavone (**1.59**), 4',5,7-trihydroxyflavone (**1.60**), and 3',4',5-trihydroxy-7-methoxyflavone (**1.61**). A phytochemical study on the defatted leaves of *A. officinalis* collected from India identified the flavone velutin (**1.62**) (Majumdar *et al.*, 1981). The flavones isolated from *Avicennia* species are listed in Figure 1.8.

1.58 $R_1 = H$ $R_2 = OCH_3$ $R_3 = H$
1.59 $R_1 = OCH_3$ $R_2 = OCH_3$ $R_3 = OCH_3$
1.60 $R1 = OH$ $R_2 = H$ $R_3 = H$
1.61 $R_1 = OCH_3$ $R_2 = OH$ $R_3 = H$

1.62
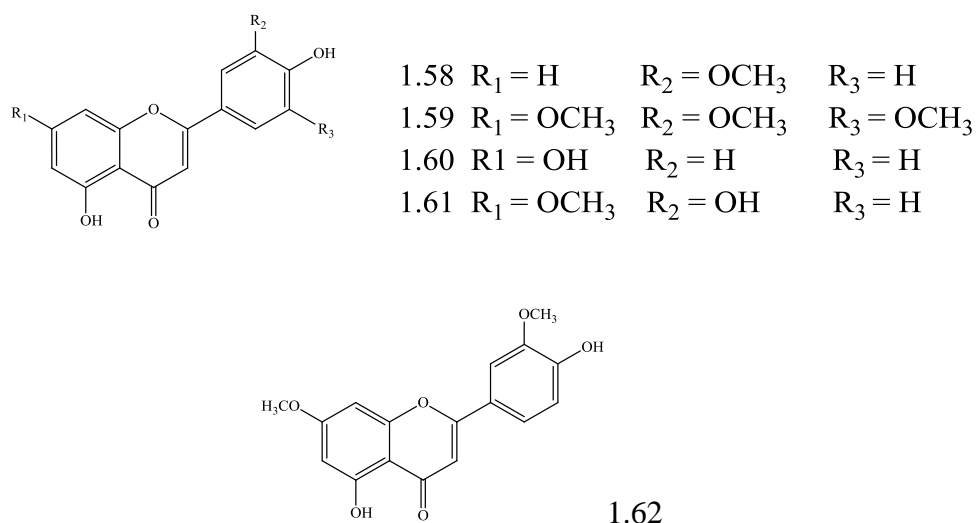
Figure 1.8: Flavones isolated from *Avicennia* sp.

1.4.6 Miscellaneous

Phyto-chemical investigation of the leaves of *A. germinans* collected from Libreville, Gabon resulted in the isolation of the megastigmane glucoside; vomifoliol 9-*O*-β-ᴅ-glucopyranoside ((6*S*,9*R*)-roseoside) (**1.63**) (Bousquet-Mélou and Fauvel, 1998). Meanwhile, a study by Sharp and his co-workers characterized two lignans, pinoresinol (**1.64**) and syringaresinol (**1.65**), which were isolated from *A. germinans* collected in Costa Rica (Sharp *et al.*, 2001). Fauvel and his colleagues identified three phenylpropanoid glycosides: verbascoside (acteoside) (**1.66**), isoverbascoside (**1.67**), and derhamnosylverbascoside (**1.68**), which were isolated from the leaves of *A. marina* collected from Java (Fauvel *et al.*, 1993). Subrahmanyam also characterized triacontan-1-ol (**1.69**) from the roots of *A. officinalis* Linn collected

from India (Subrahmanyam *et al.*, 2006) and triacontane (**1.70**) was obtained from *A. marina*, collected from Newcastle, Australia (Bell and Duewell, 1961). Investigation on aerial parts of *A. marina* collected from United Arab Emirates resulted in the isolation of betain (**1.71**) which occurred at high concentrations (Adrian-Romero *et al.*, 1998). All compounds are shown in Figure 1.9.

1.64 R = H
1.65 R = OCH$_3$

1.63

1.66 R1 = *E*-caffeoyl   R$_2$ = H
1.67 R$_1$ = H   R$_2$ = *E*-caffeoyl

1.68

1.69   1.70   1.71
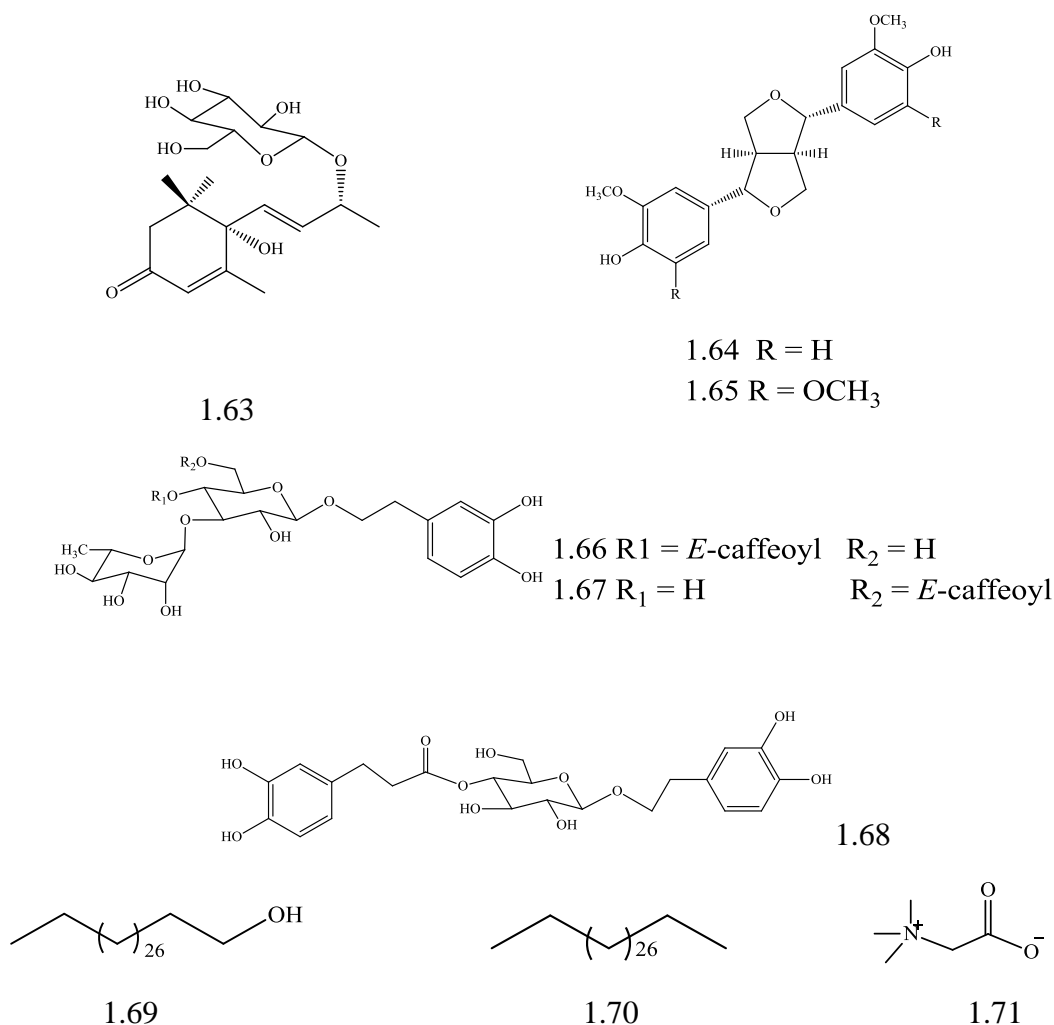
Figure 1.9: Selected compounds isolated from *Avicennia* sp.

1.5   Bioactive secondary metabolites of fungi isolated from *Avicennia* sp.

Endophytes are defined as microorganisms that live inter- and/or intracellularly in plant tissues for a short or prolonged period without producing any visible disease symptoms (Hyde and Soytong, 2008). The endophytic fungi also produce different group of compounds to promote plant growth and protect the plant from

environmental stress or animal predation. For mutualism, these above-mentioned microorganisms receive thriving space within the host plant (Nair and Padmavathy, 2014). Unique bioactive metabolites produced by endophytes are not only advantageous for the plant itself but also possess high potential for new drugs and medicines which will be able to treat certain diseases in humans. They may also be utilised in functional foods. The first report on mangrove fungi was in 1955 when Cribb did an isolation work on mangrove roots from Australia (Cribb and Cribb, 1955). Recently, the number of studies on unique and biologically active compounds produced by endophytic fungi especially from marine sources has increased due to advances in dereplication and chromatographic methodologies. *Avicennia marina* with seven varieties is one of the most abundant species from Avicenniaceae (Jun Wu *et al.*, 2008). There are a significant number of reports on metabolites isolated from *A. marina* fungal endophytes.

1.5.1 Pyrones

The fungus *Aspergillus niger* (MA-132) isolated from the fresh inner tissue of the mangrove plant *A. marina* collected from Dongzhai Harbor in Hainan, China yielded ten α-pyrone derivatives, nigerapyrones A-H (**1.72-1.79**), as well as asnipyrones B (**1.80**) and A (**1.81**) (Figure 1.10) (Liu *et al.*, 2011). Nigerapyrone E (**1.76**) exhibited significant cytotoxicity against tumour cell lines SW1990, MDA-MB-23 and A549 with IC_{50} values of 38, 48 and 43 μM, respectively. These compounds were found inactive against two bacteria, *Staphylococcus aureus* and *Escherichia coli* as well as four plant-pathogenic fungi, *Alternaria brassicae*, *Fusarium oxysporum*, *Coniella diplodiella* and *Physalospora piricola*.

1.5.2 Xyloketals and xyloallenolides

The endophytic fungus *Xylaria* sp. (No. 2508) isolated from the seeds of *A. marina* from Mai Po, Hong Kong produced xyloketals A-I (**1.82-1.90**) and xyloallenolide A (**1.91**) (Lin *et al.*, 2001, Yu Wu *et al.*, 2005b, Yu Wu *et al.*, 2005a, Liu *et al.*, 2006, Yin *et al.*, 2008). Subsequently, fermentation of the fungus in large scale yielded three metabolites named xyloketal J (**1.92**), xyloester A (**1.93**), xyloallenolide B

(**1.94**) and a known substituted dihydrobenzofuran (**1.95**) (Xu *et al.*, 2008) (Figure 1.11).

1.72 R = H
1.73 R = OCH$_3$

1.74 R = H
1.75 R = CH$_3$

1.76

1.77 R = H
1.78 R = OCH$_3$

1.79

1.80

1.81
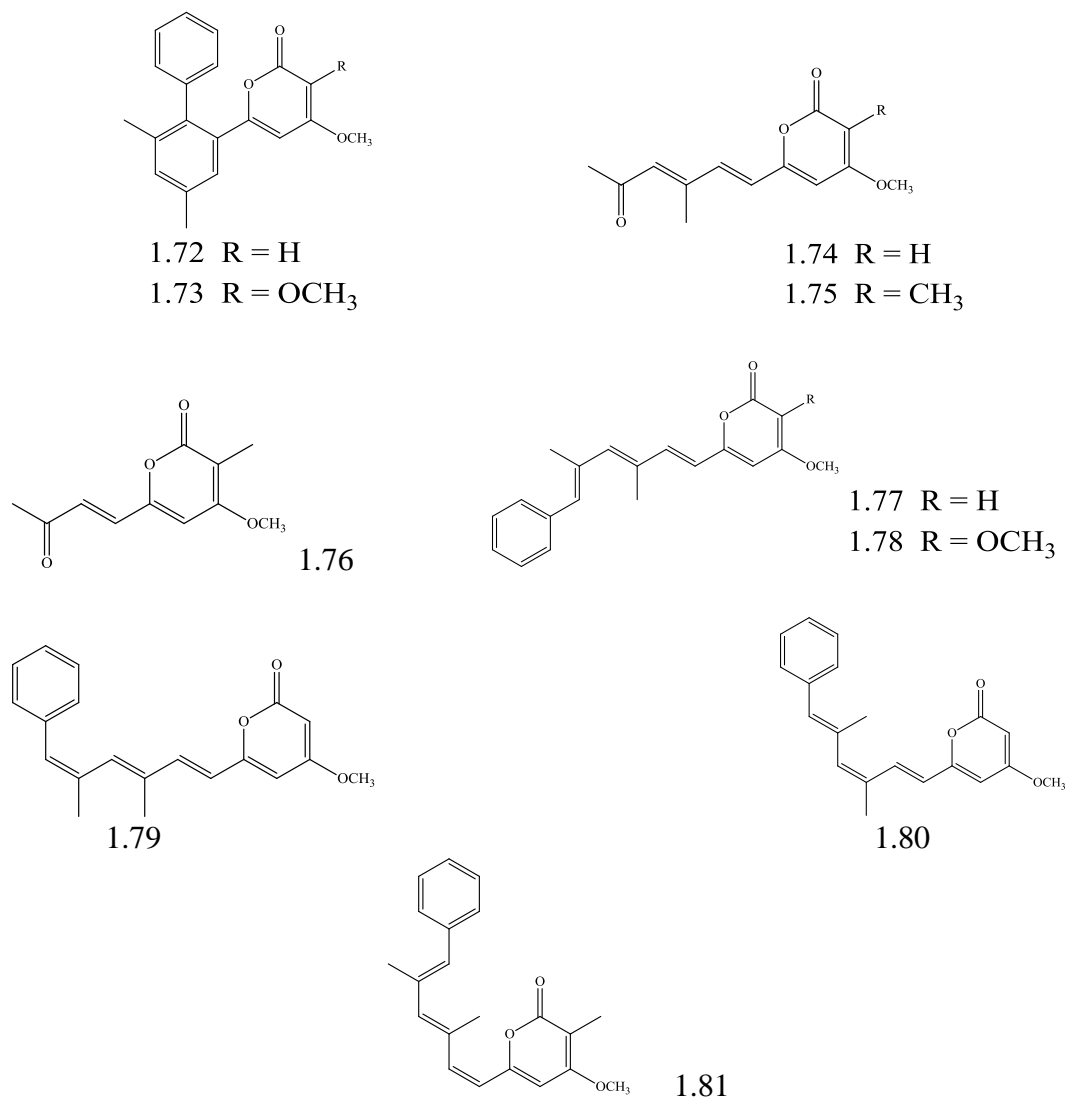
Figure 1.10: Pyrone congeners isolated from *Aspergillus niger*
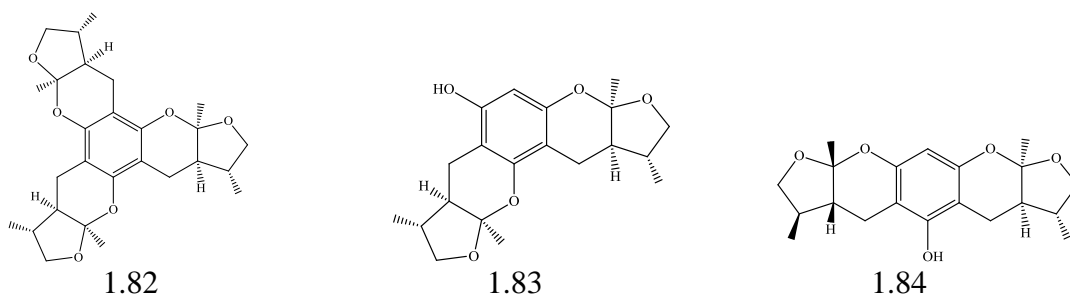
1.82

1.83

1.84

Figure 1.11: Xyloketals and xyloallenolides isolated from fungus *Xylaria* sp.

1.85

1.86

1.87

1.88

1.89

1.90

1.91

1.92

1.93

1.94

1.95
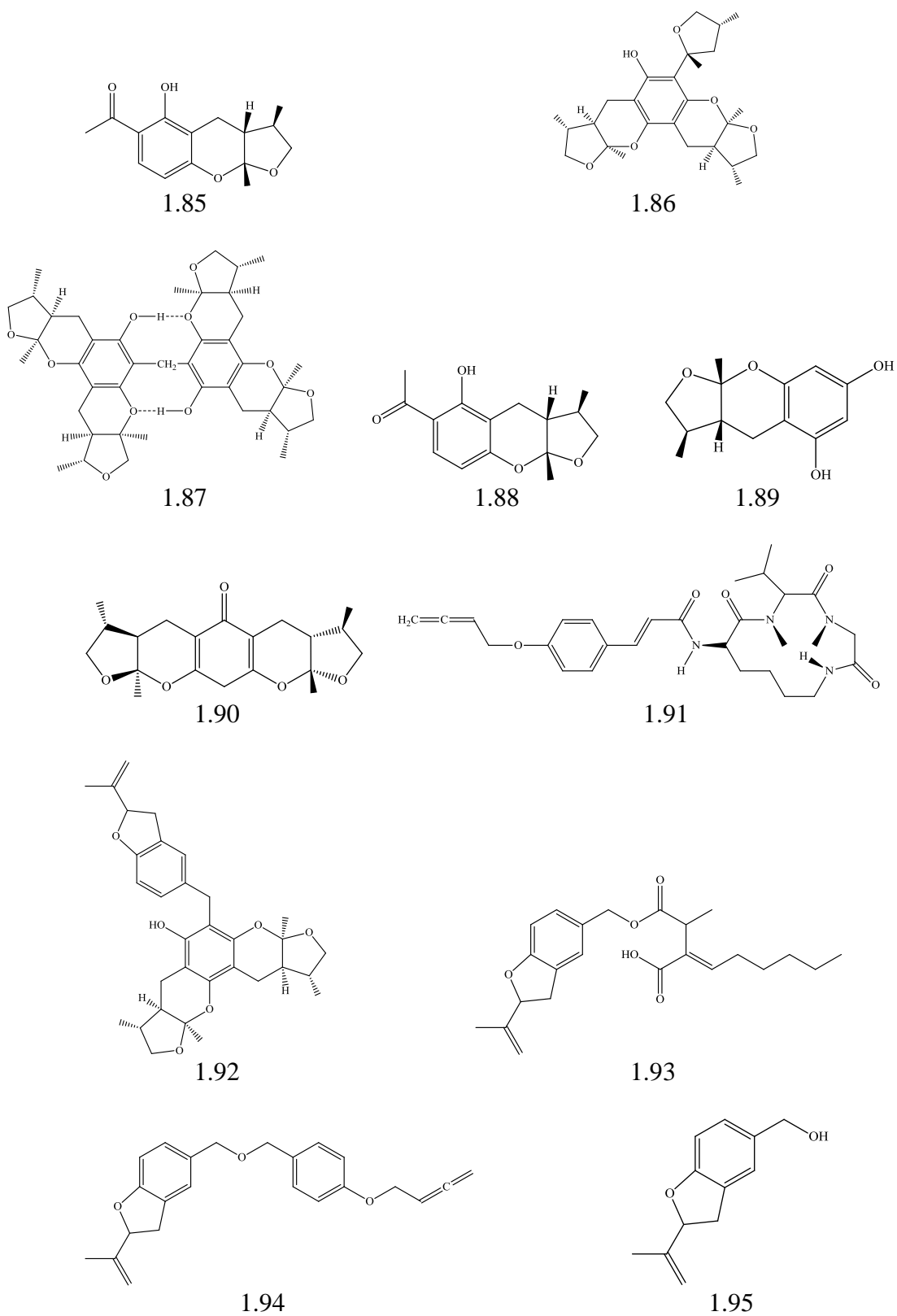
Figure 1.11: Cont'd. Xyloketals and xyloallenolides isolated from fungus *Xylaria* sp.

1.5.3 Xanthones and anthraquinones

Fungus strain no. 2526 which was isolated from a petiole of *A. marina* collected in Hong Kong produced xanthones and anthraquinones (Zhu *et al.*, 2003b). The fungus produced sterigmatocystin (**1.96**) and further large scale fermentation yielded two other xanthone derivatives, dihydrosterigmatocystin (**1.97**) and secosterigmatocystin (**1.98**), and four anthraquinones, namely averufin (**1.99**), nidurufin (**1.100**), versicolorin C (**1.101**) and physicion (**1.102**) (Zhu *et al.*, 2004) (Figure 1.12).
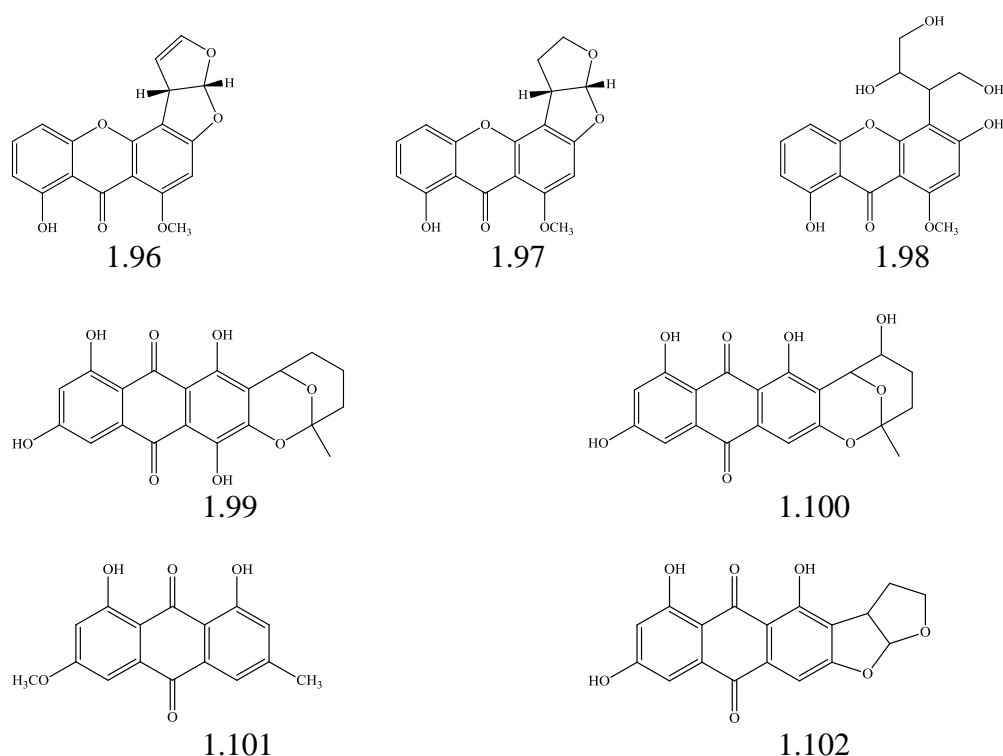
Figure 1.12: Xanthones and anthraquinones isolated from fungus strain no. 2526 (Zhu *et al.*, 2003a, Zhu *et al.*, 2004)

1.6   Metabolomics

Omics are a group of technologies expanded to explore the roles, relationships and activities of biochemical and molecular characterisations of an organism, tissue or cell type of living organism. The omics technologies include genomics (DNA and their function), transcriptomics (mRNA), proteomics (proteins) and metabolomics (metabolites involved in cellular metabolism) (Dhanapal and Govindaraj, 2015). The

use of a combination of different omics approaches for a comprehensive analysis of a biological molecular system is an effective method which is non-specific but an un-biased strategy (Figure 1.13).
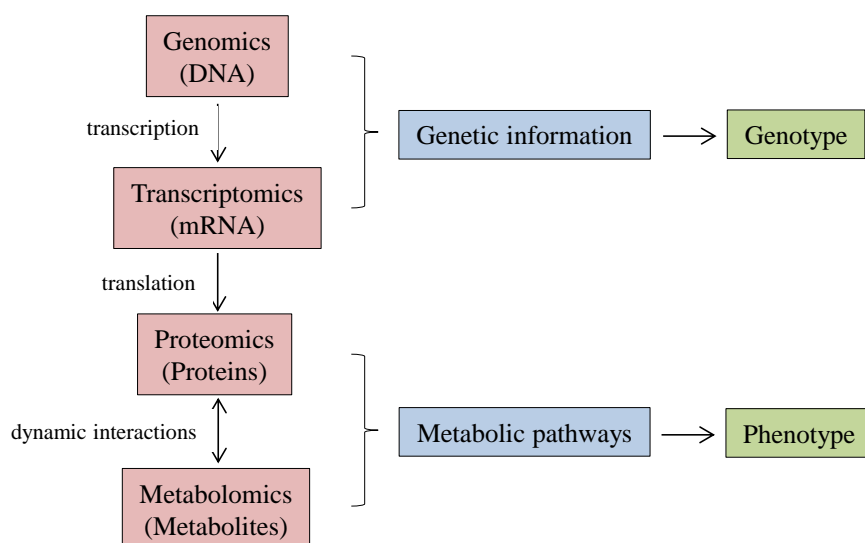
Figure 1.13: The interaction between omic technologies

These approaches allow the study of any molecules which assemble a cell, tissue or an organism leading to disclosure of genes (genomics), mRNA (transcriptomics), proteins (proteomics) and metabolites (metabolomics) in a given sample in a non-specific and non-prejudiced approach (Dhanapal and Govindaraj, 2015).

Metabolomics is a technology of integral experimental analysis of metabolites which includes four basic steps: 1) sample preparation and extraction, 2) data acquisition (analysis of the extracts), 3) data mining including data processing and multivariate analysis and 4) metabolite identification or dereplication (Kim and Verpoorte, 2010). It has been applied in multidisciplinary areas to identify and quantify metabolites such as in molecular and cell biology, functional genomics, chemical toxicology, pathology, chemical ecology, drug metabolism, disease progression and natural products chemistry of terrestrial plants, marine organisms and their associated-microorganisms (Verpoorte *et al.*, 2007, Nielsen and Oliver, 2005, Wolfender *et al.*, 2015). A pioneer study using the 'metabolite profiling' concept was published in the early 1970s (Horning and Horning, 1970, Devaux *et al.*, 1971) which reported the analysis of steroids derivatives, acids, and neutral and acidic urinary drug metabolites using GC-MS. In natural product research, the term 'metabolite' refers to a group of small molecules with a molecular weight of <1000 Da. These are classified into

primary and secondary metabolites. Primary metabolites, which include amino acids, lipids and carbohydrates, refer to molecules that are required to support the growth or function of an organism via normal metabolic process. Secondary metabolites, including polyphenols, alkaloids, terpenes, polyketides and hormones, are molecules related to signalling mechanisms for an organism's defence and survival (Grotewold, 2005). Some of these compounds possess potent activity in certain targeted biological tests, making them valuable in drug discovery and development. Metabolite profiling of the active metabolites in crude extracts of natural sources is supported by dereplication in which the novel compounds from the active groups are differentiated from known compounds which have been studied previously (Koehn and Carter, 2005). The dereplication process, when coupled with databases such as the Dictionary of Natural Products and Antimarin, assists in the isolation and purification steps of the natural product in such way as to prevent repetitive work on the same compounds. Therefore, a comprehensive analysis on different metabolites in complex mixtures can be achieved using several alternative methods such as "metabolite (or metabolic) fingerprinting," "metabolite profiling" and "metabolite target analysis" (Table 1.2). The term "metabolic" is used mostly in drug research; it is commonly used to describe the metabolic fate of an administered drug (Fiehn, 2001).

In this phytochemical study, a metabolomics approach was used to target the anti-trypanosomal active secondary metabolites as well as in preliminary screening the production of these target metabolites by the plant's endophytic fungi.

Table 1.2: Classification of metabolomics
(Fiehn, 2001)

Classification	Definition
Metabolic fingerprinting	Rapid classification of sample without extensive metabolite identification and quantitation
Metabolite profiling	Focuses on quantitative and qualitative of a large group of metabolites that is either related to a specific metabolic pathway or a class of compounds
Metabolite target analysis	Investigation of targeted metabolites

1.6.1 Techniques for metabolomics

In metabolomics, different analytical methods involve both chromatographic and spectroscopic techniques are used to characterise the chemical composition of any given biological form or extract leading to the rapid and high-throughput assessment of metabolites. The samples may be subjected to liquid chromatography (LC) or gas chromatography (GC) or direct injection and the metabolites consequently can be detected in the eluent by mass spectrometry (MS) and MS/MS fragmentation. Diverse techniques including Fourier transformed infrared spectroscopy (FT-IR), Raman spectroscopy and nuclear magnetic resonance (NMR) are also implemented. There are a lot of reports on the advantages and limitations related to the use and combination of these techniques (Sumner *et al.*, 2003, Verpoorte *et al.*, 2007, Kim *et al.*, 2011, Wolfender *et al.*, 2013). Metabolite profiling of plant or microbial crude extracts uses high resolution MS and NMR techniques for data mining and dereplication (Wolfender *et al.*, 2015). HPLC has been acknowledged to be an efficient technique for the separation of natural components from crude extracts without complicated sample preparation. A crude extract is a complex mixture with each of the natural constituents possessing different and variable physico-chemical properties that respond to different detection mechanisms. For instance, a metabolite having no chromophore will not be able to be detected by UV. Thus detection and identification of the metabolites in a given extract can be considerably improved by using MS, which is a relatively more universal detection method. HRMS is able to detect most of the metabolites at a mass tolerance of 5 ppm providing information on molecular weight, molecular formula and the partial structure of the entity. However, the use of LC-MS is not effective for all chemical compounds present in a given sample since some of the metabolites may be poorly ionised. Thus, the combination of LC-MS and NMR has been introduced. NMR spectra of a complex mixture provides structural information on the major secondary metabolites even though it is less sensitive than LC-MS (Kim and Verpoorte, 2010). The low detection limit in NMR can be complicated by the overlapping signals of primary with the secondary metabolites. Primary metabolites are much more abundant than secondary metabolites especially when the extract itself present in low quantities. One way to overcome these disadvantages is by doing simple fractionation such as liquid-liquid

partitioning; for example, *n*-BuOH-water partition was used to concentrate compounds responsible for aromatic signals resulting to higher spectral resolution (Khatib *et al.*, 2006). A summary of the metabolomics study workflow is presented in Figure 1.14.
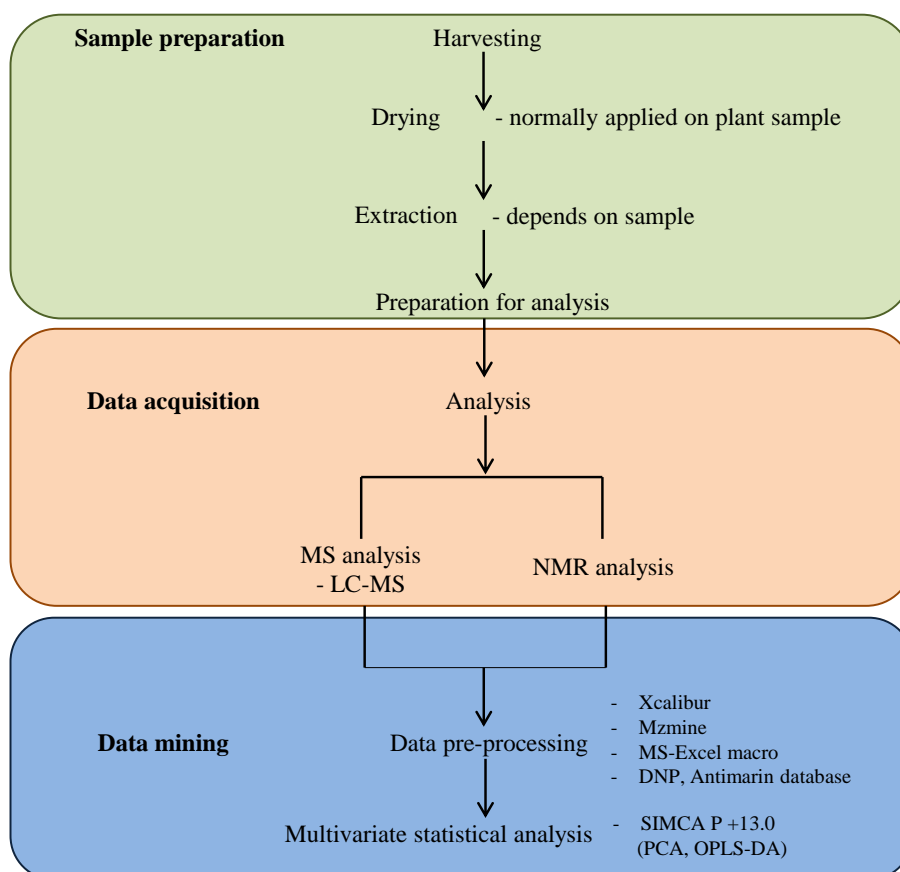
Figure 1.14: Workflow of metabolomics studies of plant and microbial extracts modified from (Macintyre *et al.*, 2014).

1.6.2 Multivariate analysis in metabolomics

The complex data generated from metabolomics based analysis (LC-MS and NMR) require statistical multivariate data analysis (MVDA) to extract the greatest amounts of useful information from the data. A basic unsupervised principal component analysis (PCA) is commonly used as the first step during MVDA to reduce data dimensionality while retaining data quality, followed by different supervised MVDAs depending on the specific data quality and research objectives (Berrueta *et al.*, 2007). In PCA, major sample components are structured to represent data variance in a two or three-dimensional coordinate scheme. This approach discloses

the grouping model of samples and visualizes the discriminant outliers which may indicate potential novel natural products which can be targeted for subsequent analysis (Krug *et al.*, 2008). One of the broadly used supervised MVDA is partial least squares (PLS); it relates a data matrix containing independent variables from samples, such as spectral intensity values (an X matrix) to a matrix containing dependent variables (e.g. measurements of response, such as toxicity scores) for those samples (a Y matrix) (Wold, 2004). OPLS can also be combined with discriminant analysis (DA) to establish the optimal position to place a discriminant surface which best separates classes. In the final step of the metabolomics approach, the selected unique biomarkers are interpreted to putatively identify the novel metabolite using databases like DNP and Antimarin.

1.7   Trypanosomiasis

Trypanosomiasis is a disease caused by trypanosomatids; a group of flagellated kinetoplastid protozoa that can infect humans. *Trypanosoma brucei* is the causal agent for a neglected tropical disease, human African trypanosomiasis (HAT) or 'African sleeping sickness' in which the parasite is transmitted to humans through the bite of a tsetse fly (*Glossina* spp) (Dumas and Bisser, 1999). *Trypanosoma cruzi* is responsible for Chagas disease (or American trypanosomiasis), a zoonotic infection which is transmitted by blood-feeding insects known as Triatominae (or kissing bugs). The insects are members of a subfamily of Reduviidae; they transmit the parasites from animals to humans (Souza, 2002).

1.7.1   Human African trypanosomiasis and Chagas disease
In HAT, the two distinctive human infective sub-species of the parasites are *T. b. gambiense* (West and Central Africa) and *T. b. rhodesiense* (East and sub-Saharan Africa). The main difference between the two infections is the rate of progression from the blood/lymphatic stage to the cerebral stage, as West African trypanosomiasis takes months and lead to a chronic phase (it is a long-developing syndrome) while East African trypanosomiasis is an acute infection (severe and

sudden in onset) with progression occuring in 1-3 weeks. Humans are the major reservoirs for the sub-species *T. b. gambiense*, whilst for *T. b. rhodesiense* animals, especially cattle, are the main reservoirs. The related sub-species, *T. b. brucei* is non-pathogenic to humans but can be found in nagana cattle (Wilkinson and Kelly, 2009). HAT occurs in two distinct phases; the early (or haemolymphatic) stage, when *T. brucei* (an extracellular parasite) replicates in both blood and lymph systems, and the late (or encephalitic) stage when the parasites migrate into the central nervous system (CNS). In the early stage, the symptoms are fever, headache, weight loss, and joint pains but may also lead to other complications such as enlarged lymph glands and spleen, local oedema and cardiac abnormalities (Barrett *et al.*, 2003, Stuart *et al.*, 2008). In the second stage, the parasites cross the blood-brain barrier, marked by the neurological symptoms including headache, changes in sleeping pattern and personality and visual impairments. The infection will lead coma and death if the patients are not treated. Meanwhile, acute Chagas disease is usually asymptomatic and rarely diagnosed; the infected patient will go on and develop chronic stage in which the disease remains asymptomatic for 10 to 30 years (Rassi and Marin-Neto, 2010). The symptoms are vomiting, nausea, hepatic intolerance, convulsion and skin disease related (Castro and Diaz, 1988, Castro *et al.*, 2006). During chronic stage, the symptoms are related to cardiac disorders (megacolon or megaeosphagus) or combination between these (Rassi and de Rezende, 2012) and Chagas heart disease is one of the main causes of mortality in endemic areas (Munoz-Saravia *et al.*, 2012).

1.7.2 Treatment state of HAT and Chagas disease

The current treatment of African sleeping sickness depends on the sub-species and disease stages. The drugs used are limited due to their toxicities (Table 1.3). There have been no new antibiotics since eflornithine was introduced in 1990 against the late stage of *T. b. gambiense* (Jacobs *et al.*, 2011). At the early stage, pentamidine is used against *T. b. gambiense* and suramin used against *T. b. rhodesiense*. They are not used at the cerebral level since these two drugs are unable to cross the blood brain barrier (Figure 1.15). In late stage treatments, eflornithine is effective against *T. b. gambiense* but is expensive. Melarsoprol is used against both *T. brucei* sub-species; however, it exhibits high toxicity due to arsenic (Matovu *et al.*, 2001).

Recently, the use of a combination of nifurtimox and eflornithine (NECT) in phase III clinical trials against *T. b. gambiense* infection was very effective and safe, and has been approved and recommended by the World Health Organization (WHO) (Priotto *et al.*, 2006, Checchi *et al.*, 2007, Priotto *et al.*, 2009). Meanwhile, nifurtimox or benznidazole are used to treat acute and chronic Chagas diseases, requiring bi- or tri-daily administration for between 60 and 90 days (Apt, 2010).

Table 1.3: Current drugs used for the treatment of HAT and its limitations

Drugs	Uses	Mechanism of actions	Limitations
Suramin	Effective against early stage of *T. b. rhodesiense*	Unknown	Ineffective against early stage of *T. b. gambiense* and late stage of both HATs
Pentamidine	Effective against early stage of *T. b. gambiense*	Unknown	Ineffective against early stage of *T. b. rhodesiense* and late stage of both HATs
Melarsoprol	Effective against late stage of both HATs	Unknown	Toxic (kills up to 5% of patients) and high resistance
Eflornithine	Effective against late stage of *T. b. gambiense*	Inhibitor of ornithine decarboxylase	Ineffective against late stage of *T. b. rhodesiense* and costly
Nifurtimox/ Eflornithine (NECT)	Effective against late stage of *T. b. gambiense*	Nifurtimox-activated by a NADH dependent mitochondrial nitroreductase leading to the generation of intracellular free radicals (Wilkinson *et al.*, 2008)	Ineffective against late stage of *T. b. rhodesiense*

Suramin
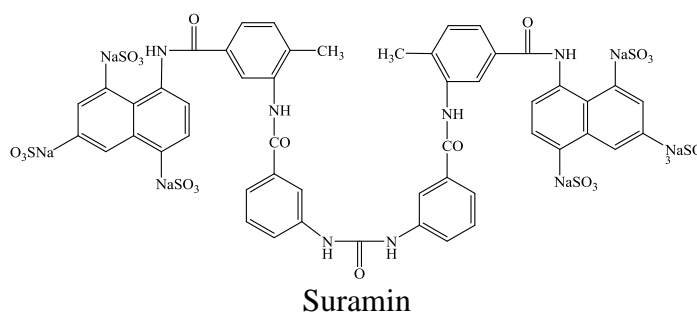
Figure 1.15: Drugs used to treat HAT and Chagas disease

Pentamidine

Melarsoprol

Eflornithine

Nifurtimox

Benznidazole
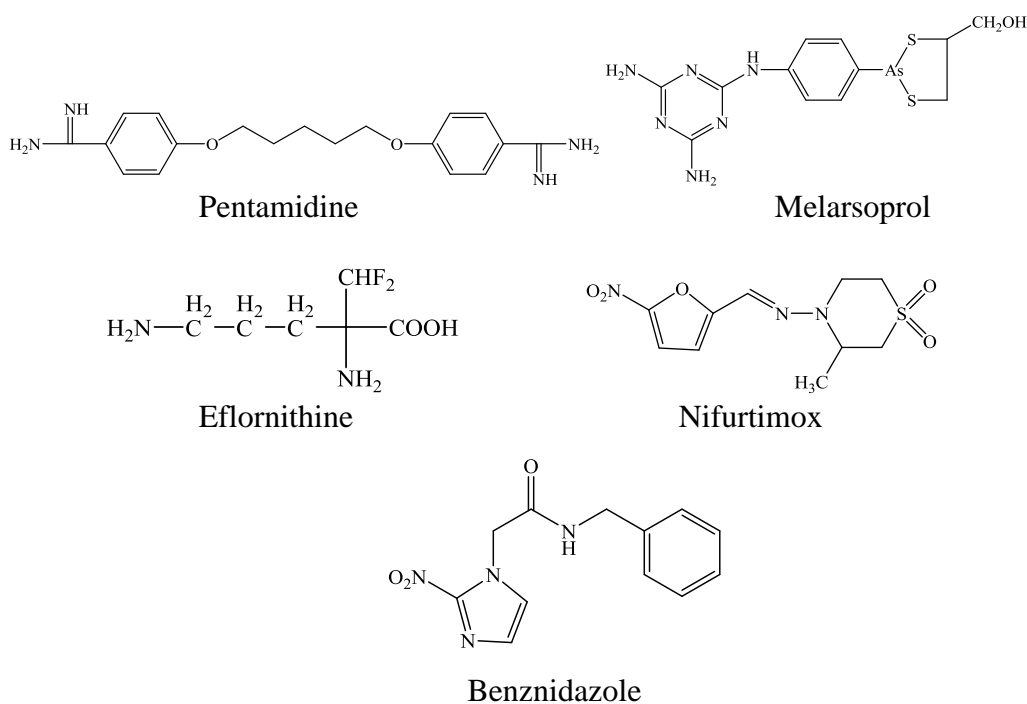
Figure 1.15: Cont'd. Drugs used to treat HAT and Chagas disease

A lot of research programs are being undertaken to target new alternative chemical compounds, either from natural substances (Onegi *et al.*, 2002, Ganapaty *et al.*, 2005, Ribeiro-Rodrigues *et al.*, 1995) or synthetic derivatives (Salmon-Chemin *et al.*, 2001, Khraiwesh *et al.*, 2012, Campos *et al.*, 2014, Ribeiro-Rodrigues *et al.*, 1995) through early screening approaches against the trypanosomal parasites. To date, none of the potential drugs have been tested in preclinical trials. The actual mechanisms on how the drugs react in human blood are aggressively being studied by numerous researchers from various fields to fight the disease especially in underdeveloped countries.

1.8   Current status of research scope

Natural products research has an important role as a resource of various biologically active substances of natural origin. Human African trypanosomiasis is a neglected disease that needs international efforts in developing new potential alternative drugs. Many of the affected rural populations live with limited access to appropriate health specialities, and the production of drugs is costly. Moreover, the available drugs used

for the treatment of trypanosomiasis depend on the sub-species as well as the stage of the disease. The requirement for drugs which are able to cross the blood brain barrier to get into contact with the parasites is also a major problem in drug design, hence some drugs are difficult to administer, are toxic and cause adverse drug reactions (Hotez *et al.*, 2007, Brun *et al.*, 2010). This circumstance necessitates the development of new, effective, cheap and safe remedies to combat the trypanosomiasis. Up until now, there is no drug of natural origins available commercially that can treat these diseases. However, the world population has used traditional medicine from natural sources for many years (Newman and Cragg, 2012, Gurnani *et al.*, 2014, Harvey *et al.*, 2015). This has driven us to further intensively search for novel anti-trypanosomal agents from natural sources. The production of the drugs from plant sources is unsustainable and un-economic, therefore, different alternative and potential resources have been developed including the discovery of the drugs from endophytic fungi. As previously described, mangrove plants produce numerous bioactive compounds (Han *et al.*, 2007) and endophytic fungi also have been explored not just for their ecological functions but for their secondary metabolites as a new source of bioactive natural products. Accordingly, many structurally unique and biologically active compounds have been obtained from the cultures of endophytic fungi. A vital question in the discovery of new potential anti-trypanosomal compounds from natural origins is, will the isolated bioactive natural product be a known compound with the same known bioactivity? Thus, to overcome this problem, the metabolomics approach is used to accelerate the identification of potential novel bioactive components from the crude extracts. The dereplication method is a process required to help researchers screen the known metabolites from the crude extracts before further scale up or isolation work is taken to avoid repetitive work. High performance liquid chromatography-electrospray ionisation-mass spectrometry (HRESI-LCMS) for both positive and negative ionization modes and spectroscopic NMR analysis are used for dereplication of plant and fungal secondary metabolites in crude extracts.

The present study reports the investigation on potential bioactive secondary metabolites from marine sources. The sea water of the east coast of Malaysia

contains valuable and countless marine biodiversity of which the majority remains unexplored. The mangrove plant *Avicennia lanata* was collected from the east coast of Peninsular Malaysia in Setiu Wetlands, Terengganu and endophytic fungal strains of *Aspergillus aculeatus* were isolated from its leaf parts, *Lasiodiplodia theobromae* from the stem, and *Fusarium* sp. from the root. In the preliminary screening, the small-scale fungal extracts were dereplicated before proceeding to scale up or purification of the secondary metabolites from the crude extracts. Hence, isolation and identification of biologically active compounds from the crude extract of *A. lanata* and associated endophytic microorganisms leading to new potent anti-trypanosomal structures has been assisted by both a targeted metabolomics approach and bioassay-guided isolation work.

The aims of this study are as follows:

    i.   To isolate bioactive metabolites from the crude extract of *A. lanata*

    ii.   To isolate and identify strains of endophytic fungi from *A. lanata*

    iii.   To preliminarily screen and identify bioactive secondary metabolites from endophytic fungi prior to scale up

    iv.   To identify and characterise the molecular structure of the bioactive compounds

    v.   To test the pure compounds agaist *Trypanosomal brucei brucei*

CHAPTER 2

2. Bioactive secondary metabolites from *Avicennia lanata*

Avicennia lanata locally known in Malaysia as *'Api-api bulu'* is found mainly in sandy or firm silt substrate of middle to higher intertidal positions (Peter and Sivasothi, 1999). In the older literature, this species was synonyms with *A. rumphiana*. *A. lanata* is native and common throughout much of Peninsular Malaysia, Philippines to New Guinea. This tree is identified by its furry fruit and furry leaves (underside). The fur; (*'bulu'* in Malay) on the leaves conserves water by trapping a layer of insulating air, thus reducing water loss through evaporation. The tree or shrub can achieve to 20 m tall; bark is dark brown to black, warty or smooth and pneumatophores 20-30 cm tall. While leaf blades are satiny dark green above and surface is dull with pale yellowish brown. The flowers are in tight bunches at the ends of a cross-like inflorescence and fruit is light green to yellowish brown with densely short-woolly, compressed and ovoid. This plant has traditionally been used as food; the seeds are boiled and eaten whereas in some places they are sold in markets as vegetables. The wood is rarely used to make charcoal and is used as firewood only to smoke fish or rubber. This fast growing mangrove tree is among the few also used in replanting mangroves to protect coastlines (the others are *Sonneratia* and *Rhizophora* species).

Avicennia lanata

Kingdom: Plantae
Phylum: Tracheophyta
Class: Magnoliopsida
Order: Lamiales
Family: Avicenniaceae
Genus: *Avicennia*
Scientific name: *Avicennia lanata* Ridley
Synonym: *Avicennia rumphiana*
Local name: *'Api-api bulu'*

Figure 2.1: Mangrove plant and leaves of *A. lanata*

2.1 Results and discussion

This chapter reports the isolation and identification of new and potentially bioactive metabolites with anti-trypanosomal activity from the stems of *A. lanata* (Figure 2.1) which were collected from Setiu Wetlands, Terengganu, Malaysia with the help of Haji Muhamad Razali Salam. A specimen was kept in the University Malaysia Terengganu herbarium with the voucher specimen code UMT-01. The dried powdered stem (4.0 kg) of *A. lanata* was macerated in methanol overnight 8L/extraction 3 times and the methanol extract was concentrated under vacuum pressure using a rotary evaporator (Büchi, Switzerland) to give 44.8160 g. The methanol extract was partitioned by liquid-liquid extraction (90% H_2O + 10% MeOH: EtOAc, 1:1, 3x) and the ethyl acetate phase was concentrated using a rotary evaporator to give a crude extract weighing 14.4115 g.

2.2 Dereplication studies on crude extract of *A. lanata* by HRESI-LCMS

The total ion chromatogram of the crude extract of *A. lanata* (Figure 2.2) showed the distribution of known and unknown compounds present in the total extract. According to the dereplication studies, the plant extract possessed certain types of

compounds, such as sterols, triterpenes and naphthoquinones which have also previously been isolated from different *Avicennia* species, mostly from *A. marina* and *A. officinalis*. Some of the putatively identified compounds have been previously isolated from *Avicennia* sp. (Table 2.1). Avicennone A (**1.8**) and D (**1.11**), naphthoquinone derivatives, were most commonly isolated from *Avicennia marina* (Han *et al.*, 2007). Most of the identified compounds have been previously isolated from marine bacteria, actinomycetes and fungi (Figure 2.3). The values and predicted formulas of unknown compounds were tabulated in Table 2.2.
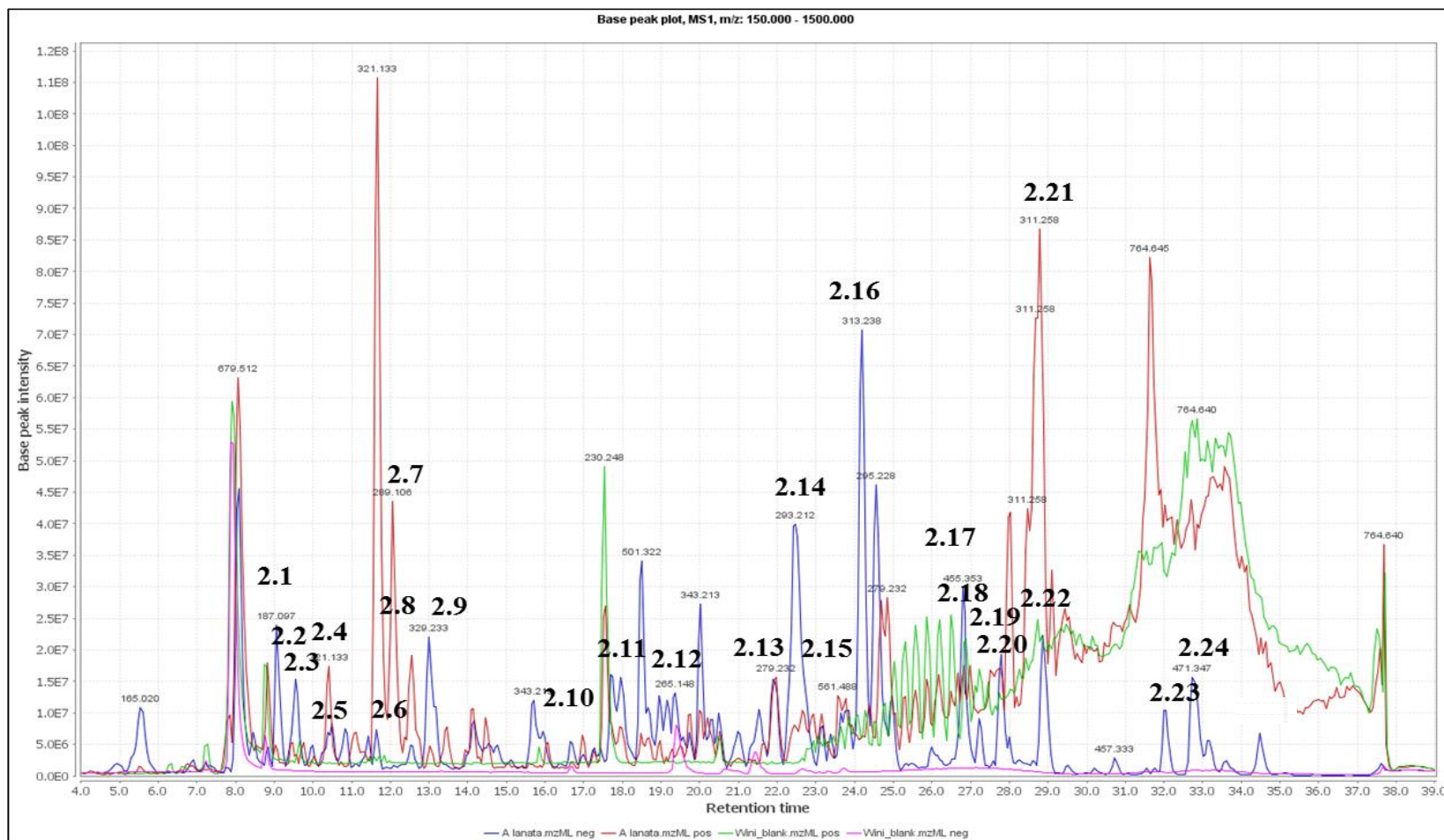
Figure 2.2: Total ion chromatogram of *A. lanata* total crude extract.
Red and blue represent the positive and negative ionisation modes, respectively, for the crude extract. Green and pink represent the positive and negative ionisation modes, respectively, for the solvent blank

Table 2.1: Compounds from the total crude extract of *A. lanata*
that were putatively identified using the DNP database (Sources; P-plant, F-fungi)

No.	ESI modes	Rt (min)	MS (m/z)	Molecular weight	Chemical formula	Name	Tolerance (ppm)	Sources	Peak Area
2.1	N	9.12	187.0976	188.1048	$C_9H_{16}O_4$	cerberidol	2.7762	*Cerbera manghas*	2.24E+8
2.2/ 1.8	P	9.31	215.0339	214.1740	$C_{12}H_6O_4$	avicennone D	0.0861	[P] *Avicennia marina*	7.07E+6
2.3	N	9.55	305.0668	306.0741	$C_{15}H_{14}O_7$	canescin-A; malignin-A; canescin	2.2779	[F] *Penicillium canescens, Aspergillus malignus*	2.78E+8
2.4	N	11.42	277.0720	278.0793	$C_{14}H_{14}O_6$	4,4'-dimethyl-2,2',3,3',6,6'-biphenylhexol;	2.8213	[F] *Penicillium rubrum*	6.69E+7
2.5/ 1.11	P	10.41	321.1331	320.3370	$C_{17}H_{20}O_6$	avicennone A	-0.4652	*Avicennia marina*	1.83E+8
2.6	P	11.66	321.1329	320.1257	$C_{17}H_{20}O_6$	cavoxin	0.6544	*Phoma cava*	1.55E+9
2.7	P	11.66	289.1069	288.0996	$C_{16}H_{16}O_5$	aloesaponol IV	0.6223	*Aloe saponaria*	1.18E+9
2.8	P	12.54	321.0968	320.0896	$C_{16}H_{21}BrN_2$	dihydroflustramine C	2.3296	Bryozoa *Flustra foliacea*	2.35E+8
2.9	N	13.01	329.2336	330.2409	$C_{18}H_{34}O_5$	5,8,12-trihydroxy-9-octadecenoic acid	0.8438	Wheat bran	2.95E+8
2.10	N	17.70	311.2231	312.2304	$C_{18}H_{32}O_4$	9-octadecenedioic acid	1.0909	*Candida tropicalis*	4.55E+8
2.11	N	18.51	501.3226	502.3298	$C_{30}H_{46}O_6$	aleurodiscal	0.8309	*Aleurodiscus mirabilis*	4.69E+8
2.12	N	18.48	291.1970	292.2042	$C_{18}H_{28}O_3$	chromomoric acid C	1.3588	*Chromolaena morii*	1.19E+8
2.13	P	21.97	279.2318	278.2245	$C_{18}H_{30}O_2$	8,13:13,17-diepoxy-14,15-inorlabdane	0.3265	*Pinus monticola*	2.85E+8
2.14	N	22.48	293.2125	294.2198	$C_{18}H_{30}O_3$	colnelenic acid	1.0570	Product of enzymic oxidation of potato lipids	9.57E+8
2.15	P	23.57	561.4880	560.4807	$C_{36}H_{64}O_4$	3-(3,4-dihydroxyphenyl)-1-propanol	0.4451	*Tsuga chinensis* var. *formosana*	2.32E+8
2.16	N	24.18	313.2385	314.2457	$C_{18}H_{34}O_4$	2-methyl-3-tridecylbutanedioic acid	0.1303	Leaves of *Didymocarpus pedicellata*	1.40E+9
2.17	N	26.79	455.3533	456.3606	$C_{30}H_{48}O_3$	3,7-dihydroxy-8-fernen-11-one	0.5897	*Balsamorhiza sagittata*	4.22E+8
2.18	P	27.56	1372.8401	1371.8328	$C_{72}H_{122}O_{24}$	amphidinol 5	0.5441	*Amphidinium klebsii*	1.00E+6
2.19	P	27.72	1328.8169	1327.8096	$C_{70}H_{118}O_{23}$	amphidinol-9	2.8393	*Amphidinium carterae*	1.23E+6

Table 2.1: Cont'd. Compounds from the total crude extract of _A. lanata_
that were putatively identified using the DNP database (Sources; P-plant, F-fungi)

2.20	N	27.80	473.3273	474.3346	$C_{29}H_{46}O_5$	17,23-epoxy-3,24,29-trihydroxy-27-norlanost-8-en-15-one	1.2499	_Muscari comosum_ (tassel hyacinth)	2.22E+8
2.21	P	28.78	311.2582	310.2509	$C_{19}H_{34}O_3$	dihydro-4-hydroxy-5-methyl-3-tetradecylidene-2(3H)-furanone	2.1839	Roots of _Litsea japonica_	2.58E+9
2.22	N	28.86	453.3375	454.3448	$C_{30}H_{46}O_3$	bacogenin A$_3$	0.2443	_Bacopa monniera_	2.84E+8
2.23	N	32.06	471.3482	472.3554	$C_{30}H_{48}O_4$	alisol B	0.3946	Rhizomes of _Alisma plantago_-aquatica	1.21E+8
2.24	N	34.48	461.3643	462.3716	$C_{29}H_{50}O_4$	stigmast-24(28)-ene-2,3,22,23-tetrol	1.4381	_Phaseolus vulgaris_ (kidney bean) seed	8.47E+7

Table 2.2: Compounds present in the crude extract of _A. lanata_
that were unidentified using the DNP database

ESI modes	Rt (min)	MS (m/z)	Molecular weight	Predicted Formula	Peak Area
N	5.54	165.0196	166.0269	$C_8H_6O_4$	2.06E+8
P	13.47	185.0597	184.0525	$C_{12}H_8O_2$	9.19E+7
P	14.14	370.1859	369.1787	$C_{19}H_{23}N_5O_3/C_{18}H_{27}NO_7$	1.16E+8
P	19.98	362.2536	361.2463	$C_{19}H_{31}N_5O_2/C_{18}H_{35}NO_6$	3.68E+8
P	28.04	589.5213	588.5140	$C_{39}H_{64}N_4/C_{28}H_{64}N_{10}O_3/C_{38}H_{68}O_4$	5.65E+8

2.1

2.2

2.3

2.4

2.5

2.6

2.7

2.8

2.9

2.10

2.11

2.12
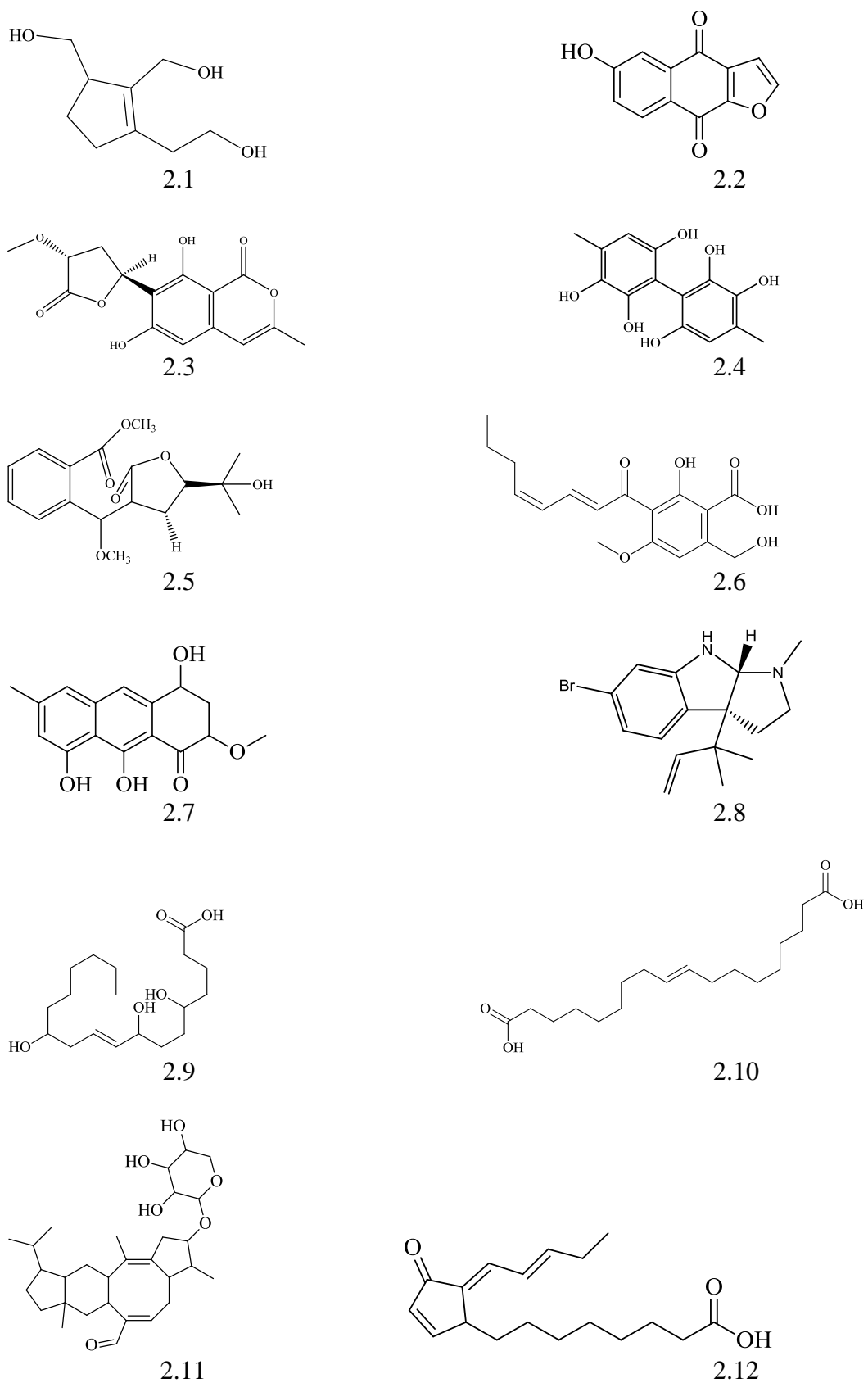
Figure 2.3: Compounds that were putatively identified through dereplication studies on *A. lanata* crude extract

2.13

2.14

2.15

2.16

2.17

2.18

2.19

2.20

2.21

2.22

Figure 2.3: Cont'd. Compounds that were putatively identified through dereplication studies on *A. lanata* crude extract

2.23　　　　　　　　　　　　　　　　　　2.24
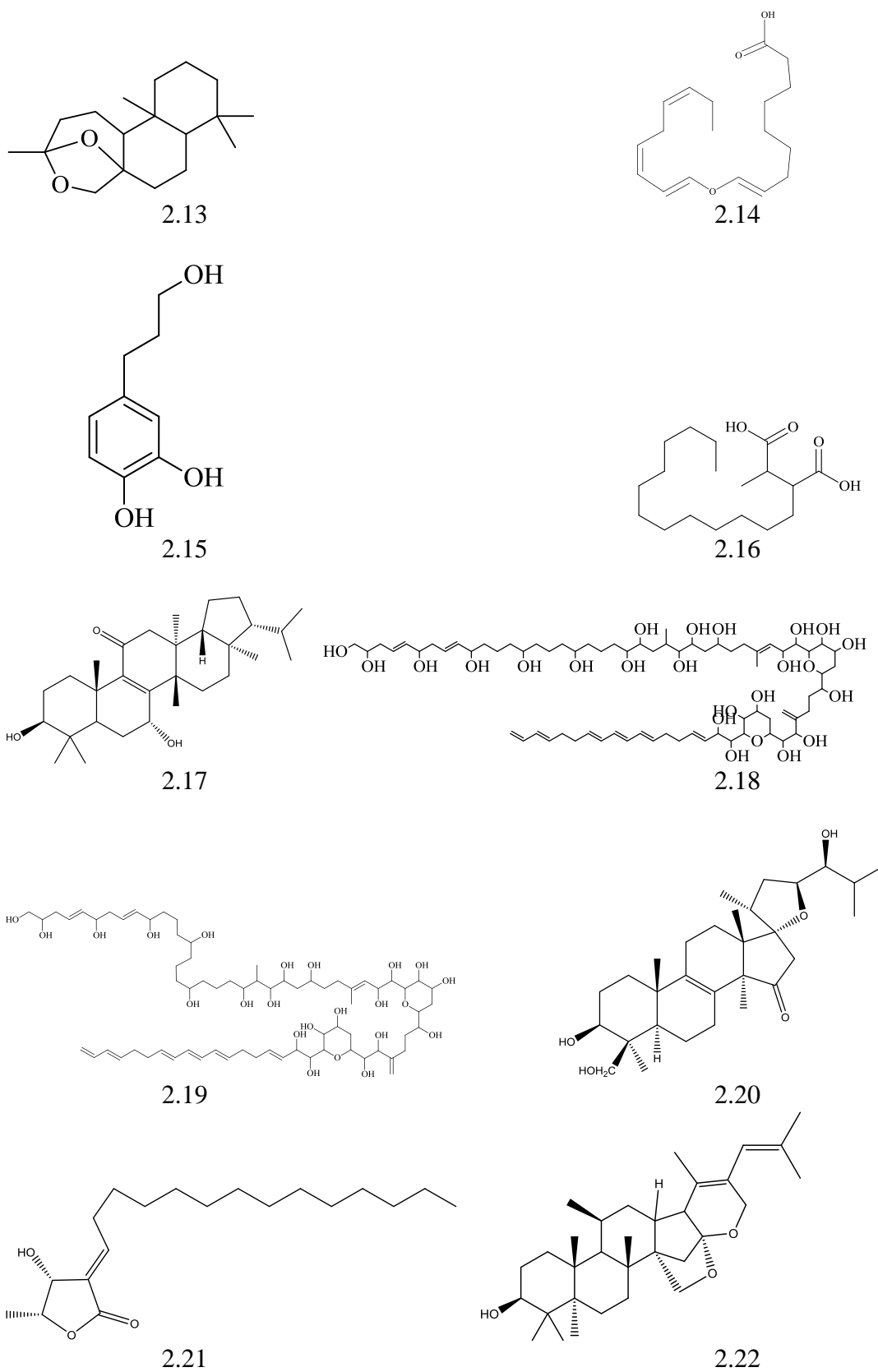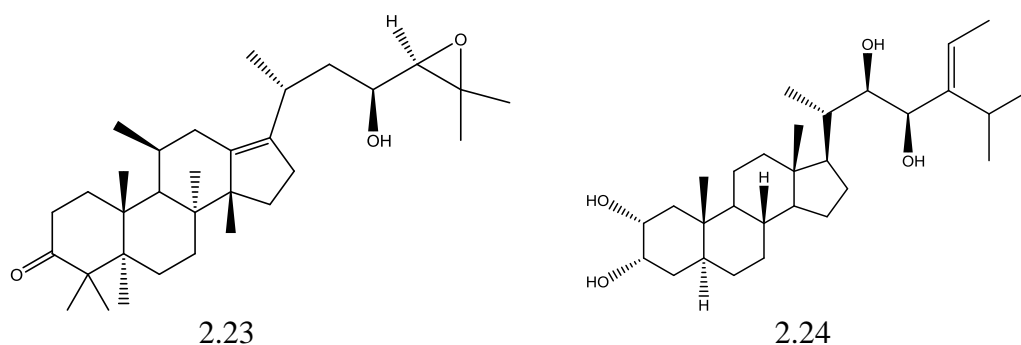
Figure 2.3: Cont'd. Compounds that were putatively identified through dereplication studies on *A. lanata* crude extract

2.3　Isolation of secondary metabolites from *A. lanata*

Further isolation and identification of bioactive metabolites from the *A. lanata* plant extract were carried out based on the bioactivity screening results of each fraction against *T. b. brucei*.

Table 2.3: Anti-trypanosomal activity of *A. lanata* crude extract and its fractions (calculated as mean value percentage viability) at different concentrations of 20, 10 and 5 μg/mL

Fractions	Yield (g)	*T. b. brucei* (% D control)		
		20 μg/mL	10 μg/mL	5 μg/mL
EtOAc extract	14.4115	35.0	73.7	107.1
TGWD-F1	6.3254	114.0	139.1	142.1
TGWD-F2	5.2059	131.0	151.6	151.4
TGWD-F3	1.7074	40.6	51.7	92.8
TGWD-F4	0.7330	42.9	49.0	61.3
TGWD-F5	0.7130	-12.3	-10.5	3.8
TGWD-F6	0.3380	0.2	-13.3	-5.1
TGWD-F7	0.1343	-5.8	-4.9	48.3
TGWD-F8	0.1200	-4.3	-3.8	32.8
TGWD-F9	0.1570	33.3	19.6	85.8

% D, percentage viability of control

2.3.1　Bioactivity test results for the *A. lanata* crude fractions

Each fraction was screened at different concentrations: 20 μg/mL, 10 μg/mL and 5 μg/mL. The assay was performed in duplicate for each sample. The results show the percentage growth of *T. b. brucei* (Table 2.3), with negative readings meaning higher growth inhibition on the trypanosomal cells. The *A. lanata* crude extract

showed marginal anti-trypanosomal activity, whereas after fractionation, the activity for fractions F5 to F8 increased, and decreased in fraction F9. Fractions F1 and F2 showed very weak anti-trypanosomal activity whereas fractions F3, F4 and F9 showed moderate activity. Meanwhile, fractions F5 until F8 showed significant activity in this screening test, thereby supporting further investigation of the biologically-active compounds from this plant extract.

2.3.2 Multivariate analysis of the *A. lanata* fractions

A dereplication study was performed on the *A. lanata* major fractions to obtain the metabolomic profile of each fraction and to evaluate the relationship between metabolites in the *A. lanata* extract and their bioactivity against *T. b. brucei*. The unsupervised PCA score plot showed moderate separation of the *A. lanata* fractions (Figure 2.4 a).
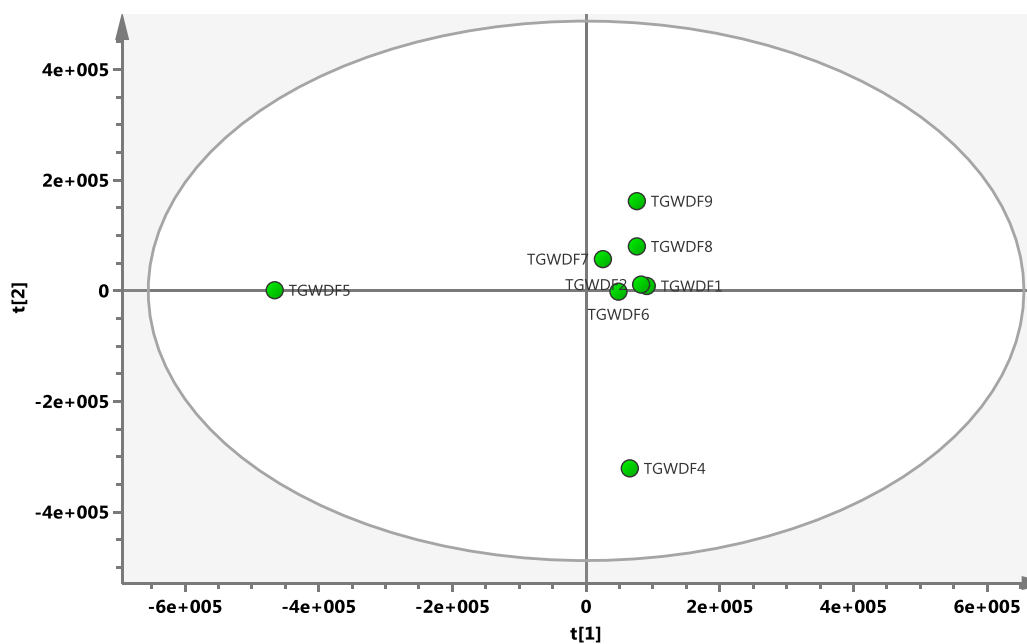
a)

Figure 2.4: Multivariate analysis on *A. lanata* fractions
(a) Unsupervised PCA score plot of the *A. lanata* fractions showed moderate separation between the datasets; (b) Supervised OPLS-DA score plot analysis showed a distinctive separation between the active and inactive groups ($R^2(Y) =1.0; Q^2(Y) =0.99$); (c) OPLS-DA S-plot exhibited the biomarkers at the end-point for each group (highlighted in red).

b)

c)
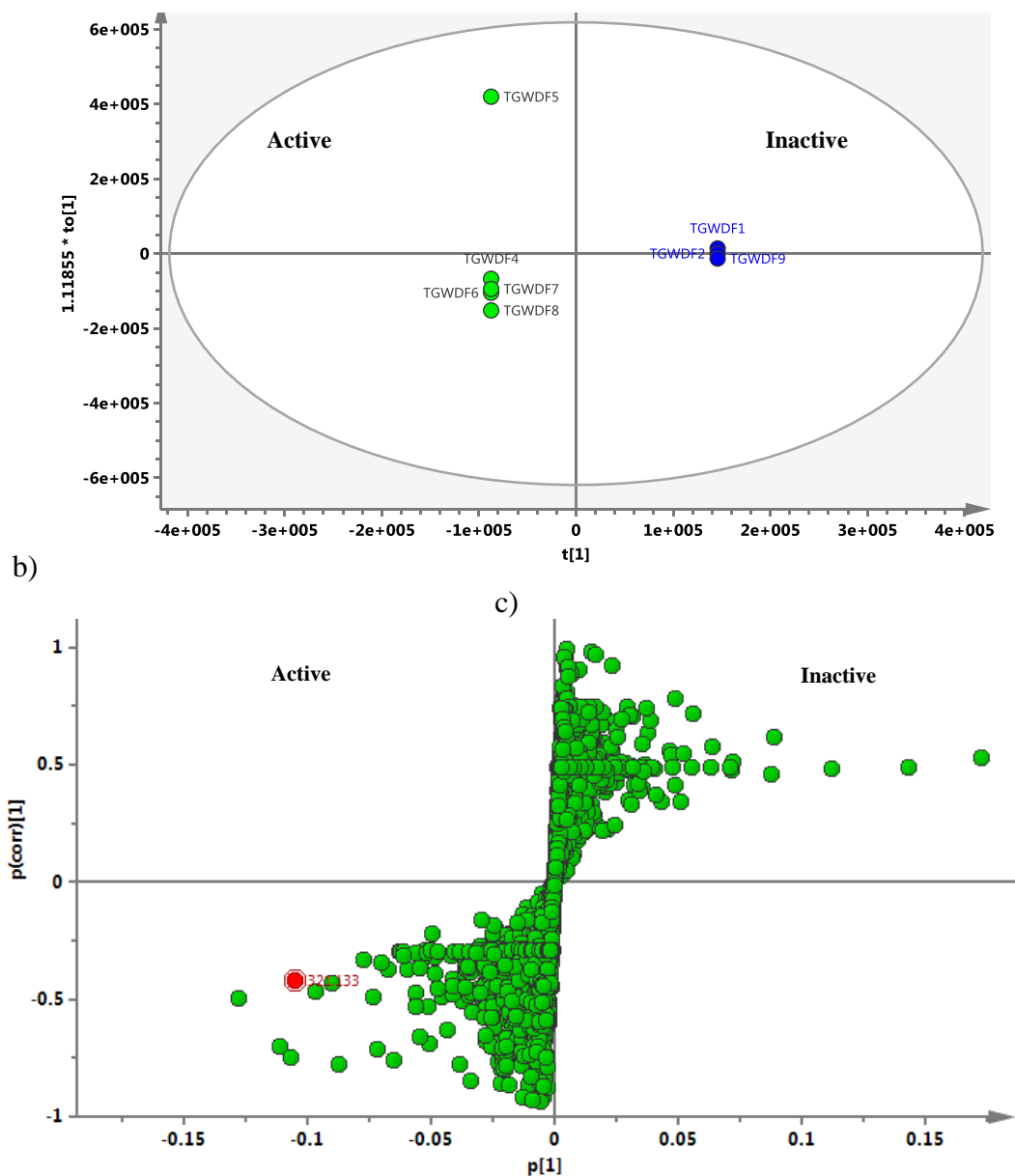
Figure 2.4: Cont'd. Multivariate analysis on *A. lanata* fractions

(a) Unsupervised PCA score plot of the *A. lanata* fractions showed moderate separation between the datasets; (b) Supervised OPLS-DA score plot analysis showed a distinctive separation between the active and inactive groups ($R^2(Y) = 1.0$; $Q^2(Y) = 0.99$); (c) OPLS-DA S-plot exhibited the biomarkers at the end-point for each group (highlighted in red).

There was clear separation between fraction F5 and the other fractions that were also active against *T. b. brucei*. Fraction F4, which also possessed moderate activity, was likewise set apart from other fractions. Meanwhile, a supervised multivariate OPLS-DA analysis exhibited two classes - fractions F1, F2, F3 and F9 were the inactive group and clustered in the same quadrant, while fractions F4, F5, F6, F7 and F8 were the active group, but fraction F5 was an outlier from the active cluster (Figure 2.4 b).

The OPLS-DA S-plot (Figure 2.4 c) showed the metabolites at the end point of both the active and inactive groups. From the DNP database, it was putatively determined that fractions F1 and F2 contained mostly fatty acid oils, while fractions F3 and F4 were comprised of terpenoid and sterol metabolites. Fractions F5 to F9 were putatively identified to have mainly aromatic compounds, with these compounds perhaps contributing towards the activity of the fractions. Some of the ion peaks in the active group have been putatively identified as presented in Table 2.1. Characteristic metabolites for the genus *Avicenna* was observed at *m/z* 321.1331 $[M+H]^+$ putatively identified as avicennone A (**1.11**), earlier described from *A. marina* (Han *et al.*, 2007). The aim of this study was to isolate potential compounds from the active fractions that are responsible for the anti-trypanosomal activity.

2.3.3 Isolation and purification of compounds from *A. lanata* fractions

All of the *A. lanata* fractions were analysed on normal silica TLC plates to monitor separation and purity. Based on the TLC profiles, the dereplication study, and the anti-trypanosomal results, fractions F3 and F4 showed similar chemical profiles thus the fractions were pooled together (and were labelled collectively as F3) in order to have a better fraction yield and to avoid repetitive isolation work (Figure 2.5). Further chromatographic separation of fraction F3 through open column chromatography gave four known compounds, which were taraxerol (F3-17 (**1.44**), 124.0 mg, 0.84%), taraxerone (F3-13 (**1.45**), 148.8 mg, 1.03%), stigmasterol (F3-19 (**1.47**), 108.9 mg, 0.76%) and β-sitosterol (F3-22, (**1.56**), 32.0 mg, 0.22%). These four compounds are the major compounds found in the *A. lanata* extract. Fraction F5 was purified using open column chromatography followed by flash chromatography (Biotage Isolera, Sweden), yielding also three pure compounds: avicenol C (F5-2-3 (**1.7**), 20.7 mg, 0.14%), avicequinone C (F5-2-6 (**1.4**), 5.7 mg, 0.04%) and glycoquinone (F5-2-9 (**2.25**), 25.7 mg, 0.18%). Further purification of fraction F6 using flash chromatography (Biotage Isolera, Sweden and Grace Reveleris, USA) afforded a new derivative hydroxyavicenol C (F6-8 (**2.26**), 6.5 mg, 0.05%), and further fractionation of F7 by preparative thin layer chromatography resulted in two new derivatives, glycosemiquinone (F7-5-2 (**2.27**), 6.0 mg, 0.04%) and

avicennpentenone carboxylate (F7-5-1 (**2.28**), 6.7 mg, 0.05%). A summary of the workflow on the *A. lanata* crude extract was shown in Figure 2.6.
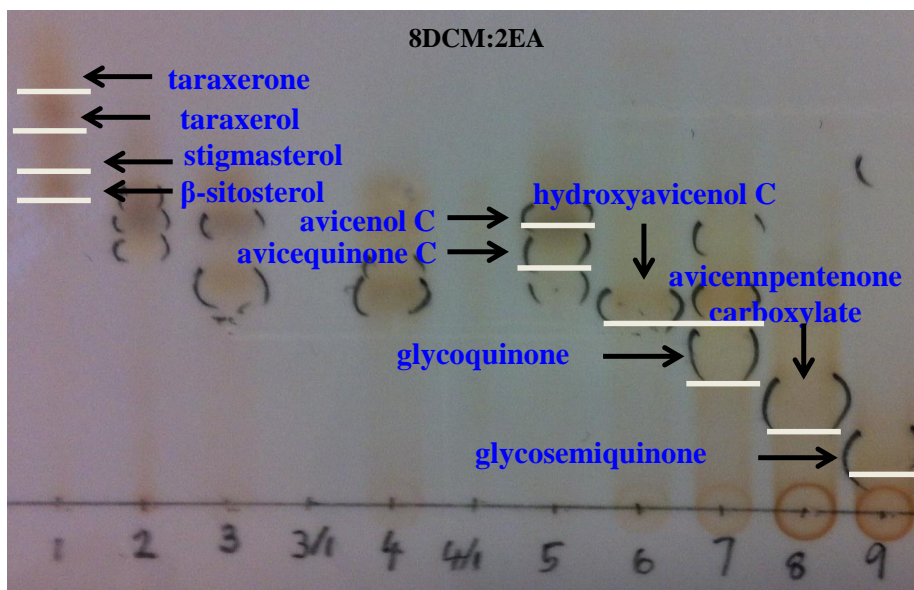
Figure 2.5: TLC of *A. lanata* fractions
after spraying with *p*-Anisaldehyde-sulphuric acid
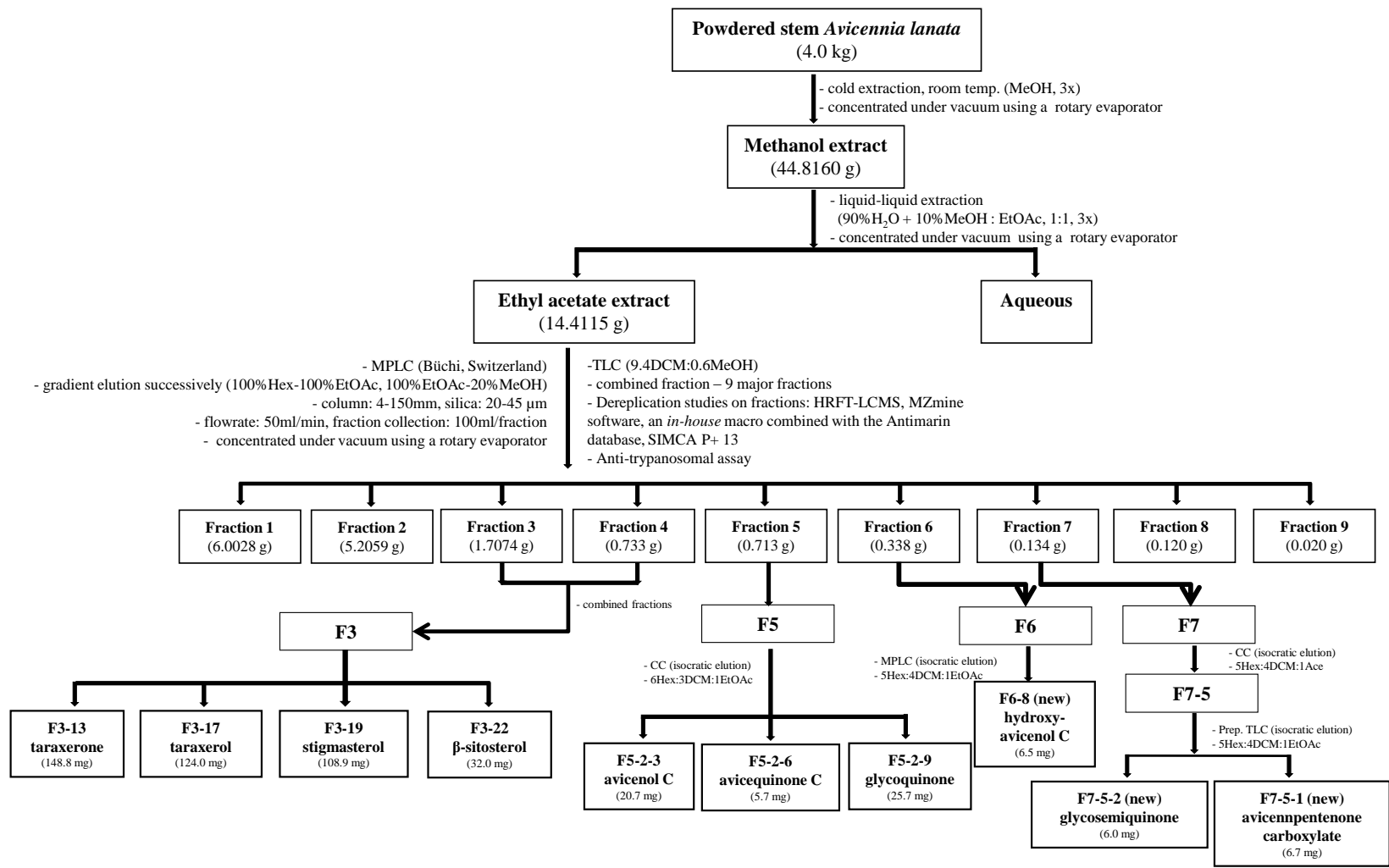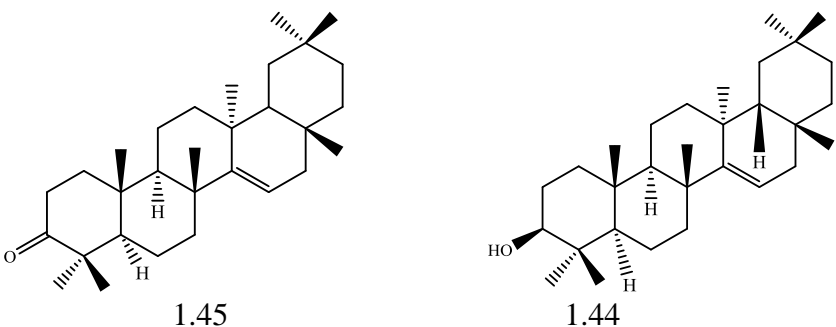
Figure 2.6: Summary of workflow on *A. lanata* crude extract

2.4 Structure elucidation and identification of secondary metabolites

In searching for novel bioactive compounds from *A. lanata*, three new compounds, derivatives of avicenol C, glycoquinone and a new carboxylate derivative, were isolated along with seven known compounds: taraxerone (**1.45**), taraxerol (**1.44**), stigmasterol (**1.47**), β-sitosterol (**1.56**), avicenol C (**1.7**), avicequinone C (**1.4**) and glycoquinone (**2.25**).

2.4.1 Compound F3-13 (taraxerone, 1.45)

Compound F3-13 (148.8 mg) was colourless crystals and identified as taraxerone with optical rotation $[\alpha]_D^{20}$ +7.4° (*c* 1.00, CHCl$_3$). High resolution mass spectrum exhibited a molecular ion peak at *m/z* 424.3705 [M]$^+$ which was consistent with the molecular formula C$_{30}$H$_{48}$O. IRν_{max} (KBr) cm^{-1}: 3401, 2936, 2962, 2872, 1708, 1457, 1375, 1054, 970. EI-MS m/z (int. rel. %): 424 (M$^+$, 26.8), 409 (19.2), 300 (84.8), 295 (66.4), 204 (100), 189 (35.6), 133 (76.0), 119 (50.8) and 107 (63.5) (Mawa and Said, 2012).

Synonyms	taraxerone, 14-taraxeren-3-one, *D*-friedoolean-14-en-3-one	taraxerol, 3-picenol, skimmiol, tiliadin, alnulin, *D*-friedoolean-14-en-3β-ol
Sample code Sources Yield (mg, %) Physical state Mol. formula Molecular weight (g/mol) R$_f$ value (2H:8DCM) Optical rotation $[\alpha]_D^{20}$	F3-13 (**1.45**) *A. lanata* stem 148.8 (1.03%) Colourless needles C$_{30}$H$_{48}$O 424.3705 [M]$^+$ 0.49 +7.4° (*c* 1.00, CHCl$_3$)	F3-17 (**1.44**) *A. lanata* stem 124.0 (0.84%) Colourless needles C$_{30}$H$_{50}$O 426.3862 [M]$^+$ 0.44 +8.7° (*c* 1.02, CHCl$_3$)

1.45   1.44

The ^{1}H NMR spectrum of F3-13 (Figure 2.7 a, Table 2.4) showed a downfield doublet of doublets at δ_H 5.55 (*dd, J*=8.2, 3.2 Hz, 1H), which corresponded to the olefinic proton at H-15. The two signals at δ_H 2.56 (*ddd, J*=15.8, 11.8, 7.0 Hz, 1H) and 2.32 (*ddd, J*=15.8, 6.3, 3.3 Hz, 1H) represented one methylene proton at C-2 that shifted to the downfield region because of the electronegativity effect of the carbonyl group, and δ_H 1.91 (*dd, J*=15.1, 3.2 Hz, 2H) represented a methylene proton at C-1. The remaining eight singlet signals observed at δ_H 1.07, 1.06, 1.08, 0.82, 1.13, 0.91, 0.94 and 0.90 corresponded to methyl groups 23, 24, 25, 26, 27, 28, 29 and 30, respectively. The presence of all methyl protons as singlet proved that the methyl protons of this compound were attached to quaternary carbons. The ^{13}C NMR results (Figure 2.7, Table 2.4) showed 30 carbon signals with one carbonyl carbon at δ_C 217.7 (C-3), and a carbon at 157.7 (C-14) that was attached through a double bond to a quaternary carbon at 117.3 (C-15). Ten methylene carbon signals were observed at 38.4 (C-1), 34.2 (C-2), 20.5 (C-6), 35.1 (C-7), 17.5 (C-11), 35.9 C-12), 36.8 (C-16), 40.7 (C-19), 33.7 (C-21) and 33.2 (C-22) and eight methyl carbon signals at δ_C 26.2 (C-23), 21.6 (C-24), 14.9 (C-25), 29.9 (C-26), 25.7 (C-27), 30.0 (C-28), 33.5 (C-29) and 21.4 (C-30) were found in the up field region. The remaining carbon signals were observed at δ_C 55.9 (C-5), 48.8 (C-9), and 48.9 (C-18), representing methine carbons, along with quaternary carbon signals at δ_C 47.7 (C-4), 39.0 (C-8), 37.8 (C-10), 37.8 (C-13), 37.6 (C-17) and 28.9 (C-20). Based on the spectroscopy results and comparison with previous reports, this compound was identified as taraxerone (Mawa and Said, 2012).
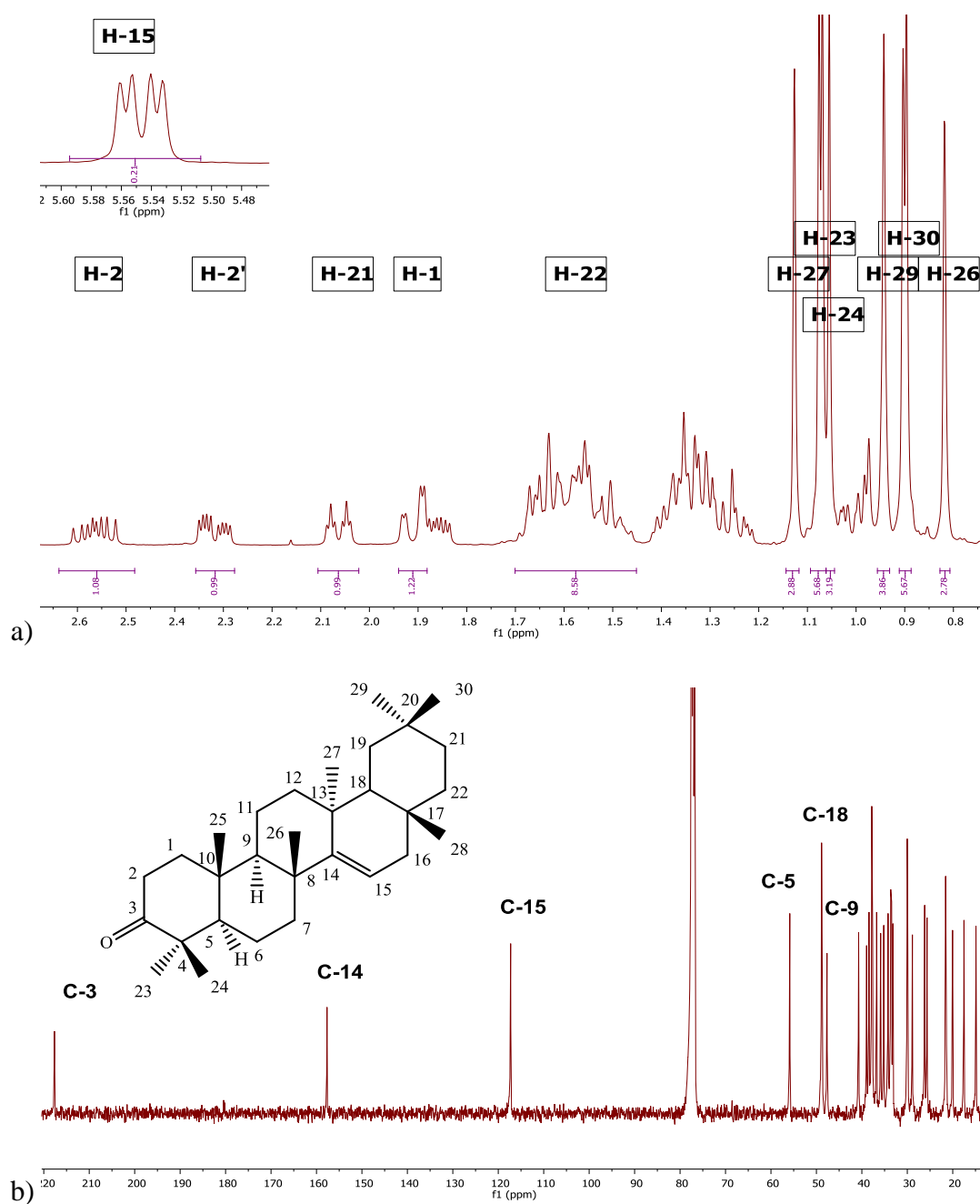
Figure 2.7: (a) ^{1}H and (b) ^{13}C NMR spectra of F3-13
(CDCl$_3$, ^{1}H 400 MHz, ^{13}C 100.5 MHz)

2.4.2 Compound F3-17 (taraxerol, 1.44)

Compound F3-17 (124.0 mg) was isolated as colourless crystals with optical rotation $[\alpha]_D^{20}$ +8.7° (*c* 1.02, CHCl$_3$) and the MS showed the [M]$^+$ at *m/z* 426.3862 corresponding to a molecular formula of C$_{30}$H$_{50}$O. IRν_{max} (KBr) cm^{-1}: 3401, 2916, 2849, 1609, 1460, 1441, 1383, 1376, 1037, 762. MS *m/z* (int. rel. %): 426 (M$^+$, 6.3), 411 (6.3), 302 (35.4), 287 (34.6), 218 (26.8), 204 (100), 189 (27.6), 135 (35.4)

(Mawa and Said, 2012). The ^{1}H and ^{13}C NMR results (Figure 2.8 a, b, Table 2.4) of this compound were consistent with the signals exhibited by compound F3-13 except for the carbonyl signal. A methine proton signal was observed at δ_H 3.18 (*m*, 1H), which was downfield because of the OH group, and an oxygen-bearing carbon linked to methine carbon was found at δ_C 79.3 (C-3). Compound F3-17 was identified as taraxerol based on spectroscopy results in which the NMR and optical rotation results matched the previous literature (Mawa and Said, 2012).
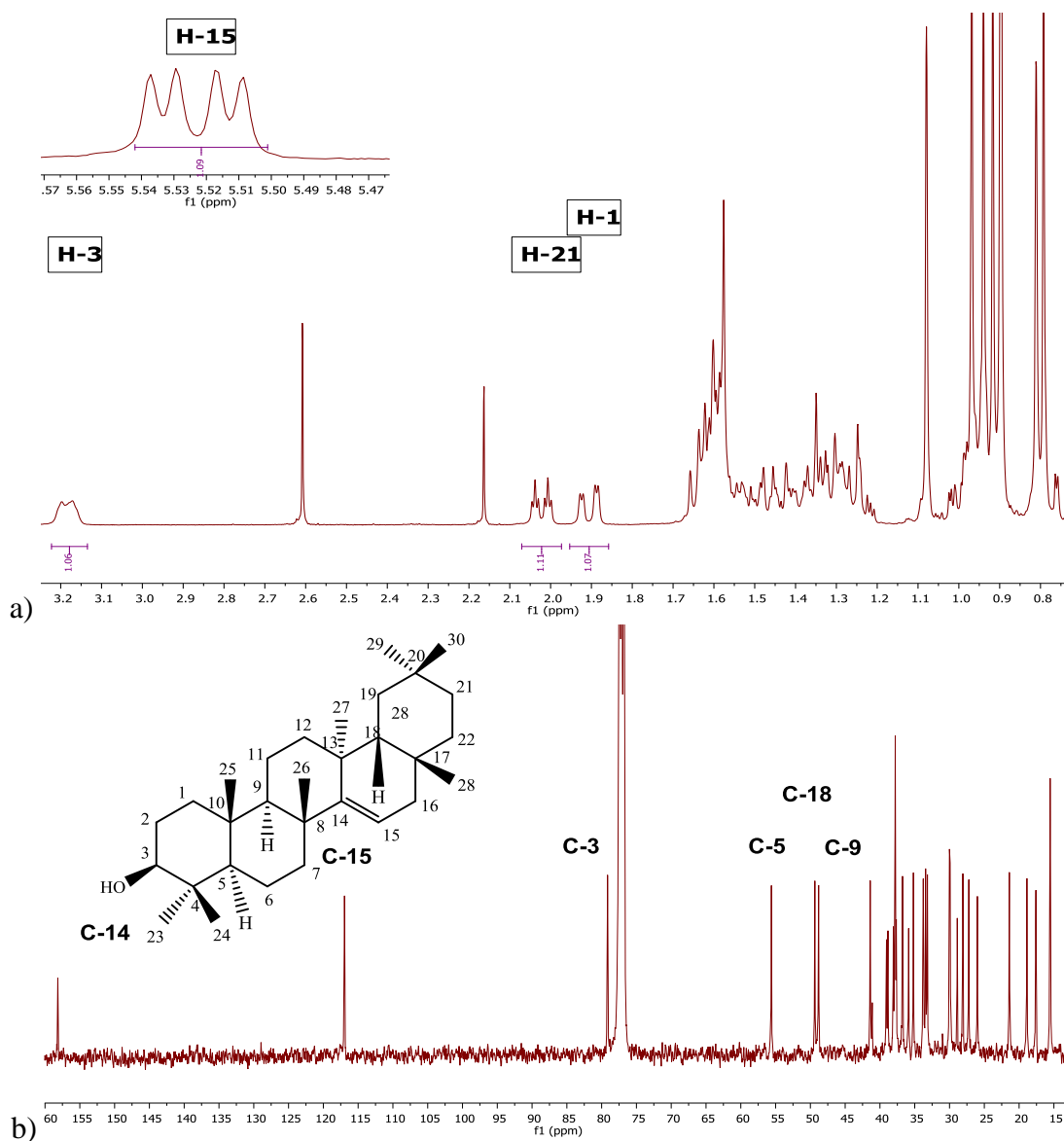
Figure 2.8: (a) ^{1}H and (b) ^{13}C NMR spectra of F3-17
(CDCl$_3$, ^{1}H 400 MHz, ^{13}C 100.5 MHz)

Table 2.4: ^{1}H and ^{13}C NMR of compounds F3-13 & F3-17
(CDCl$_3$, [1]H 400 MHz, [13]C 100.5 MHz) and comparison with previous data

No.	^{1}H NMR, δ_H (ppm, multi. J in Hz)				^{13}C NMR, δ_C (ppm)			
	F3-13	*taraxerone	F3-17	*taraxerol	F3-13	*taraxerone	F3-17	*taraxerol
1	1.91 (dd, J=15.1, 3.2 Hz, 2H)	-	1.91 (dd, J=14.8, 3.2 Hz, 2H)	-	37.4	38.5	38.2	38.2
2	2.56 (ddd, J=15.8, 11.8, 7.0 Hz, 1H) 2.32 (ddd, J=15.8, 6.3, 3.3 Hz, 1H)	-	1.59 (m, 2H)	-	34.2	34.4	27.4	27.4
3	-	-	3.18 (m, 1H)	3.20	217.7	217.0	79.3	79.1
4	-	-	-	-	47.7	47.8	39.0	39.0
5	1.29 (m, 1H)	-	-	-	55.9	56.0	55.8	55.7
6	1.58 (m, 1H)	-	-	-	20.5	20.2	19.0	19.0
7	-	-	-	-	35.1	35.3	35.4	35.3
8	-	-	-	-	39.0	39.1	39.2	39.2
9	-	-	-	-	48.8	48.9	49.0	48.9
10	-	-	-	-	38.4	37.9	38.0	37.9
11	-	-	-	-	17.5	17.7	17.8	17.7
12	-	-	-	-	35.9	36.0	36.0	36.0
13	-	-	-	-	37.8	37.8	37.8	37.8
14	-	-	-	-	157.7	157.8	158.3	158.3
15	5.55 (dd, J=8.2, 3.2 Hz, 1H)	5.56 (d, J=4.7 Hz, 1H)	5.52 (dd, J=3.27, 8.12 Hz, 1H)	5.53	117.3	117.4	117.1	117.1
16	-	-	-	-	36.8	36.9	36.9	36.9
17	-	-	-	-	37.6	37.9	38.0	37.9
18	-	-	-	-	48.9	49.0	49.5	49.5
19	-	-	-	-	33.7	40.8	41.6	41.5
20	-	-	-	-	28.9	29.0	29.1	29.0

Figure 1.5: Cont'd. ^{1}H and ^{13}C NMR of compounds F3-13 & F3-17
(CDCl$_3$, [1]H 400 MHz, [13]C 100.5 MHz) and comparison with previous data

21	2.06 (*dt, J*=12.8, 3.3 Hz, 1H)	-	2.02 (*dt, J*=12.8, 3.3 Hz, 1H)	-	40.7	33.8	33.9	33.9
22	-	-	-	-	33.2	33.3	33.3	33.3
23	1.07 (*s*, 3H)	1.09 (*s*, 3H)	0.98 (*s*, 3H)	0.98 (*s*, 3H)	26.2	26.3	28.3	28.2
24	1.06 (*s*, 3H)	1.07 (*s*, 3H)	0.93 (*s*, 3H)	0.93 (*s*, 3H)	21.6	21.7	15.3	15.6
25	1.08 (*s*, 3H)	1.08 (*s*, 3H)	0.80 (*s*, 3H)	0.81 (*s*, 3H)	14.9	15.0	15.3	16.0
26	0.82 (*s*, 3H)	0.83 (*s*, 3H)	0.91 (*s*, 3H)	0.91 (*s*, 3H)	29.9	30.1	30.1	30.1
27	1.13 (*s*, 3H)	1.14 (*s*, 3H)	1.09 (*s*, 3H)	1.09 (*s*, 3H)	25.7	25.8	26.2	26.1
28	0.91 (*s*, 3H)	0.92 (*s*, 3H)	0.82 (*s*, 3H)	0.83 (*s*, 3H)	30.0	30.2	30.1	30.0
29	0.94 (*s*, 3H)	0.96 (*s*, 3H)	0.94 (*s*, 3H)	0.96 (*s*, 3H)	33.5	33.6	33.6	33.6
30	0.90 (*s*, 3H)	0.91 (*s*, 3H)	0.90 (*s*, 3H)	0.91 (*s*, 3H)	21.4	21.5	21.6	21.5
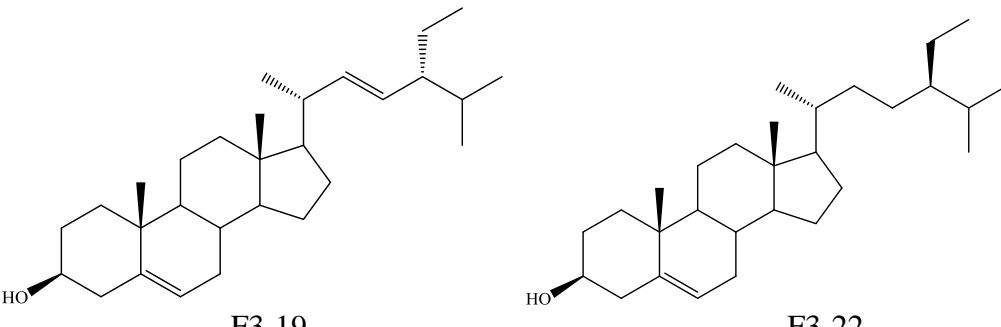
*Mawa & Said, 2012

F3-13

F3-17

Synonyms	stigmasterol, stigmasterin, (24R)-24-ethylcholesta-5,22-dien-3β-ol, (24R)-stigmast-5,22-dien-3β-ol, Δ^5-stigmasterol	β-sitosterol, 22,23-dihydrostigmasterol, stigmast-5-en-3-ol, β-sitosterin
Sample code	F3-19 (**1.47**)	F3-22 (**1.56**)
Sources	*A. lanata* stem	*A. lanata* stem
Yield (mg, %)	108.9 (0.76%)	32.0 (0.22%)
Physical state	Colourless needles	Colourless needles
Molecular formula	$C_{29}H_{48}O$	$C_{29}H_{50}O$
Mol. weight (g/mol)	412.3705 [M]$^+$	414.3862 [M]$^+$
R$_f$ value (2H:8DCM)	0.42	0.40
Optical rotation $[\alpha]_D^{20}$	+8.5° (*c* 1.05, CHCl$_3$)	-20° (*c* 0.10, (CHCl$_3$)

F3-19   F3-22

2.4.3 Compound F3-19 (1:1 ratio of stigmasterol+β-sitosterol)

Compound F3-19 (108.9 mg) was also obtained as colourless needles and HRMS (*m/z*): 412.3705 [M]$^+$, corresponded to the molecular formula $C_{29}H_{48}O$ whereas mass fragmentation were 394, 351, 314, 300, 271, 229, 213, 55 (Chaturvedula and Prakash, 2012). The ^{1}H NMR spectrum of F3-19 (Figure 2.9 a, Table 2.5) showed signals which resembled a mixture sterol type of compounds between stigmasterol and β-sitosterol (1:1, stigmasterol+β-sitosterol). This included a downfield broad doublet signal at δ_H 5.33 (H-6) and a multiplet signal at δ_H 5.12 and 5.02 for H-22 and H-23 for three olefinic protons due to the present of mixture between. A multiplet signal at δ_H 3.53 (H-3) had shifted downfield because of the electronegativity effect from the hydroxyl group attached to C-3. Six methyl proton signals were also evident. Three of them showed doublet signals at δ_H 0.92 (H-21), 0.83 (H-28), and 0.81 (H-29), one methyl triplet signal at δ_H 0.83 (H-26) and two methyl singlet signals at δ_H 0.68 (H-19) and 1.00 (H-18). The ^{13}C NMR results (Figure 2.9 b, Table 2.5) showed 29 carbon signals, including one methine carbon

51

shifted to δ_C 71.9 (C-3), a double bond carbon signal at δ_C 122.7 (C-6) and a quaternary carbon at δ_C 140.9 (C-5) on ring B, and double bond signals at δ_C 138.4 (C-22) and 129.3 (C-23) indicating that they were aliphatic chain. Remaining carbon signals appeared at δ_C 21.3, 19.5, 19.9, 19.1, and 12.4 were assigned to C-21/26, C-28, C-29, C-18 and C-19, respectively. Based on the NMR spectra and comparison with previous literature (Chaturvedula and Prakash, 2012), this compound was identified as mixture between stigmasterol and β-sitosterol (1:1 ratio).
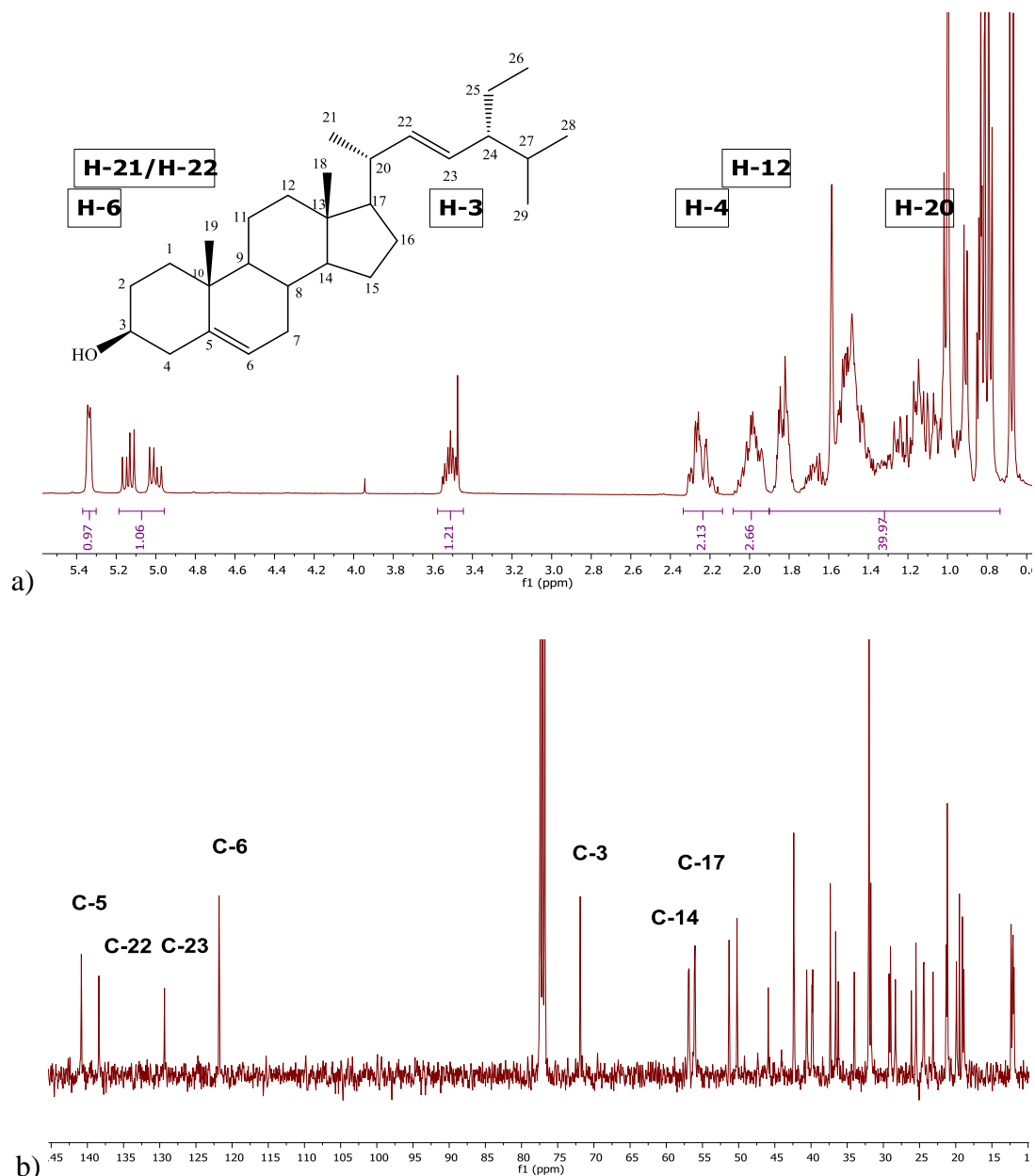
Figure 2.9: (a) ^{1}H and (b) ^{13}C NMR spectra of F3-19
(CDCl$_3$, ^{1}H 400 MHz, ^{13}C 100.5 MHz)

2.4.4 Compound F3-22 (1:1 ratio of β-sitosterol+stigmasterol, 1.56)

Compound F3-22 (32.0 mg) was obtained as colourless needles and HRMS showed exact mass at *m/z* 414.3862 [M]$^+$ corresponding to the molecular formula $C_{29}H_{50}O$ and optical rotation $[\alpha]_D^{20}$ -20° (*c* 0.10, (CHCl$_3$). The ^{1}H and ^{13}C NMR spectra of F3-22 (Figure 2.10 a, b, Table 2.5) showed proton and carbon signals similar to the compound F3-19 (1:1, a mixture between stigmasterol and β-sitosterol), which has been isolated from mangrove plant *A. lanata* crude mixture of extract except the absence of trans olefinic protons (H-22 and H-23) and its unsaturated carbon signals. The other olefinic proton at δ_H 5.36 *(t, J*=6.4 Hz, 1H) corresponded to H-6 and the oxygenated proton at δ_H 3.51 *(m,* 1H) for H-3. The ^{13}C NMR spectral data revealed 29 carbon signals. Remaining proton and carbon signals of this compound were similar to the previous compound (F3-19, stigmasterol). The NMR spectra (^{1}H and ^{13}C) and optical rotation results of this compound showed similarity to β-sitosterol $[\alpha]_D^{20}$ -29.2° (*c* 0.20, (CHCl$_3$) which has been isolated from plant *Artemisia princeps* Pampanini (Yoo *et al.*, 2006), thus the structure of F3-22 was elucidated as β-sitosterol which also has been isolated from the aqueous extract of the leaves of *Rubus suavissimus* (Chaturvedula and Prakash, 2012).

a)
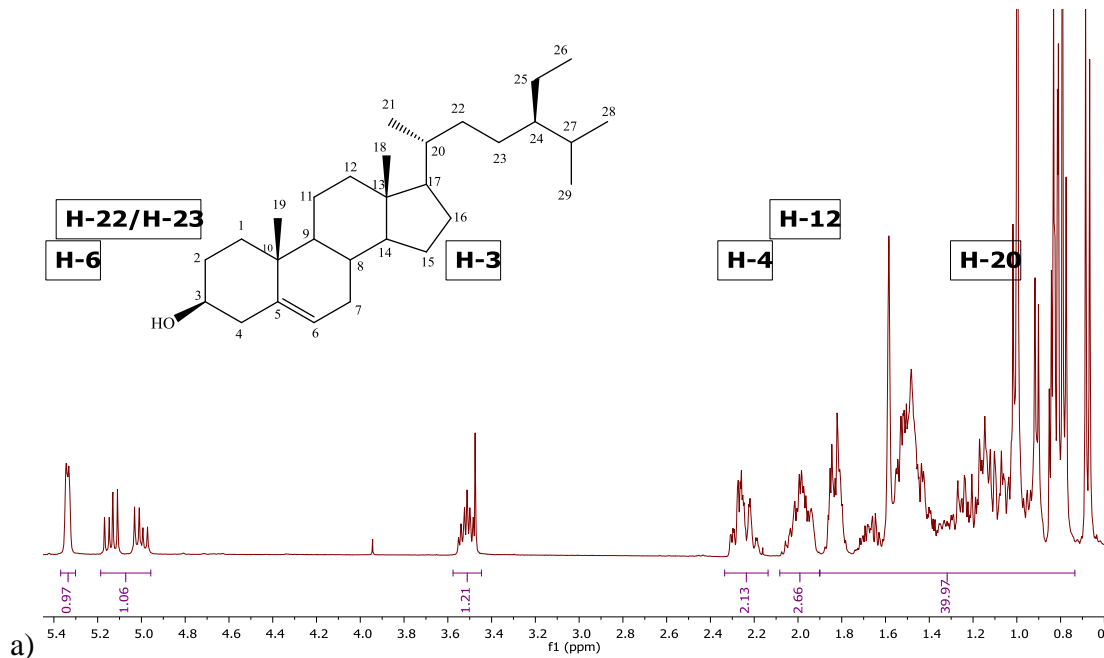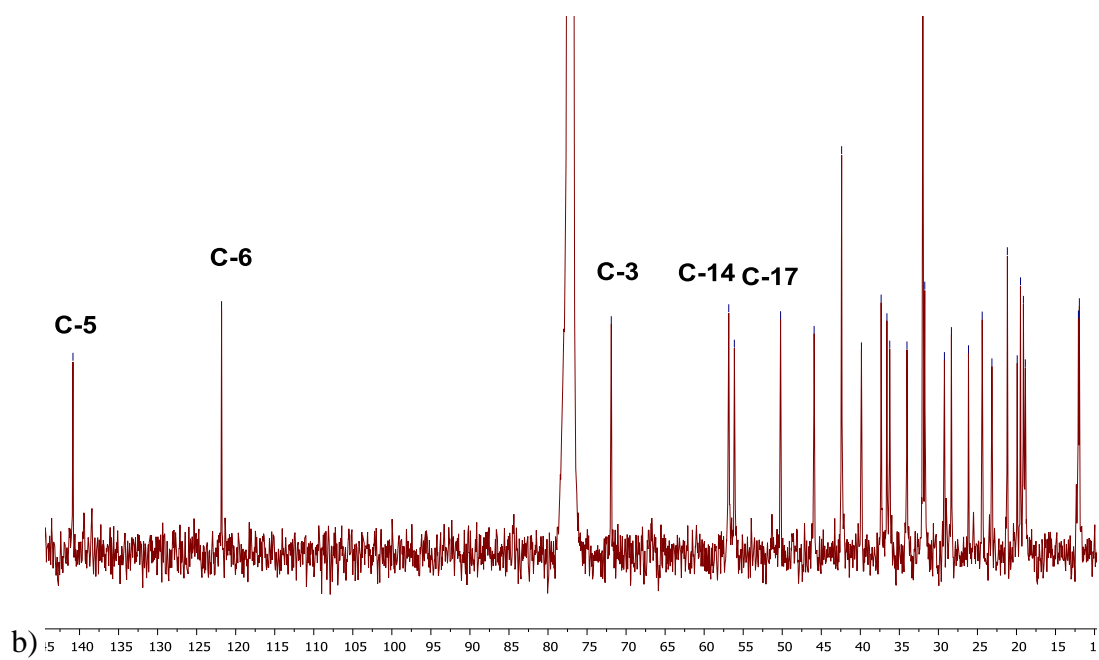
Figure 2.10: (a) ^{1}H and (b) ^{13}C NMR spectra of F3-22
(CDCl$_3$, ^{1}H 400 MHz, ^{13}C 100.5 MHz)

Table 2.5: ^{1}H and ^{13}C NMR of compounds F3-19 & F3-22
(CDCl₃, [1]H 400 MHz, [13]C 100.5 MHz) and comparison with previous data

No.	^{1}H NMR, δ_H (ppm, multi. J in Hz)				^{13}C NMR, δ_C (ppm)			
	F3-19	*stigmasterol	F3-22	*β-sitosterol	F3-19	*stigmasterol	F3-22	*β-sitosterol
1	1.08 (*m*, 2H)	-	1.05 (*m*, 2H)	-	37.3	37.6	37.3	37.5
2	-	-	-	-	33.9	32.1	31.8	31.9
3	3.51 (*m*, 1H)	3.53 (*tdd*, J=4.5, 4.2, 3.8 Hz, 1H)	3.51 (*m*, 1H)	3.53 (*tdd*, J=4.5, 4.2, 3.8 Hz, 1H)	71.9	72.1	71.9	72.0
4	2.26 (*m*, 1H)	-	2.26 (*m*, 2H)	-	42.4	42.4	42.4	42.5
5	-	-	-	-	141.8	141.1	140.8	140.9
6	5.33 (*t*, J=6.4 Hz, 1H)	5.36 (*t*, J=6.4 Hz, 1H)	5.34 (*t*, J=5.3 Hz, 1H)	5.36 (*t*, J=6.4 Hz, 1H)	121.8	121.8	121.8	121.9
7	-	-	-	-	31.7	31.8	32.0	32.1
8	1.94 (*m*, 1H)	-	1.99 (*m*, 1H)	-	31.9	31.8	32.0	32.1
9	1.82 (*m*, 1H)	-	1.84 (*m*, 1H)	-	50.2	50.2	50.2	50.3
10	-	-	-	-	36.6	36.6	36.6	36.7
11	1.50 (*m*, 1H)	-	1.48 (*m*, 1H)	-	21.2	21.5	21.2	21.3
12	1.99 (*m*, 1H)	-	1.99 (*m*, 1H)	-	39.8	39.9	39.9	39.9
13	-	-	-	-	42.1	42.4	42.4	42.6
14	-	-	-	-	56.9	56.8	56.9	56.9
15	-	-	-	-	24.4	24.4	26.2	26.3
16	-	-	-	-	29.0	29.3	28.3	28.5
17	-	-	-	-	56.1	56.2	56.1	56.3
18	1.00 (*s*, 3H)	1.01 (*s*, 3H)	1.00 (*s*, 3H)	1.01 (*s*, 3H)	12.4	12.2	12.0	12.0
19	0.68 (*s*, 3H)	0.68 (*s*, 3H)	0.67 (*s*, 3H)	0.68 (*s*, 3H)	19.1	18.9	18.9	19.0
20	1.17 (*m*, 1H)	-	1.15 (*m*, 1H)	-	40.6	40.6	36.2	36.3
21	0.92 (*d*, J=6.5 Hz, 3H)	0.93 (*d*, J=6.5 Hz, 3H)	0.91 (*d*, J=6.7 Hz, 3H)	0.93 (*d*, J=6.5 Hz, 3H)	21.3	21.7	19.5	19.2

Figure 1.5: Cont'd. ^{1}H and ^{13}C NMR of compounds F3-19 & F3-22
(CDCl$_3$, ^{1}H 400 MHz, ^{13}C 100.5 MHz) and comparison with previous data

22	5.01 (*m*, 1H)	-	1.31 (*m*, 1H)	-	138.4	138.7	34.0	34.2
23	5.14 (*m*, 1H)	-	1.24 (*m*, 1H)	-	129.3	129.6	26.2	26.3
24	-	-	-	-	45.9	46.1	45.9	46.1
25	-	-	-		25.4	25.4	23.2	23.3
26	0.83 (*t*, *J*=7.2 Hz, 3H)	0.84 *(t*, *J*=7.2 Hz, 3H)	0.83 (*s*, 3H)	0.84 *(t*, *J*=7.2 Hz, 3H)	12.1	12.1	12.1	12.2
27	-	-	-	-	29.2	29.6	29.2	29.4
28	0.83 (*d*, *J*=6.4 Hz, 3H)	0.83 (*d*, *J*=6.4 Hz, 3H)	0.81 (b*s*, 3H)	0.83 (*d*, *J*=6.4 Hz, 3H)	19.9	20.2	19.9	20.1
29	0.81 (*d*, *J*=6.4 Hz, 3H)	0.81 (*d*, *J*=6.4 Hz, 3H)	0.79 (b*s*, 3H)	0.81 (*d*, *J*=6.4 Hz, 3H)	19.5	19.8	19.5	19.6

*(Chaturvedula and Prakash, 2012)
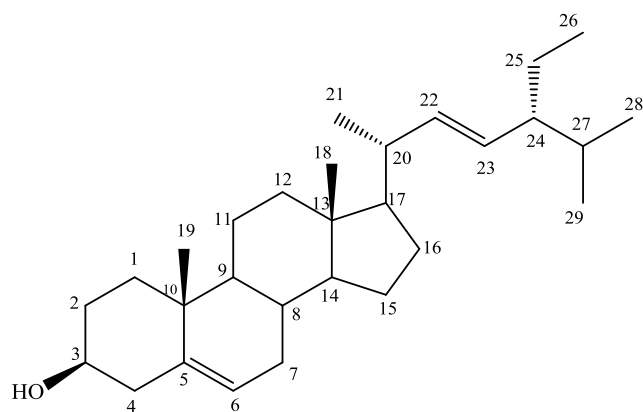
F3-19
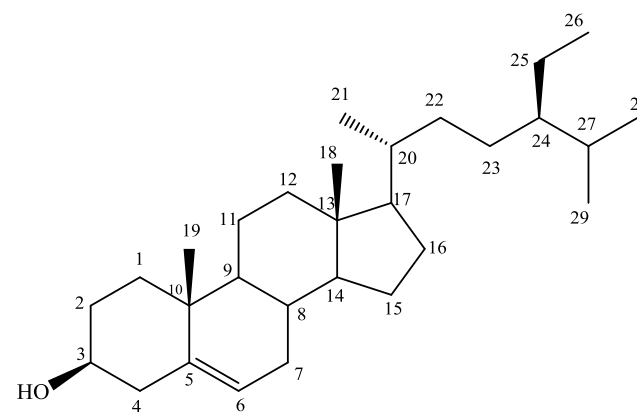
F3-22

2.4.5 Compound F5-2-3 (avicenol C, 1.7)

Compound F5-2-3 (20.7 mg) was isolated as a yellow powder and its molecular formula was assigned as $C_{17}H_{20}O_4$ by HRESI-MS at m/z 289.1431 $[M+H]^+$.

Synonyms	avicenol C, 2-(4,9-dimethoxy-2,3-dihydronaphtho[2,3-b]furan-2-yl)propan-2-ol
Sample code	F5-2-3 (**1.7**)
Sources	*A. lanata* stem
Yield (mg, %)	20.7 (0.14%)
Physical state	Yellow powder
Molecular formula	$C_{17}H_{20}O_4$
Molecular weight (g/mol)	288.1362
Exact mass (m/z)	289.1431 $[M+H]^+$
Ret. time (min)	17.57
R_f value (2H:8DCM)	0.34
Optical rotation $[\alpha]_D^{20}$	+30° (*c* 1.00, CHCl$_3$)

1.7

The optical rotation of $[\alpha]_D^{20}$ +30° (c 1.00, CHCl$_3$) compared with previous data $[\alpha]_D^{20}$ +22 (c 1.031, MeOH), UVλ_{max} nm: 227, 255, 300. IRν_{max} cm^{-1}: 3589, 3450 (br), 1672, 1595, 1537. EI-MS m/z (%): 256 (M$^+$, 12), 241 (100), 214 (18), 199 (10), 129 (10), 115 (17), 105 (22) (Ito et $al.$, 2000). The ^{1}H NMR results of F5-2-3 (Figure 2.11 a, Table 2.6) showed an ABCD system which had four different sets of proton signals. In the aromatic region, the spectrum indicated proton signals at δ_H 8.02 (d, J=7.5 Hz, 1H), 8.00 (d, J=7.5 Hz, 1H), 7.42 (br t, J=7.6 Hz, 1H), and 7.32 (br t, J=7.5 Hz, 1H) corresponding to H-5, H-8, H-7 and H-6, respectively. In the up-field region, an oxygenated methine proton was found at δ_H 4.71 as a triplet (J=8.5 Hz, 1H, H-2'). In the COSY spectrum this proton correlated to a methylene proton at δ_H 3.40 (d, J=8.5 Hz, 2H, H-1'). The remaining proton signals were two methoxy signals at δ_H 4.02 (s, 3H) and 3.97 (s, 3H). The ^{13}C NMR results (Figure 2.11 b, Table 2.8) showed 17 carbon signals. Three of them were carbonyl carbon signals with two carbon signals at δ_C 147.8 (C-4) and 147.30 (C-1) which corresponded to 4,9-dimethoxy-2,3-dihydronaphtho while 132.1 corresponded to C-2. Four quaternary carbon signals for rings A and B were found at δ_C 129.0 (C-4a), 124.3 (C-8a), and 118.7 (C-3) as well as one quaternary carbon signal on the side chain at δ_C 71.8 (C-3'). Four aromatic carbon signals were further observed at δ_C 125.9, 123.4, 121.8 and 121.2 for C-7, C-6, C-8 and C-5, respectively. The remaining carbon signals were found at δ_C 90.4 for a methine carbon attached to oxygen (C-2'), a methylene carbon δ_C 28.9 (C-1') and two methoxy carbon signals at δ_C 60.6 and 60.4.

a)
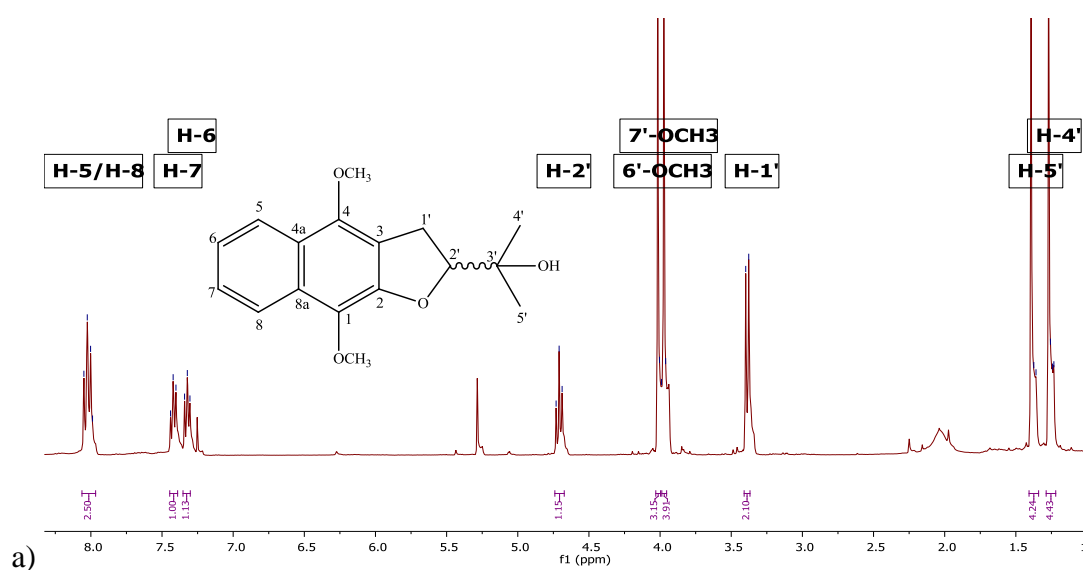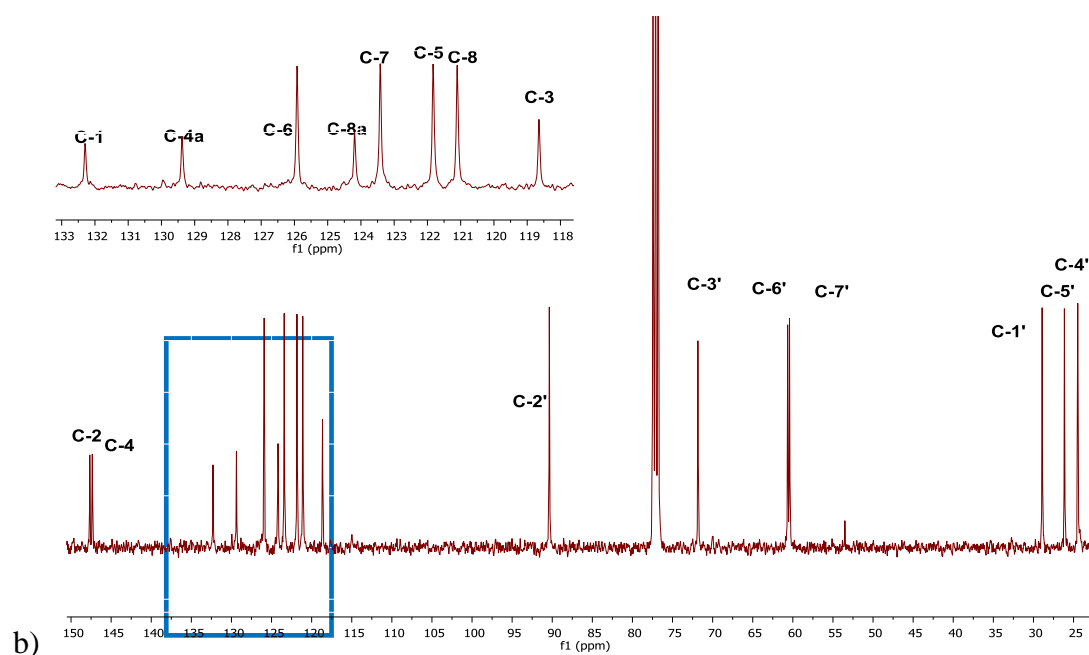
Figure 2.11: (a) ^{1}H and (b) ^{13}C NMR spectra of F5-2-3
(CDCl$_3$, ^{1}H 400 MHz, ^{13}C 100.5 MHz)

In the COSY spectrum (Figure 2.13 a), strong correlations were observed between the aliphatic doublet H-1' and triplet H-2' as well as between the aromatic protons. The positions of the carbonyl carbons (C-4 and C-1) were confirmed by the HMBC spectrum as shown in Figure 2.13 b. The other correlations between protons and carbons are depicted in Figure 2.12. Based on 1D and 2D NMR spectra, mass spectroscopy, optical rotation as well as comparison with published data, this compound was proposed to be avicenol C (2-(4,9-dimethoxy-2,3-dihydronaphtho[2,3-b]furan-2-yl)propan-2-ol) which was also previously isolated from the stem barks of *A. alba* (Han *et al.*, 2007, Ito *et al.*, 2000), *A. marina* twigs (Han *et al.*, 2007) and the roots of *A. officinalis* (Anjaneyulu *et al.*, 2003).
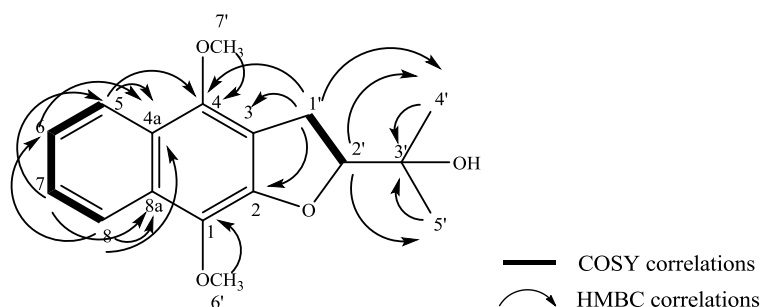
Figure 2.12: COSY and HMBC correlations of F5-2-3

59
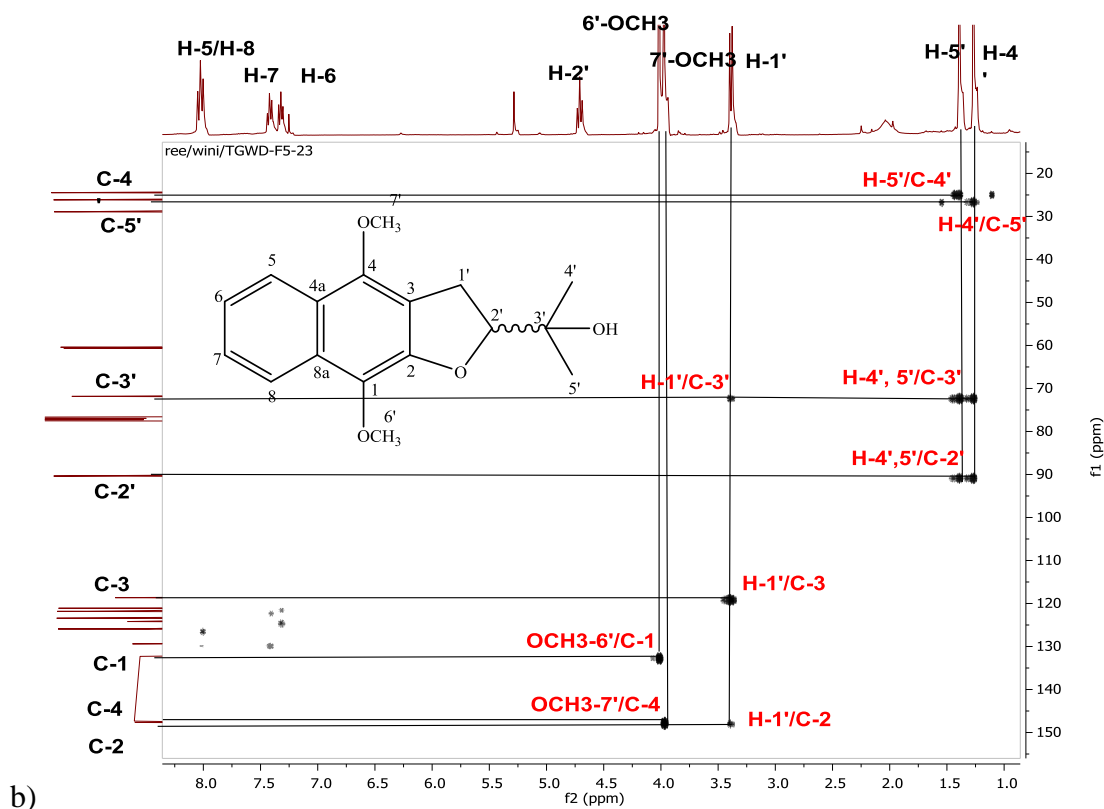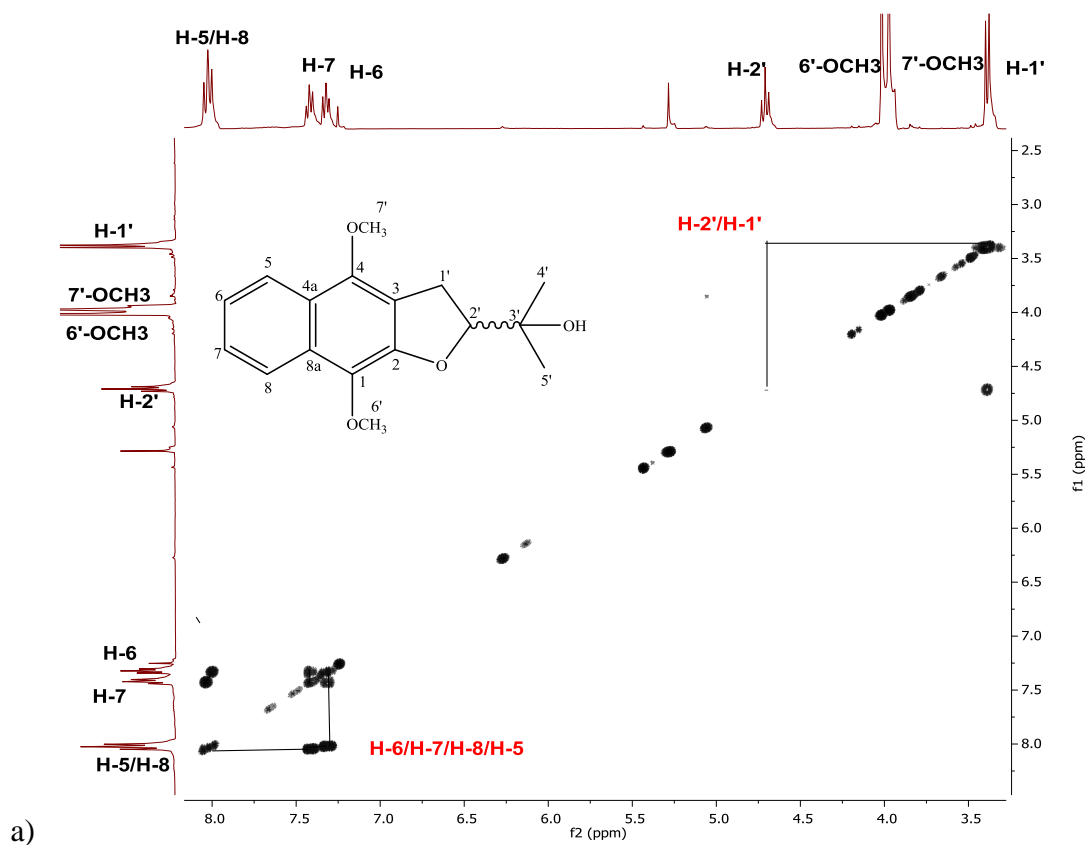
Figure 2.13: (a) COSY and (b) HMBC NMR spectra of F5-2-3
(CDCl$_3$, ^{1}H 400 MHz, ^{13}C 100.5 MHz)

Table 2.6: ^{1}H and ^{13}C NMR of compound F5-2-3
(CDCl$_3$, ^{1}H 400 MHz, ^{13}C 100.5 MHz) and comparison with previous data

No.	^{1}H NMR, δ_H (ppm, multi. J in Hz)		^{13}C NMR, δc (ppm)		COSY ^{1}H⇔^{1}H	HMBC ^{1}H⇔^{13}C
	F5-2-3	***avicenol C**	**F5-2-3**	***avicenol C**		
1	-	-	132.3	147.5	-	-
2	-	-	147.7	147.2	-	1'
3	-	-	118.7	118.3	-	1'
4	-	-	147.3	132.2	-	5, 1'
4a	-	-	129.4	129.3	-	5, 6, 8
5	8.02 (*d*, *J*=7.5 Hz, 1H)	8.02 (*d*, *J*=8.4 Hz, 1H)	121.8	121.0	-	7, 4, 4a
6	7.32 (br *t*, *J*=7.5 Hz, 1H)	7.41 (br *t*, *J*=8.4 Hz, 1H)	125.9	125.8	6	4a, 8
7	7.42 (br *t*, *J*=7.6 Hz, 1H)	7.31 (br *t*, *J*=8.4 Hz, 1H)	123.4	123.3	5, 7	5, 8a
8	8.00 (*d*, *J*=7.5 Hz, 1H)	8.00 (*d*, *J*=8.4 Hz, 1H)	121.1	121.7	6, 8	4a, 6, 8a
8a	-	-	124.2	124.1	7	7, 8, 8a
1'	3.39 (*d*, *J*=8.5 Hz, 2H)	3.38 (*d*, *J*=8.4 Hz, 2H)	28.8	28.8	-	2, 3, 4, 3'
2'	4.71 (*t*, *J*=8.5 Hz, 1H)	4.71 (*t*, *J*=8.4 Hz, 1H)	90.4	90.3	2'	3', 4', 5'
3'	-	-	71.8	71.7	1'	1', 4', 5'
4'-CH$_3$	1.26 (*s*, 3H)	1.26 (*s*, 3H)	24.5	24.3	-	2', 3'
5'-CH$_3$	1.39 (*s*, 3H)	1.39 (*s*, 3H)	26.2	26.1	-	2', 3'
6'-OCH$_3$	4.02 (*s*, 3H)	4.01 (*s*, 3H)	60.7	60.6	-	1
7'-OCH$_3$	3.97 (*s*, 3H)	3.96 (*s*, 3H)	60.4	60.3	-	4

*Han *et al.*, 2007, Ito *et al.*, 2000, Anjaneyulu *et al.*, 2003

No.	^{1}H NMR, δ_H (ppm, multi. J in Hz)				
	F5-2-3	[a,b] avicenol C	F5-2-6	[a,b,c] avicequinone C	F6-8
1	-	-		-	-
2	-	-	-	-	-
3	-	-	-	-	-
4	-	-	-	-	-
4a	-	-	-	-	-
5	8.02 (d, J=7.5 Hz, 1H)	8.02 (d, J=8.4 Hz, 1H)	8.18 (m, 1H)	8.17 (m, 1H)	8.07 (dd, J=7.4 Hz, 1H)
6	7.32 (br t, J=7.6 Hz, 1H)	7.41 (br t, J=8.4 Hz, 1H)	7.74 (m, 1H)	7.75 (m, 1H)	7.68 (dd J=7.4 , 2.1, Hz, 1H)
7	7.42 (br t, J=7.5 Hz, 1H)	7.31 (br t, J=8.4 Hz, 1H)	7.74 (m, 1H)	7.75 (m, 1H)	7.68 (dt, J=7.4, 2.1 Hz, 1H)
8	8.00 (d, J=7.5 Hz, 1H)	8.00 (d, J=8.4 Hz, 1H)	8.20 (m, 1H)	8.21 (m, 1H)	8.07 (dt, J=7.4 Hz, 1H)
1'	3.39 (d, J=8.5 Hz, 2H)	3.38 (d, J=8.4 Hz, 2H)	6.81 (s, 1H)	6.82 (s, 1H)	3.15 (d, J=10.0 Hz, 2H)
2'	4.71 (t, J=8.5 Hz, 1H)	4.71 (t, J=8.4 Hz, 1H)	-	-	4.83 (t, J=10.0 Hz, 1H)
3'	-	-		-	-
4'-CH$_3$	1.26 (s, 3H)	1.26 (s, 3H)	1.70 (s, 3H)	1.69 (s, 3H)	1.24 (s, 3H)
5'-CH$_3$	1.39 (s, 3H)	1.39 (s, 3H)	1.70 (s, 3H)	1.69 (s, 3H)	1.39 (s, 3H)
6'-OCH$_3$	4.02 (s, 3H)	4.01 (s, 3H)	-	-	-
7'-OCH$_3$	3.97 (s, 3H)	3.96 (s, 3H)	-	-	-

[a]Ito *et al.*, 2000, [b]Anjaneyulu *et al.*, 2003, [c]Williams, 2005
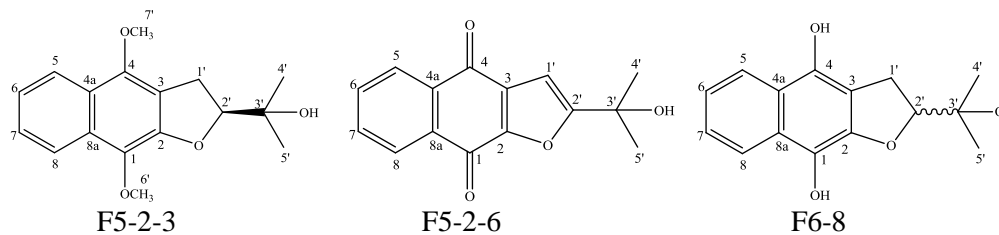
F5-2-3   F5-2-6   F6-8

Atom C	^{13}C NMR, δ_C (ppm)				
	F5-2-3	[a]avicenol C	F5-2-6	[a,b,c]avicequinone C	F6-8
1	132.3	147.5	173.5	173.3	153.7
2	147.7	147.2	151.7	151.6	139.3
3	118.7	118.3	131.4	131.2	125.1
4	147.3	132.2	180.9	180.7	159.3
4a	129.4	129.3	132.7	132.9	129.6
5	121.8	121.0	126.9	126.8	126.1
6	125.9	125.8	133.9	133.9	133.1
7	123.4	123.3	133.9	133.7	134.2
8	121.1	121.7	127.2	126.8	126.4
8a	124.2	124.1	133.3	132.3	132.5
1'	28.8	28.8	102.7	102.6	29.2
2'	90.4	90.3	168.1	168.1	92.4
3'	71.8	71.7	69.5	69.3	71.8
4'-CH$_3$	24.5	24.3	28.8	28.7	24.1
5'-CH$_3$	26.2	26.1	28.8	28.7	25.8
O-CH$_3$	60.4	60.3	-	-	-
O-CH$_3$	60.7	60.6	-	-	-

[a]Ito *et al.*, 2000, [b]Anjaneyulu *et al.*, 2003, [c]Williams, 2005

2.4.6 Compound F5-2-6 (avicequinone C, 1.4)

Compound F5-2-6 (5.7 mg) was isolated as yellow oil and its molecular formula was assigned as C$_{15}$H$_{12}$O$_4$ by HRESI-MS. It differed from the previous compound, F5-2-3, by C$_2$H$_8$.

Synonyms	avicequinone C, 2-(2-hydroxypropan-2-yl)naphtha [2,3-b]furan-4,9-dione
Sample code	F5-2-6 (**1.4**)
Sources	*A. lanata* stem
Yield (mg, %)	5.7 (0.04%)
Physical state	Yellow oil
Molecular formula	C$_{15}$H$_{12}$O$_4$
Molecular weight (g/mol)	256.2534
Exact mass (*m/z*)	257.0807 [M+H]$^+$
Ret. time (min)	14.03
R$_f$ value (2H:8DCM)	0.32

1.4
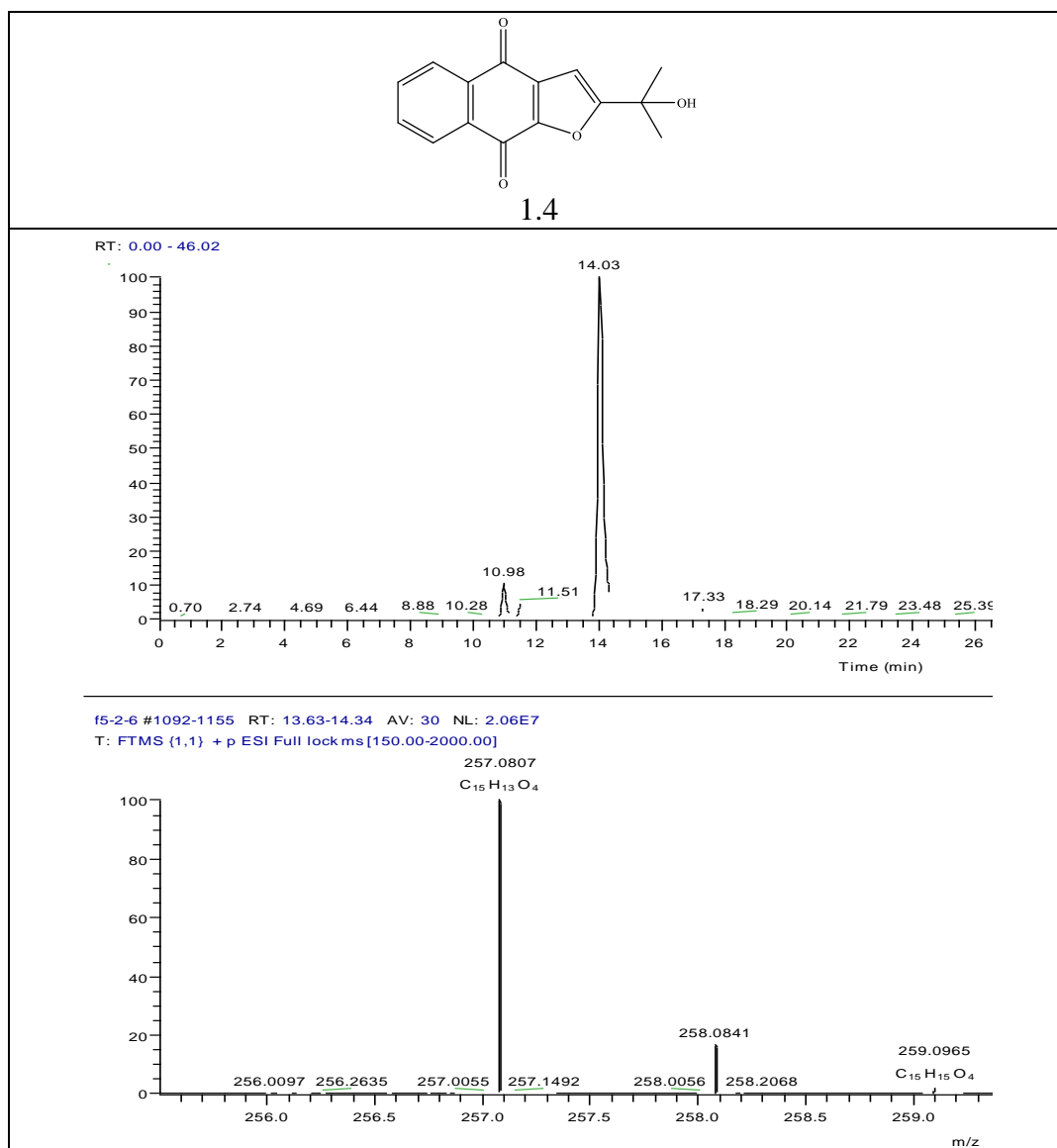
The ^{1}H and ^{13}C NMR results (Figure 2.14 a, b, Table 2.7, Table 2.8) of this compound showed similar signals to F5-2-3, except for the appearance of one sharp singlet at δ_H 6.81 (*s*, 1H) directly attached to a carbon signal at δ_C 102.6 (C-1') which was assigned to an aromatic carbon. Two unit of methyl signals were observed at more downfield 1.70 (*s*, 6H) compared to the compound earlier because of the electronegativity effect from olefinic carbon C-2'. Two carbonyl carbon signals were observed at δ_C 180.9 and 173.5, corresponding to carbons C-1 and C-4 in the aromatic ring, with strong correlations between C-4 and H-5/H-1'and C-1 with H-8. A quaternary carbon signal at δ_C 131.4 (C-3) was more downfield than a quaternary signal showed in F5-2-3 spectrum indicating that this carbon was affected by the

64

carbonyl carbons in the 1,4-naphthoquinone system. The other aromatic carbon signals remained similar to those in compound F5-2-3.

a)

b)
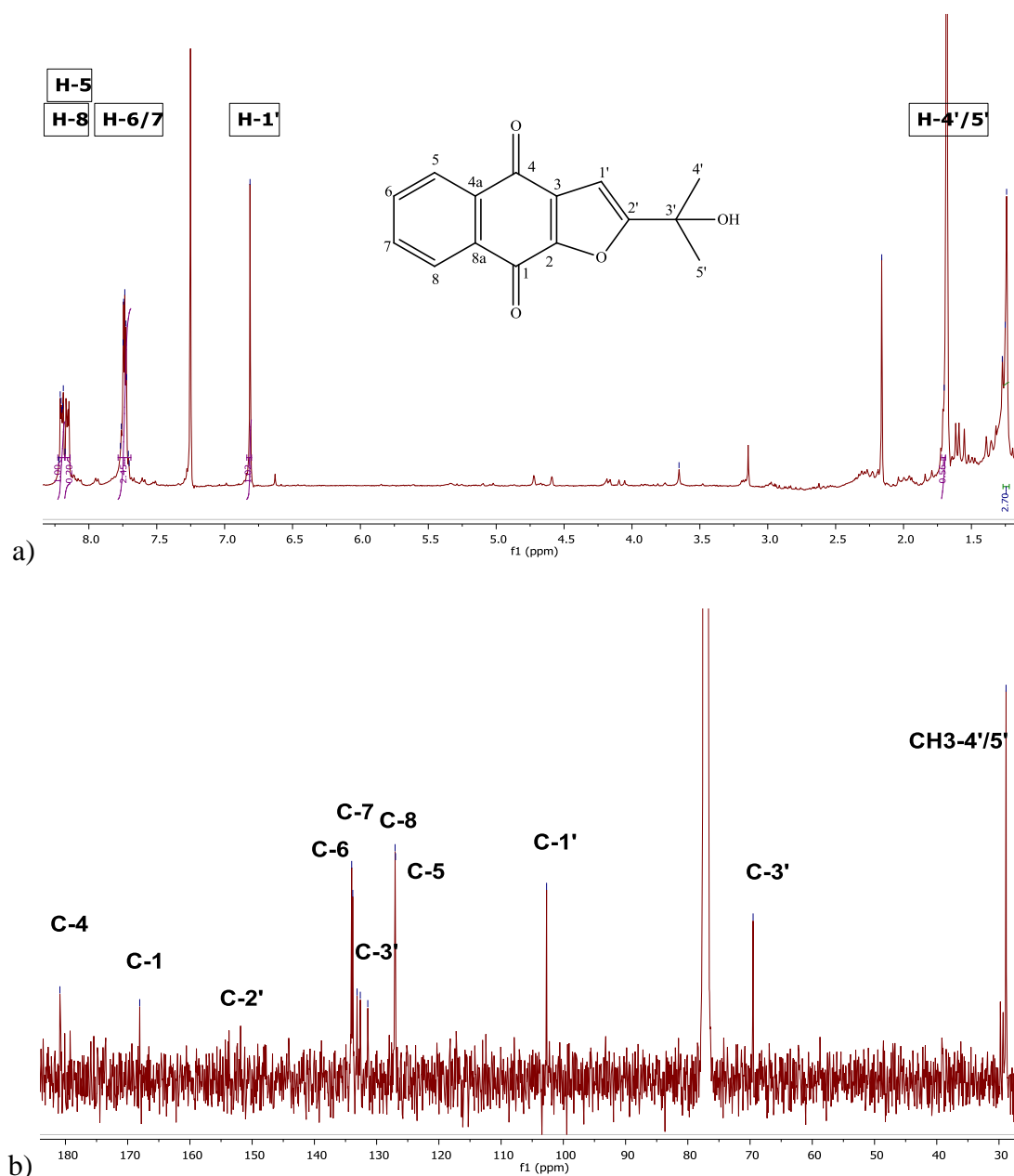
Figure 2.14: (a) ^{1}H and (b) ^{13}C NMR spectra of F5-2-6
(CDCl$_3$, ^{1}H 400 MHz, ^{13}C 100.5 MHz)

The position of protons and carbons were established by COSY (Figure 2.15 a) and HMBC (Figure 2.15 b). The spectra showed two methyl protons in the aliphatic side chain correlating with a quaternary carbon signal at δ_C 167.5 (C-2'), which was an oxygenated carbon. The other correlations between these protons and carbons were illustrated in the structure. This compound was elucidated to be avicequinone C (2-

(2-hydroxypropan-2-yl)naphtho[2, 3-b] furan-4, 9-dione) based on the spectroscopy and comparison with previous reports (Russell B Williams, 2005, Ito *et al.*, 2000)
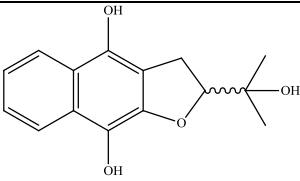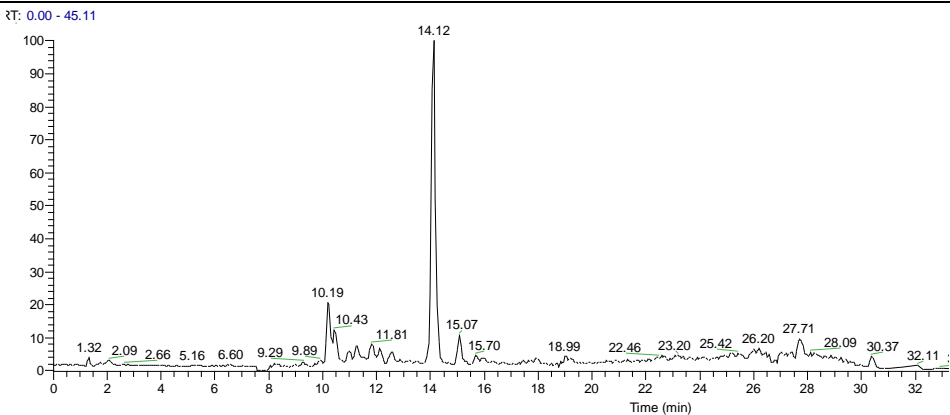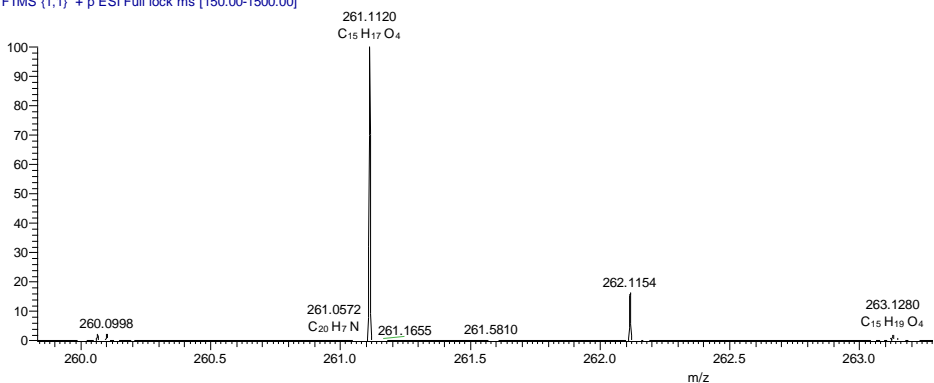
Figure 2.15: (a) COSY and (b) HMBC NMR spectra of F5-2-6
(CDCl$_3$, ^{1}H 400 MHz, ^{13}C 100.5 MHz)

2.4.7 Compound F6-8 (new compound, 2.26)

Compound F6-8 (6.5 mg) was isolated as yellow oil and its molecular formula was determined by HRESI-MS as $C_{15}H_{16}O_4$ with m/z 261.1120 $[M+H]^+$ and optical rotation $[\alpha]_D^{20}$ -8.4° (c 1.00, CHCl$_3$).

Synonyms	hydroxyavicenol C , 2-(2-hydroxypropan-2-yl)-2, 3-dihydronaphtho [2, 3-b] furan-4, 9-diol
Sample code	F6-8 (**2.26**)
Sources	*A. lanata* stem
Yield (mg, %)	6.5 (0.05%)
Physical state	Yellow oil
Molecular formula	$C_{15}H_{16}O_4$
Molecular weight (g/mol)	260.1049
Exact mass (*m/z*)	261.1120 $[M+H]^+$
Ret. time (min)	14.12
R_f value (2H:8DCM)	0.29
Optical rotation $[\alpha]_D^{20}$	-8.4 (*c* 1.00, CHCl$_3$)

2.26

It had a difference of C_2H_4 compared with compound F5-2-3. The ^{1}H NMR spectrum of F6-8 (Figure 2.16 a, Table 2.7) exhibited an ABCD spin system of aromatic protons with 2H protons for a doublet of doublet at δ_H 8.07 (*dd*, *J*=7.4 Hz, 2H) and a doublet of triplet at δ_H 7.68 (*dd J*=7.4, 2.1, Hz, 2H). The other proton signals remained the same as those found in F5-2-3. The ^{13}C NMR (Figure 2.16 b, Table 2.8) showed 15 carbon signals with two carbonyl carbon signals at δ_C 159.3 and 153.7, corresponding to C-4 and C-1, respectively that were shifted downfield because of the electronegativity effect. These two carbon signals differed from those carbon signals in F5-2-3 and F5-2-6, suggesting that F6-8 has different hydroxylated. Two quaternary carbon signals at δ_C 139.3 and 125.1 were assigned to C-2 and C-3 respectively. The other carbon signals remained the same as in compound F5-2-3.
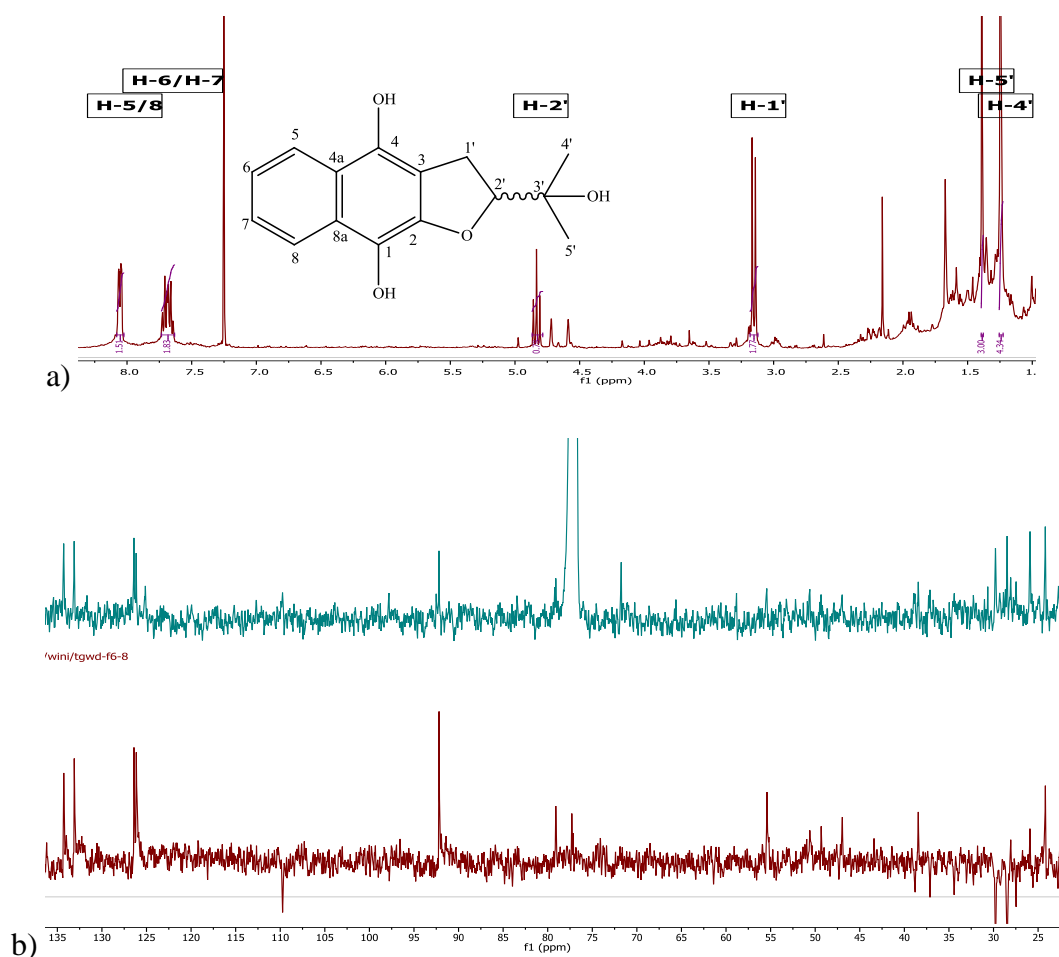
Figure 2.16: (a) ^{1}H and (b) ^{13}C NMR of F6-8
^{13}C NMR (green spectrum), DEPT NMR (red spectrum) (CDCl_3, [1]H 400 MHz, [13]C 100.5 MHz)

68

H-H correlations on the COSY spectrum (Figure 2.18 a) indicated partial structures for a tetrahydrofuran moiety, and aromatic ring and a =C-CH$_2$-COH-C= unit in the molecule. The correlations between H-1' andC-4/C-3 in the tetrahydrofuran ring were observed in the HMBC spectrum (Figure 2.18 b). Other correlations between the aromatic ABCD system and tetrahydrofuran were shown in Figure 2.17. This compound has different only at naphthalene ring at C-1 and C-4 with hydroxyl group directly attached instead of methoxy, whereas on the furan ring was the same. The optical rotation of this compound was (-) compared with avicenol C (F5-2-3), $[\alpha]_D^{20}$ +30° (c 1.00, CHCl$_3$) suggested that compound F6-8 to be a new derivative. In keeping with the nomenclature previously established the trivial name (-)-hydroxyavicenol C was proposed (2-(2-hydroxypropan-2-yl)-2,3-dihydronaphtho-[2, 3-b] furan-4, 9-diol), a *para*-hydroxyl congener of avicenol have not previously been reported.

Figure 2.17: COSY and HMBC correlations of F6-8

69
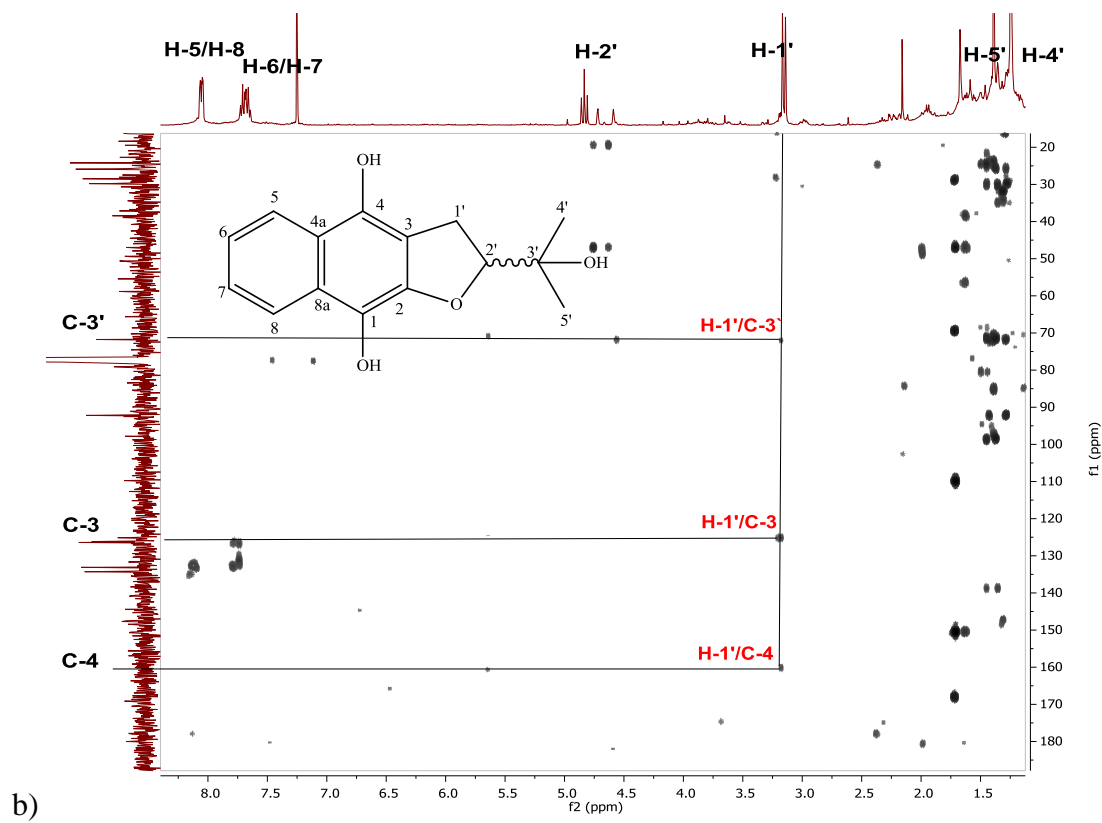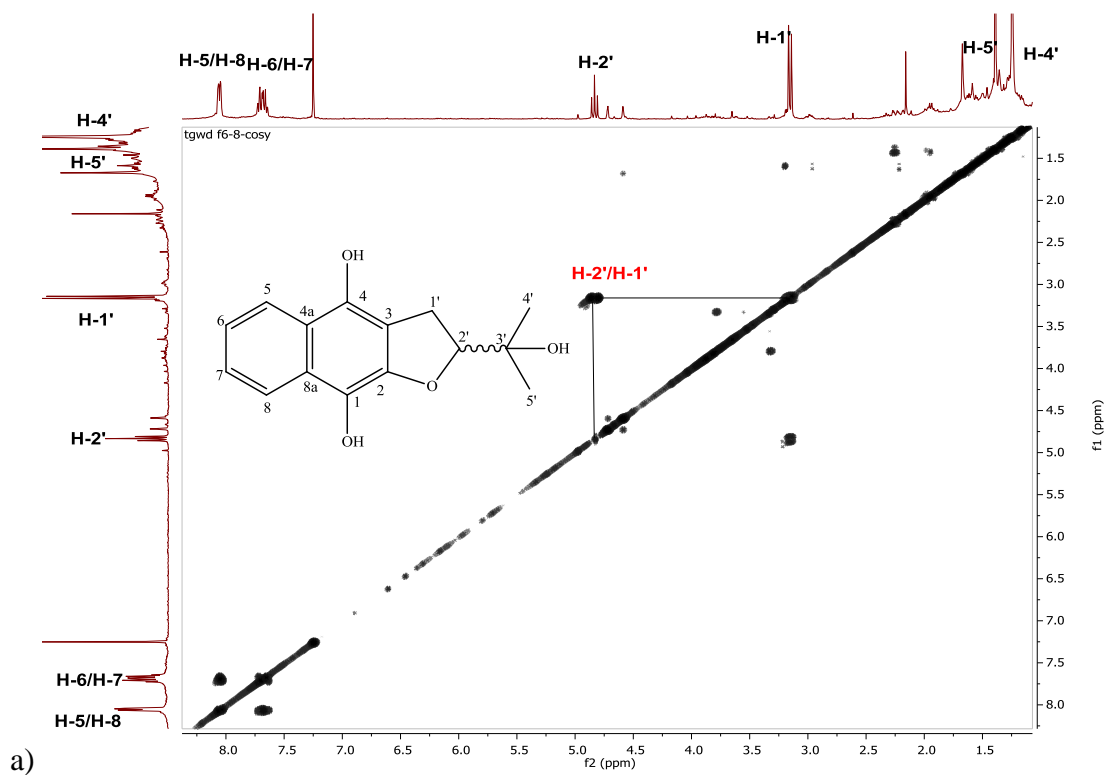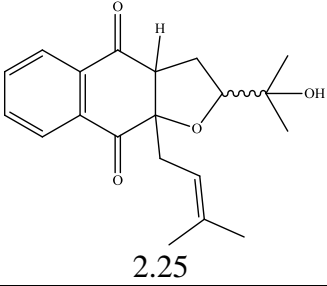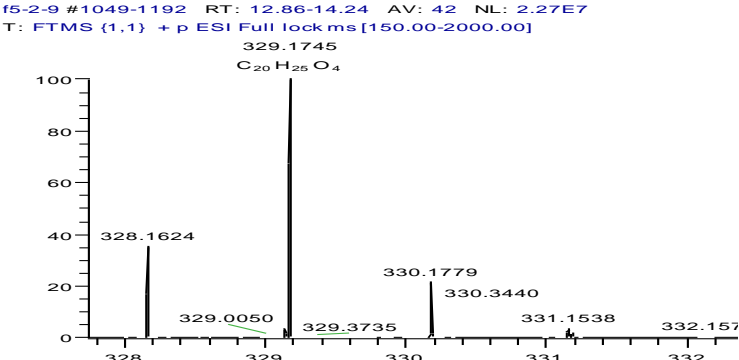
Figure 2.18: (a) COSY and (b) HMBC NMR spectra of F6-8
(CDCl$_3$, ^{1}H 400 MHz, ^{13}C 100.5 MHz)

70

2.4.8 Compound F5-2-9 (glycoquinone, 2.25)

Compound F5-2-9 (25.7 mg) was isolated as yellow oil. Its molecular formula was determined by HRESI-MS to be $C_{20}H_{24}O_4$ with m/z 329.1745 $[M+H]^+$.

Synonyms	glycoquinone, 2-(2-hydroxypropan-2-yl)-9a-(3-methylbut-2-en-1-yl)-3,3a-dihydronaphtho[2,3-b]furan-4,9(2H,9aH)-dione
Sample code	F5-2-9 (**2.25**)
Sources	*A. lanata* stem
Yield (mg, %)	25.7 (0.18%)
Physical state	Yellow oil
Molecular formula	$C_{20}H_{24}O_4$
Molecular weight (g/mol)	328.1675
Exact mass (m/z)	329.1745 $[M+H]^+$
Ret. time (min)	13.66
R_f value (2H:8DCM)	0.24
Optical rotation $[\alpha]_D^{20}$	+20° (c 1.00, CHCl$_3$)

2.25

The optical rotation $[\alpha]_D^{20} \pm 0°$ (c 0.068, MeOH), UVλ_{max} nm: 227, 255, 300. IRν_{max} cm^{-1}: 3377 (br), 1691, 1597. EI-MS m/z (%): 328 (M$^+$, 29), 260 (100), 242 (31), 239 (27), 227 (26), 189 (30), 173 (44), 159 (29), 149 (78) (Ito *et al.*, 1999). The aromatic proton signals showed ABCD system - at δ_H 8.06 and 7.75 corresponding to two unit proton signals of H-5 and H-8 and two unit proton signals for H-6 and H-7 proton, respectively. Two methyl signals located on aliphatic remained the same to avicenol C, except for the presence of a methine proton signal at δ_H 3.39 (*dd*, *J*=9.6, 10.5 Hz, H-3) assigned to a deshielded proton located at the *para*− position of the two carbonyl groups (Figure 2.19 a, Table 2.9). A methylene proton signal located on the dihydrofuran ring at δ_H 2.43 (*ddd*, *J*=4.5, 9.7, 13.7 Hz, 1H) and 1.97 (*ddd*, *J*=9.1, 10.5, 13.7 Hz, 1H) were splitt to give a doublet of doublet doublets, because of the electronegativity effect from the carbonyl group C-4 hence, an methine proton signal linked to an oxygen at δ_H 3.90 was shifted to up field which indicated by a double of doublet signal (*dd*, *J*=9.1, 4.4 Hz, 1H). The differences in ^{1}H NMR spectrum of this compound also detected with the presence of a prenyl moiety, which was indicated by one methylene proton signal at δ_H 2.54 (*m*, 2H, H-1") that correlated to a downfield proton at δ_H 5.00 (*t*, *J*=7.7 Hz, H-2") and two singlet signals of methyl proton at δ_H 1.53 (*s*, 3H, H-5") and 1.48 (*s*, 3H, H-4"), as seen in the COSY spectrum. The differences in carbon signals between this compound and avicenol C were indicated in ^{13}C NMR spectrum (Figure 2.19 b, Table 2.10), two carbonyl carbon signals at δ_C 198.2 and 196.1 for C-1 and C-4, respectively, a methine carbon at δ_C 54.7 (C-3) that was deshielded because of the electronegative effect from carbonyl C-4 as well as the carbon signals for prenyl moiety - a methylene carbon signal at δ_C 34.7 (C-1"), olefinic carbon signals at δ_C 116.6 (C-2") and 138.1 (C-3") along with two methyl carbon signals at δ_C 18.1 (C-4") and 25.8 (C-5"). The remaining carbon signals were found similar to avicenol C (F5-2-3).
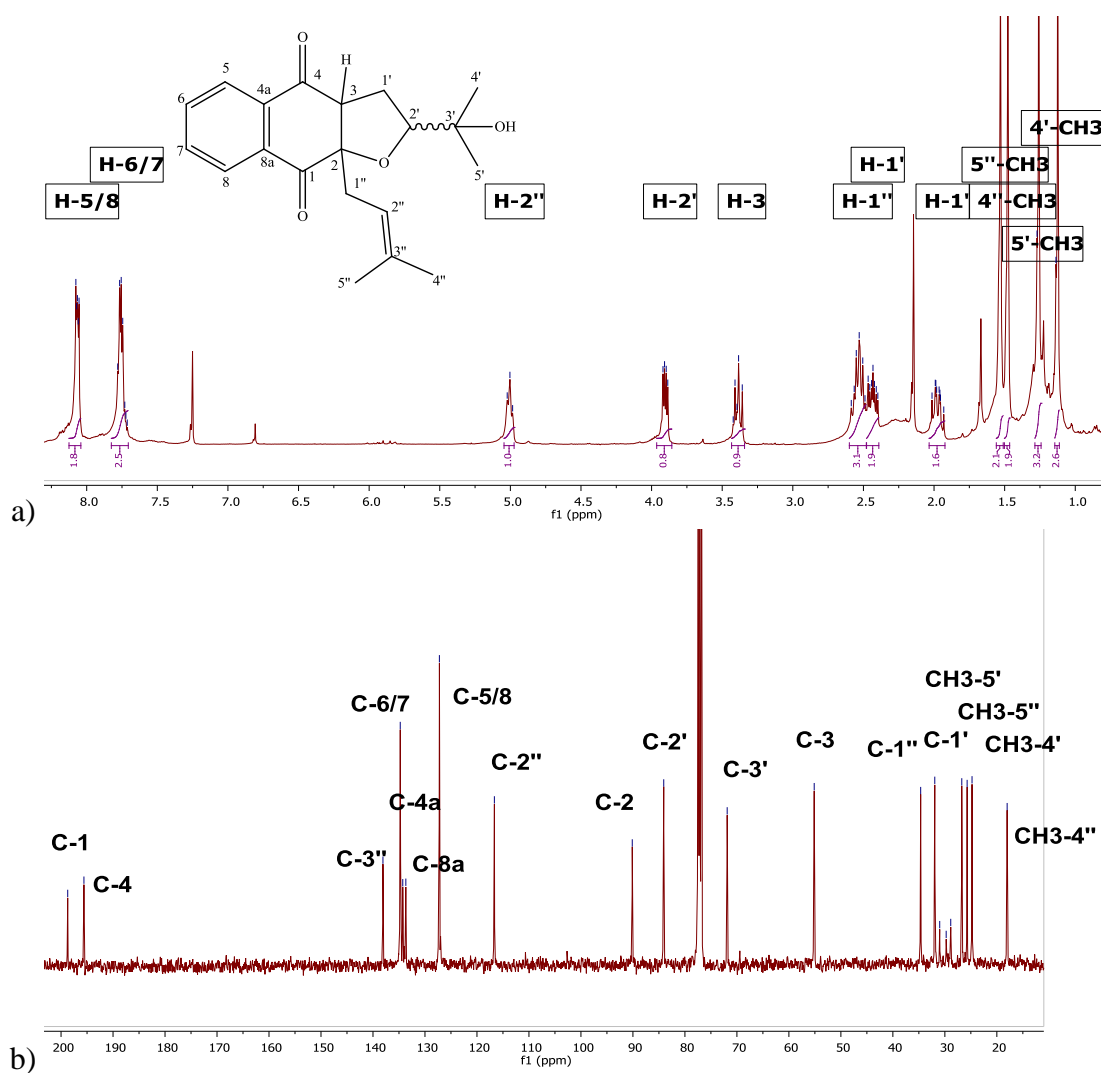
Figure 2.19: (a) ^{1}H and (b) ^{13}C NMR spectra of F5-2-9
(CDCl$_3$, ^{1}H 400 MHz, ^{13}C 100.5 MHz)

COSY and HMBC correlations were illustrated as in Figure 2.20. The COSY spectrum depicted the correlation between H-1'' and H-2'' (Figure 2.21 a). The presence of the tetrahydrofuran ring fused to the 2,3-dihydro-1,4-napthoquinone skeleton was described by the correlations of C-4 to H-5, H-3 and H-1' as seen in the HMBC spectrum (Figure 2.21 b). Other significant C-H long-range correlations were observed on the prenyl moiety between H-1'' and C-1, C-2'' and C-3'', as well as further strong correlations between H-2'', two methyl protons, and C-4'' and C-5''. Based on the spectroscopy results and comparison with a previous study, this compound was elucidated to be glycoquinone (2-(2-hydroxypropan-2-yl)-9a-(3-methylbut-2-en-1-yl)-3,3a-dihydronaphtho[2,3-b]furan-4,9(2*H*,9a*H*)-dione),   which

had also been previously isolated from the stem of *Glycomis pentaphylla* (Ito *et al.*, 1999).
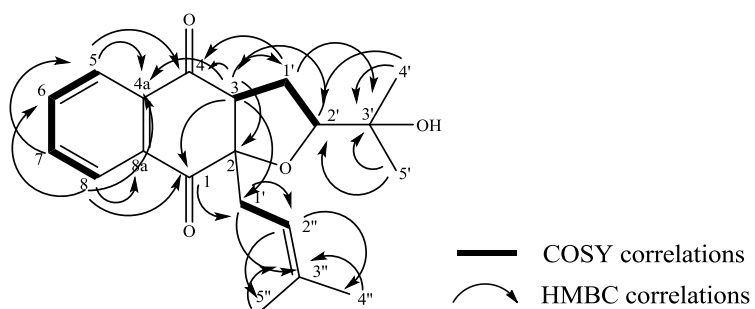
Figure 2.20: COSY and HMBC correlations of F5-2-9

a)
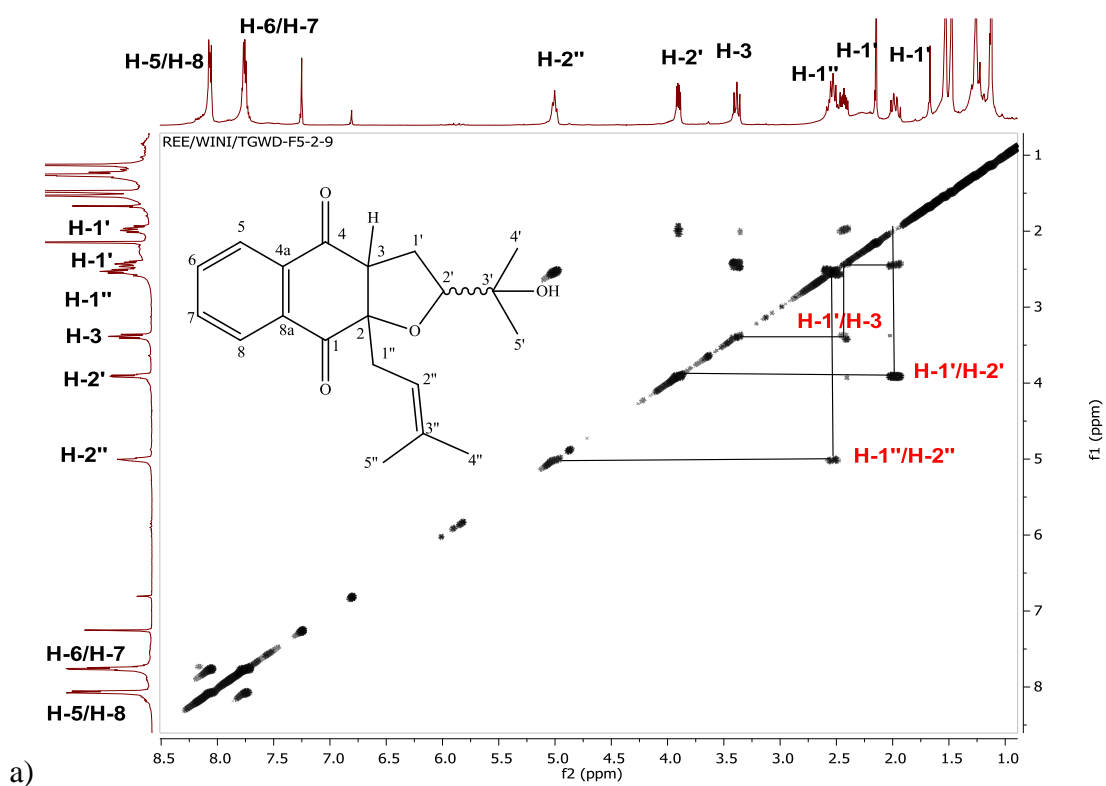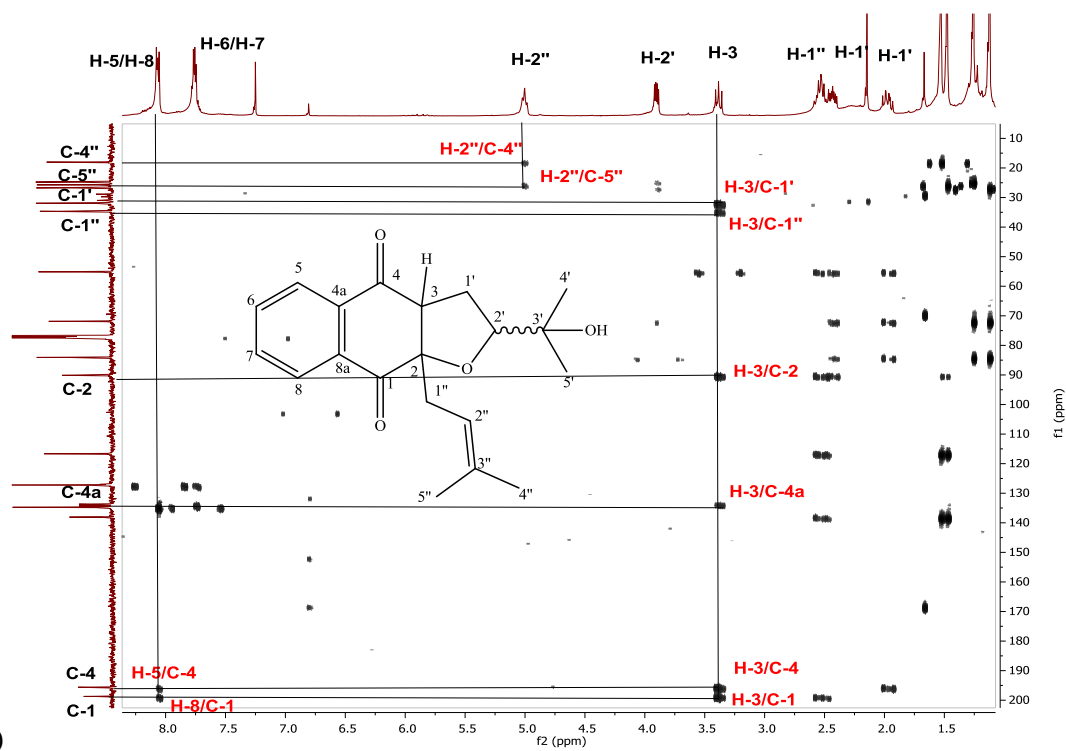
Figure 2.21: (a) COSY and (b) HMBC NMR spectra of F5-2-9
(CDCl$_3$, ^{1}H 400 MHz, ^{13}C 100.5 MHz)

Table 2.9: ^{1}H NMR of compounds F5-2-9, F7-5-2, F7-5-1
(CDCl$_3$, 400 MHz) and comparison with previous data

| Atom C | ^{1}H NMR, δ_H (ppm, multi. *J* in Hz) | | | |
	F5-2-9	*glycoquinone	F7-5-2	F7-5-1
1	-	-	-	-
2	-	-	-	-
3	3.39 (*dd*, *J*=9.6, 10.5 Hz, 1H)	3.41 (*dd*, *J*=9.5, 10.8 Hz, 1H)	-	-
4	-	-	-	-
4a	-	-	-	-
5	8.07 (*m*, 1H)	8.09 (*m*, 1H)	7.72 (*d*, *J*=7.8 Hz, 1H)	8.07 (*d*, *J*=7.7 Hz, 1H)
6	7.75 (*m*, 1H)	7.78 (*m*, 1H)	7.44 (*t*, *J*=7.6 Hz, 1H)	7.62 (*t*, *J*=8.1 Hz, 1H)
7	7.75 (*m*, 1H)	7.78 (*m*, 1H)	7.58 (*t*, *J*=7.6 Hz, 1H)	7.53 (*t*, *J*=7.7 Hz, 1H)
8	8.07 (*m*, 1H)	8.09 (*m*, 1H)	8.12 (*d*, *J*=7.9 Hz, 1H)	7.27 (*d*, *J*=7.7 Hz, 1H)
8a	-	-	-	-
1'	2.43 (*ddd*, *J*=4.5, 9.7, 13.7 Hz, 1H)	2.46 (*ddd*, *J*=4.4, 9.5, 13.4 Hz, 1H)	3.00 (*m*, 2H)	2.95 (*m*, 2H)
	1.97 (*ddd*, *J*=9.1 10.5, 13.7 Hz, 1H)	2.01 (*ddd*, *J*=9.2, 10.8, 13.4 Hz, 1H)		
2'	3.90 (*dd*, *J*=9.1, 4.4 Hz, 1H)	3.93 (*dd*, *J*=9.2, 4.4 Hz, 1H)	3.93 (*dd*, *J*=9.0, 4.3 Hz, 1H)	4.28 (*dd*, *J*=8.6, 6.3 Hz, 1H)
3'	-	-	-	-
4'-CH$_3$	1.13 (*s*, 3H)	1.14 (*s*, 3H)	1.21 (*s*, 3H)	1.27 (*s*, 3H)
5'-CH$_3$	1.26 (*s*, 3H)	1.24 (*s*, 3H)	1.35 (*s*, 3H)	1.18 (*s*, 3H)
1"	2.54 (*m*, 2H)	2.58 (*dd*, *J*=14.3, 7.7 Hz, 2H)	2.98 (*m*, 2H)	-
2"	5.00 (*t*, *J*=7.7 Hz, 1H)	5.03 (*m*, 1H)	4.77 (*dd*, *J*=8.6, 6.3 Hz, 1H)	-
3"	-	-	-	-
4"-CH$_3$	1.48 (*s*, 3H)	1.50 (*s*, 3H)	1.49 (*s*, 3H)	-
5"-CH$_3$	1.53 (*s*, 3H)	1.54 (*s*, 3H)	1.54 (*s*, 3H)	-
8''-OCH$_3$	-	-	-	3.48 (*s*, 3H)
9''-OCH$_3$	-	-	-	3.84 (*s*, 3H)

* Ito *et al.*, 1999

Atom C	^{13}C NMR, δ_c (ppm)			
	F5-2-9	* glycoquinone	F7-5-2	F7-5-1
1	198.2	198.6	181.8	101.7
2	90.1	90.1	79.8	49.1
3	55.1	55.0	112.6	171.1
4	196.1	195.5	145.6	132.9
4a	134.2	134.2	128.9	-
5	127.0	127.2	126.0	130.5
6	134.8	134.7	132.7	132.5
7	134.8	134.6	132.7	129.8
8	127.0	127.2	126.0	130.3
8a	133.7	133.6	142.0	130.1
1'	32.1	31.9	31.9	27.1
2'	84.0	84.0	92.4	81.9
3'	71.8	71.8	71.6	71.2
4'-CH$_3$	24.8	26.7	23.6	25.7
5'-CH$_3$	26.6	26.6	26.3	23.5
1"	34.7	34.5	29.6	-
2"	116.6	116.5	117.4	-
3"	138.1	138.1	138.6	-
4"-CH$_3$	18.1	18.0	18.7	-
5"-CH$_3$	25.8	25.6	26.3	-
6"	-	-	-	166.2
7"	-	-	-	165.3
8"-OCH$_3$	-	-	-	52.2
9"-OCH$_3$	-	-	-	56.5

* Ito *et al.*, 1999

F5-2-9   F7-5-2   F7-5-1
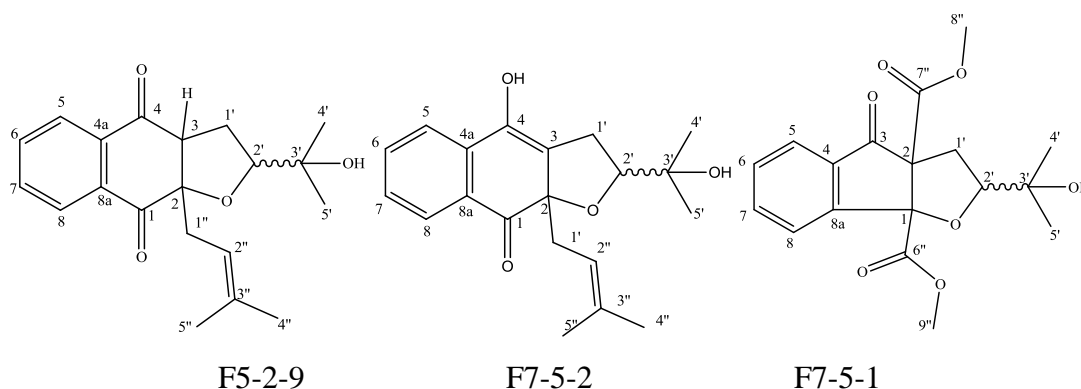
2.4.9 Compound F7-5-2 (new compound, 2.27)

Compound F7-5-2 (6.0 mg) was isolated as yellow oil and its molecular formula was determined by HRESI-MS as $C_{20}H_{24}O_4$ with m/z 329.1747 $[M+H]^+$ and optical rotation $[\alpha]_D^{20}$ +11° (c 1.00, CHCl$_3$).

Synonyms	glycosemiquinone, 4-hydroxy-2-(2-hydroxypropan-2-yl)-9a-(3-methylbut-2-en-1-yl)-2,3-dihydronaphtho[2,3-b]furan-9(9aH)-one
Sample code	F7-5-2 (**2.27**)
Sources	*A. lanata* stem
Yield (mg, %)	6.0 (0.04%)
Physical state	Yellow oil
Molecular formula	$C_{20}H_{24}O_4$
Molecular weight (g/mol)	328.1675
Exact mass (m/z)	329.1747 $[M+H]^+$
Ret. time (min)	13.36
R$_f$ value (2H:8DCM)	0.10
Optical rotation $[\alpha]_D^{20}$	+11° (c 1.00, CHCl$_3$)

2.27

Figure 2.22: (a) ^{1}H and (b) ^{13}C NMR spectra of F7-5-2
^{13}C NMR (green spectrum), DEPT (red spectrum) (CDCl$_3$, ^{1}H 400 MHz, ^{13}C 100.5 MHz)

The ^{1}H NMR results of F7-5-2 (Figure 2.22 a, Table 2.9) showed ABCD spins proton signals δ_H 8.12 (*d*, *J*=7.9 Hz, 1H), 7.72 (*d*, *J*=7.8 Hz, 1H), 7.58 (*t*, *J*=7.6 Hz, 1H) and 7.44 (*t*, *J*=7.6 Hz, 1H) corresponding to protons H-8, H-5, H-6 and H-7. The presence of a methine proton linked to an oxygen at δ_H 3.93 was indicated by a a double of doublet signal (*dd*, *J*=9.0, 4.3 Hz, H-2'). An olefinic at δ_H 4.77 was indicated by a double of doublet signal (*dd*, *J*=8.6, 6.3 Hz, H-2'') and the presence of a downfield methylene proton due to unsaturated carbon $\Delta^{3, 4}$ was indicated by a multiplet signal at δ_H 3.00 (*m*, 2H, H-1'). Remaining proton signals showed similar signals to those proton signals of compound F5-2-9 except for the absence of doublet of doublets which representing a methine proton signal at C-3. The ^{13}C NMR results (Figure 2.22 b, Table 2.10) showed 20 carbon signals, including two carbonyl carbon

79

signals at δ_C 181.8 (C-1) and a carbon signal at δ_C 145.6 (C-4) which was different compared with the carbon signal in compound F5-2-9. This compound was proposed to have a hydroxyl group attached at carbon position C-4. The remaining carbon signals were shown by four quaternary carbon signals at δ_C 128.9, 142.0, and 112.6, which corresponded to aromatic carbons C-4a, C-8a and C-3, respectively. The aromatic and prenyl moiety carbon signals remained the same as those discussed for compound F5-2-9.

The molecular structure was also established by 2D NMR using COSY and HMBC experiments (Figure 2.24 a and b). Some of the important COSY correlations were between protons H-1' and H-2' and amongst the aromatic protons. The HMBC showed important correlations between proton H-8 and carbonyl carbon C-1, C-7 and C-8a. Other correlations were between proton H-1' and C-3', proton H-7 and C-8 and C-8a, as well as correlation between prenyl proton H-2" and C-4"/5". The COSY and HMBC correlations were depicted in Figure 2.23. The NMR spectra revealed that this compound has different only at C-4 in which the carbon directly attached to a hydroxyl hence affect the splitting pattern of the aromatic protons compared with those earlier compound avicequinone C, (F5-2-9) that has been found in *Glycomis pentaphylla* (Ito *et al.*, 1999), therefore this compound was proposed to be a new derivative, (+)-glycosemiquinone (4-hydroxy-2-(2-hydroxypropan-2-yl)-9a-(3-methylbut-2-en-1-yl)-2,3-dihydronaphtho[2,3-b] furan-9(9a*H*)-one).
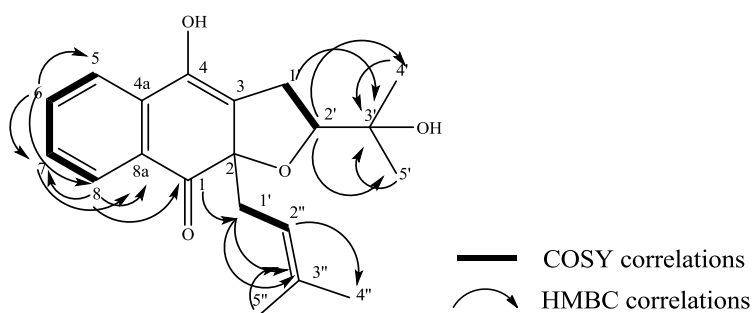
Figure 2.23: COSY and HMBC correlations of F7-5-2
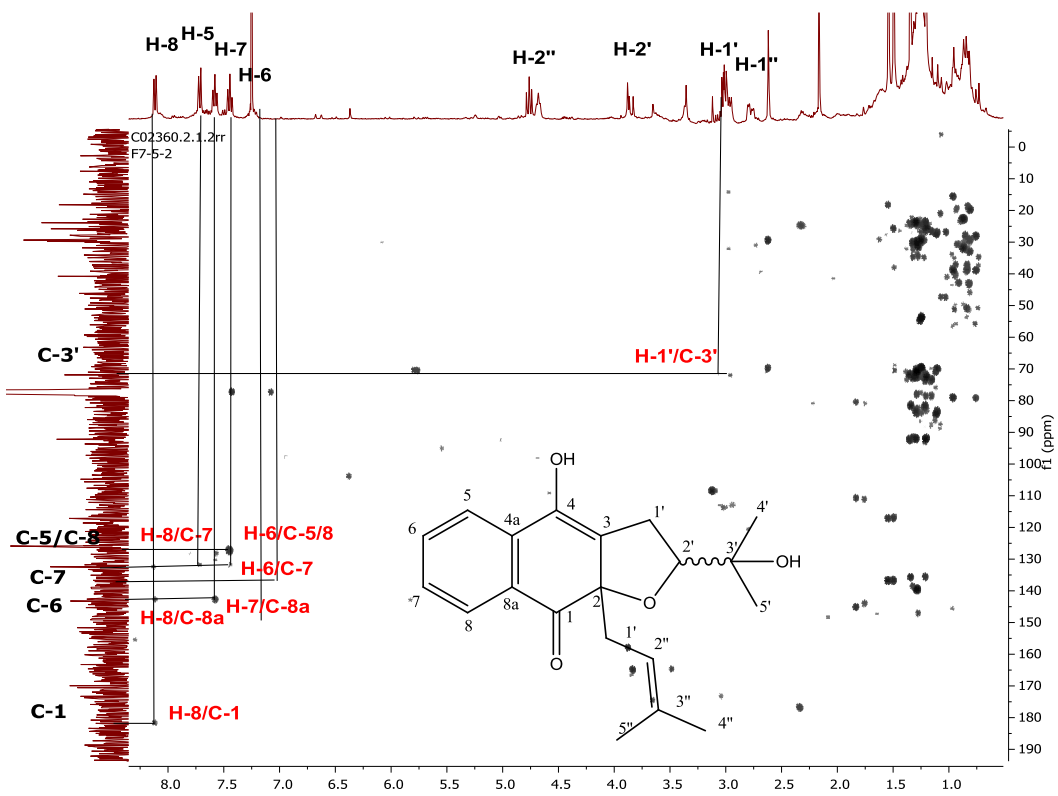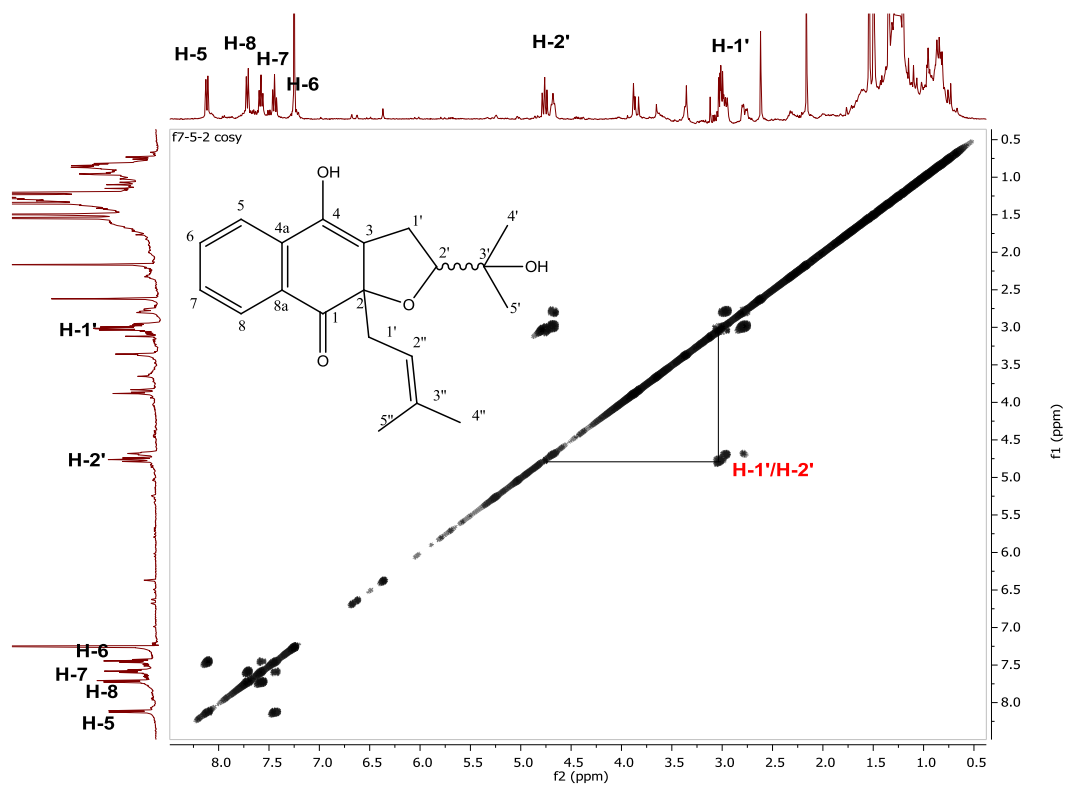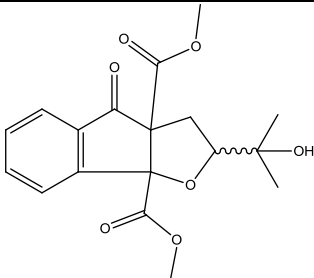
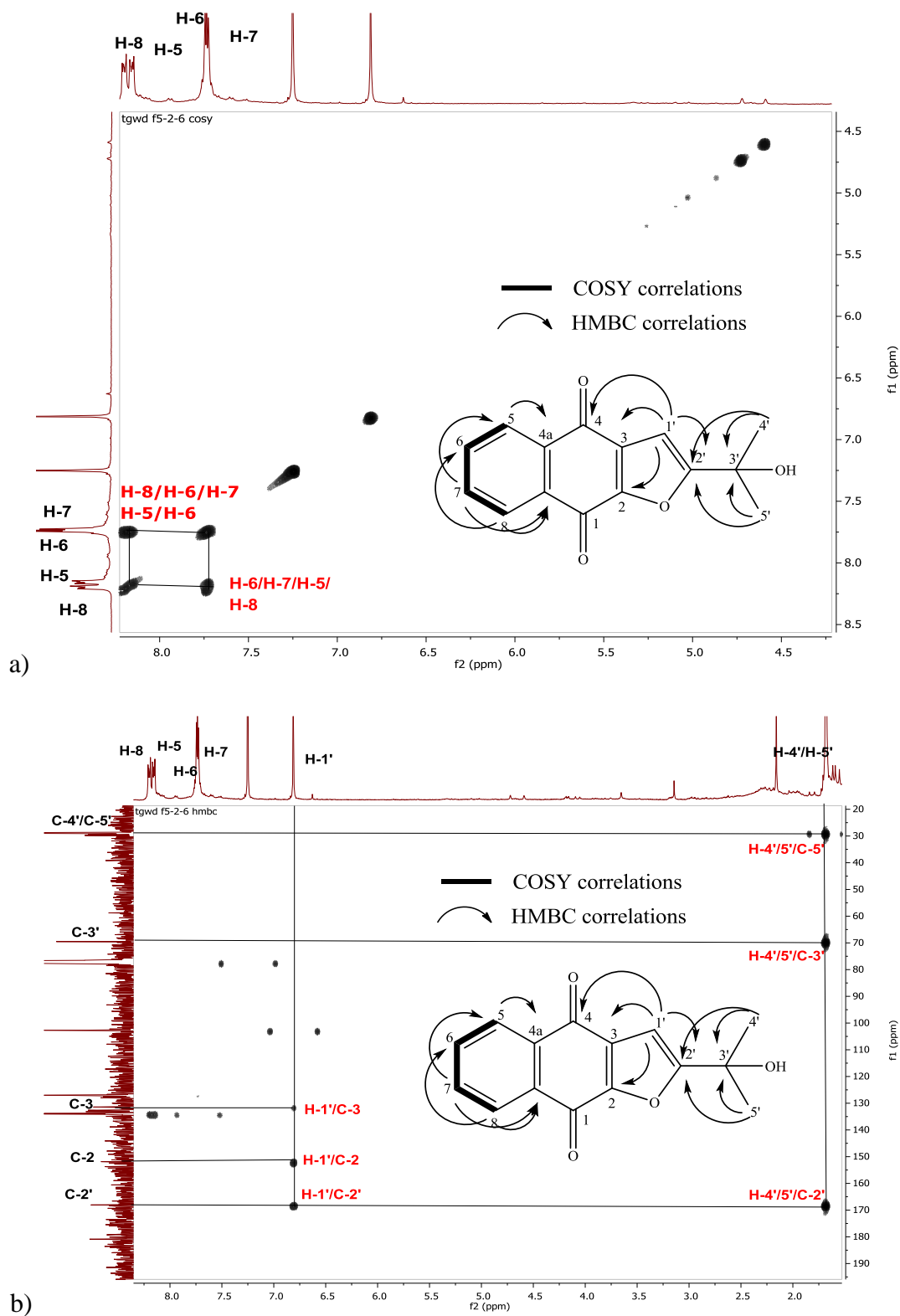**Figure 2.24:** (a) COSY and (b) HMBC NMR spectra of F7-5-2
(CDCl$_3$, ^{1}H 400 MHz, ^{13}C 100.5 MHz)
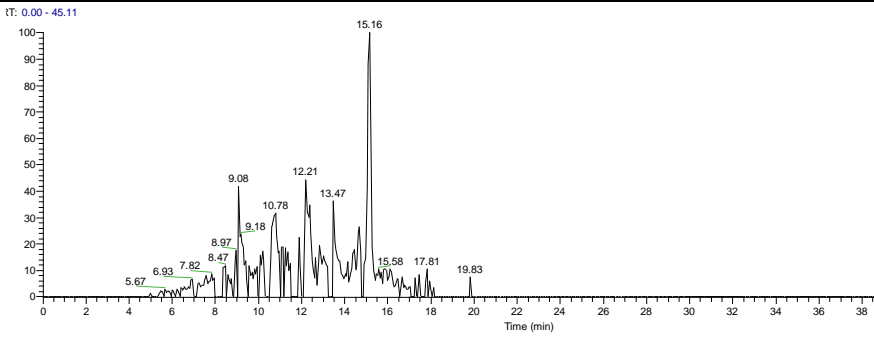
2.4.10 Compound F7-5-1 (new compound, 2.28)

Compound F7-5-1 (6.7 mg) was isolated as yellow oil. The molecular formula was determined by HRESI-MS as $C_{18}H_{20}O_7$ with an *m/z* of 349.1280 [M+H]$^+$ and optical rotation $[\alpha]_D^{20}$ +13° (*c* 1.00, CHCl$_3$).
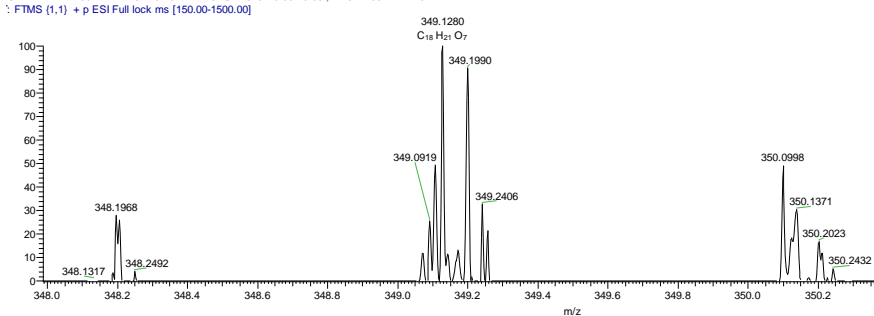
Synonym	avicennpentenone carboxylate, dimethyl 2-(2-hydroxypropan-2-yl)-4-oxo-3,3a,4,8b-tetrahydro-2*H*-indeno[1,2-b]furan-3a,8b-dicarboxylate
Sample code	F7-5-1 (**2.28**)
Sources	*A. lanata* stem
Yield (mg, %)	6.7 (0.05%)
Physical state	Yellow oil
Molecular formula	$C_{18}H_{20}O_7$
Molecular weight (g/mol)	348.1200
Exact mass (*m/z*)	349.1280 [M+H]$^+$
Ret. time (min)	15.16
R$_f$ value (2H:8DCM)	0.17
Optical rotation $[\alpha]_D^{20}$	+13° (*c* 1.00, CHCl$_3$)

2.28

The ^{1}H NMR results of F7-5-1 (Figure 2.25 a, Table 2.9) ABCD spin proton signals: one doublet was more downfield at δ_H 8.07 (*d*, *J*=7.7 Hz, H-5), a second doublet at δ_H 7.27 (*d*, *J*=7.7 Hz, H-8) and two triplets at δ_H 7.62 (*t*, *J*=8.1 Hz, H-6) and 7.53 (*t*, *J*=7.7 Hz, H-7), respectively. The aliphatic proton signals of the substituted tetrahydrofuran remained the same with avicenol C except the presence two singlet signals of methoxy at δ_H 3.84 and 3.47 were also evident. The ^{13}C NMR results (Table 2.25 b, Table 2.10) showed 18 carbon signals including three carbonyl carbon signals at δ_C 171.1 (C-3) 166.2 (C=0 a) and 165.3 (C=O b), and six aromatic carbon signals at δ_C 132.9 (C-4), 132.5 (C-6), 130.5 (C-5), 130.3 (C-8), 130.1 (C-8a) and 129.8 (C-7). The aliphatic cabon signals of the substituted tetrahydrofuran remained the same with avicenol C, except the presence of a quaternary carbon signal that was deshielded by carbonyl carbon C-3 at δ_C 49.1 (C-2) and two methoxy carbon signals at δ_C 52.2 and 56.5.

a)

b)
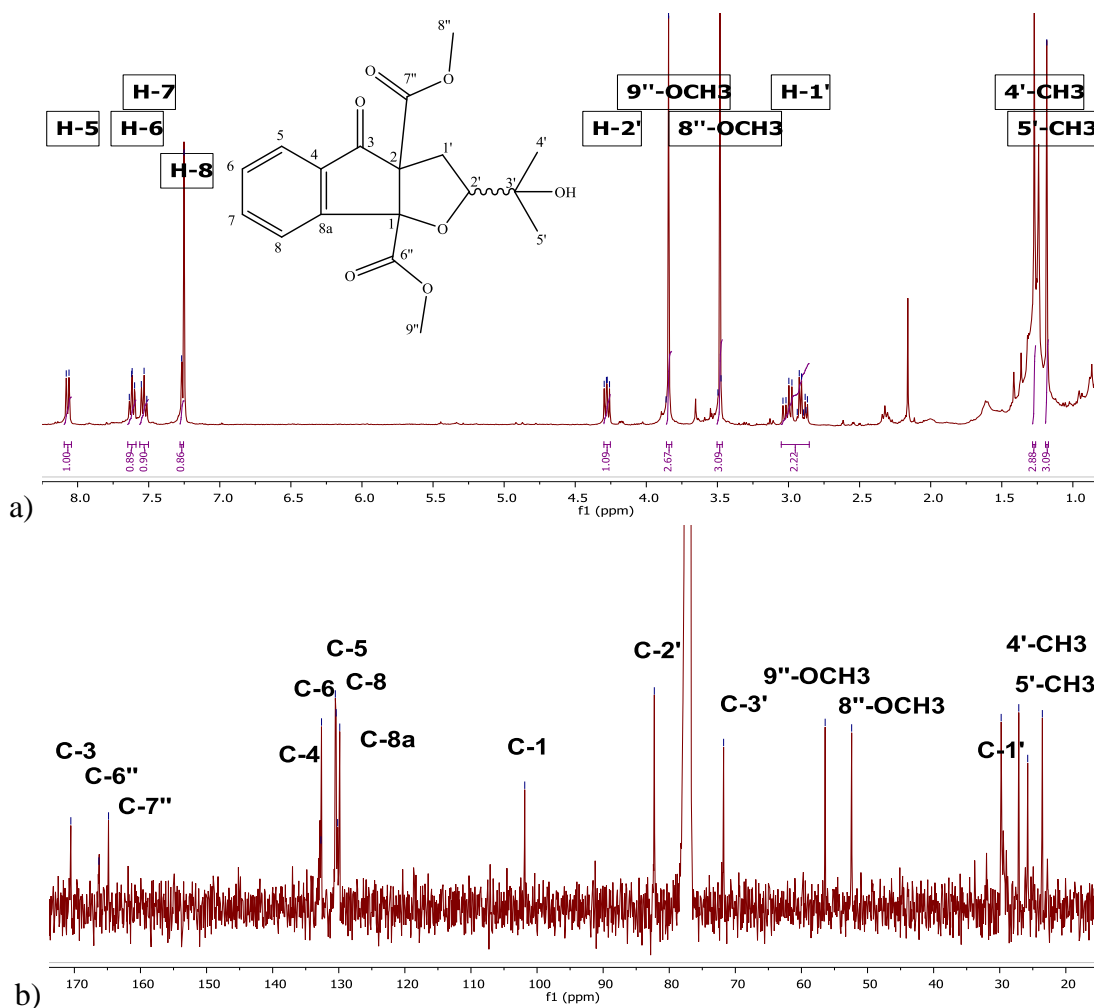
Figure 2.25: (a) ^{1}H and (b) ^{13}C NMR spectra of F7-5-1
(CDCl$_3$, ^{1}H 400 MHz, ^{13}C 100.5 MHz)

83

The important H-H COSY correlations (Figure 2.26 a) were observed amongst aromatic protons, H-5 and H-6, H-6 and H-7, H-7 and H-8, and proton H-1' and H-2'. The significant C-H long-range couplings between carbons and protons were established and supported by HMBC correlations (Figure 2.26 b). The important correlations which need to be highlighted were those from the methylene H-1' with C-1, C-2', C-3', C-7'', 8''-CH$_3$ with C-7'', 9''-CH$_3$ with C-6'', H-2' with C-2, and H-4'/5' with C-3' (Figure 2.27) in which the correlations between those new proton and carbon signals. The stereochemistry of this compound at chiral center C-2', $[\alpha]_D^{20}$ +13° (c 1.00, CHCl$_3$), was almost the same with previous compounds (F5-2-3, F5-2-9, F7-5-2). But comparison with the NMR results, this compound showed different functional group in which 1, 2-dicarboxylate attached to hydrofuran ring, but the rest signals remained the same as discussed earlier. Hence, elucidation of this compound revealed that it as a new metabolite avicennpentenone carboxylate isolated from this plant extract.

a)

b)
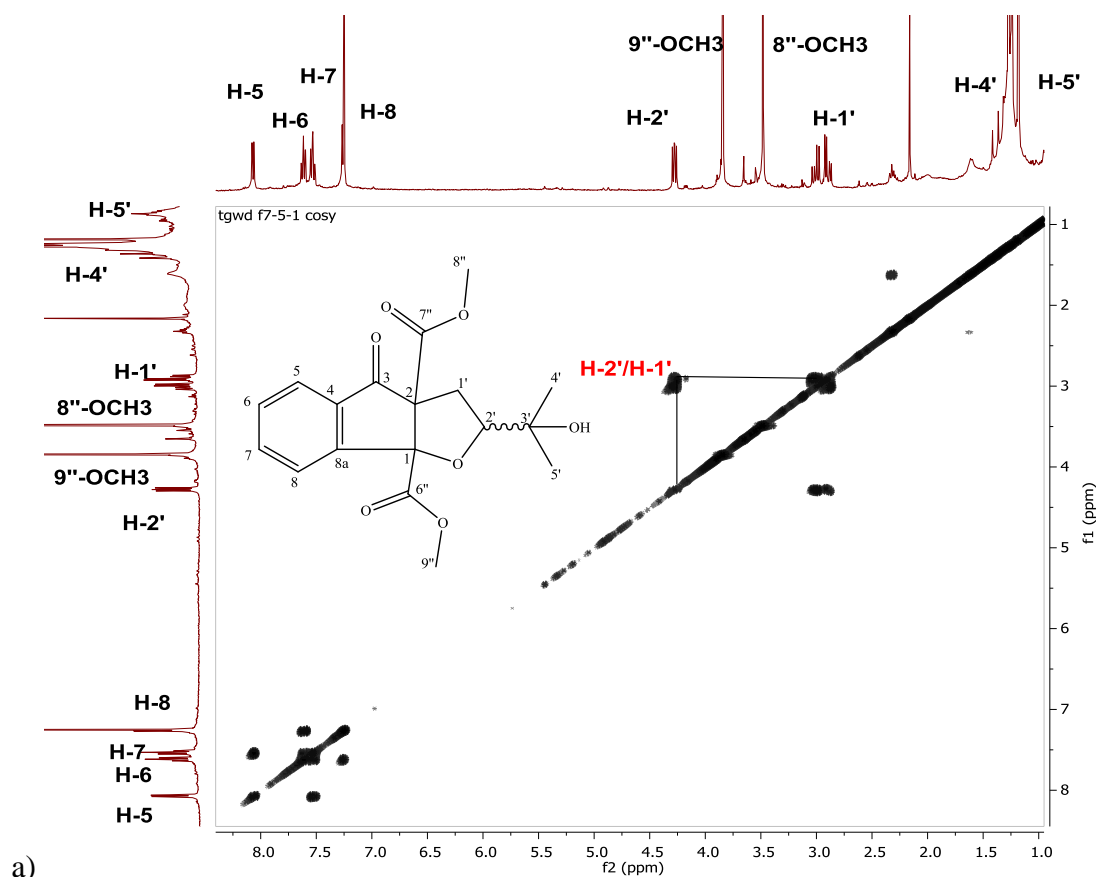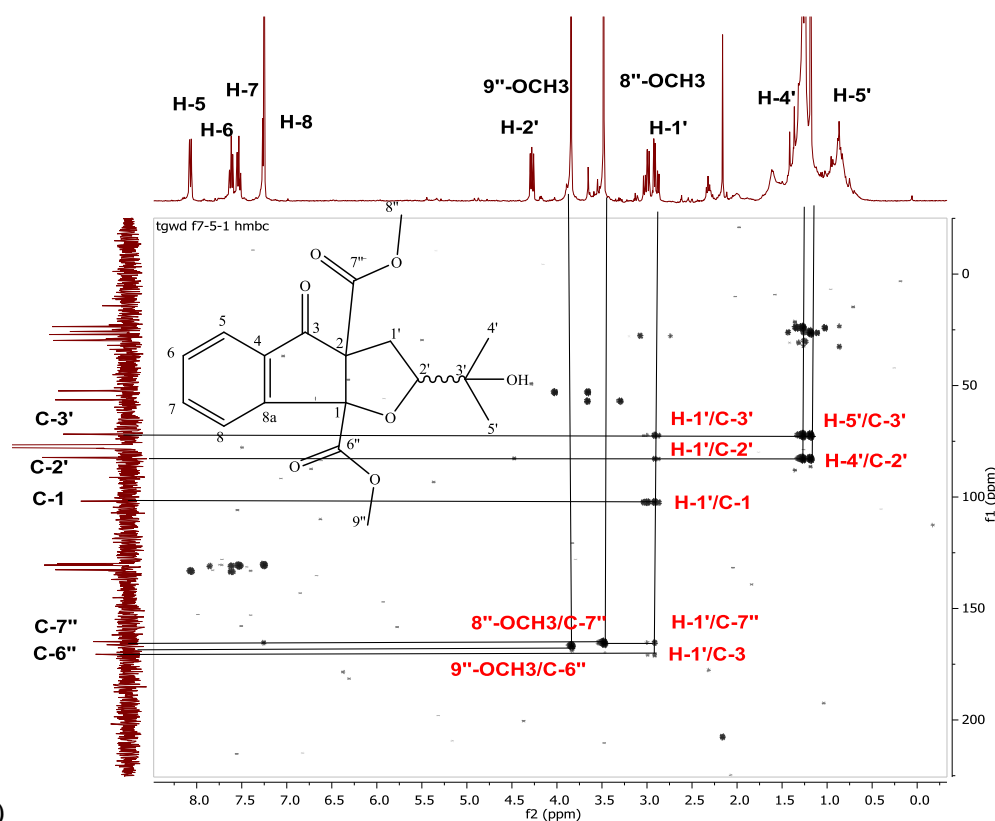
Figure 2.26: (a) COSY and (b) HMBC NMR spectra of F7-5-1
(CDCl$_3$, ^{1}H 400 MHz, ^{13}C 100.5 MHz)
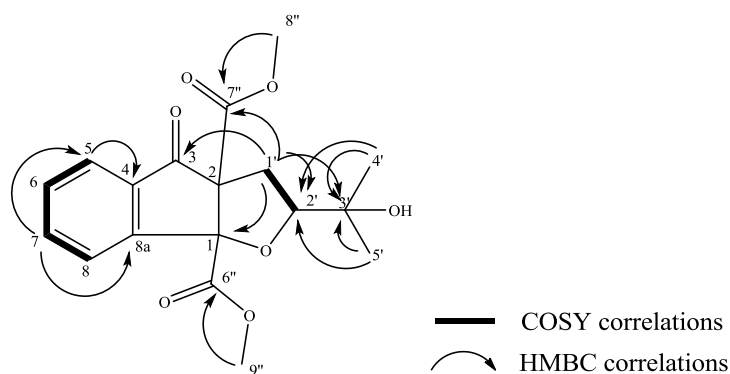
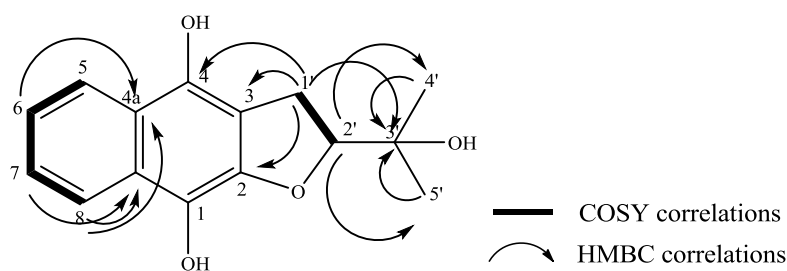**Figure 2.27:** COSY and HMBC correlations of F7-5-1

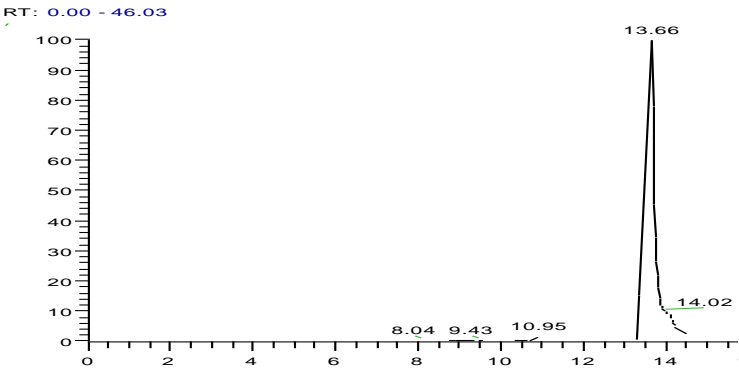## 2.5   Bioactivity test results

Pentacyclic triterpenes-taraxerol, taraxerone and β-sitosterol were inactive against the protozoa with MICs of 154.20 and 145.30 μM and 142.30 μM, respectively (Table 2.11). Meanwhile, stigmasterol had a very low effect with MIC values of 126.40 against *T. b. brucei*. Avicequinone C displayed the most potent against *T. b.*

brucei with an MIC of 3.12 μM. The next potent is avicenol C with MIC 6.25 μM, whereas its derivative hydroxyavicenol C possessed moderate activity (MIC 12.50 μM) which is less than avicenol C. Hydroxyavicenol C differed only from avicequinone C in that it possessed hydroxyl groups as opposed to *p*-dione and α,β-unsaturetaed quinone system. Glycoquinone and the closely related compound, glycosemiquinone had similar activity with MIC of 12.50 μM. In addition, the new derivative, avicennpentenone carboxylate showed significant activity with MIC 6.25 μM against the same microorganism. All active compounds against *T. b. brucei* were not toxic against PNT2A cell lines.

taraxerone

taraxerol

stigmasterol

β-sitosterol

avicenol C

avicequinone C

hydroxyavicenol C

glycoquinone   glycosemiquinone   avicennpentenone carboxylate
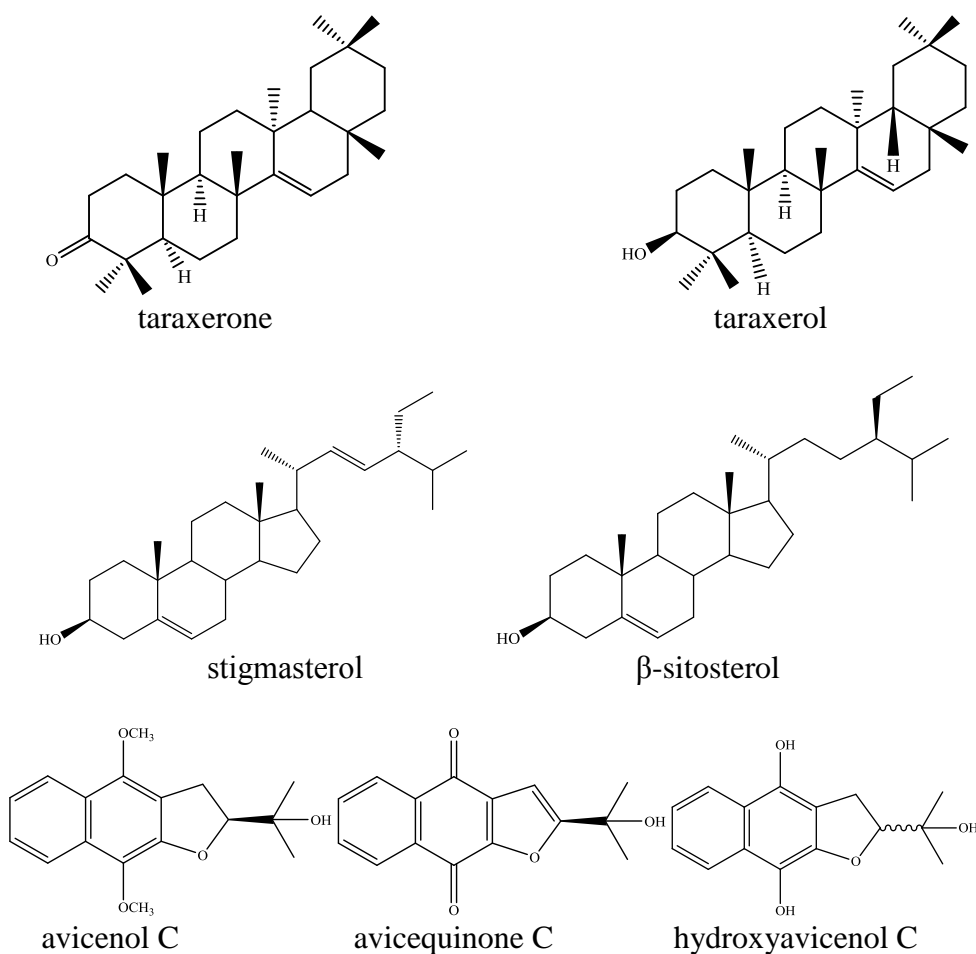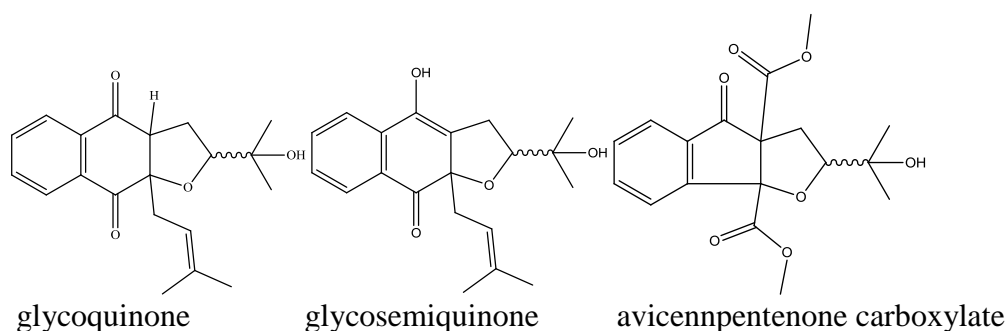
Table 2.11: Activities of the isolated compounds
from *A. lanata* against *T. b. brucei* and PNT2A cells

Compounds	[a] MICs (μM)	[b] Cytotoxicity, % D of control (100 μg/mL)
taraxerone	154.20	88.8
taraxerol	145.30	92.8
stigmasterol	126.40	98.7
β-sitosterol	142.30	96.2
avicenol C	6.25	78.3
avicequinone C	3.12	68.6
hydroxyavicenol C	12.50	86.1
glycoquinone	12.50	80.3
glycosemiquinone	12.50	86.1
avicennpentenone carboxylate	6.25	86.3
Suramin	0.11	n.d
Triton X	n.d	0.082

[a] Each sample was tested in two independent assays against *T. b. brucei*, MIC values indicate the minimum inhibitory concentration of a compound/standard in μM necessary to achieve 90% growth inhibition. MICs (MIC < 10 μM - promising; 10 μM < MIC > 20 μM - moderate; 20 μM < MIC > 30 μM - marginal/weak; 30 μM < MIC > 40 μM - limited; MIC > 40 μM - no activity);
[b] Initial screening for cytotoxicity activity against human normal prostatic epithelial cells (PNT2A) , % D of control values (at 100 μg/mL,) were determined by averaging of three independent assays results (n=3); [c, d] Positive controls; n.d.- not determined.

Chapter 3

3. Bioactive secondary metabolites of fungi isolated from *A. lanata*

3.1 Isolation and identification of endophytic fungi from *A. lanata*

3.1.1 Isolation of the endophytic fungi

In this present study, the endophytic fungi have been isolated from fresh parts of the mangrove plant *Avicennia lanata* - stems, stem barks, leaves and roots. The fungi were obtained from inner part of stems, leaves and roots of the mangrove plant *A. lanata* collected from Setiu Wetlands, Terengganu, Malaysia. The specimen was deposited in Universiti Malaysia Terengganu herbarium (UMT-01). The protocols used to isolate of the organisms have been described in Chapter 7.2. Later, the pure strain was incubated for further molecular characterization.

3.1.2 Molecular characterization of endophytic fungi

The pure strain was grown on malt agar and the mycelium was harvested, later the genomic nucleic acid (DNA) was extracted using Extraction and Dilution solution (Sigma-Aldrich, USA) as described in Chapter 7.3.1. The ITS regions of all isolates were amplified using polymerase chain reaction (PCR) using the universal ITS primers ITS1 (TCCGTAGGTGAACCTGCGG) and ITS4 (TCCTCCGCTTATTGATATGC) primer pairs (Sigma-Aldrich, USA) and REDExtract-N-Amp PCR ReadyMix (Sigma-Aldrich, UK) as discussed in Chapter 7.3.2. The PCR-amplified DNA was purified using agarose gel electrophoresis (Chapter 7.3.3), and extracted using a GenElute Gel Extraction Kit (Sigma-Aldrich, USA) according to Chapter 7.3.4. The DNA was submitted to Dr. Rothwelle Tate at University of Strathclyde for sequencing. The sequence analysis of the amplicons was performed by BLASTN (http://blast.ncbi.nlm.nih.gov/Blast.cgi) comparison using the National Centre for Biotechnology Information (NCBI) database's best hit (Sayers *et al.*, 2010) to confirm the identities of the selected strains. All fungal sequences were at least 98% identical to the best hit in the NCBI database (Taylor and Houston, 2011). A summary workflow for the isolation and identification of endophytic fungi from mangrove plant *A. lanata* was shown in Figure 3.1.

```
                    ┌─────────────────────────────────────┐
                    │  Mangrove plant Avicennia lanata     │
                    └─────────────────────────────────────┘
                                     │
                                     │  - Collected fresh parts; stems, leaves, barks and roots
          ┌──────────────────────────┼──────────────────────────┐
          │                          │                          │
     ┌─────────┐               ┌──────────┐               ┌─────────┐
     │  Stems  │               │  Leaves  │               │  Roots  │
     └─────────┘               └──────────┘               └─────────┘
          │     ┌─────────────────────────────────────────────┐     │
          │     │ Identification of endophytic fungi: DNA work │     │
          │     └─────────────────────────────────────────────┘     │
          │                          │                          │
  ┌───────────────────┐   ┌──────────────────────┐   ┌─────────────────┐
  │ Lasiodiplodia     │   │ Aspergillus aculeatus│   │ Fusarium sp.    │
  │ theobromae        │   │                      │   │                 │
  └───────────────────┘   └──────────────────────┘   └─────────────────┘
```

1) **Preliminary screening -** small scale in 500 mL of Erlenmeyer flask, room temperature
Rice culture – 7, 15, 30 days, containing 50 g rice : 50 mL water (autoclaved)
Liquid culture – 7, 15, 30 days, containing 50 mL broth (autoclaved)
2) **Dereplication studies:**
HRFT-LCMS, MZmine software, *in-house* macro combined with the Antimarin database, SIMCA P+ 13
3) **Bioactivity -** anti-trypanosomal

Scale up: *L. theobromae*	Scale up: *A. aculeatus*	Scale up: *Fusarium* sp.
Rice culture: 15 days, 30 L, room temp., containing 100 or 200 g rice in 1L or 2L Erlenmeyer flask	Rice culture: 30 days, 20 L, room temp., containing 100 or 200 g rice in 1L or 2L Erlenmeyer flask	Rice culture: 15 days, 40 L, room temp., containing 100 or 200 g rice in 1L or 2L Erlenmeyer flask

Figure 3.1: A summary workflow
for isolation and identification of endophytic fungi from mangrove plant *A. lanata*

3.2 Bioactive secondary metabolites from *Fusarium* sp.

The mangrove derived-fungus *Fusarium* sp. has been explored for its potential to yield valuable bioactive secondary metabolites. *Fusarium* are a filamentous fungus widely distributed in plants and in the soil which grow rapidly on agar plates (dextrose or malt agar) at 27 °C and produce woolly or cottony, flat, spreading colonies. From the front of the plate, the colour of the colony might be white, cream, tan, yellow, red, violet, pink or purple, while at the bottom of the plate, they are sometimes tan, red, dark purple or brown. The filtrates of some strains of *F. equiseti* were recognised to be highly phytotoxic (Brian *et al.*, 1961), *F. oxysporum* f. sp. *ciceri* (FOC 5) cause wilting in chickpea, *Cicer arietinum* which revealed bikaverin and norbikaverin as responsible for the toxigenicity (Gopalakrishnan, 2004). *F. solani* is a well-known pathogen that caused wilt and rot in citrus, peas and tomato as well as affected spinach chloroplasts and the growth of tobacco leaves in which naphthazarin toxin metabolites have been produced. Dihydrofusarubin, marticin, isomarticin, javanicin and fusarubin were successfully isolated from *F. solani*

(Tatum and Baker, 1983, Heiser *et al.*, 1998, Rensburg *et al.*, 2001, Achor *et al.*, 1993, Rehman *et al.*, 2014, Baker *et al.*, 1981). *F. graminearum* is the causal agent for a decline in cereal production instigating *Fusarium* head blight in wheat and barley (Yang *et al.*, 2013). *F. oxysporum* is the most common pathogen causing wilt in crops such as cucumber (Melo and Piccinin, 1999), pea (Sharma, 2011, Bani *et al.*, 2014). *F. solani* f. sp. *piperis* cause root rot and stem blight on black pepper (*Piper nigrum* and *Piper betle*) (Duarte and Archer, 2003). A study on *F. solani* isolated from bean hulls yielded the toxigenic metabolites solaniol and diacetoxyscirpenol (Ishii *et al.*, 1971).

Previous chemical studies on *Fusarium* sp. demostrated its capability to produce interesting bioactive metabolites. Anhydrofusarubin showed very selective cytotoxicity to both oral human carcinoma cells (KB) and human breast cancer cells (MCF-7) whereas austrocortirubin from the same isolate was active against MCF-7 (Trisuwan *et al.*, 2010). 9α-hydroxyhalorosellinia A is an octahydroanthraquinone type compound isolated from the sea fan-derived *Fusarium* sp. which showed weak anti-fungal activity (against *Cryptococcus neofomans* and *Microsporum gypseum*) (Trisuwan *et al.*, 2010) but an earlier study on the same metabolite exhibited strong anti-malarial (against *Plasmodium falciparum*, KI cell) and anti-mycobacterial activities (against *Mycobacterium tuberculosis* H37Ra) (Sommart *et al.*, 2008).

Other compounds from *Fusarium* sp., such as zearalenone and fusarielin E inhibited *Pyricularia oryzae* activity (Zhao *et al.*, 2008, Gai *et al.*, 2007). Beauvericin is a mycotoxin cyclic hexadepsipeptide belonging to the enniatin antibiotic family which was isolated from *Beaveria bassiana* and *Fusarium* sp. (Hamill *et al.*, 1969, Logrieco *et al.*, 1998). Beauvericin displayed insecticidal activity against *Aedes aegypti* (Hamill *et al.*, 1969, Grove and Pople, 1980), cytotoxicity against human leukaemia cell CCRF-CEM (Jow *et al.*, 2004) as well as two human cell lines of myeloid origin: the monocytic lymphoma cells U-937 and the promyelocytic leukaemia cells HL-60 (Calò *et al.*, 2004). Studies on combination of beauvericin and ketoconazole or miconazole showed effective anti-fungal activity to *Candida parapsilopsis* otherwise the two metabolites alone do not show any activity (Zhang *et al.*, 2007, Fukuda *et al.*,

2004). Beauvericin also exhibited anti-viral activity against HIV-1 integrase (Shin *et al.*, 2009) while beauvericin from *F. redolens* and *F. proliferatum* showed anti-bacterial activity to both Gram-positive and negative bacteria (Lijian Xu *et al.*, 2010, Meca *et al.*, 2010).

3.3 Results and discussion

3.3.1 Identified endophytic fungi from mangrove plant *A. lanata*

Four pure fungal strains were successfully isolated from mangrove *A. lanata* and were identified by DNA extraction, PCR amplification and sequencing by using polymerase chain reaction (PCR) and the universal ITS primers (Supporting Information; GenBank GQ856236 and GQ856237, respectively). The voucher specimens of all strains were deposited in Natural Product metabolomics Laboratory (SIPBS, University of Strathclyde). The isolated endophytic fungi from the mangrove plant *A. lanata* were identified as *Aspergillus aculeatus* obtained from the leaf part; *Lasiodiplodia theobromae* from the stem; *Aspergillus flavipes* from the stem bark and *Fusarium* sp. from the root part. Three strains were subjected to screening and optimization of the metabolites production in different media at different growth phases. *Aspergillus flavipes* was reported to be a causal agent of chronic necrotizing pulmonary aspergillosis (lung infection) associated with pulmonary fibrosis, allergen, irritant, hypersensitivity pneumonitis, dermatitis and lumbar vertebral osteomyelitis. Thus, the strain was discarded for health and safety issues.

3.3.2 Preliminary screening and identification of metabolite production from *Fusarium* sp.

Preliminary screening and identification of metabolite production from the small scale of *Fusarium* sp. extracts was carried out by cultivating the pure strain (Figure 3.2) as described in Chapter 7.4. The metabolites produced from the small scale of *Fusarium* sp. extracts (FRC7, FRC15, FRC30, FLC7, FLC15 and FLC30) was dissolved and analysed using HRESI-LCMS (Thermo Scientific, UK) for dereplication studies and tested for anti-trypanosomal activity.
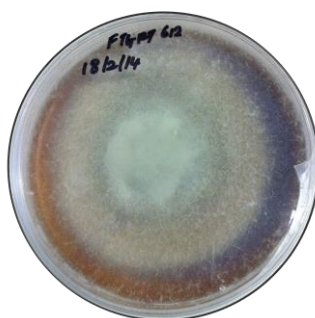
Figure 3.2: Endophytic fungus *Fusarium* sp. pure strain grown on malt agar plate

The bioactivity test results on the small scale of *Fusarium* sp. extracts (Table 3.1), showed that the small scale extract from the rice culture media on day 15 (FRC15) and 30 (FRC30), liquid culture media day 7, 15 and 30 (FRC7, FRC15, FRC30) showed intense activity. Figure 3.3 a, is an unsupervised score plot analysis showed the small extracts from rice and liquid media day 30 (FRC30 and FLC30) distributed outlier from other extracts.

Table 3.1: Anti-trypanosomal activity of *Fusarium* sp. small scale extracts (calculated as mean value of percentage viability) at concentrations of 20 µg/ mL (RC= rice culture extracts, LC = liquid culture extracts on day 7, 15 and 30)

Small scale extract *Fusarium* sp.	*T. b. brucei*, % D control (20 µg/mL)
FRC7	94.0
FRC15	0.1
FRC30	-2.9
FLC7	-8.5
FLC15	-9.3
FLC30	-2.9

% D control, percentage inhibition of control

Metabolite with *m/z* 291.1999 [M-H]⁻ was identified as 2-hydroxynorjavanicin from *Fusarium solani* (Baker *et al.*, 1990, Tatum *et al.*, 1985), *Nectria haematococca* (Parisot *et al.*, 1988), and three unidentified metabolites with *m/z* 319.2312, 305.21565 and 235.9260 [M-H]⁻ only produced in FRC30 and FLC30.
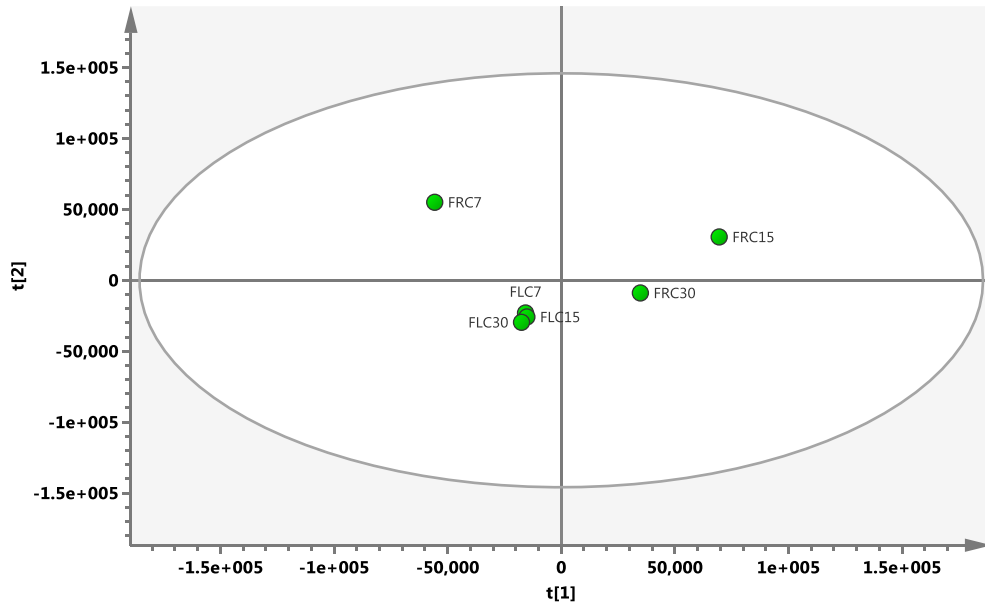
a)
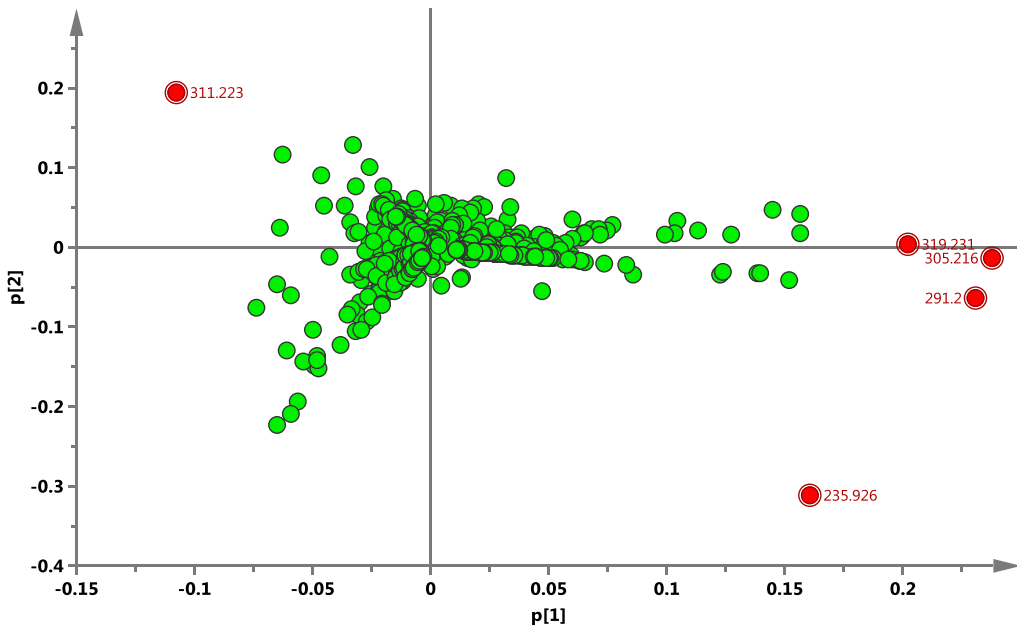
b)

Figure 3.3: PCA analysis on small scale of *Fusarium* sp. extracts

Fusarium sp. grown in rice and liquid culture media (FRC= rice culture extracts, FLC = liquid culture extracts on day 7, 15 and 30); (a) Unsupervised PCA score plot analysis of the small scale extract of *Fusarium* sp. showed distinctive separation between different extracts of different period of time day 7, 15 and 30; (b) Unsupervised PCA loading plot showed the end metabolites produced.
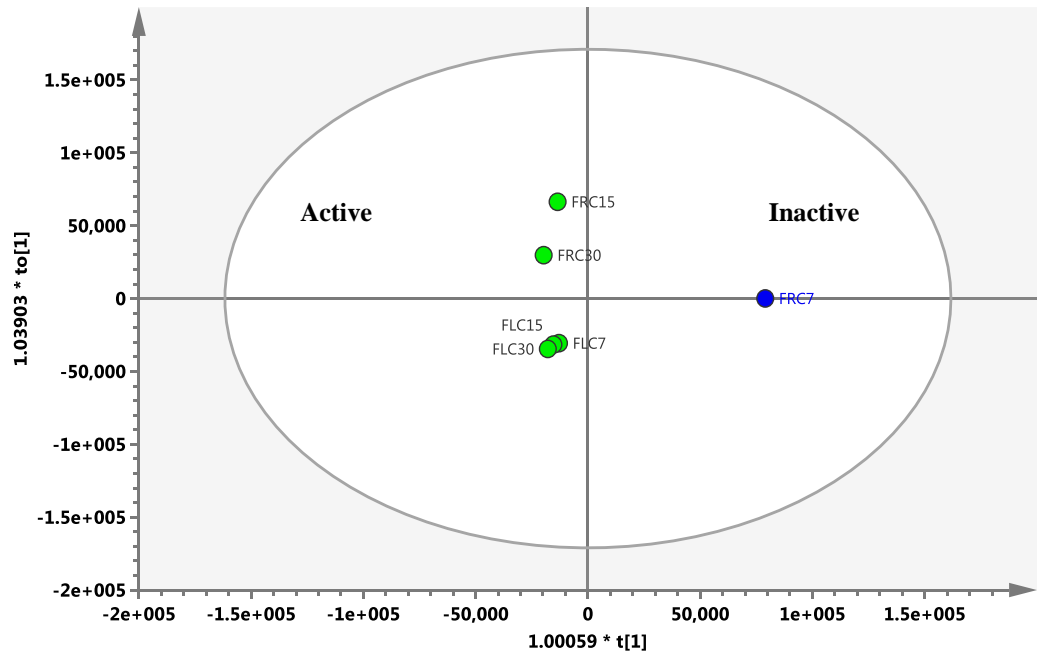
a)
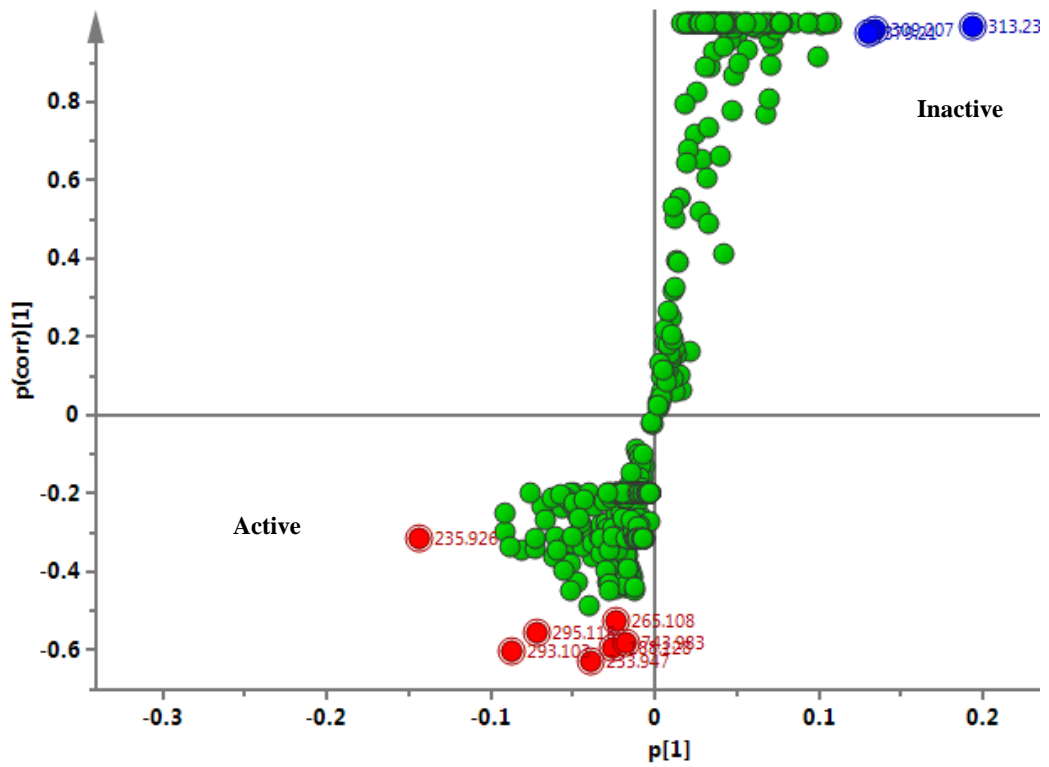
b)

Figure 3.4: OPLS-DA analysis on small scale of *Fusarium* sp. extracts

(a) Supervised OPLS-DA score plot analysis showed good separation between rice culture extract (FRC7, FRC15, FRC30) and liquid culture extract (FLC7, FLC15, FLC30). FRC15, FRC30, FLC7, FLC15, FLC30 were active (highlight in green) and FRC7 was inactive (highlight in blue) ($R^2(Y)$ =1.00; Q2(Y) =1.00); (b) OPLS-DA S-plot exhibited outlier metabolites on both active (red) and inactive (blue) groups.

Based on the anti-trypanosomal results, the datasets were grouped into active (red) and inactive (blue) extracts; only FRC7 extract were inactive, FLC30 extract showed distinctive separation between them (Figure 3.4 a). The S-plot (Figure 3.4 b) showed the end-point metabolites which have been produced; in which m/z 295.1180 [M-H]⁻ was putatively identified as fusarentin-6-methylether isolated from *F. larvarum* (Grove and Pople, 1979), 293.1030 [M-H]⁻ was identified as 6,7(Z)-phomopsolide A from *Phomopsis oblongo* (Grove, 1985) and *Penicillium* sp. (isolated from *Taxus brevifolia*) (Stierle *et al.*, 1997), and 265.1080 [M-H]⁻ was identified as 3*R*,5*R*-sonnerlactone isolated from *Sonneratia apetala* (Li *et al.*, 2010) which might responsible for the inactivity against trypanosomal activity. Whereas, four unidentified metabolites with m/z 235.9260 and 233.9470 [M-H]⁻, 743.9830 and 188.1280 [M+H]⁺ which have not been reported yet, In the inactive group (blue), the metabolites with m/z 313.2382 [M-H]⁻ was putatively identified as 6-hydroxy-4-oxo-octadecanoic acid isolated from *Hygrophorus discoxanthus* (Gilardoni *et al.*, 2006), 309.2070 [M-H]⁻ was identified as hygrophorone *H. pustulatus* (Lübken *et al.*, 2004), and 379.2100 [M-H]⁻ was not identified in the database. Among these, the small scale extracts on day 15 and 30 for both media were considered for upscaling. The other parameters need to be considered were shorter period of cultivation and yield of the extract, so that the starting material will be enough for further isolation of pure metabolites. Thus, rice culture day 15 (FRC15) was chosen as optimum condition for the production of bioactive metabolites among those extracts.
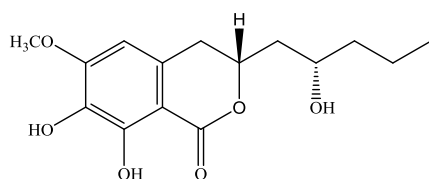
fusarentin-6-methylether
Rt: 9.62
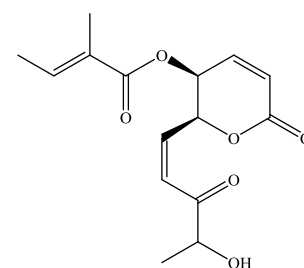
6,7(*Z*)-phomopsolide A
Rt: 7.77
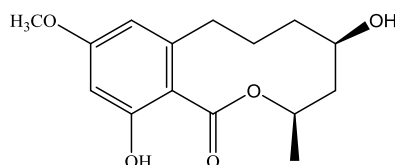
3*R*,5*R*-sonnerlactone,
Rt: 8.34

3.4 Scale up the production of bioactive metabolites on from *Fusarium* sp.

Based on the results from the dereplication studies and anti-trypanosomal activity, it can be concluded that the use of rice culture medium on day 15 was the optimum condition for the production of active secondary metabolites of *Fusarium* sp. The pure *Fusarium* sp. strain was inoculated onto a new agar plate and incubated for 8 days. The agar on which the fungi grew on was cut into small cubes and transferred into 40 x 1L containing rice media (100 g of rice: 100 mL of water) or 20 x 2 L of Erlenmeyer flasks (200 g of rice: 200 mL of water) which have been autoclaved before use and incubated at room temperature for 15 days. The metabolites were extracted using ethyl acetate (1:1, 2x) homogenized and filtered to give an organic phase which was then concentrated under vacuum rotary evaporator (Büchi, Switzerland) to give 11.0 g of crude extract. The total crude extract was analysed using HRESI-LCMS for dereplication studies (Chapter 7.6).

3.4.1 Dereplication studies on total crude of *Fusarium* sp. (FRC15)

The dereplication study on the total crude extract of *Fusarium* sp. was performed as described in Chapter 7.6. The total ion chromatogram of the *Fusarium* sp. crude extract (Figure 3.5) showed distribution of known and unknown compounds present in FRC15 total extract. Most of the metabolites were produced from both marine and terrestrial fungi; *Sclerotinia libertiana, Gibberella fujikuroi, Epidermophyton floccosum, Fusarium* sp., *Aspergillus* sp., Basidiomycetes, *Pestalotiopsis* sp. and *Sphaeropsis sapinea* (Table 3.2). The *m/z* values and predicted formulas of unknown metabolites also were listed in Table 3.3. The metabolites that were putatively identified through dereplication studies on *Fusarium* sp. crude extract (FRC15) were also illustrated in Figure 3.6.
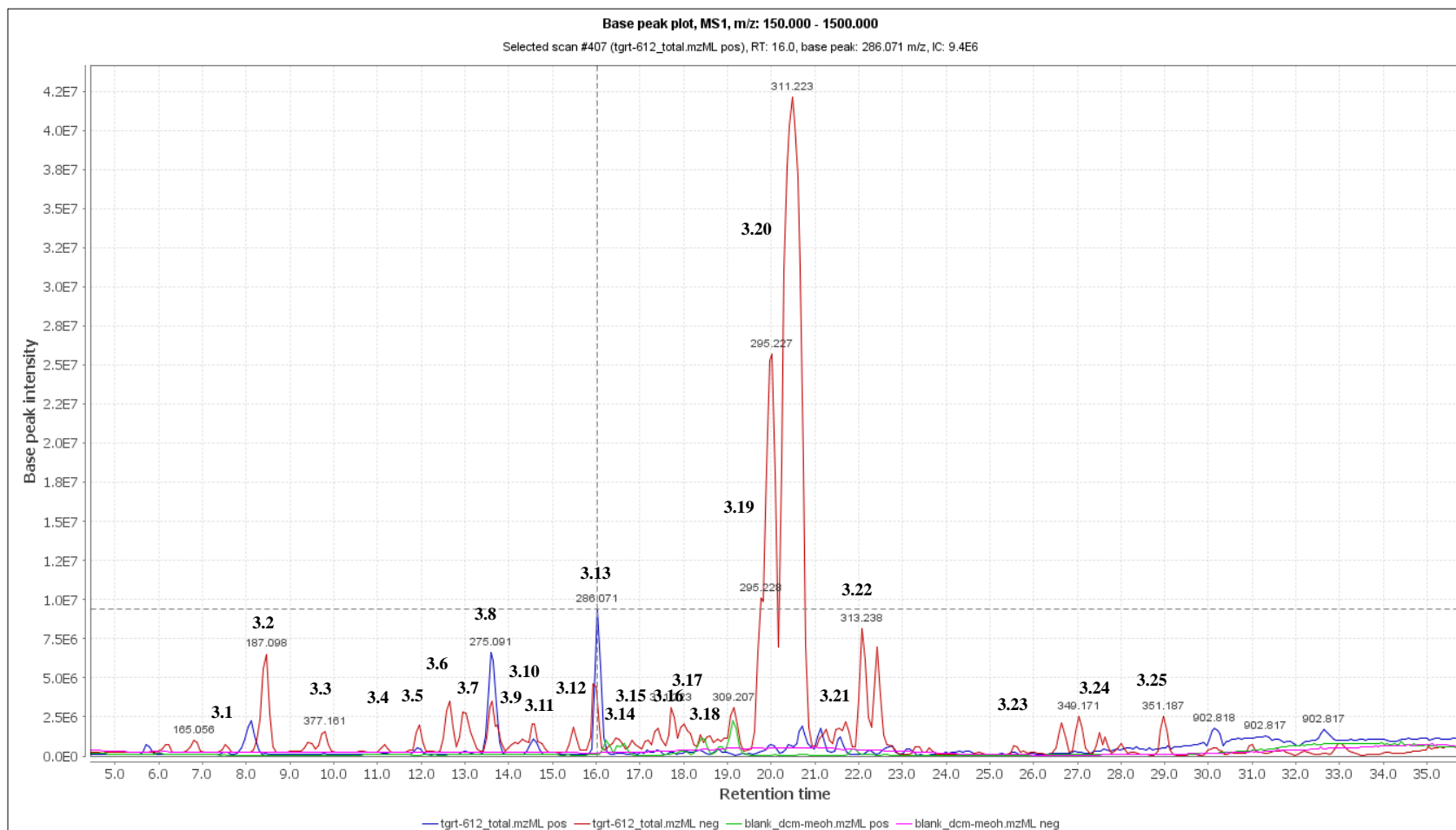
Figure 3.5: Total ion chromatogram of the crude extract of *Fusarium* sp.
in rice media day 15 (FRC15) (blue and red represent positive and negative ionisation modes respectively, for crude extract. Green and pink represent positive and negative ionisation modes respectively, for solvent blank)

Table 3.2: Compounds from the total crude extract of *Fusarium* sp. (FRC15)
that were putatively identified using the Antimarin database (Sources; F-fungi)

No.	ESI modes	Rt (min)	MS (*m/z*)	Molecular weight	Chemical formula	Name	Tolerance (ppm)	Sources	Peak area
3.1	N	7.52	233.0819	234.0892	$C_{13}H_{14}O_4$	sclerin	-0.1035	[F] *Sclerotinia libertiana, Aspergillus carneus*	1.04E+07
3.2	N	8.46	187.0976	188.1049	$C_9H_{16}O_4$	isoaspinonene	0.3467	[F] *Aspergillus ochraceus*	8.81E+07
3.3	N	9.80	377.1607	378.1680	$C_{20}H_{26}O_7$	gibberellin A13	1.7686	[F] *Gibberella fujikuroi*	2.14E+07
3.4	N	11.17	291.0511	292.0584	$C_{14}H_{12}O_7$	floccosic acid	2.0550	[F] *Epidermophyton floccosum*	1.20E+07
3.5	N	11.95	305.0667	306.2670	$C_{15}H_{14}O_7$	fusarubin	1.8790	[F] *Fusarium solani, F. decemcellulare, F. martici-pisi, F. javanicum*	2.21E+07
3.6	N	12.65	329.1396	330.3750	$C_{19}H_{22}O_5$	gibberellin A11	1.9675	[F] *Gibberella fujikuroi*	4.64E+07
3.7	N	12.96	329.2334	330.2407	$C_{18}H_{34}O_5$	9,10,11-trihydroxy-(12Z)-12-octadecenoic acid	0.1969	[F] Chinese truffle Tuber indicum	4.82E+07
3.8	P	13.59	291.0862	290.0789	$C_{15}H_{14}O_6$	javanicin; solanione; F4	1.7472	[F] *Fusarium solani, F. decemcellulare*	8.60E+07
3.9	N	13.75	347.1864	348.1937	$C_{20}H_{28}O_5$	LL-S-491g; sphaeropsidin B	1.6057	[F] *Aspergillus chevalierii* (Lederle S491), [F] Phytopathogenic fungi *Sphaeropsis sapinea, Diplodia mutila,*	2.49E+07
3.10	N	14.31	329.0668	330.0741	$C_{17}H_{14}O_7$	bisdechlorogeodin	2.1585	[F] *Aspergillus fumigatus*; (+): Penicillium [F] *frequentans*; (-) *Oospora sulphurea*	1.42E+07
3.11	P	14.57	291.0862	290.0789	$C_{15}H_{14}O_6$	fonsecin; TMC-256B1	1.5075	[F] *Aspergillus fonsecaeus; Aspergillus carbonarius*	1.54E+07
3.12	N	15.94	333.2073	334.2146	$C_{20}H_{30}O_4$	flexibilide	0.5461	Cnidaria; *Sinularia flexibilis*	5.09E+07
3.13	P	16.04	286.0709	285.0637	$C_{15}H_{11}NO_5$	bostrycoidin	1.7338	[F] *Fusarium solani, F. oxysporum, F. decemcellulare, F. bostrycoides, F. solani*-purple	9.01E+07

Table 3.2: Cont'd. Compounds from the total crude extract of *Fusarium* sp. (FRC15)

3.14	N	16.44	327.2179	328.2251	$C_{18}H_{32}O_5$	sch-725674	0.5532	[F] *Aspergillus* sp.	2.46E+07
3.15	N	16.82	343.2127	344.2200	$C_{18}H_{32}O_6$	gallicynoic acid F	1.9340	[F] Basidiomycete; *Coriolopsis gallica*	1.61E+07
3.16	N	17.20	325.2021	326.2094	$C_{18}H_{30}O_5$	pestalotiopsin B	0.3059	[F] *Pestalotiopsis* sp. (endophytic fungus of *Taxus brevifolia*)	1.76E+07
3.17	N	18.01	347.1995	348.2068	$C_{18}H_{33}ClO_4$	plakortether C	0.0423	Porifera; *Plakortis simplex*	4.81E+07
3.18	N	18.39	307.1917	308.1989	$C_{18}H_{28}O_4$	sorokinianin	0.5743	[F] Phytopathogenic fungus *Bipolaris sorokiniana*	1.47E+07
3.19	N	18.62	295.2278	296.2350	$C_{18}H_{32}O_3$	(1*S*,2*R*)-3-oxo-2-(2*Z*-(1S,2R)-3-oxo-2-pentylcyclopentane-1-octanoic acid	0.3310	*F. oxysporum*	2.67E+07
3.20	N	20.49	311.2228	312.2301	$C_{18}H_{32}O_4$	filoboletic acid	1.7144	[F] Fungus *Filoboletus* sp.	1.19E+09
3.21	N	21.69	297.2435	298.2508	$C_{18}H_{34}O_3$	D-12-hydroxy-9-octadecenoid acid; ricinoleic acid	0.0901	[F] Ascomycetes, Basidiomycetes	3.63E+07
3.22	N	22.07	313.2382	314.2458	$C_{18}H_{34}O_4$	6-hydroxy-4-oxo-octadecanoic acid	0.1789	[F] Basidiomycete; *Hygrophorus discoxanthus*	1.87E+08
3.23	N	25.54	715.5327	716.5400	$C_{47}H_{72}O_5$	variabilin 5,9-tetracosadienoate	2.8351	Porifera *Ircinia felix*	6771285
3.24	N	27.50	393.2651	394.2724	$C_{23}H_{38}O_5$	15-acetoxyhexadecylcitraconic anhydride	2.5321	[F] *Aspergillus wentii*	1.48E+07
3.25	N	28.97	351.1865	352.1937	$C_{18}H_{34}Cl_2O_2$	9,10-dichlorostearic acid	1.9680	[F] *Verticillium dahliae*	2.96E+07

* The highlighted rows were compounds isolated from *Fusarium* sp.

Table 3.3: Compounds present in the crude extract of *Fusarium* sp. (FRC15) that were unidentified using the Antimarin database

ESI modes	Rt (min)	MS (*m/z*)	Molecular weight	Peak area
N	6.23	151.0400	152.0473	1.54E+07
P	8.12	164.1071	163.0998	3.85E+07
N	13.64	929.1953	930.2026	3.72E+07
N	14.60	923.1485	924.1558	2.60E+07
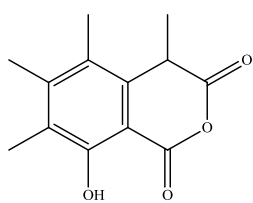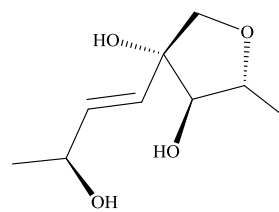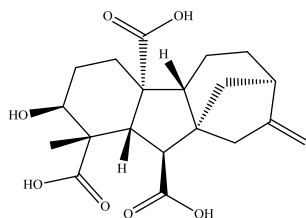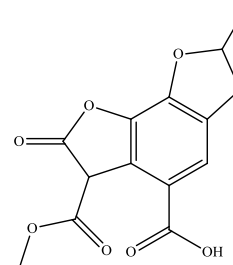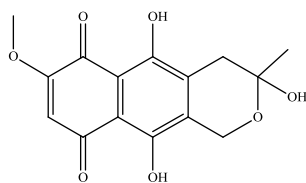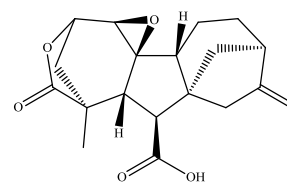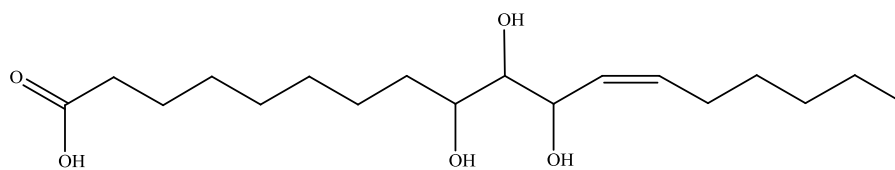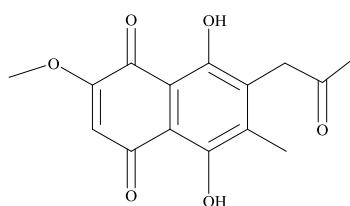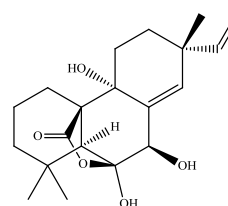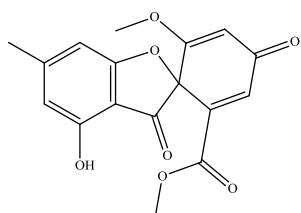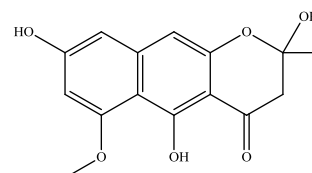
Figure 3.6: Compounds that were putatively identified through dereplication studies on *Fusarium* sp. (FRC15) crude extract
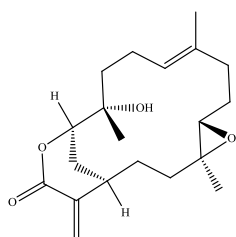
3.12
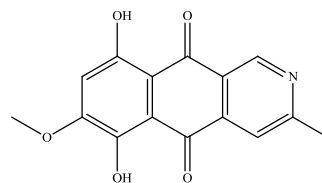
3.13
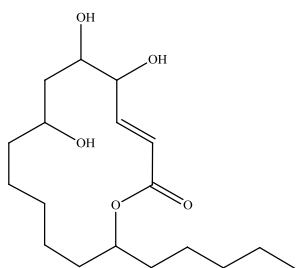
3.14
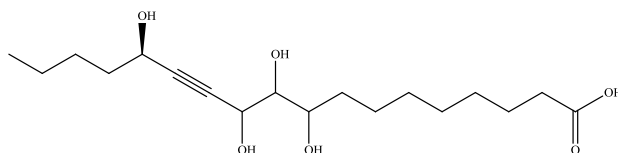
3.15
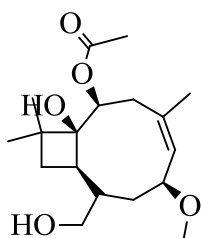
3.16
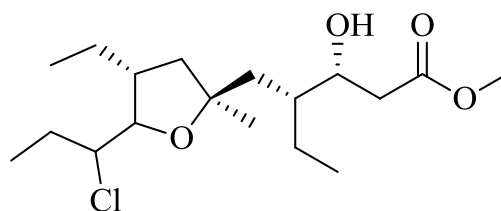
3.17
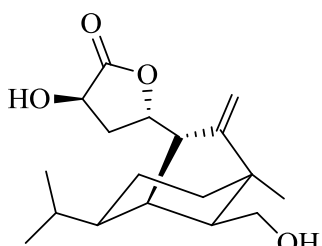
3.18
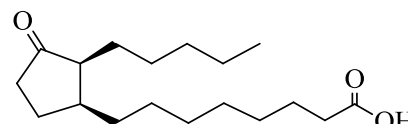
3.19
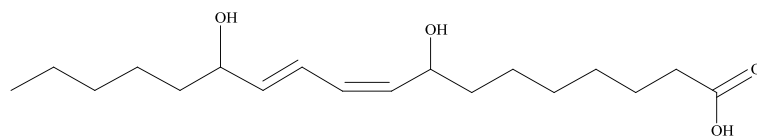
3.20
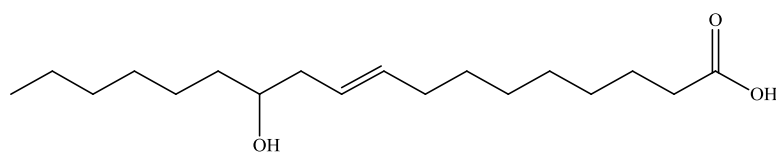
3.21

Figure 3.6: Cont'd. Compounds that were putatively identified through dereplication studies on *Fusarium* sp. (FRC15) crude extract

3.22

3.23

3.24

3.25
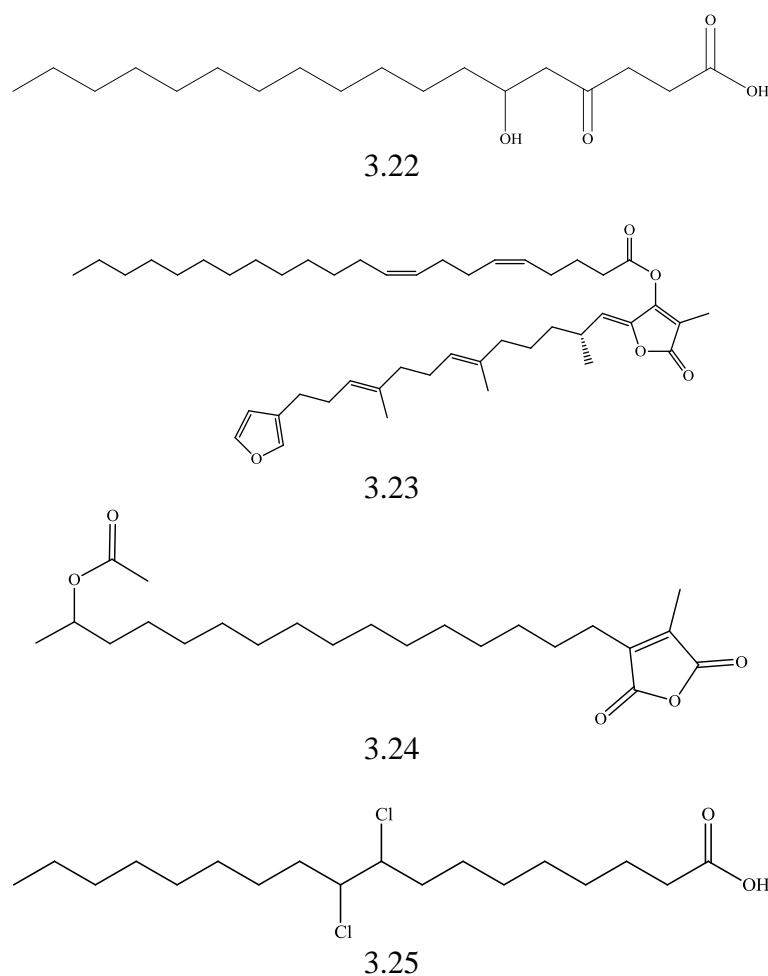
Figure 3.6: Cont'd. Compounds that were putatively identified
through dereplication studies on *Fusarium* sp. (FRC15) crude extract

3.4.2   Isolation of secondary metabolites from *Fusarium* sp.

Thin layer chromatography (TLC) was applied to the *Fusarium* sp. (FRC15) crude
extract using a range of different solvent systems to determine the polarity of
compounds. The TLC plate was examined under ultraviolet radiation (UV) to
observe the profile of UV-active compounds and the TLC plate was sprayed with a
universal reagent, anisaldehyde-sulphuric acid and heated to check for non-UV
active compounds (Chapter 7.8.1). The total crude extract of *Fusarium* sp. (11.0 g)
was fractionated by using medium pressure liquid chromatography (Büchi,
Switzerland) with gradient elution using hexane-ethyl acetate-methanol (100%
Hexane:0% ethyl acetate, up to 100% ethyl acetate, 100% ethyl acetate: 0%
methanol up to 30% ethyl acetate:70% methanol) to give a number of sub-fractions.
The sub-fractions were combined based on the TLC profiles to give 16 major

fractions of FRC15. The 16 major fractions were analysed using HRESI-LCMS for dereplication study and tested for anti-trypanosomal activity. The active major fractions were subjected to further isolation and purification using column chromatography and flash chromatography (Grace Reveleris, USA and Biotage Isolera One, Sweden) using normal and reverse phase chromatography and appropriate size columns (Reveleris, USA and SNAP, Sweden).

3.4.3 Bioactivity test results on *Fusarium* sp. (FRC15) fractions

Fractions FRC15-1, 2 and 3 showed less activity while other fractions exhibited strong anti-trypanosomal activity (Table 3.4).

Table 3.4: Anti-trypanosomal activity of *Fusarium* sp. (FRC15) fractions (calculated as mean value of percentage viability) at concentrations of 20 µg/mL

Fractions	Yield (g)	*T. b. brucei*, % D control (20 µg/mL)
FRC15-1	0.7672	45.8
FRC15-2	0.2895	26.8
FRC15-3	0.1695	39.5
FRC15-4	0.0850	1.9
FRC15-5	0.0413	5.8
FRC15-6	0.1105	1.1
FRC15-7	0.1120	-0.3
FRC15-8	0.2415	2.8
FRC15-9	0.3076	-1.6
FRC15-10	0.2264	-0.9
FRC15-11	0.2858	-4.1
FRC15-12	0.7044	-0.7
FRC15-13	0.3961	2.7
FRC15-14	0.1786	1.0
FRC15-15	0.5199	0.3
FRC15-16	0.1854	0.4

% D, percentage viability of control

3.4.4 Multivariate analysis on *Fusarium* sp. (FRC15) fractions

Further investigation on *Fusarium* sp. (FRC15) fractions was carried out by evaluating the metabolites in each fraction and its relationship with their bioactivity against *T. b. brucei*. The unsupervised PCA score plot analysis (Figure 3.7 a) showed the distribution of all fractions in which fractions FRC15-6, 10 and 12 distributed away from other fractions. Meanwhile, the supervised OPLS-DA plot

(Figure 3.7 b) showed distinctive separation on fractions FRC15-10, 11 and 12 compared with other fractions, and fractions FRC15-2 and 3 were distributed in the inactive group.
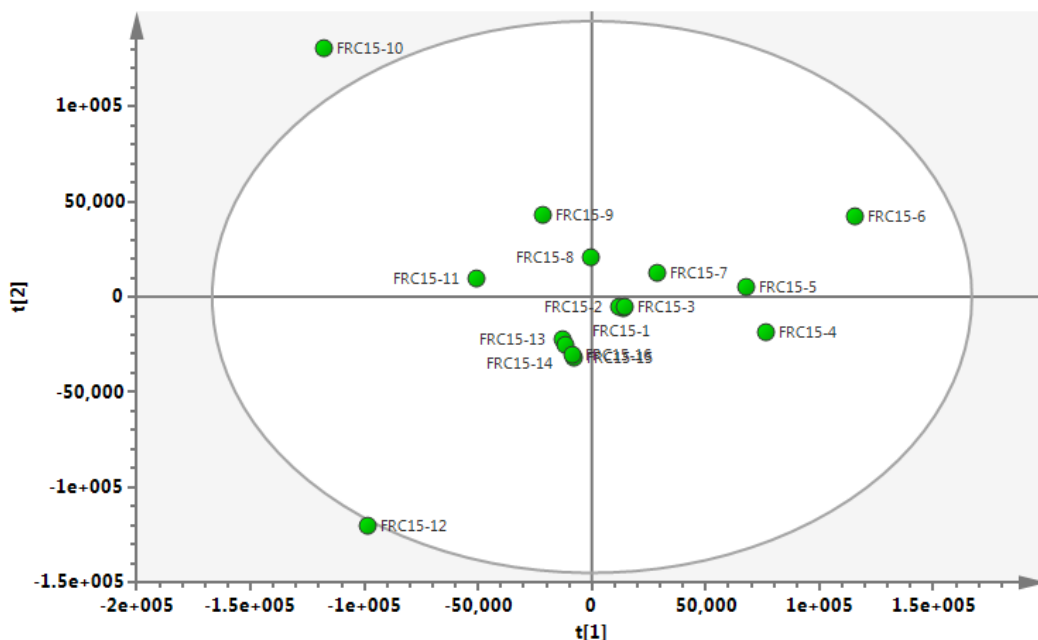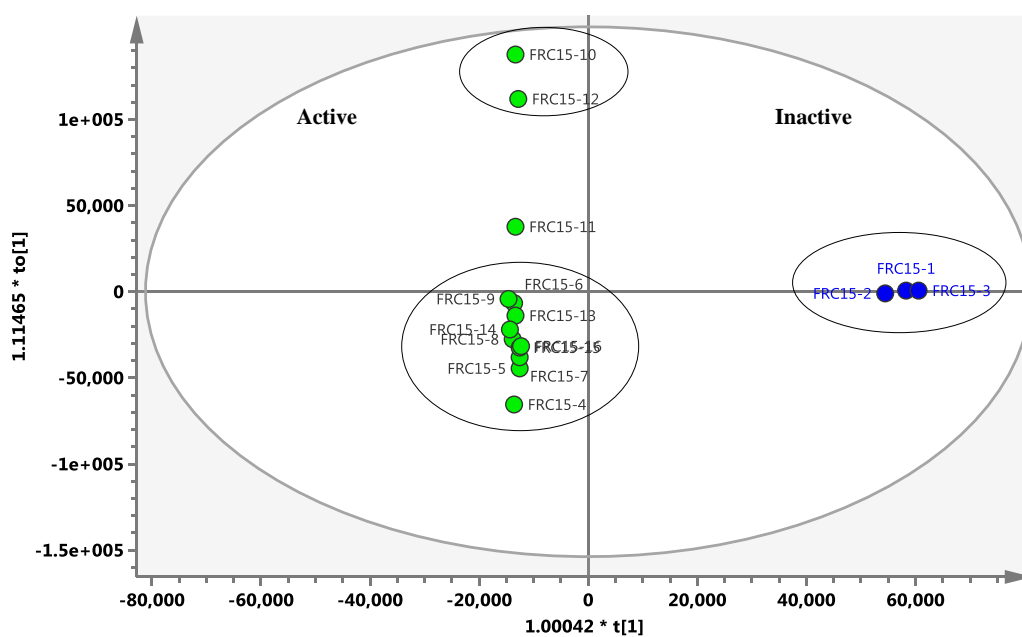
Figure 3.7: PCA analysis on *Fusarium* sp. (FRC15) fractions
(a) Unsupervised PCA score plot analysis of the *Fusarium* sp. (FRC15) fractions showed moderate separation between the datasets except for fractions FRC15-6, 10 and 12; (b) Supervised OPLS-DA score plot analysis showed good separation between active and inactive fractions; FRC15-10, 11, and 12 in active group showed distinctive separation compared with other fractions and FRC15-2 and 3 were inactive separated further ($R^2(Y) =0.998; Q2(Y) =0.390$).

The metabolites which highlighted red in S-plot were in active fractions (Figure 3.8) with *m/z* 289.0723 and 291.0862 [M+H]$^+$ were putatively identified as anhydrofusarubin (**3.28**) and javanicin (**3.8**), respectively, which have been previously isolated from *Fusarium* species-*F. decemcellulare* (Medentsev *et al.*, 1988) and *F. solani* (Tatum and Baker, 1983) . Meanwhile, the metabolite with *m/z* 291.0874 [M+H]$^+$ was not identified may due to be another isomer of javanicin. The metabolite with *m/z* 293.1031 [M+H]$^+$ was putatively identified as solaniol (**3.26**), which has been isolated from *F. solani*; "Munissi MUF2" (Kimura *et al.*, 1988). The metabolite with *m/z* 295.2280 [M-H]$^-$ was putatively identified as (1*S*,2*S*)-3-oxo-2(2Z-pentenyl)cyclopentane-1-octanoic acid (**3.19**) which has been previously isolated from *F. oxysporum* (Miersch *et al.*, 1999).
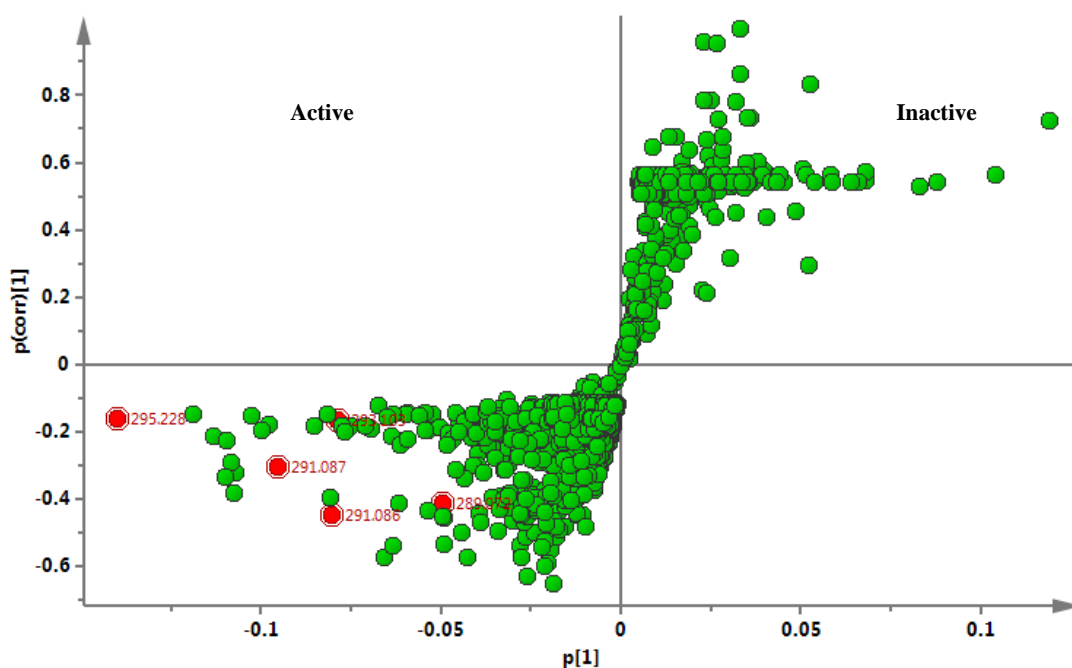
Figure 3.8: S-plot exhibited the end-point metabolites on both active and inactive groups

3.8
Rt: 14.46 mins

3.19
Rt: 19.96 mins

3.26
Rt: 10.04 mins

3.28
Rt; 14.53 mins
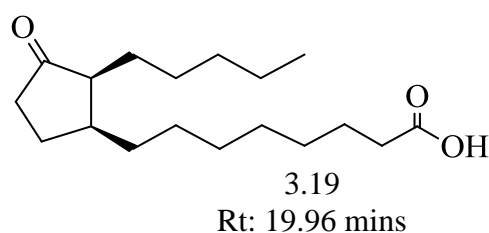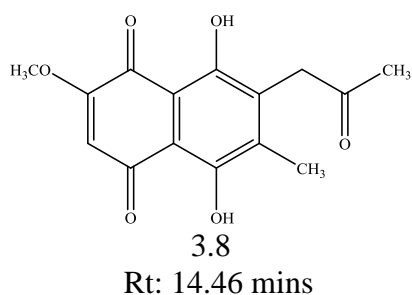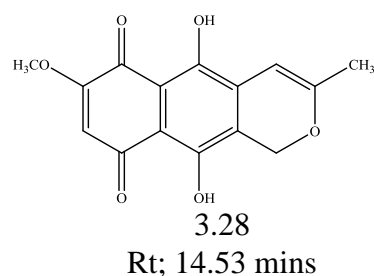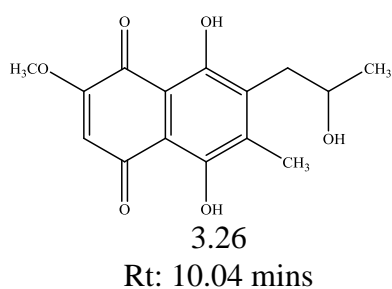
3.5   Isolation of secondary metabolites from *Fusarium* sp. (FRC15)

A summary of workflow on the *Fusarium* sp. (FRC15) crude extract was shown in Figure 3.9. All of the *Fusarium* sp. 16 fractions were monitored on TLC plate for profiling detected under UV light and after spraying the TLC plate with the reagent *p*-anisaldehyde-sulphuric acid (Figure 3.10). Each fraction was analysed using HRESI-LCMS for further dereplication study as well as tested against anti-trypanosomal activity. The active fractions were subjected to isolation and purification and yielded five compounds. Isolation work on fraction FRC15-3 gave a pale yellow oil elucidated as ergosterol peroxide (FRC15-3-r2-10, (**3.27**), 3.2 mg, 0.03%) and purification of fraction FRC15-4 yielded violet crystals of anhydrofusarubin (FRC15-4-F4, (**3.28**), 7.3 mg, 0.07%). Purification of fraction FRC15-6 gave dihydrojavanicin (FRC15-6-r2-13, (**3.29**), 2.4 mg, 0.02%). Further isolation on fraction FRC15-8 gave red crystals of javanicin (FRC15-8-F8c, (**3.8**), 5.7 mg, 0.05%). Purification of fraction FRC15-11 gave red crystals of solaniol (FRC15-11-F11, (**3.26**), 7.0 mg, 0.06%).
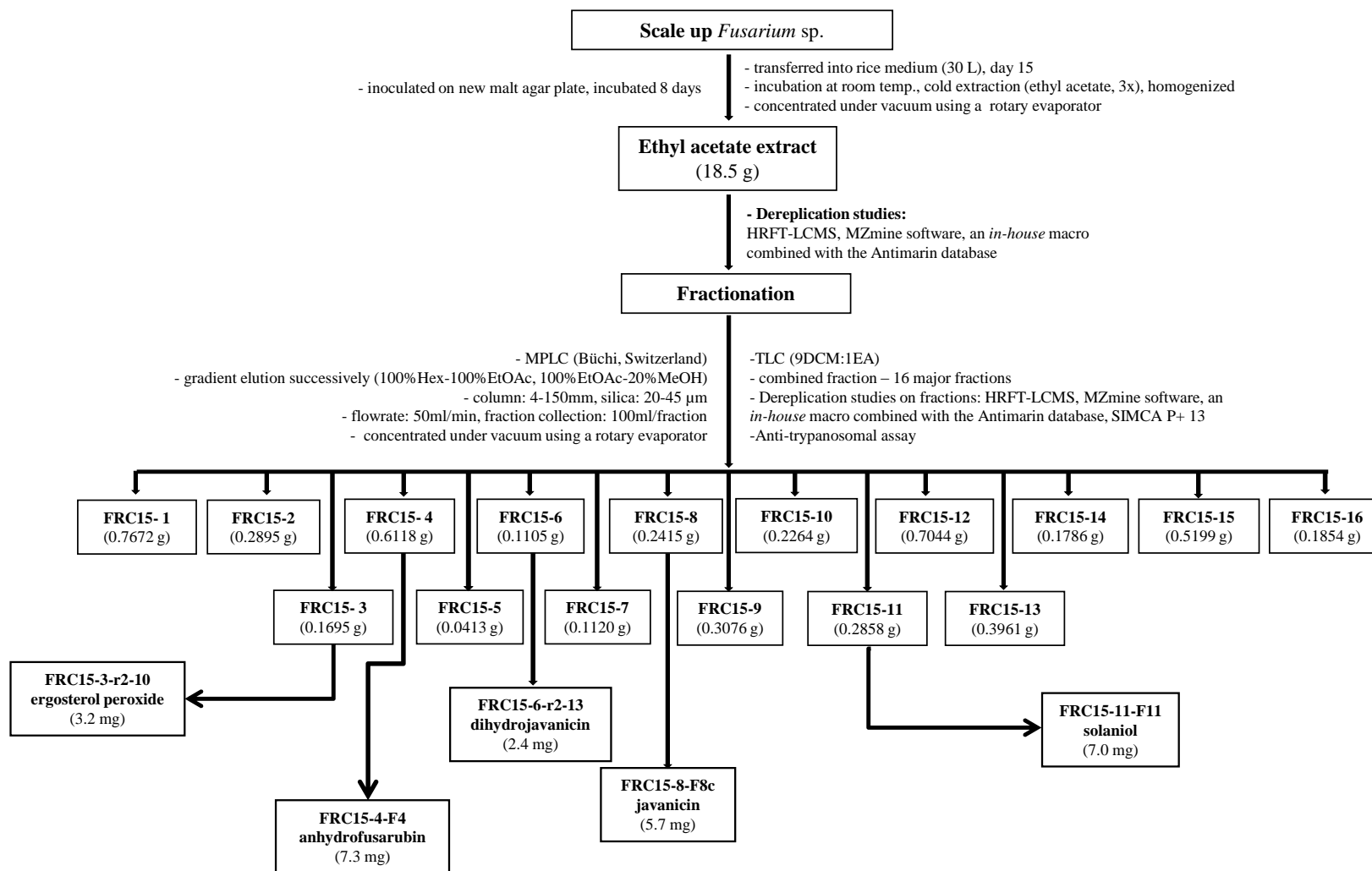
Figure 3.9: A summary of workflow on the *Fusarium* sp. (FRC15) crude extract
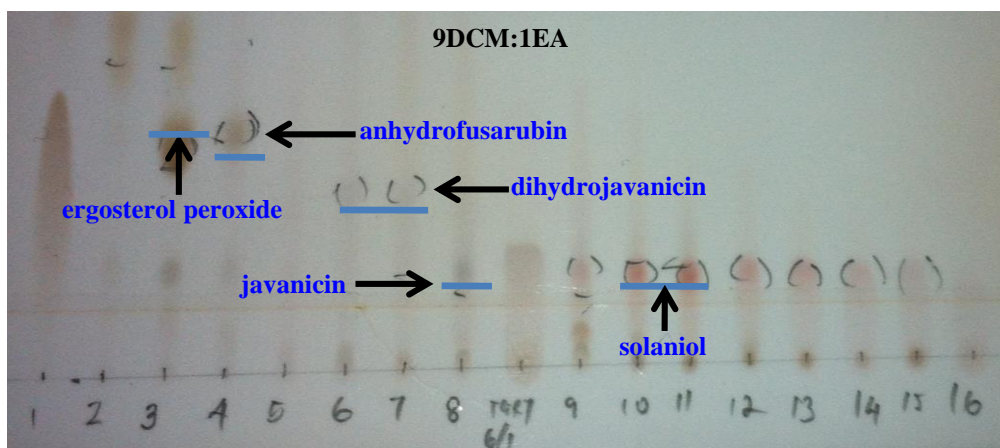
Figure 3.10: TLC summary plate on *Fusarium* sp. (FRC15) fractions
after spraying with *p*-anisaldehyde-sulphuric acid

3.6 Structure elucidation and identification on secondary metabolites from *Fusarium* sp.

The chemical constituents from a 15-day rice culture of the endophytic fungus *Fusarium* sp. (FRC15) yielded ergosterol peroxide (**3.27**) along with four metabolites with 1,4-naphthoquinones of the naphthazarin related structure.

3.6.1 Compound FRC15-3-r2-10 (ergosterol peroxide, 3.27)

Compound FRC15-3-r2-10 (3.2 mg) was obtained as light yellow oil and HRMS showed exact mass at *m/z* 428.3290 [M]$^+$ corresponding to the molecular formula $C_{28}H_{44}O_3$ and optical rotation $[\alpha]_D^{20}$ +25° (*c* 0.10, (CHCl$_3$).

Synonyms	ergosterol peroxide, ergosterol endoperoxide, peroxy-ergosterol 5α,8α-epidioxy-22*E*-ergosta-6,22-dien-3β-ol
Sample code	FRC15-3-r2-10 (**3.27**)
Sources	*Fusarium* sp.
Yield (mg, %)	3.2 mg (0.03%)
Physical state	Light yellow oil
Mol. formula	$C_{28}H_{44}O_3$
Exact mass (*m/z*)	428.3290 [M]$^+$
Mol. weight (g/mol)	428.6472
R$_f$ value (9DCM:1M)	0.73
Optical rotation $[\alpha]_D^{20}$	+25° (*c* 0.10, (CHCl$_3$)
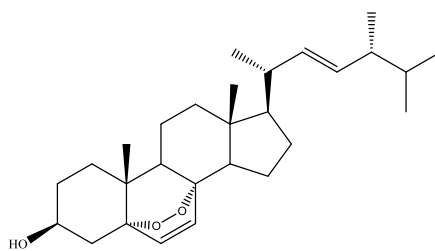
3.27

Table 3.5: ^{1}H and ^{13}C NMR of compounds FRC15-3-r2-10
(CDCl$_3$, ^{1}H 400 MHz, ^{13}C 100.5 MHz) and comparison with previous data

No.	^{1}H NMR, δ_H (ppm, multi. J in Hz)		^{13}C NMR, δ_C (ppm)	
	FRC15-3-r2-10	[a, b] ergosterol peroxide	FRC15-3-r2-10	[a, b] ergosterol peroxide
1	-	-	34.8	34.7
2	-	-	30.2	30.0
3	3.96 (*m*, 1H)	3.98 (*m*, 1H)	66.6	66.2
4	-	-	37.0	36.8
5	-	-	79.6	79.3
6	6.50 (*d*, *J*=8.5 Hz, 1H)	6.54 (*d*, *J*=8.3 Hz, 1H)	135.3	135.0
7	6.23 (*d*, *J*=8.5 Hz, 1H)	6.27 (*d*, *J*=8.3 Hz, 1H)	130.8	130.5
8	-	-	82.2	82.1
9	-	-	51.1	51.0
10	-	-	39.4	39.3
11	-	-	20.7	20.6
12	-	-	39.4	39.3
13	-	-	44.6	44.5
14	-	-	51.8	51.6
15	-	-	23.5	23.4
16	-	-	28.7	28.6
17	-	-	56.3	56.1
18	0.87 (*s*, 3H)	0.90 (*s*, 3H)	13.0	12.8
19	0.81 (*s*, 3H)	0.82 (*s*, 3H)	20.0	20.8
20	-	-	39.8	39.6
21	0.99 (*d*, *J*=6.6 Hz, 3H)	1.00 (*d*, *J*=6.6 Hz, 3H)	21.0	20.8
22	5.18 (*m*, 1H, H-22)	5.19 (*m*, 1H, H-22)	135.5	135.3
23	5.18 (*m*, 1H, H-23)	5.19 (*m*, 1H, H-23)	132.4	132.1
24	-	-	42.9	42.7
25	0.90 (*d*, *J*=6.8 Hz, 3H)	0.91 (*d*, *J*=7.3 Hz, 3H)	17.6	17.5
26	-	-	33.1	33.0
27	0.83 (b*s*, 3H)	0.83 (*d*, *J*=6.6 Hz, 3H)	18.3	19.9
28	0.80 (b*s*, 3H)	0.81 (*d*, *J*=6.6 Hz, 3H)	19.6	19.6

[a](Ramos-Ligonio *et al.*, 2012), [b](da Graça Sgarbi *et al.*, 1997)

^{1}H NMR spectrum of FRC15-3-r2-10 (Figure 3.11 a, Table 3.5) showed signals which corresponded also to a sterol compound with two downfield doublets of the olefinic proton signals were showed at δ_H 6.50 (*d*, *J*=8.5 Hz, 1H) and 6.23 (*d*, *J*=8.5 Hz, 1H) which corresponded to H-6 and H-7 respectively and the other olefinic signals were shown by δ_H 5.18 (*m*, 2H) indicated of H-22 and H-23. A downfield methine proton due to electronegative effect from oxygen on the same carbon was indicated by a signal at δ_H 3.96 (*m*, 1H, H-3). Meanwhile, six methyl proton signals were also appeared. The ^{13}C NMR results (Figure 3.11, Table 3.5) showed 28 carbon signals with two unsaturated carbon signals at δ_C 135.3 and 130.8 corresponded to C-6 and C-7 and δ_C 135.5 and 132.4 representing C-22 and C-23. Besides, three oxygenated carbon signals were observed, one of them was a methine carbon at δ_C 66.6 (C-3) and two quaternary carbon at δ_C 79.6 and 82.2 corresponded to C-5 and C-8 respectively. Based on the NMR spectra and comparison with authentic spectra data (Ramos-Ligonio *et al.*, 2012, da Graça Sgarbi *et al.*, 1997, Yoo *et al.*, 2006), this compound was identified as ergosterol peroxide.

a)
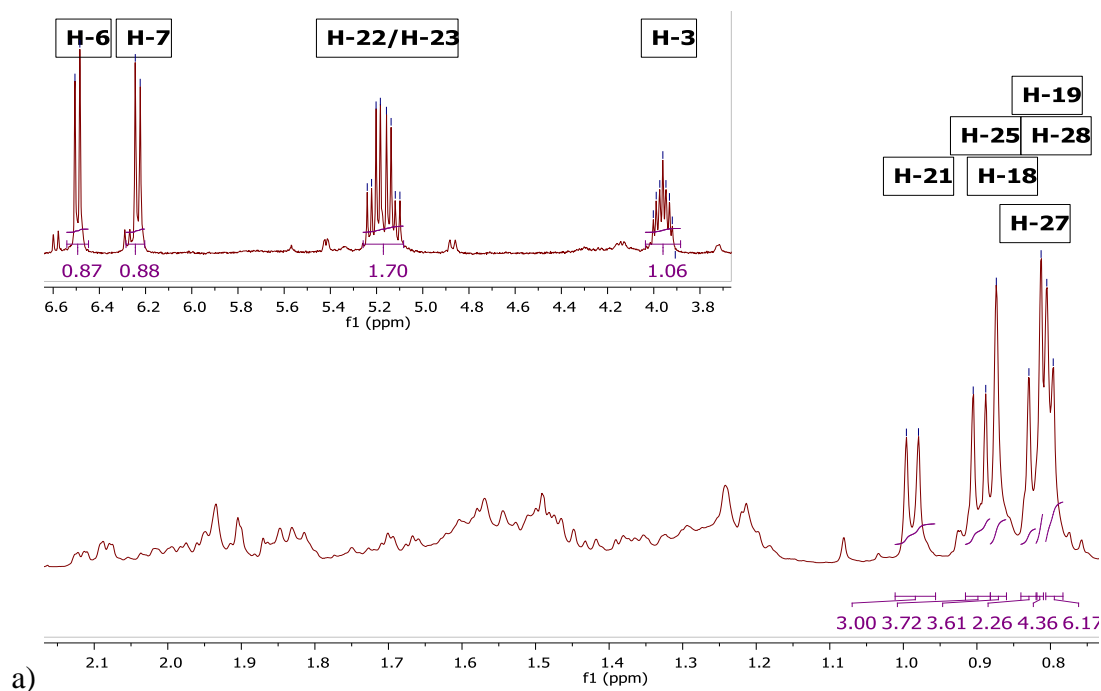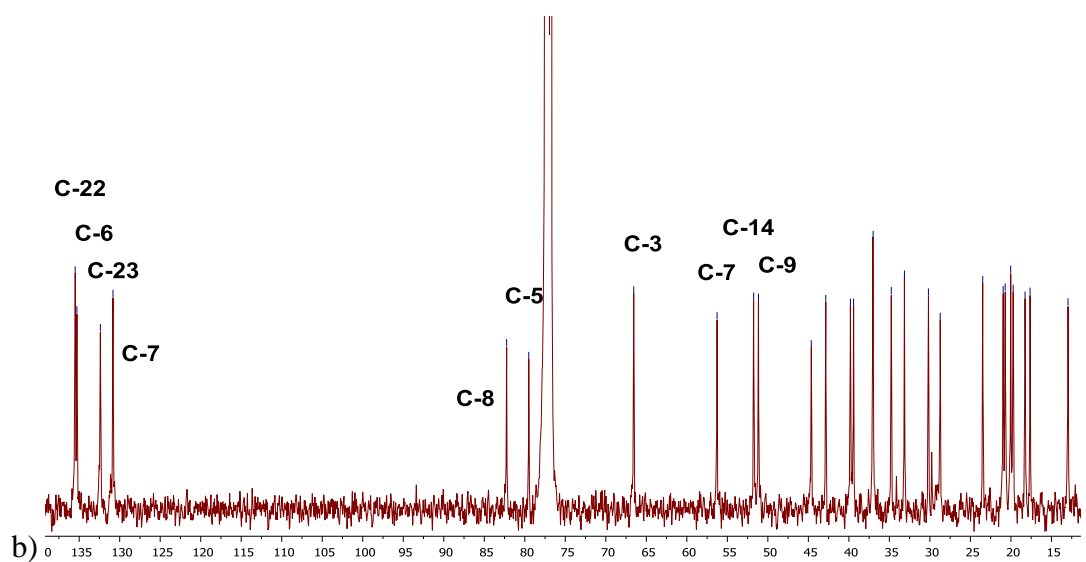
Figure 3.11: (a) ^{1}H (b) ^{13}C NMR spectra of FRC15-3-r2-10
(CDCl$_3$, ^{1}H 400 MHz, ^{13}C 100.5 MHz)
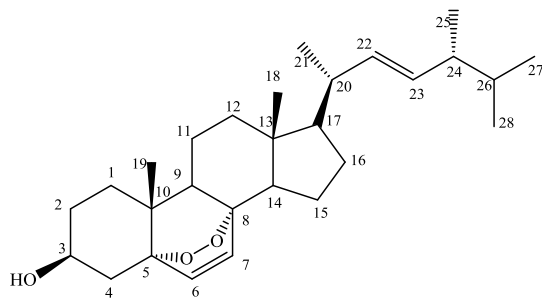
3.27

Synonyms	anhydrofusarubin, F-6	javanicin, solanione, F-4	dihydrojavanicin	solaniol, F-2
Sample code	FRC15-4-F4 (**3.28**)	FRC15-8-F8c (**3.8**)	FRC15-6-r2-13 (**3.29**)	FRC15-11-F11 (**3.26**)
Sources	*Fusarium* sp.	*Fusarium* sp.	*Fusarium* sp.	*Fusarium* sp.
Yield (mg, %)	7.3 mg (0.07%)	5.7 mg (0.05%)	2.4 mg (0.02%)	7.0 mg (0.06%)
Physical state	Violet needles	Red needles	Yellow needles	Red needles
Mol. formula	$C_{15}H_{12}O_6$	$C_{15}H_{14}O_6$	$C_{15}H_{14}O_6$	$C_{15}H_{16}O_6$
Mol. weight (g/mol)	288.0632	290.0789	290.0790	292.0944
Exact mass (*m/z*)	289.0707 [M+H]$^+$	291.0862 [M+H]$^+$	291.0860 [M+H]$^+$	293.1020 [M+H]$^+$
Ret. time (min)	18.71	14.53	13.80	13.62
R_f value (9DCM:1M)	0.66	0.34	0.29	0.22

3.28

3.8

3.29

3.26

RT: 0.00 - 45.09

18.71

5.97 7.65 8.85 11.10 13.50 15.25 17.07 19.83 20.76 23.05 24.86

Time (min)
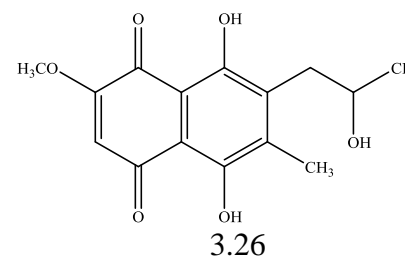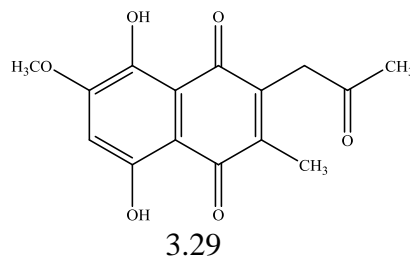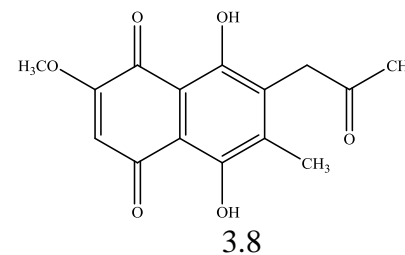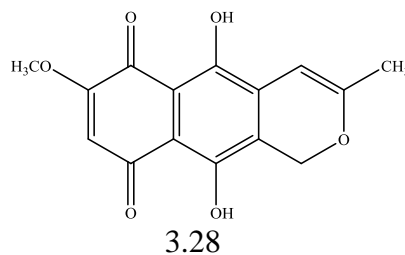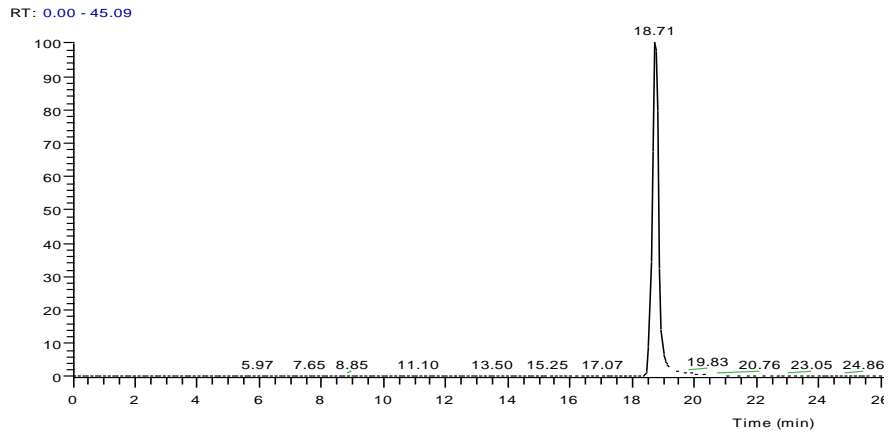
tgrt-612_4 #460-491 RT: 18.23-19.21 AV: 16 SB: 489 19.11-35.47 , 0.03-18.27 NL: 5.40E6
T: FTMS {1,1} + p ESI Full lock ms [150.00-1500.00]

289.0707
$C_{15}H_{13}O_6$

289.1117

289.0200

288.0635
$C_{15}H_{12}O_6$

288.5780

289.4194

290.0737

290.0230 290.1170

m/z

a)

RT: 0.00 - 45.09

14.53

1.63 3.56 4.68 6.79 9.26 10.38 13.85 15.34 16.90 18.80 20.62 21.99 24.88

Time (min)
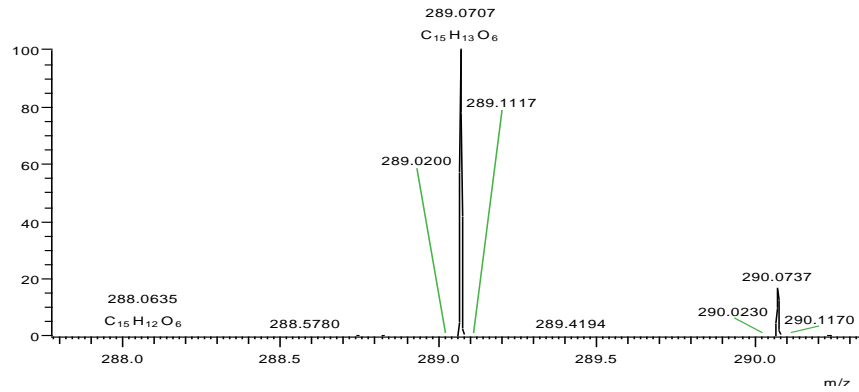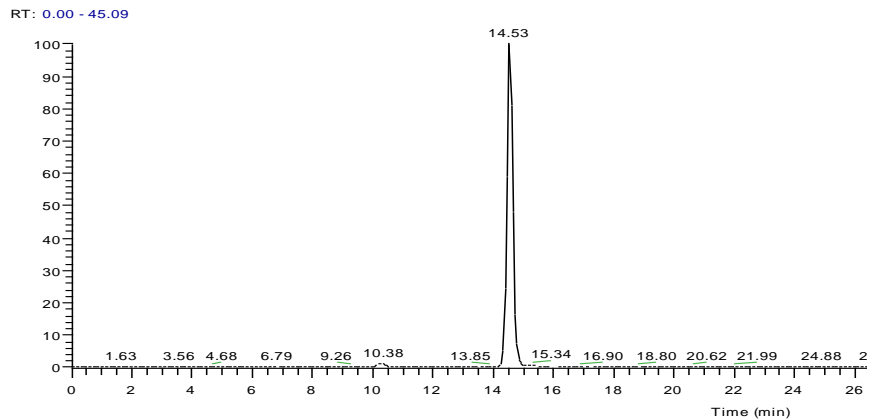
tgrt-612_8 #343-392 RT: 13.62-15.41 AV: 25 SB: 581 14.94-45.09 , 0.03-14.09 NL: 3.36E5
T: FTMS {1,1} + p ESI Full lock ms [150.00-1500.00]

291.0862
$C_{15}H_{15}O_6$

293.1017
$C_{15}H_{17}O_6$

292.0893

290.1005

290.9752

291.1821 291.6373

292.1903

293.0061

293.1723

b)

m/z

113

RT: 0.00 - 45.10
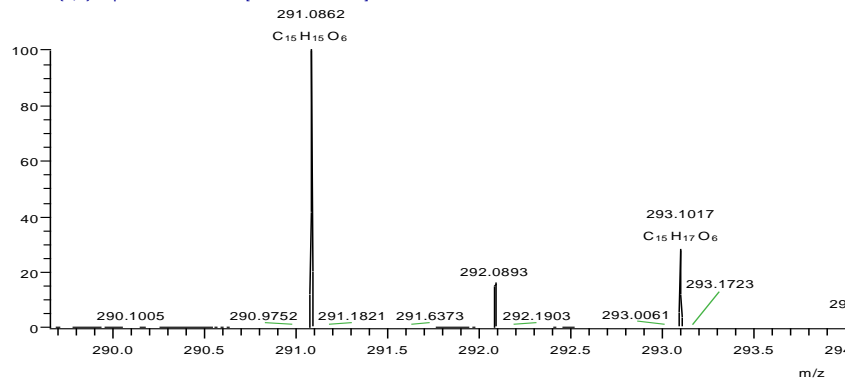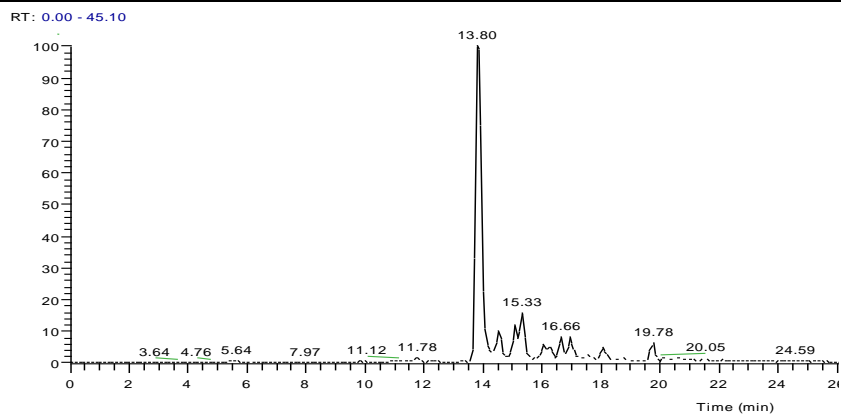
tgrt-612_6 #343-364 RT: 13.49-14.22 AV: 11 SB: 550 14.29-41.21 , 0.03-13.28 NL: 3.44E4
T: FTMS {1,1} + p ESI Full lock ms [150.00-1500.00]

c)

RT: 0.00 - 45.06
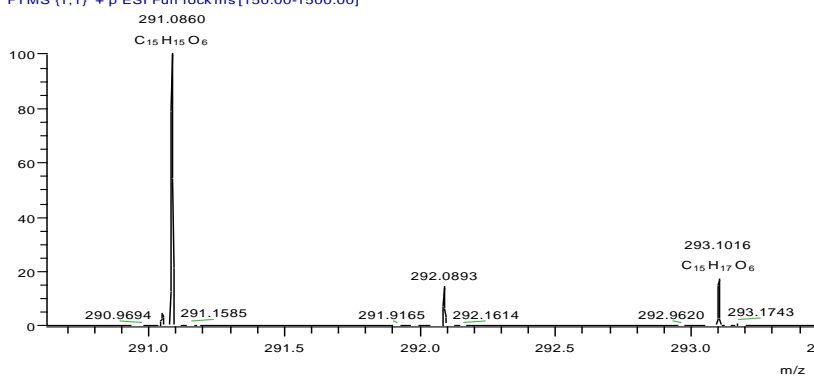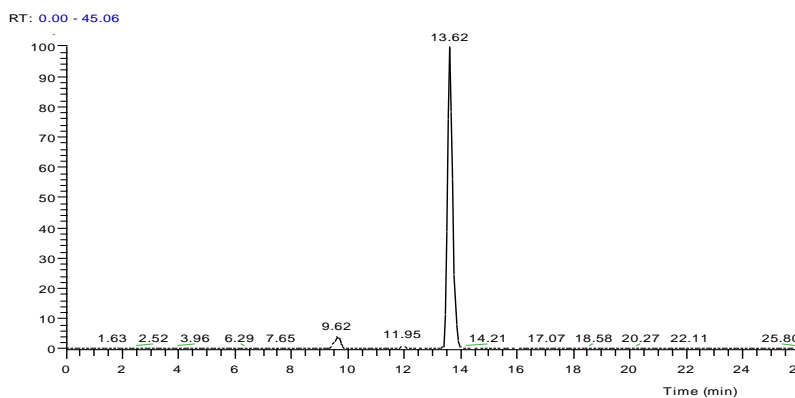
tgrt-612_11 #329-384 RT: 12.83-14.67 AV: 28 SB: 580 13.99-45.06 , 0.03-13.22 NL: 3.48E6
T: FTMS {1,1} + p ESI Full lock ms [150.00-1500.00]
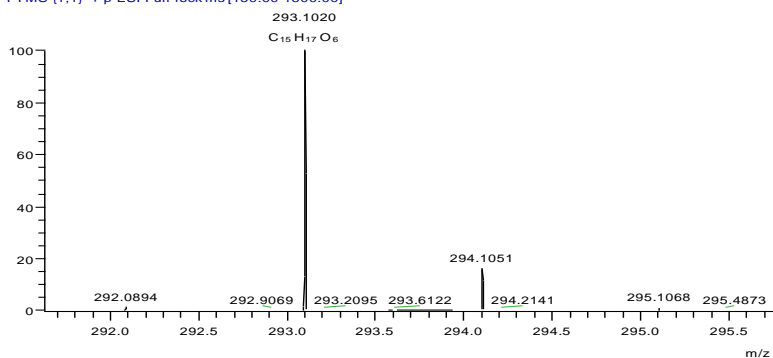
d)

The positive ionisation mode for the HRMS of a) anhydrofusarubin; b) javanicin; c)
dihydrojavanicin; and d) solaniol.

3.6.2   Compound FRC15-4-F4 (anhydrofusarubin, 3.28)

Compound FRC15-4-F4 (7.3 mg) was obtained as violet needles and the molecular formula was determined to be $C_{15}H_{12}O_6$ by HRESI-MS (exact mass at *m/z* 289.0707 [M+H]$^+$). The ^1H NMR spectrum of this compound (Figure 3.12, Table 3.6) showed the presence of two aromatic proton signals: δ_H 6.19 (*s*, 1H) and 6.01 (*s*, 1H). A methylene proton signal was found at δ_H 5.23 (*s*, 2H) directly attached to an oxygen on C ring corresponded to H-13, a methoxy at δ_H 3.92 (*s,* 3H) and a methyl at δ_H 2.01 (*s*, 3H). The ^{13}C NMR results (Table 3.7) showed eight quaternary carbon which were six of them attached to oxygen- δ_C 183.2 (C-4), 177.8 (C-1), 162.2 (C-10), 158.4 (C-5/C-8) and 160.6 (C-2), and the other two were at δ_C 133.6 (C-7) and 123.1 (C-6). Meanwhile, the HMBC spectrum (Figure 3.13) indicated that the H-3 correlated to C-1, C-2, C-4 and C-4a. The other important correlations were shown by the methylene proton H-13 with C-5, C-6, C-7 and C-10, between methyl proton H-11 and C-9 and C-10, as well as the correlation between H-9 to C-6, C-8 and C-10. The remaining correlations were described as in Figure 3.14. Therefore, this compound was identified as anhydrofusarubin which has also previously been isolated from fungus *Fusarium solani* (Kimura *et al.*, 1988).
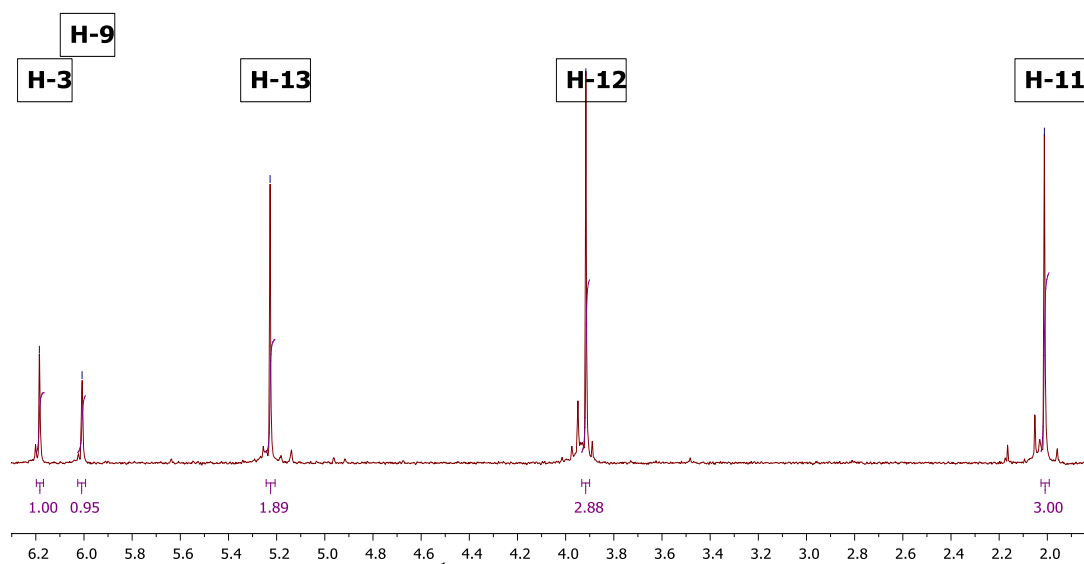
Figure 3.12: ^1H NMR spectrum of FRC15-4-F4
(CDCl$_3$, ^1H 400 MHz)
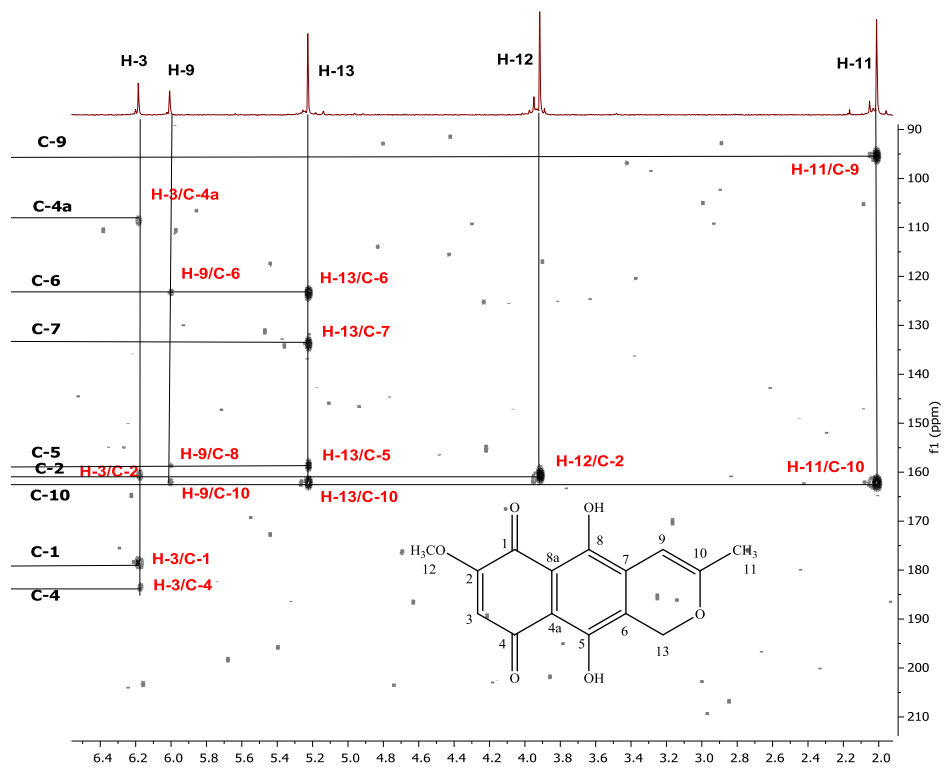
Figure 3.13: HMBC NMR spectrum of FRC15-4-F4
(CDCl$_3$, ^{1}H 400 MHz, ^{13}C 100.5 MHz)
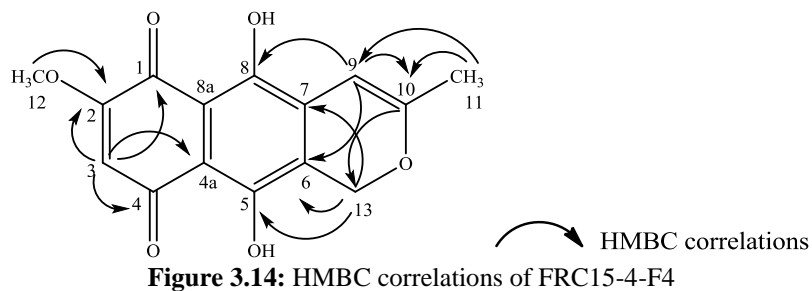
Figure 3.14: HMBC correlations of FRC15-4-F4

116

Table 3.6: ^{1}H NMR of naphthazarin derivatives related structure
FRC15-4-F4, FRC15-8-F8c, FRC15-6-r2-13, FRC15-11-F11 (CDCl₃, 400 MHz) and comparison with previous data

No.	^{1}H NMR, δ_H (multi. J in Hz)						
	FRC15-4-F4	*anhydrofusarubin	FRC15-8-F8c	*javanicin	FRC15-6-r2-13	FRC15-11-F11	*solaniol
1	-	-	-	-	-	-	-
2	-	-	-	-	-	-	-
3	6.19 (s, 1H)	6.20 (s, 1H)	6.21 (s, 1H)	6.25 (s, 1H)	7.15 (s, 1H)	6.19 (s, 1H)	6.11 (s, 1H)
4	-	-	-	-	-	-	-
4a	-	-	-	-	-	-	-
5	-		-			-	-
6	-	-	-	-	-	-	-
7	-	-	-	-	-	-	-
8	-	-	-	-	-	-	-
8a	-	-	-	-	-	-	-
9	6.01 (s, 1H)	6.02 (s, 1H)	3.91 (s, 2H)	3.92 (s, 2H)	3.77 (s, 2H)	2.94 (d, J=5.9 Hz, 2H)	2.88 (d, J=6.2 Hz, 2H)
10	-	-	-	-	-	4.13 (m, 1H)	4.19 (m, 1H)
11	2.01 (s, 3H)	2.03 (s, 3H)	2.29 (s, 3H)	2.27 (s, 3H)	2.30 (s, 3H)	1.32 (d, 6.2 Hz, 3H)	1.35 (d, 6.0 Hz, 3H)
12	3.92 (s, 3H)	3.78 (s, 3H)	3.93 (s, 3H)	3.95 (s, 3H)	3.88 (s, 3H)	3.92 (s, 3H)	3.91 (s, 3H)
13	5.23 (s, 2H)	5.23 (s, 2H)	2.23 (s, 3H)	2.34 (s, 3H)	2.10 (s, 3H)	2.35 (s, 3H)	2.35 (s, 3H)

* Kimura *et al.*, 1988
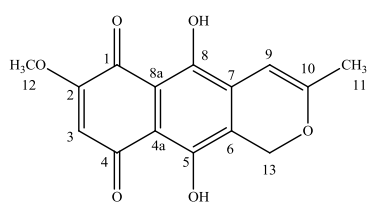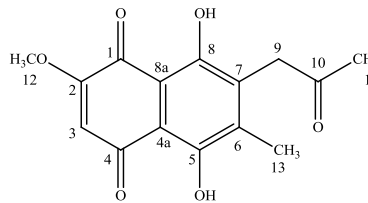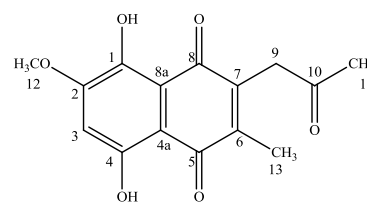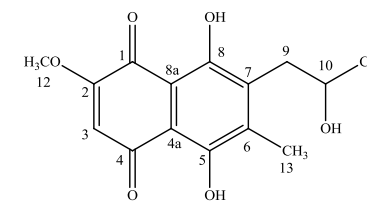
3.28   3.8   3.29   3.26

**Table 3.7: ^{13}C NMR of of naphthazarin derivatives related structure
FRC15-4-F4, FRC15-8-F8c, FRC15-6-r2-13 (CDCl$_3$, 100.5 MHz) and FRC15-11-F11**

Carbon	^{13}C NMR, δ_C (ppm)			
	FRC15-4-F4	FRC15-8-F8c	FRC15-6-r2-13	FRC15-11-F11
1	177.8	177.9	166.6	177.8
2	160.6	160.7	149.7	161.2
3	-	-	-	110.1
4	183.2	183.8	154.2	184.3
4a	108.4	108.2	-	108.4
5	158.4	160.7	188.6	161.2
6	123.1	134.2	141.6	138.9
7	133.6	143.2	146.9	142.3
8	158.4	161.8	183.9	163.2
8a	109.9	149.3	-	-
9	94.9	-	-	36.7
10	162.2	204.2	203.9	68.0
11	-	-	-	24.7
12	-	-	-	57.7
13	-	-	-	-

3.6.3   Compound FRC15-8-F8c (javanicin, 3.8)

Compound FRC15-8-F8c (5.7 mg) was obtained as red needles and the molecular formula was determined to be $C_{15}H_{14}O_6$ by HRESI-MS (exact mass at *m/z* 291.0862 [M+H]$^+$) was elucidated as compound **3.8.** The ^{1}H NMR spectrum of this compound (Figure 3.15, Table 3.6) showed the same aromatic proton signal at δ_H 6.21 (*s*, 1H) which corresponded to H-3. A few differences of the proton signals on ring C were observed which one of them was the presence of a methylene proton singlet signal at δ_H 3.91 (*s*, 2H, H-9). Strong decisive HMBC correlations were observed (Figure 3.16); proton H-3 correlated with carbon carbonyl C-1, C-2, C-4 and C-4a, the methylene proton H-9 correlated with the carbonyl carbon for C-10 and three quaternary carbons; C-6, C-7, C-8 and C-8a. Another supporting correlation recorded was the presence of two methyl groups which one of them was found at δ_H 2.28 (*s*, 3H, H-11) has strong HMBC correlation with the carbonyl group C-10 and δ_H 2.23 (*s*, 3H) for H-13 which had correlations with carbons C-5, C-6, C-7 and C-9. The remaining signals and ^3J correlations were similar with those found for FRC15-4-F4 (Figure 3.17). The differences between the congeners were supported by their different physical characteristic which appeared to be a very strong red needles colour compared with that of FRC15-4-F4 which was a violet crystal. Thus this

compound was proposed as javanicin. In earlier reports, this metabolite also has been isolated from *F. javanicum* (Arnstein and Cook, 1947), *Fusarium* sp. isolated from a mold obtained as an aerial contaminant (Chilton, 1968) and *F. solani* isolated from pollen grain of *Pinus thumbergii* Parl (Kimura *et al.*, 1988), *Chloridium* sp.; an endophytic fungus which was isolated from neem plant (Kharwar *et al.*, 2009) and from sea fan-derived fungi *Fusarium* (Trisuwan *et al.*, 2010). However, in another report (Bentley and Gatenbeck, 1965), the hydroxyl groups were attached at C-1 and C-4, respectively. Meanwhile, another metabolite with hydroxyl groups at both C-1 and C-4 was also isolated in this extract which will be discussed in section 3.6.4.
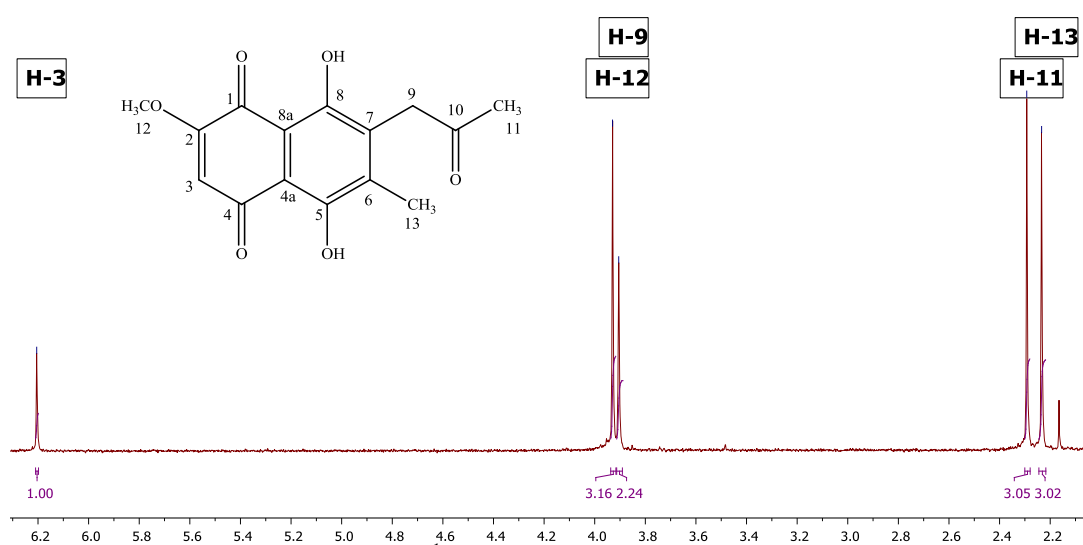
Figure 3.15: ^{1}H NMR spectrum of FRC15-8-F8c
(CDCl$_3$, ^{1}H 400 MHz)
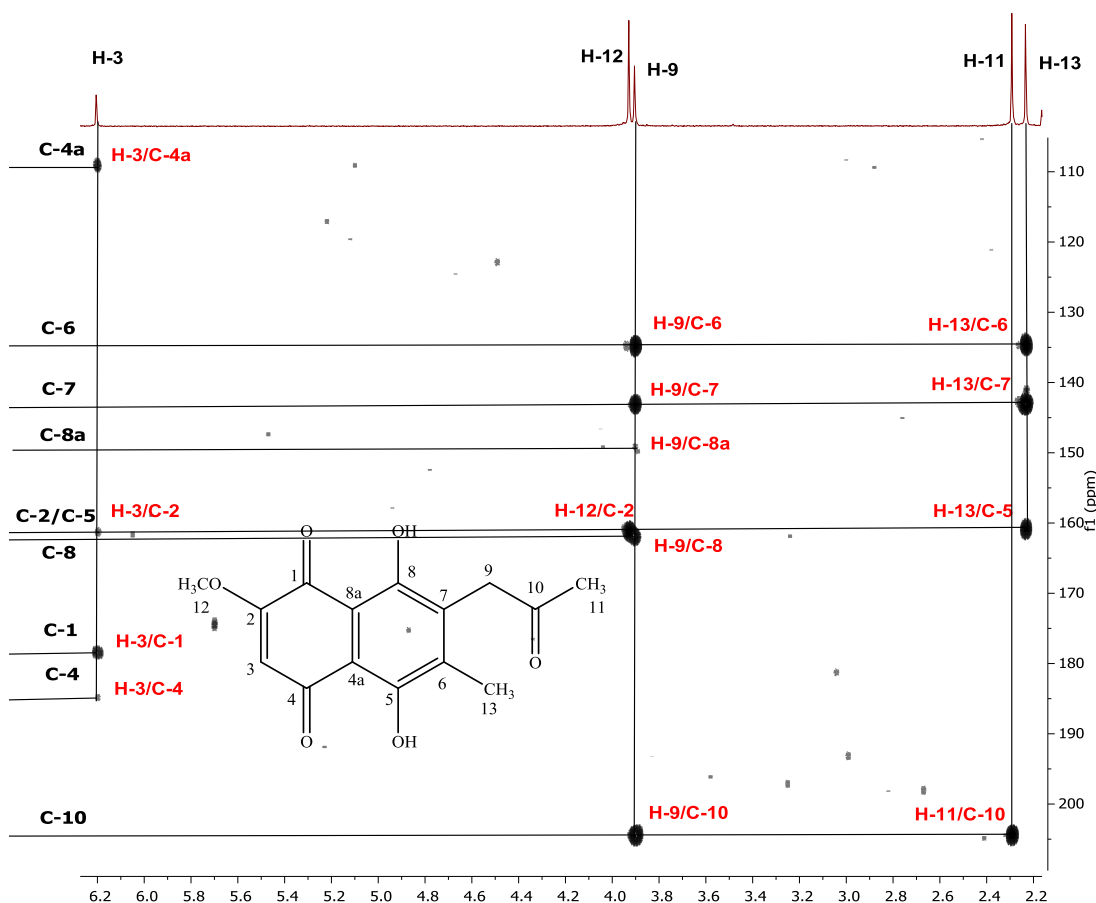
Figure 3.16: HMBC NMR spectrum of FRC15-8-F8c
(CDCl$_3$, ^{1}H 400 MHz, ^{13}C 100.5 MHz)
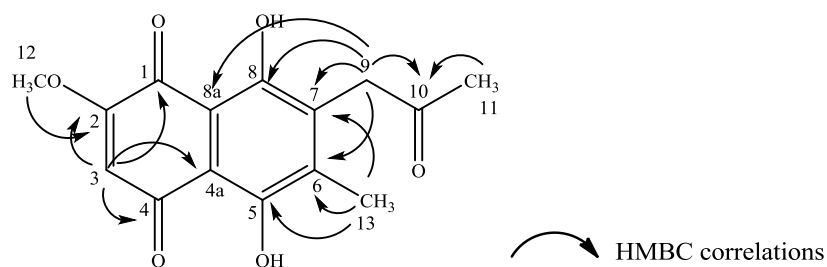
Figure 3.17: HMBC correlations of FRC15-8-F8c

3.6.4 Compound FRC15-6-r2-13 (dihydrojavanicin, 3.29)

Compound FRC15-6-r2-13 (2.4 mg) was also obtained as yellow needles and HRESI-MS showed exact mass at *m/z* 291.0860 [M+H]$^+$ corresponding to the molecular formula C$_{15}$H$_{14}$O$_{6,}$ has the same empirical formula as javanicin which was discussed under the earlier section 3.6.3. ^{1}H NMR spectrum (Figure 3.18, Table 3.6) showed the same spin system to javanicin; an aromatic proton signal H-3 at δ_H 7.15 (*s*, 1H), a methylene proton signal at δ_H 3.77 (*s*, 2H, H-9), a methoxy proton signal

120

3.88 (*s*, 3H, H-12) and two methyl proton signals at 2.30 and 2.10 assigned to CH$_3$-11 and 13 respectively. Carbon assignments were shown in Table 3.7. The important correlations between protons and carbons were observed in the HMBC NMR spectrum (Figure 3.19). The lone aromatic proton singlet (H-3) correlated with the carbon signal at δ_C 154.2 (C-4), indicating a hydroxyl-bearing carbon while the methoxy group showed strong correlation with the carbon signal at δ_C 166.6 (C-1) instead of a ketonic carbon at δ_C 180-200 ppm. Besides, the presence of correlations between the methylene proton (H-9) and quaternary carbon signals at δ_C 141.6 (C-6), 146.9 (C-7), and carbonyl carbon signals at δ_C 183.9 (C-8) and 203.9 (C-10) were also observed. Furthermore, one of the methyl protons (13-CH$_3$) also correlated to C-6/C-7 as well as to other the carbonyl carbon at δ_C 188.6 (C-5). Based on the spectral data and comparison with literature data, this compound was proposed to be dihydrojavanicin which had been derived from the javanicin skeleton with a difference in positions of the carbonyl and hydroxyl substituents. However, this compound was also assigned the trivial name javanicin in the literature (Bentley and Gatenbeck, 1965).
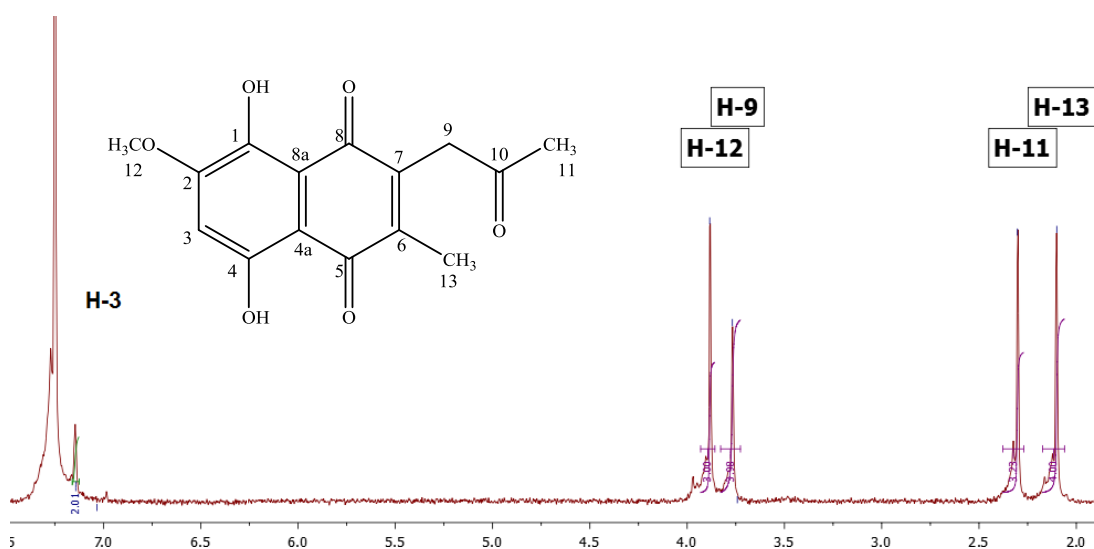
Figure 3.18: ^{1}H NMR spectrum of FRC15-6-r2-13
(CDCl$_3$, ^{1}H 400 MHz)

121
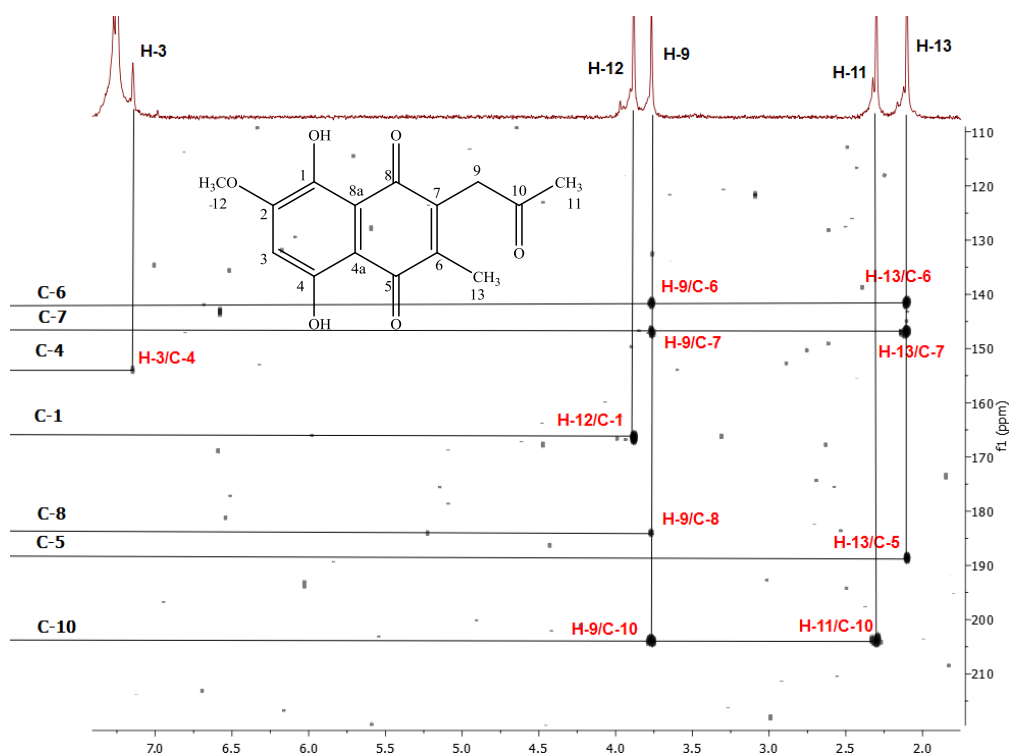
Figure 3.19: HMBC NMR spectrum of FRC15-6-r2-13
(CDCl$_3$, ^{1}H 400 MHz, ^{13}C 100.5 MHz)
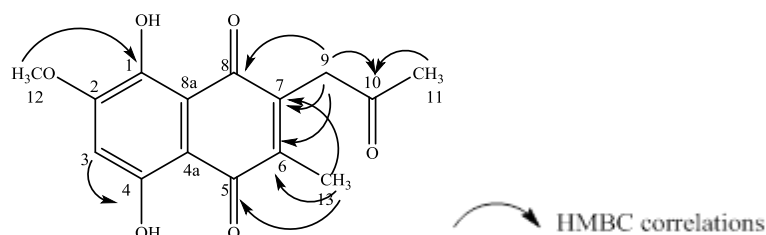
Figure 3.20: HMBC correlations of FRC15-6-r2-13

3.6.5   Compound FRC15-11-F11 (solaniol, 3.26)

Compound FRC15-11-F11 (7.0 mg) was also obtained as red crystals and HRESI-MS showed exact mass at *m/z* 293.1020 [M+H]$^+$ corresponding to the molecular formula C$_{15}$H$_{16}$O$_6$ which has extra two proton signals compared with javanicin. ^{1}H NMR spectrum (Figure 3.21, Table 3.6) showed a methylene proton doublet (H-9) which shifted up field at δ_H 2.94 (*d*, *J*=5.9 Hz, 2H) and directly correlated with a carbon signal at δ_C 36.7 (C-9), this carbon shifted to downfield indicating that this carbon has an effect from a hydroxyl linked methine carbon at δ_C 68.0 (C-10). Besides, one of the methyl groups (H-11) showed a doublet signal which means that

this proton attached to a methine proton at δ_H 4.13 (*m*, 1H, H-10) which was indicated by the strong correlations between protons H-9, H-10 and H-11 as shown in the COSY NMR spectrum (Figure 3.22 a). The HMBC NMR spectrum (Figure 3.22 b) disclosed the most important correlations between methylene protons H-9 and C-6, C-7, C-8, C-10- and C-11. The other correlations remained the same with compound FRC15-8-F8 (Figure 3.23). Thus, this compound was identified as solaniol which also has been isolated from *Fusarium* sp. (Kimura *et al.*, 1988, Trisuwan *et al.*, 2010).
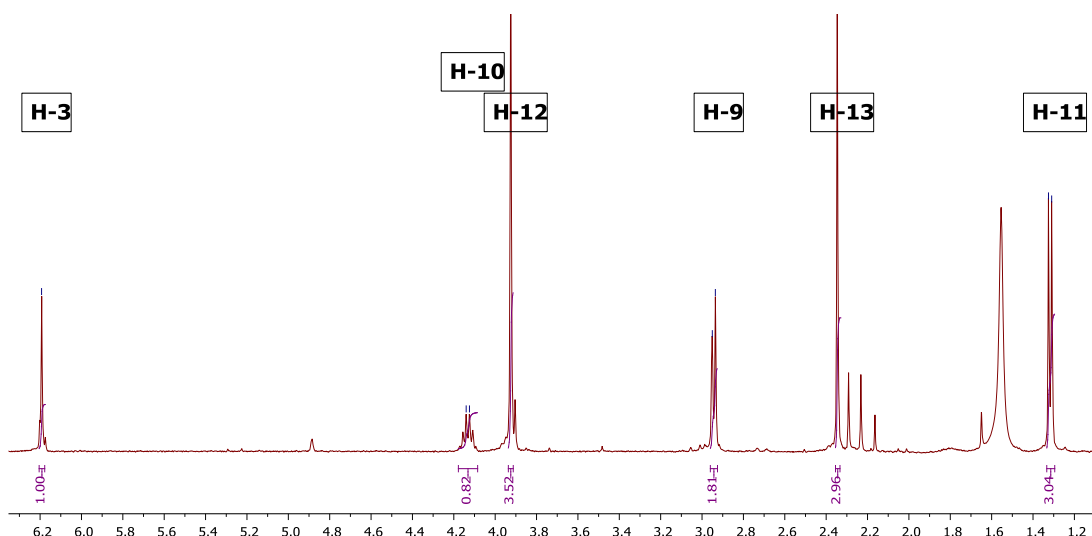
Figure 3.21: ^{1}H NMR spectrum of FRC15-11-F11
(CDCl$_3$, ^{1}H 400 MHz)
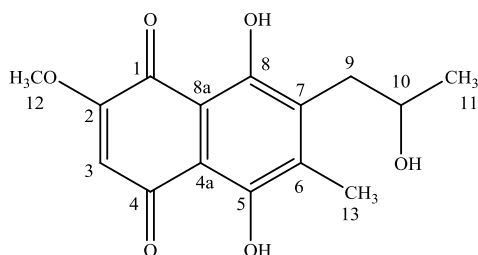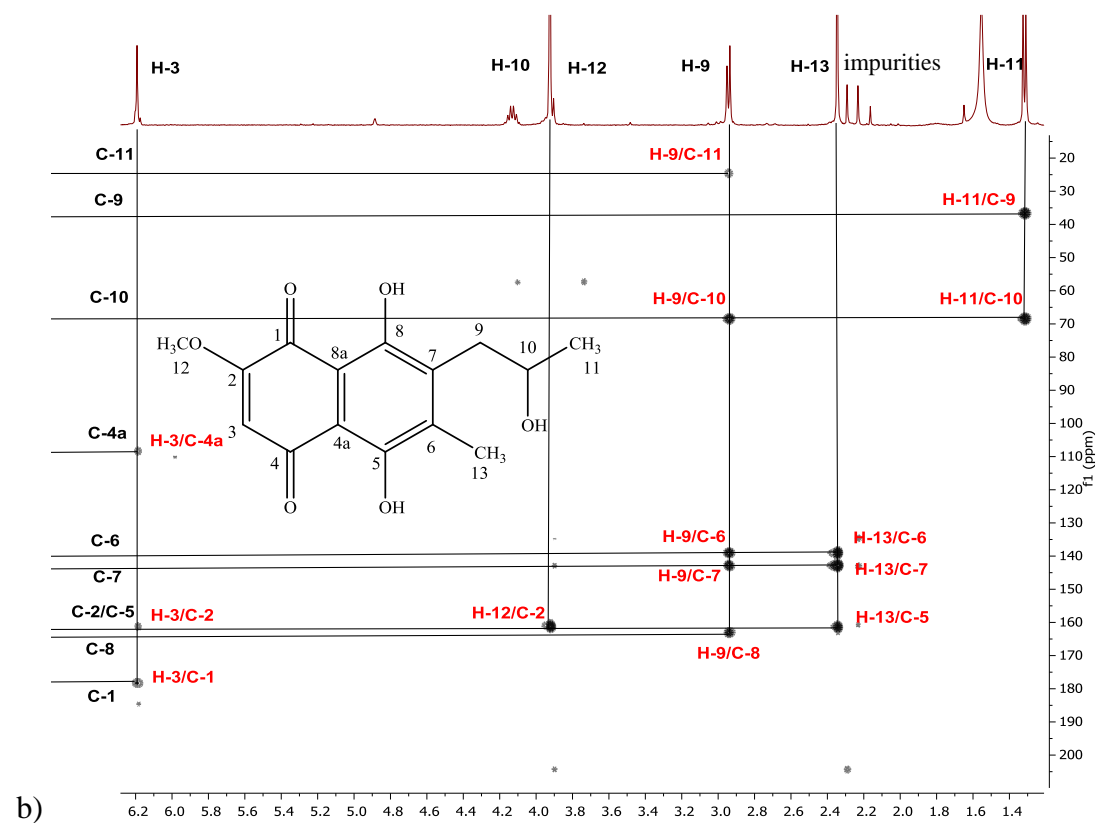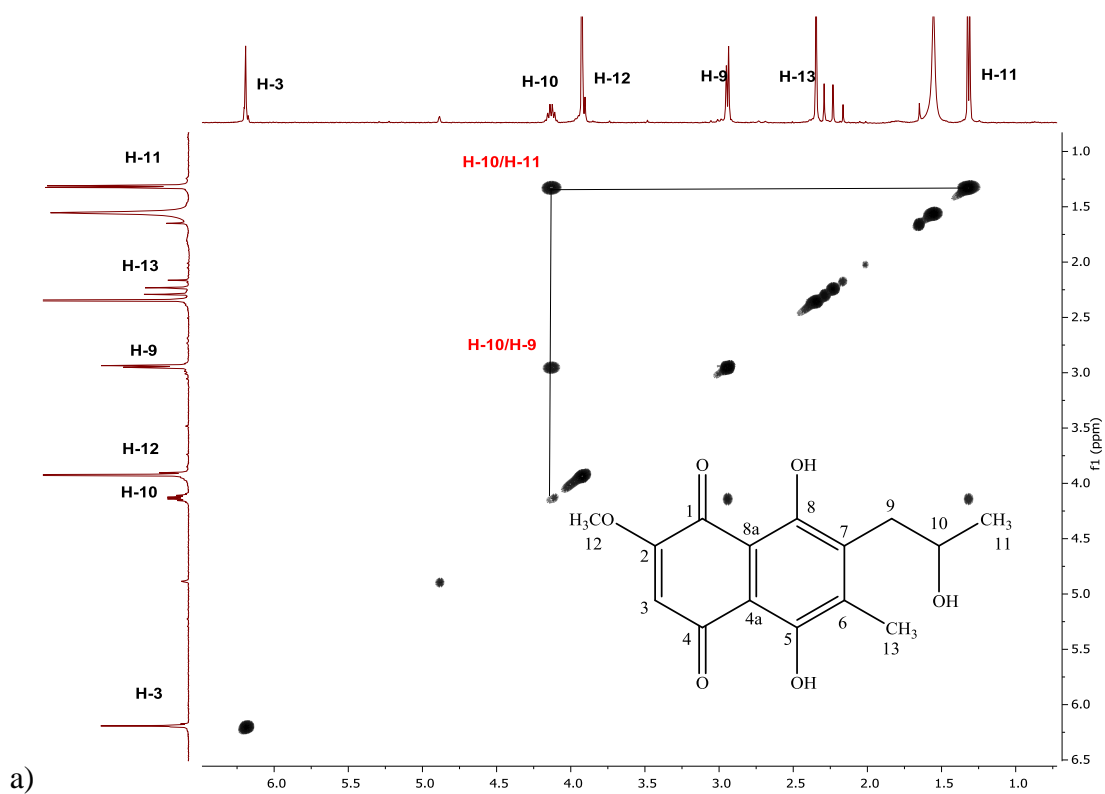
Figure 3.22: (a) COSY and (b) HMBC NMR spectra of FRC15-11-F11
(CDCl$_3$, ^{1}H 400 MHz, ^{13}C 100.5 MHz)
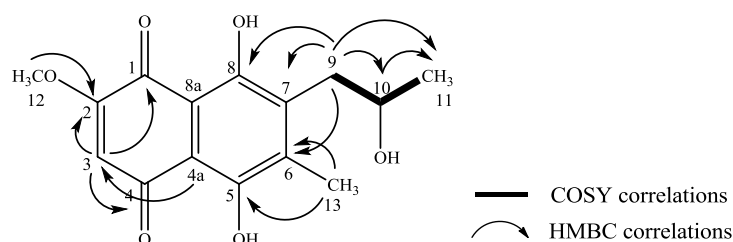
Figure 3.23: COSY and HMBC correlations of FRC15-11-F11

3.7 Bioactivity test results

Table 3.8: Activities of the isolated compounds
from *Fusarium* sp. against *T. b. brucei* and PNT2A cells

Compounds	[a] MICs (µM)	[b] Cytotoxicity, % D of control (100 µg/mL)
ergosterol peroxide	1.48	91.7
anhydrofusarubin	1.20	67.1
javanicin	0.60	61.4
dihydrojavanicin	1.90	22.3
solaniol	0.32	38.6
Suramin	0.11	n.d
Triton X	n.d	0.082

[a] Each sample was tested in two independent assays against *T. b. brucei*, MIC values indicate the minimum inhibitory concentration of a compound/standard in µM necessary to achieve 90% growth inhibition. MICs (MIC < 10 µM - promising; 10 µM < MIC > 20 µM - moderate; 20 µM < MIC > 30 µM - marginal/weak; 30 µM < MIC > 40 µM - limited; MIC > 40 µM - no activity);
[b] Initial screening for cytotoxicity activity against human normal prostatic epithelial cells (PNT2A) , % D of control values (at 100 µg/mL,) were determined by averaging of three independent assays results (n=3); [c, d] Positive controls; n.d.- not determined.

The isolation and identification of secondary metabolites from the crude extract of endophytic fungus *Fusarium* sp. revealed the presence of ergosterol peroxide, four known metabolites (1,4-naphthoquinones with naphthazarin related structures); anhydrofusarubin, dihydrojavanicin, javanicin and solaniol in which these metabolites comprised the major compounds in the total extract. The isolated naphthazarin compounds were observed in the dereplication study in which these metabolites have been isolated from the active fractions. Each compound was also subjected to anti-trypanosomal activity and cytotoxicity against PNT2A cells (Table 3.8). The results showed ergosterol peroxide and the naphthazarin compounds significantly effective against *T. b. brucei* and comparable to suramin. Ergosterol peroxide showed potent activity with an MIC of 1.48 µM and had the least toxic effects against normal prostate cells. Among the naphthazarin derivatives, solaniol

had the most potent activity against *T. b. brucei* with an MIC of 0.32 μM. The next potent was javanicin with an MIC of 0.60 μM, whereas its congener, dihydrojavanicin exhibited less activity (MIC = 1.90 μM). Solaniol and dihydrojavanicin showed more toxic effects against PNT2A cells. Meanwhile, anhydrofusarubin had an MIC of 1.20 μM. Notably, javanicin and anhydrofusarubin showed similarly weak toxic effects against PNT2A cells.
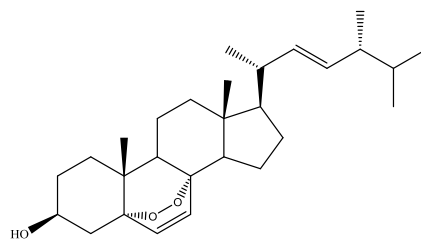
ergosterol peroxide
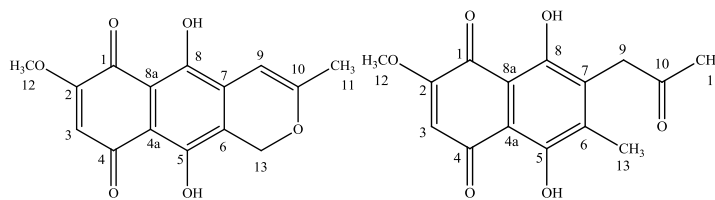
anhydrofusarubin

javanicin
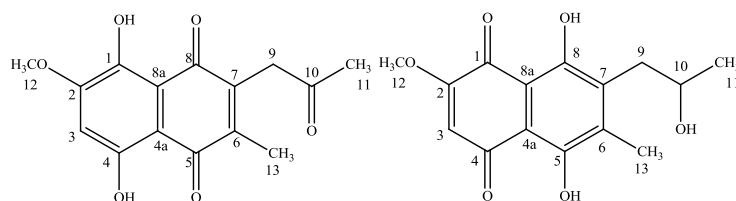
dihydrojavanicin

solaniol

Chapter 4

4. Bioactive secondary metabolites from *Aspergillus aculeatus*

Further investigations for potential new metabolites for anti-trypanosomal have been performed on *A. aculeatus* isolated from mangrove plant *A. lanata*. Previous studies reported various metabolites have been isolated from *Aspergillus* species possessed significant biological activities; for example, aspergiolide A, is an anthraquinone derivative isolated from cultures of a marine-derived fungus *Aspergillus glaucus* had selective cytotoxicities against A-549 (human lung epithelia cell), HL-60 (human leukaemia cell), BEL-7402 (human liver cancer cell) and P-388 (murine leukaemia cell) cell lines with IC_{50} values of 0.13, 0.28, 7.5 and 35.0 µM respectively (Du *et al.*, 2007). Meanwhile, a study by (Chen *et al.*, 2013) revealed naringinase isolated from *A. aculeatus* (JMUdb058) is an enzyme complex that has the capability to hydrolyse many glycosides which are important in the food and pharmaceutical industries. Spirotryprostatins E and two derivatives of fumitremorgin B, prenylated indole diketopiperazine alkaloids which have been previously isolated from the holothurian *S. japonicus*-derived fungus *A. fumigatus,* possessed significant activity against MOLT-4 (human acute lymphoblastic leukaemia cell), HL-60, and A-549 cell lines (Wang *et al.*, 2008). Here, I report the preliminary screening, isolation and identification, and the biological activity against trypanosomes of secondary metabolites from the mangrove-derived fungus *A. aculeatus*.

4.1 Results and discussion

4.1.1 Preliminary screening of metabolite production from *A. aculeatus*

A pure strain of *A. aculeatus* (Figure 4.1) was cultivated to afford the potential bioactive metabolites production (Chapter 7.4). The bioactivity test results of the small-scale extracts of *A. aculeatus* against *T. b. brucei* are reported in Table 4.1. The small-scale extract of the rice culture on day 30 (AARC30) showed significant activity compared to the other rice culture extracts. Conversely, the extracts from the liquid cultures showed less activity against *T. b. brucei*.
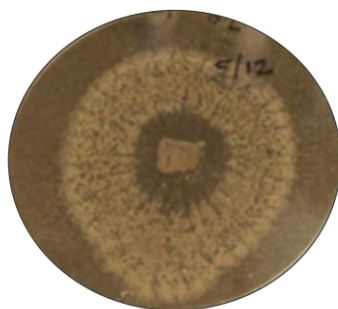
Figure 4.1: A pure strain of the endophytic fungus *A. aculeatus* grown on malt agar plate

Table 4.1: Anti-trypanosomal activity of *A. aculeatus* small-scale extract (calculated as percentage viability) at concentrations of 20 µg/mL (RC= rice culture extracts, LC = liquid culture extracts on day 7, 15 and 30)

Small scale extract *A. aculeatus*	*T. b. brucei*, % D control (20 µg/mL)
AARC7	21.4
AARC15	32.1
AARC30	4.3
AALC7	41.8
AALC15	32.3
AALC30	45.8

% D, percentage viability of control

4.1.2 Dereplication studies on small-scale *A. aculeatus* extract

The dereplication study for the small-scale extracts was accomplished to gain a metabolomic profile for monitoring and preliminary screening the relationship between the production of metabolites and different culture media (rice and liquid media) at different periods of cultivation (RC= rice culture extracts, LC = liquid culture extracts on day 7, 15 and 30). Furthermore, the relationship between the metabolites and bioactivity of the mangrove plant *A. lanata* associated endophytic fungi *A. aculeatus* also was investigated. Metabolic profiling was firstly performed on the small-scale cultures to choose the optimum conditions for cultivation which was later to be scaled up. Each extract was tested for anti-trypanosomal activity.

a)

b)
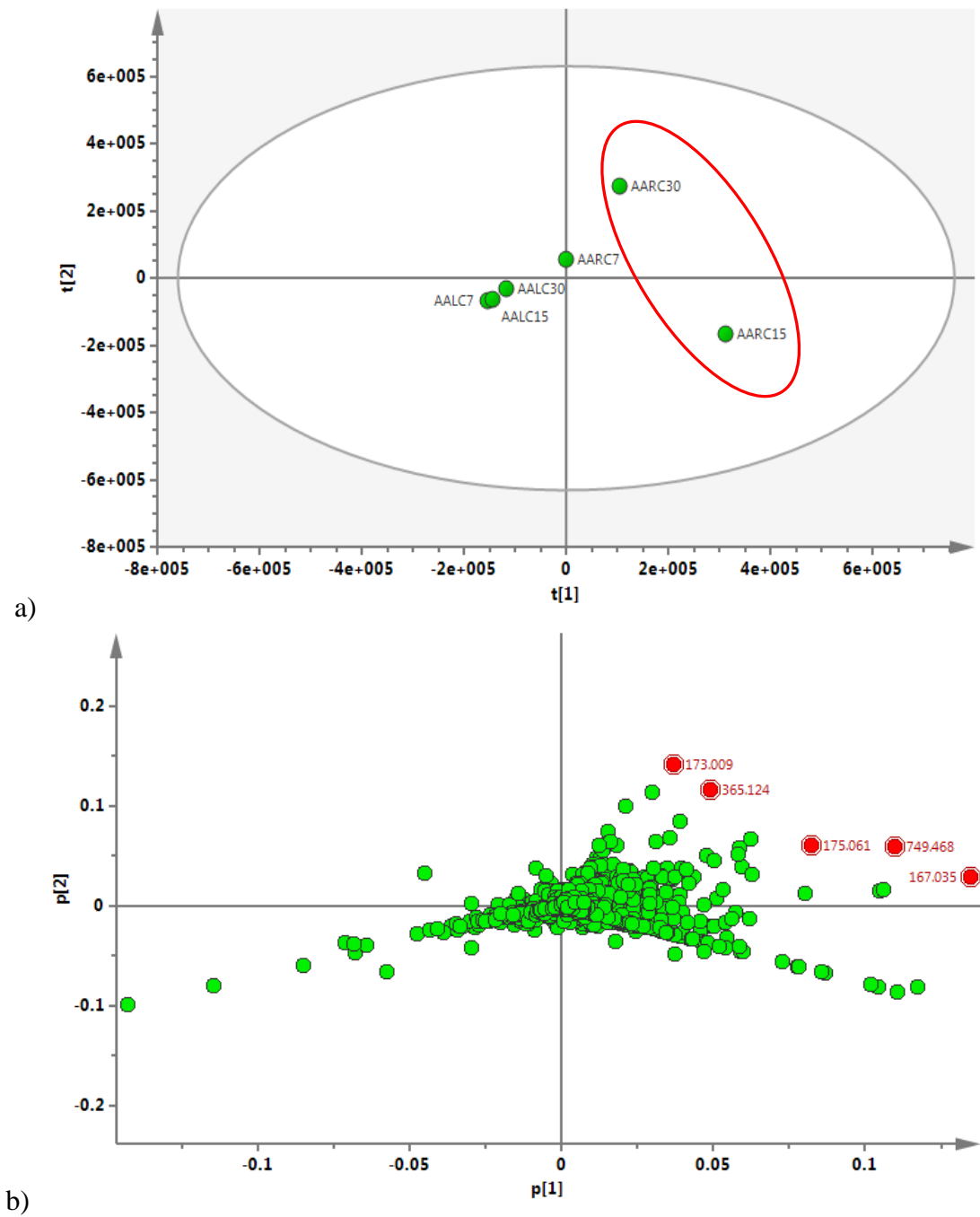
Figure 4.2: Multivariate analysis on small scale extracts of *A. aculeatus*

A. aculeatus grown in rice and liquid culture media (AARC= rice culture extracts, AALC = liquid culture extracts on day 7, 15 and 30); (a) Unsupervised PCA score plot analysis of the small-scale extract of *A. aculeatus* showed moderate separation between the datasets, except AARC15 and AARC30 showed distinctive separation; (b) PCA loading plot showed the distribution of the metabolites.
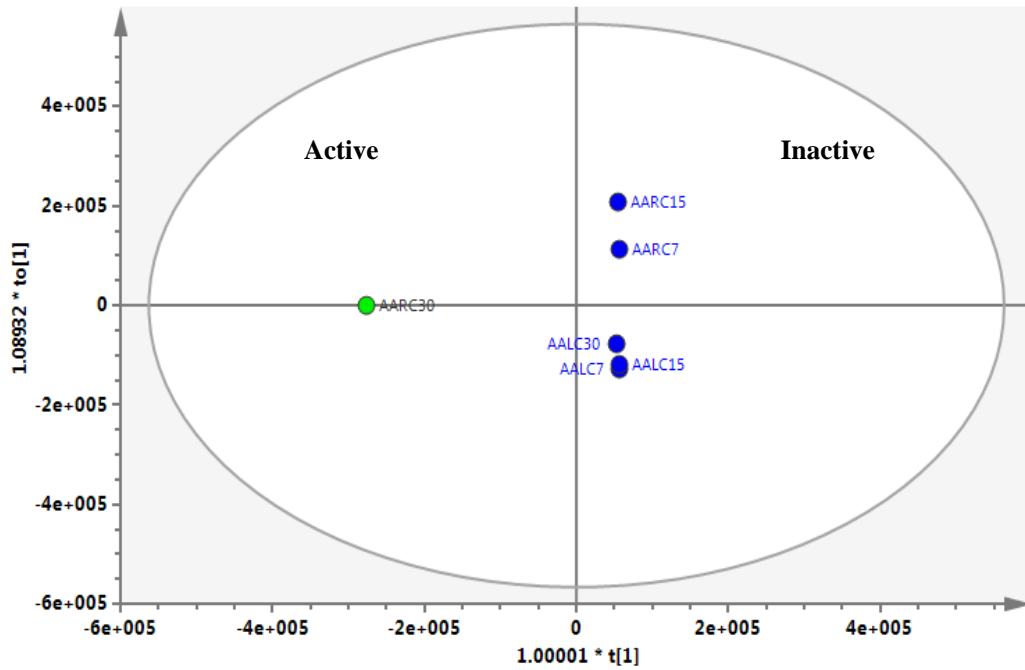
c)
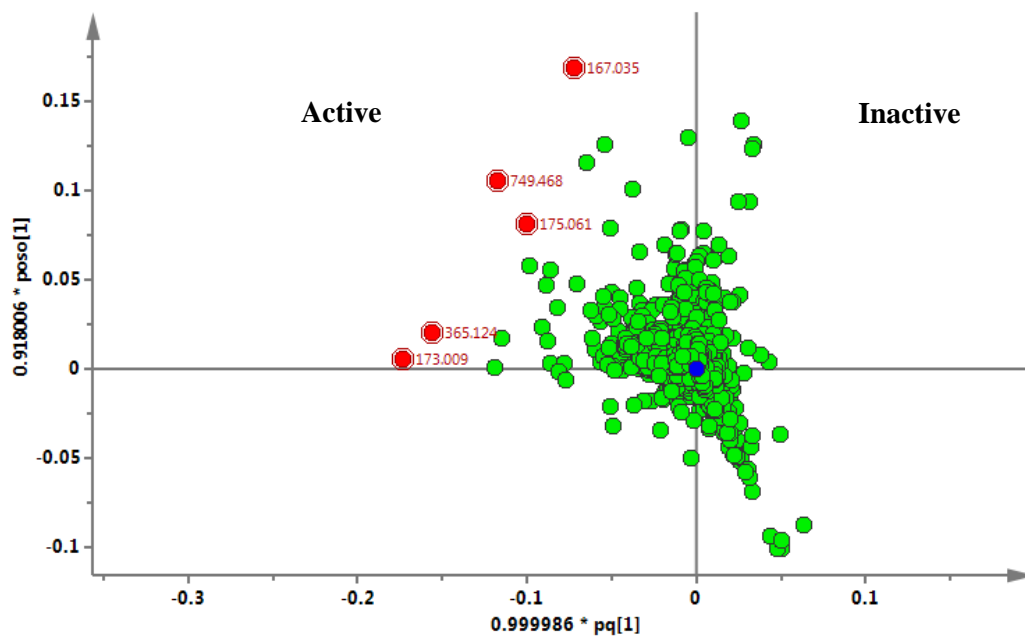
d)

Figure 4.2: Cont'd. Multivariate analysis on small scale extracts of *A. aculeatus*
c) Supervised OPLS-DA score plot analysis showed a distinctive separation between active (green) and inactive (blue) extracts when tested for anti-trypanosomal activity ($R^2(Y) =1.0$; $Q^2(Y) =0.99$); (d) OPLS-DA loading plot highlighting the outlying metabolites in the active groups.

Figure 4.2 a depicted an unsupervised score plot analysis showing that the small-scale extracts of the 15 and 30 day rice cultures were discriminant from other extracts. From the supervised OPLS-DA results, the small scale 30 day rice culture (AARC30) extract was classified as active, displaying significant activity against

T. b. brucei, whereas the other extracts were classified as inactive (Figure 4.2 b). The OPLS-DA loading plot (Figure 4.2 c) showed respective unique biomarkers that were more prevalent in the active group. Those metabolites with the strongest contribution to anti-trypanosomal activity are highlighted in red and labelled with their *m/z* values. The compound with *m/z* 173.0090 [M-H]$^-$ and 175.061 [M+H]$^+$ was putatively identified as *cis*-aconitic acid, previously isolated from *A. terreus* (Dwiarti *et al.*, 2002), whereas *m/z* 167.050 [M-H]$^-$ was identified as vanillic acid (Ayer and Trifonov, 1995). The *m/z* 749.4684 and 365.1242, both negatively ionised, were not identified from the Antimarin database. From the inactive group, the *m/z* 323.0021 and 321.0051 [M-H]$^-$ did not give any hit from the database.

cis-aconitic acid
Rt: 1.82, 4.30 mins

vanillic acid
Rt: 2.61
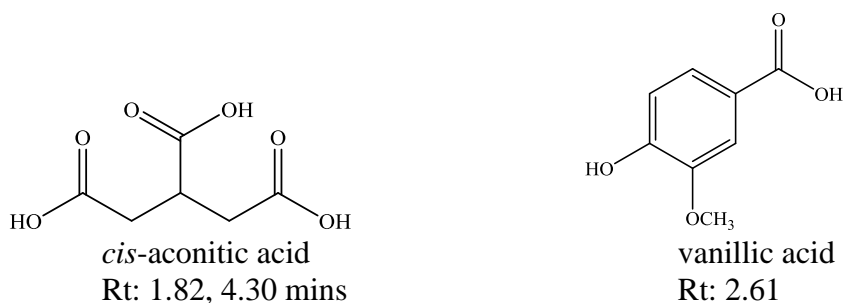
4.2   Scale-up of *A. aculeatus* for the isolation of secondary metabolites

Based on the dereplication results and bioactivity against *T. b. brucei* of the small-scale extracts, it was concluded that the cultivation of *A. aculeatus* on rice medium for 30 days was the optimum condition for the production of active secondary metabolites by the fungus. The pure *A. aculeatus* strain was inoculated onto a new agar plate and incubated for 8 days. The agar on which the fungi was grown was cut into small cubes and transferred into 20 of 2-L Erlenmeyer flasks (5 cubes per flask) containing autoclaved rice medium (200 g of rice: 200 mL of water) and incubated at room temperature for 30 days. The metabolites were extracted using ethyl acetate (1:1, 2x), to give a crude extract of 18.5 g. A dereplication study was subsequently performed on the total crude extract using HRESI-LCMS (Chapter 7.3).

4.2.1 Dereplication results on total crude extract of *A. aculeatus*

The total ion chromatogram of the crude extract (Figure 4.3) showed the distribution of known and unknown compounds present in the AARC30 total extract. Asperparaline A, MK-7607, glauconic acid, 16-keto-aspergillimide, paraherquamide E, oxaline, phomopside A, secalonic acid D were some of the putatively identified metabolites which have been previously isolated from fungal sources. Some of the identified metabolites have been isolated from *Streptomyces* sp., marine sponges, and marine bacteria (Table 4.2). The structures of the putatively identified metabolites are depicted in Figure 4.4. The *m/z* values and predicted formulas of unknown metabolites are listed in Table 4.3.
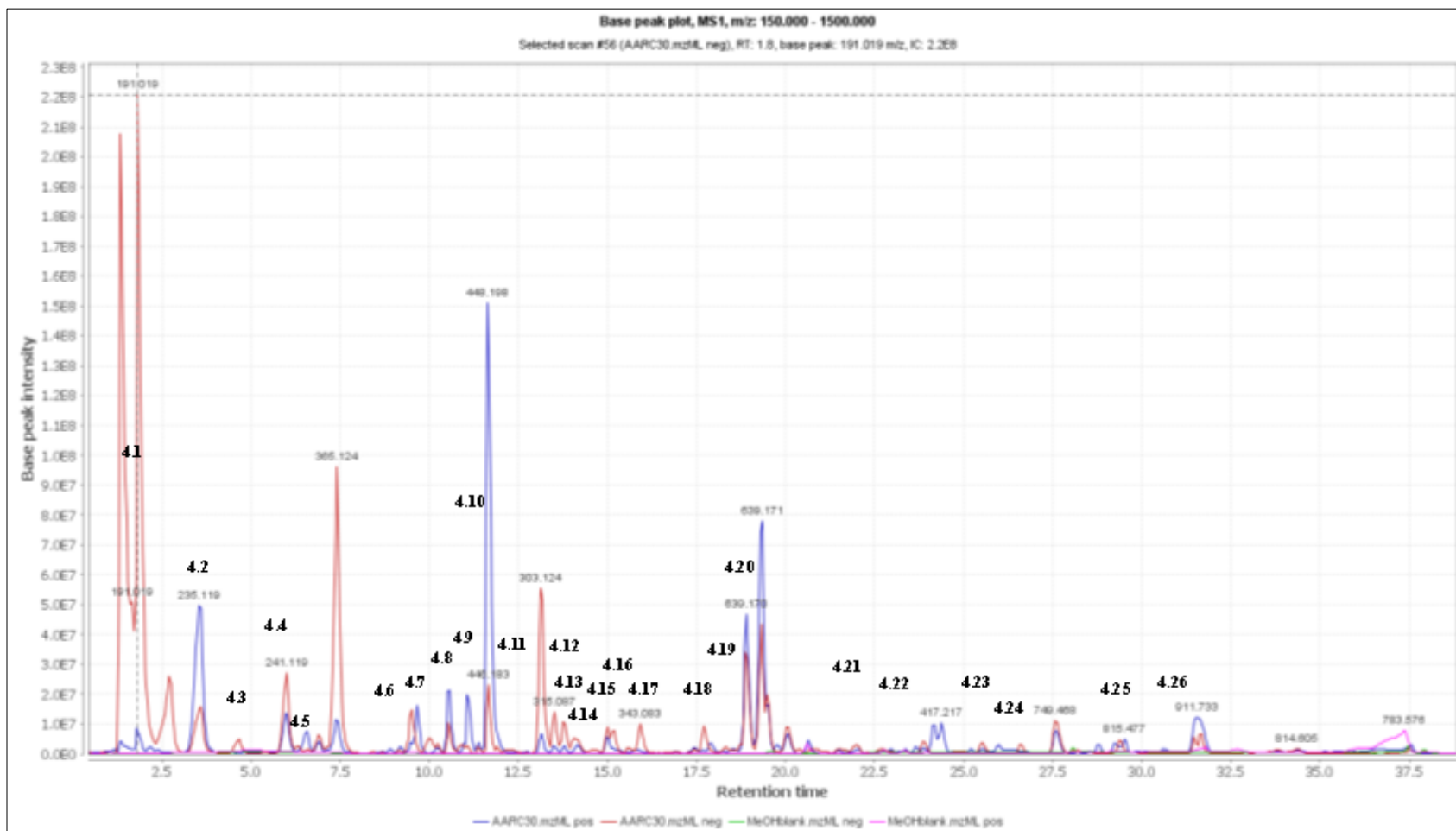
Figure 4.3: Total ion chromatograms of the crude extract of *A. aculeatus*
in rice media day 30 (AARC30) (Blue and red represent the positive and negative ionisation modes, respectively, for the crude extract. Pink and green are the positive
and negative ionisation modes, respectively, for the solvent blank)

Table 4.2: Compounds from the crude extract of *A. aculeatus* (AARC30)
that were putatively identified using the Antimarin database (Sources; F-fungi, A-algae, B-bacteria)

No.	ESI modes	Rt (min)	MS (m/z)	Molecular weight	Chemical formula	Name	Tolerance (ppm)	Sources	Peak Area
4.1	N	1.82	191.0197	192.0270	$C_6H_8O_7$	citric acid	2.9099	[F] *Aspergillus niger* var.; *Phycomyces blakesleeanus*	4.66E+09
4.2	P	3.54	235.1189	234.1116	$C_{11}H_{14}N_4O_2$	JBIR-75	1.9376	[F] *Aspergillus* sp. fS14	8.29E+08
4.3	N	4.66	175.0611	176.0684	$C_7H_{12}O_5$	MK-7607	2.7979	[F] *Curvularia eragrostidis*	6.96E+07
4.4	N	5.99	241.1195	242.1268	$C_{11}H_{18}N_2O_4$	bicycloamid	0.5511	Porifera; *Asteropus* sp	3.42E+08
4.5	P	6.59	360.2280	359.2207	$C_{20}H_{29}N_3O_3$	asperparaline A; aspergillimide; VM-55598	1.0253	[F] *Aspergillus japonicus* JV-23; *Aspergillus* sp.	1.12E+08
4.6	P	7.39	349.1280	348.1207	$C_{18}H_{20}O7$	glauconic acid	1.0960	[F] Penicillium *Purpuro genum* and *P. glaucum*	1.54E+08
4.7	N	9.52	321.1345	322.1418	$C_{17}H_{22}O_6$	tubiporone	0.4907	Cnidaria; *Tubipora musica*	1.75E+08
4.8	P	9.66	374.2073	373.2001	$C_{20}H_{27}N_3O_4$	16-keto-aspergillimide	1.1880	[F] *Aspergillus* sp.	1.45E+08
4.9	P	10.58	266.1022	265.0949	$C_{13}H_{15}NO_5$	methyl 2-[propanamide-2'-methoxycarbonyl]-benzoate	1.5601	[A] brown alga *Jolynal aminarioides*	2.18E+08
4.10	P	11.07	478.2699	477.2627	$C_{28}H_{35}N_3O_4$	paraherquamide E; VM 54159; paraherquamide VM-54159	0.9107	[F] *Penicillium charlesii* ATCC 20841, *Aspergillus* sp.	1.81E+08
4.11	P	11.64	448.1979	447.1906	$C_{24}H_{25}N_5O_4$	oxaline	1.0845	[F] *Penicillium oxalicum, P. crustosum, P.glandicola, P. atramentosum*	1.34E+09
4.12	N	11.67	446.1836	447.1909	$C_{24}H_{25}N_5O_4$	naamidine C	0.595	Porifera; *Leucetta chagosensis*	1.90E+08
4.13	N	13.52	315.0877	316.0950	$C_{17}H_{16}O_6$	nanaomycina A; OM 173aA; OM 173a1; nanaomycin A-methylester	2.7406	[B] *Streptomyces* sp. om-173 (FERM-p 6509); semisynthetic from nanaomycin A	1.43E+08
4.14	N	13.77	347.1141	348.1213	$C_{18}H_{20}O_7$	1-hydroxybyssochlamic acid	1.2526	Ascomycota	1.24E+08
4.15	N	14.08	331.0827	332.0899	$C_{17}H_{16}O_7$	phomopside A	1.0501	Ascomycota; Phomopsis sp	6.97E+07
4.16	N	15.01	365.1511	366.1584	$C_{21}H_{22}N_2O_4$	speradine A	1.2007	Ascomycota; *Aspergillus tamarensis*	8.60E+07
4.17	N	15.19	299.0927	300.1000	$C_{17}H_{16}O_5$	dihydroxy-methoxy-propyl-naphthopyranone	0.8648	Echinodermata	8.66E+07
4.18	N	15.92	343.0826	344.0899	$C_{18}H_{16}O_7$	Z-coniosclerodinol	0.9248	Ascomycota; *Coniothyrium cereale*	1.01E+08

Table 4.2: Cont'd. Compounds from the crude extract of *A. aculeatus* (AARC30)

4.19	N	17.71	345.0983	346.1056	$C_{18}H_{18}O_7$	phomosine A	2.5749	[B] *Streptomyces fradiae*	9.88E+07
4.20	N	18.88	637.1567	638.1640	$C_{32}H_{30}O_{14}$	secalonic acid A	0.7441	*Aspergillus aculeatus, Claviceps purpurea*	3.65E+08
4.21	P	19.34	639.1708	638.1635	$C_{32}H_{30}O_{14}$	secalonic acid E	0.7583	[F] *Claviceps purpurea, Pyrenochaeta terrestris, Phoma terrestris*	1.33E+09
4.22	N	22.01	295.2281	296.2354	$C_{18}H_{32}O_3$	3(Z)-hydroxy-hexadeca-4(E),6(Z)-dienoic	0.7595	Chlorophyta, *Tydemania expeditionis*	6.18E+07
4.23	N	24.53	721.4382	722.4455	$C_{40}H_{68}O_7P_2$	prephytoene pyrophosphate; prelycopersene pyrophosphate	2.7964	-	6.73E+06
4.24	P	25.51	726.5000	725.4927	$C_{37}H_{67}N_5O_9$	kailuin B	-0.8486	[B] marine gram-neg. bacterium BH-107	2.02E+07
4.25	N	26.58	509.3277	510.3349	$C_{32}H_{46}O_5$	echinolactone A	0.8305	Cnidaria Echino poralamellosa	3.70E+07
4.26	P	29.50	815.4773	814.4700	$C_{42}H_{70}O_{15}$	anthenoside C	-1.7701	Echinodermata; *Anthenea chinensis*	4.67E+07
4.27	N	31.47	299.2596	300.2669	$C_{18}H_{36}O_3$	methyl-2-methoxyhexadecanoate	1.5308	Porifera; *Amphimedon compressa*	5.10E+07

* The highlighted rows were compounds isolated from *A. aculeatus*

**Table 4.3: Compounds present in the crude extract of *A. aculeatus* (AARC30)
that were not identified using the Antimarin database**

ESI modes	Rt (min)	MS (m/z)	Molecular weight	Peak Area
P	7.39	349.1274	348.3472	1.54E+08
N	7.41	365.1245	366.1317	1.08E+09
P	17.92	536.2869	535.2796	4.39E+07
N	19.48	433.2137	434.2209	2.08E+08
P	24.37	417.2173	416.2100	2.13E+08
P	25.20	324.2896	323.2823	1.78E+07
P	26.00	425.2145	424.2072	3.54E+07
P	28.76	481.2925	480.2852	3.29E+07
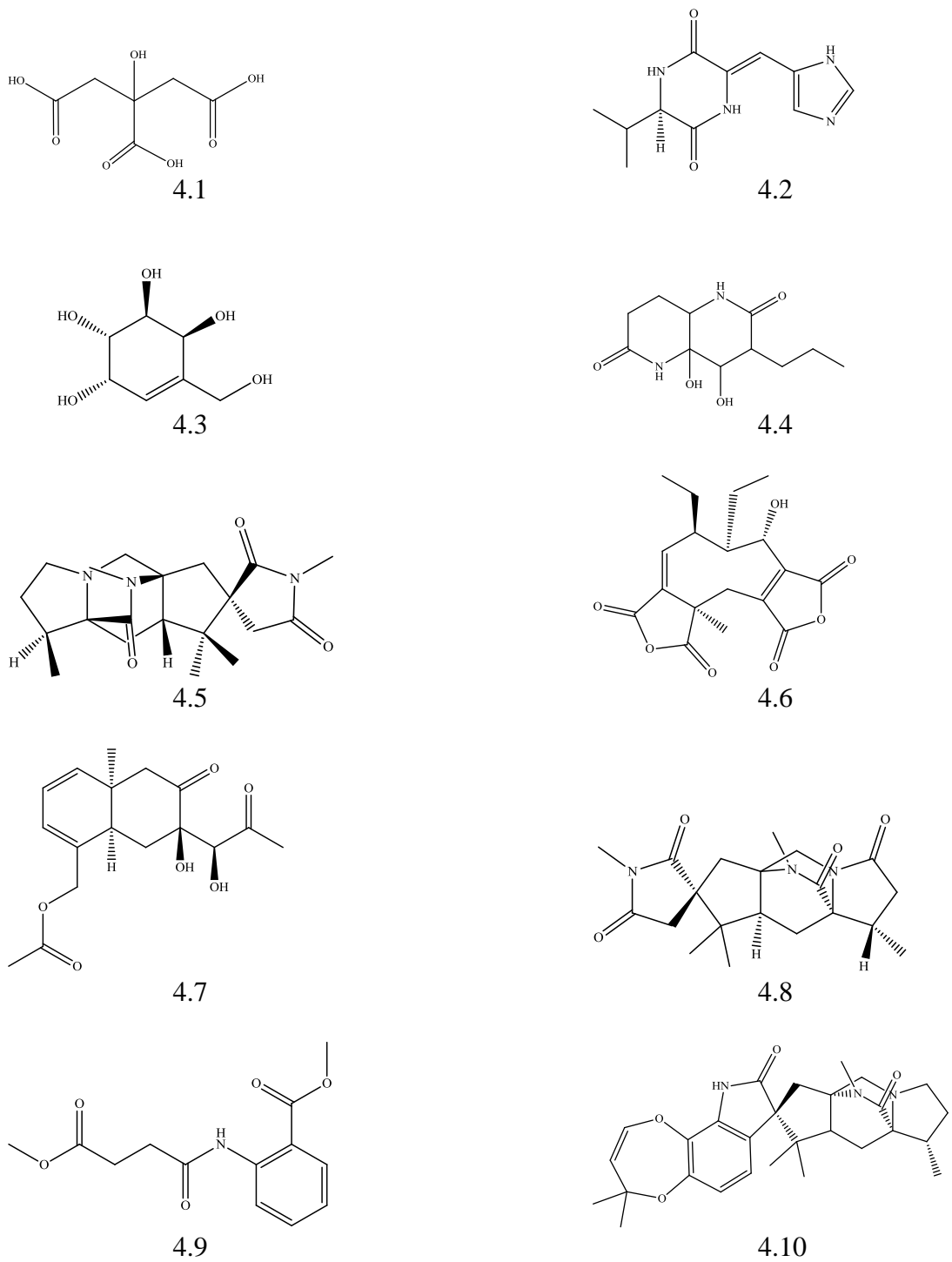
Figure 4.4: Compounds that were putatively identified
through dereplication studies on *A. aculeatus* (AARC30) crude extract
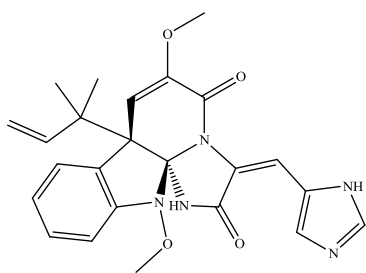
4.11
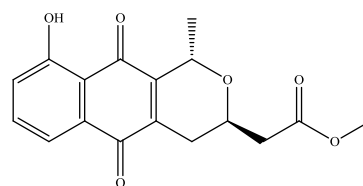
4.12
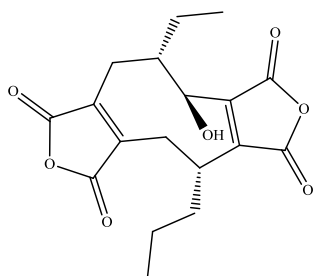
4.13
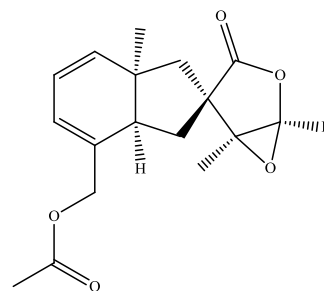
4.14
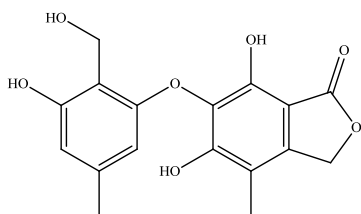
4.15
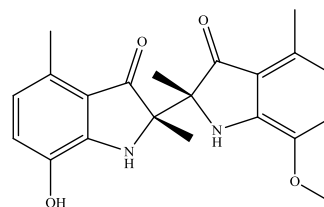
4.16
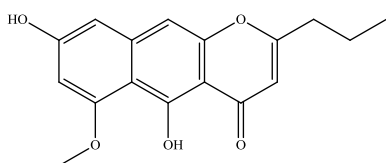
4.17
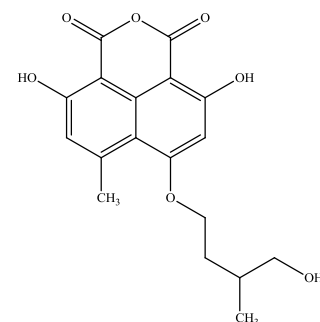
4.18
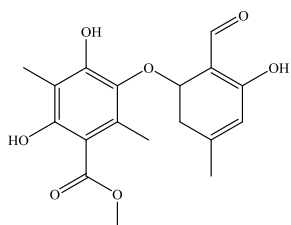
4.19
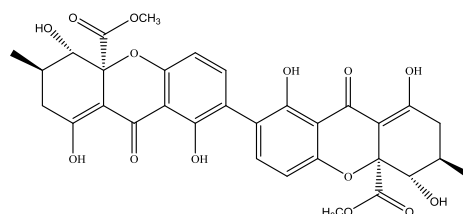
4.20

Figure 4.4: Cont'd. Compounds that were putatively identified
through dereplication studies on *A. aculeatus* (AARC30) crude extract
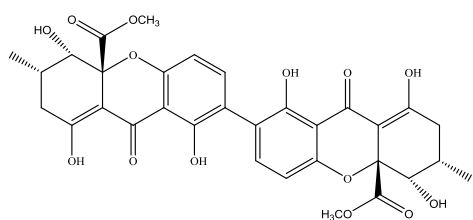
4.21
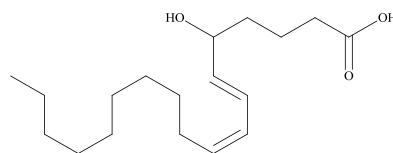
4.22
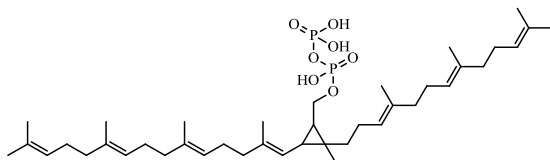
4.23
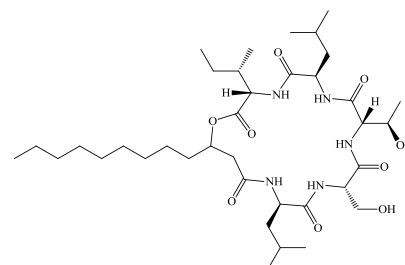
4.24
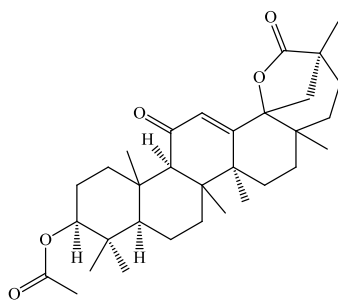
4.25
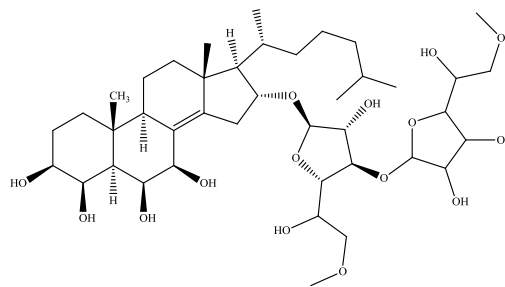
4.26
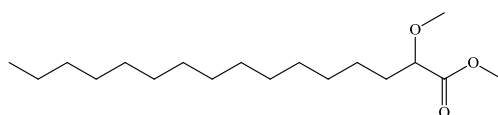
4.27

Figure 4.4: Cont'd. Compounds that were putatively identified
through dereplication studies on *A. aculeatus* (AARC30) crude extract

4.2.2   Isolation of secondary metabolites from *A. aculeatus*

Thin layer chromatography (TLC) was carried out on the *A. aculeatus* crude extract
using a combination of different solvent systems in order to determine the best
mobile phase for the fractionation of the extract. The total crude extract of *A. aculeatus* (18.5 g) was fractionated using medium pressure liquid chromatography
(MPLC) (Büchi, Switzerland) with gradient elution using hexane-ethyl acetate-
methanol (100% hexane:0% ethyl acetate, up to 100% ethyl acetate, 100% ethyl

acetate:0% methanol up to 30% ethyl acetate:70% methanol). The sub-fractions were combined based on the TLC profiles to give 16 major fractions of AARC30. These were analysed using HRESI-LCMS for dereplication and assayed for anti-trypanosomal activity. The active major fractions were subjected to further isolation and purification using column chromatography and flash chromatography (Grace Reveleris, USA and Biotage Isolera One, Sweden) using normal and reverse chromatography and various sizes of columns (Reveleris, USA and SNAP, Sweden).

4.2.3 Bioactivity results of *A. aculeatus* major fractions

The fractions (AARC30-1 until AARC30-16) were tested for anti-trypanosomal activity and the results were shown in Table 4.4. Fractions AARC30-1 until AARC30-6 showed strong activity, whereas fractions AARC30-7 until AARC30-10 showed moderate activity and fractions AARC30-11 until AARC30-16 exhibited poor activity against *T. b. brucei*.

Table 4.4: Anti-trypanosomal activity of *A. aculeatus* fractions (calculated as mean percentage viability) at concentrations of 20 µg/mL

Fractions	Yield (g)	*T. b. brucei*, % D control (20 µg/mL)
F1	1.5226	5.5
F2	0.3398	4.7
F3	0.2392	1.9
F4	0.6118	-2.9
F5	0.1260	2.5
F6	0.5669	0.5
F7	0.5688	70.3
F8	0.3723	78.2
F9	1.6133	27.6
F10	1.0144	23.1
F11	5.6037	94.7
F12	6.7248	107.2
F13	0.7601	112.6
F14	1.1238	104.4
F15	1.7252	102.4
F16	0.2068	92.3

% D, percentage viability of control

4.2.4 Multivariate analysis of *A. aculeatus* fractions

A dereplication study on *A. aculeatus* fractions was carried out to investigate the metabolic profile of each fraction and its relationship with its bioactivity against *T. b. brucei*. The unsupervised PCA score plot analysis (Figure 4.5 a) showed that the active fractions AARC30-4, AARC30-5 and AARC30-6 were the outlier fractions. Meanwhile, the PCA loading plot (Figure 4.5 b) showed that the metabolites with *m/z* 349.128 and 403.202 [M+H]$^+$ and *m/z* 347.114, 303.124, 345.098, 369.265 [M-H]$^-$ were distributed in between fractions AARC30-5 and AARC30-6. The metabolite with *m/z* 417.217 [M+H]$^+$, however only can be seen in fraction AARC30-4. The supervised OPLS-DA score plot analysis (Figure 4.5 c) showed the distribution of the fractions after they were grouped into active and inactive groups. The active group showed two distinctive clusters; that of AARC30-4, 5, 6 and of AARC30-1, 2, 3, 7, 8, 9, and 10. Fraction AARC30-5 was an outlier compared to fractions AARC30-4 and AARC30-6. In the inactive group, fractions AARC30-11 until AARC30-16 showed indistinctive distribution.
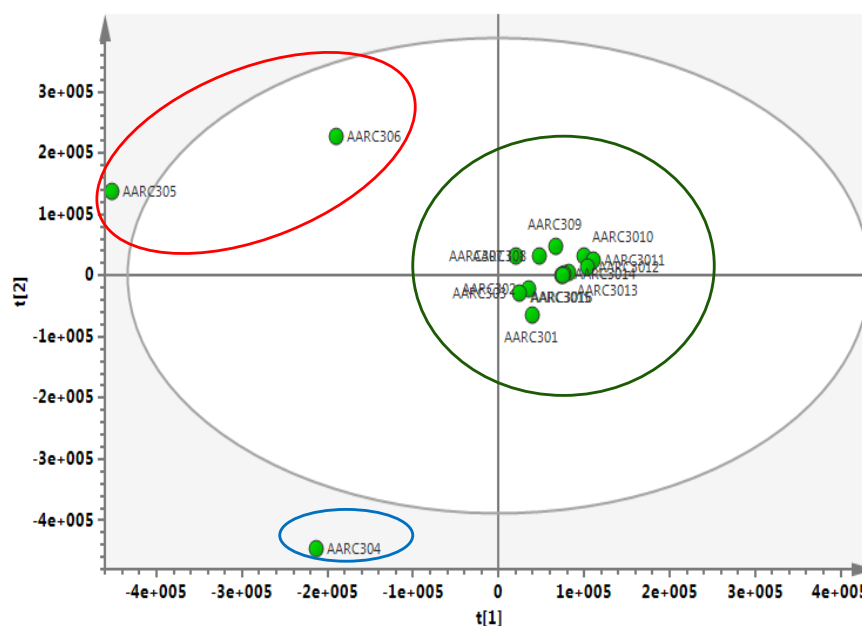
a)

Figure 4.5: Multivariate analysis of *A. aculeatus* crude fractions
(a) Unsupervised PCA score plot analysis of the *A. aculeatus* (AARC30) fractions showed that the fractions clustered together, except for fractions AARC30-4, AARC30-5 and AARC30-6, which were outliers.

b)

c)

d)
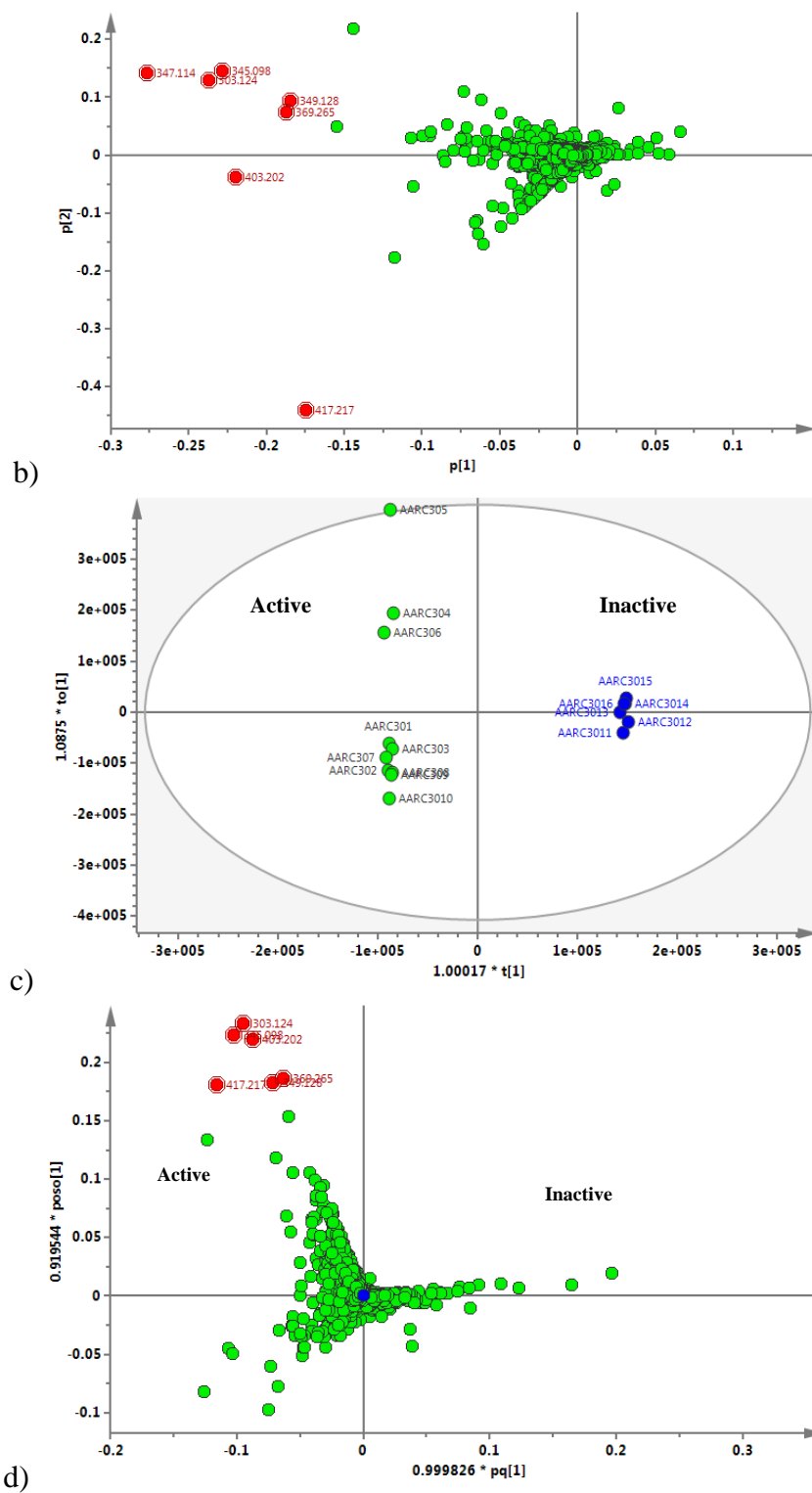
Figure 4.5: Cont'd. Multivariate analysis of *A. aculeatus* crude fractions
(b) PCA loading plot showed the distribution of the metabolites; (c) Supervised OPLS-DA score plot analysis showed a very distinctive separation between the active (green) and inactive (blue) fractions ($R^2(Y) = 0.997$; $Q^2(Y) = 0.796$); (d) OPLS-DA loading plot showed the distribution of the metabolites between the active and inactive fractions with the outlying metabolites in the active fractions highlighted in red and labelled with their *m/z* ratios.

The OPLS-DA loading plot (Figure 4.5 d) showed the distribution of the metabolites with those corresponding to the active group highlighted and labelled. Using the Antimarin database, metabolites with *m/z* 345.098 [M-H]⁻ was putatively identified as phomosine A, which have been previously isolated from *Phomopsis* sp. (Krohn *et al.*, 1995). A metabolite with *m/z* 303.124 [M-H]⁻ was identified as pestalotiopsone F isolated from *Pestalotiopsis* sp. (Jing Xu *et al.*, 2009). A metabolite with both ionisation modes- *m/z* 349.128 [M+H]⁺ and 347.114 [M-H]⁻ as well as *m/z* 403.202 and 417.217 [M+H]⁺ have not been identified when compared with the database. Further isolation and purification works focused on the active fractions which have unique metabolites, as seen by the outliers in the loading plots. Further isolation work focused more on the active fractions and unidentified metabolites.

4.19; phomosine A
Rt: 17.7 mins

pestalotiopsone F
Rt: 13.7 mins
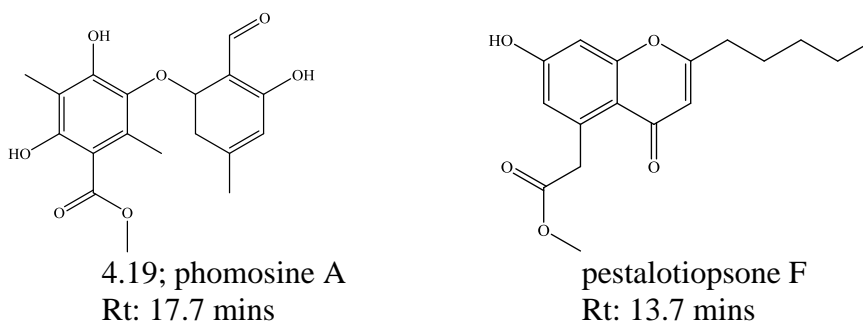
4.3   Isolation of secondary metabolites from *A. aculeatus*

All of the 16 fractions were monitored on TLC plates to aid in pooling and to determine their purity. UV light revealed the UV-active compounds, whereas the *p*-anisaldehyde-sulphuric acid spray reagent was useful for exposing the non-UV-active compounds (Figure 4.6). Each fraction was analysed using HRESI-LCMS for further dereplication study as well as being tested against trypanosomal activity. Thus, the fractions that were subsequently found to be active were subjected to further isolation and purification, ultimately revealing eight compounds. Isolation on fraction AARC30-4 gave ergosterol peoxide (AARC30-4-1, (**3.27**) 5.3 mg, 0.03%). Further several isolations on fraction AARC30-5 using flash chromatography (Grace Isolera, USA) gave one new 2,3-dihydrochromen-4-one, aspergillusenone (AARC30-5-116-3, (**4.28**), 2.3 mg, 0.01%), whereas fraction AARC30-6 yielded four acid type of compounds: vanillic acid (AARC30-6-28, (**4.29**), 5.2 mg, 0.01%),

3,4-dihydroxyphenylacetic acid (AARC30-6-11, (**4.30**), 4.3 mg, 0.02%), *o*-hydroxyphenylacetic acid (AARC30-6-50, (**4.31**), 6.23 mg, 0.03%), and *p*-hydroxyphenylacetic acid (AARC30-6-60, (**4.32**), 4.32 mg, 0.02%). Meanwhile, several purifications on fraction AARC30-9 revealed a new metabolite, 2-(3,4-hydroxyphenyl)-*N*, *N*-dimethylacetamide (AARC30-9-8-36, (**4.33**), 4.25 mg, 0.02%). Further isolation on fraction AARC30-10 gave yellow crystals, secalonic acid A (AARC30-10-18 (**4.20**), 10.3 mg, 0.06%). A summary of the workflow on the *A. aculeatus* crude extract is shown in Figure 4.7.
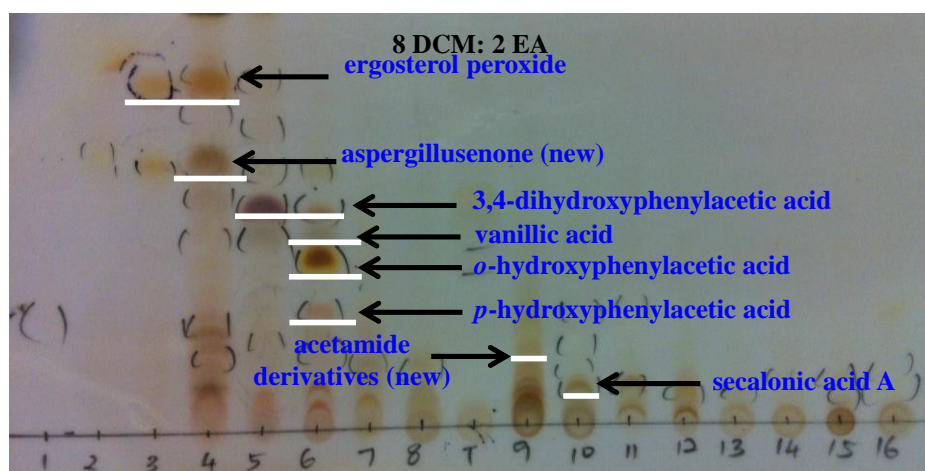
Figure 4.6: TLC summary plate of *A. aculeatus* fractions after spraying with *p*-anisaldehyde-sulphuric acid

Scale up *Aspergillus aculeatus*

- inoculated on new malt agar plate, incubated 8 days

- transferred into rice medium (20 L), day 30
- incubation at room temp., cold extraction (ethyl acetate, 3x), homogenized
- concentrated under vacuum using a rotary evaporator

Ethyl acetate extract
(18.5 g)

- **Dereplication studies:**
HRFT-LCMS, MZmine software, an *in-house* macro
combined with the Antimarin database

Fractionation

- MPLC (Büchi, Switzerland)
- gradient elution successively (100%Hex-100%EtOAc, 100%EtOAc-20%MeOH)
- column: 4-150mm, silica: 20-45 μm
- flowrate: 50ml/min, fraction collection: 100ml/fraction
- concentrated under vacuum using a rotary evaporator

-TLC (9.4DCM:0.6MeOH)
- combined fraction – 16 major fractions
- Dereplication studies on fractions: HRFT-LCMS, MZmine
software, an *in-house* macro combined with the Antimarin
database, SIMCA P+ 13
-Anti-trypanosomal assay

AARC30- 1 (1.5226 g)
AARC30-2 (0.3398 g)
AARC30- 4 (0.6118 g)
AARC30-6 (0.5669 g)
AARC30-8 (0.3723 g)
AARC30-10 (1.0144 g)
AARC30-12 (6.7248 g)
AARC30-14 (1.1238 g)
AARC30-15 (1.7252 g)
AARC30-16 (0.2068 g)

AARC30- 3 (0.2392 g)
AARC30-5 (0.1260 g)
AARC30-7 (0.5688 g)
AARC30-9 (1.6133 g)
AARC30-11 (5.6037 g)
AARC30-13 (0.7601 g)

AARC30-10-18 secalonic acid A (10.3 mg)

AARC30-4-1 ergosterol peroxide (5.30 mg)

aspergilluse-none (new) (2.30 mg)

acetamide (new) (4.25 mg)

AARC30-6-11 3, 4-dihydroxyphenylacetic acid (4.30 mg)
AARC30-6-28 vanillic acid (5.20 mg)
AARC30-6-50 *o*-hydroxyphenyl-acetic acid (6.23 mg)
AARC30-6-60 *p*-hydroxyphenylacetic acid (4.32 mg)

Figure 4.7: A summary of workflow on the *A. aculeatus* crude extract

4.4 **Structure elucidation and identification of metabolites from *A. aculeatus***

The investigation for new potential bioactive metabolites from a 30-day rice culture of the endophytic fungus *A. aculeatus* (AARC30) revealed two new compounds along with other six known compounds.

4.4.1 Compound AARC30-5-116-3 (new compound, 4.28)

Compound AARC30-5-116-3 (2.30 mg) was obtained as a yellow crystal and HRESI-LCMS showed a peak at *m/z* 349.1284 [M+H]$^+$ corresponding to the molecular formula $C_{18}H_{20}O_7$. The optical rotation was measured $[\alpha]_D^{20}$ +17.3 (*c* 1.00, acetone).

New compound	aspergillusenone, 7-hydroxy-2-(4-hydroxy-3-methoxy-3-methyl-5-oxotetrahydrofuran-2-yl)-3,5,8-trimethyl-4H-chromen-4-one
Sample code	AARC30-5-116-3 (**4.28**)
Sources	*A. aculeatus*
Yield (mg, %)	2.30 (0.01%)
Physical state	Yellow crystal
Molecular formula	$C_{18}H_{20}O_7$
Mol. weight (g/mol)	348.3472
Exact mass (*m/z*)	349.1284 [M+H]$^+$
Ret. time (min)	13.80
R_f value (8DCM: 2EA)	0.51
Optical rotation $[\alpha]_D^{20}$	+17.3 (*c* 1.00, CHCl$_3$)

4.28   6.42

(relative stereochemistry based on blennolide E, **6.42** (Zhang *et al.*, 2008)

RT: 0.00 - 45.11

AARC305 #417-457 RT: 13.37-14.42 AV: 21 SB: 494 14.19-43.49 , 0.03-13.48 NL: 5.62E7
T: FTMS {1,1} + p ESI Full lock ms [150.00-1500.00]
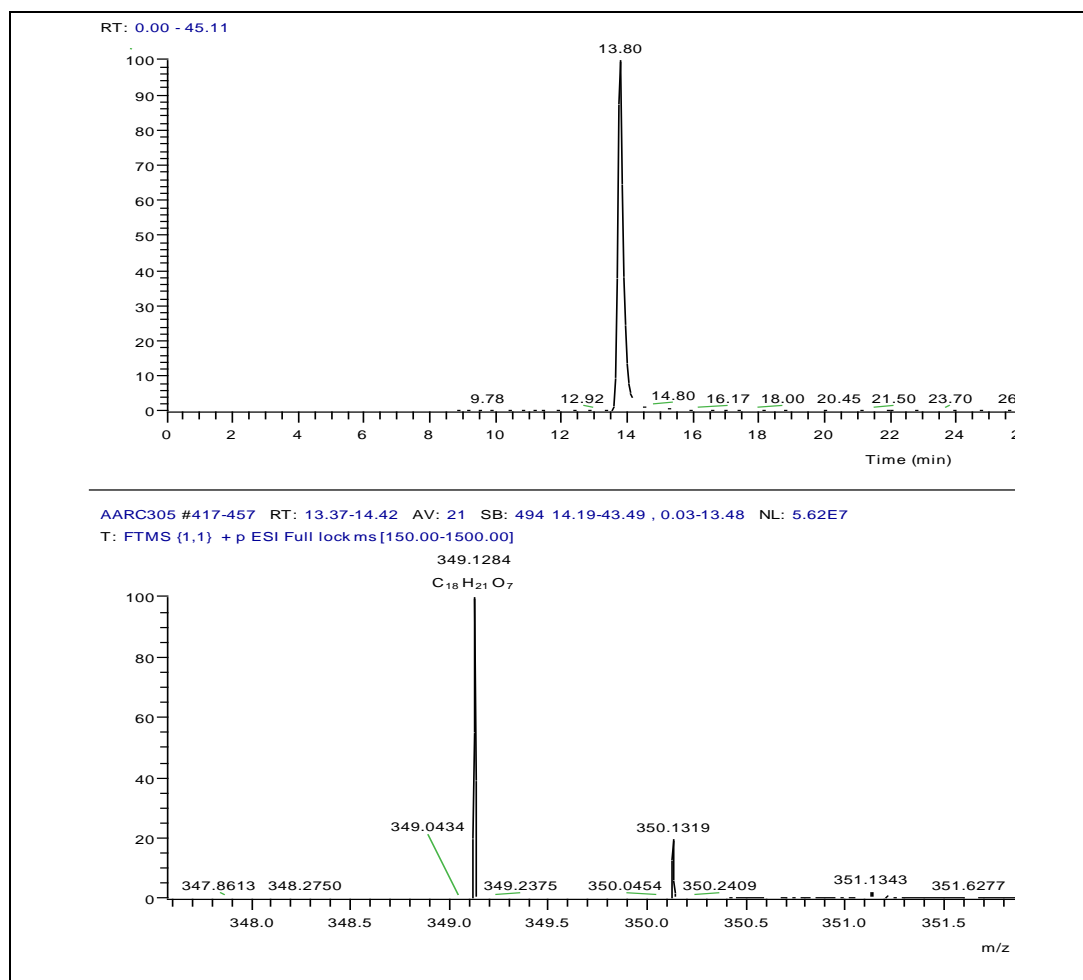
The ^{1}H NMR spectrum of AARC30-5-116-3 (Figure 4.8a, Table 4.5) showed a singlet proton signal on the aromatic region δ_H 6.60 (*s*, 1H, H-6). Two methine oxygen-linked signals were observed at δ_H 5.00 (*s*, 1H) and 4.45 (*d*, *J*=4.27 Hz, 1H) corresponded to H-9 and H-11 respectively, in which H-11 was correlated to a hydroxyl group at the same carbon, δ_H 4.13 (*d*, *J*=4.23 Hz, OH). Four methyl groups were also recorded in which three of them were on the aromatic ring: δ_H 1.73 (*s*, 3H), 2.10 (*s*, 3H) and 2.35 (*s*, 3H), whereas δ_H 1.71 (*s*, 3H) was on the furan ring. A methoxy group was also observed at δ_H 3.35 (*s*, OCH$_3$).

146
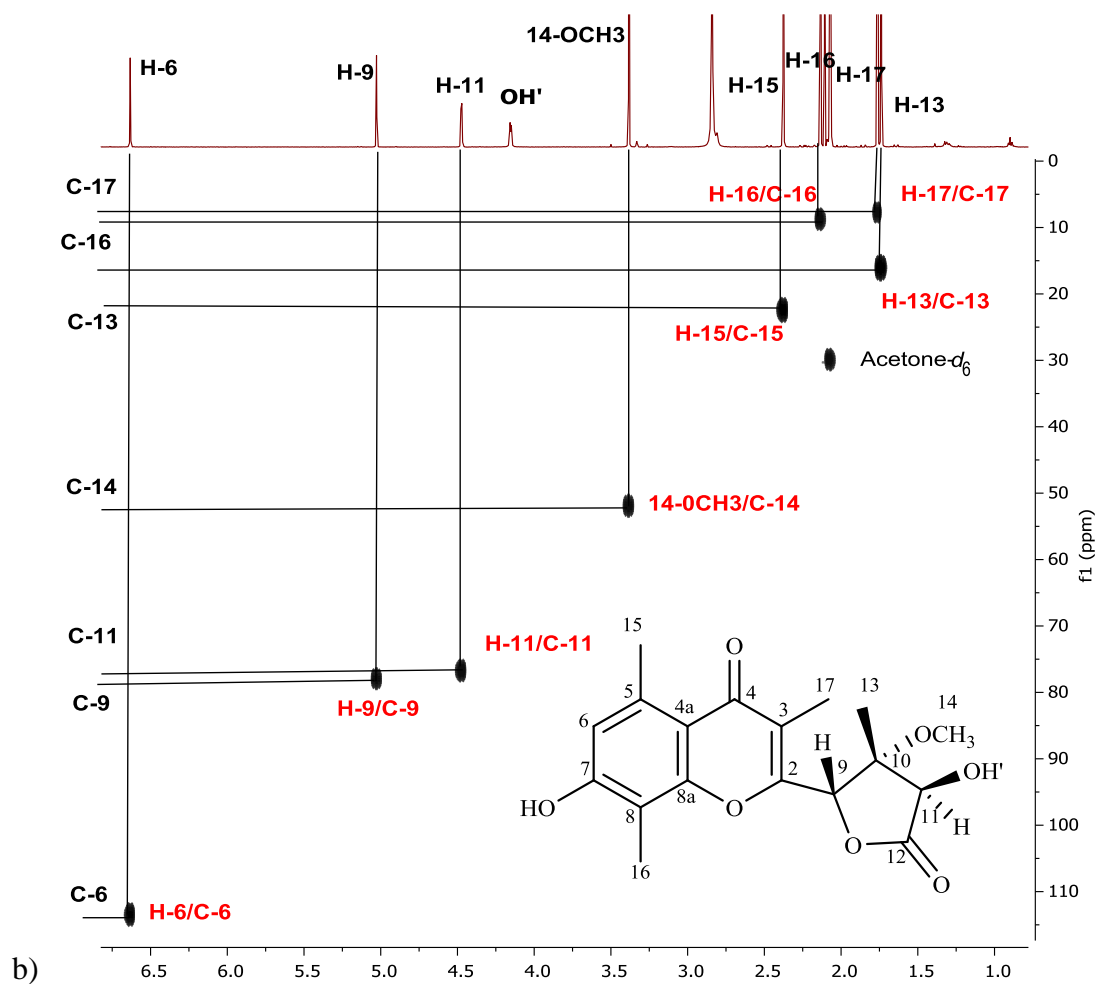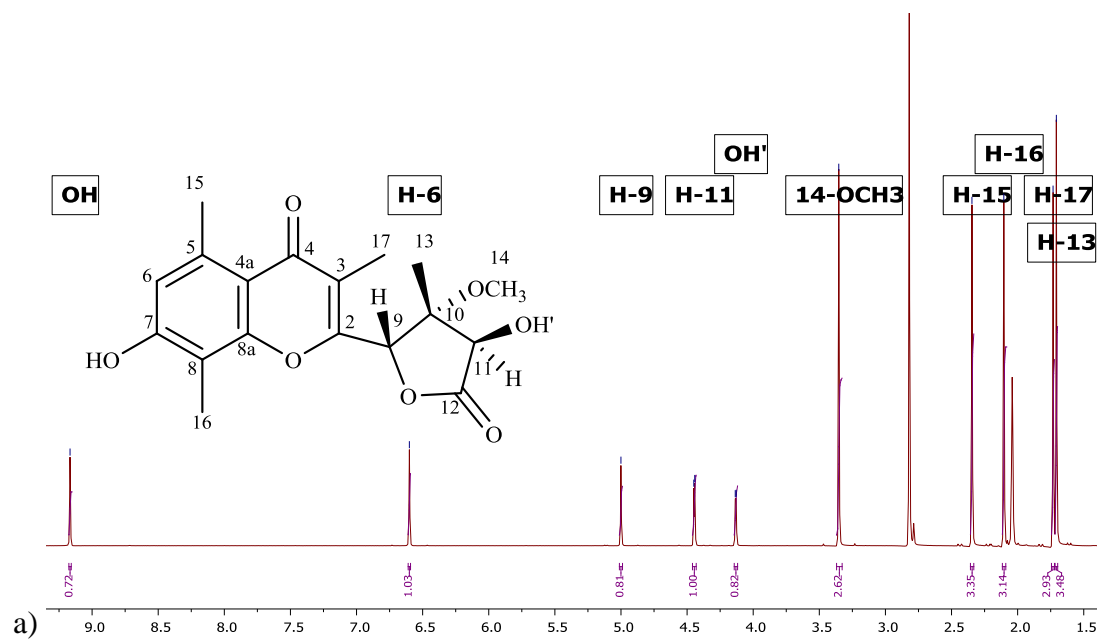
Figure 4.8: (a) ^{1}H and (b) HSQC NMR of AARC30-5-116-3
(Acetone-d_6, [1]H 600 MHz, DEPT 135, 150 MHz)

Table 4.5: ^{1}H and ^{13}C NMR of compound AARC30-5-116-3
(Acetone-d_6, ^{1}H 600 MHz, DEPT 135, 150 MHz) *Zhang *et al.*, 2008

No.	^{1}H NMR, δ_H (ppm, multi. *J* in Hz)		DEPT 135 NMR, δ_C (ppm)		COSY ^{1}H⇔^{1}H	NOESY ^{1}H⇔^{1}H	HMBC ^{1}H⇔^{13}C
	AARC30-5-116-3	*blennolide E	AARC30-5-116-3	*blennolide F (DEPT)	AARC30-5-116-3	AARC30-5-116-3	AARC30-5-116-3
2	-	-	156.3	83.6	-	-	9, 17
3	-	3.17 (*d*, *J*=17.0 Hz, 1H) 3.02 (*d*, *J*=17.0 Hz, 1H)	117.7	39.8	-	-	9, 17
4	-	-	196.9	194.0	-	-	17
4a	-	-	109.7	107.6	-	-	6, 15
5	-	-	140.7	161.9	-	-	15
6	6.60 (*s*, 1H)	6.57 (*dd*, *J*=8.3, 0.6 Hz, 1H)	113.4	110.8	5	15	4a, 7, 8, 15
7	-	7.42 (*t*, *J*=8.3 Hz, 1H)	159.6	139.0	-	-	7, OH,
8	-	6.52 (*dd*, *J*=8.2, 0.6 Hz, 1H)	111.8	107.7	-	-	6, 16, OH
8a	-	-	156.3	158.8	-	-	16
9	5.00 (*s*, 1H)	4.46 (*d*, *J*=1.8 Hz, 1H)	77.9	83.3	13	13	2, 3, 10, 11
10	-	3.01 (*m*, 1H)	80.8	39.2	-	-	9, 13, 14
11	4.45 (*d*, *J*=4.27 Hz, 1H)	4.80 (*d*, *J*=8.4 Hz, 1H)	76.7	74.2	OH'	13	12, 13
12	-	-	196.9	174.2	-	-	11
13	1.71 (*s*, 3H)	1.25 (*d*, *J*=7.3 Hz, 1H)	16.0	16.5	9	9, 11, 14	10, 11
14-OCH$_3$	3.35 (*s*, OCH$_3$)	-	51.9	168.4	-	13	10
15	2.35 (*s*, 3H)	3.73 (*s*, OCH$_3$)	22.4	53.6	-	6	4a, 5, 6
16	2.10 (*s*, 3H)	-	8.74	-	-	-	8, 8a
17	1.73 (*s*, 3H)	-	7.71	-	-	-	2, 3, 4
OH	9.17 (*s*, OH)	11.40 (*s*, OH)	-	-	-	-	6, 7, 8
OH'	4.13 (*d*, *J*=4.23 Hz, OH)	-	-	-	11	-	-
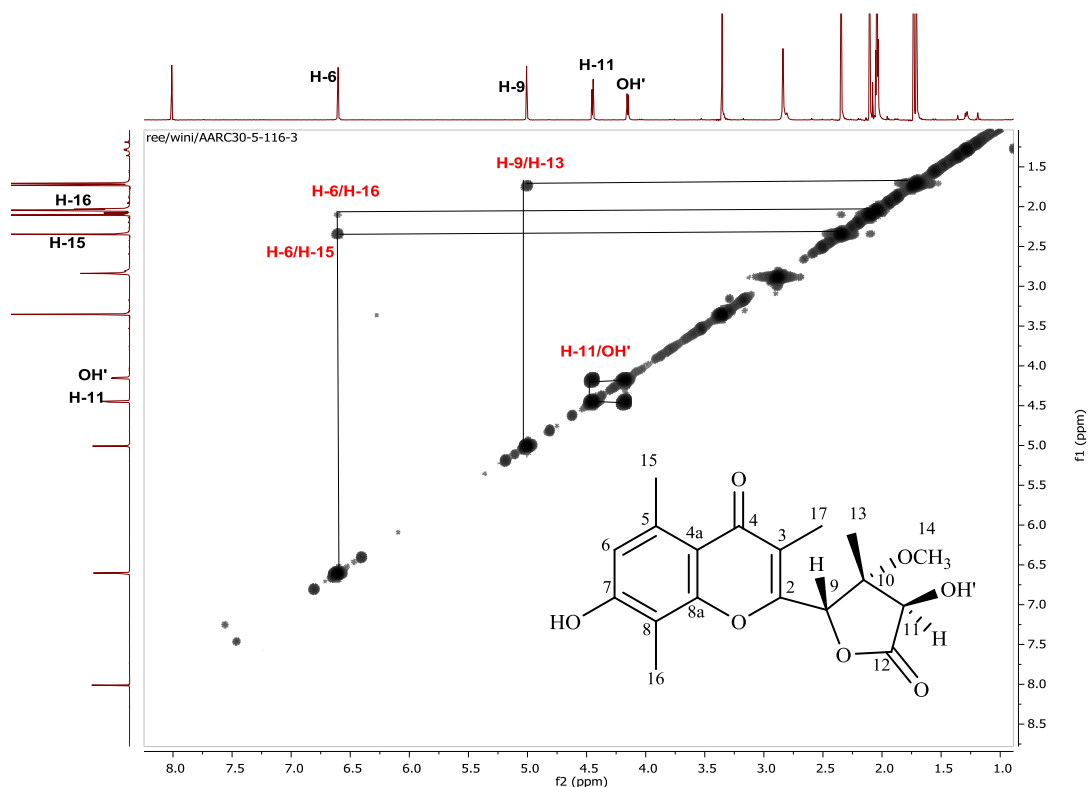
Figure 4.9: COSY NMR spectrum of AARC30-5-116-3
(Acetone-d_6, ^{1}H 600 MHz)
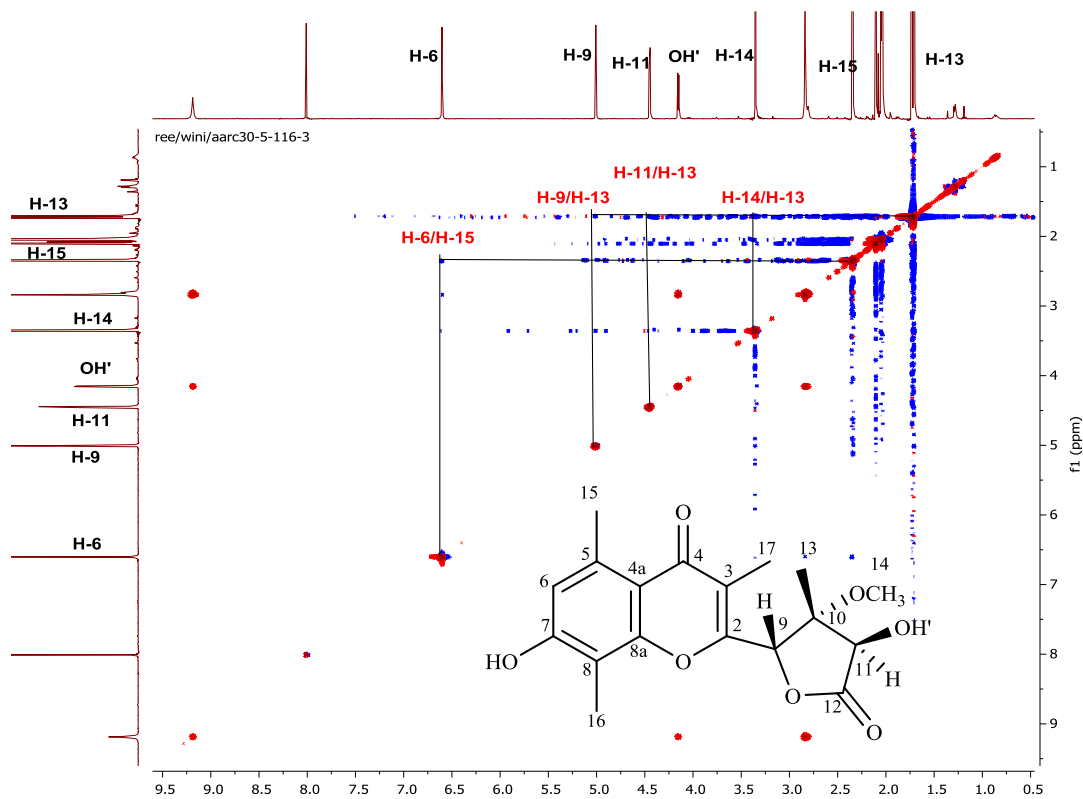
Figure 4.10: NOESY NMR spectrum of AARC30-5-116-3
(Acetone-d_6, ^{1}H 600 MHz)

Meanwhile, the COSY NMR (Figure 4.9) showed three correlations between H-6 and 15-CH$_3$, H-9 and 13-CH$_3$, and H-11 and OH'. The NOESY NMR (Figure 4.10) showed three important correlations between H-9 and 13-CH$_3$, between 13-CH$_3$ and H-11/14-OCH$_3$ as well as between H-6 and 15-CH$_3$. The HMBC NMR spectrum (Figure 4.11) showed the important correlations between proton H-6 and C-4a/C-7/C-8/C-15, H-9 and C-2/C-3/C-10/C-11, H-11 and C-12, H-14 and C-10, H-15 and C-4a/ C-5/C-6, H-16 and C-8/C-8a, H-17 and C-2/C-3/C-4. The remaining correlations between protons and carbons were depicted as in Figure 4.12.

Previous study reported some metabolites with the same skeleton have been discovered from endophytic fungus *Blennoria* sp. which has been isolated for the first time from *Carpobrotus edulis*; a native African plant called '*Hottentot-fig*' (Zhang *et al.*, 2008). The HRESI-LCMS and optical rotation for this compound is 336.0845 [M]$^+$ calculated for C$_{16}$H$_{16}$O$_8$, which is C$_2$H$_4$O$_8$ different from present metabolite and the optical rotation was measured $[\alpha]_D^{20}$ +69.0 (*c* 2.17, CHCl$_3$). Blennolide E possessed 2,3-dihydrochroman-4-one as a main skeleton and a furanone as substituent group. The presence of carbonyl in blennolide E was indicated at δ_C 168.4 (C-4), a quaternary carbon signal at δ_C 83.4 (C-2) and a methine carbon signal at δ_C 39.8 (C-3) representing the non-conjugated pyran ring (Zhang *et al.*, 2008). The same skeleton 2,3-dihydrochroman-4-one was found in microdiplodiasone isolated from fungus strain *Microdiplodia* sp. from the shrub *Lycium intricatum*, except for the two hydroxyls at *ortho-* and *meta*-positioned on the aromatic ring (Siddiqui *et al.*, 2011). Other different signals in blennolide E were also listed as in Table 4.5. In contrast, in present study shows that AARC30-5-116-3 possesses 2,3-dihydrochromen-4-one as the main skeleton with furanone ring as a substituent group attached at C-2.

4.28   6.42
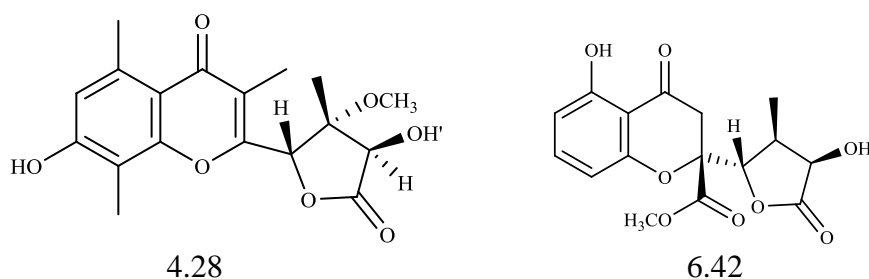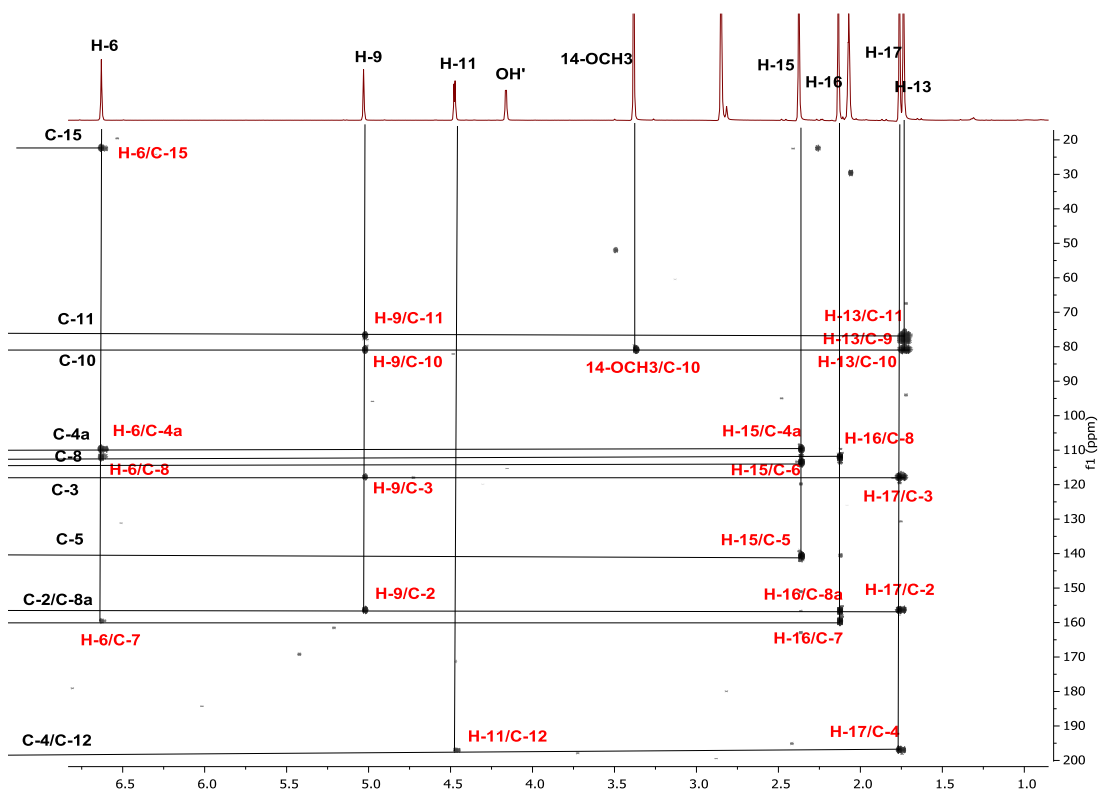
Figure 4.11: HMBC NMR spectrum of AARC30-5-116-3
(Acetone-d_6, ^{1}H 400 MHz, DEPT 135, 150 MHz)
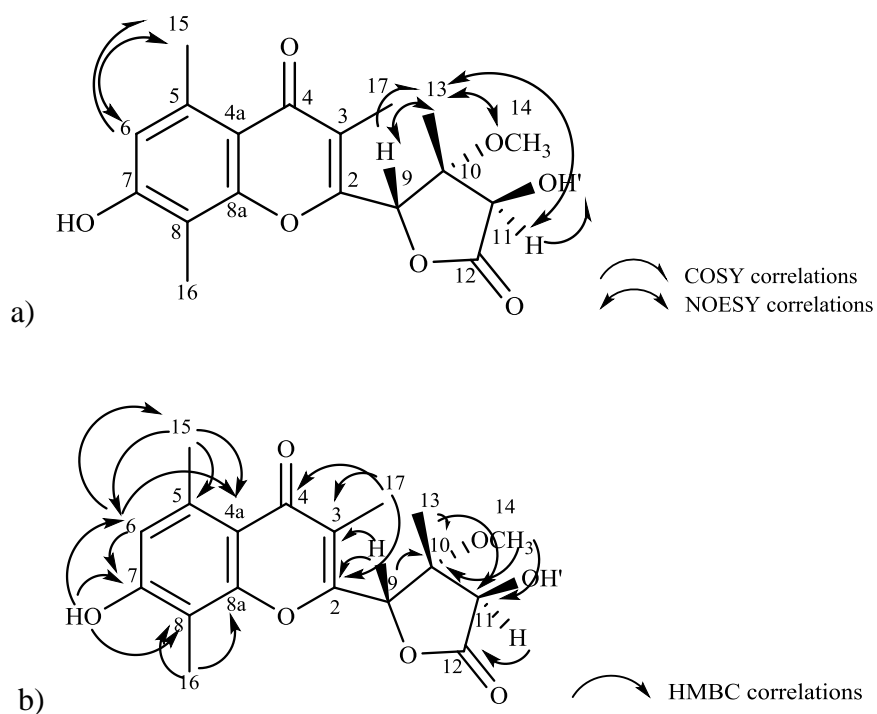
Figure 4.12: a) COSY and NOESY b) HMBC correlations of AARC30-5-116-3

Relative stereochemistry of AARC30-5-116-3 was established by means of NOESY which has been discussed earlier and circular dichroism (CD). The CD spectrum of AARC30-5-116-3 (Figure 4.13) was recorded in acetonitrile showed similar pattern to blennolide E (Zhang *et al.*, 2008), the CD consisted of three moderate positive bands in 290-370 nm region, a small positive band at 215 nm, two negative bands at 235 and 270 nm. Therefore, present compound was proposed to be a new 2,3-dihydrochromen-4-one derivative, namely as aspergillusenone (7-hydroxy-2-(4-hydroxy-3-methoxy-3-methyl-5-oxotetrahydro-furan-2-yl)-3,5,8-trimethyl-4*H*-chromen-4-one).

a)

b)
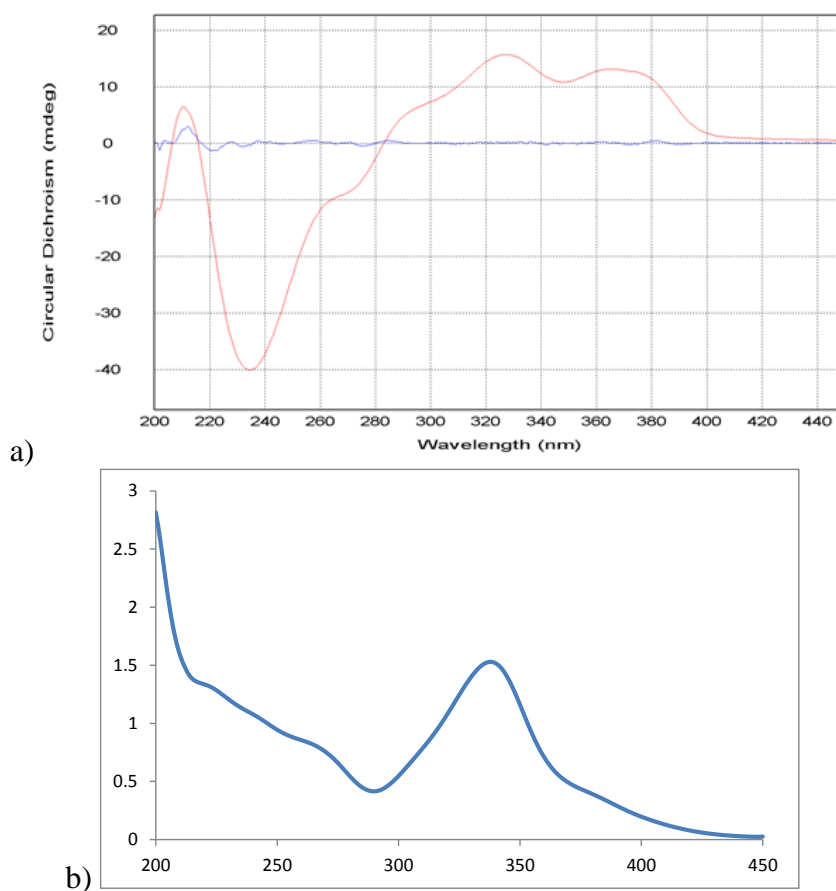
Figure 4.13: a) CD and b) UV spectra of AARC30-5-116
in acetonitrile, sample concentration at 1.44 mM, cell length 0.2 cm

Synonyms	vanillic acid, 4-hydroxy-3-methoxy-benzoic acid	3,4-dihydroxy-phenylacetic acid	o-hydroxyphenyl-acetic acid, 2-hydroxyphenylacetic acid	p-hydroxyphenyl-acetic acid, 4-hydroxyphenylacetic acid
Sample code	AARC30-6-28 (**4.29**)	AARC30-6-11 (**4.30**)	AARC30-6-50 (**4.31**)	AARC30-6-60 (**4.32**)
Sources	*A. aculeatus*	*A. aculeatus*	*A. aculeatus*	*A. aculeatus*
Yield (mg, %))	5.20 (0.01%)	4.30 (0.02%)	6.23 (0.03%)	4.32 (0.02%)
Physical state	Yellow oil	Yellow oil	Yellow oil	Yellow oil
Mol. formula	$C_8H_8O_4$	$C_8H_8O_4$	$C_8H_8O_3$	$C_8H_8O_3$
Mol. weight (g/mol)	168.1467	168.1467	152.1473	152.1473
Exact mass (*m/z*)	168.0400 $[M]^+$	168.0423 $[M]^+$	152.0473 $[M]^+$	152.0473 $[M]^+$
R_f value (8DCM: 2EA)	0.48	0.50	0.45	0.40

4.29   4.30   4.31   4.32

Table 4.6: ^{1}H NMR of phenolic acids
AARC30-6-28, AARC30-6-11, AARC30-6-50, AARC30-6-60 (Acetone-d_6, 400 MHz) and comparison with previous data

No.	^{1}H NMR, δ_H (ppm, multi. J in Hz)				
	AARC30-6-28 (4.29)	***vanillic acid**	**AARC30-6-11 (4.30)**	**AARC30-6-50 (4.31)**	**AARC30-6-60 (4.32)**
1	-	-	-	-	-
2	7.55 (*d*, *J*=2.0 Hz, 1H)	7.43 (*s*, 1H)	6.86 (*d*, *J*=2.5 Hz, 1H)	-	7.12 (*d*, *J*=8.2 Hz, 1H)
3	-	-	-	6.84 (*d*, *J*=7.7 Hz, 1H)	6.78 (*d*, *J*=8.2 Hz, 1H)
4	-	-	-	7.08 (*t*, *J*=7.7 Hz, 1H)	-
5	6.90 (*d*, *J*=8.1 Hz, 1H)	6.84 (*d*, *J*=8.7 Hz, 1H)	6.92 (*d*, *J*=8.6 Hz, 1H)	6.78 (*t*, *J*=7.7 Hz, 1H)	6.78 (*d*, *J*=8.2Hz, 1H)
6	7.58 (*dd*, *J*=8.3, 2.0 Hz, 1H)	7.45 (*d*, *J*=8.7 Hz, 1H)	6.76 (*dd*, *J*=8.6, 2.6 Hz, 1H)	7.17 (*d*, *J*=7.7 Hz, 1H)	7.12 (*d*, *J*=8.2 Hz, 1H)
7	-	-	3.78 (*s*, 2H)	3.64 (*s*, 2H)	3.50 (*s*, 2H)
O-CH₃	3.90 (*s*, OCH₃)	3.80	-	-	-
OH	8.38 (*s*, OH)		8.28 (*s*, OH)		8.21 8.28 (*s*, OH)

*Yu *et al.*, 2006 (DMSO-d_6, [1]H 300 MHz)
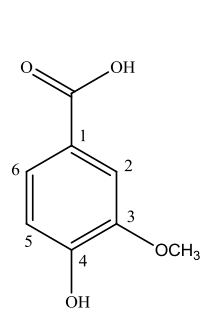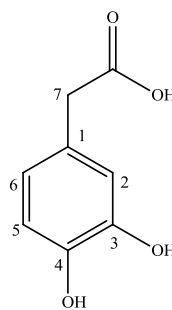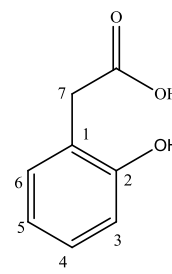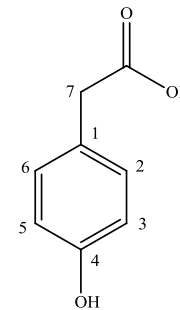
4.29   4.30   4.31   4.32

Table 4.7: ^{13}C NMR of phenolic acids AARC30-6-28, AARC30-6-11, AARC30-6-50, AARC30-6-60 (Acetone-d_6, 100.5 MHz) and comparison with previous data

Atom C	^{13}C NMR, δ_C (ppm)				
	AARC30-6-28	*vanillic acid	AARC30-6-11	AARC30-6-50	AARC30-6-60
1	122.1	121.7	125.2	121.7	125.8
2	114.7	115.1	110.6	155.3	115.2
3	147.2	147.3	154.0	115.3	130.4
4	151.2	151.1	147.9	128.2	156.4
5	112.8	112.8	112.0	119.4	130.4
6	124.1	123.5	114.6	131.7	115.2
7	-	-	33.0	34.9	39.6
C=O	166.6	167.3	174.3	172.3	172.4
O-CH$_3$	55.5	55.6	-	-	-

*Yu *et al.*, 2006 (DMSO-d_6, ^{13}C 75 MHz)

4.4.2 Compound AARC30-6-28 (vanillic acid, 4.29)

Compound AARC30-6-28 (5.20 mg) was obtained as yellow C and HRESI-MS showed the exact mass at *m/z* 168.0400 [M]$^+$, corresponding to the molecular formula $C_8H_8O_4$. The ^1H NMR spectrum of AARC30-6-28 (Figure 4.14 a, Table 4.6) showed an ABX spin system in the aromatic signals at δ_H 7.58 (*dd*, *J*=8.3, 2.0 Hz, 1H), 7.55 (*d*, *J*=2.0 Hz, 1H) and 6.90 (*d*, *J*=8.1 Hz, 1H) corresponding to the aromatic protons H-6, H-2 and H-5, respectively. A methoxy signal was also observed at δ_H 3.90 (*s*, OCH$_3$). Meanwhile, the ^{13}C NMR results (Figure 4.14 b, Table 4.7) showed a carbonyl carbon signal at δ_C 166.6 and two oxygen-linked quaternary carbon signals at δ_C 151.2 and 147.2, which were indicative of C-4 and C-3, respectively. Another quaternary carbon signal was observed at δ_C 122.1 (C-1), along with three carbon methine aromatic signals at δ_C 124.1, 114.7 and 112.1, which belong to C-6, C-2, and C-5, respectively. This compound was identified as vanillic acid (4-hydroxy-3-methoxybenzoic acid), which also has been previously isolated from the aspen blue stain fungus *Ophiostoma crassivaoinata* (Ayer and Trifonov, 1995), the fruit of *Capparis spinosa* (Yu *et al.*, 2006), the plant of *Bistorta manshuriensis* (Chang *et al.*, 2009) and from the fruit of *Amomum tsao-ko* (Martin *et al.*, 2000).
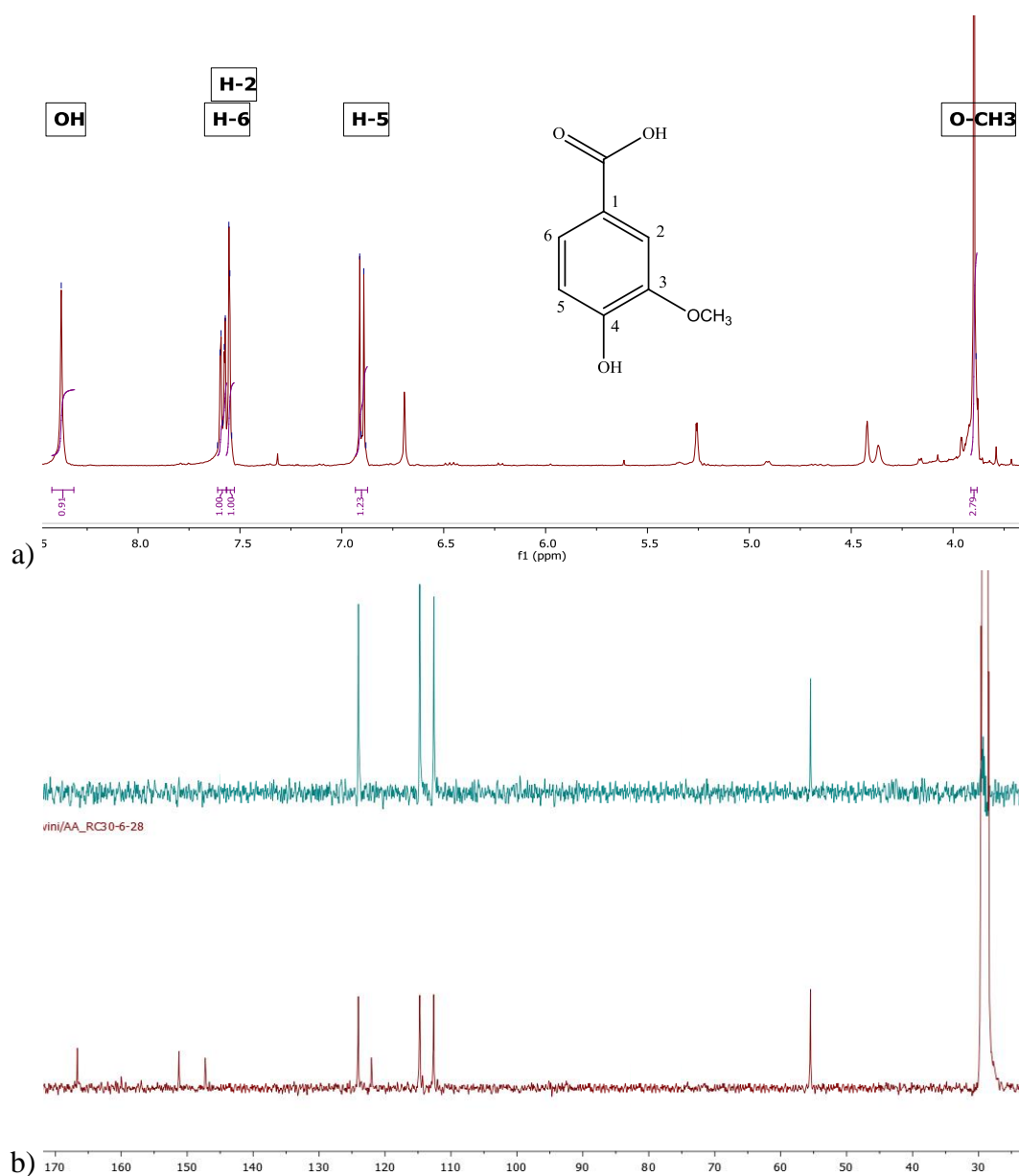
Figure 4.14: (a) ^{1}H (b) ^{13}C NMR of AARC30-6-28
DEPT 135 NMR (green), ^{13}C NMR (red) (Acetone-d_6, 400 MHz, ^{13}C 100.5 MHz)

4.4.3 Compound AARC30-6-11 (3,4-dihydroxyphenylacetic acid, 4.30)

Compound AARC30-6-11 (4.30 mg) was obtained as yellow oil and HRMS showed the exact mass at m/z 168.0423 [M]$^+$, corresponding to the molecular formula $C_8H_8O_4$. The ^{1}H NMR spectrum of AARC30-6-11 (Figure 4.15 a, Table 4.6) showed the same ABX system shown by AARC30-6-28. Three proton signals in the aromatic region at δ_H 6.92 (*d*, *J*=8.6 Hz, 1H), 6.86 (*d*, *J*=2.5 Hz, 1H) and 6.76 (*dd*, *J*=8.6, 2.6 Hz, 1H) corresponded to the *ortho* coupling H-5, *meta* coupling H-2 and *ortho* and *meta* coupling H-6, respectively. A methylene proton signal was

156

observed at δ_H 3.78 (*s*, 2H), the downfield chemical shift indicating that this proton was affected by an oxygen on the carbonyl group. Meanwhile, the ^{13}C and DEPT NMR spectra (Figure 4.15 b, Table 4.7) revealed eight carbon signals representing a phenyl with *para*-substitution. One of the signals indicated a carbonyl carbon at δ_C 174.3, while three C-H carbon signals belonged to the aromatic carbons: δ_C 110.6 (C-2), 114.6 (C-6), and 112.0 (C-5). Three quaternary carbon signals also were observed at δ_C 125.2 (C-1), δ_C 147.9 (C-4) and 154.0 (C-3). The structural elucidation of this compound was finalized and compared with a previous study on *Ophiostoma crassivaginata* (Ayer and Trifonov, 1995), thus confirming the identity of this compound as 3,4-dihydroxyphenylacetic acid.
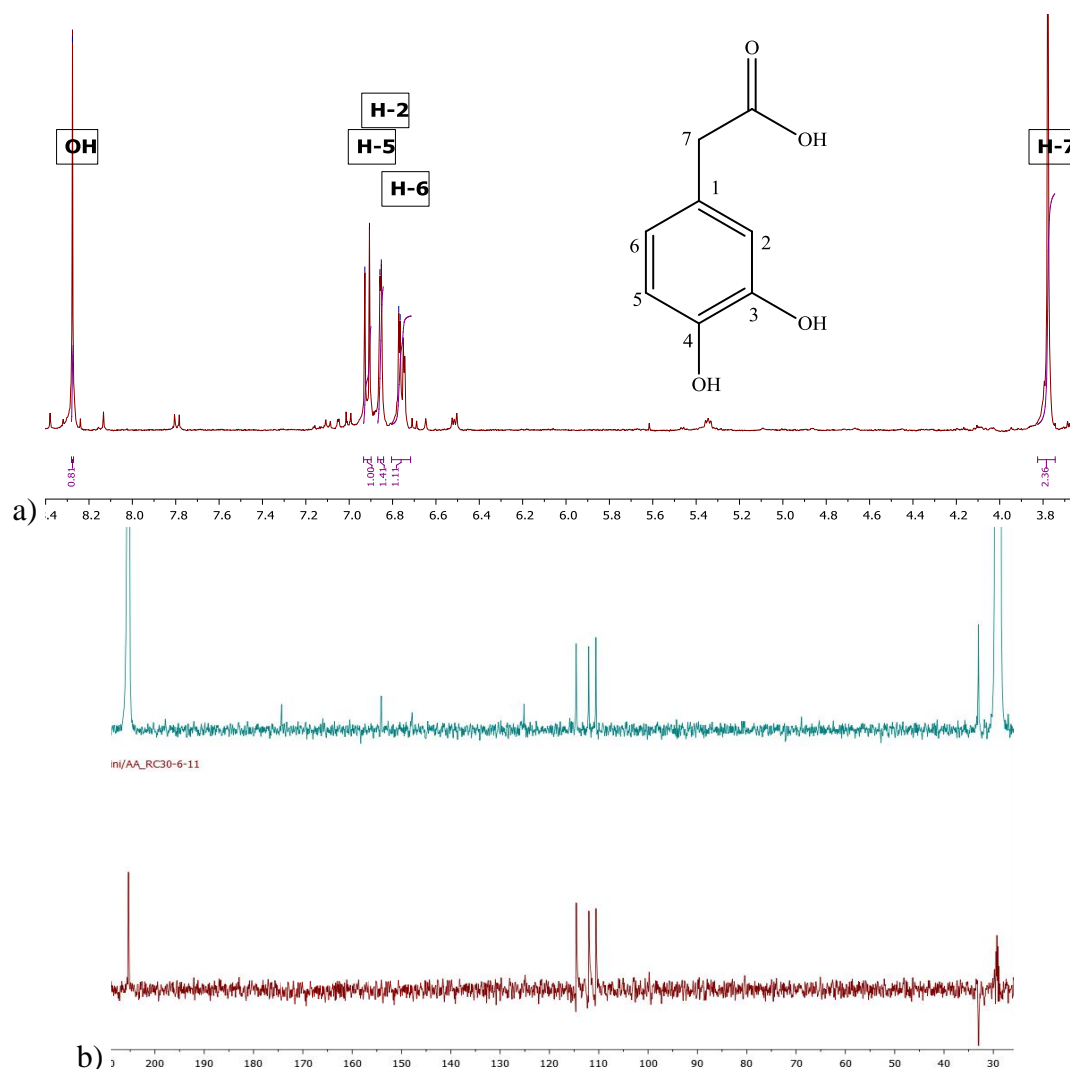
Figure 4.15: a) ^{1}H (b) ^{13}C NMR of AARC30-6-11
^{13}C NMR (green), DEPT 135 NMR (red) (Acetone-d_6, [1]H 400 MHz, [13]C 100.5 MHz)

4.4.4 Compound AARC30-6-50 (*o*-hydroxyphenylacetic acid, 4.31)

Compound AARC30-6-50 (6.23 mg) was obtained as yellow oil and HRMS showed exact mass at *m/z* 152.0473 $[M]^+$ corresponding to the molecular formula $C_8H_8O_3$. The ^1H NMR spectrum of AARC30-6-50 (Figure 4.16 a, Table 4.6) showed ABCD spin system with *ortho*-substitution; four aromatic proton signals at δ_H 6.84 (*d*, *J*=7.7 Hz, 1H), 7.08 (*t*, *J*=7.7 Hz, 1H), 6.78 (*t*, *J*=7.7 Hz, 1H), and 7.17 (*d*, *J*=7.7 Hz, 1H) corresponded to proton H-3, H-4, H-5, and H-6 respectively along with a methylene proton at δ_H 3.64 (*s*, 2H). The ^{13}C NMR results (Figure 4.17 b, Table 4.7) showed a carbonyl carbon signal at δ_C 172.3 and a carbon signal at δ_C 155.3 referred to a quaternary carbon-oxygen linked, C-2. Another quaternary carbon signal was observed at δ_C 121.7 (C-1), four methine carbon aromatic signals were shown by δ_C 115.3, 128.2, 119.4 and 131.7 corresponded to C-3, C-4, C-5 and C-6 respectively. A methylene carbon signal was also clearly observed at downfield δ_C 34.9 (C-7) which had electronegativity effect from the carbonyl on the aliphatic chain. Thus, this compound was determined as *o*-hydroxyphenylacetic acid which has been previously isolated from fermentation broth of bacteria *Micromonospora* sp. P1068 (Gutierrez-Lugo *et al.*, 2005).
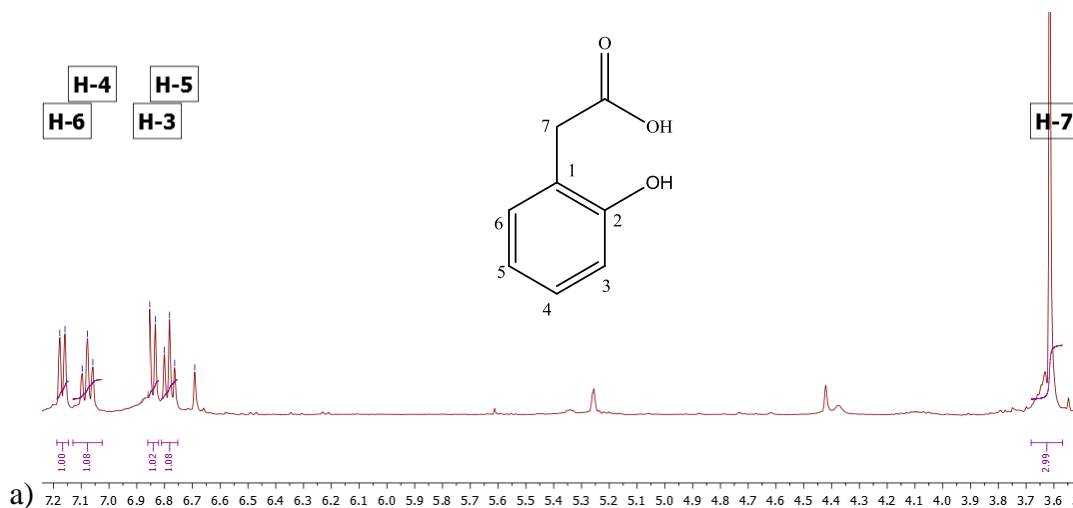
Figure 4.16: (a) ^1H (b) ^{13}C NMR spectra (red), DEPT 135 NMR (green) of AARC30-6-50 (Acetone-*d*$_6$, ^1H 400 MHz, ^{13}C 100.5 MHz)

b)

4.4.5   Compound AARC30-6-60 (*p*-hydroxyphenylacetic acid, 4.32)

Compound AARC30-6-60 (4.32 mg) was obtained as yellow oil and HRMS showed the exact mass at *m/z* 152.0473 [M]$^+$, corresponding to the molecular formula $C_8H_8O_3$. The ^{1}H NMR spectrum of AARC30-6-60 (Figure 4.17 a, Table 4.6) showed a symmetrical AA'BB' system with the aromatic signals at δ_H 7.12 (*d*, *J*=8.2 Hz, 1H) and 6.78 (*d*, *J*=8.2 Hz, 1H) corresponding to two proton signals for H-2/H-6 and for H-3/H-5. A methylene proton signal was also observed at δ_H 3.50 (*s*, 2H). The ^{13}C NMR results (Figure 4.17 b, Table 4.7) showed a carbonyl carbon signal at δ_C 172.4 and a carbon signal at δ_C 156.4 referring to an oxygen-linked quaternary carbon, C-4. Another quaternary carbon signal was observed at δ_C 125.8 (C-1), and two methine carbon aromatic signals were shown by δ_C 115.2 and 130.4, which corresponded to C-2/C-6 and C-3/C-5, respectively. A methylene carbon signal was also clearly observed downfield at δ_C 39.6 (C-7), as it had an electronegativity effect from the carbonyl on the aliphatic chain. Therefore, this compound was assigned as *p*-hydroxyphenylacetic acid which has been previously isolated from the aspen blue stain fungus *Ophiostoma crassivaginata* (Ayer and Trifonov, 1995) and marine bacteria strain T148 (Al-Zereini, 2006).

159
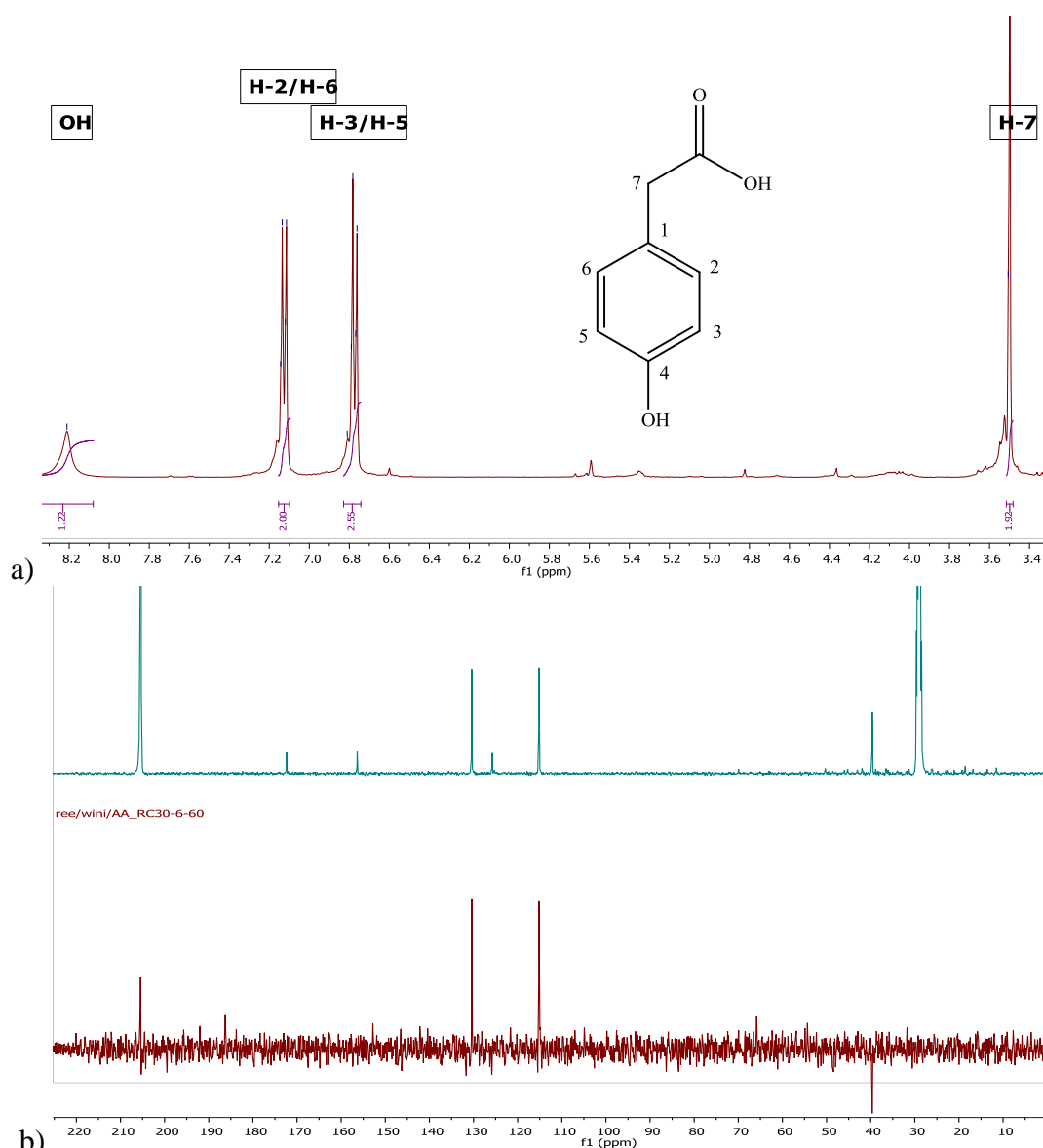
Figure 4.17: (a) ^{1}H and (b) ^{13}C NMR) of AARC30-6-60
^{13}C NMR (green), DEPT 135 NMR (red) (Acetone-d_6, ^{1}H 400 MHz, ^{13}C 100.5 MHz)

4.4.6 Compound AARC30-9-8-36 (new compound, 4.33)

Compound AARC30-9-8-36 (4.25 mg) was obtained as yellow oil and HRESI-LCMS showed a peak at *m/z* 196.1261 [M+H]$^+$ corresponding to the molecular formula $C_{10}H_{13}NO_3$. The ^{1}H NMR spectrum of AARC30-9-8-36 (Figure 4.18 a, Table 4.8) showed the presence of an ABX spin system for the aromatic proton signals: δ_H 6.67 (*d*, *J*=8.0 Hz, 1H), 6.66 (*s*, 1H) and 6.57 (*d*, *J*=8.5, 3.0 Hz, 1H) corresponded to protons H-5, H-2 and H-6, respectively. Two identical of methyl group signals were found at δ_H 3.61 (*s*, 6H). These were shifted downfield due to the effect of the nitrogen on the aliphatic chain. A methylene proton signal was

shown at δ_H 3.56 (*s*, 2H), indicating that this proton was deshielded by the carbonyl effect.

New compound	2-(3,4-dihydroxyphenyl)-*N*, *N*-dimethylacetamide
Sample code	AARC30-9-8-36 (**4.33**)
Sources	*A. aculeatus*
Yield (mg, %)	4.25 (0.02%)
Physical state	Yellow oil
Molecular formula	$C_{10}H_{13}NO_3$
Mol. weight (g/mol)	195.2151
Exact mass (*m/z*)	196.1261 [M+H]$^+$
Ret. time (min)	21.96
R_f value (8DCM: 2EA)	0.13

4.33
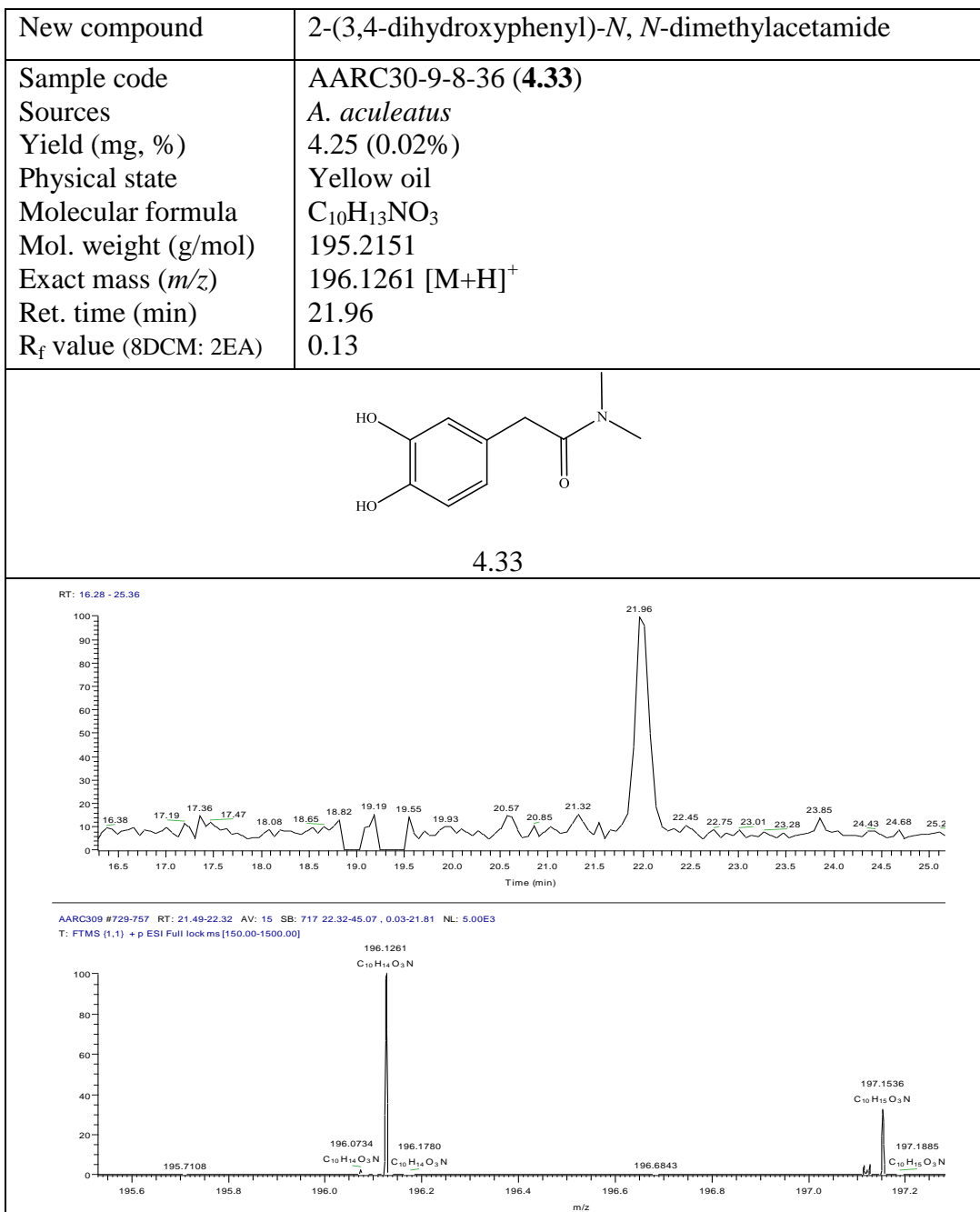
Meanwhile, the ^{13}C NMR spectrum (Figure 4.18 b, Table 4.8) revealed a carbonyl signal at δ_C 172.8 and three quaternary carbon signals, the latter two of which were directly attached to a hydroxyl group: δ_C 122.1 (C-1), 150.3 (C-4) and 148.2 (C-3). The other carbon signals were in the downfield region: δ_C 117.7, 115.8 and 114.4,

representing carbons C-2, C-5 and C-6, respectively. A methylene carbon signal at δ_C 35.2 and two carbon methyl signals at δ_C 51.0 and 50.9 directly attached to nitrogen were also observed. The correlation between the groups within the dimethyl amide, O=C-N-$(CH_3)_2$, was established by HMBC 2D NMR (Figure 4.19) and remaining correlations are shown in Figure 4.20. A substance with two ethyl groups attached to the amide group namely as 3,4-dihydroxyphenylacetic acid diethylamide has been synthetically prepared by (Carlsson *et al.*, 1962). Therefore, this compound proposed to be a new compound, 2-(3,4-dihydroxyphenyl)-*N,N*-dimethylacetamide, naturally isolated from this endophyte.
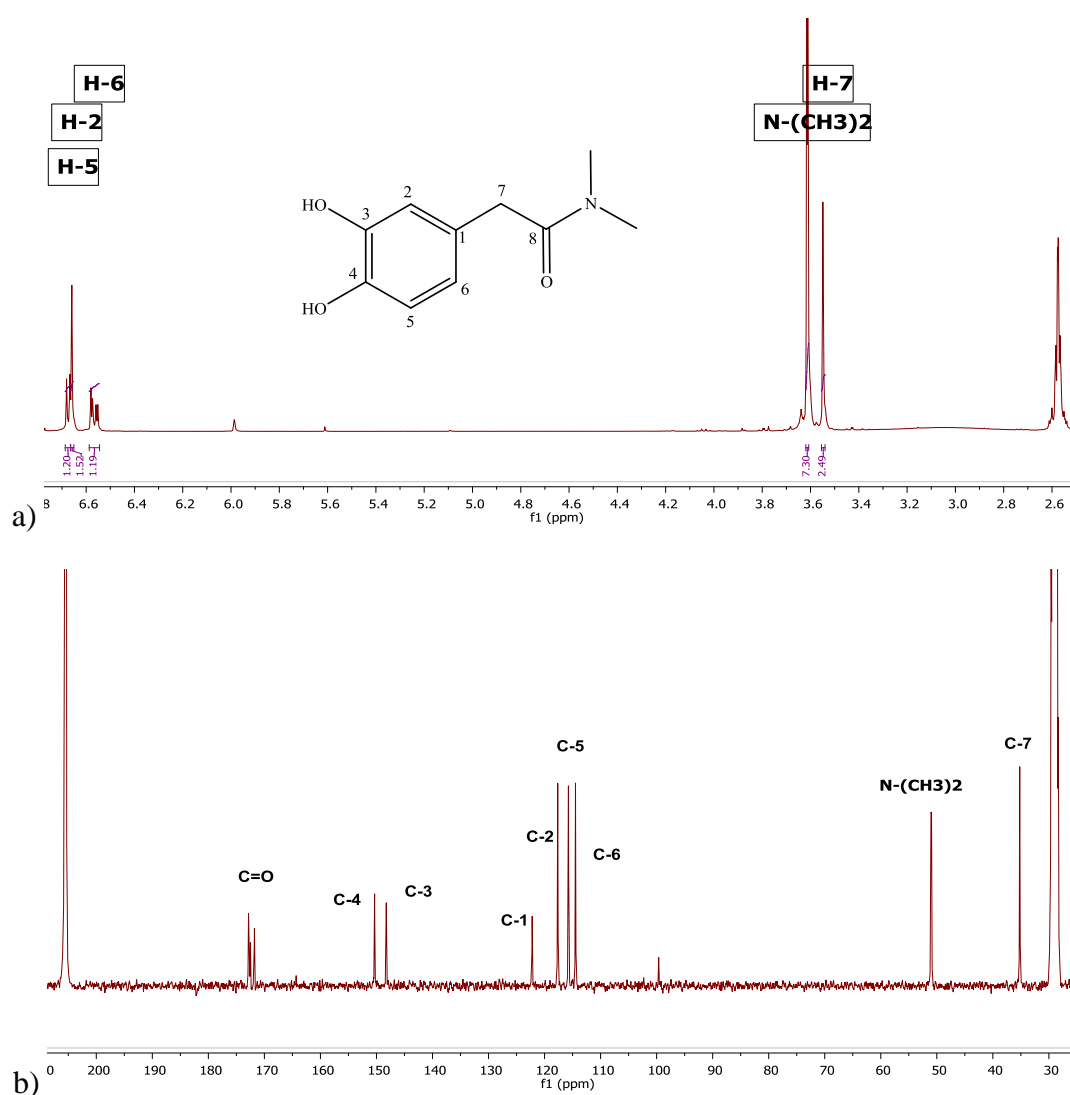
Figure 4.18: (a) ^{1}H (b) ^{13}C NMR spectra of compound AARC30-9-8-36 (Acetone-d_6, ^{1}H 400 MHz, ^{13}C 100.5 MHz)

Table 4.8: ^{1}H and ^{13}C NMR of compound AARC30-9-8-36
(Acetone-d_6, ^{1}H 400 MHz, ^{13}C 100.5 MHz)

No.	^{1}H NMR, δ_H (ppm, multi. J in Hz)	^{13}C NMR, δ_C (ppm)	HMBC H⇔C
1	-	122.1	-
2	6.66 (s, 1H)	117.7	1, 3, 4, 6, 7
3	-	148.2	-
4	-	150.3	-
5	6.67 (d, J=8.0 Hz, 1H)	115.8	1, 3, 4, 6
6	6.57 (d, J=8.5, 3.0 Hz, 1H)	114.4	2, 4, 5, 7
7	3.56 (s, 2H)	35.2	1, 2, 3, 8
8	-	172.8	-
N-CH$_3$	3.61 (s, 3H)	51.0	8
N-CH$_3$	3.61 (s, 3H)	50.9	8
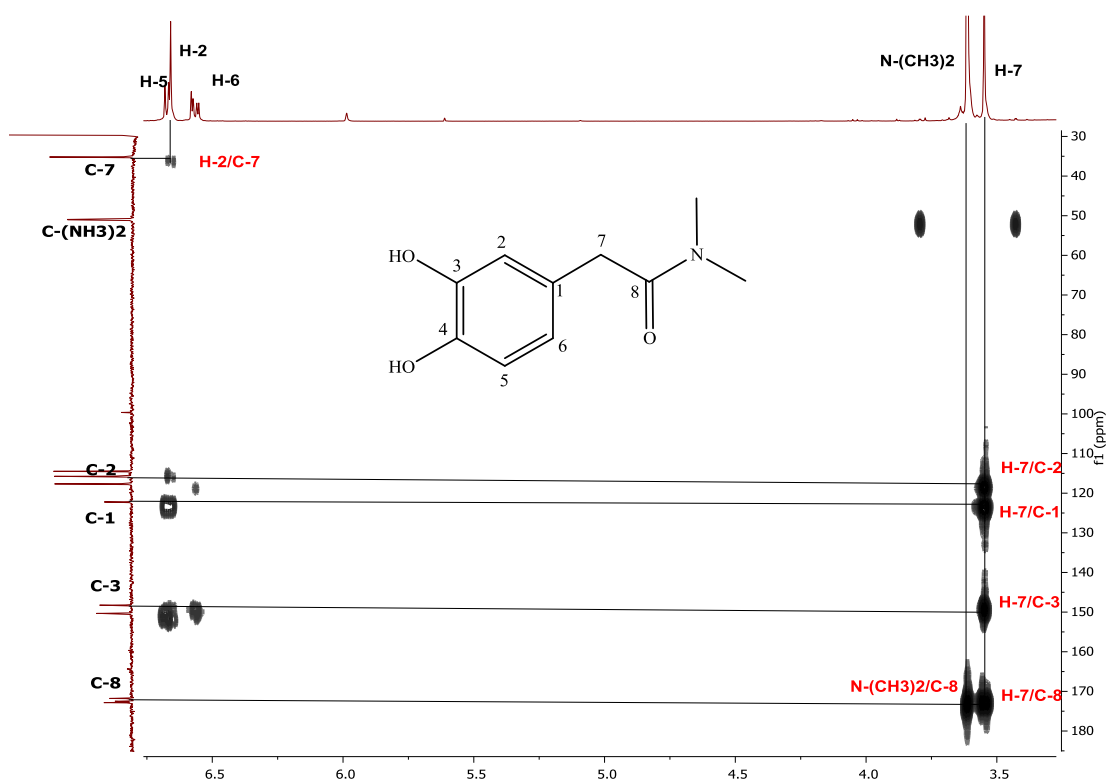
Figure 4.19: HMBC NMR spectrum of AARC30-9-8-36
(Acetone-d_6, ^{1}H 400 MHz, ^{13}C 100.5 MHz)

163
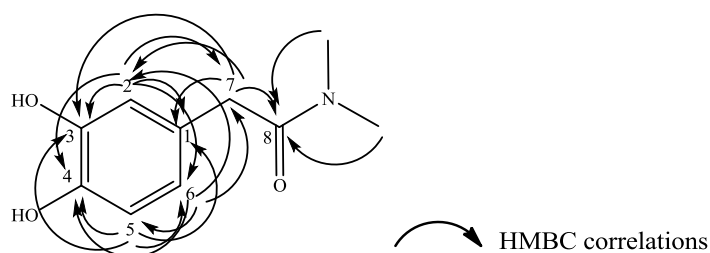
Figure 4.20: HMBC correlations of AARC30-9-8-36

4.4.7 Compound AARC30-10-18 (secalonic acid A, 4.20)

Compound AARC30-10-18 (10.30 mg) was obtained as yellow crystals. It had optical rotation of $[\alpha]_D^{20}$ +59.0 (*c* 1.00, acetone). The *m/z* 639.1713 $[M+H]^+$, corresponding to the molecular formula $C_{32}H_{30}O_{14}$, was determined by HRESI-LCMS. This metabolite was deduced by spectroscopic analysis and comparison from previous data; $[\alpha]_D^{25}$ +61.0 (*c* 0.11, $CHCl_3$), IRν_{max} (KBr) cm^{-1}: 3505 (chelated OH), 1735 (aliphatic ester C=O), 1610 (chelated O-hydroxyl C=O), 1585 (aromatic ring, C=C), 1432, 1232, 1061, UV/Vis (CH_2Cl_2): λ_{max} (ε)=338 (32840), 260 (13136), 228 nm (21086 $mol^{-1}m^3cm^{-1}$) (Ren *et al.*, 2006).

Synonyms	secalonic acid A, ergochrome AA (2,2')
Sample code	AARC30-10-18 (**4.20**)
Sources	*A. aculeatus*
Yield (mg, %)	10.30 (0.06%)
Physical state	Yellow crystals
Mol. formula	$C_{32}H_{30}O_{14}$
Exact mass (*m/z*)	639.1713 $[M+H]^+$
Mol. weight (g/mol)	638.5722
Ret. time (min)	18.88
R_f value (8DCM: 2EA)	0.28
Optical rotation $[\alpha]_D^{20}$	+59.0 (*c* 1.00, acetone)

4.20

(relative stereochemistry based on secalonic acid D, **4.34** (Anderson *et al.*, 1977)

rc30-8-18 #506-542   RT: 18.18-19.43   AV: 18   SB: 583 19.2
T: FTMS {1,1} + p ESI Full lock ms [150.00-1500.00]

639.1713
$C_{32}H_{31}O_{14}$

640.1742
$C_{32}H_{32}O_{14}$

641.1766
$C_{32}H_{33}O_{14}$

638.8417

643.4545
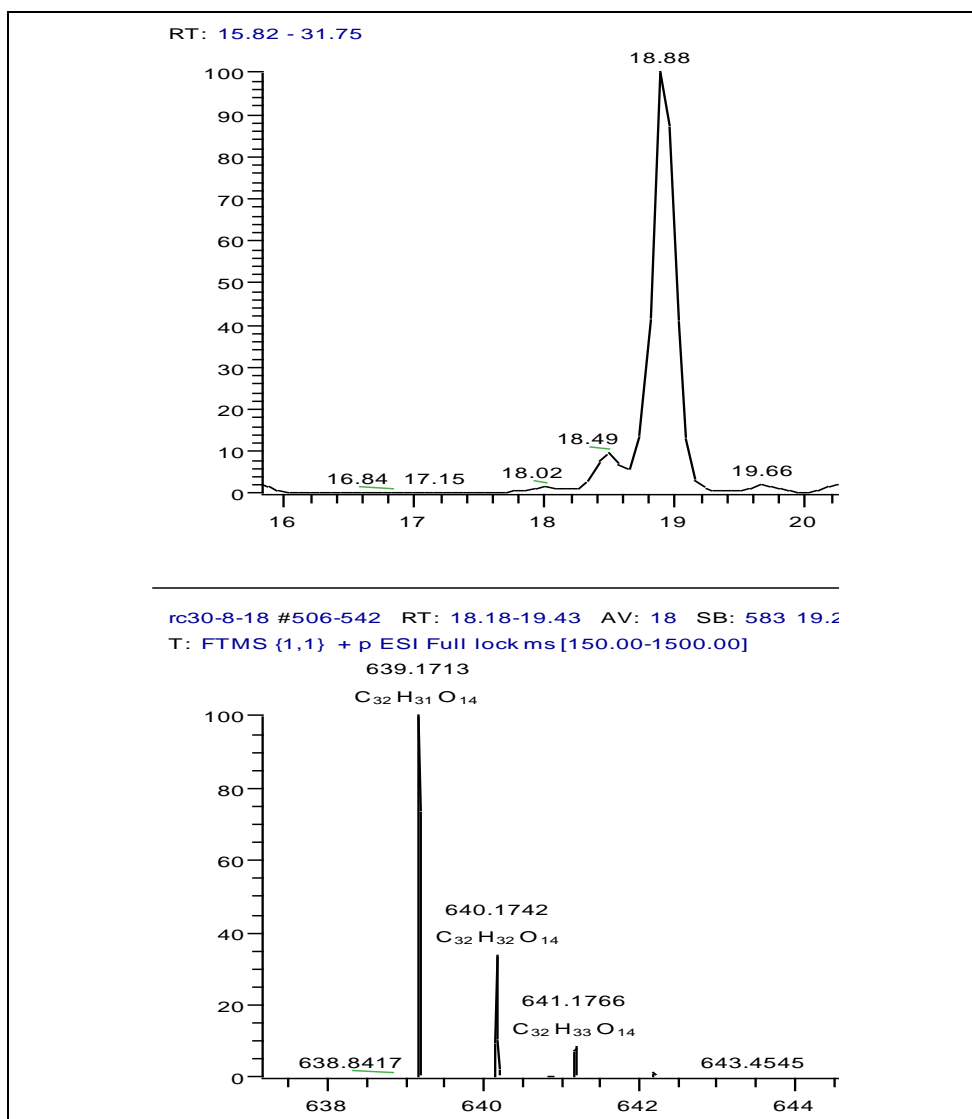
In addition, the complete assignment of all of the signals in the ^{1}H and ^{13}C NMR spectra confirmed the structure of the dimeric molecule that had been postulated. Figure 4.21 a and Table 4.9 show the proton signals of AARC30-10-18. 2H of each aromatic proton signal at δ_H 7.49 (*d*, *J*=8.5 Hz, 2H) and 6.57 (*d*, *J*=8.5 Hz, 2H) corresponded to protons H-3/3' and H-4/4'. A proton signal at δ_H 3.97 (*dd*, *J*=10.6, 4.7 Hz, 2H) indicated that this proton was affected by the electronegative effect of the hydroxyl group on the same carbon (HC-5-OH). A methine proton signal was also observed at δ_H 2.46 (*m*, 2H), which corresponded to H-6, and a methylene proton signal was shown at δ_H 2.75-2.44 (*m*, 2H). One methyl also was found at δ_H 1.16 (*d*, *J*=6.0 Hz, 6H) and assigned to CH$_3$-11/11'. Meanwhile, the presence of three proton signals at δ_H 13.76 (*s,* 2H; OH), 11.64 (*s*, 2H; OH) and 5.16 (*d*, *J*=4.7

Hz, 2H; OH) were assigned to the hydroxyl groups OH-8/8', OH-1/1' and OH-5/5', respectively.

The ^{13}C NMR spectrum (Figure 4.21 b, Table 4.9) exhibited 16 carbon signals with every signal representing two carbon atoms. Two carbonyl carbon signals were observed at δ_C 187.7 (C-9/9') and 178.7 (C-8/8'), as well as three quaternary carbon signals directly attached to hydroxyl groups: δ_C 170.2 (C12/12'), 159.4 (C-1/1') and 159.3 (C-4a/4a'). An oxygen-bound methine carbon was also seen at δ_C 76.3 (C-5/5'). The other carbon signals and optical rotation remained the same as those described in secalonic acid D (**4.34**) which has been isolated from marine lichen-derived fungus *Gliocladium* sp. (Ren *et al.*, 2006). However, relative stereochemistry of AARC30-10-18 based on CD spectrum (Figure 4.22 a) compared with its enantiomer secalonic acid D (Andersen *et al.*, 1977), the sequences of bands were similar but their signs inverted. AARC30-10-18 possessed three positive bands which were indicated by 215 nm (+11), 225 nm (+19), 270 nm (+21) and two negative bands were represented by 250 nm (-18) and a strong band at 310 nm (-33). Therefore, based on the spectroscopy results and comparison with previous literature, this compound was identified as secalonic acid A (5*S*,6*S*, 10a*R*,5'*S*,6'*S*,10a'*R*). Secalonic acid A also has been previously isolated from *A. ochraceus* (Yamazaki *et al.*, 1971) and *Paecilomyces* sp. (Zhai *et al.*, 2011).

a)

b)
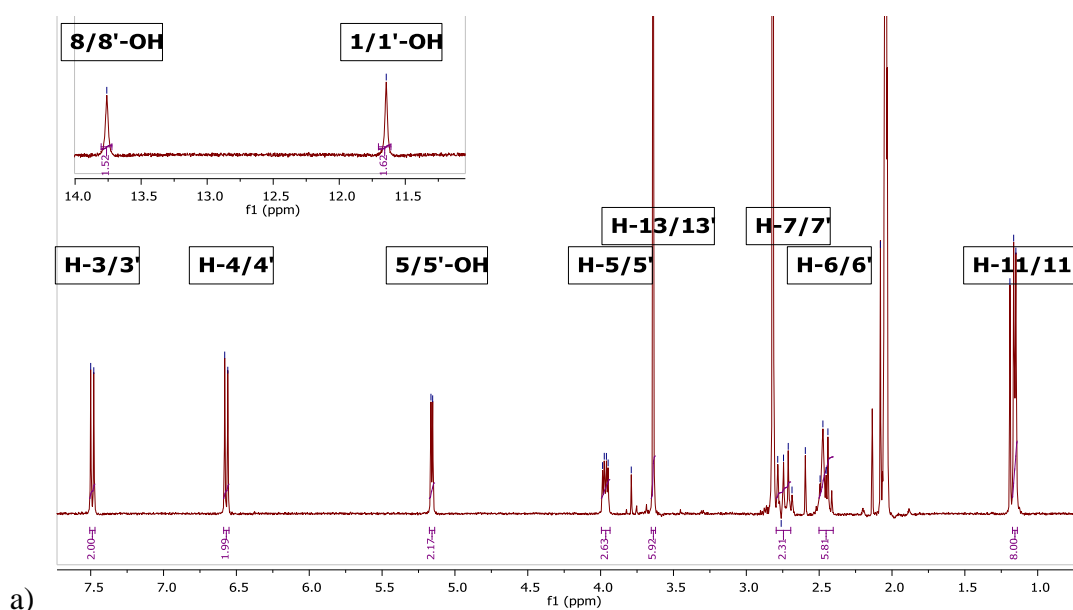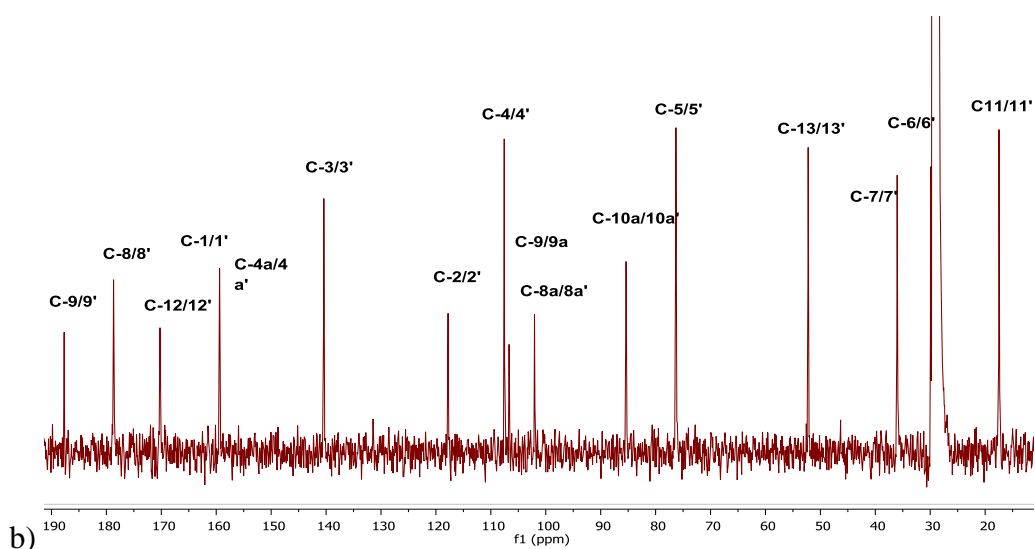
Figure 4.21: (a) ^{1}H (b) ^{13}C NMR spectra of compound AARC30-10-18
(Acetone-d_6, [1]H 400 MHz, [13]C 100.5 MHz)

Table 4.9: ^{1}H and ^{13}C NMR of compound AARC30-10-18
(Acetone-d_6, [1]H 400 MHz, [13]C 100.5 MHz) and comparison with literature

No.	^{1}H NMR, δ_H (ppm, multi. J in Hz)		^{13}C NMR, δ_C (ppm)	
	AARC30-10-18	*Secalonic acid D	AARC30-10-18	*Secalonic acid D
1/1'	-	-	159.4	158.9
2/2'	-	-	117.8	117.3
3/3'	7.49 (*d*, *J*=8.5 Hz, 2H)	7.45 (*d*, *J*=8.42 Hz, 2H)	140.4	140.2
4/4'	6.57 (*d*, *J*=8.5 Hz, 2H)	6.63 (*d*, *J*=8.42 Hz, 2H)	107.6	107.5
4a/4a'	-	-	159.3	158.5
5/5'	3.97 (*dd*, *J*=10.6, 4.7 Hz,2H)	3.81 (*d*, *J*=9.51 Hz, 2H)	76.3	75.2
6/6'	2.46 (*m*, 2H)	2.131 (*m*, 2H)	29.9	29.9
7/7'-α	2.75-2.44 (*m*, 2H)	2.65 (*dd*, *J*=8.42, 19.8 Hz, 2H)	36.0	35.8
7/7'-β		2.49 (*dd*, *J*=6.22, 19.8 Hz, 2H)	-	-
8/8'	-	-	178.7	178.2
8a/8a'	-	-	102.1	101.7
9/9'	-	-	187.7	186.6
9a/9a'	-	-	106.7	106.3
10a/10a'	-	-	85.4	85.2
11/11'	1.16 (*d*, *J*=6.0 Hz, 6H)	1.03 (*d*, *J*=6.22 Hz, 6H)	17.5	17.8
12/12'	-	-	170.2	170.0
13/13'	3.64 (*s*, 6H)	3.61 (*s*, 6H)	52.2	52.6
1/1'-OH	11.64 (*s*, 2H; OH)	11.62 (*s*, 2H; OH)	-	-
5/5'-OH	5.16 (*d*, *J*=4.7 Hz, 2H; OH)	4.08 (*s*, 2H; OH)	-	-
8/8'-OH	13.76 (*s*, 2H; OH)	13.60 (*s*, 2H; OH)	-	-

* Ren, *et al.*, 2006, ^{1}H and ^{13}C NMR (DMSO-d_6, [1]H 600 MHz, [13]C 150 MHz)

4.20   4.34

a)

b)
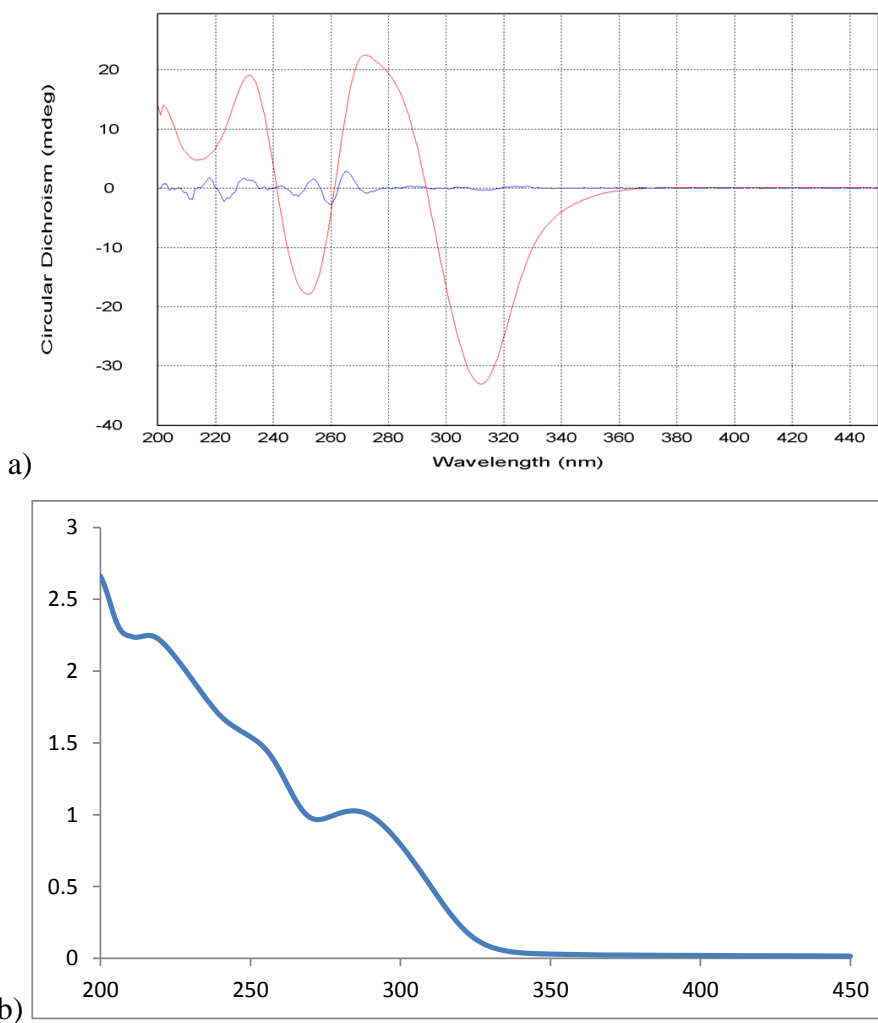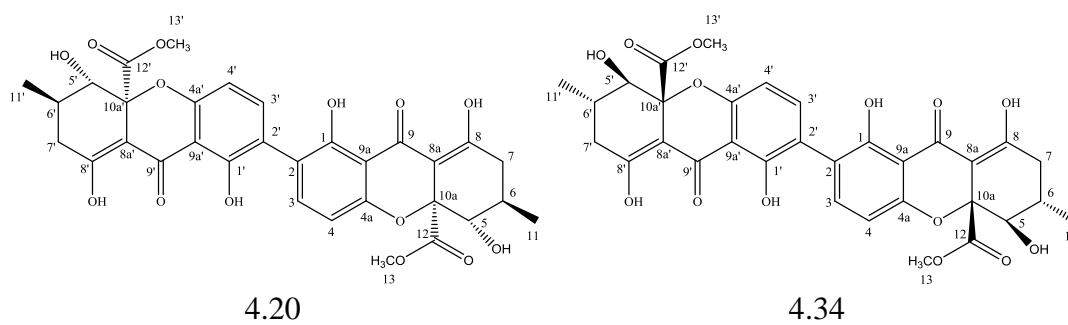
Figure 4.22: a) CD and b) UV spectra of AARC30-10-18
in acetonitrile, sample concentration at 0.39 mM, cell length 0.2 cm

Further purification on fraction AARC30-4 revealed AARC30-4-1 (ergosterol peroxide, (**3.27**), 5.30 mg), which had also been isolated from the fungus *Fusarium* sp. (Chapter 3.6.1).

4.5   Bioactivity test results

Each compound was tested against *T. b. brucei* and normal prostate cells (Table 4.10). Ergosterol peroxide, an ergosterol derivative in which a peroxide group is attached to the B ring (between C-5 and C-8) showed potent activity against *T. b. brucei* with an MIC of 1.56 μM and almost non-toxic to normal prostate cells (PNT2A). Among phenolic acids; 3,4-dihydroxyphenylacetic acid had the most potent activity with an MIC of 1.56 μM, whereas vanillic acid, *o*-hydroxyphenylacetic acid and *p*-hydroxyphenylacetic acid also had promising anti-trypanosomal activity with similar MIC of 6.25 μM. Whereas the only amide type of compound, 2-(3,4-dihydroxyphenyl)-*N,N*-dimethylacetamide also displayed good activity (MIC of 6.25 μM). The phenolic acids and amide decreased cytotoxicity against PNT2A cells. The activity shown by aspergillusenone and secalonic acid A was the most significant with MIC values of 1.26 and <0.19 μM, respectively, almost comparable to suramin. Both compounds showed cytotoxicity effects against PNT2A cells, 22.2% and 25.0% of control values, respectively. However, the initial screening concentration used against normal prostate cells was higher than their MICs, thus, it is still possible both compound can be used as a lead drugs against trypanosomal protozoa.

vanillic acid

3, 4-dihydroxyphenylacetic acid

o-hydroxyphenylacetic acid

p-hydroxyphenyl-acetic acid

ergosterol peroxide

aspergillusenone
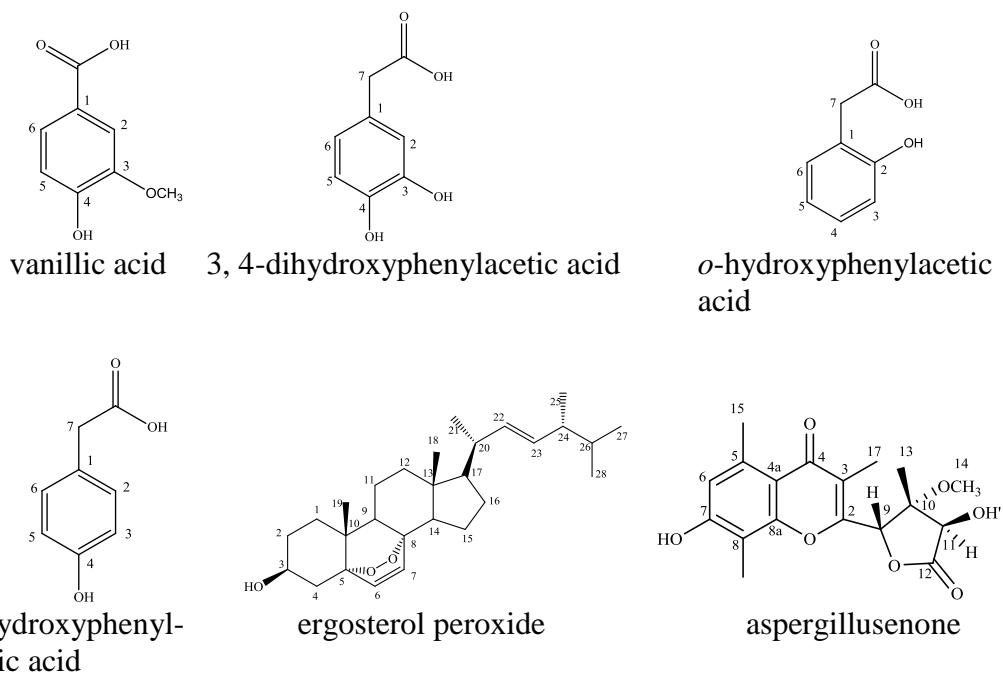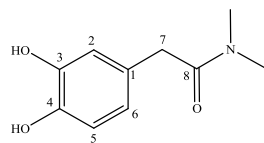
2-(3,4-dihydroxyphenyl)-*N*,*N*-dimethylacetamide
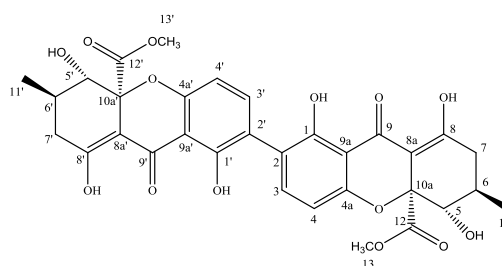
secalonic acid A

**Table 4.10: Activities of the isolated compounds
from *A. aculeatus* against *T. b. brucei* and PNT2A cells**

Compounds	[a] MICs (µM)	[b] Cytotoxicity, % D of control (100 µg/mL)
ergosterol peroxide	1.56	94.0
3,4-dihydroxyphenylacetic acid	1.56	93.0
o-hydroxyphenylacetic acid	6.25	98.1
vanillic acid	6.25	83.4
p-hydroxyphenylacetic acid	6.25	93.7
aspergillusenone	1.26	22.2
2-(3,4-dihydroxyphenyl)-*N*,*N*-dimethylacetamide	3.12	91.9
secalonic acid A	<0.19	25.0
Suramin	0.11	n.d
Triton X	n.d	0.082

[a] Each sample was tested in two independent assays against *T. b. brucei*, MIC values indicate the minimum inhibitory concentration of a compound/standard in µM necessary to achieve 90% growth inhibition. MICs (MIC < 10 µM - promising; 10 µM < MIC > 20 µM - moderate; 20 µM < MIC > 30 µM - marginal/weak; 30 µM < MIC > 40 µM - limited; MIC > 40 µM - no activity);
[b] Initial screening for cytotoxicity activity against human normal prostatic epithelial cells (PNT2A) , % D of control values (at 100 µg/mL,) were determined by averaging of three independent assays results (n=3); [c, d] Positive controls; n.d.- not determined.

170

Chapter 5

5.   Bioactive secondary metabolites from *Lasiodiplodia theobromae*

In this chapter, another fungal strain *L. theobromae* (synonym *Botryodiplodia theobromae*), isolated from *A. lanata*, was investigated for potential anti-trypanosomal substances. *L. theobromae* is a phytopathogenic fungus that causes fruit and root diseases, resulting in serious damage to agriculture in tropical and subtropical regions. Many studies have been reported on *L. theobromae* as a disease-causing agent, including studies on its effects on mango production and gummosis in Pakistan and Egypt (Khanzada *et al.*, 2004, Ismail *et al.*, 2012), respectively. The former led to a proposal of better approaches to reduce the problem in mango fields (Khanzada *et al.*, 2005). Other studies involved causal agents in *Boswellia papyrifera* trees in Ethiopa (Gezahgne *et al.*, 2014), grapevine and mamey sapote *Pouteria sapota* dieback (Al-Saadoon *et al.*, 2012, Pedraza *et al.*, 2013), and rot diseases in *Jatropha curcas* in Benin (Adanonon *et al.*, 2014) and mulberry roots in China (Adandonon *et al.*, 2014, Xie *et al.*, 2014). A recent study (Twumasi *et al.*, 2014) proved this fungus, which has been isolated from four different samples - cocoa, mango, banana and yam from the forest of Ghana, is phytopathogenic and caused rot fungus in crops. It is also known as a human pathogen causing keratomycosis (Punithalingam, 1976) and phaeohyphomycosis (Summerbell *et al.*, 2004). Previous chemical investigation of this fungus afforded some natural biologically active metabolites such as jasmonic acid which inhibits plant growth (Aldridge *et al.*, 1971, Nakamori *et al.*, 1994), lasiodiplodin and its derivatives (Aldridge *et al.*, 1971, Yang *et al.*, 2000, Li *et al.*, 2005a, Matsuura *et al.*, 1998), dihydroisocoumarins including mellein and its derivatives (Nakamori *et al.*, 1994, Aldridge *et al.*, 1971, Nunes *et al.*, 2008), cyclohexene compounds related to theobroxide (Takei *et al.*, 2008, Nakamori *et al.*, 1994, Kitaoka *et al.*, 2009) along with their derivatives, and eremophilane-type sesquiterpene and ergosterol from *L. theobromae* isolated from guava (Nunes *et al.*, 2008). The lasiodiplodin derivatives (3*R*,4*S*)-4-hydroxylasiodiplodin, (3*R*,6*R*)-6-hydroxy-de-*O*-methyllasiodiplodin and (3*R*,5*R*)-5-hydroxy-de-*O*-methyllasiodiplodin which have been isolated from *L. theobromae* proved to possesses potato micro-tuber inducing

substances (Yang *et al.*, 2000, Nakamori *et al.*, 1994, Matsuura *et al.*, 1998, Aldridge *et al.*, 1971, Li *et al.*, 2005a, Li *et al.*, 2007).

5.1 Results and discussion

Preliminary screening and identification of metabolite production from *L. theobromae* (Figure 5.1) was carried out. The anti-trypanosomal bioactivity results of the extracts of *L. theobromae* were reported in Table 5.1. LTRC15 showed the most intense activity while LTRC7 showed the least activity of the rice culture extracts. In contrast, the extracts of liquid cultures showed weak activity.
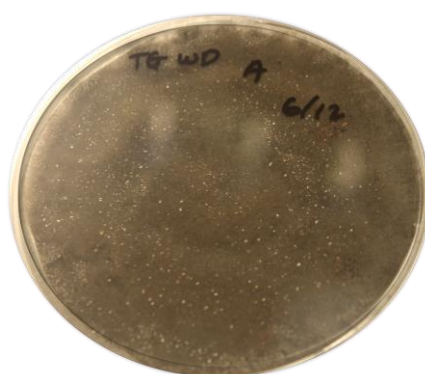
Figure 5.1: A pure strain of the endophytic fungus *L. theobromae* grown on malt agar plate

Table 5.1: Anti-trypanosomal activity of *L. theobromae* small-scale extracts (calculated as mean value of percentage viability) at concentrations of 20 µg/ mL

Small scale extracts *L. theobromae*	*T. b. brucei*, % D control (20 µg/mL)
LTRC7	47.3
LTRC15	1.9
LTRC30	15.6
LTLC7	90.0
LTLC15	61.4
LTLC30	54.5

% D, percentage viability of control

The dereplication study for the small scale extracts was accomplished to gain a metabolomic profile for monitoring and preliminary screening the relationship between the production of metabolites and different culture media at different

periods of cultivation (RC= rice culture extracts, LC = liquid culture extracts on day 7, 15 and 30).
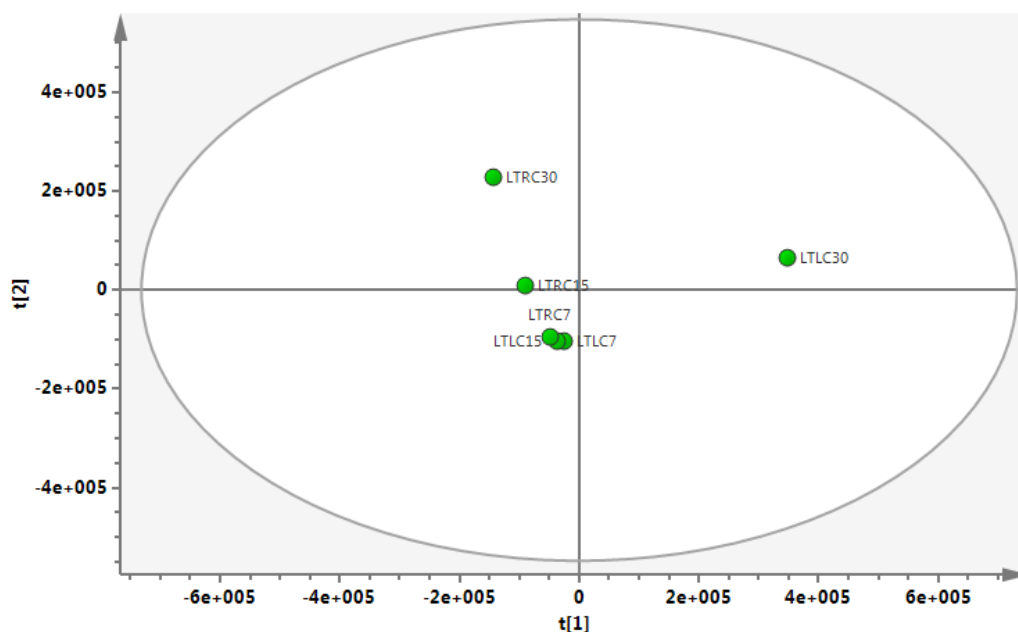
a)
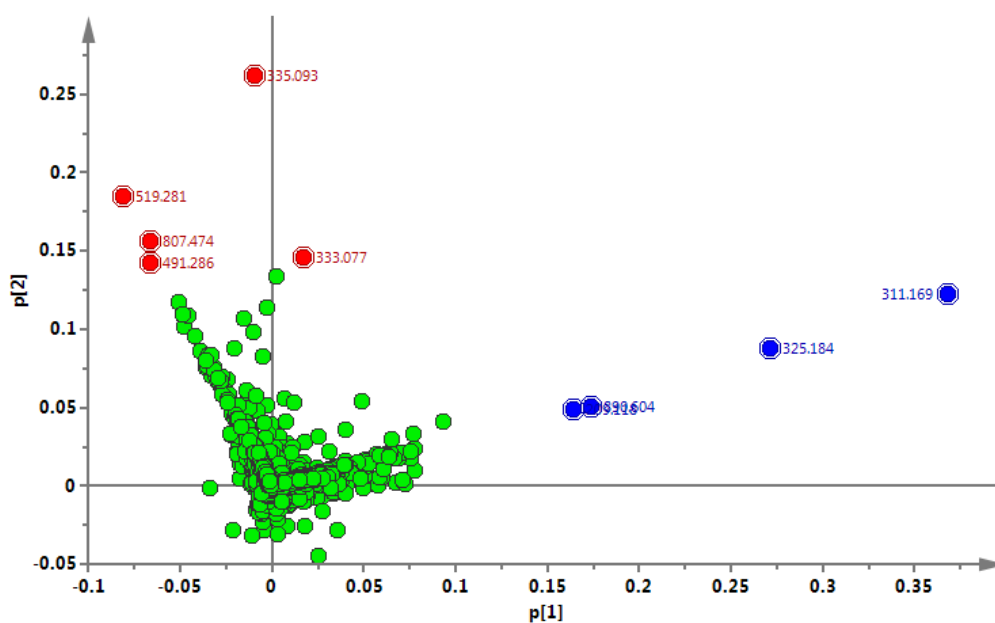
b)

Figure 5.2: PCA analysis on small scale extracts of *L. theobromae*
L. theobromae grown in rice and liquid culture media (LTRC= rice culture extracts, LTLC = liquid culture extracts on day 7, 15 and 30); The multivariate analysis on production of metabolites and different culture media at different periods of cultivation (RC= rice culture extracts, LC = liquid culture extracts on day 7, 15 and 30). (a) The PCA score plot of the small-scale extracts of *L. theobromae* showed moderate separation between LTRC30, LTLC30 and the other extracts; (b) PCA loading plot showed the metabolites were produced only in LTLC30 (blue) and LTRC30 (red).

The bioactivity of the metabolites of *L. theobromae* was also investigated. Metabolic profiling was initially performed to allow the selection of the optimum condition for cultivation to be later scaled up. Each extract was also tested for anti-trypanosomal activity. The score plot of the unsupervised PCA (Figure 5.2 a) showed that the extract of the 30-day rice culture (LTRC30) and 30-day liquid culture day (LTLC30) were well-separated from the other extracts. The PCA loading plot (Figure 5.2 b) showed biomarkers produced in LTLC30 (blue), with *m/z* 209.1180 [M-H]⁻ was putatively identified as placidene E isolated from the Mediterranean sacoglossan *Placida dendritica* (Cutignano *et al.*, 2003), and *m/z* 311.1690, 325.1840, and 890.6040 [M-H]⁻ were not identified. Whereas, the metabolites produced in LTRC30 were *m/z* 491.2860 [M-H]⁻ putatively identified as actinoramide C isolated from (red) *Streptomyces* sp. (Nam *et al.*, 2011), whereas 519.2810 and 807.4740 [M-H]⁻ were not identified with database. These three metabolites also appeared in LTRC15 but were less abundant. Besides, two metabolites were found in both LTRC30 and LTLC30 extracts; *m/z* 333.0770 [M-H]⁻ was identified as halenaquinol isolated from *Xestospongia sapra* (Motomasa Kobayashi *et al.*, 1985), and 335.0930 [M-H]⁻ was identified as xylarenol isolated from the fungus *Xylaria* sp. PSU-A80 (Rukachaisirikul *et al.*, 2007).
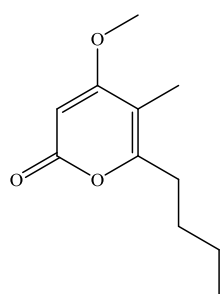
placidene E
Rt: 11.97 mins
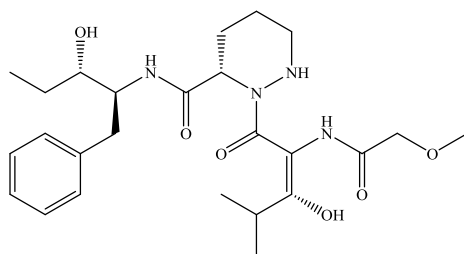
actinoramide C
Rt; 13.99 mins
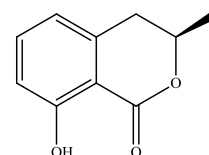
mellein
Rt: 13.60
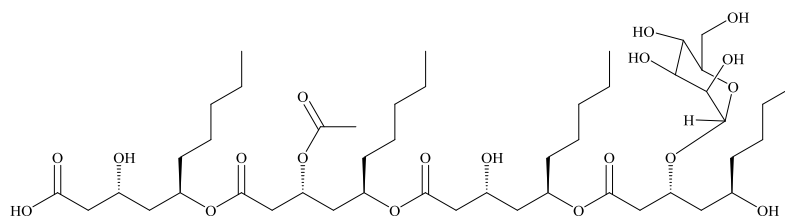
halymecin B
Rt: 18.69

174
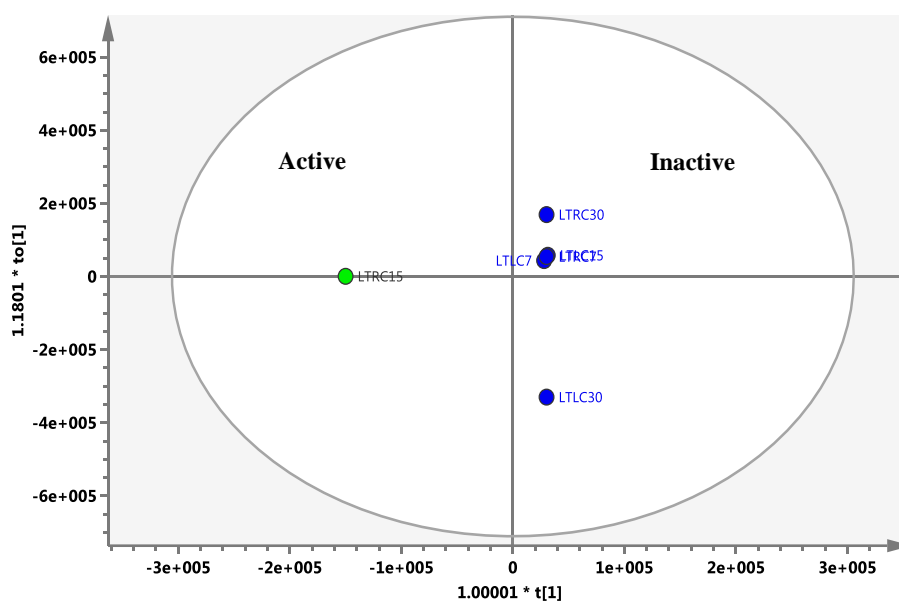
a)
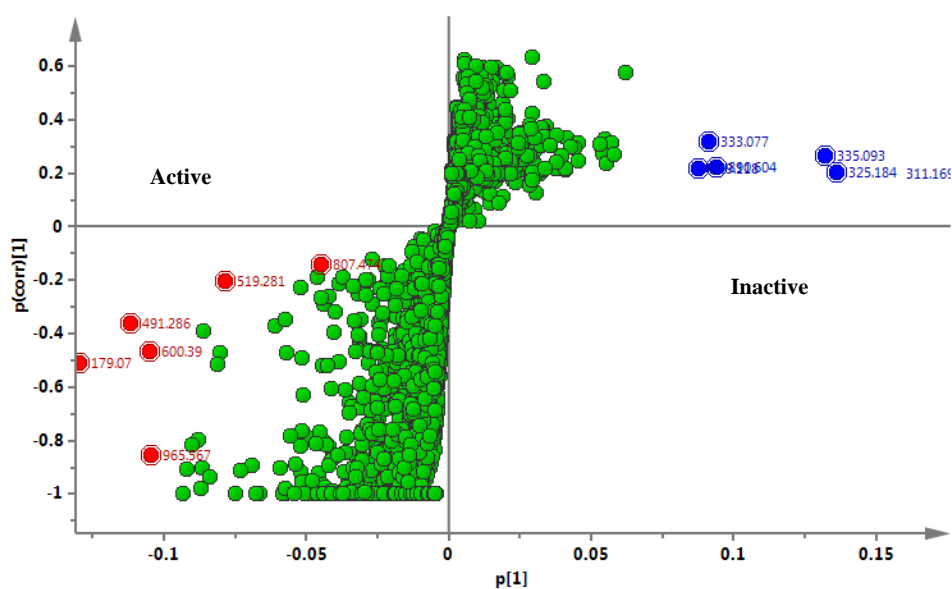
b)

Figure 5.3: OPLS-DA analysis on small scale extracts of *L. theobromae*
(a) Supervised OPLS-DA score plot analysis showed a better separation between LTRC15 (active) and LTLC30 (inactive) ($R^2(Y)$ =0.989; $Q_2(Y)$ =0.999); (b) OPLS-DA S-plot exhibited outlier compounds on both active (red) and inactive groups (blue).

However, the supervised OPLS-DA (Figure 5.3 a) showed a significant difference between small-scale extracts of the active LTRC15 and inactive LTRC7, LTRC3, LTLC7, and LTLC15. Meanwhile, the S-plot (Figure 5.3 b) showed unique biomarkers in the active (red) and inactive group (blue) in which some of them were putatively identified using Antimarin database. The metabolites that may be responsible for the anti-trypanosomal activity in LTRC15; with m/z 491.2860

[M-H]⁻ was identified earlier, 179.0700 [M+H]⁺ was identified as mellein from *L. theobromae* (Aldridge *et al.*, 1971), and 965.6570 [M-H]⁻ was identified as halymecin B isolated from *Fusarium* sp. (Chen *et al.*, 1996). Whereas, the metabolites with m/z 600.3900, 519.2810 and 807.4740 [M-H]⁻ were not identified. Meanwhile, the biomarkers were produced in inactive group (blue) with m/z 209.1180 [M-H]⁻ was putatively identified as placidene E isolated from the Mediterranean sacoglossan *Placida dendritica* (Cutignano *et al.*, 2003), 333.0770 and 335.0930 [M-H]⁻ as mentioned earlier, were also found in LTRC30 and LTLC30 extracts. Meanwhile, the metabolites with m/z 311.1690, 325.1840, and 890.6040 [M-H]⁻ were not identified from the database.

5.2 Scale up of *L. theobromae* for the isolation of metabolites

Based on the results of the dereplication study and anti-trypanosomal assays, it was concluded that the extract from the 15-day rice culture was the most active. *L. theobromae* was therefore subsequently cultured in 25 of 2 L Erlenmeyer flasks containing 200 g of rice for 15 days (LTRC15). The metabolites were extracted using ethyl acetate, yielding 24.0 g of crude extract. This was analysed using HRESI-MS for dereplication (Chapter 7.6).

5.2.1 Dereplication studies on the crude extract of *L. theobromae*

The total ion chromatogram of the crude extract of *L. theobromae* LTRC15 (Figure 3.5) shows the distribution of known and unknown compounds present in LTRC15 total extract. Those compounds previously identified using the AntiMarin database was listed in Table 3.2 and their structures illustrated in Figure 5.5. Several have been isolated from endophytic fungi; these include asparvenone from *Aspergillus parvulus,* 1,3-dihydro-3,7-dihydroxy-5-methoxy-6-methyl-4-isobenzofuran-carboxylic acid from *Aspergillus duricaulis*, and viscumamide from *Paecilomyces* sp. isolated from mangroves. Some of the identified metabolites also have been isolated from marine endophytic fungi, bacteria, lichens, chordates, and sponges. Meanwhile, the *m/z* values and predicted formulas of unknown metabolites are listed in Table 5.3.
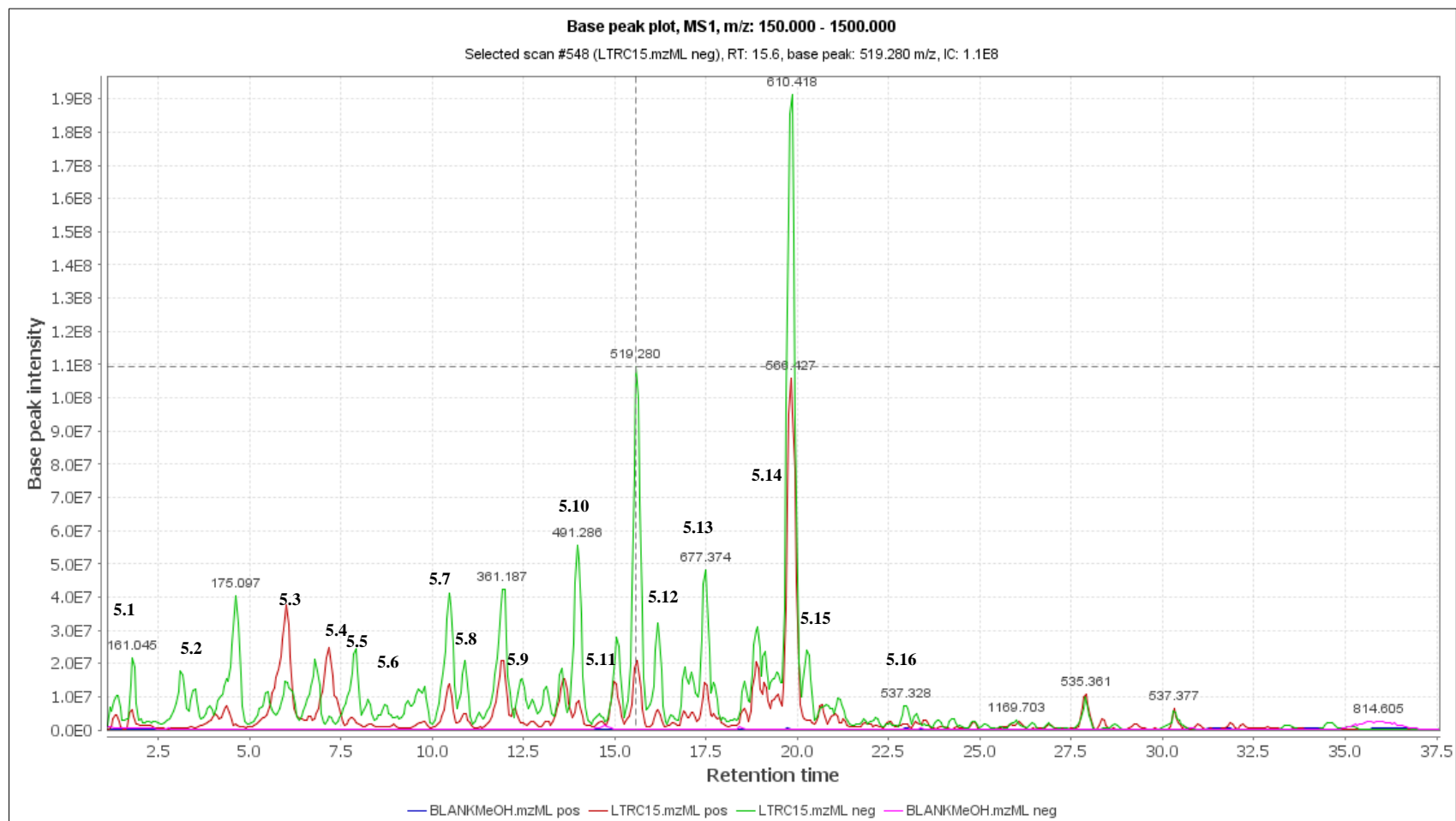
Figure 5.4: Total ion chromatogram of the crude extract of *L. theobromae*
in rice media day 15 (LTRC15) (red and green represent the positive and negative ionisation modes, respectively, for the crude extract. Pink and blue are the positive and negative ionisation modes, respectively, for the solvent blank).

Table 5.2: Compounds from the total crude extract of *L. theobromae* (LTRC15)
that were putatively identified using the Antimarin database (Sources; F-fungi, B-bacteria, M-mollusc, L-lichen, P-porifera)

No.	ESI modes	Rt (min)	MS (m/z)	Molecular weight	Chemical formula	Name	Tolerance (ppm)	Sources	Peak Area
5.1	N	1.79	161.0454	162.1410	$C_6H_{10}O_5$	pentonic acid γ-lactone	2.2059	[F] *Phycomyces blakesleeanus*	2.29E+08
5.2	N	3.50	181.0507	182.1730	$C_9H_{10}O_4$	6-ethyl-2,4-dihydroxybenzoic acid	0.1546	[F] *Penicillium baarnense*	3.12E+08
5.3	P	5.99	159.1018	158.1950	$C_8H_{14}O_3$	tetrahydro-4-hydroxy-6-propylpyran-2-one	1.2288	[F] *Botryosphaeria rhodina* PSU-M35 and PSU-M114	1.01E+09
5.4	P	7.15	231.1592	230.3010	$C_{12}H_{22}O_4$	2,3-dihydroxydodecane-4,7-dione	0.3713	[F] Basidiomycete; *Conocybe siliginea*	5.99E+08
5.5	N	7.89	221.0818	222.0891	$C_{12}H_{14}O_4$	asparvenone	1.8459	[F] *Aspergillus parvulus*	5.02E+08
5.6	N	8.23	239.0560	240.0633	$C_{11}H_{12}O_6$	1,3-dihydro-3,7-dihydroxy-5-methoxy-6-methyl-4-isobenzofurancarboxylic acid	1.8471	[F] *Aspergillus duricaulis*	2.14E+08
5.7	N	10.45	333.0770	334.1993	$C_{20}H_{14}O_5$	halenaquinol	1.9427	[P] *Xestospongia sapra*	7.42E+08
5.8	N	10.88	341.1606	342.1678	$C_{17}H_{26}O_7$	methyl 6-methoxydiperoxyhexadecaenoate	-0.0305	Porifera; *Plakortis* aff. *simplex*	3.57E+08
5.9	N	12.45	329.2334	330.4600	$C_{18}H_{34}O_5$	Penicitide B	0.1045	*Penicillium chrysogenum*	3.05E+08
5.10	N	13.97	491.2860	492.2933	$C_{25}H_{40}N_4O_6$	glidobactin F; Bu-2867T-F	-1.9457	[M] *Polyangium brachysporum*	1.08E+09
5.11	P	14.97	281.1750	280.3590	$C_{16}H_{24}O_4$	tagetolone	2.9352	[F] *Alternaria tagetica*	2.29E+08
5.12	N	16.16	649.3800	650.3873	$C_{32}H_{58}O_{13}$	glycolipid B; Rhamnolipid B; R-1; acyl-dirhamnolipid-C10,C10	0.1219	[B] *Pseudomonas aeruginosa*; [B] Rhizosphere bacterium*; Pseudomonas* sp. GRP3	8.56E+08
5.13	N	17.48	677.3750	678.3822	$C_{33}H_{58}O_{14}$	18-*O*-beta-D-glucopyranosyl-18*R*-hydroxydihydroalloprotolichesterinate-21-*O*-a-L-rhamnopyranoside	0.1905	[L] Lichens; *Acarospora gobiensis, Lecanora fructulosa, Peltigera canina, Rhizoplaca peltata, Xanthoparmelia camtschadalis,*	6.77E+08
5.14	P	19.82	566.4280	565.4208	$C_{31}H_{51}N_9O$	viscumamide	1.7923	[F] Endophytic *Paecilomyces* sp. from mangroves	1.98E+09
5.15	N	20.26	295.2278	296.2350	$C_{18}H_{32}O_3$	12-hydroxy-9*Z*,13*E*-octadecadienoic acid	1.4322	[F] *Epichloe typhina*	4.75E+08
5.16	N	22.97	537.3282	538.3355	$C_{31}H_{46}N_4O_2S$	virenamide A	2.4383	Chordata; *Diplosoma virens*	1.14E+08

**Table 5.3: Compounds present in the crude extract of *L. theobromae* (LTRC15)
that were unidentified using the Antimarin database**

ESI modes	Rt (min)	MS (m/z)	Molecular weight	Peak Area
N	5.48	172.0971	173.1053	2.98E+08
N	5.97	151.0402	152.0475	4.39E+07
N	11.92	361.1870	362.1943	8.97E+08
N	15.57	519.2809	520.2882	1.51E+09
P	16.18	668.4230	667.4158	2.13E+08
N	18.54	835.4683	836.4756	3.59E+08
N	18.90	596.4028	597.4100	4.56E+07
N	19.84	610.4186	611.4259	5.31E+08
N	21.11	580.2950	581.3023	2.29E+08
P	27.90	535.3610	534.3537	1.45E+08
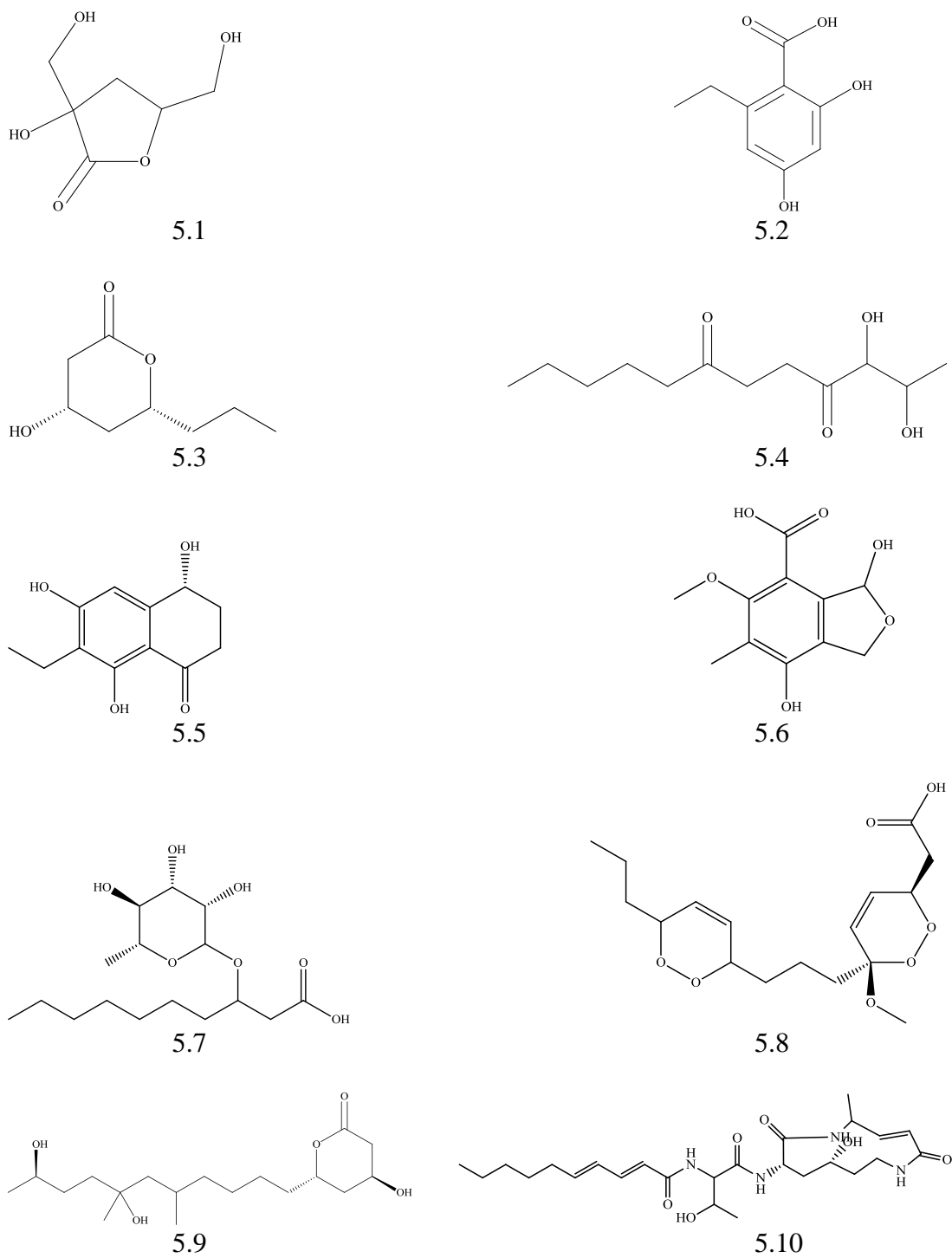
Figure 5.5: Compounds that were putatively identified
through dereplication studies *L. theobromae* (LTRC15) crude extract

5.11

5.12

5.13

5.14

5.15

5.16
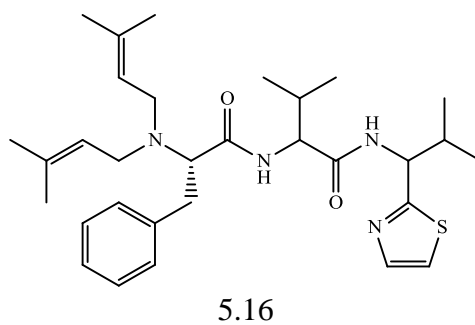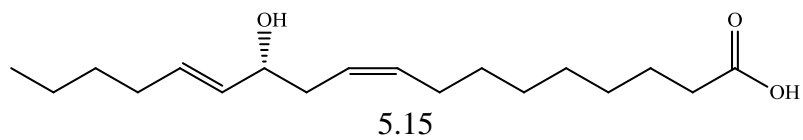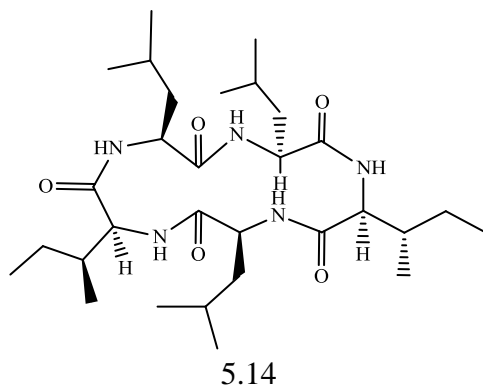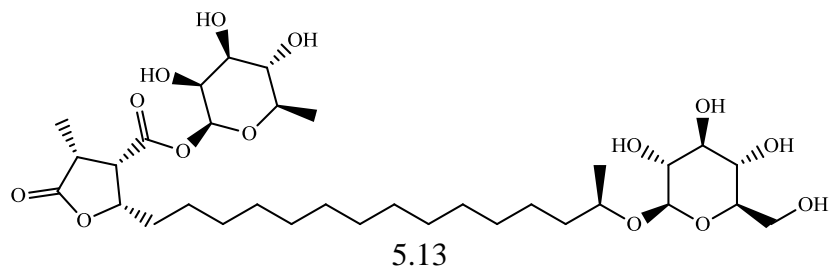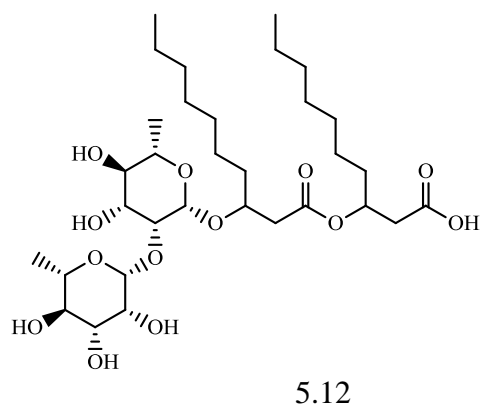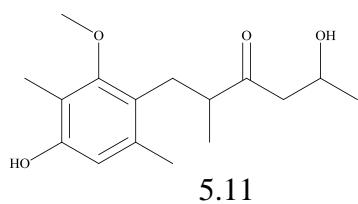
Figure 5.5: Cont'd. Compounds that were putatively identified through dereplication studies *L. theobromae* (LTRC15) crude extract

181

5.2.2 Isolation of secondary metabolites from *L. theobromae*

Thin layer chromatography (TLC) was performed on the LTRC15 crude extract using a combination of different solvent systems to obtain general ideas on the polarity of the metabolites as well as optimize the solvent system to be used for separation and isolation work. The total crude extract of *L. theobromae* (24.0 g) was fractionated using medium pressure liquid chromatography (Büchi, Switzerland). The sub-fractions were combined according to their TLC profiles to give 15 major fractions of LTRC15. The 15 fractions were tested for anti-trypanosomal activity and were analysed using HRESI-LCMS and NMR for the dereplication study. Later, the active fractions were subjected to further isolation and purification to afford pure compounds.

5.2.3 Bioactivity results of *L. theobromae* major fractions

The results of the anti-trypanosomal assay of the *L. theobromae* fractions are shown in Table 5.4. Fractions LTRC15-3, 5, 6, 7, 8, 9, 10, 11, 12 and 15 exhibited strong activity compared to fractions LTRC15-1, 2, 4, 13 and 14, which were less active.

Table 5.4: Anti-trypanosomal activity of *L. theobromae* fractions
(calculated as mean value of percentage viability) at a concentration of 20 μg/mL

Fractions	Yield (g)	*T. b. brucei,* % D control (20 μg/mL)
LTRC15-F1	4.2564	91.5
LTRC15-F2	0.7630	42.8
LTRC15-F3	0.3236	8.8
LTRC15-F4	0.3274	16.5
LTRC15-F5	0.3816	6.6
LTRC15-F6	0.7063	6.2
LTRC15-F7	0.2325	5.5
LTRC15-F8	0.8063	5.2
LTRC15-F9	2.4277	9.1
LTRC15-F10	3.6221	6.1
LTRC15-F11	3.7457	7.9
LTRC15-F12	7.5651	8.6
LTRC15-F13	2.9523	51.5
LTRC15-F14	0.7646	86.5
LTRC15-F15	0.7919	6.8

% D, percentage viability of control

5.2.4 Multivariate analysis of *L. theobromae* fractions

A dereplication study on the *L. theobromae* fractions was accomplished to investigate the metabolite profile of each fraction and its correlation with the bioactivity against *T. b. brucei*.

a)

b)
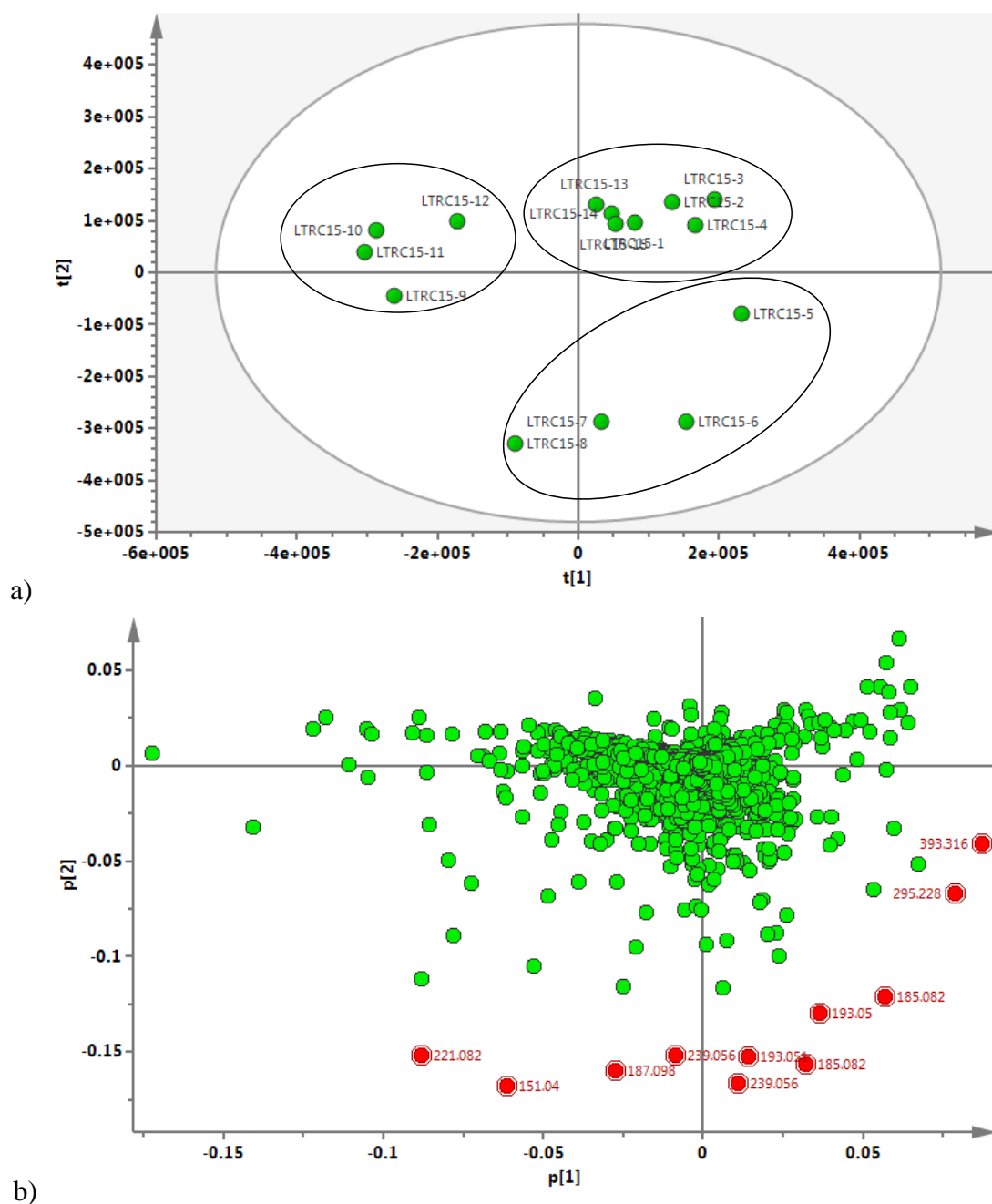
Figure 5.6: PCA analysis on *L. theobromae* crude fractions
(a) Unsupervised PCA score plot of the *L. theobromae* (LTRC15) fractions showed good separation between the datasets with three clusters in which fractions LTRC15-5, 6, 7 and 8 distributed outlier from others; (b) Unsupervised PCA loading plot showed metabolites highlighted in red representing the metabolites in fractions LTRC15-5, 6, 7 and 8.
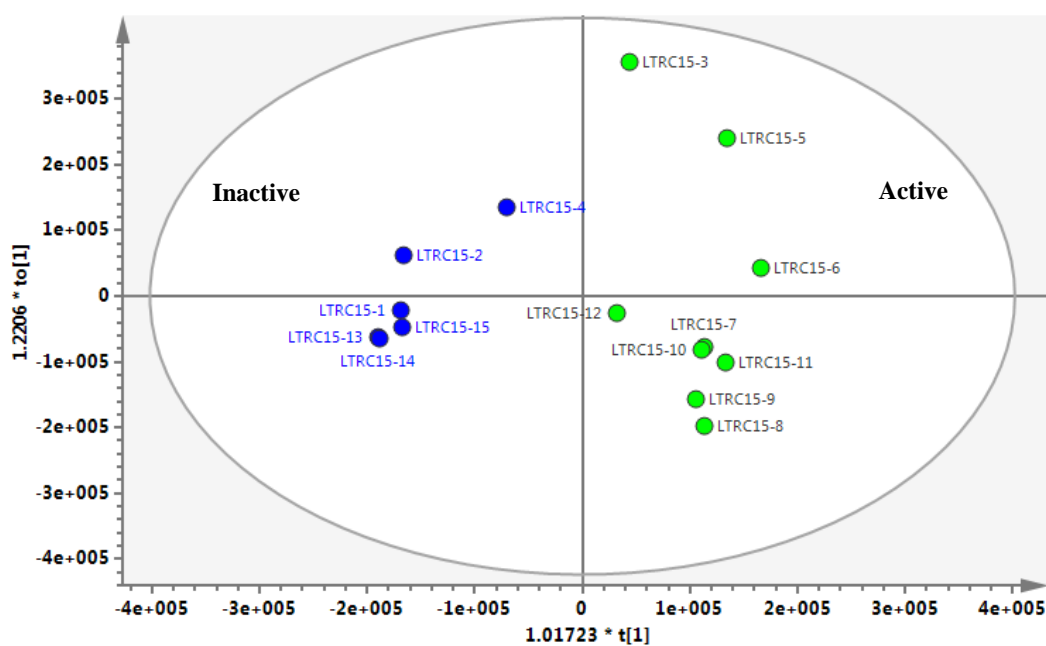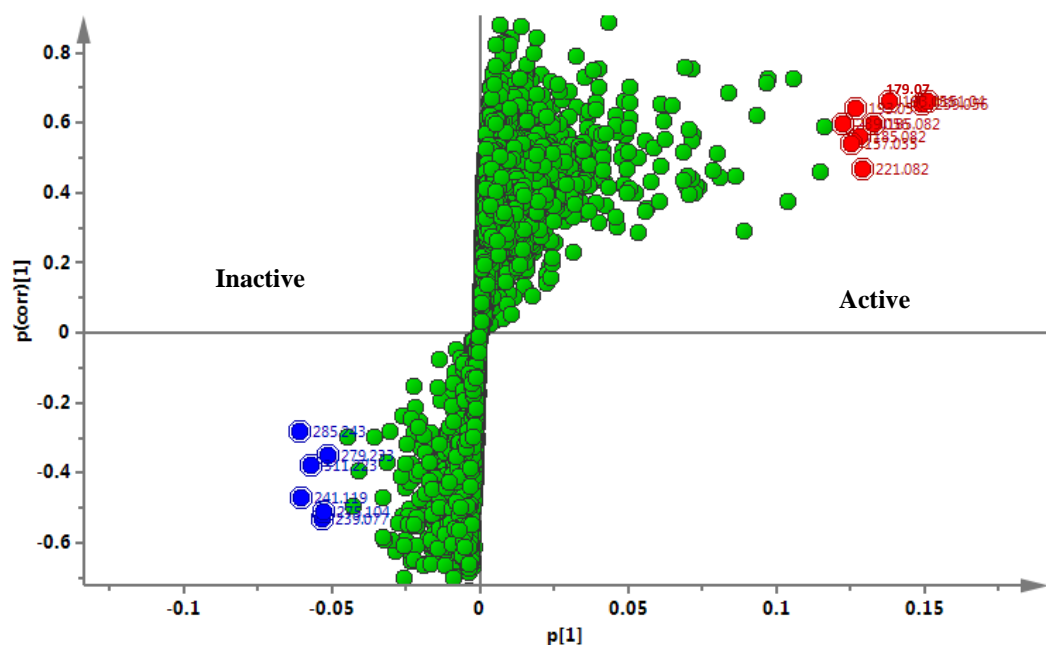
Figure 5.7: OPLS-DA analysis on *L. theobromae* crude fractions

(a) Supervised OPLS-DA score plot analysis showed moderate separation between the active (green) and inactive fractions (blue) ($R^2(Y) =0.916$; $Q_2(Y) =0.389$); (b) S-plot with outlying metabolites from active (red) and inactive groups (blue) highlighted.

The unsupervised PCA score plot (Figure 5.6 a) showed three clusters: consecutive fractions LTRC15-5 to 8, fractions LTRC15-9 to 12 and lastly, fractions LTRC15-1 to, 4, and 13 to 15 together. The loading plot (Figure 5.6 b) displayed the distribution of metabolites highlighted in red representing the metabolites in fractions LTRC15-5 to 8 in which metabolites with *m/z* 393.3160 [M+H]$^+$ was putatively identified as

24*R*-ergostatetraen-3-one isolated from *Dysidea herbacea* (Kobayashi *et al.*, 1992), 185.0820 [M-H]⁻ was identified as dihydroaspyrone isolated from *Aspergillus ochraceus* (Fuchser and Zeeck, 1997), 239.0600 [M-H]⁻ was putatively identified as coloratin B from fungus *Xylaria intracolorata* (Quang *et al.*, 2006) and 193.0650 and 193.0651 [M-H]⁻ were putatively identified as 4-hydroxymellein and 5-hydroxymellein, respectively isolated from *Uvaria hamiltonii* (Asha *et al.*, 2004) and *Penicillium* sp. (Oliveira *et al.*, 2009).

24*R*-ergostatetraen-3-one
Rt: 28.24

dihydroaspyrone
Rt: 9.46

coloratin B
Rt: 9.76

4-hydroxymellein
Rt: 8.88

5-hydroxymellein
Rt: 9.76
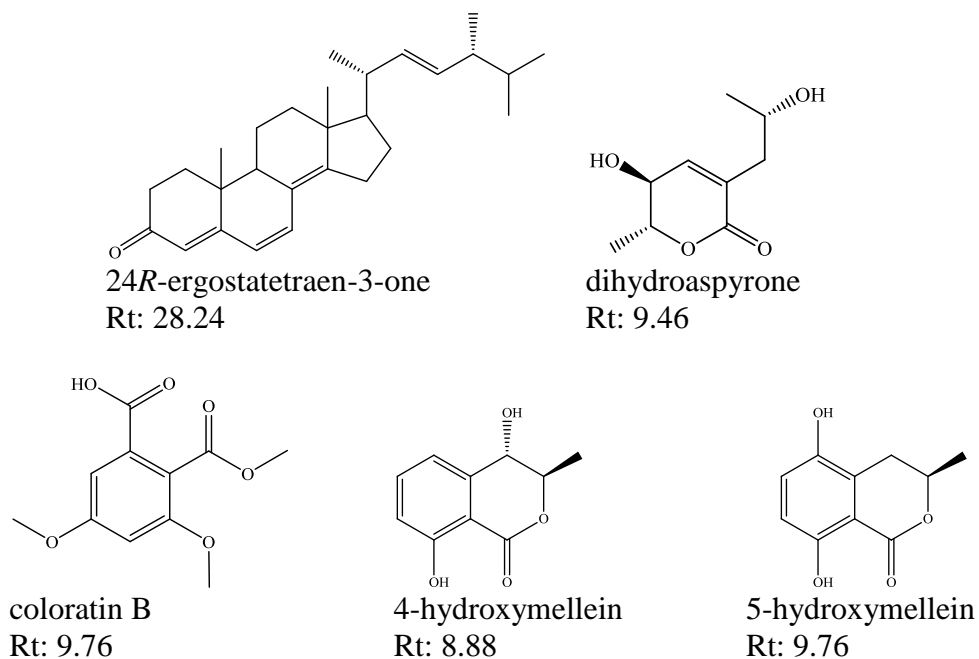
Meanwhile, the supervised OPLS-DA score plot (Figure 3.8 a) showed that fractions LTRC15-3, 5, 6 and fractions LTRC15-7 to 12 were clustered in the upper and lower right quadrants, respectively. While, the inactive fractions, LTRC15-1, 13, 14 and 15, were distinctively grouped together. The S-plot (Figure 3.8 b) showed metabolites more prevalent in respective active and inactive groups. Those which were predicted to strongly contribute to activity are highlighted in red. These metabolites, with *m/z* 239.0600, 193.0510, 193.0500, 185.0820 [M-H]⁻ and 393.3160 [M+H]⁺ have been identified earlier. Meanwhile *m/z* 519.2810 [M-H]⁻ was not identified, and has also been produced in LTRC30 which may contribute for the activity. Meanwhile metabolites in the inactive group (blue), negative ionisation mode with *m/z* 279.2330 was putatively identified as 10,13-octadecadienoic acid

pyrrolidide isolated from *Cinachyrella alloclada* (Barnathan *et al.*, 1992), 311.2230 was identified as plakortin from *Plakortis simplex* (Cafieri *et al.*, 1999), 275.1040 was a peptide identified as cyclo-(L-tyrosyl-*trans*-4-hydroxy-L-proline) from *Ruegeria* sp. from cell culture of sponge *Suberites domuncula* (Mitova *et al.*, 2004), 333.0770 and 335.0930 [M-H]⁻ as mentioned earlier also have been produced in both LTRC30 and LTLC30 small scale extract that were inactive.

5.3   Isolation of secondary metabolites from *L. theobromae*

The 15 active fractions were subjected to isolation and purification, yielding six pure compounds. Isolation work on fraction LTRC15-3 yielded colourless crystals of (-)-mellein, (LTRC15-3-19, (**5.19**), 11.0 mg, 0.05%). Further purification of fraction LTRC15-4 gave *p*-hydroxyphenethyl alcohol (LTRC15-4-22, (**5.17**), 5.3 mg, 0.02%), fraction LTRC15-5 afforded *p*-hydroxybenzaldehyde (LTRC15-5-5F-1, (**5.18**), 5.2 mg, 0.02%) and fraction LTRC15-6 gave (-)-*trans-axial*-4-hydroxymellein (LTRC15-6-31c, (**5.20**), 7.0 mg, 0.03%). Meanwhile, several purifications of fraction LTRC15-8 gave (-)-5-hydroxymellein (LTRC15-8-22c, (**5.22**), 6.0 mg, 0.03%) and another congener of (-)-*cis-equatorial*-4-hydroxymellein (LTRC15-8-41, (**5.21**), 8.7 mg, 0.04%). Figure 5.8 shows a TLC summary plate of the crude fractions labelled with the compounds purified from them. A summary of workflow on the *L. theobromae* crude extract was shown in Figure 5.9.
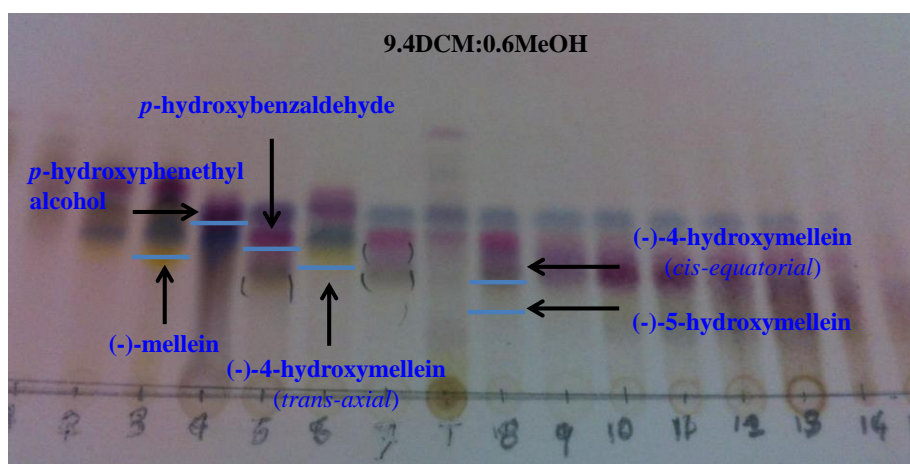
Figure 5.8: TLC summary plate of *L. theobromae* fractions
after spraying with *p*-anisaldehyde-sulphuric acid

Scale up *Lasiodiplodia theobromae*

- transferred into rice medium (40 L), incubated day 15
- inoculated on new malt agar plate, incubated 8 days
- incubation at room temp., cold extraction (ethyl acetate, 3x), homogenized
- concentrated under vacuum using a rotary evaporator

Ethyl acetate extract
(24.0 g)

- Dereplication studies:
HRFT-LCMS, MZmine software, an *in-house* macro
combined with the Antimarin database

Fractionation

-TLC (6 Hex:4 EA)
- MPLC (Büchi, Switzerland)
- combined fraction – 15 major fractions
- gradient elution successively (100%Hex-100%EtOAc, 100%EtOAc-20%MeOH)
- Dereplication studies on fractions: HRFT-LCMS, MZmine
- column: 4-150mm, silica: 20-45 µm
software, an *in-house* macro combined with the Antimarin
- flowrate: 50ml/min, fraction collection: 100ml/fraction
database, SIMCA P+ 13
- concentrated under vacuum using a rotary evaporator
- Anti-trypanosomal activity

| LTRC30- 1 (4.2564 g) | LTRC30-2 (0.7630 g) | LTRC30- 4 (0.3274 g) | LTRC30-6 (0.7063 g) | LTRC30-8 (0.8063 g) | LTRC30-10 (3.6221 g) | LTRC30-12 (7.5651 g) | LTRC30-14 (0.7646 g) | LTRC30-15 (0.7919 g) |

LTRC30- 3 (0.3236 g)

LTRC30-5 (0.3816 g)

LTRC30-7 (0.2325 g)

LTRC30-9 (2.4277 g)

LTRC30-11 (3.7457 g)

LTRC30-13 (2.9523 g)

LTRC30-3-19
(-)-mellein
(11.0 mg)

LTRC15-4-22
p-hydroxyphenethyl alcohol
(5.3 mg)

LTRC15-6-31c
(-)-4-hydroxymellein
(t*rans-axial*, 7.0 mg)

LTRC15-8-41
(-)-4-hydroxymellein
(*cis-equatorial*, 8.7 mg)

LTRC15-8-22c
(-)-5-hydroxymellein
(6.0 mg)

LTRC15-5-5F-1
p-hydroxybenzaldehyde
(5.2 mg)

Figure 5.9: A summary of the workflow on the *L. theobromae* crude extract

5.4 Structure elucidation and identification of secondary metabolites

The six known metabolites isolated from LTRC15 consisted of two simple phenolics along with mellein and three of its derivatives.

Synonyms	*p*-hydroxyphenethyl alcohol, 4-hydroxy-benzene ethanol, tyrosol, salidrosol	*p*-hydroxybenzaldehyde, 4-hydroxybenzaldehyde, *p*-formylphenol
Sample code	LTRC15-4-22 (**5.17**)	LTRC15-5-5F-1 (**5.18**)
Sources	*L. theobromae*	*L. theobromae*
Yield (mg, %)	5.3 (0.02%)	5.2 (0.02%)
Physical state	Yellow oil	Yellow oil
Mol. formula	$C_8H_{10}O_2$	$C_7H_6O_2$
Mol. weight (g/mol)	138.1638	122.1213
R_f value (9.4DCM:0.6MeOH)	0.50	0.45

5.17   5.18

5.4.1 Compound LTRC15-4-22 (*p*-hydroxyphenethyl alcohol, 5.17)

Compound LTRC15-4-22 (5.3 mg) was obtained as yellow oil with molecular formula $C_8H_{10}O_2$. The ^1H NMR spectrum of LTRC15-4-22 (Figure 5.10, Table 5.5) showed an AA'BB' system in the aromatic region integrating for 2H each at δ_H 7.32 (*dd*, *J*=8.0, 2.0 Hz, 2H) and 7.23 (*dd*, *J*=8.0, 2.0 Hz, 2H) corresponding to the aromatic protons H-2/H-6 and H-3/H-5, respectively, due to the equivalence of the protons on the di-substituted benzene ring. The spectrum showed typical patterns associated with a *para*-substituted benzene ring. In addition, two methylene proton signals were observed. One of them was at δ_H 2.86 (*s*, 2H, H-8) while the other shifted downfield due to the hydroxyl group, was at δ_H 3.84 (*s*, 2H, H-7). Thus, the compound was identified as *p*-hydroxyphenethyl alcohol or also trivially known as tyrosol. It has been isolated from the fungus *Papulaspora immerse* (Gallo *et al.*, 2010), the aspen blue stain fungus *Ophiostoma crassivaoinata* (Ayer and Trifonov,

1995), the phyto-pathogen fungus *Ceratocystis adiposa* (Guzmán-López *et al.*, 2007) and *Botryosphaeria obtuse* (Venkatasubbaiah *et al.*, 1991), and is naturally found in wine and virgin olive oil (Covas *et al.*, 2003).

Table 5.5: ^{1}H NMR of LTRC15-4-22 and LTRC15-5-5F-1
(CDCl$_3$, 400 MHz)
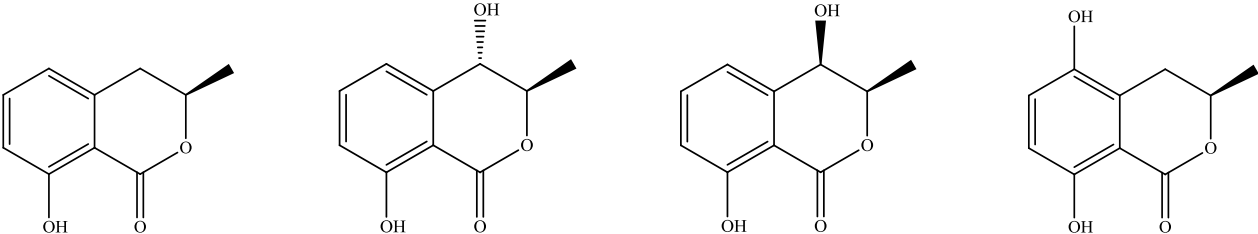
No.	^{1}H NMR, δ_H (ppm, multi. *J* in Hz)		
	LTRC15-4-22	**LTRC15-5-5F-1**	***p*-hydroxybenzaldehyde**
1	-	-	
2	7.32 (*dd*, *J*=8.0, 2.0 Hz, 1H)	7.81 (*d*, *J*=8.4 Hz, 1H)	7.81 (*d*, *J*=8.4 Hz, 1H)
3	7.23 (*dd*, *J*=8.0, 2.0 Hz, 1H)	6.96 (*d*, *J*=8.4 Hz, 1H)	6.96 (*m*, 1H)
4	-	-	-
5	7.23 (*dd*, *J*=8.0, 2.0 Hz, 1H)	6.96 (*d*, *J*=8.4 Hz, 1H)	6.96 (*m*, 1H)
6	7.32 (*dd*, *J*=8.0, 2.0 Hz, 1H)	7.81 (*d*, *J*=8.4 Hz, 1H)	7.81 (*d*, *J*=8.4 Hz, 1H)
7	2.86 (*t*, *J*=6.7 Hz, 2H)	9.86 (*s*, 1H, CHO)	9.87 (*s*, 1H, CHO)
8	3.84 (*t*, *J*=6.6 Hz, 2H)	-	-
O-H	-	6.12 (*s*, OH)	6.12 (*s*, OH)

*Bao *et al.*, 2009

5.4.2 Compound LTRC15-5-5F-1 (*p*-hydroxybenzaldehyde, 5.18)

Compound LTRC15-5F-1 (5.2 mg) was obtained as yellow substance with molecular formula C$_7$H$_6$O$_2$. The ^{1}H NMR spectrum of LTRC15-5F-1 (Figure 5.11, Table 5.5) showed a symmetrical AA'BB' system in the aromatic region with 2H at δ_H 7.81 (*d*, *J*=8.4 Hz, 2H) and 6.96(*d*, *J*=8.4 Hz, 2H) corresponding to the four aromatic protons H-2/H-6 and H-3/H-5, respectively. This revealed the presence of a di-substituted benzene ring. One proton signal at δ_H 9.86 (*s*, 1H) indicated the presence of an aldehyde proton, whereas another signal at δ_H 6.12 (*s*, OH) signified a hydroxyl group. This compound was therefore elucidated as *p*-hydroxybenzaldehyde which has been previously isolated from the bark of *Vitex negundo* (Dhakal *et al.*, 2009) and *Phycomyces blakesleeanus* strain NRRL1555 (Barrero *et al.*, 1996).

Figure 5.10: ^{1}H NMR spectrum of LTRC15-4-22
(CDCl$_3$, 400 MHz)

Figure 5.11: ^{1}H NMR spectrum of LTRC15-5-5F-1
(CDCl$_3$, 400 MHz)

Synonyms	(-)-mellein, (-)-8-hydroxy-3-methylisochroman-1-one, 3,4-dihydro-8-hydroxy-3-methylisocoumarin	(-)-4-hydroxy-mellein, (-)-4,8-dihydroxy-3-methylisochroman-1-one, 3,4-dihydro-4,8-dihydroxy-3-methylisocoumarin	(-)-4-hydroxy-mellein, (-)-4,8-dihydroxy-3-methyl-isochroman-1-one, 3,4-dihydro-4,8-dihydroxy-3-methylisocoumarin	(-)-5-hydroxy-mellein, (-)-5,8-dihydroxy-3-methylisochroman-1-one, 3,4-dihydro-5,8-dihydroxy-3-methylisocoumarin
Sample code	LTRC15-3-19 (**5.19**)	LTRC15-6-31c (**5.20**)	LTRC15-8-41 (**5.21**)	LTRC15-8-22c (**5.22**)
Sources	*L. theobromae*	*L. theobromae*	*L. theobromae*	*L. theobromae*
Yield (mg, %)	11.0 (0.05%)	7.0 (0.03%)	8.7 (0.04%)	6.0 (0.03%)
Physical state	Colourless needles	Colourless needles	Colourless needles	Colourless needles
Mol. formula	$C_{10}H_{10}O_3$	$C_{10}H_{10}O_4$	$C_{10}H_{10}O_4$	$C_{10}H_{10}O_4$
Mol. weight (g/mol)	178.1846	194.1840	194.1840	194.1840
Exact mass (*m/z*)	179.0705 [M-H]$^-$	195.0650 [M+H]$^+$	195.0650 [M+H]$^+$	195.0651 [M+H]$^+$
Ret. time (min)	13.83	9.77	8.24	10.86
R_f value (9.4DCM:0.6M)	0.50	0.35	0.33	0.23
$[\alpha]_D^{20}$ (*c* 1.00, CHCl$_3$)	-119.0	-31.0	-44.0	-69.0 (*c* 1.00,CHCl$_3$)

5.19   5.20 (*trans-axial*)   5.21 (*cis-equatorial*)   5.22

(relative stereochemistry based on previous studies)

a)

b)

c)

d)
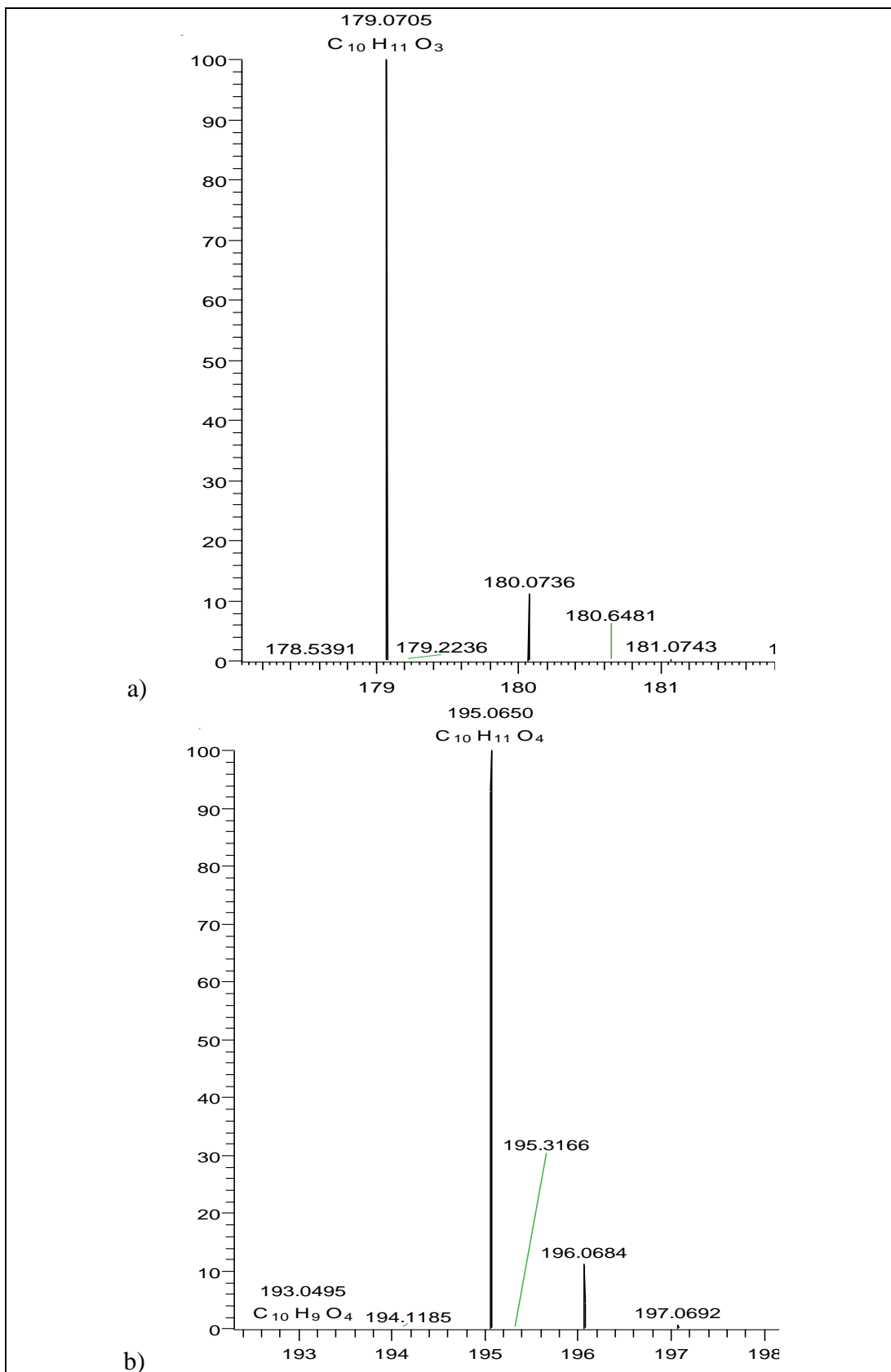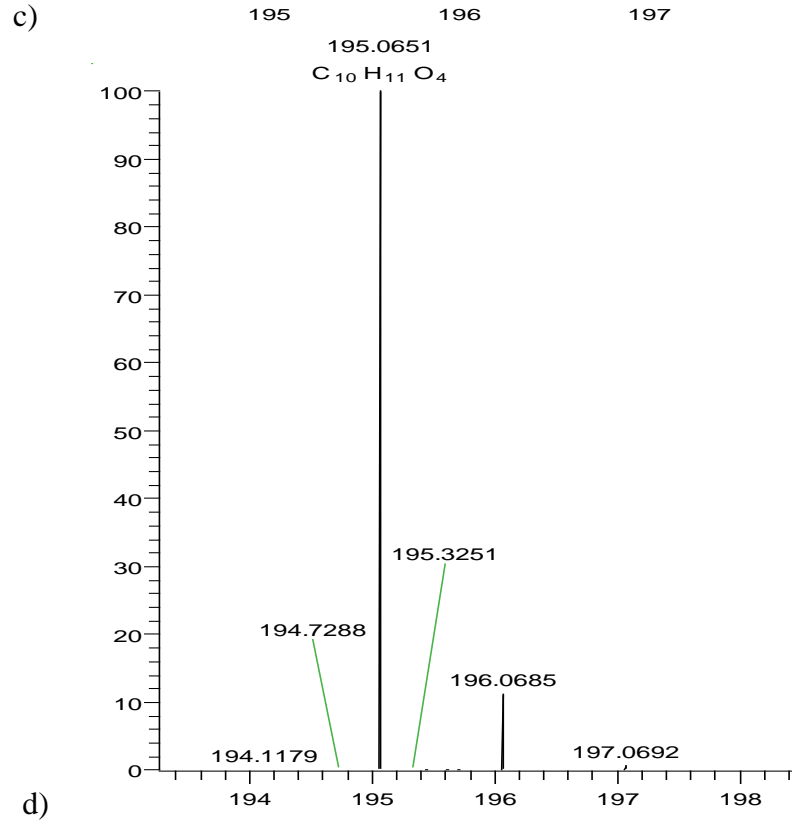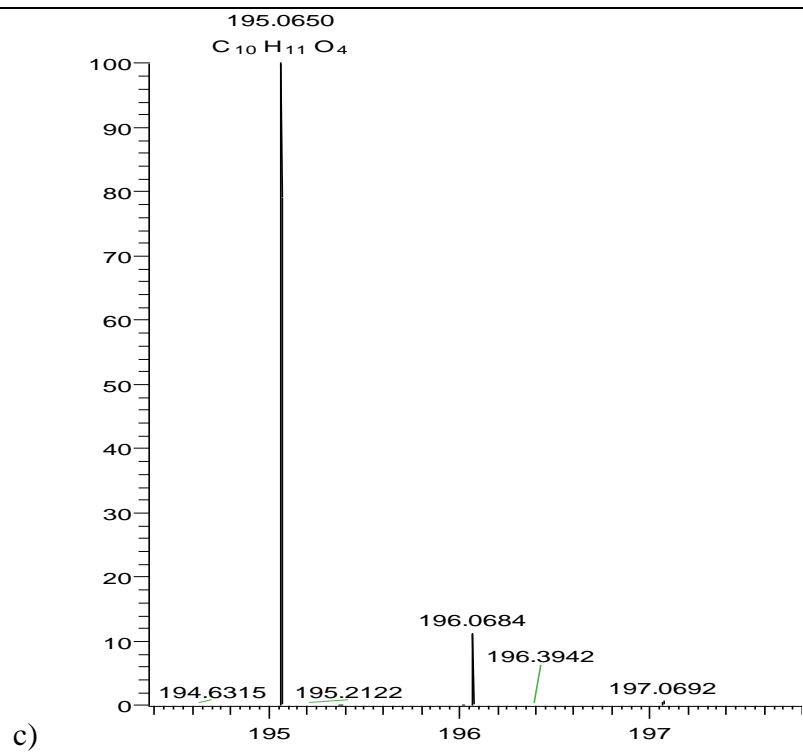
The negative ionisation mode for the HRMS of a) (-)-mellein, positive ionisation mode for the HRMS of b) (-)-*trans-axial*-4-hydroxymellein c) (-)-*cis-equatorial*-4-hydroxymellein d) (-)-5-hydroxymellein

5.4.3 Compound LTRC15-3-19 ((-)-mellein, 5.19)

Compound LTRC15-3-19 (11.0 mg) was obtained as colourless needles having an optical rotation of $[\alpha]_D^{20}$ -119.0 (c 1.00, CHCl$_3$) and HRMS showed the mass ion peak at m/z 179.0705 corresponding to the molecular formula C$_{10}$H$_9$O$_3$ [M-H]$^-$. The ^{1}H NMR spectrum of LTRC15-3-19 (Figure 5.12, Table 5.6) showed the presence of an ABC system for the aromatic proton signals. Peaks at δ_H 7.40 (t, J=8.0 Hz, 1H), 6.88 (d, J=7.4 Hz, 1H), and 6.68 (d, J=7.4 Hz, 1H) corresponded to protons H-6, H-7 and H-5, respectively. A methylene proton signal at δ_H 2.92 (d, J=7.3 Hz, 2H) corresponded to H-4, and a methine proton (H-3) which was directly attached to an oxygen showed a peak at δ_H 4.73 (m, 1H). A methyl signal was observed at δ_H 1.52 (d, J=6.3 Hz, 3H) and a hydroxyl group at δ_H 11.02 (s, 8-OH). Meanwhile, the ^{13}C NMR spectrum (Table 5.7) deduced from the ^{1}H and ^{13}C correlation in HMBC spectrum showed ten carbon signals, in which two of them are quaternary carbon: δ_C 139.5 (C-8a) and 108.6 (C-4a), two carbonyl carbon signals at δ_C 169.6 (C-1), 162.4 (C-8), three aromatic carbon signals δ_C 118.5 (C-5), 136.9 (C-6), and 116.7 (C-7), a methine carbon at δ_C 76.2 (C-3) directly attached to oxygen, carbon CH$_2$ at δ_C 35.2 (C-4) and 21.5 (CH$_3$). Meanwhile, the COSY NMR (Figure 5.13) clearly showed the correlations between the aromatic protons, and a correlation between H-4 and the oxygenated proton H-3. The HMBC spectrum (Figure 3.13) indicated that the methylene (H-4) and methine protons (H-3) on the aliphatic region were correlating to the methyl group. The other important correlations were between protons H-4/H-5/H-6 and the quaternary carbon at δ_C 139.5 (C-4a), proton H-3/H-4/H-7 and quaternary carbon at δ_C 108.6 (C-8a). A search of previous literature revealed that compound LTRC15-3-19 had similar ^{1}H and ^{13}C NMR spectra to mellein ($[\alpha]_D^{25}$ -102 (c 0.969, CHCl$_3$)), which has been isolated from an endophytic coniferous tree *Pezicula* sp. (Schulz *et al.*, 1995), thus this compound was identified as (-)-mellein (8-hydroxy-3-methylisochroman-1-one). This compound was isolated for the first time from *Aspergillus melleus* (Nishikawa, 1933), and later isolated from the fungi *Lasiodiplodia theobromae* (Aldridge *et al.*, 1971), *Aspergillus ochraceus, Botryosphaeria obtusa* (Cole *et al.*, 1971, Djoukeng *et al.*, 2009), a mangrove ascomycete *Helicascus kanaloanus* (Poch and Gloer, 1989), and a fungus causing the citrus disease, *Phoma tracheipilla* (Parisi *et al.*, 1993).
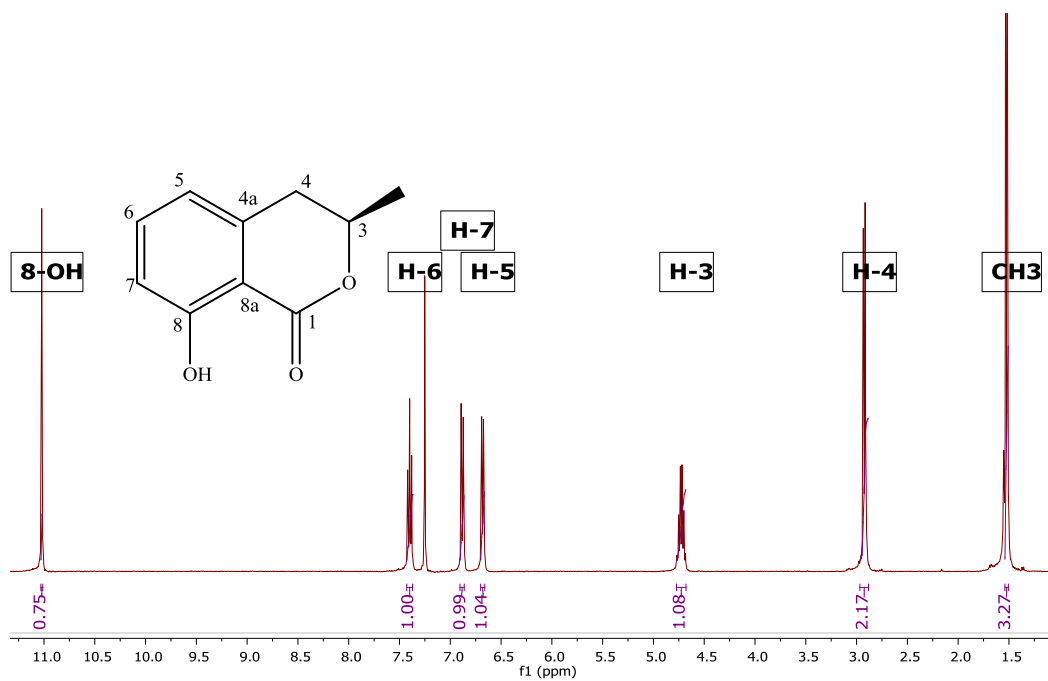
Figure 5.12: ¹H NMR spectrum of LTRC15-3-19
(CDCl₃, ¹H 400 MHz)

Table 5.6: ^{1}H NMR of mellein and its derivatives
LTRC15-3-19, LTRC15-6-31c, LTRC15-8-41 (CDCl$_3$, 400 MHz), LTRC-8-22c (Acetone-d_6, 400 MHz) & comparison with literature

No.	LTRC15-3-19	[a](-)-mellein	LTRC15-6-31c (*trans-axial*)	LTRC15-8-41 (*cis-equatorial*)	[b](-)-4-hydroxymellein (*cis*)	LTRC15-8-22c
			^{1}H NMR, δ_H (ppm, multi. *J* in Hz)			
1	-	-	-	-	-	-
2	-	-	-	-	-	-
3	4.73 (*m*, 1H)	4.73 (*m*, 1H)	4.59 (*dd*, *J*=6.6, 5.8 Hz, 1H)	4.70 (*d*, *J*=1.0 Hz, 1H)	4.71 (*d*, *J*=1.0 Hz, 1H)	4.75 (*m*, 1H)
4	2.92 (*d*, *J*=7.3 Hz, 2H)	2.93 (*d*, *J*=7.3 Hz, 2H)	4.59 (*dd*, *J*=6.6, 5.8 Hz, 1H)	4.60 (*d*, *J*=1.5 Hz, 1H)	4.59 (*d*, *J*=2.0 Hz, 1H)	2.65 (*dd*, *J*=17.0, 11.5 Hz, 1H)
4'	-	-	-	-	-	3.19 (*dd*, *J*=16.9, 3.4 Hz, 1H)
4a	-	-	-	-	-	-
5	6.68 (*d*, *J*=7.4 Hz, 1H)	6.69 (*d*, *J*=7.4 Hz, 1H)	7.02 (*d*, *J*=8.5 Hz, 1H)	7.02 (*d*, *J*=8.5 Hz, 1H)	7.04 (*d*, *J*=8.5 Hz, 1H)	-
6	7.40 (*t*, *J*=8.0 Hz, 1H)	7.41 (*dd*, *J*=8.0 Hz, 1H)	7.54 (*t*, *J*=8.5 Hz, 1H)	7.53 (*t*, *J*=8.5 Hz, 1H)	7.54 (*dd*, *J*=8.5 Hz, 1H)	7.11 (*d*, *J*=8.9 Hz, 1H)
7	6.88 (*d*, *J*=8.2 Hz, 1H)	6.89 (*d*, *J*=8.1 Hz, 1H)	6.99 (*d*, *J*=7.1 Hz, 1H)	6.92 (*d*, *J*=7.2 Hz, 1H)	6.93 (*d*, *J*=7.0 Hz, 1H)	6.71 (*d*, *J*=8.9 Hz, 1H)
8	-	-	-	-	-	-
8a	-	-	-	-	-	-
CH$_3$	1.52 (*d*, *J*=6.3 Hz, 3H)	1.53 (*d*, *J*=6.3 Hz, 3H)	1.51 (*d*, *J*=6.0 Hz, 3H)	1.59 (*d*, *J*=6.6 Hz, 3H)	1.60 (*d*, *J*=6.5 Hz, 3H)	1.50 (*d*, *J*=6.2 Hz, 3H)
5-OH	-	-	-	-	-	8.26 (*s*, OH)
8-OH	11.02 (*s*, OH)	11.04 (*s*, OH)	11.00 (*s*, OH)	11.01 (*s*, OH)	-	10.57 (*s*, OH)

[a]Schulz *et al.*, 1995, [b]Montenegro *et al.*, 2012 (CDCl$_3$, 400 MHz)
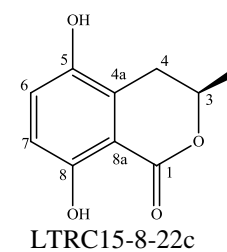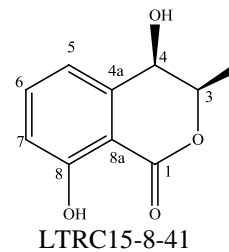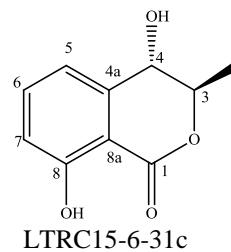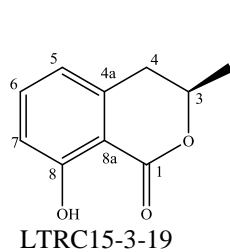
LTRC15-3-19   LTRC15-6-31c   LTRC15-8-41   LTRC15-8-22c

No.	^{13}C NMR, δ_C (ppm)		
	LTRC15-3-19	***(-)-mellein**	**LTRC15-8-22c**
1	169.6	169.96	169.9
2	-	-	-
3	76.2	76. 1	76.7
4	35.2	34.6	28.8
4a	139.5	139.4	125.8
5	118.5	116.2	146.4
6	136.9	136.1	124.5
7	116.7	117.9	115.9
8	162.4	162.1	156.6
8a	108.6	108.3	108.8
CH$_3$	21.5	20.7	20.9

*Schulz *et al.*, 1995
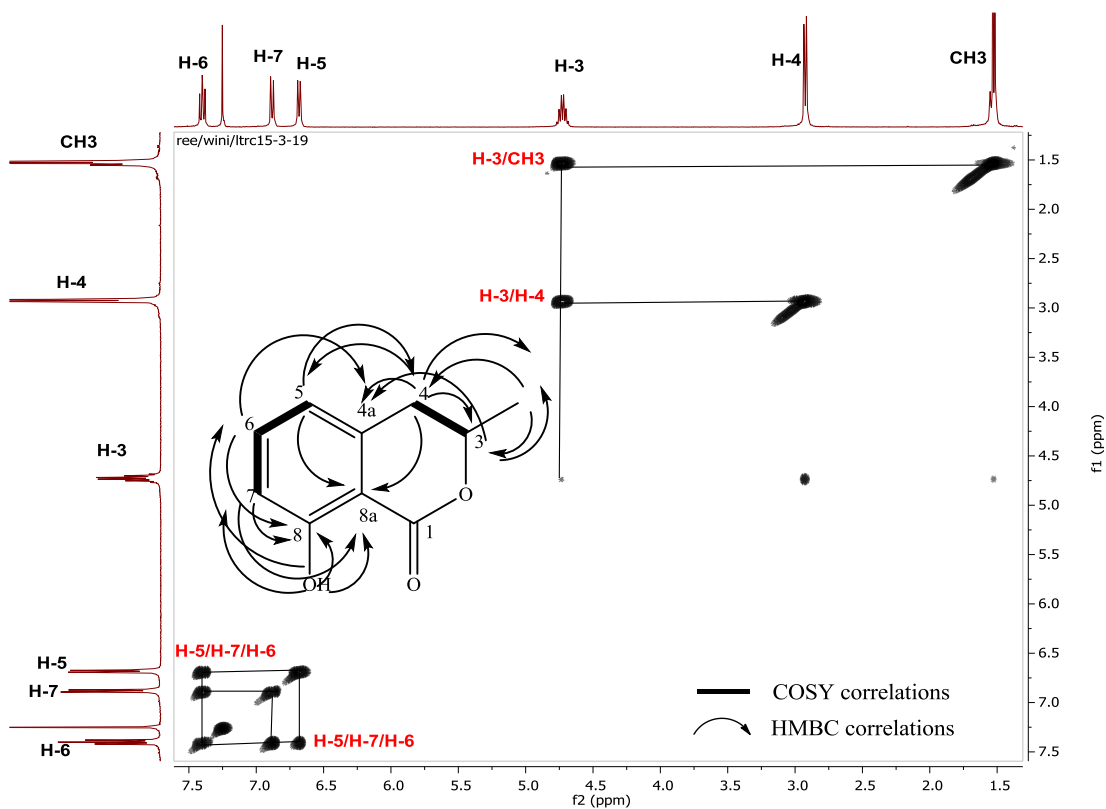
Figure 5.13: COSY NMR spectrum of LTRC15-3-19
(CDCl$_3$, ^{1}H 400 MHz)
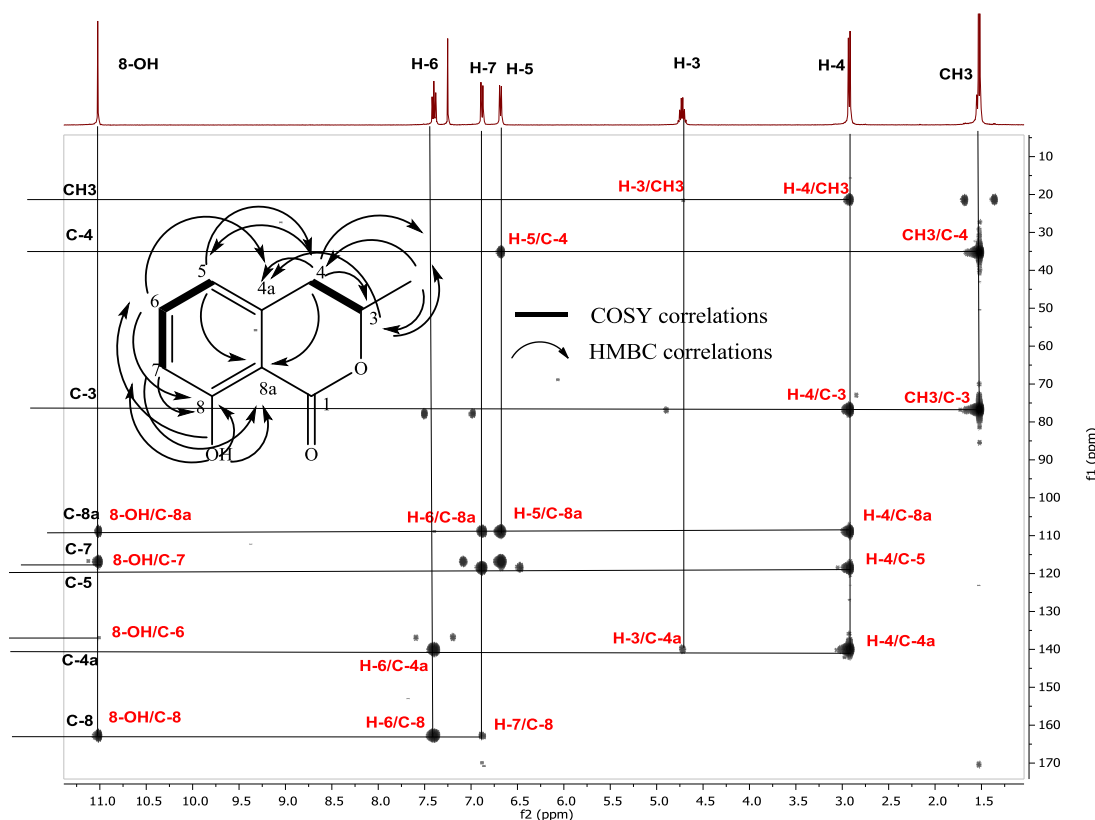
Figure 5.14: HMBC NMR spectrum of LTRC15-3-19
(CDCl$_3$, ^{1}H 400 MHz)

5.4.4   LTRC15-6-31c ((-)-*trans-axial*-4-hydroxymellein, 5.20)

Compound LTRC15-6-31c (7.0 mg) was obtained as colourless needles with an optical rotation of $[\alpha]_D^{20}$ -31.0 (*c* 1.00, CHCl$_3$) and an exact mass at *m/z* 195.0650 [M+H]$^+$ corresponding to the molecular formula C$_{10}$H$_{11}$O$_4$ and ion fragmentation as in Figure 5.16. The ^{1}H NMR spectrum of LTRC15-6-31c (Figure 3.15, Table 5.6) showed the same ABC system as compound LTRC15-3-19: peaks at δ_H 7.54 (*t*, *J*=8.5 Hz, 1H), 7.02 (*d*, *J*=8.5 Hz, 1H), and 6.99 (*d*, *J*=7.1 Hz, 1H) corresponded to protons H-6, H-5 and H-7, respectively. Two methine proton signals were observed at δ_H 4.59 (*dd*, *J*=6.6, 5.8 Hz, 2H), corresponding to H-3 and H-4 with bigger coupling constant 5.8 Hz, indicating that these two protons were in the *trans-axial* position. A methyl signal was found at δ_H 1.51 (*d*, *J*=6.0 Hz, 3H), as well as a hydroxyl group at δ_H 11.05 (*s*, 8-OH), revealing the same pattern shown by the compound mentioned before (Chapter 5.4.3). While finalizing the elucidation of the structure, a search of previous data showed that a compound, 4-hydroxymellein ($[\alpha]_D^{20}$ -28 (*c* 0.50, CHCl$_3$)) possessed a similar ^{1}H NMR spectrum to LTRC15-6-31c, thus this

198

compound was identified as (-)-*trans-axial*-4-hydroxymellein (4,8-dihydroxy-3-methylisochroman-1-one). This compound was earlier isolated by biotransformation of the marine bacterium *Stappia* sp. (Zhile Feng *et al.*, 2010), as well as from the fungi *Aspergillus ochraceus, A. oniki, Seimatosporium* sp. and an endophytic fungus of the conifer tree *Canoplea elegantula* (Cole *et al.*, 1971, Sasaki *et al.*, 1970, Hussain *et al.*, 2012, Findlay *et al.*, 1995), *Uvaria hamiltonii* (Asha *et al.*, 2004), *Apiospora camptospora* (Aldridge *et al.*, 1971) and *Penicillium* sp. (Oliveira *et al.*, 2009).
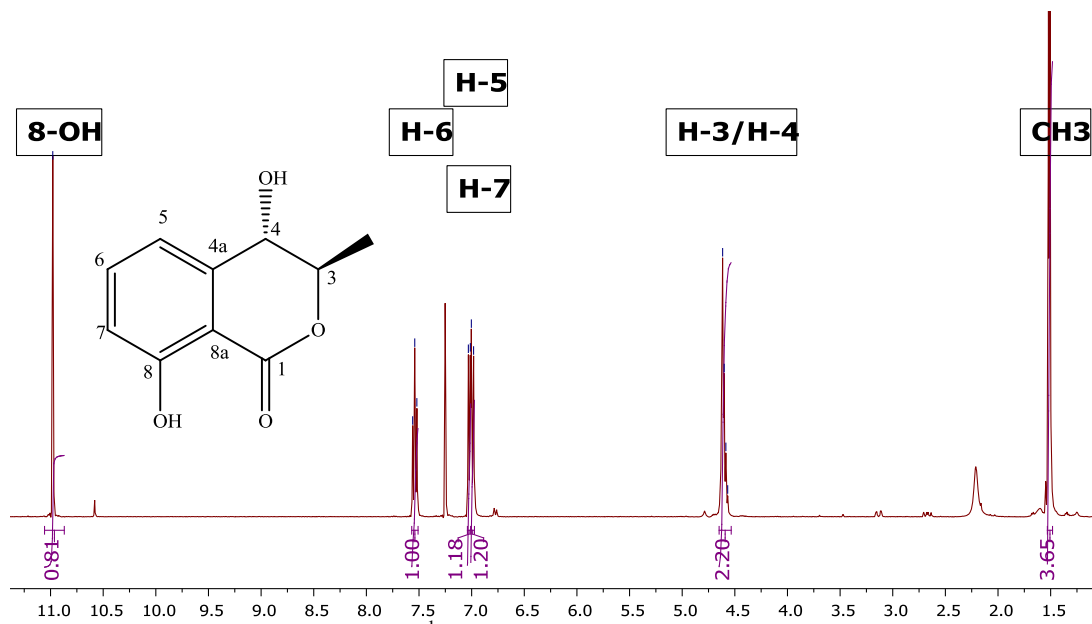
Figure 5.15: ^{1}H NMR spectrum of LTRC15-6-31c
(CDCl$_3$, ^{1}H 400 MHz)
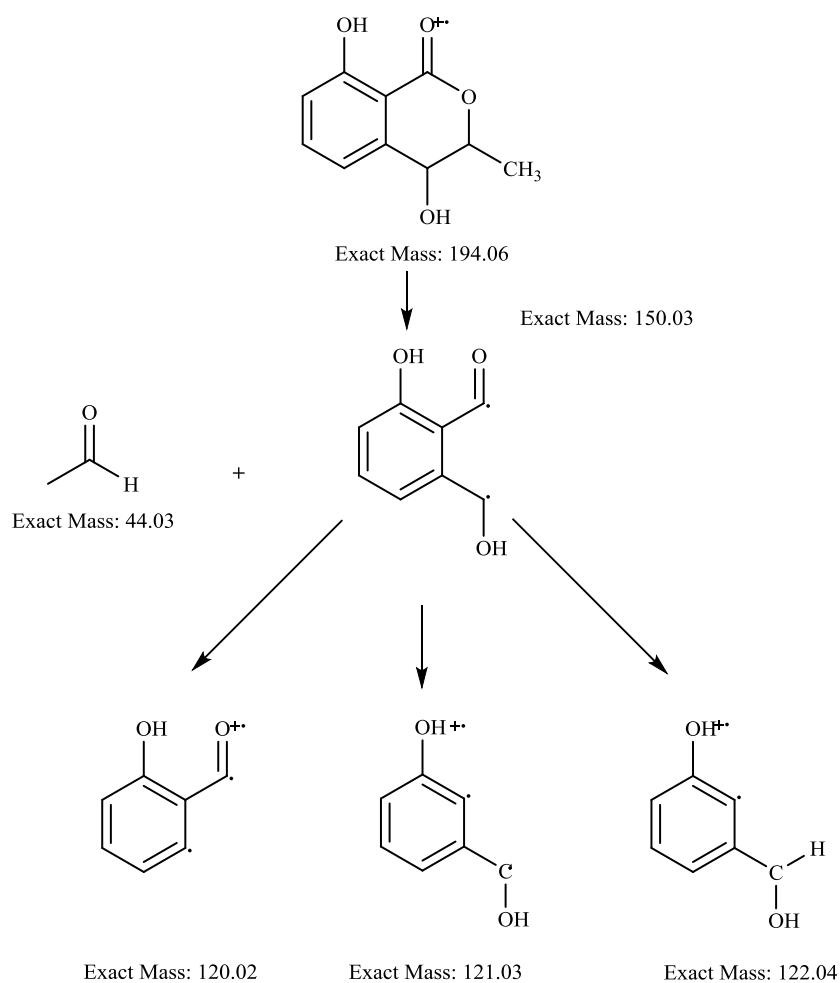
Figure 5.16: Ion fragmentation mass spectrometer of 4-hydroxymellein

5.4.5 LTRC15-8-41 ((-)-*cis-equatorial*-4-hydroxymellein, 5.21)

Compound LTRC15-8-41 (8.7 mg) was obtained as colourless needles. It had an optical rotation of $[\alpha]_D^{20}$ -44.0 (*c* 1.00, CHCl$_3$), which was slightly different from latter isolated compound, LTRC15-6-31c. However, the HRESI-MS showed a similar mass ion peak at *m/z* 195.0650 [M+H]$^+$ corresponding to the molecular formula C$_{10}$H$_{11}$O$_4$ [M+H]$^+$ as in compound LTRC15-6-31c. The ^{1}H NMR spectrum of LTRC15-8-41 (Figure 5.17, Table 5.6) showed the same spin system of aromatic protons with LTRC15-6-31c: δ_H 7.53 (*t*, *J*=8.5 Hz, 1H), 7.02 (*d*, *J*=8.5 Hz, 1H), and 6.92 (*d*, *J*=7.2 Hz, 1H) which corresponded to protons H-6, H-5 and H-7, respectively. However, the methine proton signals were observed at δ_H 4.60 (*d*, *J*=1.5 Hz, 1H) and 4.70 (*d*, *J*=1.5 Hz, 1H), corresponding to H-4 and H-3, respectively; the coupling constant 1.0-1.5 Hz indicated that these protons were *cis-equatorial* to each

other. A methyl signal was observed at δ_H 1.59 (*d*, *J*=6.0 Hz, 3H), as well as a hydroxyl group at δ_H 11.05 (*s*, 8-OH). This compound was identified as (-)-*cis-equatorial*-4-hydroxymellein   (4,8-dihydroxy-3-methylisochroman-1-one).   The compound has been previously reported from the fungi *L. theobromae* (Aldridge *et al.*, 1971), *A. ochraceus, Seimatosporium* sp. and the ascidian *Eudistoma vannamei* (Cole *et al.*, 1971, Hussain *et al.*, 2012, Montenegro *et al.*, 2012), *Uvaria hamiltonii* (Asha *et al.*, 2004), *Cercospora taiwanensis* (Camarda *et al.*, 1976) and *Aspergillus melleus* (Garson *et al.*, 1984, Holker and Simpson, 1981).
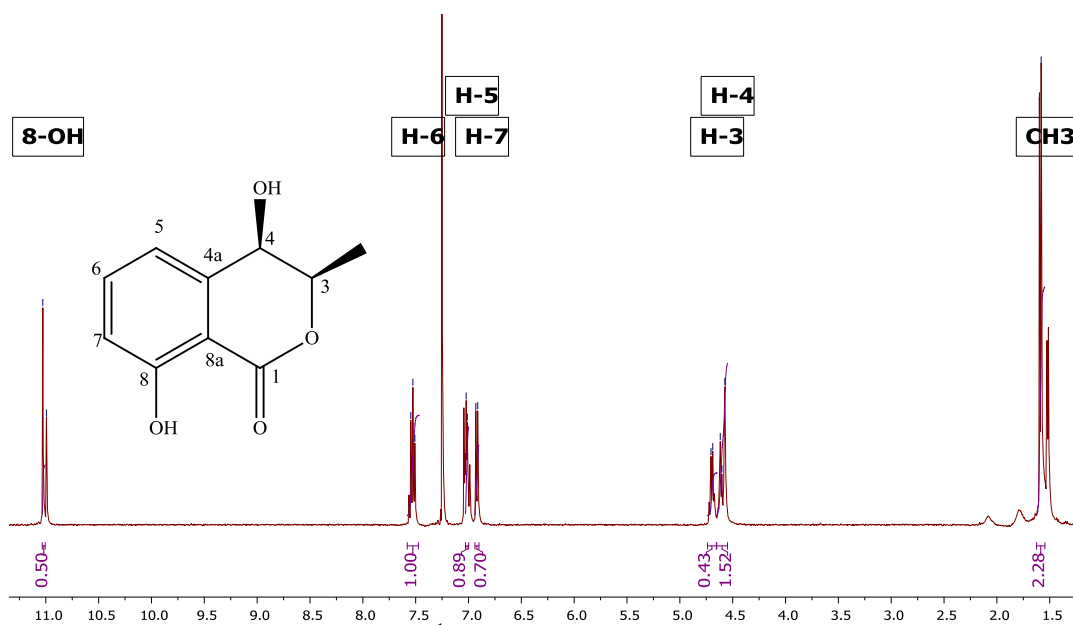
Figure 5.17: ^{1}H NMR spectrum of LTRC15-8-41
(CDCl$_3$, [1]H 400 MHz)

5.4.6   Compound LTRC15-8-22c ((-)-5-hydroxymellein, 5.22)

Compound LTRC15-8-22c (6.0 mg) was obtained as colourless needles with an optical rotation of $[\alpha]_D^{20}$ -69.0 (*c* 1.00, acetone). HRMS showed a mass ion peak at *m/z* 193.0506 corresponding to the molecular formula C$_{10}$H$_{11}$O$_4$ 195.0651 [M+H]$^+$ which was the same as 4-hydroxymellein. A difference was observed in the aromatic proton signals that showed an AB spin system (Figure 3.21) instead. Two aromatic doublets were observed at δ_H 7.11 (*d*, *J*=8.9 Hz, 1H) and 6.71 (*d*, *J*=8.9 Hz, 1H), referring to H-6 and H-7, respectively, which were in the *ortho* position. Methylene proton signals were shown by two of doublet of doublets at δ_H 3.19 (*dd*, *J*=16.9, 3.4 Hz, 1H), corresponding to H-4', while 2.65 (*dd*, *J*=17.0, 11.5 Hz, 1H) was assigned

201

to H-4. These protons were correlating to a methine proton at δ_H 4.75 (*m*, 1H, H-3) as seen in the COSY NMR (Figure 3.22 a). The methyl signal was shown at δ_H 1.50 (*d*, *J*=6.2 Hz, 3H). Meanwhile, the important correlation between proton H-4, H-6 and H-7 and the aromatic carbon at δ_C 146.4 (C-5) were observed in its HMBC spectrum (Figure 3.22 b); carbon C-5 was shifted downfield due to the hydroxyl group attached to this carbon. The other correlations that need to be highlighted were between the protons H-4 and H-6 with quaternary carbon at δ_C 139.5 (C-4a), and proton H-7 with quaternary carbon at δ_C 108.8 (C-8a). A compound having the same NMR spectra (^{1}H and ^{13}C) and (-) optical rotation was isolated from *Seimatosporium* sp. (Hussain *et al.*, 2012); hence, this compound was elucidated as (-)-5-hydroxymellein (5,8-dihydroxy-3-methylisochroman-1-one). It has also been previously reported from the fungi *Septoria nodorum* (Devys *et al.*, 1994) and *Botryosphaeria obtuse* (Venkatasubbaiah and Chilton, 1990, Djoukeng *et al.*, 2009) and *Penicillium* sp. (Oliveira *et al.*, 2009).
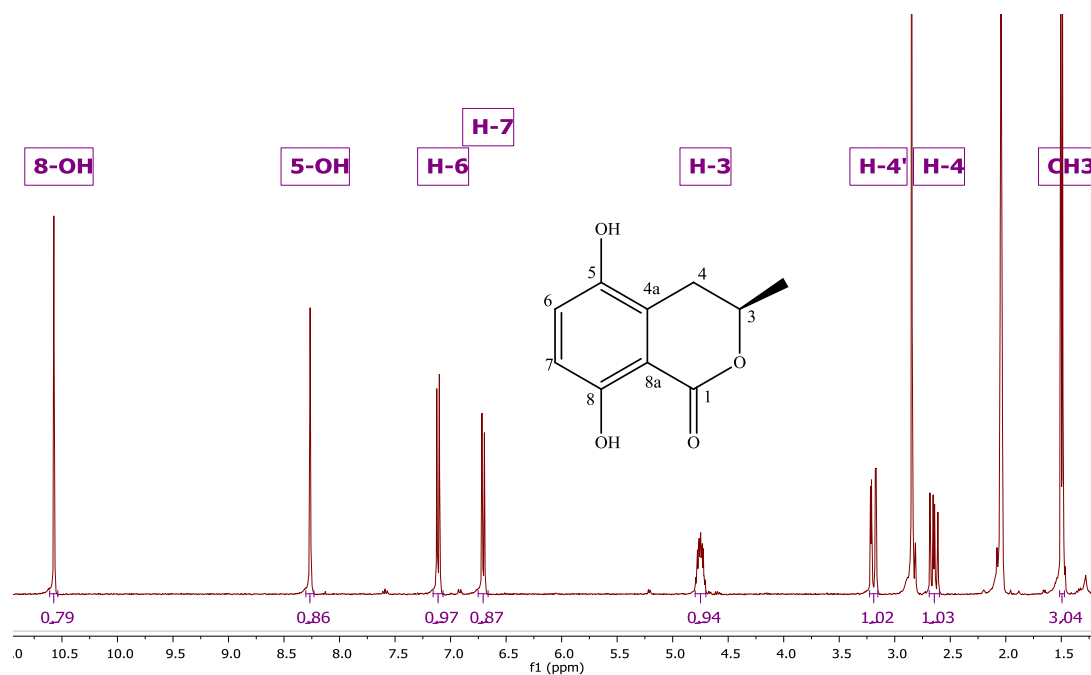
Figure 5.18: ^{1}H NMR spectrum of LTRC-8-22c
(Acetone-*d*6, [1]H 400 MHz)
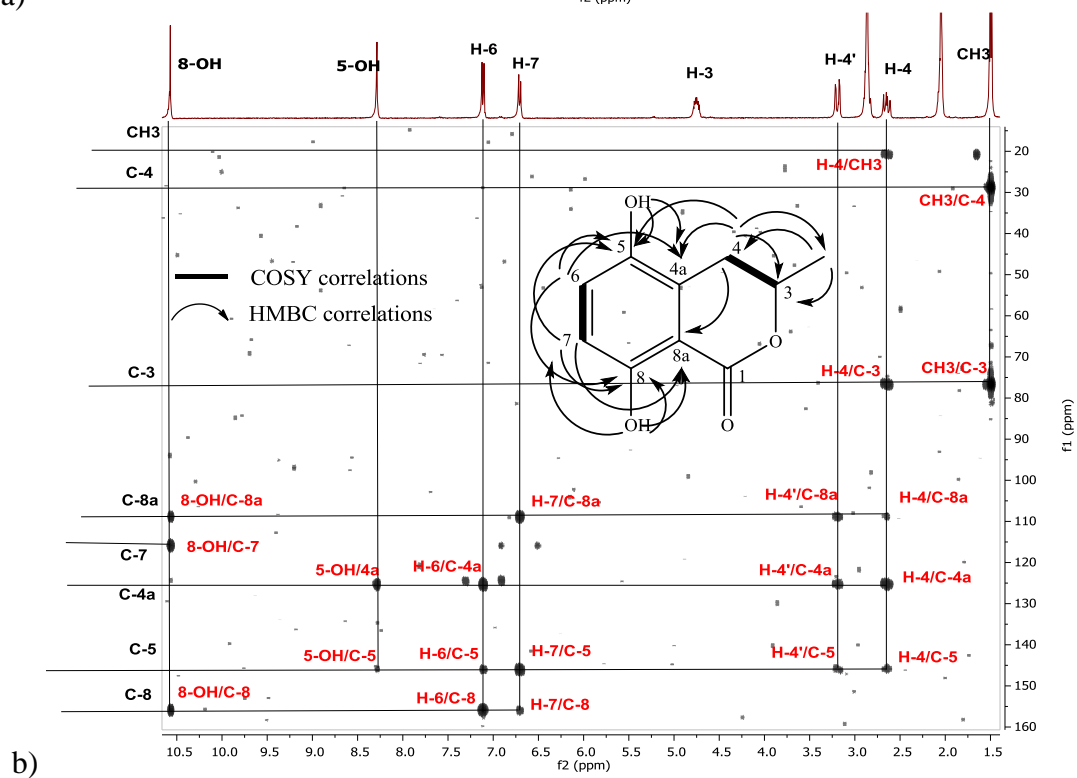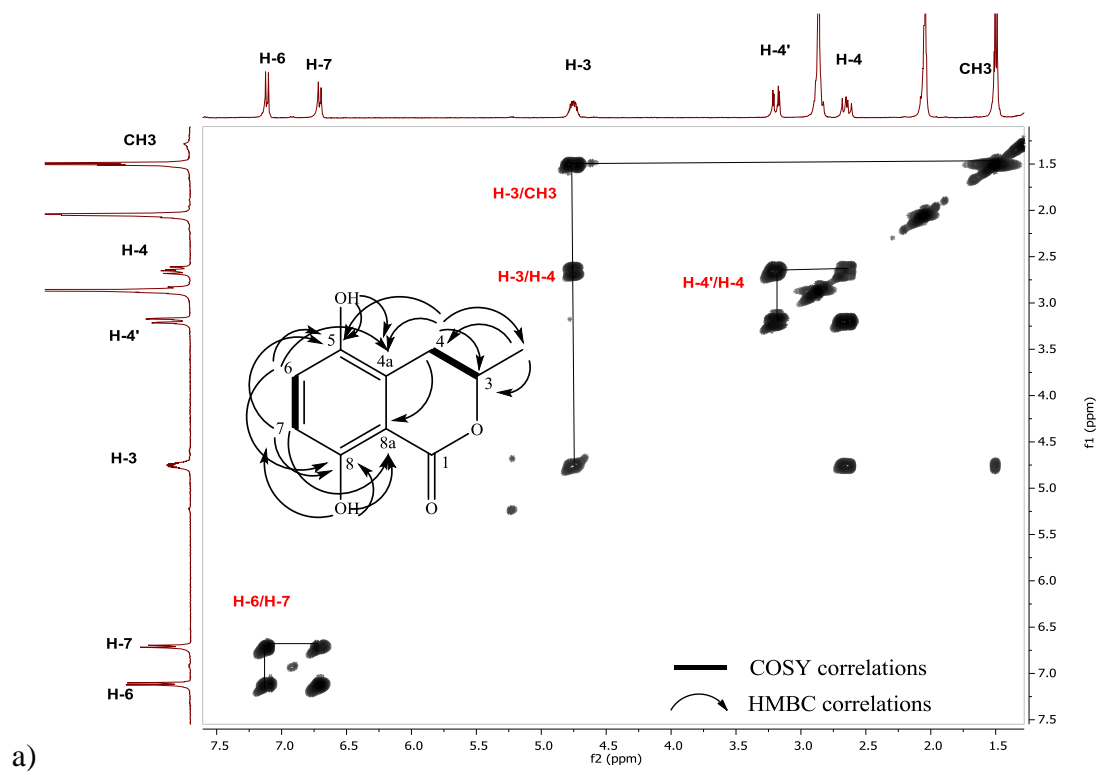
Figure 5.19: (a) COSY and (b) HMBC NMR spectra of LTRC-8-22c
(Acetone-d_6, ^{1}H 400 MHz)

203

5.5 Bioactivity test results

Four metabolites with *m/z* 179.0705 $[M+H]^+$ (mellein), 195.0650 $[M+H]^+$ (two epimers of 4-hydroxymellein) and 195.0651 $[M+H]^+$ (5-hydroxymellein), were identified in the dereplication study (Figure 5.6 and Figure 5.7) and were successfully isolated and identified. The metabolites isolated from LTRC15 were tested for anti-trypanosomal activity and cytotoxicity against PNT2A (Table 5.8). Two phenolic metabolites, *p*-hydroxyphenethyl alcohol and *p*-hydroxybenzaldehyde possessed potent activity against the protozoa *T. b. brucei* with MIC of 12.50 and 6.25 μM, respectively. Mellein and its derivatives also showed activity against *T. b. brucei*, with (-)-5-hydroxymellein possessing slightly higher potency (MIC of 2.40 μM) compared with (-)-mellein and (-)-4-hydroxymellein derivatives. The phenolics and mellein derivatives showed relatively non-toxic against PNT2A cells.

Table 5.8: Activities of the isolated compounds
from *L. theobromae* against *T. b. brucei* and PNT2A cells

Compounds	[a] MICs (μM)	[b] Cytotoxicity, % D of control (100 μg/mL)
p-hydroxyphenethyl alcohol	12.5	81.5
p-hydroxybenzaldehyde	6.25	86.6
(-)-mellein	5.80	84.4
(-)-*trans-axial*-4-hydroxymellein	3.20	82.3
(-)-*cis-equatorial*-4-hydroxymellein	8.20	87.8
(-)-5-hydroxymellein	2.40	89.7
Suramin	0.11	n.d
Triton X	n.d	0.082

[a] Each sample was tested in two independent assays against *T. b. brucei*, MIC values indicate the minimum inhibitory concentration of a compound/standard in μM necessary to achieve 90% growth inhibition. MICs (MIC < 10 μM - promising; 10 μM < MIC > 20 μM - moderate; 20 μM < MIC > 30 μM - marginal/weak; 30 μM < MIC > 40 μM - limited; MIC > 40 μM - no activity);
[b] Initial screening for cytotoxicity activity against human normal prostatic epithelial cells (PNT2A) , % D of control values (at 100 μg/mL,) were determined by averaging of three independent assays results (n=3); [c, d] Positive controls; n.d.- not determined.

p-hydroxyphenethyl alcohol   p-hydroxybenzaldehyde   (-)-mellein

(-)-*trans-axial*-   (-)-*cis-equatorial*-   (-)-5-hydroxymellein
4-hydroxymellein   4-hydroxymellein

The investigation of the anti-trypanosomal activity of mellein and its derivatives, tyrosol and p-hydroxybenzaldehyde was reported for the first time in this study. These compounds demostrated that they are potential anti-protozoal agents for *T. b. brucei*. Previously, the anti-trypanosomal activity of simple phenolic compounds *in vitro* has also been reported from *Aspergillus aculetaus* (Chapter 4). This study is encouraging in that it shows the potential of marine endophytic fungi as sources of anti-trypanosomal compounds.

Chapter 6

6.   Discussions

It is a known fact that Malaysia possesses more sea than land within its territory. The water of the east coast of Malaysia contains great marine biodiversity, the majority of which remains unexplored. Mangrove plants have been used for different medicinal purposes; for example, the extract of *Ipomoea pescaprae* is used as an anti-inflammatory and in the treatment of headache, sinusitis and rheumatic pains and is also used in baths to treat scabies (Bandaranayake, 1998). In this study, the *Avicennia lanata* crude extract was found to possess promising structural diversity and bioactive metabolites. The investigation for novel active chemical components is challenging as many studies have been performed on natural sources. However, endophytic fungi are easier to handle and sustainable since their production of metabolites can be optimised in the laboratory by using different culture conditions. Moreover, the use of high-throughput techniques such as metabolomics tools and advanced chromatography techniques facilitate the targeting and isolation of new metabolites.

In the present study, a mangrove plant (*A. lanata*) extract and three endophytic fungal strains, *Fusarium* sp., *Aspergillus aculeatus* and *Lasiodiplodia theobromae* were investigated for the presence of bioactive compounds. Various classes of metabolites have been isolated and identified including naphthofuranquinones and their new derivatives, hydroxyavicenol C, glycosemiquinone and avicennpentenone carboxylate, two triterpenes and two sterols from the mangrove *A. lanata*, an ergosterol peroxide from *Fusarium* sp. and *A. aculeatus*, 1,4-naphthoquinones with a naphthazarin structure from *Fusarium* sp., four dihydroisocoumarins (mellein and its derivatives) from *L. theobromae*, secalonic acid A and a new 2,3-dihydrochromen-4-one derivative, aspergillusenone from *A. aculeatus* as well as simple phenolic and carboxylic acids from both *A. aculeatus* and *Fusarium* sp.. As evidenced above, the chemical constituents from plants and endophytic fungi that live in the plant tissues are manifold, and some of these constituents may be biochemically active

metabolites that can serve as lead compounds for new candidates' drug. All extracts and fractions were tested for trypanocidal activity against the bloodstream form of *T. b. brucei,* using suramin as the positive control. Unlike *T. b. gambiense* and *T. b. rhodesiense*, *T. b. brucei* is non-pathogenic to humans; it is only harmful to domestic mammals and antelopes. The parasite is usually used in early drug discovery screening tests to identify bioactive metabolites (Stevens *et al.*, 2004, Pink *et al.*, 2005). Complementary to the bioassay screening, advanced metabolomic and dereplication studies were used to screen and evaluate all the potential bioactive metabolites in those extracts during preliminarily screening in order to be able to prioritise the extracts and samples. To pinpoint the active compound, the active extracts and fractions were further subjected to isolation and purification using various high-throughput and normal chromatography techniques, and the isolated compounds were subsequently tested against *T. b. brucei*. Different classes of the isolated compounds have been discussed in previous chapters, some of which were potent against the protozoa.

6.1 Triterpene and sterol compounds

Two pentacyclic triterpenes possessing the same taraxerane-type skeleton, taraxerol (**1.44**) and taraxerone (**1.45**), have been isolated from the mangrove *A. lanata*, differ only at C-3 where taraxerone has a carbonyl and taraxerol a β-OH. Stigmasterol (**1.47**) and β-sitosterol (**1.56**) have been also isolated from this plant. The only difference between these structures is the presence of a double bond at $\Delta^{22, 23}$ on the side chain. Ergosterol peroxide (**3.27**), an ergosterol-derived compound which has been isolated from the endophytic fungi *Fusarium* sp. and *A. aculeatus*, possesses an endo-peroxide, represented by an O-O bridge between C-5 and C-8 on tetracyclic ring, and two unsaturated double bonds at $\Delta^{6, 7}$ on the ring and $\Delta^{22, 23}$ on the side chain. The mechanism for the production of ergosterol peroxide through the photo-oxidation of ergosterol has been proposed by Trigos and Ortega-Regules (2002). This mechanism was later used to aid in the classification of natural antioxidant scavengers of free radicals as photosensitizers or quenchers of singlet oxygen (Lagunes and Trigos, 2015).
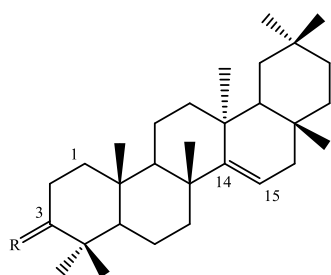
1.44; R=OH
1.45; R=O
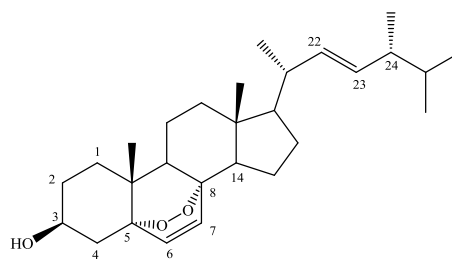
3.27
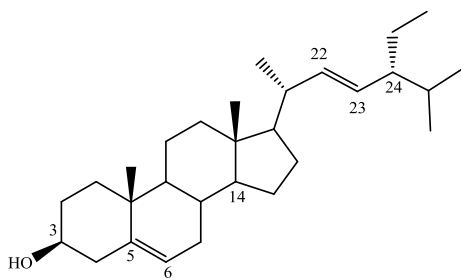
1.47; $\Delta^{22,\,23}$
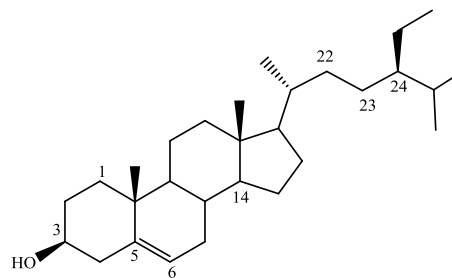
1.56
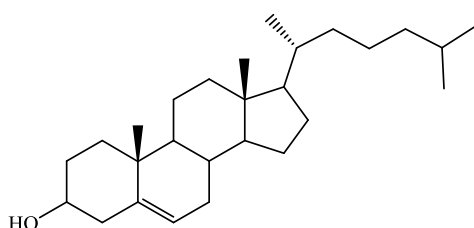
1.54
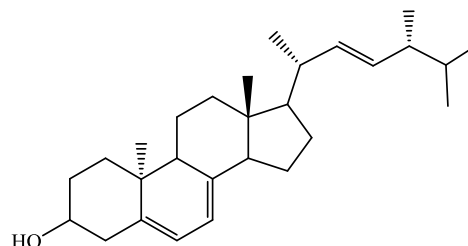
6.1

6.1.1   Biosynthesis of sterols

Sterols are an important component of cell membranes, supporting their structure and growth. Cholesterol (**1.54**), the main sterol in mammals, and ergosterol (**6.1**) with other 24-methylsterols, which are mainly found in fungi and trypanosomatids, are formed from lanosterol. Phytosterols, the main sterols in plants, are formed from cycloartenol (9,19-cyclic derivative). The biosynthesis pathway of sterols in mammalian cells, fungi and trypanosomatids, algae and higher plants is illustrated in Figure 6.1. The intermediates lanosterol and cycloartenol have $\Delta^{24,\,25}$ on the side chain; in mammalian cells the double bond is reduced to cholesterol whereas alkylation at C-24 and hydrogenation at C-25 produces alkylated sterols in fungi, trypanosomatids, algae and higher plants (Shujiro Seo *et al.*, 1992). The presence of

3β–OH on the tetracyclic ring is essential to promote the growth of the organism whereas the methyl groups at C-14 or C-4 inhibit growth. These sites are crucial for
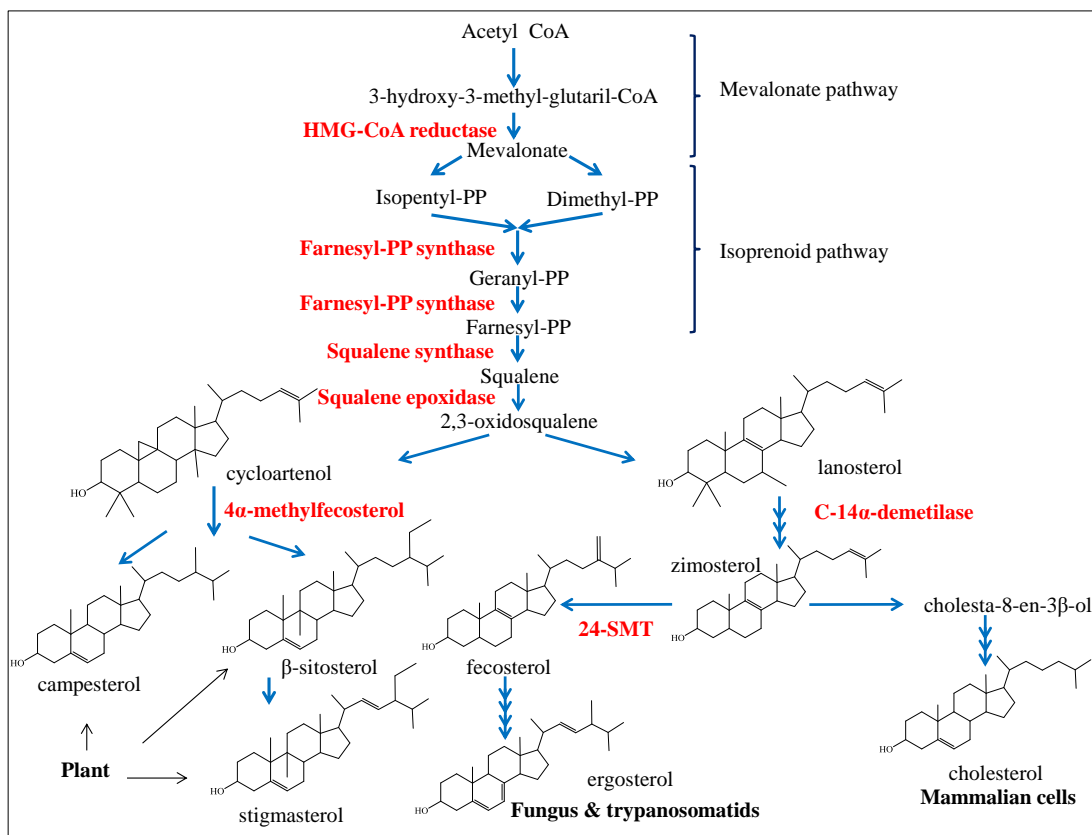
Figure 6.1: The biosynthesis of ergosterol
in fungi and trypanosomatids, cholesterol in mammalian cells, and stigmasterol and campesterol in plants showing the main steps and the enzymes involved which are highlighted in red. A β-methyl at C-24 and the double bond at C-22 in the side chain are essential in ergosterol and other 24-methylsterols to support fungal and trypanosomatid growth. C-14α-demethylase and 24-sterolmethyltransferase (24-SMT) are important to regulate the production of ergosterol in fungi and trypanosomatids (de Souza and Rodrigues, 2009).

the activity of the sterols in the cellular membranes (de Souza and Rodrigues, 2009). Cholesterol (**1.54**) and ergosterol (**1.61**) differ in that cholesterol has only one double bond on the ring at $\Delta^{5,\ 6}$ and is absent of methyl-24 on the saturated side chain, whereas ergosterol has two double bonds at $\Delta^{5,\ 7}$ on the ring and $\Delta^{22,\ 23}$ on the side chain, and a β-24-methyl on the side chain, which are important in fungi and trypanosomatids to maintain growth. The enzyme 24-sterolmethyltranferase (24-SMT) is important to regulate the production of ergosterol in fungi and trypanosomatids. This pathway thus serves as a good target for anti-trypanosomal and anti-fungal drugs. Earlier study reported that the ergosterol peroxide was an

artefact of isolation of ergosterol, found in the extracts of sporophores of *Piptoporus betulinus* or *Daedalea quercina* which have been exposed to daylight for several days (Adam *et al.*, 1967). However, later study on the formation of epidioxy sterols in *Penicillium rubrum* and *Gibberella fujikuro*, proved that the transformation of ergosterol to ergosterol peroxide was via simultaneous photo-oxidative and enzymatic pathways (Bates *et al.*, 1976).

6.1.2 Biological evaluation of taraxerone and taraxerol

In this study, taraxerol (**1.44**) and taraxerone (**1.45**) from *A. lanata* showed very limited activity against *T. b. brucei* with MICs of 145.30 and 154.20 μM, respectively (Table 6.1). A previous study has shown that β-amyrin (**1.49**) showed poor activity against blood stream strain of *T. b. brucei* with an IC_{50} of 126.9 μM (Hoet *et al.*, 2007). The molecular structure of β-amyrin is similar to taraxerol, and the only difference is the double bond shifted from $\Delta^{14, 15}$ to $\Delta^{12, 13}$. Taraxerol has also been isolated from the Ecuadorian plant *Cupania cinerea* and showed IC_{50} values of <10 μM against *T. b. rhodesiense in vitro* bloodstream trypomastigotes with low cytotoxicity (Gachet *et al.*, 2011). A study on activity of taraxerol and taraxerone, which have been isolated from the bark of *Cupania dentata* (Sapindaceae), against flagellate protozoan *Giardia lamblia* trophozoites, both were also found to have potential giardicidal activity with IC_{50} values of 26.7 and 37.8 μM, respectively (Hernández-Chávez *et al.*, 2012). The compounds also exhibited anti-plasmodial (*Plasmodium falciparum*), analgesic (Biswas *et al.*, 2009a) and anti-inflammatory (Biswas *et al.*, 2009b) activities. Other biological activities have shown that taraxerone and taraxerol were also allelopathic (Macías-Rubalcava *et al.*, 2007) and displayed anti-fungal activity (Magadula and Erasto, 2009).

6.1.3 Biological evaluation of sterols

β-sitosterol (**1.56**), which possessed a saturated side chain was inactive against the protozoan with an MIC value of 142.30 μM. However, stigmasterol (**1.47**) which has a double bond on the side chain, showed slightly increased activity but still a very low inhibitory effect on *T. b. brucei* (MIC of 126.40 μM).

Compounds	Sources	[a] *T. b. brucei*, MICs (μM)	[b] PNT2A cells, % D of control (100 μg/mL)
Triterpene-taraxerane types			
taraxerol (**1.44**)	*A. lanata* stems	145.30	92.8
taraxerone (**1.45**)	*A. lanata* stems	154.20	88.8
Sterols			
stigmasterol (**1.47**)	*A. lanata* stems	126.40	98.7
β-sitosterol (**1.56**)		142.30	96.2
ergosterol peroxide (**3.27**)	*A. aculeatus*	1.56	94.0
	Fusarium sp.	1.48	91.7
Naphthouinones			
Naphthofuranquinones			
avicenol C (**1.7**)	*A. lanata* stems	6.25	78.3
avicequinone C (**1.4**)	*A. lanata* stems	3.12	68.6
hydroxyavicenol C (**2.26**, new)	*A. lanata* stems	12.50	86.1
glycoquinone (**2.25**)	*A. lanata* stems	12.50	80.3
glycosemiquinone (**2.27**, new)	*A. lanata* stems	12.50	86.1
avicennpentenone carboxylate (**2.28**, new)	*A. lanata* stems	6.25	86.3
Naphthazarin structures			
anhydrofusarubin (**3.28**)	*Fusarium* sp.	1.20	67.1
javanicin (**3.8**)	*Fusarium* sp.	0.60	61.4
dihydrojavanicin (**3.29**)	*Fusarium* sp.	1.90	22.3
solaniol (**3.26**)	*Fusarium* sp.	0.32	38.6
Simple phenolic acids			
vanillic acid (**4.29**)	*A. aculeatus*	6.25	83.4
3,4-dihydroxyphenylacetic acid (**4.30**)	*A. aculeatus*	1.56	93.0
o-hydroxyphenylacetic acid (**4.31**)	*A. aculeatus*	6.25	98.1
p-hydroxyphenylacetic acid (**4.32**)	*A. aculeatus*	6.25	93.7
2-(3,4-dihydroxyphenyl)-*N*, *N*-dimethylacetamide (**4.33**, new)	*A. aculeatus*	3.12	91.9
p-hydroxyphenethyl alcohol (**5.17**)	*L. theobromae*	12.50	81.5
p-hydroxybenzaldehyde (**5.18**)	*L. theobromae*	6.25	86.6
Dihydroisocoumarins			
(-)-mellein (**5.19**)	*L. theobromae*	5.80	84.4
trans-axial-4-hydroxymellein (**5.20**)	*L. theobromae*	3.20	82.3
cis-equatorial-4-hydroxymellein (**5.21**)	*L. theobromae*	8.20	87.8
(-)-5-hydroxymellein (**5.22**)	*L. theobromae*	2.40	89.7
Xanthones			
aspergillusenone (**4.28**, new)	*A. aculeatus*	1.26	22.2
secalonic acid A (**4.21**)	*A. aculeatus*	<0.19	25.0
[c] Suramin	-	0.11	n.d
[d] Triton X	-	n.d	0.082

[a] Each sample was tested in two independent assays against *T. b. brucei*, MIC values indicate the minimum inhibitory concentration of a compound/standard in μM necessary to achieve 90% growth inhibition. MICs (MIC < 10 μM - promising; 10 μM < MIC > 20 μM - moderate; 20 μM < MIC > 30 μM - marginal/weak; 30 μM < MIC > 40 μM - limited; MIC > 40 μM - no activity); [b] Initial screening for cytotoxicity activity against human normal prostatic epithelial cells (PNT2A) , % D of control values (at 100 μg/mL,) were determined by averaging of three independent assays results (n=3); [c, d] Positive controls; n.d.- not determined.

A study by Hoet and co-workers reported the *in vitro* anti-trypanosomal activity of a few sterol derivatives. Stigmasterol (**1.47**) and clerosterol (**6.2**), which also has the double bond on the side chain (C-27), showed very weak activity against *T. b. brucei* with IC$_{50}$ values of 134.6 and 129.8 μM, respectively (Hoet *et al.*, 2007). In the same report, stigmastanol (**6.3**) and β-sitosterol (**1.56**), both of which have a saturated side chain, were also found to be inactive against the protozoa with IC$_{50}$ values of >240 μM and > 241.1 μM, respectively. Another sterol isolated from the Turkish sponge *Agelas oroides*, 24-ethyl-cholest-5α-7-en-3-β-ol (**1.57**)*,* has a $\Delta^{7, 8}$ double bond and also showed limited activity against *T. b. rhodesiense* with IC$_{50}$ value of 34.2 μM (Tasdemir *et al.*, 2007). Saringosterol (**6.4**) which possesses two unsaturated double bonds ($\Delta^{5, 6}$ and $\Delta^{25, 26}$) and a hydroxyl group on the side chain (C-24), has increased activity against *T. b. brucei* (IC$_{50}$ = 7.8 μM) (Hoet *et al.*, 2007). The activity of 24-vinyl-cholest-9-ene-3β,24-diol (**6.5**), a saringosterol derivative isolated from *Haliclona simulans* showed increased activity against *T. b. brucei* with an MIC of 4.58 μM (Viegelmann *et al.*, 2014). The only difference between the two is the double bond shifted from $\Delta^{5, 6}$ to $\Delta^{9, 11}$. Vernoguinosterol (**6.6**) and vernoguinoside (**6.7**) have furan rings on the side chain, and gave potent activity against the bloodstream trypomastigotes of *T. b. rhodesiense* with IC$_{50}$ values of 4-11 μM (Tchinda *et al.*, 2002).

6.2

6.3

1.57

6.4; R=H
6.8; R=OH

6.5

6.6; R=H
6.7; R=Glucose
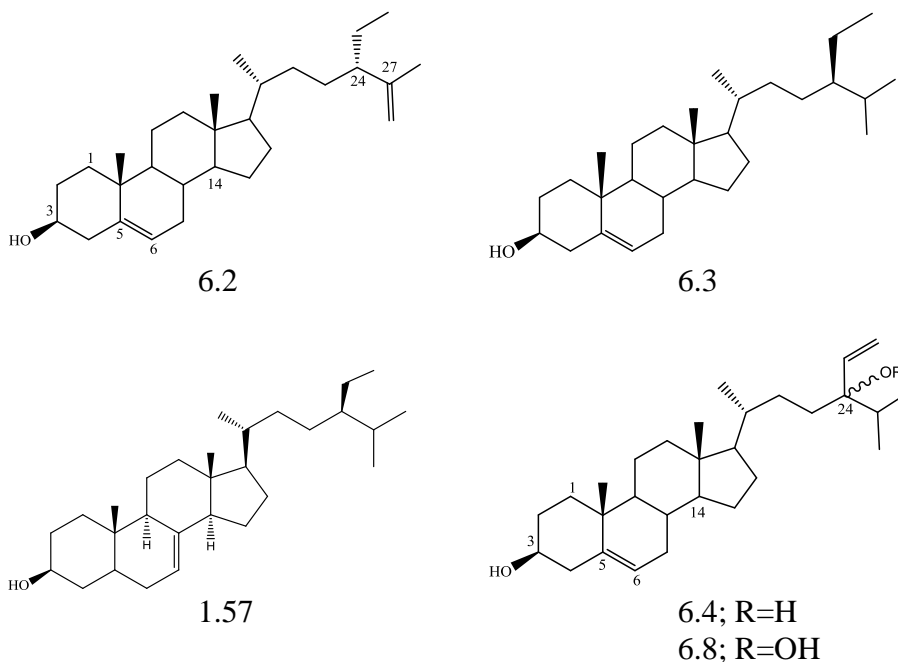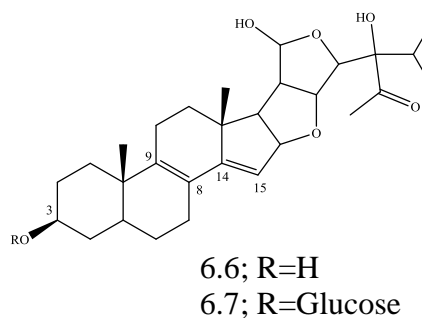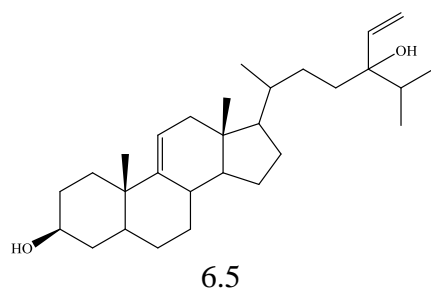
It is interesting to note that a natural compound which has a peroxide group (R-O-O-R), can possess a range of biological activities including anti-protozoa (Ramos-Ligonio *et al.*, 2012, Meza-Menchaca *et al.*, 2015), anti-microbial (Zhao *et al.*, 2010, Huang *et al.*, 2009, Lu *et al.*, 2000, Li *et al.*, 2005b), anti-tumour (Jong and Donovick, 1989, Bok *et al.*, 1999, Wu *et al.*, 2012, Sawadsitang *et al.*, 2015) and cytotoxic (Nam *et al.*, 2001, Sawadsitang *et al.*, 2015) activities. Ergosterol peroxide (**3.27**) isolated from *Fusarium* sp. and *A. aculeatus* displayed potent activity against *T. b. brucei* with MIC values of 1.48 μM and 1.56 μM, respectively. This slight variation might be due to impurities that may be present in the samples. A previous study reported that this compound showed strong trypanocidal activity (IC$_{50}$ 0.156 μM) against the intracellular form of *T. cruzi*, the parasite responsible for Chagas disease, without causing cytotoxic effects to the mammalian cells (HeLa) (Ramos-Ligonio *et al.*, 2012). The exoperoxide functional group on the side chain of 24-hydroperoxy-24-vinylcholesterol (**6.8**), which is a derivative of saringosterol (**6.4**), increased its anti-trypanosomal activity against *T. b. brucei* with an IC$_{50}$ of 3.2 μM compared to 7.8 μM for saringosterol. Besides, a study on 24-methylenecholesterol (**6.9**), is a derivative of cholesterol and an epidioxy sterol; 20-methyl-pregn-6-en-3β-ol,5α,8α-epidioxy (**6.10**), both have been isolated from the sponge of *H. simulans* showed potent activity against *T. b. brucei* with an MIC of 9.01 μM (Viegelmann *et al.*, 2014).

6.9

6.10
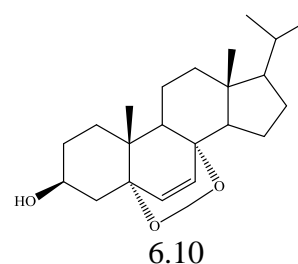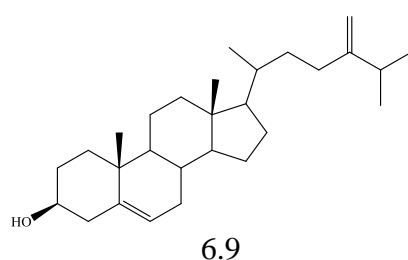
Ergosterol is a part of the cellular membrane constituents of fungi and trypanosomatids that are required for their growth and function. As the structure of ergosterol peroxide is similar to that used by the parasite in its cell membranes to support growth, the selectivity of this metabolite is enhanced, allowing it to target the parasite without causing any toxicity to its host. The results of cytotoxicity assays on ergosterol peroxide against mammalian host cells or human erythrocytes showed that this compound has no cytotoxicity (Mohandas and Gallagher, 2008, Ramos-Ligonio *et al.*, 2012, Kuria *et al.*, 2002, Viegelmann *et al.*, 2014). It is probably that when ergosterol peroxide replaces the ergosterol in the cell membrane of trypanosomatids during the growth stages, the endoperoxide bridge breaks and triggers the formation of reactive oxygen species (ROS), free radicals which are known to disrupt the parasite plasma membrane (Villamil *et al.*, 2004). These findings suggest that the presence of olefinic and oxygenated groups on the sterol as endo (cyclic ring) or exo side chain plays a significant role in enhancing anti-trypanosomal activity in which this was corroborated by the activities obtained by the compounds in this study. The modification of sterol with these functional groups could result in an increase of the anti-trypanosomal activities.

Other reports on ergosterol peroxides show that this compound possesses various biological activities. A structure-activity comparison between ergosterol and ergosterol peroxide for anti-melanogenic activity on B16 10F7 cells showed that the peroxide had inhibited accumulation of the melanin pigment by the suppression of the melanogenic enzyme in B16 10F7 cells with IC_{50} 15.7 µM (Mukaiyama *et al.*, 2009). Ergosterol peroxide isolated from *Sarcodon aspratus* (Berk.) has been reported to induce apoptosis, causing the inhibition of HL-60 (human leukaemia cells) (Toshiyuki Takei *et al.*, 2005) and human prostate cancer cells, PC-3 (Russo *et al.*, 2010). Ergosterol peroxide has the potential to treat kidney disease as it suppressed TGF-β1-induced fibroblast activation in NRK-49F (fibroblast cells) (Rong Zhu *et al.*, 2014). In addition, its ability to suppress the NF-κ B signalling pathway, causing the inhibition of TNF-α production and COX-2 expression in ergosterol peroxide-treated RAW 264.7 macrophages, indicates its potential as an anti-inflammatory agent (Kuo *et al.*, 2011). Therefore, the peroxide moiety has a

potent role in anti-trypanosomal activity and ergosterol peroxide could also serve as a new resource to treat various diseases.

6.2 Naphthoquinones

6.2.1 Naphthofuranquinone type of compounds

Six 1,4-naphthofuranquinone-derived compounds, three of which are being reported here for the first time, have been isolated from the mangrove plant *A. lanata*. The three known compounds were identified as avicenol C (**1.7**), avicequinone C (**1.4**) and glycoquinone (**2.25**). Avicenol C (**1.7**) possessed two methoxy groups which were attached at C-1 and C-4 and a hydroxyisopropyl group attached at C-2' indicating the presence of the side chain on the 2-substituted benzofuran skeleton. Hydroxyavicenol C (**2.26**), is a new derivative of avicenol C, the only difference being two hydroxyl groups attached on both carbon C-1 and C-4 instead of the two methoxy groups in avicenol C. The furan side chain remained the same. Meanwhile, avicequinone C (**1.4**) possessed a *p*-dione with an α,β-unsaturated quinone system ring and an unsaturated double bond on the side chain furan ring ($\Delta^{1', 2'}$).
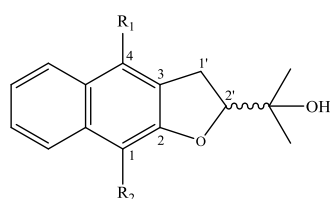
1.7; R$_1$=OCH$_3$, R$_2$=OCH$_3$
2.26; R$_1$=OH, R$_2$=OH
1.4; R$_1$=O, R$_2$=O, $\Delta^{1', 2'}$
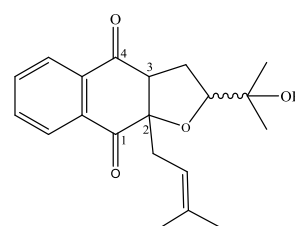
2.25
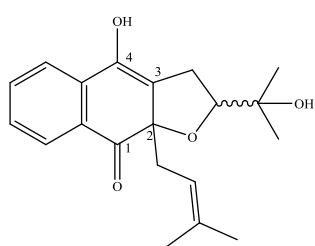
2.27
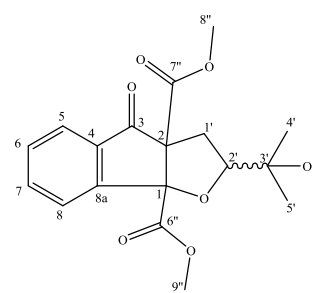
2.28

Another known compound, glycoquinone (**2.25**), also has a *p*-dione with the addition of a prenylated side chain at C-2. The furan side chain remained the same as before.

However, its new derivative, glycosemiquinone (**2.27**), exhibited a hydroxyl group attached to C-4 and a keto group at C-1 while the furan side chain was maintained. The new furan derivative, avicennpentenone carboxylate (**2.28**), lost one carbon on ring B with the addition of two carboxylate groups at C-1 and C-2 compared to other derivatives. Again, the presence of the furan side chain remained the same.

6.2.2 Biosynthesis of 1,4-naphthoquinones naphthazarin structure

Further isolation and identification of secondary metabolites from the crude extract of the endophytic fungus *Fusarium* sp. isolated from *A. lanata* revealed four known 1,4-naphthoquinones of the naphthazarin related structures: anhydrofusarubin (**3.28**), javanicin (**3.8**) and its derivative, dihydrojavanicin (**3.29**) and solaniol (**3.26**). All derivatives have a quinoidal core (C-1 and C-4) with a substituted methoxy group at C-2, a benzene ring with two hydroxyls at both C-5 and C-8, differed only with the presence of substitutuents at C-6 and C-7. Anhydrofusarubin is a violet crystal with a 5,8-dihydroxy-2-methoxy-naphthalene-1,4-dione and a pyran ring which were attached at C-6 and C-7, while javanicin is a red crystal of 5,8-dihydroxy-2-methoxy-naphthalene-1,4-dione with 2-oxopropyl side chain attached at C-7. The yellow crystalline derivative has two hydroxyl groups at C-1 and C-4 instead of C-5 and C-8, compared with the red crystals of javanicin. Solaniol, is a red crystal with a 5,8-dihydroxy-2-methoxy-naphthalene-1,4-dione and a 2-hydroxypropyl side chain attached at C-7. The presence of fully conjugated rings in these metabolites resulted in a very strongly coloured crystal.

3.28

3.26

3.8

3.29
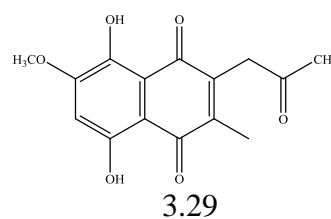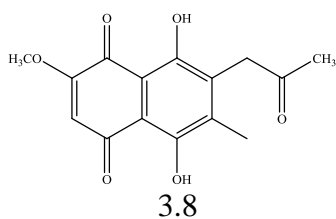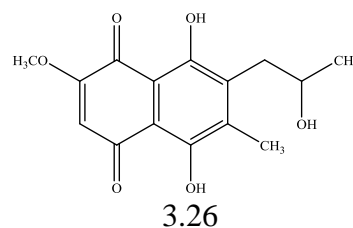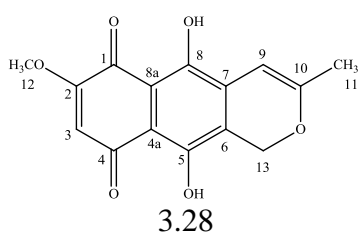
The biogenesis of naphthoquinones produced in *Fusarium* sp. (Figure 6.2) begins with precursors from the acetate malonate pathway. Gatenbeck and Bentley, (1965) and Arsenault, (1968) suggest that the primary metabolite in pigment synthesis is an aromatic acid which is later methylated to fusarubinic acid; isolated from the fungus *Nectria haematococca* (Parisot *et al.*, 1988). The successive reduction of fusarubinic acid subsequently results to aromatic aldehyde and the primary alcohol fusarubin, and leads to the production of javanicin, solaniol, and bostrycoidin. Dehydration of fusarubin and javanicin produced anhydrofusarubin and anhydrojavanicin, respectively. The formation of anhydrofusarubin lactone is the result of direct conversion from fusarubinic acid, and reduction of anhydrofusarubin lactone gave anhydrofusarubin lactol.
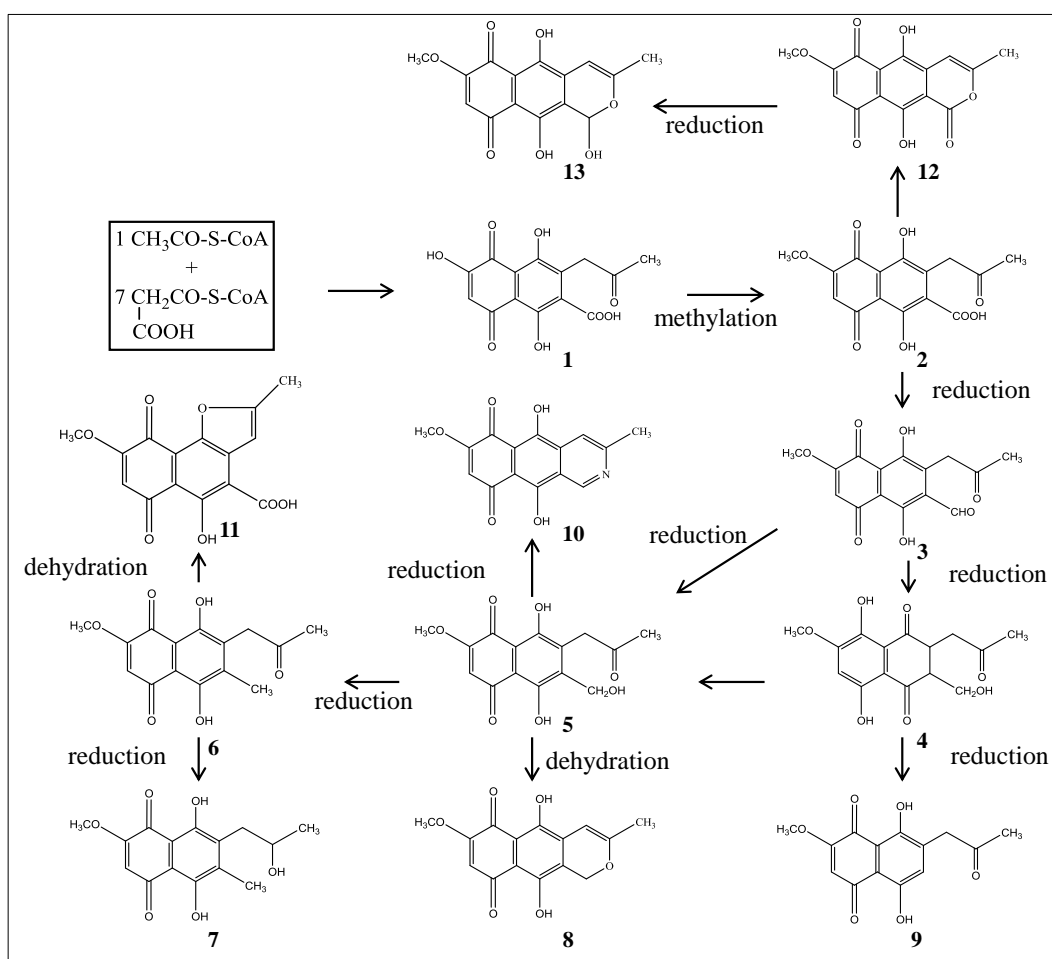
Figure 6.2: Biogenesis relations of various naphthoquinones
synthesized by *Fusarium* sp. is illustrated (Medentsev *et al.*, 1988). The proposed pathway proceeds by formation of acetate malonate to produce 1. aromatic acid (Gatenbeck and Bentley, 1965), 2. fusarubinic acid, 3. aromatic aldehyde, 4. dihydrofusarubin, 5. fusarubin, 6. javanicin, 7. solaniol, 8. anhydrofusarubin, 9. norjavanicin, 10. bostrycoidin, 11. anhydrojavanicin, 12. anhydrofusarubin lactone, 13. anhydrofusarubin lactol.

6.2.3 Biological evaluation of naphthoquinones

Naphthoquinones are compounds, have been isolated from various sources, with structural properties that promote toxicity and exhibit biological activities such as anti-inflammatory, anti-cancer, and anti-leishmania. The fully aromatic system of quinones is characterised by a *p*-dione ring with an α,β-unsaturated quinone system which is able to take part in redox reactions, resulting to the generation of free radicals (Pinto and de Castro, 2009). The biological redox cycle of naphthoquinone derivatives can be triggered by one- or two-electron reduction (Figure 6.3). The one-electron reduction involves the absorption of the quinone by the parasites and subsequent reduction to semiquinones and quinols. Unstable forms are capable of reacting with molecular oxygen leading to the formation of hydrogen peroxide and superoxide anions, followed by the formation of hydroxyl radicals (Docampo *et al.*, 1978). These free radicals are highly reactive and are known to cause damage by reacting with DNA, lipids and proteins (Villamil *et al.*, 2004). Meanwhile, the two-electron reduction is associated with DT-diphorase, leading to the formation of unstable hydroquinones, consequently increasing the quinone toxicities (Munday, 2000).
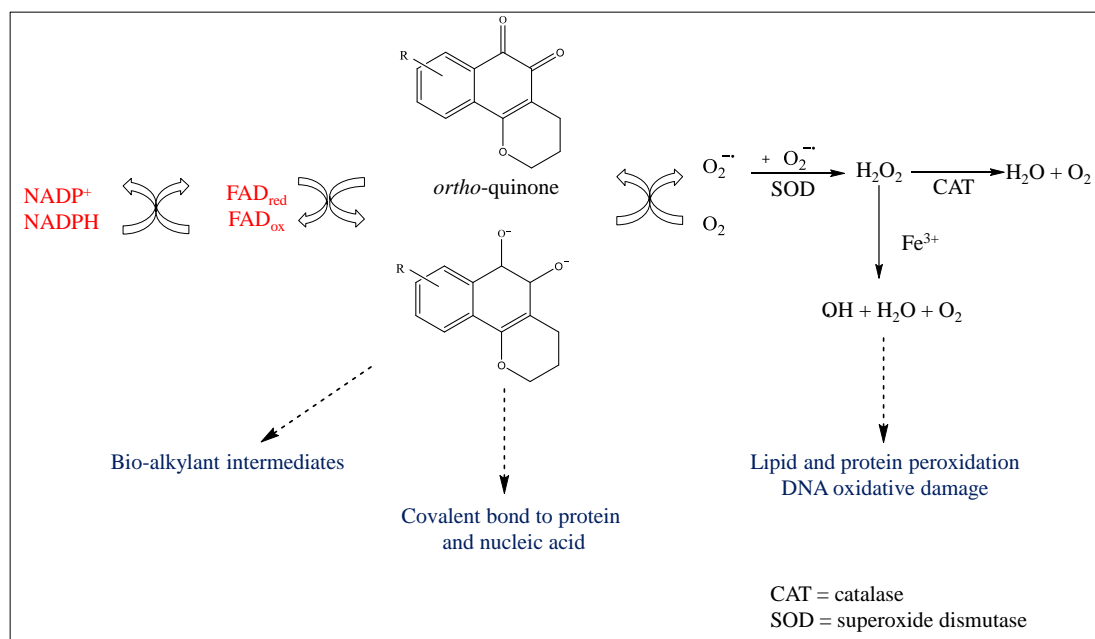
Figure 6.3: The schematic diagram representing the redox cycle and generation of metabolites by quinones (Pinto and de Castro, 2009)

A review by Pinto and de Castro, (2009) compared the activities of the original naphthoquinones to synthetic compounds and suggested structural characteristics that lead to an increase in lipophilicity, allowing better penetration of the 1,4-naphthoquinone compounds through the plasma membrane of the parasite. The functional groups that might be responsible for increasing trypanocidal activity are the presence of a furan moiety, hydroxyl or methoxy groups either on the quinoidal or benzene ring or an aliphatic side chain. Other reports on the structure and anti-leishmanial activity relationship study of naphthoquinones (Ali *et al.*, 2011), suggested that the introduction of methyl or methoxy groups at C-2 on the quinoid ring of the 1,4-naphthoquinones, slightly increased the activity against the parasite *Leishmanial* sp.. While the presence of hydroxyl groups at C-5 and C-8 was able to enhance the activity. In contrast, the presence of hydroxyl at C-2 and substituted prenyl or methyl moiety at C-3 on naphthazarin derivatives decreased the activity.
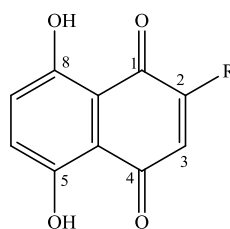
1) R; CH_3 or OCH_3 - increases the anti-leishmanial activity
2) R; OH - decreases the anti-leishmanial activity

6.2.4 Biological evaluation of naphthofuranquinone derivatives

The naphthofuranquinone derivatives from *A. lanata* showed promising anti-trypanosomal activity. Among these derivatives, avicequinone C (**1.4**) was the most potent with an MIC of 3.12 µM. The differences in this structure compared with the other derivatives have been described before. The presence of *p*-dione with α,β-unsaturation on the quinone ring system resulted in increased anti-trypanocidal activity compared to the other derivatives. In contrast, avicenol C (**1.7**) had methoxy groups as opposed to the quinoid and lacked the $\Delta^{1', 2'}$ unsaturation and gave an MIC of 6.25 µM. The presence of the hydroxyl groups, instead of the quinoid group in (-)-hydroxyavicenol C (**2.26**) had decreased the trypanocidal activity with the MIC value of 12.50 µM. There was no difference in the anti-trypanosomal activity of

glycoquinone (**2.25**) and its derivative, (+)-glycosemiquinone (**2.27**), as the MIC for both compounds was 12.50 µM. It showed that the presence of prenyl group on both **2.25** and **2.27** decreased the activity against the protozoa. The new derivative, avicennpentenone carboxylate, showed potent activity with an MIC of 6.25 µM. The loss of one carbon and the addition of two carboxylate groups may have also contributed towards the increased activity. All naphthofuranquinone derivatives showed weak toxicities against normal prostate cells (PNT2A).

A study on synthetic (**6.11**) and natural (**6.12**) naphthofuranquinones isolated from the trunk wood of *Tabebuia ochracea* (Zani *et al.*, 1991) *in vitro* against different strains of the epimastigotes of *T. cruzi*, had showed that the compounds possessing only one methoxy group on the benzene ring showed the most potent activity against the protozoa with growth inhibition (GI) 100% at 13-17 µM of the tested compounds (Ribeiro-Rodrigues *et al.*, 1995). In contrast, the same study also showed that two natural products (**6.13** and **6.14**) and two synthetic compounds (**6.15** and **6.16**) of naphthofuranquinone derivatives possessing two methoxy groups on the benzene ring had decreased the trypanocidal activity against the protozoa with (GI) 45% and 22% respectively. A naphthofuranquinone, (**6.17**)**,** isolated from *Calceolaria sessilis,* had three methyl groups attached to the side chain of the furan ring increased the trypanocidal activity against the epimastigotes of *T. cruzi* with 50% culture growth inhibition (GI$_{50}$) values of 2.1-5.2 µM (Morello *et al.*, 1995). The bioactivity-guided isolation on the extracts of the root barks and stem barks of *Kigelia pinnata* (Bignoniaceae) yielded a naphthofuranquinone with a hydroxyl moiety on the benzene ring (**6.18**), showed potent *in vitro* activity against *T. b. brucei* and *T. b. rhodesiense*, with IC$_{50}$ values of 0.12 and 0.045 µM, respectively, as well as its derivative (**6.19**), which has been synthetically prepared showed potent trypanocidal activity (Moideen *et al.*, 1999). A furanoeremophilane derivative, maturone (**6.20**), which has been isolated from the roots of *Psacalium beamanii*, (Pérez-Castorena *et al.*, 2004), and a mixture of **6.20** and its derivative, isomaturone, (**6.21**) produced by Lewis acid catalysed Diels-Alder reaction of benzofuranquinone with piperylene, exhibited potent trypanocidal activity against *T. cruzi* (Aso *et al.*, 1993).
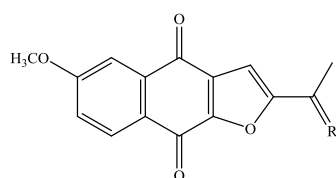
6.11; R=O; IC50 0.40-0.60 µM
6.12; R=H, OH; IC50 2.0-3.0 µM
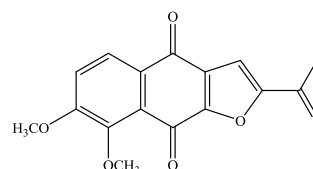
6.13; R=O
6.14; R=H, OH
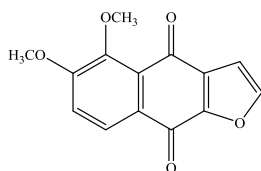
6.15
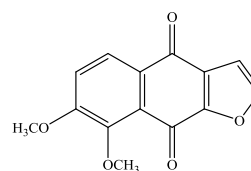
6.16
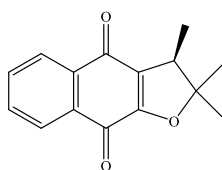
6.17
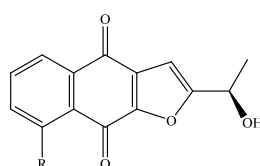
6.18; R=OH
6.19; R=H
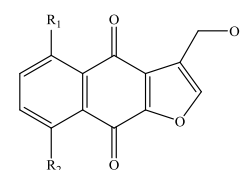
6.20; R$_1$=CH$_3$; R$_2$=H
6.21; R$_1$=H; R$_2$=CH$_3$

6.2.5 Biological evaluation of naphthazarin derivatives

The four naphthazarin derivatives possess a quinoid element in the naphthoquinone core (C-1 and C-4), one methoxy on the quinoid ring (C-2) and two hydroxyl groups on the benzene ring (C-5 and C-8). The presence of different functional groups at C-7 and C-8 was observed among the derivatives. In the present study, four derivatives have been tested for anti-trypanosomal activity. All derivatives showed greater activity against *T. b. brucei* when compared to naphthofuranquinone derivatives, with MICs ranging between 0.30-1.90 µM. Javanicin (**3.8**), has a ketone side chain at C-7 and showed potent anti-protozoal activity with MIC value of 0.60 µM. Interestingly, solaniol (**3.26**) a reduced analogue of javanicin (**3.8**) , with an alcohol chain at C-7 showed the most prominent anti-trypanosomal activity with MIC value of 0.32 µM. The presence of the free hydroxyl group interestingly represents a major attributing factor to enhance the trypanocidal activity. Anhydrofusarubin (**3.28**), with a pyran functional group, also showed pronounced effects against the protozoa with MIC 1.20 µM but the activity was reduced when compared with solaniol (**3.26**) and javanicin (**3.8**). In contrast, dihydrojavanicin (**3.29**), a congener of javanicin, only different in positions of the carbonyl and hydroxyl substituents, showed less activity

with MIC of 1.90 μM. Both dihydrojavanicin (**3.29**) and solaniol (**3.26**) showed more toxic compared with other naphthazarin derivatives. Previous reports on other naphthazarin related structures possessing the quinoid character with α,β-unsaturated system contributed to potent activity against trypanocidal activity have been described (Docampo *et al.*, 1977, Bringmann *et al.*, 2003, Ganapaty *et al.*, 2006).

Another naphthoquinone congener with the naphthazarin structure which displays various biological activities is lapachol (**1.1**); naturally occurring in the genus *Tabebuia* (family Bignoniaceae). A review on lapachol (Hussain *et al.*, 2007), stated that this compound was first isolated from *Tabebuia avellanedae* by Paterno in 1882. A study on lapachol which has been isolated from the wood of *Tabebuia heptaphylla* displayed weak activity against the amastigote form of the parasite *Leishmania donovani* in peritoneal mice macrophages (Schmeda-Hirschmann and Papastergiou, 2003). Another natural analogue of lapachol, β-lapachone (**6.22**), was reported to demonstrate potent trypanocidal activity (Docampo *et al.*, 1977). A well-known naphthazarin monomer, plumbagin (**6.23**), isolated from the tropical lianas belonging to the Ancistrocladaceae and Dioncophyllaceae families, was characterised with a hydroxyl at C-5 and a methyl at C-2 showed potent activity against *T. b. brucei* strain TC 221, with EC_{50} value of 0.034 μM (Bringmann *et al.*, 2003). The presence of a naphthalene derivative, namely 4-hydroxy-3,5-dimethoxy-2-naphthaldehyde (**6.24**), exhibited moderate activity against *T. cruzi* with IC_{50} value of 12.38 μM but weak activity against *T. b. rhodesiense* with the IC_{50} value of 19.82 μM (Ganapaty *et al.*, 2006). In the same report, two commonly occurring naphthoquinone dimers, diospyrin (**6.25**) and 8'-hydroxyisodiospyrin (**6.26**) showed potent activity against *T. b. rhodesiense* with the IC_{50} values of 1.12 and 12.94 μM, respectively, but were inactive against *T. cruzi*, showing that they were more selective. Both **6.25** and **6.26,** increased cytotoxicity with IC_{50} of 6.38 and 9.30 μM, respectively, contradict with compound **6.24** which had weak cytotoxicity (174.94 μM). The three compounds have been isolated from the roots of *Diospyros assimilis* (Ganapaty *et al.*, 2006).

1.1   6.22   6.23   6.24

6.25   6.26
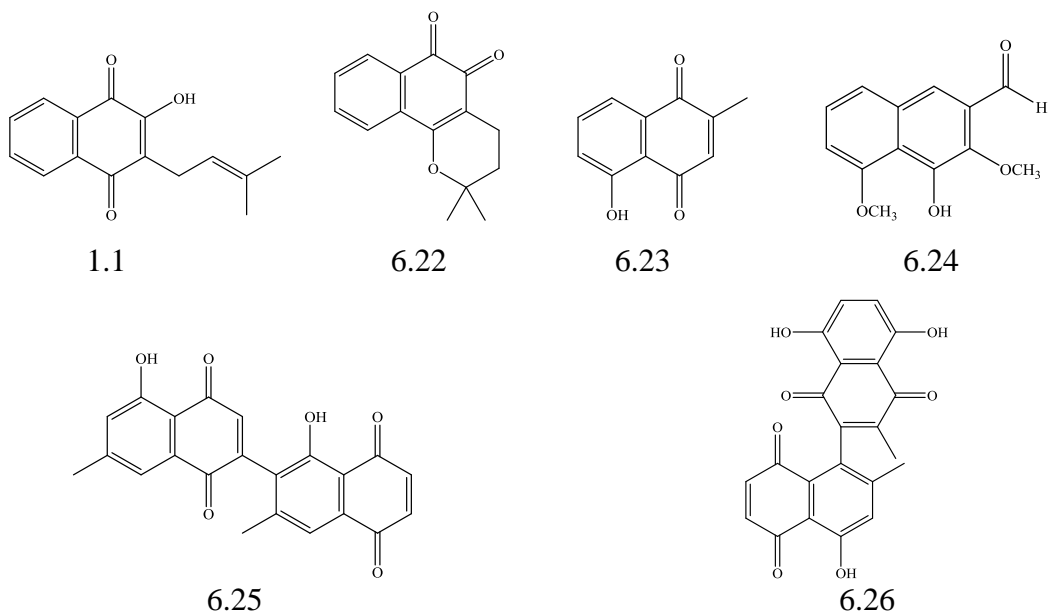
The activity of synthetically prepared lapachol derivatives against the epimastigotes of *T. cruzi*; which included α-lapachone (**6.27**), β-lapachone (**6.22**) and its hydroxylic-β-lapachone (**6.28**) from a commercially available lapachol, showed that β-lapachone (**6.22**) and its hydroxylic-β-lapachone (**6.28**) had potent activity with IC_{kc5} of 0.21 and 3.75 μM, respectively compared with current drugs; nifurtimox and benznidazole (IC_{kc50} of 9.5 and 20.6 μM) whereas, lapachol and α-lapachone showed weak activity (IC_{kc5} of 31.3 and 24.7 μM), respectively, (Salas *et al.*, 2008). In the same study, a synthetically produced α-lapachone derivative with a pyridine (**6.29**) instead of a benzene ring increased trypanocidal activity at IC_{kc5} of 20.1 μM.

6.27   6.28   6.29
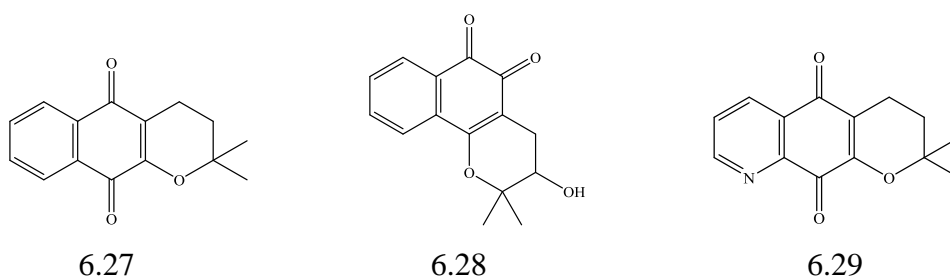
6.2.6 Other biological activities of 1,4-naphthoquinones

Other biological activities was exhibited by naturally occurring avicequinone C (**1.4**) and stenocarpoquinone B (**1.15**) isolated from *Avicennia marina*, possessing a *p*-dione group with an α,β-unsaturated quinone system, were both found to be strongly

anti-proliferative against L-929 (mouse fibroblasts), K-562 (human chronic myeloid leukaemia) and HeLa (human cervix carcinoma) cell lines with GI_{50} of 0.2-4.3 μg/mL (Han *et al.*, 2007). These compounds also showed potent anti-microbial activity against *Candida albicans, Mycobacterium smegmatis, Mycobacterium aurum, Mycobacterium vaccae, Mycobacterium fortuitum* and *Staphylococcus aureus* (Han *et al.*, 2007). The α,β-unsaturated quinone system has been proven to contribute to the anti-cancer activity; a study has shown that the α,β-unsaturated quinone derivatives isolated from the roots of *Ekmanianthe longiflora* have potent cytotoxicity against human cancer and murine cell lines, whereas the absence of this system results in the loss of anti-cancer activity (Peraza-Sánchez *et al.*, 2000). Two natural naphthofuranquinones isolated from the bark of *Tecoma ipe* (synonym *Tabebuia avellanedae*), (**6.30** and **6.31**), exhibited *in vitro* anti-tumour activity against proliferation of human adenocarcinomic epithelial tumour cell (A-549) and colic adenocarcinoma cell (WiDr) with average IC_{50} values of 1.48 and 1.44 μM, respectively (Hirai *et al.*, 1998).

6.30; R=H
6.31; R=OH
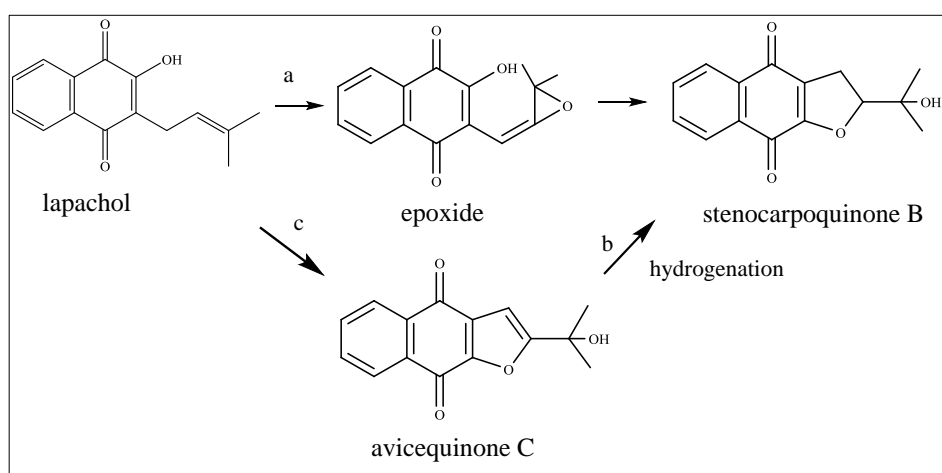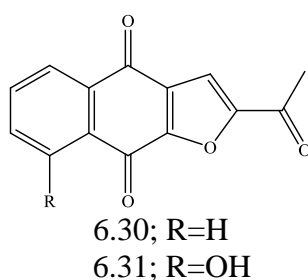
Figure 6.3: The proposed biosynthesis of stenocarpoquinone B
a) peroxidation of lapachol, via an eposide intermediate involving the side-chain double bond (Adams and Lewis, 1978) and b) hydrogenation of avicequinone C (Williams *et al.*, 2006). c) The biosynthesis of avicequinone C from lapachol (Doroshow *et al.*, 1990).

Synthetic stenocarpoquinone B (**1.15**) from peroxidation of lapachol, (**1.1**) (Figure 6.3), was also active against KB (human epidermoid carcinoma of the nasopharynx cell culture) (Adams and Lewis, 1978). A lot of studies have shown that the naphthazarin core is responsible forvarious bioactivities which included anti-cancer (Takemoto *et al.*, 2014) (Jow *et al.*, 2004), anti-bacterial (Kharwar *et al.*, 2009), and HIV-1 integrase inhibition (Shin *et al.*, 2009). A study on anhydrofusarubin (**3.28**) which has been isolated from a gorgonian sea fan (*Annella* sp.) displayed potent selective cytotoxicity comparable to resazurin, a standard that is used against oral human carcinoma (KB) and human breast cancer (MCF-7) cell lines (Trisuwan *et al.*, 2010). The same compound has also been isolated from *Fusarium* sp. (isolated from soil sample) exhibiting strong anti-microbial activities against Gram-positive bacteria, *Bacillus subtilis* and *Staphylococcus aureus,* and Gram-negative bacteria, *Escherichia coli* and *Pseudomonas aeruginosa* as well as anti-fungal activity against *Magnaporthe grisea*, *Aspergillus oryzae, Penicillium citrinum* (Suzuki *et al.*, 2013). An earlier study by Kharwar *et al.*, (2009) on javanicin (**3.8**) isolated from *Chloridium* sp. (neem fungal endophyte) showed that it was active against human pathogens such as yeast (*Candida albicans*), Gram-positive bacteria (*Bacillus* sp.), Gram-negative bacteria (*E. coli, P. aeruginosa,* and *P. fluorescens*), and against fungal plant pathogens such as *Fusarium oxysporum*, *Rhizoctonia solani*, *Verticillium dahliae* and *Cercospora arachidicola*. A previous study also indicated that solaniol (**3.26**) caused toxicity in male mice (ddyS strain) leading to 'radiomimetic' morphological changes, in which karyorrhexis was observed in the actively dividing cells in the thymus, lymph nodes, spleen, bone marrow, intestine and testes (Ishii *et al.*, 1971). A screen for hepatic glucose production inhibitors in rat hepatoma cells (H4IIE-C3) revealed that javanicin and solaniol, along with other naphthoquinone derivatives inhibited hepatic glucose production. However, after 48 hours of incubation, all the compounds showed cytotoxicity against the hepatic cells (Hashimoto *et al.*, 2009). It is also possible that this system may contribute to anti-trypanosomal activity in which avicequinone C (**1.4**) isolated from *A. lanata* showed potent anti-trypanosomal activity and anti-cancer properties.

6.3   Phenolic compounds

Natural phenolic acids in free or conjugated forms usually appear as esters. From the endophytic fungus *A. aculeatus,* vanillic acid (**4.29**), 3,4-dihydroxyphenylacetic acid (**4.30**), *o*-hydroxyphenylacetic acid (**4.31**), *p*-hydroxyphenylacetic acid (**4.32**) and a new amide derivative 2-(3,4-dihydroxyphenyl)-*N*,*N*-dimethylacetamide (**4.33**) were isolated. Meanwhile, *p*-hydroxyphenethyl alcohol (**5.17**) and *p*-hydroxybenzaldehyde (**5.18**) were isolated from endophytic fungus *L. theobromae*.
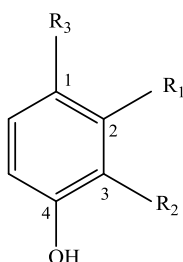
4.29; R_1=H, R_2=OCH$_3$, R_3=COOH
4.30; R_1=H, R_2=OH, R_3= CH$_2$COOH
4.31; R_1=OH, R_2=H, R_3=CH$_2$COOH
4.32; R_1=H, R_2=H, R_3=CH$_2$COOH
5.17; R_1=H, R_2=H, R3=CH$_2$CH$_2$OH
5.18; R_1=H, R_2=H, R_3=CHO
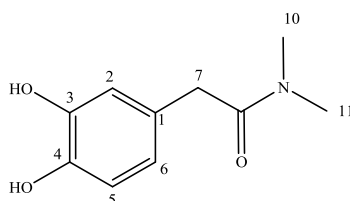
4.33

6.3.1   Biological evaluation phenolic acids

Among the phenylacetic acids, 3,4-dihydroxyphenylacetic acid (**4.30**) and the new amide derivative (**4.33**) exhibited pronounced activity against *T. b. brucei* with MIC values of 1.56 and 3.12 µM, respectively. In contrast, the introduction of nitrogen instead of an oxygen on the aliphatic chain in **4.33** resulted in slightly decreased anti-protozoal activity. Both compounds had an *ortho*-dihydroxyphenyl substituent.

Structure-activity relationship studies on some phenolic acids (Tasdemir *et al.*, 2006) revealed that caffeic (**6.32**) and hydrocaffeic acid (**6.33**) also possessing a similar *ortho*-hydroxyl unit were the most potent growth inhibition against *T. b rhodesiense* with IC_{50} of 6.1 and 6.6 μM, with decreasing cytotoxicity IC_{50} of 94.4 and 93.3 μM, respectively. The same study reported increased trypanocidal activities with catechol (**6.34**), pyrogallol (**6.35**), gallic acid (**6.36**) and 3,4-dihydrobenzoic acid (**6.37**), all having two or three OH groups *ortho*-positioned to each other, exhibiting IC_{50} values ranging from 7.3 to 18.8 μM. Other phenolic acids, such as *o*-hydroxyphenylacetic acid (**4.31**), *p*-hydroxyphenylacetic acid (**4.32**), and *p*-hydroxybenzaldehyde (**5.18**) also showed potent activity with MICs of 6.25 μM. *p*-hydroxyphenethyl alcohol (**5.17**), showed moderate activity with an MIC of 12.50 μM. The introduction of an *ortho*-methoxy instead of a hydroxyl moiety in vanillic acid (**4.29**) decreased the activity to an MIC of 6.25 μM when compared to **4.30**. All tested phenolic compounds showed less cytotoxicity against PNT2A cells.

6.32   6.33   6.34

6.35   6.36   6.37
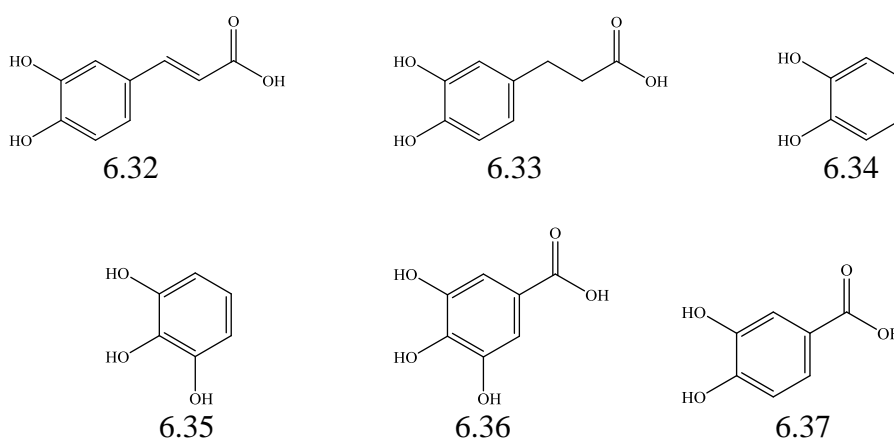
6.3.2   Other biological activities of phenolic acids

Vanillic acid showed potent anti-oxidative effects on tomato germination and growth (Ghareib *et al.*, 2010). Both vanillic acid and *p*-hydroxybenzoic acid displayed weak anti-oxidant activity (Martin *et al.*, 2000). 3,4-dihydrophenylacetic acid produced from human microbial fermentation of tea, citrus and soy showed anti-proliferative activity (Gao *et al.*, 2006). Phenylacetic acid produced from *Bacillus licheniformis* showed anti-microbial activity against *S. aureus, E. coli, C. albicans* (Yoon Kim *et al.*, 2004) and completely inhibited the growth or proliferation of *Phytium ultimum,*

Phytophthora capsici, Rhizoctonia solani, Saccharomyces cerevisiae and *Pseudomonas syringgae* (Hwang *et al.*, 2001). *p*-hydroxyphenethyl alcohol, also known as tyrosol, was reported as a strong phenolic antioxidant substance found in the Mediterranean diet particularly in wine and virgin olive oil (Covas *et al.*, 2003). It also has anti-thrombotic activity (Fragopoulou *et al.*, 2007) and, due to its strong antioxidant properties, it is capable of reducing hypercholesterolemia and hypertriglyceridemia (Gris *et al.*, 2011). Tyrosol isolated from *Neofusicocum parvum* showed moderate phytotoxicity on tomato plants (Evidente *et al.*, 2010). Various synthetic 4-benzaldehyde derivatives, such as *p*-hydroxybenzaldehyde (**5.18**), were reported as potential tyrosinase inhibitors which were found valuable in food industries and skin whitening products. Compound **5.18** was found to occur from natural sources such as higher plants and fungi (Seo *et al.*, 2003).

6.4 Mellein and its derivatives

Four dihydroisocoumarin derivatives were isolated from *L. theobromae*: (-)-mellein (**5.19**), (-)-*trans-axial* and (-)-*cis-equatorial* stereoisomers of 4-hydroxymellein (**5.20** and **5.21**), and (-)-5-hydroxymellein (**5.22**). The difference between these compounds was indicated by the presence of a hydroxyl group at C-4 for *trans-axial* and *cis-equatorial* 4-hydroxymellein and at C-5 for 5-hydroxymellein. The *trans-axial* and *cis-equatorial* stereoisomers of 4-hydroxymellein were identified by the $J_{3,4}$ coupling constants using NMR. The bigger coupling constant, 5.8 Hz, indicated *trans-axial* position, whereas 1.5 Hz denoted the *cis-equatorial* stereoisomer.
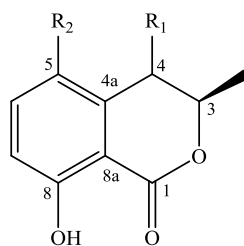
R$_1$=H, R$_2$=H: (-)-mellein
R$_1$=OH, R$_2$=H: *trans-axial*, *cis-equatorial*-4-hydroxymellein
R$_1$=H, R$_2$=OH: (-)-5-hydroxymellein

6.4.1 Biosynthesis of mellein

The proposed biosynthesis of mellein suggests it is derived from a pentaketide intermediate with eight carbon atoms from malonate and two carbon units from acetyl-CoA as illustrated in Figure 6.4. The biosynthesis commences with decarboxylative Claisen condensation of acyl groups to produce a diketide intermediate. The addition of malonyl and subsequent condensation are repeated four times to produce a pentaketide intermediate, consequently, the pentaketide intermediate undergoes aldol cyclization and dehydration, resulting in aromatization whereas the stereospesific cyclization process forms (*R*)-mellein, the most common stereoisomer isolated from natural sources (Sun *et al.*, 2012).
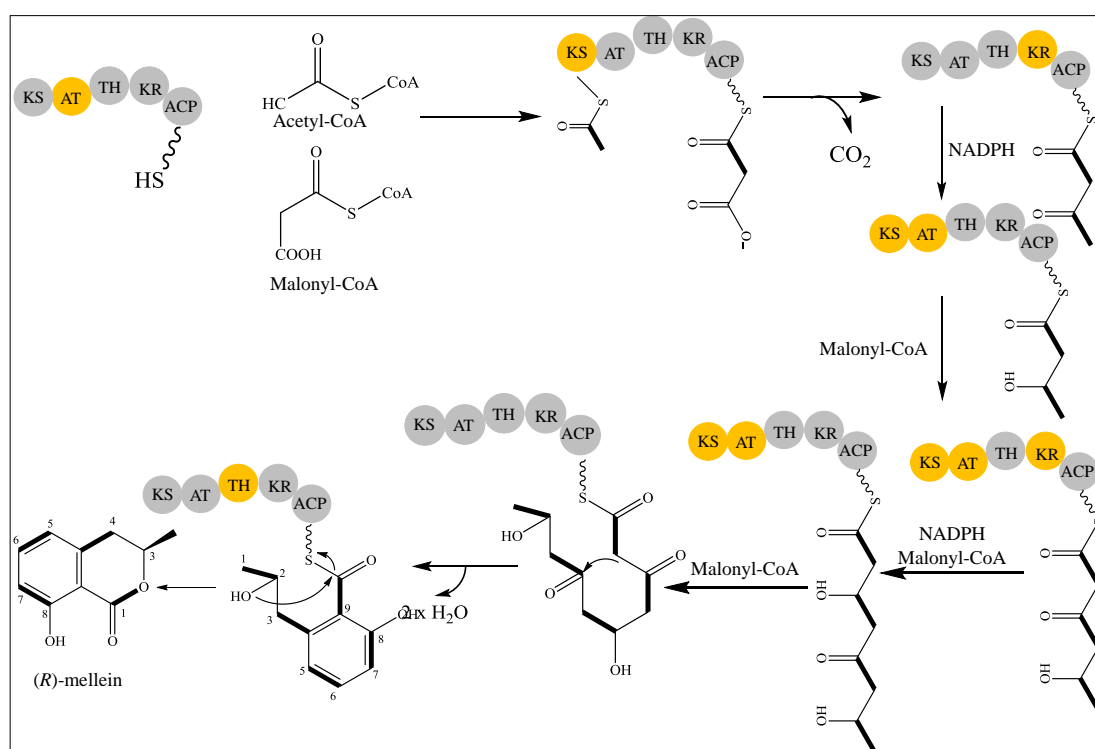
Figure 6.4: Proposed biosynthesis of mellein suggested that the product was derived from an eight carbon pentaketide intermediate from malonic and two carbons from an acetyl-CoA unit (Sun *et al.*, 2012).

6.4.2 Biological evaluation of mellein and its derivatives

Mellein is a dihydroisocoumarin derivative, which was first isolated in 1933 from *Aspergillus mellus* (Nishikawa, 1933). In this study, mellein and its other derivatives were isolated from *L. theobromae*: (-)-mellein, the (-)-*trans-axial*-, (-)-*cis-equatorial*-

forms of 4-hydroxymellein and (-)-5-hydroxymellein. The derivatives exhibited strong anti-trypanosomal activities. Mellein (**5.19**) showed an MIC of 5.8 μM whereas (-)-5-hydroxymellein (**5.22**) showed the most potent activity with an MIC of 2.4 μM. Interestingly, introduction of two hydroxyl moieties on the benzene ring at C-5 and C-8, enhanced the activity against *T. b. brucei*. The *trans-axial* streoisomer with two hydroxyl groups may promote better activity than the *cis-equatorial* stereoisomer, with MICs of 3.2 μM and 8.2 μM, respectively. This suggested that the *trans-equatorial* orientation helped to bind to the correct active sites on the target. Notably, mellein and its derivatives exhibited less toxic against PNT2A cells. Mellein and *cis*-4-hydroxymellein, isolated from *Arthrinium state* of *Apiospora montagnei*, completely killed both male and female adult trematode *Schistosoma mansoni* parasites, *in vitro* at 200 and 50 μg/mL, respectively (Ramos *et al.*, 2013).

Although these compounds have not been tested against trypanosomal protozoa, there are some reports in previous literature of which other coumarins exhibited potent trypanosomal activity against epimastigote and trypomastigote stages of *T. cruzi* (Guinez *et al.*, 2013, Vazquez-Rodriguez *et al.*, 2013, Reyes-Chilpa *et al.*, 2008, Rodriguez *et al.*, 2015). Previous studies also described that coumarins inhibited the enzyme glycosomal glyceraldehyde 3-phosphate dehydrogenase (gGAPDH) presence in *T. cruzi* (Freitas *et al.*, 2009, Souza-Neta *et al.*, 2014, Alvim *et al.*, 2005). The enzyme gGAPDH is an important protein in trypanosomatid glycolytic pathway (Ladame *et al.*, 2003), that can play an essential role in targeting new potential drugs to treat Chagas's disease.

6.4.3   Other biological activities of mellein and its derivatives

Dihydroisocoumarin derivatives also showed other various bioactivities. (-)-mellein displayed strong anti-fungal activities against *Ustilago violacea*, *Mycotypha microspom*, *Eurotium repens,* and *Fusarium oxysporum*; herbicidal activity against *Chiarella fusca* (Schulz *et al.*, 1995), and was found to be toxic against the brine shrimp *A. salina* exhibiting 100% larval mortality after 24 hr incubation (Parisi *et al.*, 1993). Mellein also acts as a pheromone and repellent agent against ants (Blum *et al.*, 1992) and is insecticidal against *Calliphora erytrocephala* (Claydon *et al.*, 1979).

The presence of *R*-(-)-mellein in *Sphaeropsis sapinea* strain isolated from *Pinus radiata* was found to be phytotoxic and anti-fungal (Cabras *et al.*, 2006). Both (+) and (-) enantiomers of 4-hydroxymellein are only active as phytotoxins and anti-fungals when in synergism with each other (Cabras *et al.*, 2006). The (3*R*,4*R*) and (3*R*,4*S*)-4-hydroxymellein were reported to be phytotoxic against grapevine canker (Evidente *et al.*, 2010). 4-hydroxmellein also has been isolated from the fungus *Ascochyta* sp. from the plant *Meliotus dentatus* and showed potential anti-bacterial activity (Krohn *et al.*, 2007). A study on 5-hydroxymellein against chloroquine-resistant *Plasmodium falciparum*, showed potent activity (Jiménez-Romero *et al.*, 2008). Phytotoxins (-)-mellein, (-)-*cis*-4-hydroxymellein, 5-hydroxymellein and tyrosol were isolated from *Botryosphaeria obtusa* (synonym *Physalospora obtusa*), a pathogen responsible for frogeye leaf mark on apple leaves and black rot of apple fruit (Venkatasubbaiah and Chilton, 1990).

6.5   Xanthones

Xanthones are yellow substances that occur as monomers or dimers/heterodimers based on their substitution and the level of oxidation of the xanthone C-ring. Fully aromatic, dihydro-, tetrahydro-, and hexahydro-xanthones occur in fungi, lichens and bacteria (Masters and Bräse, 2012). The monomer of tetrahydroxanthones occur as blennolides/hemisecalonic acids (Zhang *et al.*, 2008), dihydroglobosuxanthone, diversonol/diversonolic esters and globosuxanthone B (Rezanka and Sigler, 2007).
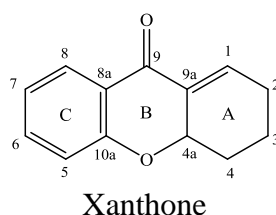
Xanthone

6.5.1   Biosynthesis of xanthone

Xanthone biosynthesis in fungi is generated from structures associated with many phenolic natural products (Birch and Donovan, 1953). Eight acetate units (Figure 6.5) are cyclized to form an anthroquinone followed by oxidative cleavage to form

benzophenone carboxylic ester. The production of xanthone occurs via cyclization directly from a benzophenone intermediate in which the biosynthetic pathways are dependent on the producing organism (pathway 1) or in some cases the fully aromatic species may result by elimination from, or allylic rearrangement of, polyhydrogenated intermediate xanthones in pathway 2 (Krohn *et al.*, 2009). Xanthone dimerisation of phenolic aromatics were found to occur commonly through biaryl linkage either with C–C bond or ether C–O–C linkage (Bringmann *et al.*, 2001), in which dimeric secalonic acids are connected to 2,2 (*ortho−ortho*)-linkage, due to the presence of a free methine at *para*-position to the phenolic moiety (Aberhart *et al.*, 1965). Ergochromes are diastereomeric at positions 6,6', 5,5', 10, and 10'.
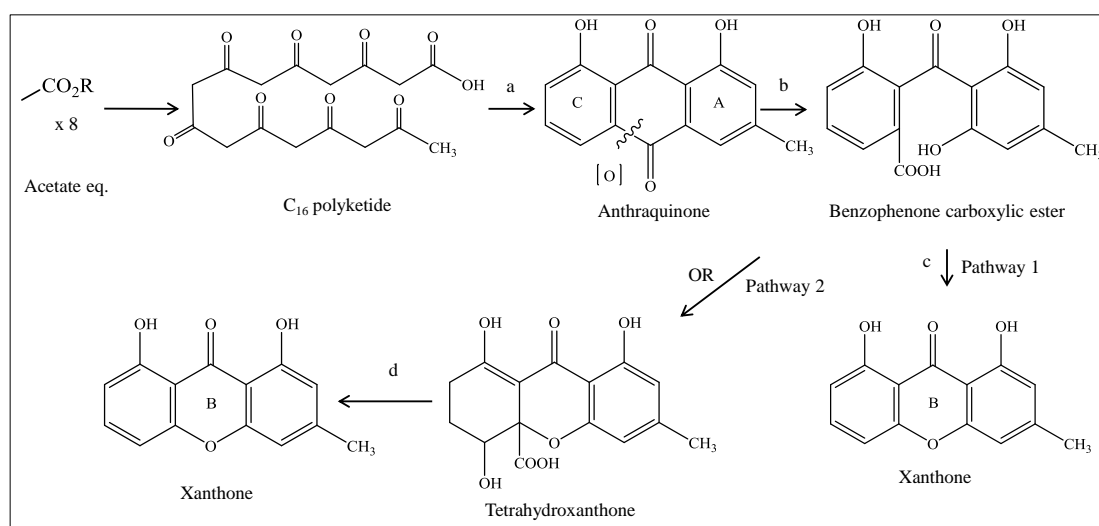
Figure 6.5: Xanthone biosynthesis pathways in fungi
showing a) cyclization; b) oxidative cleavage; c) cyclization; d) elimination or allylic arrangement of polyhydrogenated intermediate xanthones (Krohn *et al.*, 2009).

Aspergillusenone (**4.28**), a new 2,3-ddihydrochromen-4-one derivative, that is a monomer of secalonic acids, was isolated from *A. aculeatus* in this study. Six tetrahydroxanthone monomer derivatives; blennolides A-F, (**6.38-6.43**) (blennolides or hemisecalonic acids) are 2,3-dihydrochroman-4-one derivatives along with a tetrahydroxanthone dimer, secalonic acid B have been isolated from *Blennoria* sp., an endophytic fungus from *Carpobrotus edulis* (Zhang *et al.*, 2008). Zhang and co-workers proposed that the arrangement of the hydroaromatic ring in monomer of

blennolides A and B gave monomers of blennolides D–F. A study on endophytic fungus *Microdiplodia* sp. isolated from the shrub *Lycium intricatum* yielded xanthone derivatives; microdiplodiasone (**6.44**), microdiplodiasolol (**6.45**), diversonol (**6.46**), microdiplodiasol (**6.47**), 1,8-dihydroxy-3-methoxy-6-methylxanthone (**6.48**), and methyl 3,8-dihydroxy-6-methyl-9-oxo-9*H*-xanthene-1-carboxylate (**6.49**) (Siddiqui *et al.*, 2011). A study on the *fungus Chaetomium* sp., isolated from an algal species (taxonomy was not identified) from Greece, gave three heterocyclic-substituted xanthone analogues **6.50-6.52** (Pontius *et al.*, 2008).

4.28

6.38

6.39

6.40

6.41

6.42

6.43

6.44

6.45

6.46; R=CH₃
6.47; R=CH₂OH
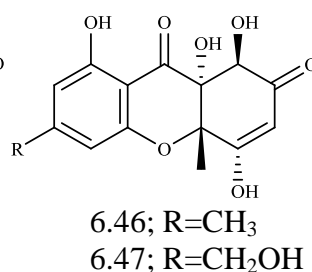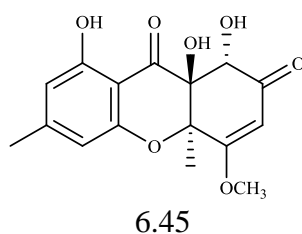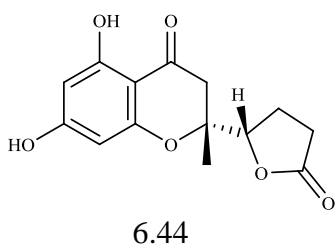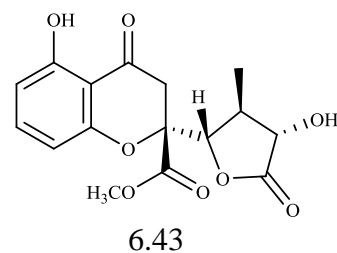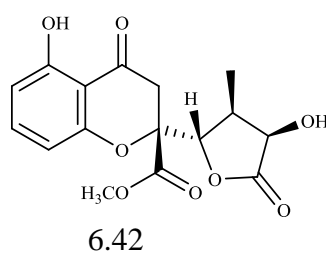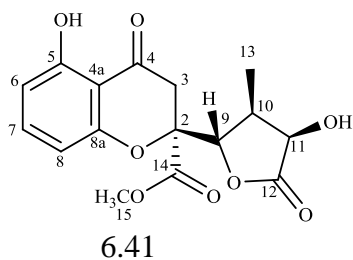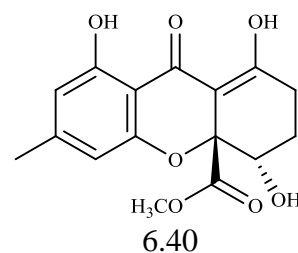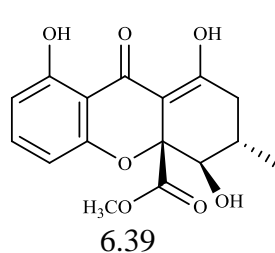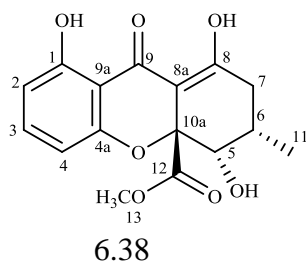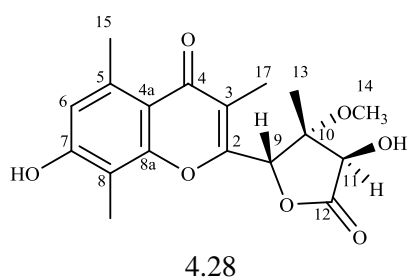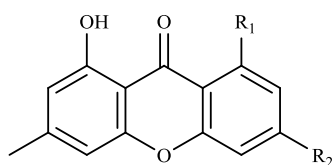
6.48; R₁=OH, R₂=OCH₃
6.49; R₁=COOCH₃, R₂=OH
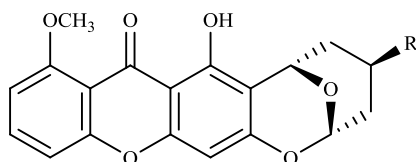
6.50; R=OH
6.51; R=H
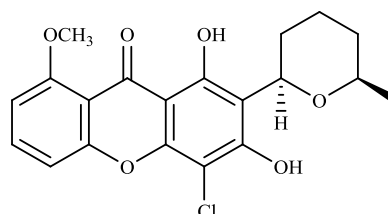
6.52

Secalonic acid A, SAA (**4.20**), is a homodimer ergochrome of two esters with a 2,2'-linkage of the monomeric unit of blennolide B (**6.39**) (Steyn, 1970). SAA is one of an important group of ergochromes, which are highly biologically active yellow mycotoxins produced by different microorganisms. All known ergochromes are dimers of monoxanthones A-F (blennolides or hemisecalonic acids) (Franck, 1980, Kurobane *et al.*, 1978) and the position of methyl and methoxycarbonyl substituents are found to be *trans*-configured (Wezeman *et al.*, 2015). The ergochrome dimers were reported for first time from *Claviceps purpurea* (Kraft, 1906). Secalonic acid A (**4.20**) has been previously isolated from *A. ochraceus* (Yamazaki *et al.*, 1971) and *Paecilomyces* sp. (Zhai *et al.*, 2011).
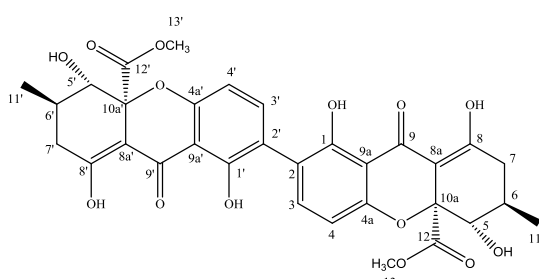
4.20
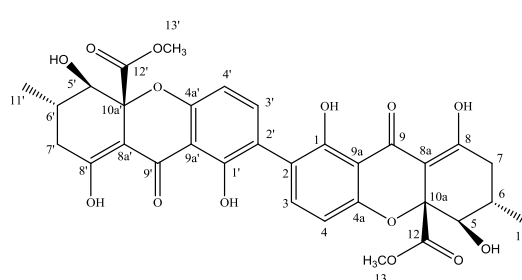
4.34

6.5.2 Biological evaluation of xanthone derivatives

The new monomer, aspergillusenone (**4.28**) and tetrahydroxanthone dimer, secalonic acid A (**4.20**), showed potent activity against *T. b. brucei* with MICs of 1.26 and <0.19 μM respectively, which is almost comparable to the activity shown by

suramin, which has an MIC of 0.11 µM. Both of these compounds possess the α,β-unsaturated carbonyl system that enhanced the anti-trypanosomal activity, in a way which has been discussed earlier (Section 6.2.4 and 6.2.5). Both compounds showed strong cytotoxicity against normal prostate cells. Although this is the first study on both compounds against the protozoa, previous study showed that the heterocyclic-xanthone **6.50,** was potent and selective against *T. b. rhodesiense* with IC_{50} value of 13.3 µM, but slightly active against *T. cruzi* (IC_{50} value of >28 µM) (Pontius *et al.*, 2008). In contrast, the activity of its hydroxyl derivative (**6.51),** against both protozoa were slightly lower than its parent analogue **6.50**, showed IC_{50} values of 25 and 19 µM, respectively. Meanwhile, **6.52** exhibited pronounced activity and was very selective against *T. cruzi* with IC_{50} value of 3.8 µM, demonstrating that the chlorine substituent influenced the increase in bioactivity.

Other than that, studies on xanthone derivatives with a similar backbone to the new derivative aspergillusenone (**4.28**), blennolides D (**6.41)** and E (**6.42**), showed potent anti-algal activity to *Chlorella fusca* and anti-fungal activity to *Microbotryum violaceum,* while **6.44-6.47**, and **6.49,** isolated from the fungus *Microdiplodia* sp. inhibited *Legionella pneumophila* Corby with MIC values of 3.12, 3.59, 3.27, 0.39-0.78, and 3.33 µM respectively (Siddiqui *et al.*, 2011).

Although secalonic acid A (**4.20)** has not been previously tested for anti-trypanosomal activity, SAA was reported to be strong anti-tumor and phlogistic activities (Harada, 1974, Kurobane *et al.*, 1986), anti-neurodegenerative (Zhai *et al.*, 2011) anti-biotic and anti-fungal activities have also been reported (Kurobane *et al.*, 1985). Meanwhile, its enantiomer secalonic acid D, SAD (**4.34**) has been previously isolated from *A. aculeatus* (Andersen *et al.*, 1977, Petersen *et al.*, 2014), *Penicillium oxalicum* (Steyn, 1970, Ciegler *et al.*, 1980), *Paecilomyces* sp. (Guo *et al.*, 2007), the lichen-derived fungus *Gliocladium* sp. T31 (Ren *et al.*, 2006), *Diploicia canescens* (Millot *et al.*, 2009) and *Penicillium chrysogenum* and *P. confertum* (Frisvad *et al.*, 2004). Previous study on SAD which has been isolated from *Gliocladium* sp. T31, showed anti-cancer activity against different tumour cell lines which was indicated by its strong cytotoxicity to K-562 (human chronic myeloid leukaemia), A-549

(human lung epithelia) and P-388 (murine leukaemia) cells at IC_{50} values of 0.03, 0.26, and 5.76 μM, respectively, but very weak cytotoxicity against BEL-7402 (liver adenocarcinoma cell, 15.50 μM) (Ren *et al.*, 2006). A further study on **4.34** showed strong inhibition on DNA topoisomerase I with MIC value of 0.4 μM and IC_{50} at 0.25 μM (Hong, 2011, Guo *et al.*, 2007). Secalonic acid D isolated from the mangrove endophytic fungus ZSU44 showed potent toxicity against HL-60 (human promyelocytic leukaemia cells) and K-562 cells by down regulation of c-Myc with IC_{50} of 0.38 and 0.43 μmol/L, respectively (Jian-ye Zhang *et al.*, 2009) and with KB cells, IC_{50} was less than 1 μg/mL (Guo *et al.*, 2007). In another report, secalonic acid D isolated from *A. aculeatus* showed potent anti-microbial activity to *Bacillus megaterium* (Andersen *et al.*, 1977).

6.6 Structure-activity relationship

Both triterpenes; taraxerol (**1.44**) and taraxerone (**1.45**) from *A. lanata* were inactive against *T. b. brucei* with MICs of 145.30 and 154.20 μM, respectively. β-sitosterol with a saturated side chain (**1.56**), the activity decreased with MIC of 142.30 μM. In contrast, the trypanocidal activity slightly increased (MIC of 126.40 μM) with stigmasterol (**1.47**), possessing an olefinic unit on the aliphatic side chain. Both sterols have been isolated from mangrove plant *A. lanata*. Meanwhile, the presence of endoperoxide in ergosterol (**3.27**) which has been isolated from *Fusarium* sp. and *A. aculeatus* gave notable increased in trypanocidal activity with MIC values of 1.48 and 1.56 μM. Ergosterol plays an important role in cellular membrane of fungi and trypanosomatids in order to sustain their growth and function. Thus, the use of ergosterol-based metabolite is a good strategy, favouring the potential drug for better binding site onto the plasma membrane of the parasite, and disruption of parasite membrane occurs when the endoperoxide moiety generates the free radical without giving any toxicity effect to its host.

The anti-trypanosomal activity exhibited by 1,4-naphthoquinones with naphthazarin related structures were greater than the activity of naphthofuranquinone derivatives. Interestingly, the presence of a quinoid core with an α,β-unsaturated system in

avicequinone C (**1.4**) isolated from *A. lanata* and four naphthazarin derivatives from *Fusarium* sp., enhanced the bioactivity. The trypanocidal activity shown by avicequinone C (**1.4**), increased with an MIC of 3.12 μM, when compared with other naphthofuranquinone derivatives. In contrast, the introduction of two methoxy groups to the quinoid core system of avicenol C (**1.7**), and two hydroxyl units to the new derivative, hydroxyavicenol C (**2.26**) at C-1 and C-4, had decreased the activity with MIC values of 6.25 and 12.50 μM, respectively. However, the ability of a hydroxyl moiety to decrease the bioactivity might slightly be different to the effect of a methoxy group. The addition of a prenyl group at C-2 of glycoquinone (**2.25**) also decreased the activity (MIC of 12.50 μM). The new glycosemiquinone derivative (**2.27**) with a ketone at C-1 and a hydroxyl at C-4 showed the same activity as the parent analogue. The loss of one carbon in naphthofuranquinones produced avicennpentenone carboxylate, (**2.28**) and the activity against the protozoa was as potent as hydroxyavicenol C (MIC = 6.25 μM). The naphthazarin derivatives exhibited the most pronounced activity against *T. b. brucei*, four of them having a similar quinoid structure with an α,β-unsaturated system in avicequinone C (**1.4**), hydroxylation at C-5 and C-8 on the benzene ring and the presence of different substituted functional groups such as pyran, ketone or alcohol onto the side chains, gave different potencies against *T. b. brucei*. The presence of a free hydroxyl group on the side chain of solaniol (**3.26**) gave better anti-trypanosomal activity, but also higher cytotoxicity. However, the introduction of a ketone and a pyran moiety on the side chain in javanicin (**3.8**) and anhydrofusarubin (**3.28**), respectively, decreased their trypanocidal activity when compared to solaniol, with MIC values of 0.60 and 1.20 μM. Dihydrojavanicin (**3.29**) was derived from a javanicin skeleton (**3.8**), with a difference in positions of the carbonyl and hydroxyl substituents, gave slightly lower activity than **3.8** with MIC of 1.90 μM and greater cytotoxicity. Comparison between the naphthofuranquinone and the naphthazarin derivatives, suggested that the quinoid with an α,β-unsaturated system on the core of 1,4-naphthoquinone and the presence of hydroxyls on the benzene ring, as well as the substitution on the side chain were able to enhance the anti-trypanocidal activity. Indeed, the substituents on the naphthazarin derivatives interfered in the redox potential of the quinoid ring thus giving slightly different trypanocidal potencies. Although solaniol (**3.26**) and

dihydrojavanicin (**3.29**) showed greater cytotoxicity compared to other naphthazarin derivatives and naphthofuranquinones, the MIC values of these two compounds against *T. b. brucei* were less than the concentration used in initial screening (at 100 µg/mL). Therefore, both **3.26** and **3.29** still could serve as lead drugs for trypanosomiasis.

The trypanocidal activity displayed by 3,4-dihydroxyphenylacetic acid (**4.30**), with a *ortho*-dihydroxyphenyl moiety gave a potent activity against *T. b. brucei* with MIC of 1.56 µM. In contrast, the introduction of a nitrogen atom as in the new amide derivative (**4.33**) and an *ortho*-methoxy moiety in vanillic acid (**4.29**) decreased the anti-protozoal activity with MIC values of 3.12 and 6.25 µM, respectively. Other phenolic acids, *o*-hydroxyphenylacetic acid (**4.31**), and *p*-hydroxyphenylacetic acid (**4.32**), as well as *p*-hydroxybenzaldehyde (**5.18**) also showed potent activity with MICs of 6.25 µM. Meanwhile, *p*-hydroxyphenethyl alcohol (**5.17**) showed a moderate activity with an MIC of 12.50 µM. All phenolic compounds were less toxic against PNT2A cells.

Among dihydroisocoumarins, 5-hydroxymellein (**5.22**) with two hydroxyl units on the benzene ring at C-5 and C-8 showed the most potent activity against *T. b. brucei* (MIC of 2.40 µM). *Trans-axial*-4-hydroxymellein (**5.20**) had a higher potency than its isomer, *cis-equatorial*-4-hydroxymellein (**5.21**) with MIC values of 3.20 and 8.20 µM, respectively. Mellein (**5.19**) possesses only one hydroxyl moiety and was less active than other dihydroisocoumarins with MIC of 5.80 µM. Mellein and its derivatives also showed weak effects on the normal prostatic epithelial cells (PNT2A). Finally, the new monomer, aspergillusenone (**4.28**) also had a potent activity (MIC of 1.26 µM). The tetrahydroxanthone dimer, secalonic acid A (**4.20**) exhibited the most potent anti-protozoal activity with MIC value less than 0.19 µM which is almost comparable to suramin (MIC of 0.11 µM). Both compounds had an α,β-unsaturated carbonyl system, that subsequently generates free radical thus enhancing the anti-trypanosomal activity, but also toxic to normal cell. As mentioned earlier, their MIC values were lesser than cytotoxicity against PNT2A, thus these compounds might give lower toxicity effects when testing at lower concentration.

7.   Materials and Methods

7.1   Isolation of secondary metabolites from *Avicennia lanata*

7.1.1   Plant materials

The stems of *Avicennia lanata* were collected from Setiu Wetlands, Terengganu, Malaysia with the help of Haji Muhamad Razali Salam. The specimen was deposited in the Universiti Malaysia Terengganu herbarium with the voucher specimen code UMT-01.

7.1.2   Extraction, fractionation and isolation of metabolites from *A. lanata*

The dried powdered stem (4 kg) of *A. lanata* was macerated in methanol overnight (8L/extraction, 3x,) and the methanol extract was concentrated under vacuum using a rotary evaporator (Büchi, Switzerland) to give 44.8160 g. The methanol extract was partitioned by liquid-liquid extraction (90%H_2O + 10%MeOH: EtOAc, 1:1, 3x) and concentrated using a rotary evaporator to give a crude ethyl acetate extract weighing 14.4115 g. Thin layer chromatography (TLC) analysis was carried on *A. lanata* crude extract. The total *A. lanata* crude extract was fractionated by using medium pressure liquid chromatography (Büchi, Switzerland) with gradient elution using hexane-ethyl acetate-methanol yielding 25 fractions. Each sub-fraction was concentrated using a vacuum rotary evaporator and TLC was carried out to monitor the separation and sub-fractions with the similar profile were pooled together to give nine major fractions. Further purification of fraction F3 gave four compounds, which were taraxerol (F3-17 (**1.44**), 124.0 mg, 0.84%), taraxerone (F3-13 (**1.45**), 148.8 mg, 1.03%), stigmasterol (F3-19 (**1.47**), 108.9 mg, 0.76%) and β-sitosterol (F3-22, (**1.56**), 32.0 mg, 0.22%). Fraction F5 was purified using open column chromatography followed by flash chromatography (Biotage Isolera, Sweden), yielding also three pure compounds: avicenol C (F5-2-3 (**1.7**), 20.7 mg, 0.14%), avicequinone C (F5-2-6 (**1.4**), 5.7 mg, 0.04%) and glycoquinone (F5-2-9 (**2.25**), 25.7 mg, 0.18%). Further purification of fraction F6 using flash chromatography (Biotage Isolera, Sweden and Grace Reveleris, USA) afforded a new derivative hydroxyavicenol C (F6-8 (**2.26**), 6.5 mg, 0.05%), and   further fractionation of F7 by preparative thin layer

chromatography resulted in two new derivatives, glycosemiquinone (F7-5-2 (**2.27**), 6.0 mg, 0.04%) and avicennpentenone carboxylate (F7-5-1 (**2.28**), 6.7 mg, 0.05%).

7.2   Isolation and identification of pure fungal strain from *A. lanata*
7.2.1   Chemicals and reagents
(a)   Chemicals for culture media

Agar	Oxoid, UK
Chloramphenicol	Acros Organics, Belgium
Glucose	Alfa Aesar, UK
Malt extract	Oxoid, UK
Peptone	Fisher, UK
Rice (long grain)	various brand, Glasgow, UK
Yeast extract	Oxoid, UK
Sodium hydroxide (NaOH)	Merck KGaA, Germany
Hydrochloric acid (HCl)	Fischer Chemical, UK

(b)   Chemicals for DNA extraction and PCR amplification

Extraction and Dilution solution	Sigma-Aldrich, UK
Forward primer (ITS1)	Life Technologies, UK
Reverse primer (ITS4)	Life Technologies, UK
REDExtract-N-Amp PCR ReadyMix	Sigma-Aldrich, UK

(c)   Chemicals for agarose gel electrophoresis

Agarose	Sigma-Aldrich, UK
Ethidium bromide	Sigma-Aldrich, UK
Tris/Borate/EDTA (TBE) buffer	Sigma-Aldrich, UK
Hypper ladder II	Sigma-Aldrich, UK

(d)   Chemicals for extraction of PCR products

GenElute Gel Extraction Kit	Sigma-Aldrich, UK

7.2.2 Equipment

Microbiology safety laminar hood (BioMAT^2)   Medical Air Technology, UK

Incubator   Vindon Scientific Ltd., UK

Thermal cycler   Perkin Elmer, USA

Nitrogen gas cylinder (BOC UNI066)   University of Strathclyde

Disposable scalpels sterile   Swann-Morton, UK

pH meter (Jenway 3020)   Keison, UK

Isopropanol (to prep. 70% isopropanol solution)   Sigma-Aldrich, UK

Disinfectant spray   Reckitt-Beckinser, Germany

7.2.3 Fungal materials

Fresh parts of the mangrove plant *A. lanata* which included the stems, leaf, bark, and root (10 cm each) were collected from Setiu Wetlands, Terengganu, Malaysia. The respective plant parts were packed and kept in a cold box and transferred to the University of Strathclyde. Upon arrival, the materials were washed under running tap water for a few minutes and cut into 2 cm x 2 cm segments. The plant tissue was immersed with 70% isopropanol in order to surface sterilize the exposed external tissue and was rinsed with sterilized distilled water. The plant parts were dissected to retrieve thin slices of the inner tissue parts which were laid onto a malt nutrient agar (MA). Duplicate plates were prepared. Control malt nutrient agar plate was also prepared as a blank and left opened under microbiological safety cabinet BioMAT^2 (Medical Air Technology, UK) during the seeding process. The plates were incubated at 27 $\pm$ 2 °C (Vindon Scientific Ltd., UK) for 7-15 days. All morphologically different colonies were observed and isolated based on the colour of the colony, shape or texture of the mycelial pellicle. A 5 mm x 5 mm diameter plug was cut from the edge of the colony and placed in the middle of a new malt agar plate to establish a pure colony. The plates were incubated again for 7-15 days. The purity of the single strain was verified by visual examination. When colonies were not pure, the isolation step was repeated until a pure colony was achieved. Pure strains were re-inoculated and incubated for further taxonomical characterization by molecular biological methods.

7.2.4 Composition of media

(a)   Composition of malt agar (MA) medium

MA medium was used for fungal inoculation.

Agar	20.0 g
Malt extract	15.0 g
Distilled water	to 1000 mL
pH	7.4 - 7.8 (adjusted with 10% NaOH or 36.5% HCl)

Chloramphenicol (0.2 g) was added to the medium to suppress bacterial growth.

(b)   Composition of rice medium for solid cultures

Rice	100 g
Distilled water	100 mL

Water was added to the rice and kept overnight before autoclaved.

(c)   Composition of Wickerham medium for liquid cultures (1000 mL)

Yeast extract	3.0 g
Malt extract	3.0 g
Peptone	5.0 g
Glucose	10.0 g
Distilled water	to 1000 mL
pH	7.2 - 7.4 (adjusted with 10% NaOH or 36.5% HCl)

7.3   Identification of fungal strains

Four pure fungal strains were successfully isolated from the mangrove *A. lanata* and were identified by DNA extraction, PCR amplification and sequencing by using polymerase chain reaction (PCR) with a universal ITS primers (Supporting Information; GenBank GQ856236 and GQ856237, respectively). The voucher specimens of all strains were deposited at the Natural Product Metabolomics Laboratory (SIPBS, University of Strathclyde). Three strains were chosen for further screening and were optimized to produce bioactive metabolites using different media. The chemical profile at different growth phases was analysed.

7.3.1 DNA extraction

A small cube (1 cm x 1 cm) of active growing mycelium of each fungus was excised and transferred into a 2 mL of Eppendorf tube using a sterile scalpel. 100 μL of extraction solution (Sigma-Aldrich, UK) was subsequently added to the Eppendorf tube and briefly vortexed. The disk was thoroughly covered with the extraction solution. The sample was incubated at 95 °C for 10 mins. At this stage, the fungal tissues usually do not appear to be degraded after this treatment. Then, 100 μL of Dilution solution (Sigma-Aldrich, UK) was added to equal volumes of the extraction solution and vortexed to mix. The dissolved sample was stored at 2-8 °C for PCR procedure. All steps for DNA extraction were carried out at room temperature.

7.3.2 DNA amplification

The DNA extract was amplified by polymerase chain reaction (PCR) with a universal ITS primers. ITS1 (TCCGTAGGTGAACCTGCGG) was used as a forward primer and ITS4 (TCCTCCGCTTATTGATATGC) as the reverse primer (Life Technologies, UK). PCR was carried out by using REDExtract-N-Amp PCR ReadyMix (Sigma-Aldrich, UK). The following reagents were added into a thin-walled PCR micro-centrifuge tube (the reagent should be prepared for the samples and a blank): 25 μL of REDExtract-N-Amp PCR ReadyMix, 18 μL of RNA-free water, 3 μL of ITS 1 and ITS 4 primers and 4 μL of fungal DNA with a total volume 53 μL (the PCR reagents for one sample). The components were mixed gently and centrifuged and the supernatant was collected. The supernatant was applied to the thermal cycler (Perkin Elmer, USA) using Genofun/Gfun TD1 PCR cycle as in Table 7.1.

Table 7.1: PCR cycle step using thermal cycler			
Steps	**Temperature (°C)**	**Time (mins)**	**Cycles**
Initial denaturation	95	15	1
Denaturation	95	1	35
Annealing	56	0.5	35
Extension	72	1	35
Final Extension	72	10	1
Hold	4	Indefinitely	

7.3.3 Purification of PCR products by gel electrophoresis

The PCR-amplified DNA was purified on 1% agarose gel using gel electrophoresis at 60 V for 45 minutes in Tris/Borate/EDTA (TBE) buffer. 0.5 g of agarose was added into 50 mL of TBE solution into a 100-mL wide neck Duran bottle then weighted and tared. The mixture was heated in the microwave for 1 min 30 sec, then again weighed (the value should be negative). Later, water was added until the reading was zero. Under a fume cupboard, 2 μL of 1% ethidium bromide solution was added as a staining agent. The solution was immediately poured into a gel electrophoresis plate in which a cellulose barrier was attached inside at the bottom of the plate and left for 15 mins until it solidified. The TBE buffer was added into the plate before the barrier was removed as to avoid any formation of air bubbles. The TBE buffer was added until the edge top of the plate. 15 μL of PCR-amplified DNA products were pipetted carefully into the well. The 6 μL DNA ladder was pipetted into the other well as reference. Before the run, every button was switch off and the voltage must be at minimum level, to ensure there is no electricity flowing. At t=0, the voltage was turned down to 150 V and the voltage was increased to 60 V as the gel plate was allowed to run for 45 mins. The stained DNA fragment was observed under UV camera then carefully sliced from the agarose gel plate and transferred into an Eppendorf tube.

7.3.4 Extraction of PCR products from agarose gel and DNA sequencing

The PCR-amplified DNA was purified using GenElute Gel Extraction Kit (Sigma-Aldrich, UK) which consisted of a column preparation solution, Gel Solubilisation solution, Wash solution concentrate G, Elution solution (10 mM Tris-HCl, pH 9.0), GenElute binding column G and collection tubes. The sliced gel was mixed with the Gel Solubilisation solution, incubated at 50-60^{0}C for 10 min and vortexed for 2-3 minutes. The mixture was mixed with isopropanol and then centrifuged. The solubilised gel solution mixture was loaded into the binding column and centrifuged for 1 min. The flow-through liquid was discarded. 700 μL of Wash solution was added into the binding column and centrifuged for 1 min. The Wash solution was removed from the column. 700 μL Elution solutions was added into the binding column in which the PCR product was incorporated and incubated for 1 min at 37 °C

in order to elute the product. The binding column was then centrifuged and the flow-through liquid was collected in which the PCR product had dissolved in the elution solution. The sequence analysis of the amplicons was submitted to Dr. Rothwelle Tate and the base sequence was performed by available online databases GenBank with the help of the Basic Local Alignment Search Tool (BLAST) on the webpage (http://blast.ncbi.nlm.nih.gov/Blast.cgi) using 'BLASTN' option with comparison with the National Centre for Biotechnology Information (NCBI) database's best hit (Sayers *et al.*, 2010) to confirm the identities of the selected strains. All fungal sequences were at least 98% identical to the best hit in the NCBI database (Taylor and Houston, 2011). The identified fungi with accession data was presented in Table 7.2.

Table 7.2: Identification of isolated fungi using GenBank

No. of samples	Sample ID	Fungal strains	Accession Data
1	FTGLFB 2	*Aspergillus aculeatus*	HE578070
2	FTGWD	*Lasiodiplodia theobromae*	KC960898
3	FTGRT 612	*Fusarium* sp.	FJ487927

7.3.4.1 *Aspergillus aculeatus* (FTGLFB 2)

The fungus was aseptically isolated from the leaf of *Avicennia lanata*. The strain was cultivated on malt agar (MA) media. According to (Hawksworth, 1991) *Aspergillus aculeatus* is classified as follow:

Phylum:	Ascomycota
Class:	Eurotiomycetes
Order:	Eurotiales
Family:	Trichocomaceae
Genus:	*Aspergillus*
Species:	*Aspergillus aculeatus*
Morphology:	Greenish black-spored

7.3.4.2 *Lasiodiplodia theobromae* (FTGWD)

The fungus was isolated from the twig of *A. lanata*. Taxonomy of *L. theobromae* is described below (Hawksworth, 1991). Stromata are black and the fungus still was in vegetative status.

245

Phylum: Ascomycota
Class: Dothideomycetes
Order: Botryosphaeriales
Family: Botryosphaeriaceae
Genus: *Lasiodiplodia*
Species: *Lasiodiplodia theobromae*
Morphology: Black stromata, vegetative

7.3.4.3 *Fusarium* sp. (FTGRT 612)

The fungus was isolated from root of *A. lanata*. Taxonomy of *Fusarium* sp. is described below (Hawksworth, 1991). Stromata are white and the fungus still was in vegetative status.

Phylum: Ascomycota
Class: Sordariomycetes
Order: Hypocreales
Family: Hypocreaceae
Genus: *Fusarium*
Species: *Fusarium* sp.
Morphology: White stromata, vegetative

7.4   Fungal cultivation for preliminary screening

7.4.1   Materials and equipment

IKA RW16 basic overhead stirrer   Werker Staufen, Germany

IKA T18 basic Ultra-Turrax   Werker Staufen, Germany

Cotton wool (non-absorbent)   Fischer Scientific, UK

Filter paper Fisherbrand (QL100, 110 mm)   Fischer Scientific, UK

7.4.2   Rice fermentation

The pure strains were inoculated on malt agar plates and incubated at 27 ℃ for 7-15 days. Malt agar blocks (0.5 cm x 0.5 cm) of actively growing culture of pure strains were placed on sterilized rice medium (50 g of rice + 50 mL of filtered water) and cultivated for 7, 15 and 30 days representing the different growth phases. Fermentation was stopped at the respective days by covering the culture with 100 mL of ethyl acetate and left overnight.

7.4.3   Liquid fermentation

The pure strains were inoculated on malt agar plates and incubated at 27 ºC for 7-10 days. The pure strain was cultivated on Wickerham medium (Chapter 7.2.4) and processed as was done for the rice culture media.

7.5   Extraction of metabolites from small and large scales fungal cultures
7.5.1   Extraction of metabolites from fungal grown on solid rice medium

The metabolites produced from the rice media on 7, 15 and 30 days were extracted with 100 mL of ethyl acetate, homogenized using IKA RW16 basic overhead stirrer (Werker Staufen, Germany) and filtered through a non-absorbent cotton wool (Fischer Scientific, UK). The filtrate was concentrated under a rotary vacuum evaporator (Büchi, Switzerland). The filtered mycelial was further extracted two times with ethyl acetate and pooled together with the initial filtrate then concentrated under vacuo to yield the total crude extract. In order to get rid of the excess amount of fats and oils from the crude extract, the extract was dissolved in (90%MeOH +10%H_2O) and partitioned by liquid-liquid extraction between (1:1, 90%MeOH +10%H_2O : hexane, 3x) which later was concentrated using a rotary evaporator to give the crude extract RC7, RC15, RC30.

7.5.2   Extraction of metabolites from fungal grown in liquid Wickerham

The metabolites from the liquid Wickerham medium cultivated on 7, 15 and 30 days were homogenized using IKA T18 basic Ultra-Turrax homogenizer (Werker Staufen, Germany), and filtered through a non-absorbent cotton wool (Fischer Scientific, UK). The residue was extracted with equal volumes of ethyl acetate, 3x and partitioned by liquid-liquid partitioning. The organic phase was concentrated under vacuo using a rotary evaporator (Büchi, Switzerland) to give the crude extract LC7, LC15, LC30.

7.6   Dereplication studies by using HRESI-LCMS

The dereplication study on the total crude extract and fractions of the samples were performed using HRESI-LCMS, and then processed with the MZmine software, an *in-house* macro coupled with the Dictionary of Natural Products (DNP) 2012 and AntiMarin 2012, a combination of Antibase and MarinLit, and SIMCA P+ 13 (Umetrics AB, Umeå, Sweden). The procedure and program for HRESI-LCMS was set up as described below.

The total crude extract of 1 mg/mL in methanol was analysed on an Accela HPLC (Thermo Scientific, UK) coupled with a UV detector at 280 and 360 nm and an Exactive-Orbitrap high-resolution mass spectrometer (Thermo Scientific, UK). A methanol blank was also analyzed. The column attached to the HPLC was a HiChrom, ACE (Berkshire, UK) C_{18}, 75 mm × 3.0 mm, 5 μm column. The mobile phase consisted of micropore water (A) and acetonitrile (B) with 0.1 % formic acid for each solvent. The gradient program started with 10 % B linearly increased to 100 % B within 30 mins at a flow rate of 300 μL/min and remained isocratic for 5 min before linearly decreasing back to 10 % B in 1 min. The column was then re-equilibrated with 10% B for 9 min before the next injection. The total analysis time for each sample was 45 mins. The injection volume was 10 μL and the tray temperature was maintained at 12 $^{\circ}$C. High-resolution mass spectrometry was carried out in both positive and negative ESI ionization switch modes with a spray voltage of 4.5 kV and capillary temperature at 320 $^{\circ}$C. The mass range was set from *m/z* 150-1500 for ESI-MS range.

The mass spectral data was processed using the procedure by Macintyre *et al.*, (2014) which was established in the Natural Products Metabolomics Group Laboratory at SIPBS as described here. The LC-MS chromatograms and spectra were viewed using Thermo Xcalibur 2.1 or MZmine 2.10. Raw data were initially sliced into negative and positive data sets using the MassConvert software package from ProteoWizard (pwiz). The sliced data sets were subsequently exported into MZmine 2.10. The spectra were crop-filtered from 4 to 40 mins. The peaks in the samples and solvent

and media blanks (where applicable) were detected using the chromatogram builder. Mass ion peaks were isolated using a centroid detector threshold that is greater than the noise level set at 1.0E4 using an MS level of 1. The chromatogram builder was used with a minimum time span set at 0.2 min, and the minimum height and m/z tolerance at 1.0E4 and 0.001 m/z or 5.0 ppm, respectively. Chromatogram deconvolution was then performed to detect the individual peaks. The local minimum search algorithm (chromatographic threshold: 90 %, search minimum in RT range: 0.4 min, minimum relative height: 5 %, minimum absolute height: 3.0E4, minimum ratio of peak top/edge: 2, and peak duration range: 0.3-5 min) was applied. Isotopes were also identified using the isotopic peaks grouper (m/z tolerance: 0.001 m/z or 5.0 ppm, retention time tolerance: 0.2 absolute (min), maximum charge: 2, and representative isotope: most intense). The retention time normalizer (m/z tolerance: 0.001 m/z or 5.0 ppm, retention time tolerance: 5.0 absolute (min), and minimum standard intensity: 5.0E3) was used to reduce inter-batch variation. The peak lists were all aligned using the join aligner parameters set at m/z tolerance: 0.001 m/z or 5.0 ppm, weight for m/z: 20, retention time tolerance: 5.0 relative (%), weight for RT: 20. Missing peaks were detected using the gap-filling peak finder (intensity tolerance: 1.0 %, m/z tolerance: 0.001 m/z or 5.0 ppm, and retention time tolerance of 0.5 absolute (min). An adduct search was performed for both negative and positive mode. For ESI negative mode, the adducts searched for were formate and ACN-H (RT tolerance: 0.2 absolute (min), m/z tolerance: 0.001 m/z or 5.0 ppm, max relative adduct peak height: 30 %). A complex search was also performed with ionization method [M-H]$^-$. For ESI positive mode, adducts searched for were Na+H, K+H, NH_4 and ACN+H. A complex search was performed with ionization method [M+H]$^+$, retention time tolerance: 0.2 absolute (min), m/z tolerance: 0.001 m/z or 5.0 ppm, and with maximum complex peak height of 50 %. The processed data set was then subjected to molecular formula prediction and peak identification. The data sets were exported to csv (comma delimited) to be imported to the *in-house* macro workstation. By using the macro, both the negative and positive data sets were imported for preparation followed by the removal of all media blanks and the samples. The macro combined all processed data from different media and samples and then prepared final data set for SIMCA P+ 13.0.2 followed by the dereplication

step using the Antimarin database. The combined data set was imported into SIMCA P+ 13.0.2 for multivariate analysis. Pareto scaling was applied. PCA and supervised OPLS-DA were used compare the metabolic profiles of different samples and to evaluate their unique secondary metabolites.

7.7   Bioassays

The MIC values of the isolated compounds against *T. b. brucei* were determined by averaging the results of two independent assays. The concentrations at which cell viability became less than 10% were averaged and converted to μM. MIC assays were performed by testing various concentrations of the compounds (μg/mL) against the test organism, only for the samples having >90% inhibition in initial screening (at concentration of 20 μM). Meanwhile, the initial screening for cytotoxicity activity of the isolated compounds was carried out against human normal prostatic epithelial cells (PNT2A) at 100 μg/mL. The % D of control was determined by averaging the results of three independent assays. In initial screening, if the cell viability is less than 60%, concentration response tests at 300-0.3 μg/mL will be proceded. IC_{50} values of the tested compounds were determined using Graph pad prism software and converted to μM.

7.7.1   Anti-trypanosomal assay

The activity of the plant and fungal extracts along with its pure compounds were tested *in vitro* against the blood stream form of *Trypanosomal brucei brucei* (*T. b. brucei*) S427. All the tests were done by Mrs. Carol Clements in Strathclyde Innovations in Drug Research (SIDR), University of Strathclyde. The activity of the samples was determined using the well-established Alamar blue™ 96-well microplate assay, in which the screening procedure was modified from the microplate Alamar blue assay (Räz *et al.*, 1997), to determine drug sensitivity of African trypanosomes. The samples were initially screened at one concentration (20 μg/mL crude extracts or fractions, 20 μM for pure compounds) to determine their *in vitro* activity. Stock solutions of tested samples in DMSO (Fischer Scientific, UK) were prepared at concentrations of 10 mg/mL (extracts) or 10 mM for pure

compounds. The concentration of DMSO should not exceed 0.5% of the final test solution. The 10 mg/mL stock solutions of the samples were diluted 1 in 10 with HMI-9 and 4 µL was pipetted into 96 µL HMI-9 in the 96-well plate. Sterility and DMSO control samples were placed in column 1 of the 96-well plates, test samples in columns 2 to 11 and a concentration range of suramin as a positive control in column 12. Trypanosomes were counted using a haemocytometer and diluted to a concentration of 3.0×10^4 trypanosomes per mL, and 100 µL of this suspension was added to each well of the assay plate with the exception of A1 well which contained the sterility control. The assay plate was incubated at 37ºC, 5% CO_2 under humidified atmosphere for 48 hours. Later, 20 µL of Alamar blue was added and further incubated for 24 hours. Fluorescence was then determined using the Wallac Victor 2 microplate reader (Perkin Elmer, Cambridge, UK) (excitation: 530 nm, emission: 590 nm). The results were calculated as % of the DMSO control values.

Minimum inhibitory concentration values (MIC) were determined for pure compounds with less than 10% growth compared to the control values. MIC determinations were carried out in duplicate. Test solutions at 200 µg/mL were prepared in column 2 by pipetting 4µL of 10 mg/mL test stock solution and 196 µL of HMI-9 medium into each well. 100 µL of HMI-9 medium was pipetted into columns 1 and 3 to 12, and serial 1:1 dilutions are carried out using a multi-channel pipette from columns 2 to 11. 20 µl of x 10 concentration of suramin was added to column 12 (different concentrations, ranging from 0.008 to 1.0 µM). An inoculum of 100 µL of trypanosomes at a concentration of 3.0×10^4 per mL was added to each well except A1, and the procedure continued as previously described (Räz *et al.*, 1997) The MIC values were determined as the concentration calculated to have less than 5% of control values.

Final assay concentrations in µg/mL   +ve control

	1	**2**	**3**	**4**	**5**	**6**	**7**	**8**	**9**	**10**	**11**	**12**
A	control	100	50	25	12.5	6.25	3.1	1.55	0.78	0.34	0.17	1.0µM suramin
B	control	100	50	25	12.5	6.25	3.1	1.55	0.78	0.34	0.17	0.5µM suramin
C	control	100	50	25	12.5	6.25	3.1	1.55	0.78	0.34	0.17	0.25µM suramin
D	control	100	50	25	12.5	6.25	3.1	1.55	0.78	0.34	0.17	0.125µM suramin
E	control	100	50	25	12.5	6.25	3.1	1.55	0.78	0.34	0.17	0.062µM suramin
F	control	100	50	25	12.5	6.25	3.1	1.55	0.78	0.34	0.17	0.031µM suramin
G	control	100	50	25	12.5	6.25	3.1	1.55	0.78	0.34	0.17	0.015µM suramin
H	control	equivalent solvent control e.g. DMSO										0.008µM suramin

Figure 7.1: The template map for the 96-well plate
used in anti-trypanosomal activity

7.7.2 Cytotoxicity assay

The pure compounds from mangrove plant *A. lanata* and its endophytic fungi were tested for cytotoxicity *in vitro* against human normal prostatic epithelial cell line (PNT2A) derived from ECACC (Sigma-Aldrich, Dorset, UK). All the tests were done by Mr. Yahia Tabaza and Miss Yusnaini Md. Yusoff in Strathclyde Institute of Pharmacy and Biomedical Sciences (SIPBS), University of Strathclyde.

The cytotoxicity activity of the pure compounds was determined using the well-established Alamar Blue™ redox-based 96-well microplate assay, in which the screening procedure was modified from O'Brien *et al.*, (2000). PNT2A cells were seeded into 96-well microplate assay at density of 0.5 x 10^4 cells/well in 100 µL Dulbecco's modified Eagle's medium (DMEM; Invitrogen, Paisley, UK) and

incubated at 37 ℃, 5% CO_2 with a humidified atmosphere for 24 hours. The tested compound was prepared at desired concentrations in DMEM solutions, while DMSO and Triton X as a negative and positive controls, respectively, were added into the microplate to give a total volume of 200 μL. The microplate plate was incubated at 37 ℃, 5% CO_2 with a humidified atmosphere for 24 hours, then 10 μL of Alamar blue was added. The microplate was further incubated for another 20 hours, then the fluorescence was measured using a Wallac Victor 2 microplate reader (Perkin Elmer, Cambridge, UK) (excitation: 530 nm, emission 590 nm). The results were calculated as % of the DMSO control values. Concentration response tests (300 to 0.3 μg/ml) were then proceeded (in triplicate) for samples with less than 60% of control values in the initial screen. IC_{50} values of the tested compounds were determined using Graph pad prism software.

7.8 General experimental procedures for fractionation and isolation

7.8.1 Chemical and reagents

Acetone	Sigma-Aldrich, Germany
	Fischer Chemical, UK
Acetonitrile	VWR Chemical, CE
Dichloromethane	Fischer Chemical, UK
Ethyl acetate	Sigma-Aldrich, Poland
Hexane	Fischer Scientific, UK
Silica gel 60 (Kieselgel 60)	Alfa Aesar, UK
TLC silica gel 60 F_{254}	Merck KGaA, Germany
Celite S	Sigma-Aldrich, Mexico
Pre-packed silica column	
- Silica 20-45μm, 40 x 150 mm, 96 g	VersaFlash/Supelco,Sigma-Aldrich, UK
- Silica 40 μm, 12 g, 24 g & 40 g	Grace Reveleris, USA
- Silica SNAP/Ultra HP-Spehere 10 g, 25 g	Biotage, Sweden

7.8.2 Equipment

Open column chromatography	Sigma-Aldrich, UK
Medium flash chromatography or medium	Büchi, Switzerland

pressure liquid chromatography (MPLC)

- Büchi MPLC, pump module C-601 &
  pump manager C-615
- Grace MPLC, ELSD and UV detector   Grace Reveleris, Illinois, USA
- Biotage Isolera One MPLC, UV detectors   Biotage Isolera One, Uppsala, Sweden
  (UV 1, UV 2 and PDA 200-400 nm)

UVGL-55 Handheld UV Lamp	UVP, Cambridge, UK
Heating gun HL 2010 E	Steinel, Germany
Sonicator Ultrawave	Scientific Laboratory Supplies Ltd., UK
Stuart block heater (SBH 130D/3)	Bibby Scientific Ltd., Staffordshire, UK
Freeze dryer (Christ L1, Alpha 2-4)	Martin Christ Gefriertrocknungsanlagen GmbH, Germany
Safety fume hood (SCALA)	Waldner, Germany
Balance Oertling (NA 164)	European Instruments Ltd., Oxford, UK
Rotary evaporator (Rotavapor R-3)	Büchi, Switzerland
Stuart magnetic stirrer (CB 161)	Scientific Laboratory Supplies Ltd., UK
Micropipettes - Pipetmann	Gilson, France
- Finnpipette F2	Thermo Scientific, Finland

7.8.3   Thin layer chromatography (TLC)

Thin layer chromatography (TLC) analysis was carried on crude extract by using a TLC plates contained with TLC silica gel 60 F_{254} (Merck KGaA, Germany). After elution of the sample, the plate was examined under ultraviolet radiation (UV) at λ_{254} and λ_{365} nm using a UVGL-55 Handheld UV Lamp (UVP, Cambridge, UK) to observe the profile of any UV-active compounds. It was then sprayed with a universal reagent, *p*-Anisaldehyde-sulphuric acid inside a safety fume hood (SCALA, Waldner, Germany) and heated with a heating gun HL 2010 E (Steinel, Germany) at 170℃ to check for non-UV active compounds in various colours.

7.8.4   Open column chromatography

Open column chromatography was used with various column sizes and silica gel 60 (Kieselgel 60), 0.035-0.070 mm (220-440 mesh ASTM) (Alfa Aesar, UK).

7.8.5 Medium pressure flash chromatography

The total crude extract was dissolved in any suitable solvent, mixed with Celite S (Sigma-Aldrich, Mexico) then fractionated by medium pressure liquid chromatography (Büchi, Switzerland) through gradient elution commencing with 100% hexane to 100% ethyl acetate for 20 mins, followed by 100% ethyl acetate to 30% ethyl acetate and 70% methanol for 30 mins at a flow rate of 50 mL/min. A silica column (VersaFlash/Supelco, UK) with dimensions of 4 x 150 mm and a particle size of 20-45 μm was used. The fraction collection volume was set at 100 mL/tube. TLC was carried out to monitor the separation profiles of the fractions and similar fractions were pooled together. The pooled fractions were concentrated under vacuo by a rotary evaporator. The fractions were tested for anti-trypanosomal activity and further isolation work were carried out on the active fractions. Further isolation and purification of these fractions was performed using either the conventional gravity column or by flash chromatography (Grace Reveleris, USA and Biotage Isolera One, Sweden) which can be either normal or reverse phase fitted with the respective commercially available pre-packed column either from Reveleris USA or SNAP Sweden. The two flash chromatography instruments are used to isolate and purify the active fractions or small quantity of the crude extracts. The non-UV active metabolites are purified by using Grace, since dual detectors were coupled to the instrument. Whereas, the UV active metabolites were purified by using Biotage, since this machine able to detect the UV active compounds in the 200-400 nm range.

7.8.6 *p*-Anisaldehyde - sulphuric acid spray reagent composition

The *p*-Anisaldehyde - sulphuric acid spray reagent was the universal reagent used to detect the presence of phenols, sugars, steroids and terpenes in crude extract, fractions or pure compounds separated on TLC plates. The TLC plate was sprayed with the reagent and heated at 170℃ to check for non-UV active compounds that appear in various colours. The spray reagent was stored in aluminium foil-packed glass bottle to avoid light and kept in refrigerator prior to use.

p-Anisaldehyde (Sigma-Aldrich, USA)	0.5 mL
Methanol (VWR Chemicals, EC)	85 mL
Glacial acetic acid (Sigma-Aldrich, Germany)	10 mL
Conc. H_2SO_4 (Fischer Chemical, UK)	5 mL (added slowly)

7.9 Isolation of secondary metabolites from *Fusarium* sp.

The crude extract, FRC15, of *Fusarium* sp. (11.0 g) was fractionated to give 16 major fractions. The active fractions were subjected to isolation and purification and yielded five compounds. Isolation work on fraction FRC15-3 gave a pale yellow oil elucidated as ergosterol peroxide (FRC15-3-r2-10, (**3.27**), 3.2 mg, 0.03%) and purification of fraction FRC15-4 yielded violet crystals of anhydrofusarubin (FRC15-4-F4, (**3.28**),7.3 mg, 0.07%). Purification of fraction FRC15-6 gave dihydrojavanicin (FRC15-6-r2-13, (**3.29**), 2.4 mg, 0.02%). Further isolation on fraction FRC15-8 gave red crystals of javanicin (FRC15-8-F8c, (**3.8**), 5.7 mg, 0.05%). Purification of fraction FRC15-11 gave red crystals of solaniol (FRC15-11-F11, (**3.26**), 7.0 mg, 0.06%).

7.10 Isolation of secondary metabolites from *A. aculeatus*

The crude extract, AARC30 of *A. aculeatus* (18.50 g) was fractionated resulting to 16 major fractions in which the active fractions were subjected to further isolation work and purification by flash chromatography (Grace Reveleris or Biotage Isolera) which gave eight pure compounds. Isolation on fraction AARC30-4 gave ergosterol peoxide (AARC30-4-1, (**3.27**) 5.3 mg, 0.03%). Further several isolations on fraction AARC30-5 using flash chromatography (Grace Isolera, USA) gave one new 2,3-dihydrochromen-4-one, aspergillusenone (AARC30-5-116-3, (**4.28**), 2.3 mg, 0.01%), whereas fraction AARC30-6 yielded four acid type of compounds: vanillic acid (AARC30-6-28, (**4.29**), 5.2 mg, 0.01%), 3,4-dihydroxyphenylacetic acid (AARC30-6-11, (**4.30**), 4.3 mg, 0.02%), *o*-hydroxyphenylacetic acid (AARC30-6-50, (**4.31**),

6.23 mg, 0.03%), and *p*-hydroxyphenylacetic acid (AARC30-6-60, (**4.32**), 4.32 mg, 0.02%). Meanwhile, several purifications on fraction AARC30-9 revealed a new metabolite, 2-(3,4-hydroxyphenyl)-*N*,*N*-dimethylacetamide (AARC30-9-8-36, (**4.33**), 4.25 mg, 0.02%). Further isolation on fraction AARC30-10 gave yellow crystals, secalonic acid A (AARC30-10-18 (**4.20**), 10.3 mg, 0.06%).

7.11   Isolation of secondary metabolites from *L. theobromae*

The crude extract, LTRC15, of *L. theobromae* (24.0 g) was fractionated by medium pressure liquid chromatography (Büchi, Switzerland) to give 15 major fractions. The active major fractions were also subjected to further isolation work and purification by flash chromatography (Grace Reveleris or Biotage Isolera) to yield six compounds. Purification work on fraction LTRC15-3 yielded colourless crystals of (-)-mellein, (LTRC15-3-19, (**5.19**), 11.0 mg, 0.05%). Further purification of fraction LTRC15-4 gave *p*-hydroxyphenethyl alcohol (LTRC15-4-22, (**5.17**), 5.3 mg, 0.02%), fraction LTRC15-5 afforded *p*-hydroxybenzaldehyde (LTRC15-5-5F-1, (**5.18**), 5.2 mg, 0.02%) and fraction LTRC15-6 gave (-)-*trans-axial*-4-hydroxymellein (LTRC15-6-31c, (**5.20**), 7.0 mg, 0.03%). Meanwhile, several purifications of fraction LTRC15-8 gave (-)-5-hydroxymellein (LTRC15-8-22c, (**5.22**), 6.0 mg, 0.03%) and another congener of (-)-*cis-equatorial*-4-hydroxymellein (LTRC15-8-41, (**5.21**), 8.7 mg, 0.04%).

7.12   Structure elucidation, identification and analysis of metabolites
7.12.1 General instruments
Structure determination of the isolated compounds was based on MS and NMR spectroscopy data. One dimensional NMR (1D NMR) data consisted of ^{1}H and ^{13}C NMR Jeol ([1]H 400 MHz, [13]C 100.5 MHz, SIPBS, University of Strathclyde) and Bruker ([1]H 600 MHz, [13]C 150 MHz, Department of Pure and Applied Chemistry, University of Strathclyde) and was confirmed by two dimensional NMR (2D NMR) spectra such as HMQC or HSQC, HMBC, COSY and NOESY as well as comparisons with the literature. A pure sample was dissolved in 500 μL of a suitable deuterated solvent and transferred to 5 mm Norell NMR tube (Sigma-Aldrich, USA).

Small quantity samples were analysed in Shigemi tubes (Sigma-Aldrich, USA) with 180 μL of the appropriate deuterated solvent. Dimethyl sulfoxide-d_6, chloroform-d, acetone-d_6, and methanol-d_3 bought from Sigma-Aldrich (USA) were the deuterated solvents used. The spectra were then processed with MestReNova-9.0 (MNova) 2.8 by Mestrelab Research, S.L, (Santiago de Compostela, Spain).

7.12.2 Optical rotation

The optical rotation of optically-active compounds was measured with the digital polarimeter 341 (Perkin Elmer, USA) in which the pure compound was dissolved in in 2 mL of the suitable solvent (chloroform or acetone) to a concentration of 1 mg/mL. A cuvette was filled with the test solution and was placed in the polarimeter compartment. Ten readings were averaged and the specific rotation was calculated (the spectral wavelength of Na at 589 nm at 20 °C) with the following equation

$$[\alpha]_D^{20} = \frac{a}{l + c}$$

Where:

a = average rotation value in degree (°, + or -)

l = the cell volume in mL (value of l for the micro test cell is 1)

c = concentration in g per 100 mL (e.g. if the concentration is 20 mg per 2 mL, c = 1)

7.12.3 Circular dichroism

Circular dichroism (CD) is the difference in the absorption of left-handed circularly polarised light (L-CPL) and right-handed circularly polarised light (R-CPL) and occurs when a molecule contains one or more chiral chromophores (light-absorbing groups).

Circular dichroism = ΔA(λ)

       = A(λ)$_{LCPL}$ - A(λ)$_{RCPL,}$

where λ is the wavelength

Circular dichroism (CD) spectroscopy is a spectroscopic technique where the CD of molecules is measured over a range of wavelengths. CD spectroscopy is used

extensively to study chiral molecules of all types and sizes, but it is in the study of large biological molecules where it finds its most important applications. A primary use is in analysing the secondary structure or conformation of macromolecules can be derived from circular dichroism spectroscopy.

Measurements carried out in the visible and ultra-violet region of the electromagnetic spectrum monitor electronic transitions. If the molecule under study contains one or more chiral chromophores, then one CPL state will be absorbed to a greater extent than the other. The CD signal over the corresponding wavelengths will be non-zero. A circular dichroism signal can be positive or negative, depending on whether L-CPL is absorbed to a greater extent than R-CPL (CD signal positive) or to a lesser extent (CD signal negative). CD spectrum may exhibit both positive and negative peaks when a sample with multiple CD peaks varies as a function of wavelength.

CD instrument used was Chirascan-plus spectrophotometer (Applied Photophysics Limited, Surrey, United Kingdom) in continuous manufacturing and crystallisation (CMAC) lab, Technology Innovation Centre, University of Strathclyde. Samples were prepared by dissolving in acetonitrile with appropriate concentration. Parameters used were set up on Pro-data spectrometer control panel (Figure 7.2). Under signal menu- milidegrees and absorbance; sample handling unit temperature-22.1°C; monochromator menu- wavelength (450 nm), bandwidth (1 nm), low wavelength 200 nm and high wavelength (450 nm), sampling: time per point(s): 1.000 (takes approx. 2 min), sequencer: 2 minutes; sequences menu- repeats (3 times), spectrum were set up. Firstly, background button under baseline menu was clicked (background baseline run in 30 s in which no sample inside the instrument). Meanwhile, the sample was transferred into a cuvette (cell length of 2 mm) and placed inside the instrument. To start running, acquire button was clicked, the scans took about 2 minutes. CD spectrum (from 3 repeats) was opened in Pro-data viewer, the spectrum was processed under trace manipulation dialog box, in which CD spectra from solvent and samples (from three spectra) were averaged separately, solvent (acetonitrile) was set as baseline, the averaged spectrum from each sample

was subtracted to remove solvent baseline. Then, smooth button was clicked for better spectrum. The averaged and smooth spectrum was saved as .txt or Microsoft-Excel.csv files for further analysis.
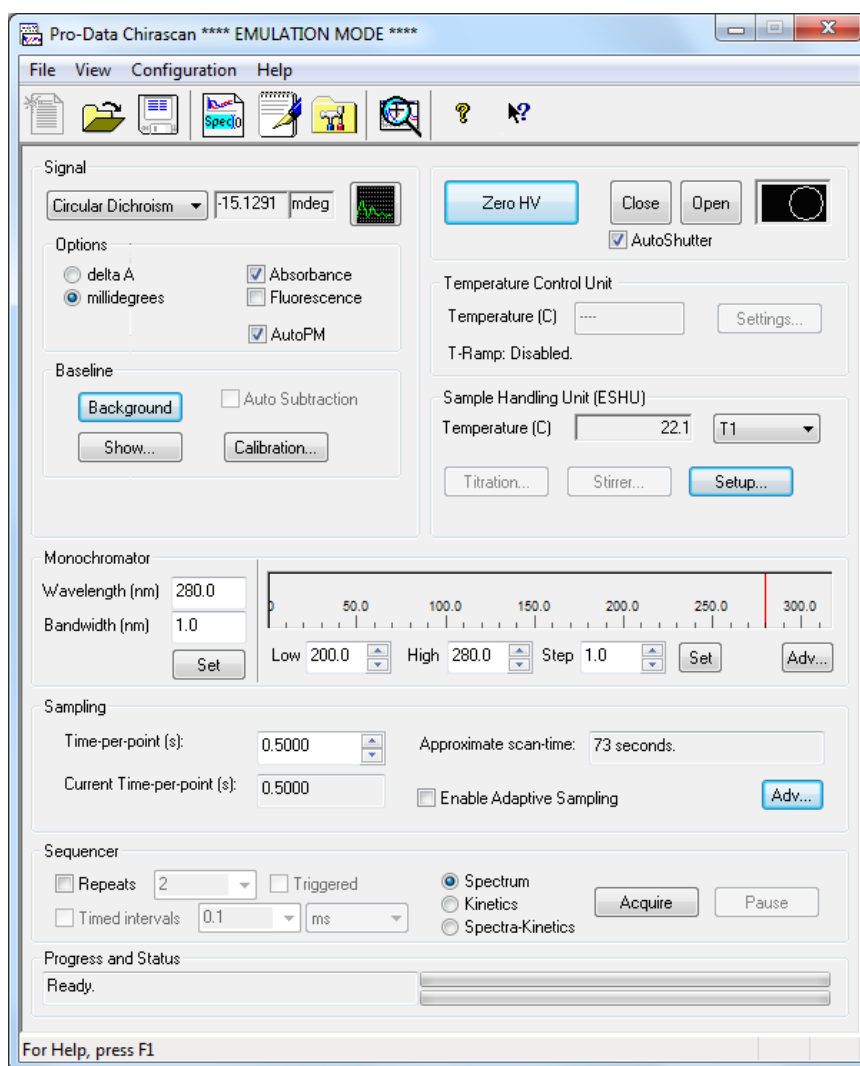
Figure 7.2: Pro-data spectrometer control panel

Chapter 8

8.   Conclusions

The main aims in the present work were to isolate secondary metabolites for anti-trypanosomal derived drugs from the mangrove plant, *Avicennia lanata* and its endophytic fungi by utilising metabolomics and bioassays-guided approaches to aid in the preliminary screening, fractionation and purification of the targeted bioactive compounds. In recent years, marine-derived metabolites have been explored widely for their biologically purposes. To achieve the goal in the discovery for new potential active secondary metabolites, the use of metabolomics tools assisted in the decision making of which fractions or the optimum medium for production of metabolites should be prioritized. By means of high resolution mass spectrometry, novel potentially bioactive molecules were identified and targeted from the crude extracts. Dereplication study was used to screen the known metabolites from the crude extracts prior to further scale up or purification work to avoid repetitive work. Three fungal strains were isolated from the fresh parts of the mangrove plant *A. lanata*, from which *Fusarium* sp. was isolated from the root part, *Aspergillus aculeatus* from the leaf part, and *Lasiodiplodia theobromae* from the twigs which were taxonomically identified by molecular biology. Small scale inoculation of the endophytes was accomplished in both solid rice and liquid broth culture media for 7, 15 and 30 days. Crude plant extracts and ethyl acetate extracts obtained from the fungal mycelia were preliminarily screened by using high resolution liquid chromatography-mass spectrometer and NMR for bioactive molecules against *T. b. brucei* and were analysed by multivariate analysis such as PCA and OPLS-DA. Hence, metabolomic and bioassay-guided isolation of potential anti-trypanosomal secondary metabolites were identified from the crude extracts of *A. lanata* and its endophytic fungi, which included quinone natural products, three of them were known naphthofuranquinone congeners and three new derivatives, four naphthazarin-related naphthoquinones, four dihydroisocoumarins (mellein and three derivatives), a new amide, a new xanthone monomer derivative and a known homodimer tetrahydroxanthone, phenolic acids, two triterpenes, two sterols and an ergosterol

peroxide, in which 25 out of 29 compounds were active against the protozoa, *T. b. brucei,* with MIC values of 0.32-12.5 μM.

8.1   Bioactive metabolites from *Avicennia lanata*

Avicennia species are known to yield naphthofuranquinones. In this study, five naphthofuranquinone derivatives were isolated from *A. lanata* crude extract in which two of them along with a carboxylate derivative were reported for the first time. All derivatives have the same benzene and furan ring system except for glycoquinone and its new derivative glycosemiquinone, which have an additional prenyl group with the similar MIC values of 12.50 μM.   Among the naphthofuranquinones isolated, avicequinone C exhibited the most potent activity against *T. b. brucei* with an MIC value of 3.12 μM. Avicenol C had an MIC value of 6.25 μM, in contrast to its new derivative; hydroxyavicenol C had an MIC of 12.50 μM which was less than its parent analogue. The present work is the first report on the new carboxylate derivative, avicennpentenone carboxylate which had an MIC of 12.50 μM. Besides the quinones, taraxerone, taraxerone, stigmasterol and β-sitosterol have been also isolated from this plant, in which all of them were inactive except for stigmasterol which showed slightly increased in activity against *T. b. brucei* with an MIC value of 126.40 μM. The presence of *p*-dione with an α,β-unsaturated system in naphthofuranquinones contributed to the prominent activity which opposed to the decreased activity in the presence of methoxy and hydroxyl moieties on a quinone system that may interfere the redox cycle resulting in lower activity than other isolates. Meanwhile, the modification in sterol compounds with an olefinic chain also slightly increased the activity.

8.2   Bioactive metabolites from *Fusarium* sp.

The small scale fungal extract from the rice culture media on days 15 and 30, as well as liquid culture media on days 7, 15, and 30 showed potent activities against *T. b. brucei* except the rice culture extract obtained from day 7. Based on the dereplication studies and multivariate analysis for the small scale extracts, *Fusarium* sp. was

scaled up in the rice culture medium for 15 days, which led to the isolation of four naphthazarin-related naphthoquinones as the major bioactive metabolites in the extract, along with ergosterol peroxide and two acids. The four naphthazarin derivatives showed intense bioactivity, in which solaniol had the most potent anti-protozoal activity with an MIC of 0.32 μM, followed by javanicin with an MIC of 0.60 μM. Interestingly, all of the naphthazarin derivatives shared the same quinone core and benzene ring systems, differing only on the side chains except for dihydrojavanicin, where the position of the hydroxyl on benzene ring and carbonyl substituents for quinone ring was different from javanicin (MIC of 1.90 μM). The next potent activity is anhydrofusarubin with an MIC of 1.20 μM. The presence of a quinoid ring with an α,β-unsaturated system, the introduction of functional groups such as hydroxyls and methoxy groups on the benzene ring as well as presence of substituents on the side chain increases the anti-protozoal bioactivity. Meanwhile, the presence of endo-peroxide bridge in ergosterol also showed potency comparable to the naphthazarin derivatives.

8.3   Bioactive metabolites from *Aspergillus aculeatus*

Preliminary screening on the production of secondary metabolites by *A. aculeatus* in small scale extracts from the rice and liquid culture media on days 7, 15 and 30 along with their activities against *T. b. brucei*, revealed that only the extract from the 30 days rice culture medium showed potent anti-protozoal activity. Further scale up of the fungus in rice culture medium for 30 days, revealed two new bioactive metabolites, an amide derivative with an MIC value of 3.12 μM and aspergillusenone, a xanthone monomer with a 2,3-dihydrochromen-4-one backbone exhibited potent activity against the protozoa with an MIC of 1.26 μM, opposed to its dimer analogue. The homodimer of tetrahydroxanthone, secalonic acid A displayed the highest potency with an MIC of <0.19 μM, which is comparable to suramin (MIC of 0.11 μM). Whereas among the isolated phenolic acids, 3,4-dihydroxyphenylacetic acid showed pronounced activity with an MIC of 1.56 μM. The other three phenolic acids were also active with similar MICs of 6.25 μM. The epidioxy sterol gave an MIC of 1.56 μM, which can be also considered as a potential anti-trypanosomal

drug. The presence of xanthone derivatives in the extract, as well as the *ortho*-hydroxy phenolic acids had enhanced the activity against the protozoa.

8.4   Bioactive metabolites from *Lasiodiplodia theobromae*

The preliminary studies on the small scale extracts of *L. theobromae* from the rice and liquid culture media from days 7, 15 and 30, revealed that only the 15th day rice culture medium exhibited anti-protozoal activity. Further scale up of this fungus yielded four dihydroisocoumarins; mellein with three of its derivatives and two phenolic acid congeners. The isolated compounds displayed potent bioactivity, in which 5-hydroxymellein showed the most potent activity with an MIC value of 2.40 µM, followed by *trans-axial*-4-hydroxymellein had an MIC value of 3.20 µM. In contrast to its enantiomer, *cis-equatorial*-4-hydroxymellein exhibited less activity (MIC of 8.20 µM). These two derivatives possessed two hydroxyls substituents, one of them on the benzene ring and the other on the pyranone ring. Meanwhile, the activity showed by *p*-hydroxybenzaldehyde and *p*-hydroxyphenethyl alcohol was also significant, with MIC values of 6.25 and 12.50 µM, respectively. The presence of the isochromanone molecules also proved to contribute to the trypanocidal activity.

8.5   Future work recommendations

The use of more than three fungal extract replicates during the preliminary screening of the small scale extracts from the rice and liquid culture media on days 7, 15 and 30 will ensure reproducibility of the production of metabolites for further scale up. Furthermore, the small scale extracts of *Fusarium* sp. from the 30th day rice medium as well as the small extract of *L. theobromae* from the 30th day rice culture medium showed unique biomarkers, which differentiated them from the other extracts exhibiting potent activity against *T. b. brucei*. In the present study, it can be concluded that the endophytic fungi grown in the rice culture medium produces more bioactive metabolites against *T. b. brucei* compared to the liquid culture medium. Hence, these two fungi can be further scaled up using the rice culture medium. The

production of secondary metabolites from these fungi can be further studied in different growth stages by using different nutrients in liquid medium may also lead to the discovery of more new potential active metabolites.

The present comparative studies on the anti-trypanosomal activity of the isolated triterpenes, sterols, naphthoquinones, phenolic acids, dihydroisocoumarins, xanthones and their derivatives, have indicated that the presence of different classes of secondary metabolites from natural sources with different substituted functional groups either on the main core or side chains served promising trypanocidal activity. The trypanocidal activity against *T. b. brucei* is used usually in a preliminary stage of the screening process of lead compounds, in which the blood stream form parasite is non-pathogenic to human. Further work using different type of parasite *in vitro* activities such as *T. b. rhodesiense*, *T. b. gambiense* or *T. cruzi* as well as the use of different parasite at their amastigote, epimastigote or trypomastigote stages, will help in the better determination of the effectiveness of the respective secondary metabolites against a specific protozoa cycle. Meanwhile, the use of more commercially available naphthoquinone and phenolic acid derivatives, along with other current drugs used to treat trypanosomiasis will establish the quantitative structure-activity relationship. Despite the excellent *in vitro* activities of the isolated compounds, it is also suggested that the *in vivo* potential of the selected active metabolites will eventually lead to a deeper understanding of their exact mechanisms of action.

One of the important criteria to bear in mind when searching for active compounds against protozoa parasites is that no toxic effects to mammalian host cells is crucial. Some of the isolated compounds showed activity against the protozoa parasite with no toxic or slightly lower toxicities. Although some of the isolated metabolites showed potent activity against *T. b. brucei* with increasing in cytotoxicity, it is best to determine their toxicities against mammalian cells at lower concentration. Thus, concentration response tests at 300-0.3 μg/mL for the samples with cell viability less than 60% of control values in the initial screening against PNT2A cells will be

carried out. IC_{50} values of the tested compounds will be determined in developing future safe drugs of trypanosomiasis treatment.

Previous reports on the isolated active metabolites against the parasitic protozoa have also showed anti-cancer properties, such as avicequinone C which had potent activity against L-929, K-562 and HeLa cell lines, thus would be suggested that some of the isolated compounds might have anti-cancer drug properties against different cancer cell lines.

In the present work, the three endophytic fungi which have been isolated from different parts of the mangrove plant, *A. lanata*, showed potent activity against *T. b. brucei*. These three fungi had produced different classes of chemical compounds in which the metabolites were also different with those metabolites produced from the organics extract of *A. lanata*. A study on the relationship of the isolated metabolites and their derivatives that link to certain biosynthetic gene clusters would thus be one of the interests to gain genome sequences leading to the prediction of new metabolite clusters.

Nowadays, the discovery of novel secondary metabolites from endophytes becomes more challenging in natural products chemistry. Different approaches have been applied in order to optimise the production of new bioactive fungal metabolites. Bacteria and fungi interact within the host plant and stimulate competition for nutrients and spaces regarded as a major ecological factor that induce bioactive secondary metabolites. A lot of studies proved that bacteria and fungi produce active secondary metabolites. Thus, co-culturing two different microbes in the same media vessel rather than strains cultured independently, leads to direct interaction which may trigger the expression of "silent" biosynthetic pathways to produce novel secondary metabolites. It will be interesting to try to co-culture of two different fungal strains using different culture media and harvesting them at different growth stages, in which the preliminary screening on the production of metabolites will be monitored using metabolomic approaches.

In summary, the screening of marine-derived metabolites by using metabolomic approaches, multivariate analysis and bioassays-guided lead to the isolation, structure elucidation and biological investigation of trypanosomal active compounds. The use of these techniques helps to target the potential of new biomarkers which active against the protozoa.

REFERENCES

Aberhart, D., Chen, Y., De Mayo, P. & Stothers, J. (1965) 'Mould metabolites—IV: The isolation and constitution of some ergot pigments'. *Tetrahedron,* 21 (6), pp.1417-1432.

Abraham, E.P. & Newton, G.G.F. (1961) 'The structure of cephalosporin C'. *Biochemical Journal,* 79 (2), pp.377-393.

Achor, D., Nemec, S. & Baker, R. (1993) 'Effects of *Fusarium solani* naphthazarin toxins on the cytology and ultrastructure of rough lemon seedlings'. *Mycopathologia,* 123 (2), pp.117-126.

Adam, H., Campbell, I. & McCorkindale, N. (1967) 'Ergosterol peroxide: a fungal artefact'.

Adams, J.H. & Lewis, J.R.J. (1978) '($\pm$)-2,3-dihydro-2-(1-hydroxy-1-methylethyl) naphtha [2,3-b] furan-4,9-quinone; an anti-tumour active peroxidation product of lapachol'. *Chem. Res. (M),* pp.0186-0192.

Adandonon, A., Datinon, B., Baimey, H. & Toffa, J. (2014) 'First report of *Lasiodiplodia theobromae* (Pat.) Griffon & Maubl causing root rot and collar rot disease of *Jatropha curcas* L. in Benin'. *Journal of Applied Biosciences,* 79 pp.6873-6877.

Adrian-Romero, M., Wilson, S.J., Blunden, G., Yang, M.-H., Carabot-Cuervo, A. & Bashir, A.K. (1998) 'Betaines in coastal plants'. *Biochemical Systematics and Ecology,* 26 (5), pp.535-543.

Al-Saadoon, A.H., Ameen, M.K., Hameed, M.A., Al-Badran, A. & Ali, Z. (2012) 'First report of grapevine dieback caused by *Lasiodiplodia theobromae* and *Neoscytalidium dimidiatum* in Basrah, Southern Iraq'. *African Journal of Biotechnology,* (11 (95)), pp.16165-16171.

Al-Zereini, W. (2006) 'Natural products from marine bacteria'. *Unpublished doctoral dissertation). University of Kaiserslautern, Germany.*

Aldridge, D., Galt, S., Giles, D. & Turner, W. (1971) 'Metabolites of *Lasiodiplodia theobromae'. Journal of the Chemical Society C: Organic,* pp.1623-1627.

Ali, A., Assimopoulou, A.N., Papageorgiou, V.P. & Kolodziej, H. (2011) 'Structure/antileishmanial activity relationship study of naphthoquinones and dependency of the mode of action on the substitution patterns'. *Planta medica,* 77 (18), pp.2003-2012.

Alvim Jr, J., Dias, R.L., Castilho, M.S., Oliva, G. & Corrêa, A.G. (2005) 'Preparation and evaluation of a coumarin library towards the inhibitory activity of the enzyme gGAPDH from Trypanosoma cruzi'. *Journal of the Brazilian Chemical Society,* 16 (4), pp.763-773.

Andersen, R., Buechi, G., Kobbe, B. & Demain, A.L. (1977) 'Secalonic acids D and F are toxic metabolites of *Aspergillus aculeatus'. The Journal of organic chemistry,* 42 (2), pp.352-353.

Anjaneyulu, A., Murthy, Y., Rao, V. & Sreedhar, K. (2003) 'Chemical examination of the mangrove plant *Avicennia officinalis'. Indian Journal of Chemistry Section B-Organic Chemistry Including Medicinal Chemistry,* 42 (12), pp.3117-3119.

Apt, W. (2010) 'Current and developing therapeutic agents in the treatment of Chagas disease'. *Drug design, development and therapy,* 4 pp.243.

Arnstein, H.R.V. & Cook, A.H. (1947) '189. Production of antibiotics by fungi. Part III. Javanicin. An antibacterial pigment from *Fusarium javanicum*'. *Journal of the Chemical Society (Resumed),* (0), pp.1021-1028.

Arsenault, G. (1968) 'Fungal metabolites—III: Quinones from *Fusarium solani* D2 purple and structure of (+)-solaniol2'. *Tetrahedron,* 24 (13), pp.4745-4749.

Asha, K.N., Chowdhry, R., Hasan, C.M. & Rashid, M.A. (2004) 'Steroids and polyketides from *Uvaria hamiltonii* stem bark'. *Aata Pharmaceutica-Zagreb-,* 54 (1), pp.57-64.

Aso, M., Ojida, A., Yang, G., Cha, O.J., Osawa, E. & Kanematsu, K. (1993) 'Furannulation strategy for synthesis of the naturally occurring fused 3-methylfurans: efficient synthesis of evodone and menthofuran and regioselective synthesis of maturone via a Lewis acid catalyzed Diels-Alder reactions. Some comments for its mechanistic aspects'. *The Journal of Organic Chemistry,* 58 (15), pp.3960-3968.

Ayer, W.A. & Trifonov, L.S. (1995) 'Phenolic and polyketide metabolites of the aspen blue stain fungus *Ophiostoma crassivaginata*'. *Phytochemistry,* 38 (2), pp.371-372.

Baker, R.A., Tatum, J.H. & Nemec Jr, S. (1981) 'Toxin production by *Fusarium solarti* from fibrous roots of blight-diseased citrus'. *Phytopathology,* 71 pp.951-954.

Baker, R.A., Tatum, J.H. & Nemec Jr, S. (1990) 'Antimicrobial activity of naphthoquinones from Fusaria'. *Mycopathologia,* 111 (1), pp.9-15.

Bandaranayake, W.M. (1998) 'Traditional and medicinal uses of mangroves'. *Mangroves and Salt Marshes,* 2 (3), pp.133-148.

Bandaranayake, W.M. (2002) 'Bioactivities, bioactive compounds and chemical constituents of mangrove plants'. *Wetlands Ecology and Management,* 10 (6), pp.421-452.

Bani, M., Rispail, N., Evidente, A., Rubiales, D. & Cimmino, A. (2014) 'Identification of the Main Toxins Isolated from *Fusarium oxysporum* f. sp. pisi Race 2 and Their Relation with Isolates' Pathogenicity'. *Journal of agricultural and food chemistry,* 62 (12), pp.2574-2580.

Bao, K., Fan, A., Dai, Y., Zhang, L., Zhang, W., Cheng, M. & Yao, X. (2009) 'Selective demethylation and debenzylation of aryl ethers by magnesium iodide under solvent-free conditions and its application to the total synthesis of natural products'. *Organic & Biomolecular Chemistry,* 7 (24), pp.5084-5090.

Barnathan, G., Mirallès, J., Gaydou, E.M., Boury-Esnault, N. & Kornprobst, J.-M. (1992) 'New phospholipid fatty acids from the marine sponge *Cinachyrella alloclada* uliczka'. *Lipids,* 27 (10), pp.779-784.

Barrero, A.F., Oltra, J.E. & Poyatos, J.A. (1996) 'Acidic metabolites from *Phycomyces blakesleeanus*'. *Phytochemistry,* 42 (5), pp.1427-1433.

Barrett, M.P., Burchmore, R.J., Stich, A., Lazzari, J.O., Frasch, A.C., Cazzulo, J.J. & Krishna, S. (2003) 'The trypanosomiases'. *The Lancet,* 362 (9394), pp.1469-1480.

Bates, M.L., Reid, W.W. & White, J.D. (1976) 'Duality of pathways in the oxidation of ergosterol to its peroxide in vivo'. *Journal of the Chemical Society, Chemical Communications,* (2), pp.44-45.

Bell, K. & Duewell, H. (1961) 'Triterpenoids from the bark of *Avicennia marina*'. *Australian Journal of Chemistry,* 14 (4), pp.662-663.

Bentley, R. & Gatenbeck, S. (1965) 'Naphthoquinone Biosynthesis in Molds. The Mechanism for Formation of Mollisin*'. *Biochemistry,* 4 (6), pp.1150-1156.

Berrueta, L.A., Alonso-Salces, R.M. & Héberger, K. (2007) 'Supervised pattern recognition in food analysis'. *Journal of Chromatography A,* 1158 (1), pp.196-214.

Birch, A. & Donovan, F. (1953) 'Studies in relation to Biosynthesis. I. Some possible routes to derivatives of Orcinol and Phloroglucinol'. *Australian Journal of Chemistry,* 6 (4), pp.360-368.

Biswas, M., Biswas, K., Ghosh, A. & Haldar, P. (2009a) 'A pentacyclic triterpenoid possessing analgesic activity from the fruits of *Dregea volubilis*'. *Pharmacognosy Magazine,* 5 (19), pp.90.

Biswas, M., Biswas, K., Ghosh, A. & Haldar, P. (2009b) 'A pentacyclic triterpenoid possessing anti-inflammatory activity from the fruits of *Dregea volubilis*'. *Pharmacognosy Magazine,* 5 (19), pp.64.

Blum, M.S., Foottit, R. & Fales, H.M. (1992) 'Defensive chemistry and function of the anal exudate of the thrips *Haplothrips leucanthemi*'. *Comparative Biochemistry and Physiology Part C: Comparative Pharmacology,* 102 (1), pp.209-211.

Blunt, J.W., Copp, B.R., Keyzers, R.A., Munro, M.H.G. & Prinsep, M.R. (2015) 'Marine natural products'. *Natural Product Reports,* 32 (2), pp.116-211.

Bok, J.W., Lermer, L., Chilton, J., Klingeman, H.G. & Towers, G.H.N. (1999) 'Antitumor sterols from the mycelia of *Cordyceps sinensis*'. *Phytochemistry,* 51 (7), pp.891-898.

Borges Coutinho Gallo, M., Coêlho Cavalcanti, B., Washington Araújo Barros, F., Odorico de Moraes, M., Veras Costa-Lotufo, L., Pessoa, C., Kenupp Bastos, J. & Tallarico Pupo, M. (2010) 'Chemical Constituents of *Papulaspora immersa*, an Endophyte from *Smallanthus sonchifolius* (Asteraceae), and Their Cytotoxic Activity'. *Chemistry & Biodiversity,* 7 (12), pp.2941-2950.

Bournot, K. (1913) 'Gewinnung von Lapachol aus dem Kernholz von *Avicennia tomentosa*'. *Archiv der Pharmazie,* 251 (5), pp.351-354.

Bousquet-Mélou, A. & Fauvel, M.-T. (1998) 'Inter-specific variation in the concentration of two iridoid glucosides in *Avicennia* L. (Avicenniaceae Endl.)'. *Biochemical Systematics and Ecology,* 26 (8), pp.935-940.

Breivik, H., rretzen, B.B., Dahl, K.H., Krokan, H.E. & naa, K.H.B. (1997) '*Fatty acid composition'*. Google Patents.

Brian, P.W., Dawkins, A.W., Grove, J.F., Hemming, H.G., Lowe, D. & Norris, G.L.F. (1961) 'Phytotoxic Compounds produced by *Fusarium equiseti*'. *Journal of Experimental Botany,* 12 (1), pp.1-12.

Bringmann, G., Günther, C., Ochse, M., Schupp, O. & Tasler, S. (2001) *Biaryls in nature: a multi-facetted class of stereochemically, biosynthetically, and pharmacologically intriguing secondary metabolites.* Springer.

Bringmann, G., Hoerr, V., Holzgrabe, U. & Stich, A. (2003) 'Antitrypanosomal naphthylisoquinoline alkaloids and related compounds'. *Die Pharmazie - An International Journal of Pharmaceutical Sciences,* 58 (5), pp.343-346.

Brun, R., Blum, J., Chappuis, F. & Burri, C. (2010) 'Human african trypanosomiasis'. *The Lancet,* 375 (9709), pp.148-159.

Cabras, A., Mannoni, M.A., Serra, S., Andolfi, A., Fiore, M. & Evidente, A. (2006) 'Occurrence, isolation and biological activity of phytotoxic metabolites produced in vitro by *Sphaeropsis sapinea*, pathogenic fungus of *Pinus radiata*'. *European Journal of Plant Pathology,* 115 (2), pp.187-193.

Cafieri, F., Fattorusso, E., Taglialatela-Scafati, O. & Ianaro, A. (1999) 'Metabolites from the sponge *Plakortis simplex*. Determination of absolute stereochemistry of plakortin. Isolation and stereostructure of three plakortin related compounds'. *Tetrahedron,* 55 (22), pp.7045-7056.

Calò, L., Fornelli, F., Ramires, R., Nenna, S., Tursi, A., Caiaffa, M.F. & Macchia, L. (2004) 'Cytotoxic effects of the mycotoxin beauvericin to human cell lines of myeloid origin'. *Pharmacological Research,* 49 (1), pp.73-77.

Camarda, L., Merlini, L. & Nasini, G. (1976) 'Metabolites of *Cercospora. Taiwapyrone*, an α-pyrone of unusual structure from *Cercospora taiwanensis*'. *Phytochemistry,* 15 (4), pp.537-539.

Campos, M.C.O., Leon, L.L., Taylor, M.C. & Kelly, J.M. (2014) 'Benznidazole-resistance in *Trypanosoma cruzi*: Evidence that distinct mechanisms can act in concert'. *Molecular and Biochemical Parasitology,* 193 (1), pp.17-19.

Carlsson, A., Lindqvist, M., Fila-Hromadko, S. & Corrodi, H. (1962) 'Synthase von Catechol-*O*-methyl-transferase-hemmendem Verbindungen. In de Catecholaminmetabolismus eingreifende substanzen. 1. Mitteilung'. *Helvetica Chimica Acta,* 45 pp.270-276.

Castro, J. & Diaz, d.T.E. (1988) 'Toxic effects of nifurtimox and benznidazole, two drugs used against American trypanosomiasis (Chagas' disease)'. *Biomedical and environmental sciences: BES,* 1 (1), pp.19-33.

Castro, J.A., Montalto deMecca, M. & Bartel, L.C. (2006) 'Toxic side effects of drugs used to treat Chagas' disease (American trypanosomiasis)'. *Human & experimental toxicology,* 25 (8), pp.471-479.

Chang, S.W., Lee, I.K. & Ryu, S.Y. (2009) 'Articles: Phytochemical Constituents of *Bistorta manshuriensis*'. *Natural Product Sciences,* 15 (4), pp.234-240.

Chapman, V.J. (1976) 'Mangrove vegetation'. *Vaduz.: J. Cramer,* 581.

Chaturvedula, V.S.P. & Prakash, I. (2012) 'Isolation of Stigmasterol and β-Sitosterol from the dichloromethane extract of *Rubus suavissimus*'. *International Current Pharmaceutical Journal,* 1 (9), pp.239-242.

Checchi, F., Piola, P., Ayikoru, H., Thomas, F., Legros, D. & Priotto, G. (2007) 'Nifurtimox plus eflornithine for late-stage sleeping sickness in Uganda: a case series'.

Chen, C., Imamura, N., Nishijima, M., Adachi, K., Sakai, M. & Sano, H. (1996) 'Halymecins, new antimicroalgal substances produced by fungi isolated from marine algae'. *J Antibiot (Tokyo),* 49 (10), pp.998-1005.

Chen, Y., Ni, H., Chen, F., Cai, H., Li, L. & Su, W. (2013) 'Purification and Characterization of a Naringinase from *Aspergillus aculeatus* JMUdb058'. *Journal of Agricultural and Food Chemistry,* 61 (4), pp.931-938.

Chilton, W.S. (1968) 'Isolation and structure of norjavanicin'. *The Journal of Organic Chemistry,* 33 (11), pp.4299-4300.

Ciegler, A., Hayes, A.W. & Vesonder, R.F. (1980) 'Production and biological activity of secalonic acid D'. *Applied and environmental microbiology,* 39 (2), pp.285-287.

Claydon, N., Grove, J.F. & Pople, M. (1979) 'Insecticidal secondary metabolic products from the entomogenous fungus *Fusarium larvarum*'. *Journal of Invertebrate Pathology,* 33 (3), pp.364-367.

Cole, R.J., Moore, J.H., Davis, N.D., Kirksey, J.W. & Diener, U.L. (1971) '4-Hydroxymellein. New metabolite of *Aspergillus ochraceus*'. *Journal of Agricultural and Food Chemistry,* 19 (5), pp.909-911.

Covas, M.I., Miro-Casas, E., Fito, M., Farre-Albadalejo, M., Gimeno, E., Marrugat, J. & De La Torre, R. (2003) 'Bioavailability of tyrosol, an antioxidant phenolic compound present in wine and olive oil, in humans'. *Drugs Exp Clin Res,* 29 (5-6), pp.203-206.

Cribb, A.B. & Cribb, J.W. (1955) 'Marine fungi from Queensland'. *Brisbane: University of Queensland Press.*

Cutignano, A., Fontana, A., Renzulli, L. & Cimino, G. (2003) 'Placidenes CF, Novel α-Pyrone Propionates from the Mediterranean Sacoglossan *Placida dendritica*'. *Journal of natural products,* 66 (10), pp.1399-1401.

da Graça Sgarbi, D., da Silva, A., Carlos, I., Silva, C., Angluster, J. & Alviano, C. (1997) 'Isolation of ergosterol peroxide and its reversion to ergosterol in the pathogenic fungus *Sporothrix schenckii*'. *Mycopathologia,* 139 (1), pp.9-14.

de Souza, W. & Rodrigues, J.C.F. (2009) 'Sterol biosynthesis pathway as target for anti-trypanosomatid drugs'. *Interdisciplinary perspectives on infectious diseases,* 2009.

Demuth, H., Jensen, S.R. & Nielsen, B.J. (1989) 'Iridoid glucosides from *Asystasia bella*'. *Phytochemistry,* 28 (12), pp.3361-3364.

Devaux, P., Horning, M. & Horning, E. (1971) 'Benzyloxime derivatives of steroids. A new metabolic profile procedure for human urinary steroids human urinary steroids'. *Analytical Letters,* 4 (3), pp.151-160.

Devys, M., Barbier, M., Bousquet, J.-F. & Kollmann, A. (1994) 'Isolation of the (−)-(3R)-5-hydroxymellein from the fungus *Septoria nodorum*'. *Phytochemistry,* 35 (3), pp.825-826.

Dhakal, R.C., Rajbhandari, M., Kalauni, S.K., Awale, S. & Gewali, M.B. (2009) 'Phytochemical Constituents of the Bark of *Vitex negundo* L'. *Journal of Nepal Chemical Society,* 23 pp.89-92.

Dhanapal, A.P. & Govindaraj, M. (2015) 'Unlimited Thirst for Genome Sequencing, Data Interpretation, and Database Usage in Genomic Era: The Road towards Fast-Track Crop Plant Improvement'. *Genetics Research International,* 2015 pp.684321.

Djoukeng, J.D., Polli, S., Larignon, P. & Abou-Mansour, E. (2009) 'Identification of phytotoxins from *Botryosphaeria obtusa*, a pathogen of black dead arm disease of grapevine'. *European journal of plant pathology,* 124 (2), pp.303-308.

Docampo, R., Cruz, F.S., Boveris, A., Muniz, R.P.A. & Esquivel, D.M.S. (1978) 'Lipid peroxidation and the generation of free radicals, superoxide anion, and

hydrogen peroxide in β-lapachone-treated *Trypanosoma cruzi* epimastigotes'. *Archives of Biochemistry and Biophysics,* 186 (2), pp.292-297.

Docampo, R., Lopes, J.N., Cruz, F.S. & Souza, W. (1977) '*Trypanosoma cruzi*: ultrastructural and metabolic alterations of epimastigotes by beta-lapachone'. *Exp Parasitol,* 42 (1), pp.142-149.

Donia, M. & Hamann, M.T. (2003) 'Marine natural products and their potential applications as anti-infective agents'. *The Lancet infectious diseases,* 3 (6), pp.338-348.

Doroshow, J.H., Akman, S., Chu, F.-F. & Esworthy, S. (1990) 'Role of the glutathione-glutathione peroxidase cycle in the cytotoxicity of the anticancer quinones'. *Pharmacology & Therapeutics,* 47 (3), pp.359-370.

Du, L., Zhu, T., Fang, Y., Liu, H., Gu, Q. & Zhu, W. (2007) 'Aspergiolide A, a novel anthraquinone derivative with naphtho[1,2,3-de]chromene-2,7-dione skeleton isolated from a marine-derived fungus *Aspergillus glaucus*'. *Tetrahedron,* 63 (5), pp.1085-1088.

Duarte, M.d.L.R. & Archer, S.A. (2003) 'In vitro toxin production by *Fusarium solani* f. sp. piperis'. *Fitopatologia Brasileira,* 28 (3), pp.229-235.

Duke, N.C., Ball, M. & Ellison, J. (1998) 'Factors influencing biodiversity and distributional gradients in mangroves'. *Global Ecology & Biogeography Letters,* 7 (1), pp.27-47.

Duke, N.C. & Pinzon, S.M. (1992) 'Ageing Rhizophora seedlings from leaf scar nodes: A technique for studying recruitment and growth in mangrove forests'. *Biotropica,* 24 (29), pp.173-118.

Dumas, M. & Bisser, S. (1999) '*Clinical aspects of human African trypanosomiasis'. Progress in human African trypanosomiasis, sleeping sickness.* Springer, pp. 215-233.

Dwiarti, L., Yamane, K., Yamatani, H., Kahar, P. & Okabe, M. (2002) 'Purification and characterization of cis-aconitic acid decarboxylase from *Aspergillus terreus* TN484-M1'. *J Biosci Bioeng,* 94 (1), pp.29-33.

Evidente, A., Punzo, B., Andolfi, A., Cimmino, A., Melck, D. & Luque, J. (2010) 'Lipophilic phytotoxins produced by *Neofusicoccum parvum*, a grapevine canker agent'. *Phytopathologia Mediterranea,* 49 (1), pp.74-79.

Fauvel, M.-t., Bon, M., Moulis, C., Fourasté, I. & Crasnier, F. (1999) 'Megastigmane and Iridoid glucosides from *Avicennia Germinans*: Two Isomeric Forms of an Iridoid'. *Natural Product Letters,* 14 (2), pp.99-106.

Fauvel, M.-t., Bousquet-Melou, A., Moulis, C., Gleye, J. & Jensen, S.R. (1995) 'Iridoid glucosides from *Avicennia germinans*'. *Phytochemistry,* 38 (4), pp.893-894.

Fauvel, M.-t., Moulis, C., Bon, M. & Fourasté, I. (1997) 'A New Iridoid Glucoside from African *Avicennia Germinans*'. *Natural Product Letters,* 10 (2), pp.139-142.

Fauvel, M.-t., Taoubi, K., Gleye, J. & Fouraste, I. (1993) 'Phenylpropanoid glycosides from *Avicennia marina*'. *Planta medica,* 59 (4).

Feng, Y., Li, X.M., Duan, X.J. & Wang, B.G. (2006) 'Iridoid glucosides and flavones from the aerial parts of *Avicennia marina*'. *Chem Biodivers,* 3 (7), pp.799-806.

Feng, Z., Nenkep, V., Yun, K., Zhang, D., Choi, H.D., Kang, J.S. & Son, B.W. (2010) 'Biotransformation of bioactive (-)-mellein by a marine isolate of bacterium *Stappia* sp'. *Journal of microbiology and biotechnology,* 20 (6), pp.985-987.

Fiehn, O. (2001) 'Combining genomics, metabolome analysis, and biochemical modelling to understand metabolic networks'. *Comparative and functional genomics,* 2 (3), pp.155-168.

Findlay, J.A., Buthelezi, S., Lavoie, R., Peña-Rodriguez, L. & Miller, J.D. (1995) 'Bioactive Isocoumarins and Related Metabolites from Conifer Endophytes'. *Journal of Natural Products,* 58 (11), pp.1759-1766.

Fragopoulou, E., Nomikos, T., Karantonis, H.C., Apostolakis, C., Pliakis, E., Samiotaki, M., Panayotou, G. & Antonopoulou, S. (2007) 'Biological activity of acetylated phenolic compounds'. *J Agric Food Chem,* 55 (1), pp.80-89.

Franck, B. (1980) 'The Biosynthesis of the Ergochromes, in The Biosynthesis of Mycotoxins: A Study in Secondary Metabolism (Ed.: P. S. Steyn)'. *Academic Press, New York,* pp.157 – 191.

Freitas, R.F., Prokopczyk, I.M., Zottis, A., Oliva, G., Andricopulo, A.D., Trevisan, M.T.S., Vilegas, W., Silva, M.G.V. & Montanari, C.A. (2009) 'Discovery of novel *Trypanosoma cruzi* glyceraldehyde-3-phosphate dehydrogenase inhibitors'. *Bioorganic & Medicinal Chemistry,* 17 (6), pp.2476-2482.

Frisvad, J.C., Smedsgaard, J., Larsen, T.O. & Samson, R.A. (2004) 'Mycotoxins, drugs and other extrolites produced by species in *Penicillium subgenus* Penicillium'. *Stud Mycol,* 49 pp.201-241.

Fuchser, J. & Zeeck, A. (1997) 'Secondary Metabolites by Chemical Screening, 34.– Aspinolides and Aspinonene/Aspyrone Co-Metabolites, New Pentaketides Produced by *Aspergillus ochraceus*'. *Liebigs Annalen,* 1997 (1), pp.87-95.

Fukuda, T., Arai, M., Yamaguchi, Y., Masuma, R., Tomoda, H. & Omura, S. (2004) 'New beauvericins, potentiators of antifungal miconazole activity, Produced by *Beauveria* sp. FKI-1366. I. Taxonomy, fermentation, isolation and biological properties'. *The Journal of antibiotics,* 57 (2), pp.110-116.

Gachet, M.S., Kunert, O., Kaiser, M., Brun, R., Zehl, M., Keller, W., Muñoz, R.A., Bauer, R. & Schuehly, W. (2011) 'Antiparasitic Compounds from *Cupania cinerea* with Activities against *Plasmodium falciparum* and *Trypanosoma brucei rhodesiense*'. *Journal of Natural Products,* 74 (4), pp.559-566.

Gai, Y., Zhao, L.L., Hu, C.Q. & Zhang, H.P. (2007) 'Fusarielin E, a new antifungal antibiotic from *Fusarium* sp'. *Chinese Chemical Letters,* 18 (8), pp.954-956.

Ganapaty, S., Steve Thomas, P., Karagianis, G., Waterman, P.G. & Brun, R. (2006) 'Antiprotozoal and cytotoxic naphthalene derivatives from *Diospyros assimilis*'. *Phytochemistry,* 67 (17), pp.1950-1956.

Ganapaty, S., Thomas, P.S., Mallika, B.N., Balaji, S., Karagianis, G. & Waterman, P.G. (2005) 'Dimeric naphthoquinones from *Diospyros discolor*'. *Biochemical Systematics and Ecology,* 33 (3), pp.313-315.

Gao, C., Yi, X., Xie, W., Chen, Y., Xu, M., Su, Z., Yu, L. & Huang, R. (2014) 'New Antioxidative Secondary Metabolites from the Fruits of a Beibu Gulf Mangrove, *Avicennia marina*'. *Marine Drugs,* 12 (8), pp.4353-4360.

Gao, K., Xu, A., Krul, C., Venema, K., Liu, Y., Niu, Y., Lu, J., Bensoussan, L., Seeram, N.P., Heber, D. & Henning, S.M. (2006) 'Of the Major Phenolic

Acids Formed during Human Microbial Fermentation of Tea, Citrus, and Soy Flavonoid Supplements, Only 3,4-Dihydroxyphenylacetic Acid Has Antiproliferative Activity'. *The Journal of Nutrition,* 136 (1), pp.52-57.

Garson, M.J., Staunton, J. & Jones, P.G. (1984) 'New polyketide metabolites from *Aspergillus melleus*: structural and stereochemical studies'. *Journal of the Chemical Society, Perkin Transactions 1,* pp.1021-1026.

Gatenbeck, S. & Bentley, R. (1965) 'Naphthaquinone biosynthesis in moulds: the mechanism for formation of javanicin'. *Biochemical Journal,* 94 (2), pp.478-481.

Gezahgne, A., Yirgu, A. & Kassa, H. (2014) 'First report of *Lasiodiplodia theobromae* causing canker on tapped Boswellia papyrifera trees in Ethiopia'. *New Disease Reports,* 29.

Ghareib, H.R.A., Abdelhamed, M.S. & Ibrahim, O.H. (2010) 'Antioxidative effects of the acetone fraction and vanillic acid from *Chenopodium murale* on tomato plants'. *Weed biology and management,* 10 (1), pp.64-72.

Ghosh, A., Misra, S., Dutta, A.K. & Choudhury, A. (1985) 'Pentacyclic triterpenoids and sterols from seven species of mangrove'. *Phytochemistry,* 24 (8), pp.1725-1727.

Gilardoni, G., Clericuzio, M., Marchetti, A., Finzi, P.V., Zanoni, G. & Vidari, G. (2006) 'New Oxidized 4-Oxo Fatty Acids from *Hygrophorus discoxanthus*'. *Natural product communications,* 1 (12), pp.1079-1084.

Gopalakrishnan, S. (2004) *Toxigenicity of Fusarium species causing wilt of chickpea.* University College London.

Gris, E.F., Mattivi, F., Ferreira, E.A., Vrhovsek, U., Filho, D.W., Pedrosa, R.C. & Bordignon-Luiz, M.T. (2011) 'Stilbenes and tyrosol as target compounds in the assessment of antioxidant and hypolipidemic activity of *Vitis vinifera* red wines from southern Brazil'. *J Agric Food Chem,* 59 (14), pp.7954-7961.

Grotewold, E. (2005) 'Plant metabolic diversity: a regulatory perspective'. *Trends in plant science,* 10 (2), pp.57-62.

Grove, J.F. (1985) 'Metabolic products of *Phomopsis oblonga*. Part 2. Phomopsolide A and B, tiglic esters of two 6-substituted 5, 6-dihydro-5-hydroxypyran-2-ones'. *Journal of the Chemical Society, Perkin Transactions 1,* pp.865-869.

Grove, J.F. & Pople, M. (1979) 'Metabolic products of *Fusarium larvarum* fuckel. The fusarentins and the absolute configuration of monocerin'. *Journal of the Chemical Society, Perkin Transactions 1,* pp.2048-2051.

Grove, J.F. & Pople, M. (1980) 'The insecticidal activity of beauvericin and the enniatin complex'. *Mycopathologia,* 70 (2), pp.103-105.

Guinez, R.F., Matos, M.J., Vazquez-Rodriguez, S., Santana, L., Uriarte, E., Olea-Azar, C. & Maya, J.D. (2013) 'Synthesis and evaluation of antioxidant and trypanocidal properties of a selected series of coumarin derivatives'. *Future Med Chem,* 5 (16), pp.1911-1922.

Guo, Z., She, Z., Shao, C., Wen, L., Liu, F., Zheng, Z. & Lin, Y. (2007) '^{1}H and ^{13}C NMR signal assignments of Paecilin A and B, two new chromone derivatives from mangrove endophytic fungus *Paecilomyces* sp.(tree 1–7)'. *Magnetic resonance in chemistry,* 45 (9), pp.777-780.

Gurnani, N., Mehta, D., Gupta, M. & Mehta, B. (2014) 'Natural Products: Source of Potential Drugs'. *African Journal of Basic & Applied Sciences,* 6 (6), pp.171-186.

Gutierrez-Lugo, M.-T., Woldemichael, G.M., Singh, M.P., Suarez, P.A., Maiese, W.M., Montenegro, G. & Timmermann, B.N. (2005) 'Isolation of three new naturally occurring compounds from the culture of *Micromonospora* sp. P1068'. *Natural Product Research,* 19 (7), pp.645-652.

Guzmán-López, O., Trigos, A., Fernández, F.J., de Jesús Yañez-Morales, M. & Saucedo-Castaneda, G. (2007) 'Tyrosol and tryptophol produced by *Ceratocystis adiposa*'. *World Journal of Microbiology and Biotechnology,* 23 (10), pp.1473-1477.

Haefner, B. (2003) 'Drugs from the deep: marine natural products as drug candidates'. *Drug discovery today,* 8 (12), pp.536-544.

Hamdan, O. (2012) *Status of mangroves in Peninsular Malaysia.* Forest Research Institute Malaysia.

Hameed, T.K. & Robinson, J.L. (2002) 'Review of the use of cephalosporins in children with anaphylactic reactions from penicillins'. *The Canadian Journal of Infectious Diseases,* 13 (4), pp.253-258.

Hamill, R.L., Higgens, C., Boaz, H. & Gorman, M. (1969) 'The structure op beauvericin, a new depsipeptide antibiotic toxic to *Artemia salina*'. *Tetrahedron Letters,* 10 (49), pp.4255-4258.

Han, L., Huang, X., Dahse, H.M., Moellmann, U., Fu, H., Grabley, S., Sattler, I. & Lin, W. (2007) 'Unusual naphthoquinone derivatives from the twigs of *Avicennia marina*'. *J Nat Prod,* 70 (6), pp.923-927.

Harada, M. (1974) 'Phlogistic Activity of Secalonic Acid A'.

Harvey, A.L., Edrada-Ebel, R. & Quinn, R.J. (2015) 'The re-emergence of natural products for drug discovery in the genomics era'. *Nature Reviews Drug Discovery,* 14 (2), pp.111-129.

Hashimoto, J., Motohashi, K., Sakamoto, K., Hashimoto, S., Yamanouchi, M., Tanaka, H., Takahashi, T., Takagi, M. & Shin-ya, K. (2009) 'Screening and evaluation of new inhibitors of hepatic glucose production'. *J Antibiot,* 62 (11), pp.625-629.

Hawksworth, D.L. (1991) 'The fungal dimension of biodiversity: magnitude, significance, and conservation'. *Mycological Research,* 95 (6), pp.641-655.

Heiser, I., Osswald, W., Baker, R., Nemec, S. & Elstner, E.F. (1998) 'Activation of Fusarium naphthazarin toxins and other p-quinones by reduced thioctic acid'. *Journal of Plant Physiology,* 153 (3–4), pp.276-280.

Hernández-Chávez, I., Torres-Tapia, L.W., Simá-Polanco, P., Cedillo-Rivera, R., Moo-Puc, R. & Peraza-Sánchez, S.R. (2012) 'Antigiardial activity of *Cupania dentata* bark and its constituents'. *Journal of the Mexican Chemical Society,* 56 (2), pp.105-108.

Hirai, K.-I., Koyama, J., Pan, J., Simamura, E., Shimada, H., Yamori, T., Sato, S., Tagahara, K. & Tsuruo, T. (1998) 'Furanonaphthoquinone analogs possessing preferential antitumor activity compared to normal cells'. *Cancer detection and prevention,* 23 (6), pp.539-550.

Hirata, Y. & Uemura, D. (1986) 'Halichondrins-antitumor polyether macrolides from a marine sponge'. *Pure and Applied Chemistry,* 58 (5), pp.701-710.

Hoet, S., Pieters, L., Muccioli, G.G., Habib-Jiwan, J.-L., Opperdoes, F.R. & Quetin-Leclercq, J. (2007) 'Antitrypanosomal activity of triterpenoids and sterols from the leaves of *Strychnos spinosa* and related compounds'. *Journal of natural products,* 70 (8), pp.1360-1363.

Holker, J.S. & Simpson, T.J. (1981) 'Studies on fungal metabolites. Part 2. Carbon-13 nuclear magnetic resonance biosynthetic studies on pentaketide metabolites of *Aspergillus melleus*: 3-(1, 2-epoxypropyl)-5, 6-dihydro-5-hydroxy-6-methylpyran-2-one and mellein'. *Journal of the Chemical Society, Perkin Transactions 1,* pp.1397-1400.

Hong, R. (2011) 'Secalonic acid D as a novel DNA topoisomerase I inhibitor from marine lichen-derived fungus *Gliocladium* sp. T31'. *Pharm Biol,* 49 (8), pp.796-799.

Horning, E. & Horning, M. (1970) 'Metabolic profiles: chromatographic methods for isolation and characterization of a variety of metabolites in man'. *Methods in medical research,* 12 pp.369.

Hotez, P.J., Molyneux, D.H., Fenwick, A., Kumaresan, J., Sachs, S.E., Sachs, J.D. & Savioli, L. (2007) 'Control of neglected tropical diseases'. *New England Journal of Medicine,* 357 (10), pp.1018-1027.

Huang, Y., Zhao, J., Zhou, L., Wang, M., Wang, J., Li, X. & Chen, Q. (2009) 'Antimicrobial compounds from the endophytic fungus *Fusarium* sp. Ppf4 isolated from the medicinal plant *Paris polyphylla* var. yunnanensis'. *Natural product communications,* 4 (11), pp.1455-1458.

Hussain, H., Krohn, K., Ahmad, V.U., Miana, G.A. & Green, I.R. (2007) 'Lapachol: an overview'. *Arkivoc,* 2 pp.145-171.

Hussain, H., Krohn, K., Schulz, B., Draeger, S., Nazir, M. & Saleem, M. (2012) 'Two new antimicrobial metabolites from the endophytic fungus, *Seimatosporium* sp'. *Nat Prod Commun,* 7 (3), pp.293-294.

Huyck, T.K., Gradishar, W., Manuguid, F. & Kirkpatrick, P. (2011) 'Eribulin mesylate'. *Nature Reviews Drug Discovery,* 10 (3), pp.173-174.

Hwang, B.K., Lim, S.W., Kim, B.S., Lee, J.Y. & Moon, S.S. (2001) 'Isolation and In Vivo and In Vitro Antifungal Activity of Phenylacetic Acid and Sodium Phenylacetate from *Streptomyces humidus*'. *Applied and Environmental Microbiology,* 67 (8), pp.3739-3745.

Hyde, K. & Soytong, K. (2008) 'The fungal endophyte dilemma'. *Fungal Divers,* 33 pp.163-173.

Ibrahim, Z.Z., Arshad, A., Chong, L.S., Bujang, J.S., Theem, L.A., Abdullah, N.M.R. & Marghany, M.M. (2000) 'East Coast of Peninsular Malaysia'. *Seas at the millennium - an environmental evaluation - Volume 2,* pp.345-359.

Ishii, K., Sakai, K., Ueno, Y., Tsunoda, H. & Enomoto, M. (1971) 'Solaniol, a toxic metabolite of *Fusarium solani*'. *Applied microbiology,* 22 (4), pp.718.

Ismail, A., Cirvilleri, G., Polizzi, G., Crous, P., Groenewald, J. & Lombard, L. (2012) 'Lasiodiplodia species associated with dieback disease of mango (*Mangifera indica*) in Egypt'. *Australasian Plant Pathology,* 41 (6), pp.649-660.

Ito, C., Katsuno, S., Kondo, Y., Tan, H.T. & Furukawa, H. (2000) 'Chemical constituents of *Avicennia alba*. Isolation and structural elucidation of new

naphthoquinones and their analogues'. *Chem Pharm Bull (Tokyo),* 48 (3), pp.339-343.

Ito, C., Kondo, Y., Rao, K.S., Tokuda, H., Nishino, H. & Furukawa, H. (1999) 'Chemical constituents of *Glycosmis pentaphylla*. Isolation of a novel naphthoquinone and a new acridone alkaloid'. *Chem. Pharm. Bull,* 47 (11), pp.1579-1581.

Jacobs, R.T., Nare, B. & Phillips, M.A. (2011) 'State of the art in African trypanosome drug discovery'. *Curr Top Med Chem,* 11 (10), pp.1255-1274.

Janse van Rensburg, J., Labuschagne, N. & Nemec, S. (2001) 'Occurrence of Fusarium-produced naphthazarins in citrus trees and sensitivity of rootstocks to isomarticin in relation to citrus blight'. *Plant pathology,* 50 (2), pp.258-265.

Jimeno, J.M. (2002) 'A clinical armamentarium of marine-derived anti-cancer compounds'. *Anti-Cancer Drugs,* 13 pp.S15-S19.

Jiménez-Romero, C., Ortega-Barría, E., Arnold, A.E. & Cubilla-Rios, L. (2008) 'Activity against *Plasmodium falciparum* of lactones isolated from the endophytic fungus *Xylaria* sp'. *Pharmaceutical Biology,* 46 (10-11), pp.700-703.

Jong, S.-C. & Donovick, R. (1989) 'Antitumor and antiviral substances from fungi'. *Advances in Applied Microbiology,* 34 pp.183.

Jow, G.-M., Chou, C.-J., Chen, B.-F. & Tsai, J.-H. (2004) 'Beauvericin induces cytotoxic effects in human acute lymphoblastic leukemia cells through cytochrome c release, caspase 3 activation: the causative role of calcium'. *Cancer letters,* 216 (2), pp.165-173.

Kathiresan, K. & Bingham, B.L. (2001) 'Biology of mangroves and mangrove ecosystems'. *Advances in marine biology,* 40 pp.81-251.

Khanzada, M., Lodhi, A.M. & Shahzad, S. (2004) 'Pathogenicity of *Lasiodiplodia theobromae* and *Fusarium solani* on mango'. *Pakistan journal of Botany,* 36 (1), pp.181-190.

Khanzada, M., Lodhi, A.M. & Shahzad, S. (2005) 'Chemical control of *Lasiodiplodia theobromae*, the causal agent of mango decline in Sindh'. *Pakistan Journal of Botany,* 37 (4), pp.1023.

Kharwar, R., Verma, V., Kumar, A., Gond, S., Harper, J., Hess, W., Lobkovosky, E., Ma, C., Ren, Y. & Strobel, G. (2009) 'Javanicin, an Antibacterial Naphthaquinone from an Endophytic Fungus of Neem, *Chloridium sp*'. *Current Microbiology,* 58 (3), pp.233-238.

Khatib, A., Wilson, E.G., Kim, H.K., Lefeber, A.W., Erkelens, C., Choi, Y.H. & Verpoorte, R. (2006) 'Application of two-dimensional J-resolved nuclear magnetic resonance spectroscopy to differentiation of beer'. *Analytica chimica acta,* 559 (2), pp.264-270.

Khoon, G.W. (1987) 'P. B. Tomlinson 1986. The botany of mangroves. Cambridge University Press, Cambridge. 413 pages.'. *Journal of Tropical Ecology,* 3 (02), pp.188-189.

Khraiwesh, M.H., Lee, C.M., Brandy, Y., Akinboye, E.S., Berhe, S., Gittens, G., Abbas, M.M., Ampy, F.R., Ashraf, M. & Bakare, O. (2012) 'Antitrypanosomal activities and cytotoxicity of some novel imidosubstituted

1, 4-naphthoquinone derivatives'. *Archives of pharmacal research,* 35 (1), pp.27-33.

Kijjoa, A. & Sawangwong, P. (2004) 'Drugs and cosmetics from the sea'. *Marine Drugs,* 2 (2), pp.73-82.

Kim, H.K., Choi, Y.H. & Verpoorte, R. (2011) 'NMR-based plant metabolomics: where do we stand, where do we go?'. *Trends in biotechnology,* 29 (6), pp.267-275.

Kim, H.K. & Verpoorte, R. (2010) 'Sample preparation for plant metabolomics'. *Phytochemical Analysis,* 21 (1), pp.4-13.

Kim, Y., Cho, J.-Y., Kuk, J.-H., Moon, J.-H., Cho, J.-I., Kim, Y.-C. & Park, K.-H. (2004) 'Identification and antimicrobial activity of phenylacetic acid produced by *Bacillus licheniformis* isolated from fermented soybean, Chungkook-Jang'. *Current microbiology,* 48 (4), pp.312-317.

Kimura, Y., Shimada, A., Nakajima, H. & Hamasaki, T. (1988) 'Structures of Naphthoquinones Produced by the Fungus, *Fusarium* sp., and Their Biological Activity toward Pollen Germination'. *Agricultural and Biological Chemistry,* 52 (5), pp.1253-1259.

Kitaoka, N., Nabeta, K. & Matsuura, H. (2009) 'Isolation and structural elucidation of a new cyclohexenone compound from *Lasiodiplodia theobromae*'. *Bioscience, biotechnology, and biochemistry,* 73 (8), pp.1890-1892.

Kobayashi, M., Krishna, M.M., Ishida, K. & Anjaneyulu, V. (1992) 'Marine Sterols. XXII. Occurrence of 3-Oxo-4, 6, 8(14)-triunsaturated Steroids in the Sponge *Dysidea herbacea*'. *Chemical & Pharmaceutical Bulletin,* 40 (1), pp.72-74.

Kobayashi, M., Shimizu, N., Kitagawa, I., Kyogoku, Y., Harada, N. & Uda, H. (1985) 'Absolute stereostructures of halenaquinol and halenaquinol sulfate, pentacyclic hydroquinones from the Okinawan marine sponge *Xestospongia sapra*, as determined by theoretical calculation of CD spectra'. *Tetrahedron letters,* 26 (32), pp.3833-3836.

Koehn, F.E. & Carter, G.T. (2005) 'The evolving role of natural products in drug discovery'. *Nat Rev Drug Discov,* 4 (3), pp.206-220.

Kong, D.-X., Jiang, Y.-Y. & Zhang, H.-Y. (2010) 'Marine natural products as sources of novel scaffolds: Achievement and concern'. *Drug discovery today,* 15 (21), pp.884-886.

Kraft, F. (1906) 'Ueber das Mutterkorn'. *Archiv der Pharmazie,* 244 (4-5), pp.336-359.

Krohn, K., Kock, I., Elsässer, B., Flörke, U., Schulz, B., Draeger, S., Pescitelli, G., Antus, S. & Kurtán, T. (2007) 'Bioactive Natural Products from the Endophytic Fungus *Ascochyta* sp. from *Meliotus dentatus*–Configurational Assignment by Solid-State CD and TDDFT Calculations'. *European journal of organic chemistry,* 2007 (7), pp.1123-1129.

Krohn, K., Kouam, S.F., Kuigoua, G.M., Hussain, H., Cludius-Brandt, S., Flörke, U., Kurtán, T., Pescitelli, G., Di Bari, L., Draeger, S. & Schulz, B. (2009) 'Xanthones and Oxepino[2, 3-b]chromones from Three Endophytic Fungi'. *Chemistry – A European Journal,* 15 (44), pp.12121-12132.

Krohn, K., Michel, A., Römer, E., Flörke, U., Aust, H.-J., Draeger, S., Schulz, B. & Wray, V. (1995) 'Biologically Active Metabolites from Fungi 61);

Phomosines AC Three New Biaryl Ethers from *Phomopsis* sp'. *Natural Product Letters,* 6 (4), pp.309-314.

Krug, D., Zurek, G., Revermann, O., Vos, M., Velicer, G.J. & Müller, R. (2008) 'Discovering the hidden secondary metabolome of *Myxococcus xanthus*: a study of intraspecific diversity'. *Applied and environmental microbiology,* 74 (10), pp.3058-3068.

Kuo, C.-F., Hsieh, C.-H. & Lin, W.-Y. (2011) 'Proteomic response of LAP-activated RAW 264.7 macrophages to the anti-inflammatory property of fungal ergosterol'. *Food Chemistry,* 126 (1), pp.207-212.

Kuria, K.A., Chepkwony, H., Govaerts, C., Roets, E., Busson, R., de Witte, P., Zupko, I., Hoornaert, G., Quirynen, L. & Maes, L. (2002) 'The Antiplasmodial Activity of Isolates from *Ajuga remota*'. *Journal of natural products,* 65 (5), pp.789-793.

Kurobane, I., Iwahashi, S. & Fukuda, A. (1986) 'Cytostatic activity of naturally isolated isomers of secalonic acids and their chemically rearranged dimers'. *Drugs under experimental and clinical research,* 13 (6), pp.339-344.

Kurobane, I., Vining, L.C. & McInnes, A.G. (1978) 'A new secalonic acid. Linkage between tetrahydroxanthone units determined from deuterium isotope 13C chemical shifts'. *Tetrahedron Letters,* 19 (47), pp.4633-4636.

König, G. & Rimpler, H. (1985) 'Iridoid glucosides in *Avicennia marina*'. *Phytochemistry,* 24 (6), pp.1245-1248.

König, G., Rimpler, H. & Hunkler, D. (1987) 'Iridoid glucosides in *Avicennia officinalis*'. *Phytochemistry,* 26 (2), pp.423-427.

Ladame, S., Castilho, M.S., Silva, C.H., Denier, C., Hannaert, V., Perie, J., Oliva, G. & Willson, M. (2003) 'Crystal structure of *Trypanosoma cruzi* glyceraldehyde-3-phosphate dehydrogenase complexed with an analogue of 1,3-bisphospho-d-glyceric acid'. *Eur J Biochem,* 270 (22), pp.4574-4586.

Lagunes, I. & Trigos, Á. (2015) 'Photo-oxidation of ergosterol: Indirect detection of antioxidants photosensitizers or quenchers of singlet oxygen'. *Journal of Photochemistry and Photobiology B: Biology,* 145 pp.30-34.

Li, K.-K., Lu, Y.-J., Song, X.-H., She, Z.-G., Wu, X.-W., An, L.-K., Ye, C.-X. & Lin, Y.-C. (2010) 'The metabolites of mangrove endophytic fungus Zh6-B1 from the South China Sea'. *Bioorganic & medicinal chemistry letters,* 20 (11), pp.3326-3328.

Li, P., Takahashi, K., Matsuura, H. & Yoshihara, T. (2005a) 'Novel potato micro-tuber-inducing compound,(3 R, 6 S)-6-hydroxylasiodiplodin, from a strain of *Lasiodiplodia theobromae*'. *Bioscience, biotechnology, and biochemistry,* 69 (8), pp.1610-1612.

Li, P., Takei, R., Takahashi, K. & Nabeta, K. (2007) 'Biosynthesis of theobroxide and its related compounds, metabolites of *Lasiodiplodia theobromae*'. *Phytochemistry,* 68 (6), pp.819-823.

Li, Y., Song, Y., Liu, J., Ma, Y. & Tan, R. (2005b) 'Anti-Helicobacter pylori substances from endophytic fungal cultures'. *World Journal of Microbiology and Biotechnology,* 21 (4), pp.553-558.

Lichter *et al.* (1972) 'Worthen LW, ed. "Food-drugs from the sea. Proc: Aug 20–23, 1972."'. *Marine Tech Soc.,* (173), pp.117-127.

Lin, Y., Wu, X., Feng, S., Jiang, G., Zhou, S., Vrijmoed, L. & Jones, E. (2001) 'A novel cinnamoylcyclopeptide containing an allenic ether from the fungus *Xylaria* sp.(strain# 2508) from the South China Sea'. *Tetrahedron Letters,* 42 (3), pp.449-451.

Liu, D., Li, X.M., Meng, L., Li, C.S., Gao, S.S., Shang, Z., Proksch, P., Huang, C.G. & Wang, B.G. (2011) 'Nigerapyrones A-H, alpha-pyrone derivatives from the marine mangrove-derived endophytic fungus *Aspergillus niger* MA-132'. *J Nat Prod,* 74 (8), pp.1787-1791.

Liu, X., Xu, F., Zhang, Y., Liu, L., Huang, H., Cai, X., Lin, Y. & Chan, W. (2006) 'Xyloketal H from the mangrove endophytic fungus *Xylaria* sp. 2508'. *Russian chemical bulletin,* 55 (6), pp.1091-1092.

Logrieco, A., Moretti, A., Castella, G., Kostecki, M., Golinski, P., Ritieni, A. & Chelkowski, J. (1998) 'Beauvericin Production by *Fusarium* Species'. *Applied and Environmental Microbiology,* 64 (8), pp.3084-3088.

Lu, H., Zou, W.X., Meng, J.C., Hu, J. & Tan, R.X. (2000) 'New bioactive metabolites produced by *Colletotrichum* sp., an endophytic fungus in *Artemisia annua*'. *Plant science,* 151 (1), pp.67-73.

Lübken, T., Schmidt, J., Porzel, A., Arnold, N. & Wessjohann, L. (2004) 'Hygrophorones A–G: fungicidal cyclopentenones from *Hygrophorus* species (Basidiomycetes)'. *Phytochemistry,* 65 (8), pp.1061-1071.

Macintyre, L., Zhang, T., Viegelmann, C., Martinez, I., Cheng, C., Dowdells, C., Abdelmohsen, U., Gernert, C., Hentschel, U. & Edrada-Ebel, R. (2014) 'Metabolomic Tools for Secondary Metabolite Discovery from Marine Microbial Symbionts'. *Marine Drugs,* 12 (6), pp.3416-3448.

Macnae, W. (1968) 'A general account of a fauna and flora of mangrove swamps and forest in the Indo-Pacific region'. *Advances in Marine Biology,* (6), pp.73-270.

Magadula, J.J. & Erasto, P. (2009) 'Bioactive natural products derived from the East African flora'. *Natural product reports,* 26 (12), pp.1535-1554.

Mahera, S.A., Ahmad, V.U., Saifullah, S.M., Mohammad, F.V. & Ambreen, K. (2011) 'Steroids and Triterpenoids from Grey Mangrove *Avicennia Marina*'. *Pakistan Journal of Botany,* 43 (2), pp.1417-1422.

Majumdar, S.G. & Ghosh, P. (1979) 'Chemical investigation on some mangroves species. 1. Genus Avicennia'. *Journal of the Indian Chemical Society,* 56 (1), pp.111-113.

Majumdar, S.G., Ghosh, P. & Thakur, S. (1981) Velutin from *Avicennia Officinalis Linn.* Council of Scientific and Industrial Research.

Martin, T.S., Kikuzaki, H., Hisamoto, M. & Nakatani, N. (2000) 'Constituents of *Amomum tsao-ko* and their radical scavenging and antioxidant activities'. *Journal of the American Oil Chemists' Society,* 77 (6), pp.667-673.

Masters, K.-S. & Bräse, S. (2012) 'Xanthones from fungi, lichens, and bacteria: the natural products and their synthesis'. *Chemical reviews,* 112 (7), pp.3717-3776.

Matovu, E., Geiser, F., Schneider, V., Mäser, P., Enyaru, J.C., Kaminsky, R., Gallati, S. & Seebeck, T. (2001) 'Genetic variants of the TbAT1 adenosine transporter from African trypanosomes in relapse infections following melarsoprol therapy'. *Molecular and biochemical parasitology,* 117 (1), pp.73-81.

Matsui, T., Ito, C., Oda, M., Itoigawa, M., Yokoo, K., Okada, T. & Furukawa, H. (2011) 'Lapachol suppresses cell proliferation and secretion of interleukin-6 and plasminogen activator inhibitor-1 of fibroblasts derived from hypertrophic scars'. *Journal of Pharmacy and Pharmacology,* 63 (7), pp.960-966.

Matsuura, H., Nakamori, K., Omer, E., Hatakeyama, C., Yoshihara, T. & Ichihara, A. (1998) 'Three lasiodiplodins from *Lasiodiplodia theobromae* IFO 31059'. *Phytochemistry,* 49 (2), pp.579-584.

Mawa, S. & Said, I.M. (2012) 'Chemical constituents of *Garcinia prainiana*'. *Sains Malaysiana,* 41 (5), pp.585-590.

Mayer, A.M., Glaser, K.B., Cuevas, C., Jacobs, R.S., Kem, W., Little, R.D., McIntosh, J.M., Newman, D.J., Potts, B.C. & Shuster, D.E. (2010) 'The odyssey of marine pharmaceuticals: a current pipeline perspective'. *Trends in pharmacological sciences,* 31 (6), pp.255-265.

Meca, G., Sospedra, I., Soriano, J., Ritieni, A., Moretti, A. & Mañes, J. (2010) 'Antibacterial effect of the bioactive compound beauvericin produced by *Fusarium proliferatum* on solid medium of wheat'. *Toxicon,* 56 (3), pp.349-354.

Medentsev, A., Baskunov, B. & Akimenko, V. (1988) 'Formation of naphthoquinone pigments by the fungus *Fusarium decemcellulare* and their influence on the oxidative metabolism of the producer'. *Biochemistry (USA).*

Melo, I.S.d. & Piccinin, E. (1999) 'Toxic metabolites from culture filtrate of *Fusarium oxysporum* and its effects on cucumber cells and plantlets'. *Revista de microbiologia,* 30 (2), pp.104-106.

Meza-Menchaca, T., Suarez-Medellin, J., Del Angel-Pina, C. & Trigos, A. (2015) 'The Amoebicidal Effect of Ergosterol Peroxide Isolated from *Pleurotus ostreatus*'. *Phytother Res.*

Miersch, O., Bohlmann, H. & Wasternack, C. (1999) 'Jasmonates and related compounds from *Fusarium oxysporum*'. *Phytochemistry,* 50 (4), pp.517-523.

Millot, M., Tomasi, S., Studzinska, E., Rouaud, I. & Boustie, J. (2009) 'Cytotoxic constituents of the lichen *Diploicia canescens*'. *Journal of natural products,* 72 (12), pp.2177-2180.

Mitova, M., Tommonaro, G., Hentschel, U., Muller, W.E. & De Rosa, S. (2004) 'Exocellular cyclic dipeptides from a Ruegeria strain associated with cell cultures of S*uberites domuncula*'. *Mar Biotechnol (NY),* 6 (1), pp.95-103.

Mohandas, N. & Gallagher, P.G. (2008) 'Red cell membrane: past, present, and future'. *Blood,* 112 (10), pp.3939-3948.

Moideen, S.V., Houghton, P.J., Rock, P., Croft, S.L. & Aboagye-Nyame, F. (1999) 'Activity of extracts and naphthoquinones from *Kigelia pinnata* against *Trypanosoma brucei brucei* and *Trypanosoma brucei rhodesiense*'. *Planta medica,* 65 (6), pp.536-540.

Montenegro, T.G.C., Rodrigues, F.A.R., Jimenez, P.C., Angelim, A.L., Melo, V.M.M., Rodrigues Filho, E., de Oliveira, M.d.C.F. & Costa-Lotufo, L.V. (2012) 'Cytotoxic Activity of Fungal Strains Isolated from the Ascidian *Eudistoma vannamei*'. *Chemistry & Biodiversity,* 9 (10), pp.2203-2209.

Morello, A., Pavani, M., Garbarino, J.A., Chamy, M.C., Frey, C., Mancilla, J., Guerrero, A., Repetto, Y. & Ferreira, J. (1995) 'Effects and mode of action of

1,4-naphthoquinones isolated from *Calceolaria sessilis* on tumoral cells and Trypanosoma parasites'. *Comp Biochem Physiol C Pharmacol Toxicol Endocrinol,* 112 (2), pp.119-128.

Mukaiyama, T., Tsujimura, N., Otaka, S., Kosaka, Y., Hata, K., Hori, K. & Sakamoto, K. (2009) '*Anti-melanogenic Activity of Ergosterol Peroxide from Ganoderma lucidum on a Mouse Melanoma Cell Line'. Animal Cell Technology: Basic & Applied Aspects.* Springer, pp. 273-277.

Munday, R. (2000) 'Autoxidation of naphthohydroquinones: effects of pH, naphthoquinones and superoxide dismutase'. *Free radical research,* 32 (3), pp.245-253.

Munoz-Saravia, S.G., Haberland, A., Wallukat, G. & Schimke, I. (2012) 'Chronic Chagas' heart disease: a disease on its way to becoming a worldwide health problem: epidemiology, etiopathology, treatment, pathogenesis and laboratory medicine'. *Heart failure reviews,* 17 (1), pp.45-64.

Nair, D.N. & Padmavathy, S. (2014) 'Impact of Endophytic Microorganisms on Plants, Environment and Humans'. *The Scientific World Journal,* 2014 pp.250693.

Nakamori, K., Matsuura, H., Yoshihara, T., Ichihara, A. & Koda, Y. (1994) 'Potato micro-tuber inducing substances from *Lasiodiplodia theobromae'. Phytochemistry,* 35 (4), pp.835-839.

Nam, K.S., Jo, Y.S., Kim, Y.H., Hyun, J.W. & Kim, H.W. (2001) 'Cytotoxic activities of acetoxyscirpenediol and ergosterol peroxide from *Paecilomyces tenuipes'. Life sciences,* 69 (2), pp.229-237.

Nam, S.-J., Kauffman, C.A., Jensen, P.R. & Fenical, W. (2011) 'Isolation and characterization of actinoramides A–C, highly modified peptides from a marine *Streptomyces* sp'. *Tetrahedron,* 67 (35), pp.6707-6712.

Nass, R. & Rimpler, H. (1996) 'Distribution of iridoids in different populations of *Physostegia virginiana* and some remarks on iridoids from *Avicennia officinalis* and *Scrophularia ningpoensis'. Phytochemistry,* 41 (2), pp.489-498.

Newman, D.J. & Cragg, G.M. (2004) 'Marine natural products and related compounds in clinical and advanced preclinical trials'. *Journal of natural products,* 67 (8), pp.1216-1238.

Newman, D.J. & Cragg, G.M. (2012) 'Natural products as sources of new drugs over the 30 years from 1981 to 2010'. *Journal of natural products,* 75 (3), pp.311-335.

Nielsen, J. & Oliver, S. (2005) 'The next wave in metabolome analysis'. *Trends in biotechnology,* 23 (11), pp.544-546.

Nishikawa, H. (1933) 'Biochemistry of Filamentous Fungi. II: A Metabolic Product of *Aspergillus melleus* Yukawa. Part I'. *Journal of the Agricultural Chemical Society of Japan,* 9 (7-9), pp.107-109.

Nunes, F.M., Oliveira, M.d.C.F.d., Arriaga, Â., Lemos, T.L., Andrade-Neto, M., Mattos, M.C.d., Mafezoli, J., Viana, F.M., Ferreira, V.M. & Rodrigues-Filho, E. (2008) 'A new eremophilane-type sesquiterpene from the phytopatogen fungus *Lasiodiplodia theobromae* (Sphaeropsidaceae)'. *Journal of the Brazilian Chemical Society,* 19 (3), pp.478-482.

O'Brien, J., Wilson, I., Orton, T. & Pognan, F. (2000) 'Investigation of the Alamar Blue (resazurin) fluorescent dye for the assessment of mammalian cell cytotoxicity'. *European Journal of Biochemistry,* 267 (17), pp.5421-5426.

Oliveira, C.M., Silva, G.H., Regasini, L.O., Zanardi, L.M., Evangelista, A.H., Young, M.C., Bolzani, V.S. & Araujo, A.R. (2009) 'Bioactive metabolites produced by *Penicillium* sp. 1 and sp. 2, two endophytes associated with *Alibertia macrophylla* (Rubiaceae)'. *Z Naturforsch C,* 64 (11-12), pp.824-830.

Onegi, B., Kraft, C., Köhler, I., Freund, M., Jenett-Siems, K., Siems, K., Beyer, G., Melzig, M.F., Bienzle, U. & Eich, E. (2002) 'Antiplasmodial activity of naphthoquinones and one anthraquinone from *Stereospermum kunthianum*'. *Phytochemistry,* 60 (1), pp.39-44.

Parisi, A., Piattelli, M., Tringali, C. & Di San Lio, G.M. (1993) 'Identification of the phytotoxin mellein in culture fluids of *Phoma tracheiphila*'. *Phytochemistry,* 32 (4), pp.865-867.

Parisot, D., Devys, M. & Barbier, M. (1988) 'Fusarubinoic acid, a new naphthoquinone from the fungus *Nectria haematococca*'. *Phytochemistry,* 27 (9), pp.3002-3004.

Pattanaik, C., Reddy, C., Dhal, N. & Das, R. (2008) 'Utilisation of mangrove forests in Bhitarkanika wildlife sanctuary, Orissa'. *Indian journal of traditional knowledge,* 7 (4), pp.598-603.

Pedraza, J.M.T., Aguilera, J.A.M., Díaz, C.N., Ortiz, D.T., Monter, Á.V. & Mir, S.G.L. (2013) 'CONTROL OF Lasiodiplodia theobromae, The Causal Agent of Dieback of Sapot Mamey [*Pouteria sapota* (Jacq.) HE Moore and Stearn] GRAFTS IN MÉXICO'. *Revista Fitotecnia Mexicana,* 36 (3), pp.233-238.

Peraza-Sánchez, S.R., Chávez, D., Chai, H.-B., Shin, Y.G., García, R., Mejía, M., Fairchild, C.R., Lane, K.E., Menendez, A.T., Farnsworth, N.R., Cordell, G.A., Pezzuto, J.M. & Kinghorn, A.D. (2000) 'Cytotoxic Constituents of the Roots of *Ekmanianthe longiflora*'. *Journal of Natural Products,* 63 (4), pp.492-495.

Peter, K.L.N. & Sivasothi, N. (1999) *A Guide to the Mangroves of Singapore 1: The Ecosystem & Plant Diversity.* Singapore Science Centre; revised edition (2002).

Petersen, L.M., Hoeck, C., Frisvad, J.C., Gotfredsen, C.H. & Larsen, T.O. (2014) 'Dereplication guided discovery of secondary metabolites of mixed biosynthetic origin from *Aspergillus aculeatus*'. *Molecules,* 19 (8), pp.10898-10921.

Pink, R., Hudson, A., Mouriès, M.-A. & Bendig, M. (2005) 'Opportunities and challenges in antiparasitic drug discovery'. *Nature Reviews Drug Discovery,* 4 (9), pp.727-740.

Poch, G.K. & Gloer, J.B. (1989) 'Helicascolides A and B: New Lactones from the Marine Fungus *Helicascus kanaloanus*'. *Journal of Natural Products,* 52 (2), pp.257-260.

Pomponi, S.A. (1999) 'The bioprocess–technological potential of the sea'. *Journal of Biotechnology,* 70 (1), pp.5-13.

Pontius, A., Krick, A., Kehraus, S., Brun, R. & Konig, G.M. (2008) 'Antiprotozoal activities of heterocyclic-substituted xanthones from the marine-derived fungus *Chaetomium* sp'. *J Nat Prod,* 71 (9), pp.1579-1584.

Priotto, G., Fogg, C., Balasegaram, M., Erphas, O., Louga, A., Checchi, F., Ghabri, S. & Piola, P. (2006) 'Three drug combinations for late-stage *Trypanosoma brucei gambiense* sleeping sickness: a randomized clinical trial in Uganda'. *PLoS Clin Trials,* 1 (8), pp.e39.

Priotto, G., Kasparian, S., Mutombo, W., Ngouama, D., Ghorashian, S., Arnold, U., Ghabri, S., Baudin, E., Buard, V. & Kazadi-Kyanza, S. (2009) 'Nifurtimox-eflornithine combination therapy for second-stage African *Trypanosoma brucei gambiense* trypanosomiasis: a multicentre, randomised, phase III, non-inferiority trial'. *The Lancet,* 374 (9683), pp.56-64.

Punithalingam, E. (1976) '*Botryodiplodia theobromae*. CMI descriptions of pathogenic fungi and bacteria, No.519'. *Commonwealth Mycological Institute, Key, Surrey, England.*

Pérez-Castorena, A.L., Arciniegas, A., Villaseñor, J.L. & de Vivar, A.R. (2004) 'Furanoeremophilane derivatives from *Psacalium beamanii*'. *Rev. Soc. Quím. Méx,* 48 pp.21-23.

Quang, D.N., Bach, D.D., Hashimoto, T. & Asakawa, Y. (2006) 'Chemical constituents of the Vietnamese inedible mushroom *Xylaria intracolorata*'. *Natural product research,* 20 (04), pp.317-321.

Ramos, H.P., Simão, M.R., de Souza, J.M., Magalhães, L.G., Rodrigues, V., Ambrósio, S.R. & Said, S. (2013) 'Evaluation of dihydroisocoumarins produced by the endophytic fungus Arthrinium state of *Apiospora montagnei* against *Schistosoma mansoni*'. *Natural Product Research,* 27 (23), pp.2240-2243.

Ramos-Ligonio, A., López-Monteon, A. & Trigos, Á. (2012) 'Trypanocidal activity of ergosterol peroxide from *Pleurotus ostreatus*'. *Phytotherapy Research,* 26 (6), pp.938-943.

Rassi, A. & de Rezende, J.M. (2012) 'American trypanosomiasis (Chagas disease)'. *Infectious disease clinics of North America,* 26 (2), pp.275-291.

Rassi, A. & Marin-Neto, J.A. (2010) 'Chagas disease'. *The Lancet,* 375 (9723), pp.1388-1402.

Rawat, D.S., Joshi, M.C., Joshi, P. & Atheaya, H. (2006) 'Marine Peptides and Related Compounds in Clinical Trial'. *Anti-Cancer Agents in Medicinal Chemistry (Formerly Current Medicinal Chemistry-Anti-Cancer Agents),* 6 (1), pp.33-40.

Rehman, A., Javed, N., Malik, A. & Mehboob, S. (2014) 'Toxin production by *Fusarium solani* from declining citrus plants and its management'. *African Journal of Biotechnology,* 11 (9), pp.2199-2203.

Ren, H., Tian, L., Gu, Q. & Zhu, W. (2006) 'Secalonic acid D; A cytotoxic constituent from marine lichen-derived fungus *Gliocladium* sp. T31'. *Archives of pharmacal research,* 29 (1), pp.59-63.

Reyes-Chilpa, R., Estrada-Muniz, E., Vega-Avila, E., Abe, F., Kinjo, J. & Hernandez-Ortega, S. (2008) 'Trypanocidal constituents in plants: 7. Mammea-type coumarins'. *Mem Inst Oswaldo Cruz,* 103 (5), pp.431-436.

Rezanka, T. & Sigler, K. (2007) 'Hirtusneanoside, an unsymmetrical dimeric tetrahydroxanthone from the lichen *Usnea hirta*'. *Journal of natural products,* 70 (9), pp.1487-1491.

Ribeiro-Rodrigues, R., dos Santos, W.G., Zani, C.L., Oliveira, A.B., Snieckus, V. & Romanha, A.J. (1995) 'Growth inhibitory effect of naphthofuran and naphthofuranquinone derivatives on *Trypanosoma cruzi* epimastigotes'. *Bioorganic and Medicinal Chemistry Letters,* 5 (14), pp.1509-1512.

Rinehart, K.L., Holt, T.G., Fregeau, N.L., Stroh, J.G., Keifer, P.A., Sun, F., Li, L.H. & Martin, D.G. (1990) 'Ecteinascidins 729, 743, 745, 759A, 759B, and 770: potent antitumor agents from the Caribbean tunicate *Ecteinascidia turbinata*'. *The Journal of Organic Chemistry,* 55 (15), pp.4512-4515.

Rodriguez, S., Guíñez, R., Matos, M., Azar, C. & Maya, J. (2015) 'Synthesis and Trypanocidal Properties of New Coumarin-Chalcone Derivatives'. *Med chem,* 5 pp.173-177.

Rukachaisirikul, V., Sommart, U., Phongpaichit, S., Hutadilok-Towatana, N., Rungjindamai, N. & Sakayaroj, J. (2007) 'Metabolites from the xylariaceous fungus PSU-A80'. *Chemical and Pharmaceutical Bulletin,* 55 (9), pp.1316-1318.

Russo, A., Cardile, V., Piovano, M., Caggia, S., Espinoza, C.L. & Garbarino, J.A. (2010) 'Pro-apoptotic activity of ergosterol peroxide and (22E)-ergosta-7,22-dien-5α-hydroxy-3,6-dione in human prostate cancer cells'. *Chemico-Biological Interactions,* 184 (3), pp.352-358.

Räz, B., Iten, M., Grether-Bühler, Y., Kaminsky, R. & Brun, R. (1997) 'The Alamar Blue® assay to determine drug sensitivity of African trypanosomes (Tb rhodesiense and Tb gambiense) in vitro'. *Acta tropica,* 68 (2), pp.139-147.

Salas, C., Tapia, R.A., Ciudad, K., Armstrong, V., Orellana, M., Kemmerling, U., Ferreira, J., Maya, J.D. & Morello, A. (2008) '*Trypanosoma cruzi*: Activities of lapachol and α- and β-lapachone derivatives against epimastigote and trypomastigote forms'. *Bioorganic & Medicinal Chemistry,* 16 (2), pp.668-674.

Salmon-Chemin, L., Buisine, E., Yardley, V., Kohler, S., Debreu, M.-A., Landry, V., Sergheraert, C., Croft, S.L., Krauth-Siegel, R.L. & Davioud-Charvet, E. (2001) '2- and 3-Substituted 1,4-Naphthoquinone Derivatives as Subversive Substrates of Trypanothione Reductase and Lipoamide Dehydrogenase from *Trypanosoma cruzi*: Synthesis and Correlation between Redox Cycling Activities and in Vitro Cytotoxicity'. *Journal of Medicinal Chemistry,* 44 (4), pp.548-565.

Sasaki, M., Kaneko, Y., Oshita, K., Takamatsu, H., Asao, Y. & Yokotsuka, T. (1970) 'Studies on the Compounds Produced by Molds: Part VII. Isolation of Isocoumarin Compounds'. *Agricultural and Biological Chemistry,* 34 (9), pp.1296-1300.

Sawadsitang, S., Mongkolthanaruk, W., Suwannasai, N. & Sodngam, S. (2015) 'Antimalarial and cytotoxic constituents of *Xylaria cf. cubensis* PK108'. *Nat Prod Res,* 29 (21), pp.2033-2036.

Sayers, E.W., Barrett, T., Benson, D.A., Bolton, E., Bryant, S.H., Canese, K., Chetvernin, V., Church, D.M., DiCuccio, M., Federhen, S., Feolo, M., Geer, L.Y., Helmberg, W., Kapustin, Y., Landsman, D., Lipman, D.J., Lu, Z.,

Madden, T.L., Madej, T., Maglott, D.R., Marchler-Bauer, A., Miller, V., Mizrachi, I., Ostell, J., Panchenko, A., Pruitt, K.D., Schuler, G.D., Sequeira, E., Sherry, S.T., Shumway, M., Sirotkin, K., Slotta, D., Souvorov, A., Starchenko, G., Tatusova, T.A., Wagner, L., Wang, Y., John Wilbur, W., Yaschenko, E. & Ye, J. (2010) 'Database resources of the National Center for Biotechnology Information'. *Nucleic Acids Research,* 38 (Database issue), pp.D5-D16.

Schmeda-Hirschmann, G. & Papastergiou, F. (2003) 'Naphthoquinone derivatives and lignans from the Paraguayan crude drug "tayï pytá"(*Tabebuia heptaphylla*, Bignoniaceae)'. *Zeitschrift für Naturforschung C,* 58 (7-8), pp.495-501.

Schulz, B., Sucker, J., Aust, H.J., Krohn, K., Ludewig, K., Jones, P.G. & Döring, D. (1995) 'Biologically active secondary metabolites of endophytic *Pezicula* species'. *Mycological Research,* 99 (8), pp.1007-1015.

Seo, S., Uomori, A., Yoshimura, Y., Takeda, K.i., Noguchi, H., Ebizuka, Y., Sankawa, U. & Seto, H. (1992) 'Biosynthesis of the 24-methylcholesterols dihydrobrassicasterol and campesterol in cultured cells of *Amsonia elliptica*: incorporation of [1,2-13C2]acetate and [2-13C,2H3]acetate'. *Journal of the Chemical Society, Perkin Transactions 1,* (5), pp.569-572.

Seo, S.Y., Sharma, V.K. & Sharma, N. (2003) 'Mushroom tyrosinase: recent prospects'. *J Agric Food Chem,* 51 (10), pp.2837-2853.

Sharma, P. (2011) 'Alarming occurrence of Fusarium wilt disease in pea (*Pisum sativum* L.) cultivations of Jabalpur district in Central India revealed by an array of pathogenicity tests'. *Agric. Biol. JN Am,* 2 (6), pp.981-994.

Sharp, H., Thomas, D., Currie, F., Bright, C., Latif, Z., Sarker, S.D. & Nash, R.J. (2001) 'Pinoresinol and syringaresinol: two lignans from *Avicennia germinans* (Avicenniaceae)'. *Biochemical Systematics and Ecology,* 29 (3), pp.325-327.

Shetty, N. & Gupta, S. (2014) 'Eribulin drug review'. *South Asian journal of cancer,* 3 (1), pp.57.

Shin, C.-G., An, D.-G., Song, H.-H. & Lee, C. (2009) 'Beauvericin and enniatins H, I and MK1688 are new potent inhibitors of human immunodeficiency virus type-1 integrase'. *The Journal of antibiotics,* 62 (12), pp.687-690.

Siddiqui, I.N., Zahoor, A., Hussain, H., Ahmed, I., Ahmad, V.U., Padula, D., Draeger, S., Schulz, B., Meier, K., Steinert, M., Kurtán, T., Flörke, U., Pescitelli, G. & Krohn, K. (2011) 'Diversonol and Blennolide Derivatives from the Endophytic Fungus *Microdiplodia* sp.: Absolute Configuration of Diversonol'. *Journal of Natural Products,* 74 (3), pp.365-373.

Sommart, U., Rukachaisirikul, V., Sukpondma, Y., Phongpaichit, S., Sakayaroj, J. & Kirtikara, K. (2008) 'Hydronaphthalenones and a dihydroramulosin from the endophytic fungus PSU-N24'. *Chemical and Pharmaceutical Bulletin,* 56 (12), pp.1687-1690.

Souza, W. (2002) 'Basic cell biology of *Trypanosoma cruzi'*. *Current pharmaceutical design,* 8 (4), pp.269-285.

Souza-Neta, L.C., Menezes, D., Lima, M.S., Cerqueira, M.D., Cruz, F.G., Martins, D. & Vannier-Santos, M.A. (2014) 'Modes of action of arjunolic acid and

derivatives on *Trypanosoma cruzi* cells'. *Curr Top Med Chem,* 14 (8), pp.1022-1032.

Spalding, M. (2010) *World atlas of mangroves.* Routledge.

Stevens, J., Brisse, S., Maudlin, I., Holmes, P. & Miles, M. (2004) 'Systematics of trypanosomes of medical and veterinary importance'. *The trypanosomiases,* pp.1-23.

Steyn, P.S. (1970) 'The isolation, structure and absolute configuration of secalonic acid D, the toxic metabolite of *Penicillium oxalicum*'. *Tetrahedron,* 26 (1), pp.51-57.

Stierle, D.B., Stierle, A.A. & Ganser, B. (1997) 'New Phomopsolides from a *Penicillium* sp'. *Journal of natural products,* 60 (11), pp.1207-1209.

Stuart, K., Brun, R., Croft, S., Fairlamb, A., Gürtler, R.E., McKerrow, J., Reed, S. & Tarleton, R. (2008) 'Kinetoplastids: related protozoan pathogens, different diseases'. *The Journal of clinical investigation,* 118 (4), pp.1301.

Subrahmanyam, C., Kumar, S. & Reddy, G. (2006) 'Bioactive diterpenes from the mangrove *Avicennia officinalis* Linn'. *Indian Journal of Chemistry Section B-Organic Chemistry Including Medicinal Chemistry,* 45 (11), pp.2556-2557.

Summerbell, R.C., Krajden, S., Levine, R. & Fuksa, M. (2004) 'Subcutaneous phaeohyphomycosis caused by *Lasiodiplodia theobromae* and successfully treated surgically'. *Medical mycology,* 42 (6), pp.543-547.

Sumner, L.W., Mendes, P. & Dixon, R.A. (2003) 'Plant metabolomics: large-scale phytochemistry in the functional genomics era'. *Phytochemistry,* 62 (6), pp.817-836.

Sun, H., Ho, C.L., Ding, F., Soehano, I., Liu, X.-W. & Liang, Z.-X. (2012) 'Synthesis of (R)-Mellein by a Partially Reducing Iterative Polyketide Synthase'. *Journal of the American Chemical Society,* 134 (29), pp.11924-11927.

Suzuki, M., Nishida, N., Ishihara, A. & Nakajima, H. (2013) 'New 3-O-Alkyl-4a, 10a-dihydrofusarubins Produced by Fusarium sp. Mj-2'. *Bioscience, biotechnology, and biochemistry,* 77 (2), pp.271-275.

Swami, U., Chaudhary, I., Ghalib, M.H. & Goel, S. (2012) 'Eribulin—a review of preclinical and clinical studies'. *Critical reviews in oncology/hematology,* 81 (2), pp.163-184.

Takei, R., Takahashi, K., Matsuura, H. & Nabeta, K. (2008) 'New potato micro-tuber-inducing cyclohexene compounds related to theobroxide from *Lasiodiplodia theobromae*'. *Biosci Biotechnol Biochem,* 72 (8), pp.2069-2073.

Takei, T., Yoshida, M., Ohnishi-Kameyama, M. & Kobori, M. (2005) 'Ergosterol peroxide, an apoptosis-inducing component isolated from *Sarcodon aspratus* (Berk.) S. Ito'. *Bioscience, biotechnology, and biochemistry,* 69 (1), pp.212-215.

Takemoto, K., Kamisuki, S., Chia, P.T., Kuriyama, I., Mizushina, Y. & Sugawara, F. (2014) 'Bioactive Dihydronaphthoquinone Derivatives from *Fusarium solani*'. *Journal of natural products,* 77 (9), pp.1992-1996.

Tasdemir, D., Kaiser, M., Brun, R., Yardley, V., Schmidt, T.J., Tosun, F. & Rüedi, P. (2006) 'Antitrypanosomal and Antileishmanial Activities of Flavonoids and Their Analogues: In Vitro, In Vivo, Structure-Activity Relationship, and

Quantitative Structure-Activity Relationship Studies'. *Antimicrobial Agents and Chemotherapy,* 50 (4), pp.1352-1364.

Tasdemir, D., Topaloglu, B., Perozzo, R., Brun, R., O'Neill, R., Carballeira, N.M., Zhang, X., Tonge, P.J., Linden, A. & Ruedi, P. (2007) 'Marine natural products from the Turkish sponge *Agelas oroides* that inhibit the enoyl reductases from *Plasmodium falciparum*, *Mycobacterium tuberculosis* and *Escherichia coli*'. *Bioorg Med Chem,* 15 (21), pp.6834-6845.

Tatum, J., Baker, R. & Berry, R. (1985) 'Three further naphthoquinones produced by *Fusarium solani*'. *Phytochemistry,* 24 (12), pp.3019-3021.

Tatum, J.H. & Baker, R.A. (1983) 'Naphthoquinones produced by *Fusarium solani* isolated from citrus'. *Phytochemistry,* 22 (2), pp.543-547.

Taylor, D.L. & Houston, S. (2011) '*A bioinformatics pipeline for sequence-based analyses of fungal biodiversity'. Fungal Genomics.* Springer, pp. 141-155.

Tchinda, A.T., Tsopmo, A., Tane, P., Ayafor, J.F., Connolly, J.D. & Sterner, O. (2002) 'Vernoguinosterol and vernoguinoside, trypanocidal stigmastane derivatives from *Vernonia guineensis* (Asteraceae)'. *Phytochemistry,* 59 (4), pp.371-374.

Trisuwan, K., Khamthong, N., Rukachaisirikul, V., Phongpaichit, S., Preedanon, S. & Sakayaroj, J. (2010) 'Anthraquinone, Cyclopentanone, and Naphthoquinone Derivatives from the Sea Fan-Derived Fungi *Fusarium* spp. PSU-F14 and PSU-F135'. *Journal of Natural Products,* 73 (9), pp.1507-1511.

Twumasi, P., Ohene-Mensah, G. & Moses, E. (2014) 'The rot fungus *Botryodiplodia theobromae* strains cross infect cocoa, mango, banana and yam with significant tissue damage and economic losses'. *African Journal of Agricultural Research,* 9 (6), pp.613-619.

Uemura, D., Takahashi, K., Yamamoto, T., Katayama, C., Tanaka, J., Okumura, Y. & Hirata, Y. (1985) 'Norhalichondrin A: an antitumor polyether macrolide from a marine sponge'. *Journal of the American Chemical Society,* 107 (16), pp.4796-4798.

Vazquez-Rodriguez, S., Figueroa-Guinez, R., Matos, M.J., Santana, L., Uriarte, E., Lapier, M., Maya, J.D. & Olea-Azar, C. (2013) 'Synthesis of coumarin-chalcone hybrids and evaluation of their antioxidant and trypanocidal properties'. *MedChemComm,* 4 (6), pp.993-1000.

Venkatasubbaiah, P. & Chilton, W.S. (1990) 'Phytotoxins of *Botryosphaeria obtusa*'. *Journal of natural products,* 53 (6), pp.1628-1630.

Venkatasubbaiah, P., Sutton, T. & Chilton, W. (1991) 'Effect of phytotoxins produced by *Botryosphaeria obtusa*, the cause of black rot of apple fruit and frogeye leaf spot'. *Phytopathology,* 81 (3), pp.243-247.

Ventura Pinto, A. & Lisboa de Castro, S. (2009) 'The Trypanocidal Activity of Naphthoquinones: A Review'. *Molecules,* 14 (11), pp.4570-4590.

Verpoorte, R., Choi, Y. & Kim, H. (2007) 'NMR-based metabolomics at work in phytochemistry'. *Phytochemistry reviews,* 6 (1), pp.3-14.

Viegelmann, C., Parker, J., Ooi, T., Clements, C., Abbott, G., Young, L., Kennedy, J., Dobson, A. & Edrada-Ebel, R. (2014) 'Isolation and Identification of Antitrypanosomal and Antimycobacterial Active Steroids from the Sponge *Haliclona simulans*'. *Marine Drugs,* 12 (5), pp.2937-2952.

Villamil, S.F., Stoppani, A.O. & Dubin, M. (2004) 'Redox Cycling of β-Lapachone and Structural Analogues in Microsomal andCytosol Liver Preparations'. *Methods in enzymology,* 378 pp.67-87.

Wang, F., Fang, Y., Zhu, T., Zhang, M., Lin, A., Gu, Q. & Zhu, W. (2008) 'Seven new prenylated indole diketopiperazine alkaloids from holothurian-derived fungus *Aspergillus fumigatus*'. *Tetrahedron,* 64 (34), pp.7986-7991.

Wezeman, T., Bräse, S. & Masters, K.-S. (2015) 'Xanthone dimers: a compound family which is both common and privileged'. *Natural product reports,* 32 (1), pp.6-28.

Wilkinson, S.R. & Kelly, J.M. (2009) 'Trypanocidal drugs: mechanisms, resistance and new targets'. *Expert Reviews in Molecular Medicine,* 11 pp.null-null.

Wilkinson, S.R., Taylor, M.C., Horn, D., Kelly, J.M. & Cheeseman, I. (2008) 'A mechanism for cross-resistance to nifurtimox and benznidazole in trypanosomes'. *Proceedings of the National Academy of Sciences,* 105 (13), pp.5022-5027.

Williams, R.B. (2005) *Searching for anticancer natural products from the rainforest plants of Suriname and Madagascar.* Virginia Polytechnic Institute and State University.

Williams, R.B., Norris, A., Miller, J.S., Razafitsalama, L.J., Andriantsiferana, R., Rasamison, V.E. & Kingston, D.G.I. (2006) 'Two New Cytotoxic Naphthoquinones from *Mendoncia cowanii* from the Rainforest of Madagascar'. *Planta medica,* 72 (6), pp.564-566.

Wold, H. (2004) '*Partial Least Squares*'. *Encyclopedia of Statistical Sciences.* John Wiley & Sons, Inc., pp.

Wolfender, J.-L., Marti, G., Thomas, A. & Bertrand, S. (2015) 'Current approaches and challenges for the metabolite profiling of complex natural extracts'. *Journal of Chromatography A,* 1382 pp.136-164.

Wolfender, J.-L., Rudaz, S., Hae Choi, Y. & Kyong Kim, H. (2013) 'Plant metabolomics: from holistic data to relevant biomarkers'. *Current medicinal chemistry,* 20 (8), pp.1056-1090.

Wright, A.E., Forleo, D.A., Gunawardana, G.P., Gunasekera, S.P., Koehn, F.E. & McConnell, O.J. (1990) 'Antitumor tetrahydroisoquinoline alkaloids from the colonial ascidian *Ecteinascidia turbinata*'. *The Journal of Organic Chemistry,* 55 (15), pp.4508-4512.

Wu, J., Xiao, Q., Xu, J., Li, M.-Y., Pan, J.-Y. & Yang, M.-h. (2008) 'Natural products from true mangrove flora: source, chemistry and bioactivities'. *Natural product reports,* 25 (5), pp.955-981.

Wu, Q.-P., Xie, Y.-Z., Deng, Z., Li, X.-M., Yang, W., Jiao, C.-W., Fang, L., Li, S.-Z., Pan, H.-H. & Yee, A.J. (2012) 'Ergosterol peroxide isolated from *Ganoderma lucidum* abolishes microRNA miR-378-mediated tumor cells on chemoresistance'. *PLoS One,* 7 (8), pp.e44579.

Wu, X.Y., Liu, X.H., Jiang, G.C., Lin, Y.C., Chan, W. & Vrijmoed, L. (2005a) 'Xyloketal G, a novel metabolite from the mangrove fungus *Xylaria* sp. 2508'. *Chemistry of Natural Compounds,* 41 (1), pp.27-29.

Wu, X.Y., Liu, X.H., Lin, Y.C., Luo, J.H., She, Z.G., Houjin, L., Chan, W.L., Antus, S., Kurtan, T. & Elsässer, B. (2005b) 'Xyloketal F: A Strong L-Calcium Channel Blocker from the Mangrove Fungus *Xylaria* sp.(# 2508) from the

South China Sea Coast'. *European journal of organic chemistry,* 2005 (19), pp.4061-4064.

Xie, H.H., Wei, J.G., Liu, F., Pan, X.H. & Yang, X.B. (2014) 'First Report of Mulberry Root Rot Caused by *Lasiodiplodia theobromae* in China'. *Plant Disease,* 98 (11), pp.1581-1581.

Xu, F., Zhang, Y., Wang, J., Pang, J., Huang, C., Wu, X., She, Z., Vrijmoed, L.L., Jones, E.B. & Lin, Y. (2008) 'Benzofuran derivatives from the mangrove endophytic Fungus *Xylaria* sp. (#2508)'. *J Nat Prod,* 71 (7), pp.1251-1253.

Xu, J. (2015) 'Bioactive natural products derived from mangrove-associated microbes'. *RSC Advances,* 5 (2), pp.841-892.

Xu, J., Kjer, J., Sendker, J., Wray, V., Guan, H., Edrada, R., Lin, W., Wu, J. & Proksch, P. (2009) 'Chromones from the endophytic fungus *Pestalotiopsis* sp. isolated from the Chinese mangrove plant *Rhizophora mucronata*'. *Journal of natural products,* 72 (4), pp.662-665.

Xu, L., Wang, J., Zhao, J., Li, P., Shan, T., Li, X. & Zhou, L. (2010) 'Beauvericin from the endophytic fungus, *Fusarium redolens*, isolated from *Dioscorea zingiberensis* and its antibacterial activity'. *Natural product communications,* 5 (5), pp.811-814.

Yamazaki, M., Maebayashi, Y. & Miyaki, K. (1971) 'The Isolation of Secalonic Acid A from *Aspergillus ochraceus* cultured on Rice'. *Chemical & Pharmaceutical Bulletin,* 19 (1), pp.199-201.

Yang, F., Jacobsen, S., Jørgensen, H.J.L., Collinge, D.B., Svensson, B. & Finnie, C. (2013) '*Fusarium graminearum* and its interactions with cereal heads: studies in the proteomics era'. *Frontiers in Plant Science,* 4.

Yang, Q., Asai, M., Matsuura, H. & Yoshihara, T. (2000) 'Potato micro-tuber inducing hydroxylasiodiplodins from *Lasiodiplodia theobromae*'. *Phytochemistry,* 54 (5), pp.489-494.

Yin, W., Lin, Y., She, Z., Vrijmoed, L. & Jones, E.G. (2008) 'A new compound: Xyloketal H from mangrove fungus *Xylaria* sp. from the South China Sea Coast'. *Chemistry of Natural Compounds,* 44 (1), pp.3-5.

Yonghong, L. (2012) 'Renaissance of marine natural product drug discovery and development'. *Journal of Marine Science Research & Development*.

Yoo, J.S., Ahn, E.M., Bang, M.H., Song, M.C., Yang, H.J., Kim, D.H., Lee, D.Y., Chung, H.G., Jeong, T.S. & Lee, K.T. (2006) 'Steroids from the aerial parts of *Artemisia princeps* Pampanini'. *Hanguk Yakyong Changmul Hakhoe Chi,* 14 pp.273-277.

Yu, Y., Gao, H., Tang, Z., Song, X. & Wu, L. (2006) 'Several phenolic acids from the fruit of *Capparis spinosa*'. *Asian Journal of Traditional Medicines,* 1 (3/4), pp.1-4.

Zani, C.L., De Oliveira, A.B. & De Oliviera, G.G. (1991) 'Furanonaphthoquinones from *Tabebuia ochracea*'. *Phytochemistry,* 30 (7), pp.2379-2381.

Zhai, A., Zhang, Y., Zhu, X., Liang, J., Wang, X., Lin, Y. & Chen, R. (2011) 'Secalonic acid A reduced colchicine cytotoxicity through suppression of JNK, p38 MAPKs and calcium influx'. *Neurochemistry International,* 58 (1), pp.85-91.

Zhang, J.-y., Tao, L.-y., Liang, Y.-j., Yan, Y.-y., Dai, C.-l., Xia, X.-k., She, Z.-g., Lin, Y.-c. & Fu, L.-w. (2009) 'Secalonic acid D induced leukemia cell

apoptosis and cell cycle arrest of G1 with involvement of GSK-3β/β-catenin/c-Myc pathway'. *Cell Cycle,* 8 (15), pp.2444-2450.

Zhang, L., Yan, K., Zhang, Y., Huang, R., Bian, J., Zheng, C., Sun, H., Chen, Z., Sun, N. & An, R. (2007) 'High-throughput synergy screening identifies microbial metabolites as combination agents for the treatment of fungal infections'. *Proceedings of the National Academy of Sciences,* 104 (11), pp.4606-4611.

Zhang, W., Krohn, K., Florke, U., Pescitelli, G., Di Bari, L., Antus, S., Kurtan, T., Rheinheimer, J., Draeger, S. & Schulz, B. (2008) 'New mono- and dimeric members of the secalonic acid family: blennolides A-G isolated from the fungus *Blennoria* sp'. *Chemistry,* 14 (16), pp.4913-4923.

Zhao, J., Mou, Y., Shan, T., Li, Y., Zhou, L., Wang, M. & Wang, J. (2010) 'Antimicrobial metabolites from the endophytic fungus *Pichia guilliermondii* isolated from *Paris polyphylla* var. yunnanensis'. *Molecules,* 15 (11), pp.7961-7970.

Zhao, L.L., Gai, Y., Kobayashi, H., Hu, C.Q. & Zhang, H.P. (2008) '5′-Hydroxyzearalenol, a new β-resorcylic macrolide from *Fusarium* sp. 05ABR26'. *Chinese Chemical Letters,* 19 (9), pp.1089-1092.

Zhu, F., Lin, Y. & Zhou, S. (2004) 'Anthraquinone derivatives isolated from marine fungus #2526 from the South China Sea'. *Chinese Journal of Organic Chemistry ,* 24 (9), pp.1114-1117.

Zhu, F., Lin, Y., Zhou, S. & Vrijmode, L. (2003a) 'Xanthone Derivatives Isolated from two Mangrove EndophyticFungi #2526 and #1850 from the South China Sea'. *Natural Product Research and Development,* 16 (5), pp.406-409.

Zhu, F., Lin, Y.-C., Zhou, S.-N. & Vrijmoed, L. (2003b) 'Sterigmatocystin isolated from mangrove endophytic fungus no. 2526'. *Chinese Journal of Applied Chemistry*, 20 (3), pp.272-274.

Zhu, R., Zheng, R., Deng, Y., Chen, Y. & Zhang, S. (2014) 'Ergosterol peroxide from *Cordyceps cicadae* ameliorates TGF-β1-induced activation of kidney fibroblasts'. *Phytomedicine,* 21 (3), pp.372-378.